ZooKeys 1205: 1–15 (2024)
DOI: 10.3897/zookeys.1205.124081

Research Article

# *Poxyaibamberus* Andersen & Dantas, gen. nov. (Diptera, Chironomidae, Orthocladiinae) from Brazil

Trond Andersen[1], Galileu P. S. Dantas[2], Viktor Baranov[3], Annui M. Sanz-laParra[1], Humberto F. Mendes[4], Neusa Hamada[2]

1 *Department of Natural History, University Museum of Bergen, University of Bergen, P.O. Box 7800, NO-5020 Bergen, Norway*
2 *Instituto Nacional de Pesquisas da Amazônia, Coordenação de Biodiversidade (CoBio), PPG_ENTO, Av. André Araújo, 2936, 69067–375, Manaus, Amazonas, Brazil*
3 *Estación Biológica de Doñana-CSIC / Doñana Biological Station-CSIC, C. Américo Vespucio, s/n, 41092 Seville, Spain*
4 *Department of Biology, Instituto de Ciências da Natureza, Universidade Federal de Alfenas, Rua Gabriel Monteiro da Silva, 700, 37130-001 Alfenas, Mato Grosso, Brazil*
*Corresponding author: Viktor Baranov (viktor.baranov@ebd.csic.es)*

## Abstract

*Poxyaibamberus* Andersen & Dantas, **gen. nov.** is erected based on the males of two species, *P. jamanximensis* Andersen & Dantas, **sp. nov.** from Jamanxim National Park, Pará State, Brazil, and *P. ubajarensis* Andersen & Dantas, **sp. nov.** from Ubajara National Park, Ceará State, Brazil. Both species have a comparatively short and wide head, with large eyes and short, five-segmented palps; a strong subapical seta on the ultimate flagellomere; scalpellate acrostichals; no setae on the wing veins except for one seta on the brachiolum; a long costal extension; and a large triangular anal point and a very long heel on the gonostylus. The systematic position of the new genus is briefly discussed.

**Key words:** Aquatic insects, new species, Neotropical Region, taxonomy

Academic editor: Fabio L. da Silva
Received: 27 March 2024
Accepted: 15 May 2024
Published: 14 June 2024

ZooBank: https://zoobank.org/8D5E77EA-DD32-4E89-868B-17475C16DBA7

Citation: Andersen T, Dantas GPS, Baranov V, Sanz-laParra AM, Mendes HF, Hamada N (2024) *Poxyaibamberus* Andersen & Dantas, gen. nov. (Diptera, Chironomidae, Orthocladiinae) from Brazil. ZooKeys 1205: 1–15. https://doi.org/10.3897/zookeys.1205.124081

## Introduction

The number of orthoclad species known from Brazil has increased rapidly during the last three decades. In their catalog of the Neotropical and Mexican chironomids Spies and Reiss (1996) recorded eight Orthocladiinae species in six genera from Brazil; one of these, *Ichthyocladius neotropicus* Fittkau, 1974, was listed as uncertain and has later been proven to not occur in Brazil (Mendes et al. 2004). Today more than 144 species in 44 genera are known to occur in the country (Pinho et al. 2024), although there is still a significant gap in the North and Northeast regions, where only 23 and 14 species of Orthocladiinae have been recorded. Many orthoclads encountered in Brazil do not readily fit into any described genus, and many new genera have been described. Several genera, namely *Gynocladius* Mendes, Sæther & Andrade-Morraye, 2005; *Oleia* Andersen & Mendes, 2007; *Saetherocladius* Andersen & Mendes, 2007; *Saetherocryptus* Andersen & Mendes, 2007; *Saetherolabis* Andersen & Mendes, 2007; *Saetherops* Andersen & Mendes, 2007; *Lyrocladius* Mendes & Andersen, 2008; *Ubatubaneura* Wiedenbrug & Trivinho-Strixino, 2009; *Iporangomberus* Mendes & Andersen, 2012; *Pebapomberus*

Mendes & Andersen, 2012; *Miambera* Andersen & Mendes, 2012; *Maximberus* Andersen & Mendes, 2012; *Jururumberus* Mendes & Andersen, 2013; *Uirassubrillia* Mendes, Andersen & Pinho, 2013; *Caaporangombera* Andersen, Pinho & Mendes, 2015; *Mariambera* Andersen, Mendes & Pinho, 2015; and *Urubicimbera* Andersen, Pinho & Mendes, 2015 are so far endemic to Brazil (Mendes et al. 2005, 2013; Andersen and Mendes 2007, 2012a, 2012b; Mendes and Andersen 2008, 2012a, 2012b, 2013; Wiedenbrug and Trivinho-Strixino 2009; Andersen et al. 2015a, 2015b, 2015c). However, several of these genera are expected to be more widely distributed when the chironomid fauna of neighboring countries is better studied.

Below we describe a new genus based on the males of two new species collected in Pará and Ceará states in northern and northeastern Brazil. Both species have a comparatively wide head with large eyes and short, five-segmented palps, a strong subapical seta on the ultimate flagellomere, scalpellate acrostichals, a long costal extension, no setae on the wing membrane and veins except for one seta on the brachiolum, a large triangular anal point, and a gonostylus with a very long heel. The systematic position of the new genus is briefly discussed.

## Materials and methods

The specimens were collected with Shannon traps (Shannon 1939) or light traps and preserved in 80% ethanol during the fieldwork. Prior to examination they were mounted in Euparal following the procedure outlined by Sæther (1969). Morphological terminology follows Sæther (1980). Coloration is based on the slide mounted specimen.

For the phylogenetic analysis we have used a morphological character matrix with 45 taxa and 83 characters. Characters were sampled from larvae, pupae, and adult males and females. Fossils were of course underrepresented in terms of characters available for observation (see https://github.com/chironomus/Poxyaibamberus-). The character matrix for the phylogenetic analysis was built using NEXUS DATA EDITOR v. 0.5. 0 (Page 2001).

First, a Bayesian analysis of the morphological matrix alone in MRBAYES 3.2.2. (Ronquist et al. 2012) was conducted using the Bayesian implementation of Lewis' Markov models (Lewis 2001). In Bayesian inference, two Markov chains were run simultaneously for 10 million generations using a discrete Dirichlet distribution with equal state frequencies (Lewis 2001). Substitution model was set to "gamma" (Nylander et al. 2004). The first 25 0000 generations were discarded as a burn-in (number of MRBAYES generations of the tree topology before the apparent stationary condition) (Nylander et al. 2004). Consensus trees showing all compatible groups and 50% compatible groups were computed in MRBAYES. Ancestral character state analysis was conducted on the allcompat consensus tree based on morphology alone using ANCTRESH in the PHYTOOLS package v. 0.7-80 (Revell 2012). R code for this analysis, alongside the data is provided in https://github.com/chironomus/Poxyaibamberus-.

To deal with the uncertainty of the positions of the genus on the tree caused by the lack of knowledge of character states, the Klopfstein and Spasojevic ROGUEPLOTS approach was applied (Klopfstein and Spasojevic 2019). A morphological allcompat tree from MRBAYES (as described above) was used to place *Poxyaibamberus* into the high posterior probability regions. ROGUEPLOTS for every species and accompanying R code are provided in the https://github.com/chironomus/Poxyaibamberus-.

Both holotypes are kept in the Invertebrate collection at the Instituto Nacional de Pesquisas da Amazônia (**INPA**), Manaus, Brazil.

## Taxonomic account

### Family Chironomidae Newman, 1834
### Subfamily Orthocladiinae Kieffer, 1911

### Genus *Poxyaibamberus* Andersen & Dantas, gen. nov.
https://zoobank.org/2FE0E263-AB8C-4240-8CB7-9FF8AF3907A4

**Type species.** *Poxyaibamberus jamanximensis* Andersen & Dantas, sp. nov.

**Diagnosis.** Small species, wing length 1.1–1.3 mm.

**Description.** ***Male antenna*** with 13 flagellomeres, strongly plumose, groove beginning on flagellomere 4, few sensilla chaetica apparently only present on flagellomere 13, with strong subapical seta. Antennal ratio 0.9.

***Head*** short and wide. Eye bare, large, reniform, without dorsomedian extension. Temporal setae in single row, consisting of inner and outer verticals. Frontal tubercle absent. Tentorium and stipes normal. Clypeus with few setae. Palp short, with 5 segments, third palpomere without sensilla clavata subapically.

***Thorax*.** Antepronotum well developed, with lobes meeting medially at anterior margin of scutum, with few ventrolateral antepronotals. Acrostichals small, scalpellate, in two rows starting some distance from antepronotum; dorsocentrals simple, uniserial; prealars few; supraalar absent. Scutellum apparently without setae.

***Wing*.** Membrane without setae, with fine punctuation. Anal lobe reduced. With long costal extension. $R_{2+3}$ running and ending close to $R_{4+5}$; $R_{4+5}$ ending distal to $M_{3+4}$; FCu far distal to RM; $Cu_1$ curved. Brachiolum with 1 seta, other veins bare. Squama bare. Sensilla campaniformia 3 above seta on brachiolum.

***Legs*.** Tibial spurs normal, comb with few setae. Pseudospurs and sensilla chaetica absent, pulvilli vestigial.

***Abdomen*.** Tergites with few setae, mostly in anterior band; sternites with few setae.

***Hypopygium*.** Anal point long, triangular, with microtrichia, with or without strong setae at base, originating high on tergite IX or at posterior margin. Tergite IX with or without setae; laterosternite IX with few setae. Phallapodeme with aedeagal lobe well developed. Transverse sternapodeme arched or straight, without oral projections. Virga apparently consists of small spines. Gonocoxite long, without volsellae. Gonostylus without crista dorsalis, with long, weakly to strongly curved heel; megaseta normal.

**Etymology.** From Tupi *Poxyaiba*, ugly and *Mberu*, fly, meaning “the ugly fly”, referring to the spiny hypopygium of *P. jamanximensis* Andersen & Dantas, sp. nov. with a very large anal point. The name is masculine.

### ***Poxyaibamberus jamanximensis*** **Andersen & Dantas, sp. nov.**

https://zoobank.org/AC19B7F6-BE94-4368-B494-44A65957202E
Figs 1A, B, 2, 3

**Type locality.** Brazil, Pará State, Itaituba, Jamanxim National Park; 05°41'58"S, 55°48'13"W; 170 m a.s.l.; 20 November 2017; Gilberto Nicácio leg.

**Type specimen.** ***Holotype*** male adult, slide-mounted in Euparal under six coverslips. Original label: "Brasil, PA, 20/11/2017, Floresta # 41, Shannon trap, Orthocladiinae, leg. G. Nicasio, ♂". (INPA).

**Diagnostic characters.** The new species can easily be separated from *P. ubajarensis* Andersen & Dantas, sp. nov. by the shape of the gonostylus, as it has a rather narrow, weakly curved, tapering heel that is slightly longer than the gonostylus proper.

**Description. Adult male** (*n* = 1). Total length 2.17 mm. Wing length 1.23 mm. Total length / wing length 1.77. Wing length / length of profemur 2.51.

***Coloration.*** Head, thorax, and legs light yellowish brown; abdomen pale yellowish brown. Wing hyaline.

***Antenna*** (Fig. 1B). With 13 segments. AR = 0.94. Terminal flagellomere 340 μm long, with 21 μm long subapical seta.

***Head*** (Fig. 1A). Inner verticals 5, outer verticals 4, postorbitals not discernable. Clypeus with 4 setae. Tentorium 99 μm long, 17 μm wide. Stipes 76 μm long. Anterior margin of cibarial pump slightly convex. Palp with palpomere 4 and 5 not measurable; palpomere 1–3 lengths (in μm) as: 14, 25, 38. Third palpomere without sensilla clavata.

***Thorax.*** Antepronotum with 2 ventrolateral setae. Acrostichals about 8, scalpellate, in double row starting some distance from antepronotum; dorsocentrals 8, uniserial; prealars 3. Scutellum apparently without setae.

***Wing*** (Fig. 2). VR = 1.33. Brachiolum with 1 seta, other veins and membrane bare. Squama bare. Costal extension 123 μm long.

***Legs.*** Fore tibia with 33 μm long spur, mid tibia with 28 and 15 μm long spurs, hind tibia with 45 and 21 μm long spurs. Width at apex of fore tibia 27 μm, of mid tibia 28 μm, of hind tibia 29 μm. Hind tibia with comb of 4 bristles, longest apparently about 28 μm long. Lengths and proportions of legs as in Table 1.

***Hypopygium*** (Fig. 3A–C). Anal point large, broadly triangular with rounded apex, starting high on tergite IX, with microtrichia and 12 strong setae in basal 1/3; 76 μm long, 39 μm wide near base, 18 μm wide medially. Laterosternite IX with 1 seta. Phallapodeme 76 μm long. Transverse sternapodeme arched, without oral projections, 62 μm long. Virga apparently consisting of field with small spines. Gonocoxite 203 μm long. Gonostylus straight, 104 μm long; heel weakly curved, tapering, 119 μm long; megaseta 7 μm long. HR = 1.95; HV = 2.09.

**Table 1.** Lengths (in μm) and proportions of legs of *Poxyaibamberus jamanximensis* Andersen & Dantas, sp. nov., male (*n* = 1).

| | Fe | Ti | $ta_1$ | $ta_2$ | $ta_3$ | $ta_4$ | $ta_5$ | LR | BV | SV | BR |
|---|---|---|---|---|---|---|---|---|---|---|---|
| $P_1$ | 490 | 596 | 547 | 270 | 155 | 82 | 49 | 0.918 | 2.941 | 1.985 | 2.10 |
| $P_2$ | 564 | 572 | 343 | 172 | 98 | 49 | 33 | 0.600 | 4.209 | 3.310 | 2.30 |
| $P_3$ | 605 | 629 | 417 | 212 | 163 | 82 | 41 | 0.662 | 3.311 | 2.961 | 2.40 |

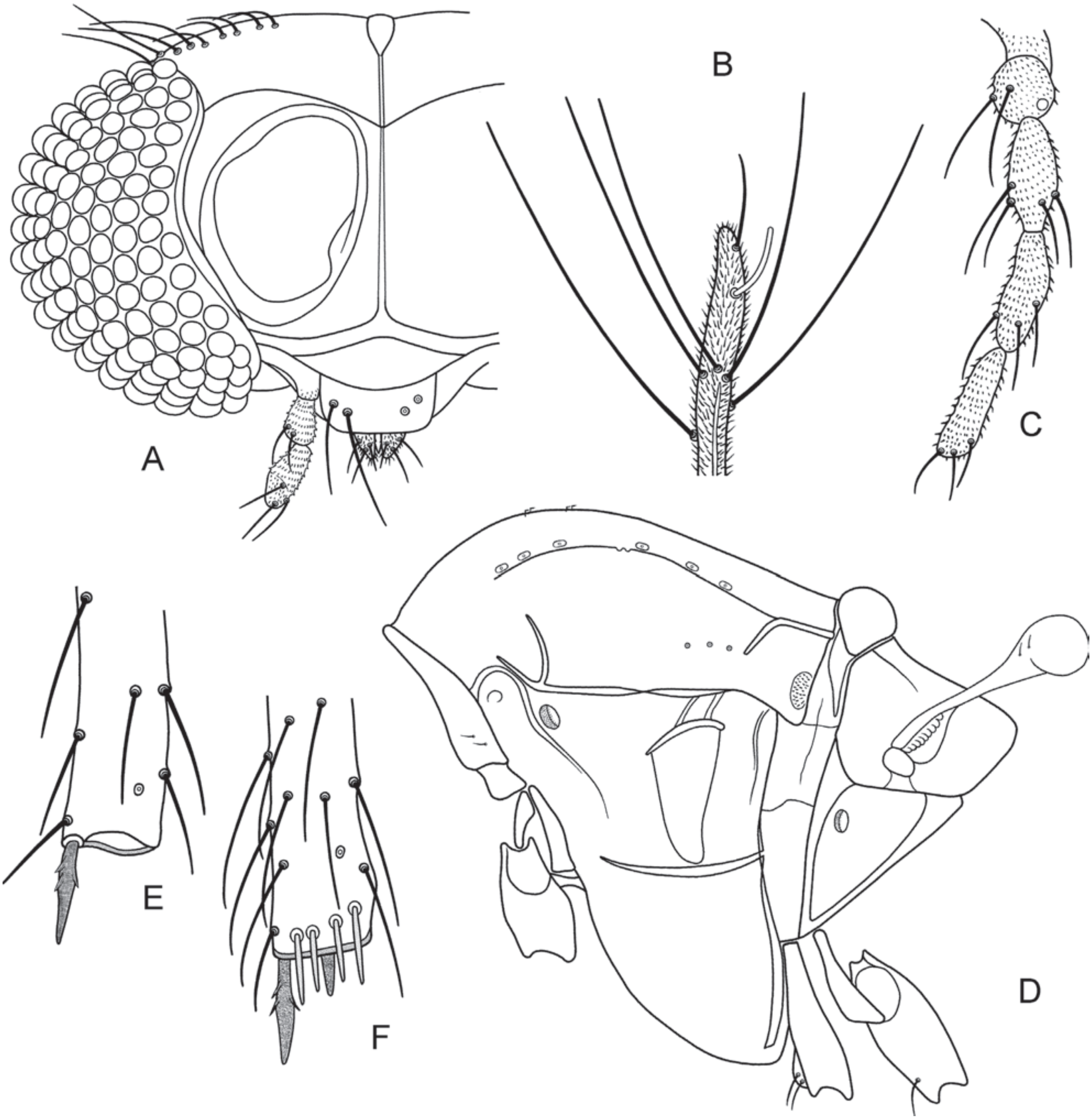

**Figure 1.** *Poxyaibamberus jamanximensis* Andersen & Dantas, sp. nov. male (**A, B**) and *P. ubajarensis* Andersen & Dantas, sp. nov., male (**C–F**) **A** head, palpomere 4 and 5 not drawn **B** apex of ultimate flagellomere **C** palp **D** thorax **E** apex of fore tibia **F** apex of hind tibia.

**Figure 2.** *Poxyaibamberus jamanximensis* Andersen & Dantas, sp. nov. male. Wing.

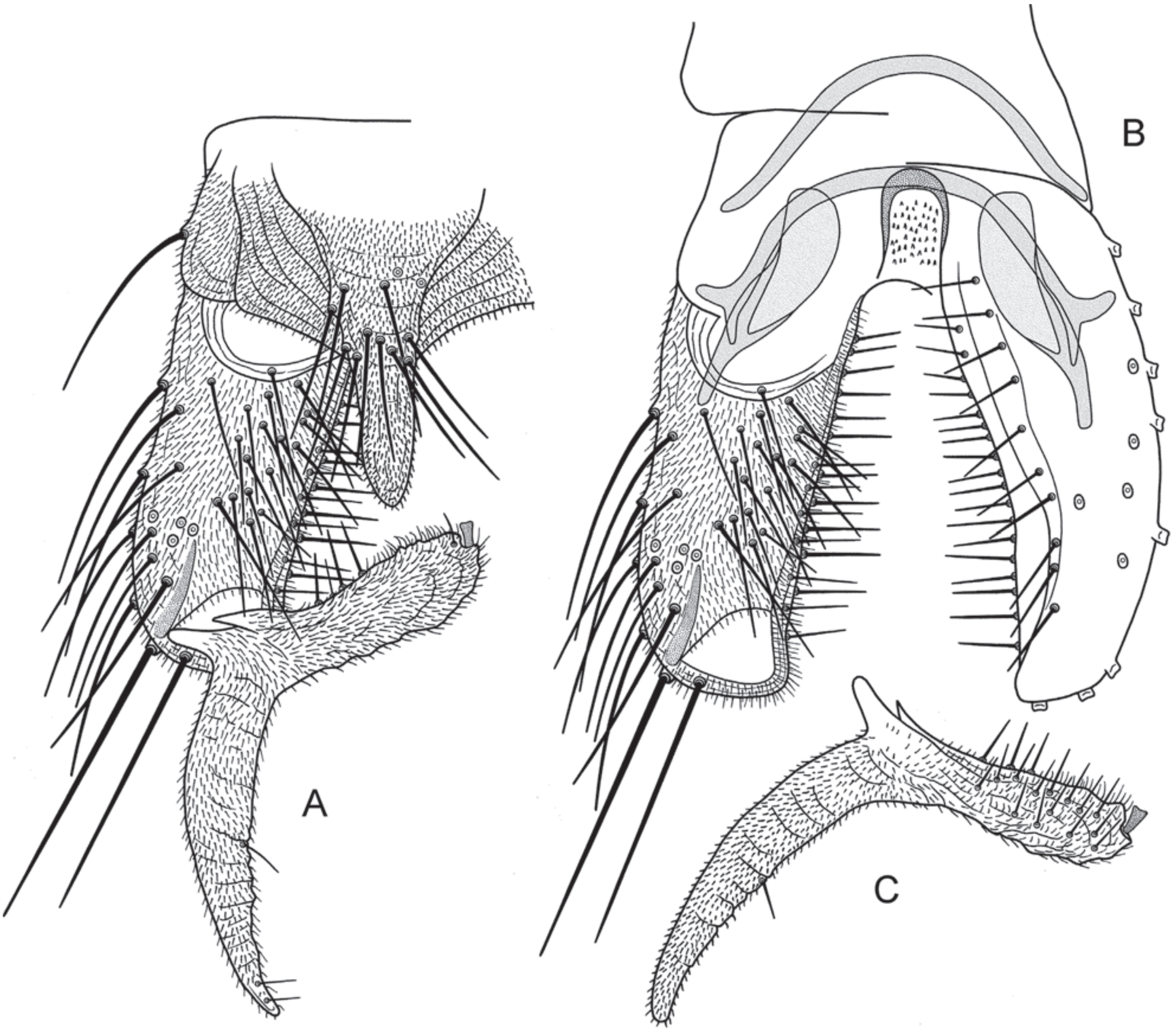

**Figure 3.** *Poxyaibamberus jamanximensis* Andersen & Dantas, sp. nov. male. **A** hypopygium, dorsal view **B** hypopygium with tergite IX and anal point removed, left dorsal aspect, right ventral aspect **C** gonostylus, ventral view.

**Immatures and female.** Larva, pupa, and female are unknown.

**Etymology.** The epithet, *jamanximensis*, is used as an adjective and meaning "from Jamanxim" in reference to the place of origin of the holotype.

**Distribution.** The species is only known from the type locality in Jamanxim National Park, Pará State, in northern Brazil, where it was collected in a Shannon trap placed near a lower-order stream. Only a single male was collected despite intensive sampling effort during the expedition with successive sampling using several types of traps. According to data from the National Institute for Space Research, the Jamanxim National Park ranks among the conservation units with the highest deforestation rates in the Amazon. This situation underscores the need to increase the knowledge of the biodiversity in this region to better understand the anthropogenic impacts on the biota and to utilize this knowledge as tools for developing conservation strategies. The discovery of a new genus of Chironomidae in the park highlights the importance of further research to understand and preserve its unique biodiversity.

### *Poxyaibamberus ubajarensis* Andersen & Dantas, sp. nov.

https://zoobank.org/E8261BAB-A560-419E-AF25-4951A909D760
Figs 1C–F, 4

**Type locality.** Brazil, Ceará State, Ubajara, Ubajara National Park, Cafundó waterfall, 03°50'13"S, 40°54'35"W, 805 m a.s.l., 25–26 February 2023, N. Hamada, J. Silva, J.M.C. Nascimento, G.P. Amorim Jr. leg.

**Type specimen.** ***Holotype*** male adult, slide-mounted in Euparal under five coverslips. Original label: "Brasil, CE, Ubajara, Parque Nacional de Ubajara, Cachoeira do Cafundó, 25-26/02/2023, light-trap, N. Hamada" (INPA).

**Diagnostic characters.** The new species can easily be separated from *P. jamanximensis* Andersen & Dantas, sp. nov. on the shape of the gonostylus, as it has a rather broad, curved, tapering heel that is slightly shorter than the gonostylus proper.

**Description. Adult male** (*n* = 1). Total length 2.02 mm. Wing length 1.13 mm. Total length / wing length 1.70. Wing length / length of profemur 2.38.

***Coloration*.** Head, thorax, and legs light brown; abdomen pale brown. Wing hyaline.

***Antenna*.** Antenna broken. With 44 µm long subapical setae.

***Head*.** Inner verticals 5, outer verticals 3, postorbitals not discernable. Clypeus with 5 setae. Tentorium 90 µm long, 13 µm wide. Stipes not discernable. Anterior margin of cibarial pump slightly concave. Palp (Fig. 1C) with five segments; palpomere lengths (in µm): 17, 22, 35, 39, 37. Third palpomere without sensilla clavata.

***Thorax*** (Fig. 1D). Antepronotum with 2 ventrolateral setae. Acrostichals very small, at least 4 in double row in anterior part of scutum; dorsocentrals 6, uniserial; prealars 3. Scutellum apparently without setae.

***Wing*.** VR = 1.33. Brachiolum with 1 seta, other veins and membrane bare. Squama bare. Costal extension 113 µm long.

***Legs*.** Fore tibia (Fig. 1E) with 30 µm long spur, mid tibia with 29 µm and 14 µm long spurs, hind tibia (Fig. 1F) with 35 µm and 18 µm long spurs. Width at apex of fore tibia 28 µm, of mid tibia 29 µm, of hind tibia 30 µm. Hind tibia with comb of 4 bristles, longest 22 µm long. Lengths and proportions of legs as in Table 2.

***Hypopygium*** (Fig. 4A, B). Anal point large, narrowly triangular with rounded apex, projecting from posterior margin of tergite IX, with microtrichia, 55 µm long, 28 µm wide near base, 8 µm wide medially. Tergite IX with 9 setae medially. Laterosternite IX with 2 setae. Phallapodeme 68 µm long. Transverse sternapodeme straight, without oral projections, 41 µm long. Virga apparently consisting of balloon-shaped ball of lamella with small spines. Gonocoxite 168 µm long. Gonostylus 79 µm long; heel curved, tapering, 72 µm long, 24 µm wide medially; megaseta 8 µm long. HR = 2.13; HV = 2.56.

**Table 2.** Lengths (in µm) and proportions of legs of *Poxyaibamberus ubajarensis* Andersen & Dantas, sp. nov., male (*n* = 1).

| | Fe | Ti | $ta_1$ | $ta_2$ | $ta_3$ | $ta_4$ | $ta_5$ | LR | BV | SV | BR |
|---|---|---|---|---|---|---|---|---|---|---|---|
| $P_1$ | 474 | 507 | – | – | – | – | – | – | – | – | – |
| $P_2$ | 507 | 515 | 310 | 155 | 98 | 53 | 45 | 0.602 | 3.795 | 3.297 | 1.92 |
| $P_3$ | 605 | 629 | – | – | – | – | – | – | – | – | – |

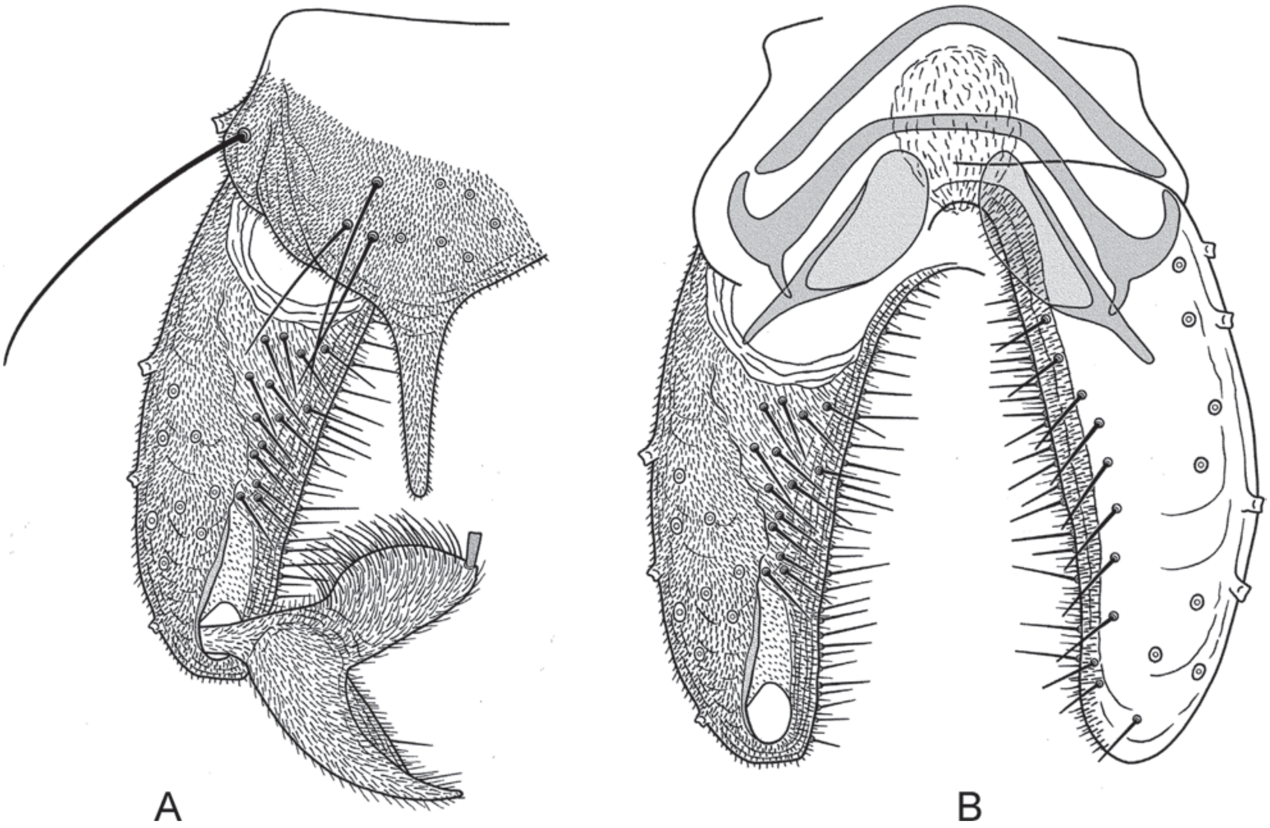

**Figure 4.** *Poxyaibamberus ubajarensis* Andersen & Dantas, sp. nov. male **A** hypopygium, dorsal view **B** hypopygium with tergite IX and anal point removed, left dorsal aspect, right ventral aspect.

**Immatures and female.** Larva, pupa, and female are unknown.

**Etymology.** The epithet, *ubajarensis*, is used as an adjective and meaning "from Ubajara" in reference to the place of origin of the holotype.

**Distribution.** The species is known only from the type locality in the Ubajara National Park in northeastern Brazil. The park covers an area of 6.288 ha and receives abundant rainfall, averaging 1.400 mm annually, while temperatures typically range between 22 °C and 26 °C. The vegetation in the park is characterized by its high diversity, with higher elevations adorned by lush humid forests (Figueiredo 1997; Souza 1997). Lower elevations feature semi-deciduous tropical rainforest on sloping areas and arboreal Caatinga (thorny deciduous forest) in the lower regions. The specimens were collected using a light trap placed about 20 m upstream of a waterfall (Fig. 5) at an elevation of 805 m a.s.l. At the sampling time, water temperature was 21.5 °C, pH was 7.05, and electric conductivity was 137.6 µS/cm.

## Discussion

In a consensus tree produced in the Bayesian analysis neighboring search, *Poxyaibamberus* falls out with *Mesosmittia* Brundin, 1956, *Pseudosmittia* Goetghebuer, 1932, *Eretmoptera* Kellog, 1900, *Thalassosmittia* Strenzke & Remmert, 1957, and *Petalocladius* Sublette & Wirth, 1972 (Fig. 6). Both *Pseudosmittia*, with more than 100 species, and *Mesosmittia*, with 18 species, are distributed in most parts of the world (Ferrington and Sæther 2011; Ashe and O'Connor 2012). The Neotropical species have been treated by Andersen et al. (2010) and Andersen and Mendes

**Figure 5.** The type locality of *Poxyaibamberus ubajarensis* Andersen & Dantas, sp. nov. in Ubajara National Park where the holotype was collected in a light trap near the Cafundó waterfall.

(2002). However, a position close to *Thalassosmittia*, *Eretmoptera*, and *Petalocladius* is notable. *Thalassosmittia* has 11 named species distributed in the Afrotropical, Nearctic, Neotropical, and Palaearctic regions (Ashe and O'Connor 2012). With few exceptions, *Thalassosmittia* representatives are marine shore dwellers (Andersen et al. 2013). However, the only *Thalassosmittia* described from the Neotropical Region is *T. amazonica* Andersen & Pinho, 2014, which was collected in the Amazon rainforest near Manaus (Andersen and Pinho 2014). *Eretmoptera* is a genus with two named species that are distributed in the Nearctic Region and in Antarctica. The adults are wingless. *Eretmoptera browni* Kellog, 1900 is distributed in California, while *E. murphyi* Schaeffer, 1914, was described from the island of South Georgia and is later introduced to Signy Island in the South Orkney Islands (Ashe and O'Connor 2012). The species is apparently parthenoge-

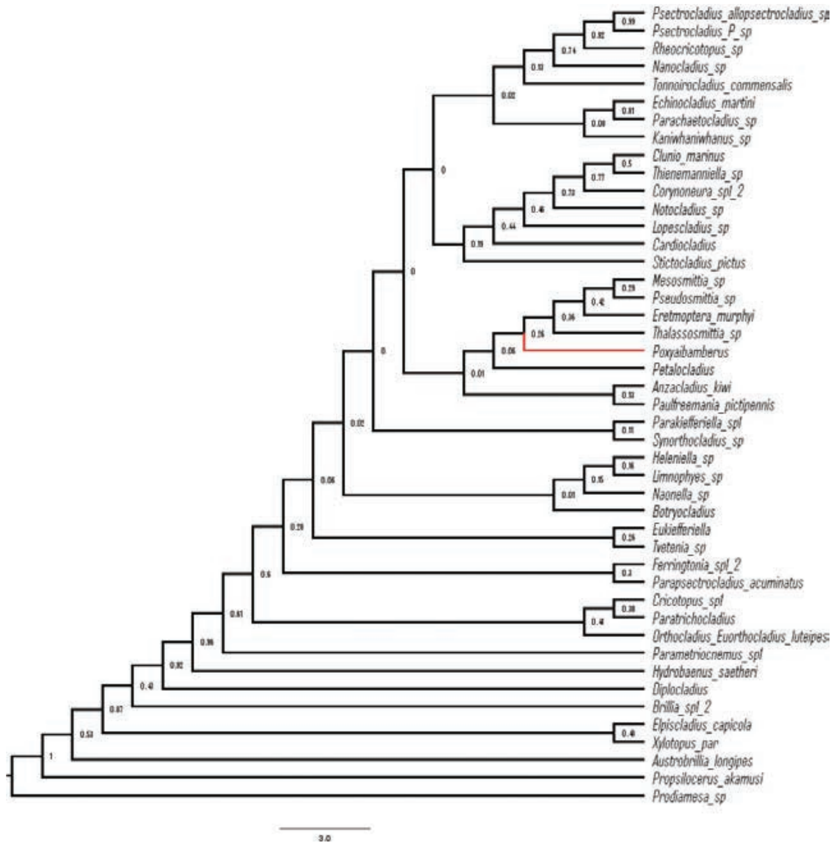

**Figure 6.** Position of *Poxyaibamberus* Andersen & Dantas, gen. nov. (marked in red) in the phylogenetic tree of Orthocladiinae, reconstructed with Bayesian inference (all posterior probabilities of the nodes are displayed, regardless of the value). This is a majority-rule consensus tree based on morphology only.

netic; the larva has a two-year life cycle and lives in damp moss and peat where they are thought to feed on decaying vegetation (Cranston 1985; Convey 1992). *Petalocladius*, with two included species, is distributed on the Caribbean Islands Jamaica and Hispaniola (Andersen et al. 2024). Both species have been collected in mountainous areas, and *P. dominiensis* Andersen & Baranov, 2024 was trapped close to a rather rapid, small river with rocky and stony substrates.

When posterior position probability mapping ("Rogue plots") was applied, *Poxyaibamberus* was plotted in approximately 20% of the cases next to *Stictocladius* Edwards, 1931 and in approximately 20% of the cases next to *Pseudosmittia* / *Eretmoptera* (Fig. 7). While these were the most frequent positions within the generated trees, it plots near *Eretmoptera* in the consensus tree due to cumulatively more frequent occurrence (ca 40%) in or near this clade (Fig. 6). The position of *Stictocladius* in relation to *Poxyaibamberus* remains highly uncertain due to the lack of knowledge of the immature stages of the new genus. It is difficult to elaborate on the character distribution in the tree, as we have used an mcmc-based Bayesian approach, rather than maximum parsimony, which precludes more detailed analysis of the characters distribution. We have used the Bayesian approach, rather than maximum parsimony because of a deficiency in knowledge of many characters in the new genus. Thus, a more detailed analysis of the character distribution and sister relationships of *Poxyaibamberus* will have to wait until description of the additional life stages of the genus.

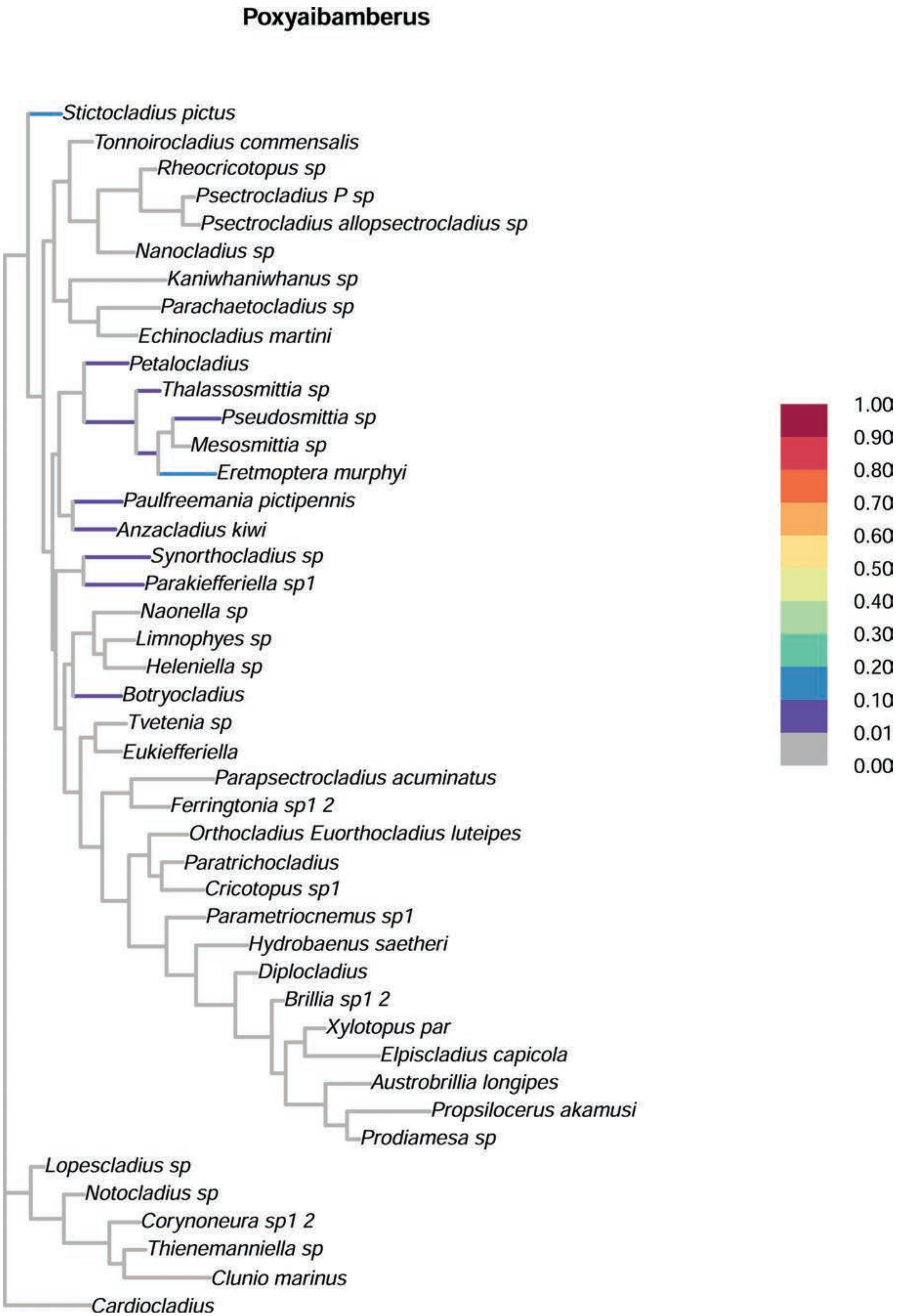

**Figure 7.** Rogue plot of the frequency of placement of *Poxyaibamberus* Andersen & Dantas, gen. nov. in the Bayesian tree from Fig. 6, based on the frequency of occurrence of *Poxyaibamberus* at a given node, based on the 50,001 most congruent trees from the Bayesian analysis of the genus's morphology.

## Acknowledgements

We are indebted to Jeane M.C. Nascimento, Jeferson O. da Silva, and Gilson P. Amorim Jr. for their invaluable support during the fieldwork in the Ubajara National Park, and to Gilberto Nicácio for providing us with the male from the Jamanxim National Park. NH received a CNPq research fellowship (process 308970/2019-5). GPSD is granted a postdoctoral fellowship by FAPEAM (process 01.02.016301.03271/2021-93). The following projects provided partial financial support: Sistemática integrada de insetos aquáticos na América do Sul (CNPq and Instituto Nacional de Pesquisas da Amazônia-INPA), and INCT ADAPTA II funded by CNPq (465540/2014–7) and FAPEAM (0621187/2017). Collection in Ubajara National Park was made under the SISBIO permit no. 82848-1. The University Museum of Bergen provided office space, microscope, and other equipment for TA.

## Additional information

### Conflict of interest

The authors have declared that no competing interests exist.

### Ethical statement

No ethical statement was reported.

### Funding

V. Baranov's work is also funded by the State Agency of Innovation, within the Ramon y Cajal Program, grant number RYC2021-032144-I. The funders had no role in study design, data collection and analysis, decision to publish, or preparation of the manuscript. Vktor Baranov received funds supporting the payment of this publication fees through the CSIC Open Access Publication Support Initiative from the CSIC Unit of Information Resources for Research (URICI). CNPq research fellowship (Process 308970/2019-5) to N. Hamada. FAPEAM postdoctoral fellowship (Process 01.02.016301.03271/2021-93) to GPSD. CNPq and Instituto Nacional de Pesquisas da Amazônia-INPA funded the project "Sistemática integrada de insetos aquáticos na América do Sul". CNPq (465540/2014–7) and FAPEAM (0621187/2017) funded the project "INCT ADAPTA II". University Museum of Bergen, Bergen, Norway.

### Author contributions

Trond Andersen – describing the new taxa, drawing the figures, preparation of manuscript, review of manuscript. Galileu P.S. Dantas – sorting and slide preparations, identification of specimens, preparation of manuscript. Viktor Baranov – phylogenetic analysis. Annui M. Sanz-laParra – photo, preparation of manuscript, review of manuscript. Humberto F. Mendes – preparation of manuscript. Neusa Hamada – organizing fieldwork, review of manuscript.

### Author ORCIDs

Trond Andersen https://orcid.org/0000-0003-2201-1870
Galileu P. S. Dantas https://orcid.org/0000-0002-9155-533X
Viktor Baranov https://orcid.org/0000-0003-1893-3215
Annui M. Sanz-laParra https://orcid.org/0000-0003-0580-6890
Humberto F. Mendes https://orcid.org/0000-0002-8261-3665
Neusa Hamada https://orcid.org/0000-0002-3526-5426

## Data availability

All of the data that support the findings of this study are available in the main text or in https://github.com/chironomus/Poxyaibamberus-.

## References

Andersen T, Mendes HF (2002) Neotropical and Mexican *Mesosmittia* Brundin, with the description of four new species (Insecta, Diptera, Chironomidae). Spixiana 25: 141–155.

Andersen T, Mendes HF (2007) Five enigmatic new orthoclad genera from Brazil (Diptera: Chironomidae: Orthocladiinae). In: Andersen T (Ed.) Contributions to the systematics and ecology of aquatic Diptera. A tribute to Ole A. Sæther. The Caddis Press, Columbus, Ohio, 17–52.

Andersen T, Mendes HF (2012a) *Miambera miae* n. gen., n. sp. from southern Brazil (Diptera: Chironomidae, Orthocladiinae). Biota Neotropica 12(1): 105–109. https://doi.org/10.1590/S1676-06032012000100009

Andersen T, Mendes HF (2012b) *Maximberus maxi* n. gen., n. sp. from Southern and Southeastern Brazil (Diptera: Chironomidae, Orthocladiinae). Biota Neotropica 12(1): 117–122. https://doi.org/10.1590/S1676-06032012000100011

Andersen T, Pinho LC (2014) A new *Thalassosmittia* Strenzke and Remmert, 1957 out of the sea: *T. amazonica* n. sp. from the Amazon rainforest, Brazil (Diptera: Chironomidae, Orthocladiinae). Chironomus 27(27): 25–30. https://doi.org/10.5324/cjcr.v0i27.1702

Andersen T, Sæther OA, Mendes HF (2010) Neotropical *Allocladius* Kieffer, 1913 and *Pseudosmittia* Edwards, 1932 (Diptera: Chironomidae). Zootaxa 2472(1): 1–77. https://doi.org/10.11646/zootaxa.2472.1.1

Andersen T, Sæther OA, Cranston PS, Epler JH (2013) 9. The larvae of Orthocladiinae (Diptera: Chironomidae) of the Holarctic Region — keys and diagnoses. In: Andersen T, Cranston PS, Epler JH (Eds) Chironomidae (Diptera) of the Holarctic Region. Keys and diagnoses — larvae. Insect Systematics & Evolution, (Supplement 66): 189–386.

Andersen T, Mendes HF, Pinho LC (2015a) *Caaporangombera*, a new Orthocladiinae genus from Brazil (Diptera, Chironomidae). Norwegian Journal of Entomology 62: 69–79. http://www.entomologi.no/journals/nje/2015-1/pdf/nje-vol62-no1-69-79-andersen.pdf

Andersen T, Mendes HF, Pinho LC (2015b) *Mariambera*, a new genus of Orthocladiinae from Brazil (Insecta: Diptera, Chironomidae). Studies on Neotropical Fauna and Environment 50(1): 24–30. https://doi.org/10.1080/01650521.2014.991589

Andersen T, Mendes HF, Pinho LC (2015c) *Urubicimbera*, a new Orthocladiinae genus from Brazil (Diptera, Chironomidae). Norwegian Journal of Entomology 62: 160–166. http://www.entomologi.no/journals/nje/2015-2/pdf/nje-vol62-no2-160-166-andersen.pdf

Andersen T, Höcherl A, Sanz-laParra AM, Bastardo RH, Baranov V (2024) A new species of *Petalocladius* Sublette & Wirth, 1972 (Diptera, Chironomidae, Orthocladiinae) from the Dominican Republic, with an emended generic diagnosis. Chironomus. Journal of Chironomidae Research 38: 4–13.

Ashe P, O'Connor JP (2012) A world catalogue of Chironomidae (Diptera). Part 2. Orthocladiinae (Section A & B). Irish Biogeographical Society and National Museum of Ireland, Dublin, 968 pp.

Convey P (1992) Aspects of the biology of the midge, *Eretmoptera murphyi* Schaeffer (Diptera: Chironomidae), introduced to Signy Island, maritime Antarctic. Polar Biology 12(6–7): 653–657. https://doi.org/10.1007/BF00236988

Cranston PS (1985) *Eretmoptera murphyi* Schaeffer (Diptera: Chironomidae), an apparently parthenogenetic Antarctic midge. British Antarctic Survey Bulletin 66: 35–45.

Ferrington Jr LC, Sæther OA (2011) A revision of the genera *Pseudosmittia* Edwards, 1932, *Allocladius* Kieffer, 1913, and *Hydrosmittia* gen. n. (Diptera: Chironomidae, Orthocladiinae). Zootaxa 2849(1): 1–314. https://doi.org/10.11646/zootaxa.2849.1.1

Figueiredo MA (1997) Unidades fitoecológicas. In: Iplance (Ed.) Atlas do Estado do Cerá. Fundaçào Instituto de Planejamento do Ceará, Governo do Estado do Ceará, Seplan, Fortaleza, 28–29.

Fittkau JE (1974) *Ichthyocladius* n. gen., eine neotropische Gattung der Orthocladiinae (Chironomidae, Diptera) deren Larven epizoisch auf Welsen (Astroblepidae und Loricariidae) leben. Entomologisk Tidskrift (Supplement 95): 91–106.

Kellog VL (1900) An extraordinary new maritime fly. The Biological Bulletin 1(2): 81–87. https://doi.org/10.2307/1535751

Klopfstein S, Spasojevic T (2019) Illustrating phylogenetic placement of fossils using RoguePlots: An example from ichneumonid parasitoid wasps (Hymenoptera, Ichneumonidae) and an extensive morphological matrix. PLoS ONE 14(4): e0212942. https://doi.org/10.1371/journal.pone.0212942

Lewis PO (2001) A likelihood approach to estimating phylogeny from discrete morphological character data. Systematic Biology 50(6): 913–925. https://doi.org/10.1080/106351501753462876

Mendes HF, Andersen T (2008) A review of *Antillocladius* Sæther and *Litocladius* Mendes, Andersen et Sæther, with the description of two new Neotropical genera (Diptera, Chironomidae, Orthocladiinae). Zootaxa 1887(1): 1–75. https://doi.org/10.11646/zootaxa.1887.1.1

Mendes HF, Andersen T (2012a) *Iporangomberus pei* n. gen., n. sp. from southeastern Brazil (Diptera: Chironomidae: Orthocladiinae). Biota Neotropica 11(4): 67–71. https://doi.org/10.1590/S1676-06032011000400006

Mendes HF, Andersen T (2012b) *Pebapomberus*, a new orthoclad genus from Brazil (Diptera: Chironomidae, Orthocladiinae). Biota Neotropica 12(2): 25–31. https://doi.org/10.1590/S1676-06032012000200003

Mendes HF, Andersen T (2013) *Jururumberus*, a new genus of Orthocladiinae (Diptera: Chironomidae) from Brazil. Biota Neotropica 13(4): 71–76. https://doi.org/10.1590/S1676-06032013000400007

Mendes HF, Andersen T, Sæther OA (2004) New species of *Ichtyocladius* Fittkau, a member of the *Corynoneura*-group (Diptera: Chironomidae: Orthocladiinae) with a review of the genus. Studies on Neotropical Fauna and Environment 39(1): 15–35. https://doi.org/10.1080/01650520412331270936

Mendes HF, Sæther OA, Andrade-Morraye M (2005) *Gynocladius scalpellosus* n. gen., n. sp. from Brazil (Diptera: Chironomidae: Orthocladiinae). Zootaxa 979(1): 1–12. https://doi.org/10.11646/zootaxa.979.1.1

Mendes HF, Andersen T, Pinho LC (2013) *Uirassubrillia beckeri* gen. n., sp. n. (Diptera: Chironomidae, Orthocladiinae) from northeastern Brazil. Zootaxa 3716(1): 65–74. https://doi.org/10.11646/zootaxa.3716.1.5

Nylander JAA, Ronquist F, Huelsenbeck JP, Nieves-Aldrey J (2004) Bayesian phylogenetic analysis of combined data. Systematic Biology 53(1): 47–67. https://doi.org/10.1080/10635150490264699

Page RDM (2001) *NDE*: *NEXUS data editor 0.5. 0.* University of Glasgow, Glasgow.

Pinho LC, Fusari LM, Mendes H (2024) Chironomidae. In: Catálogo Taxonômico da Fauna do Brasil. PNUD. http://fauna.jbrj.gov.br/fauna/faunadobrasil/3962

Revell J (2012) Phytools: An R package for phylogenetic comparative biology (and other things). Methods in Ecology and Evolution 3(2): 217–223. https://doi.org/10.1111/j.2041-210X.2011.00169.x

Ronquist F, Teslenko M, van der Mark P, Ayres DL, Darling A, Höhna S, Larget B, Liu L, Suchard MA, Huelsenbeck JP (2012) MrBayes 3.2: Efficient Bayesian phylogenetic inference and model choice across a large model space. Systematic Biology 61(3): 539–542. https://doi.org/10.1093/sysbio/sys029

Sæther OA (1969) Some Nearctic Podonominae, Diamesinae and Orthocladiinae (Diptera: Chironomidae). Bulletin - Fisheries Research Board of Canada 107: 1–154.

Sæther OA (1980) Glossary of Chironomid morphology terminology (Diptera: Chironomidae). Entomologica Scandinavica (Supplement 14): 1–51.

Schaeffer C (1914) Collembola, Siphonaptera, Diptera, and Coleoptera of the South Georgia Expedition. Science Bulletin. Museum of the Brooklyn Institute of Arts and Sciences 2(4): 90–94.

Shannon RC (1939) Methods for collecting and feeding mosquitoes in jungle yellow fever studies. The American Journal of Tropical Medicine and Hygiene 19(2): 131–140. https://doi.org/10.4269/ajtmh.1939.s1-19.131

Souza MJN (1997) Geomorfologia. In: Iplance (Ed.) Atlas do Estado do Cerá. Findaçâo Instituto de Planejamento do Cerá, Governo do Estado do Cerá, Seplan, Fortaleza, 18–19.

Spies M, Reiss F (1996) Catalog and bibliography of Neotropical and Mexican Chironomidae (Insecta, Diptera). Spixiana (Supplement 22): 61–119. https://www.zobodat.at/pdf/SpixSupp_022_0061-0119.pdf

Wiedenbrug S, Trivinho-Strixino S (2009) *Ubatubaneura*, a new genus of the *Corynoneura* group (Diptera: Chironomidae: Orthocladiinae) from the Brazilian Atlantic Forest. Zootaxa 1993(1): 41–52. https://doi.org/10.11646/zootaxa.1993.1.4

ZooKeys 1205: 17–38 (2024)
DOI: 10.3897/zookeys.1205.123579

Research Article

# Three new species of *Oocyclus* Sharp, 1882, with additional records from China (Coleoptera, Hydrophilidae, Laccobiini)

Feng-long Jia[1], Zu-qi Mai[1,2]

1 Institute of Entomology, Life Sciences School, Sun Yat-sen University, Guangzhou, 510275, Guangdong, China
2 Faculty of Environmental Sciences, Department of Ecology, Czech University of Life Sciences Prague, Czech Republic
Corresponding author: Zu-qi Mai (maizq5@mail2.sysu.edu.cn; zuqimai@gmail.com)

## Abstract

Three new species of the water scavenger beetle genus *Oocyclus* Sharp, 1882 from China (*Oocyclus extensus* **sp. nov.**, from Xizang, *O. latiorificialis* **sp. nov.** and *O. ximaensis* **sp. nov.** from Yunnan) are described and illustrated in detail. Additional faunistic data, illustrations of habitus and male genitalia, and a key to Chinese species are provided.

**Key words:** Identification key, Oriental Region, water scavenger beetles, Xizang, Yunnan

Academic editor: Mariano Michat
Received: 21 March 2024
Accepted: 22 May 2024
Published: 19 June 2024

ZooBank: https://zoobank.org/EB9D907F-1554-484A-9399-79FA6C6A4F7B

Citation: Jia F-long, Mai Z-qi (2024) Three new species of *Oocyclus* Sharp, 1882, with additional records from China (Coleoptera, Hydrophilidae, Laccobiini). ZooKeys 1205: 17–38. https://doi.org/10.3897/zookeys.1205.123579

## Introduction

*Oocyclus* Sharp, 1882 is a pantropical genus of water scavenger beetle that is highly adapted to waterfalls and seepages. All known species are restricted to rock-face seeps, margins of waterfalls, and various kinds of vertical surfaces with water (Hebauer and Wang 1998; Short and Garcia 2010, Short et al. 2013; Short and Perkins 2004; Short and Swanson 2005; Toussaint and Short 2018). Currently, a total of 81 species have been described, of which 20 are known from the Oriental Region and 61 from the Neotropical Region (Minoshima 2009; Short 2009; Toussaint and Short 2018; Jordão et al. 2018; Santana et al. 2023; Alencar et al. 2022). Only six species have been recorded in China so far, of which *O. bhutanicus* Satô, 1976, cited from Taiwan by Hebauer and Wang (1998), needs to be confirmed (Short and Swanson 2005). Previous reports of *Oocyclus* in China have been limited to the southeastern part of the country (Hebauer and Wang 1998; Short and Jia 2011; Jia and Mate 2012). The distribution of the genus in other parts of China is still unknown.

Recently, we had the opportunity to visit some nature reserves in Yunnan and Xizang and discovered several *Oocyclus* species, of which three are described here as new to science. We also studied the *Oocyclus* collections at the Biological Museum, Sun Yat-sen University, and added information about the distribution of Chinese species.

## Materials and methods

Some of the specimens were dissected. Dissected male genitalia were transferred to a drop of distilled water, remaining membranes were removed under a compound microscope, and the cleaned genitalia were then mounted in a drop of soluble resin on a paper card attached below the respective specimen. For photography, the cleaned and relaxed male genitalia were placed in a drop of glycerin. Photographs of genitalia were taken using a Zeiss AxioCam HRc camera mounted on a Zeiss AX10 microscope with the Axio Vision SE64 software. These images were then stacked in Helicon Focus v. 7.0.2. Habitus photographs were taken using a Nikon DS-Ri2 mounted on a Nikon SMZ25; layers were captured and stacked in the NIS-Elements software. Habitat images were taken using Canon 7D digital camera. The generic characters are described in detail by Hansen (1991) and Short and Perkins (2004). Morphological terminology largely follows Hansen (1991) and Short and Perkins (2004). For a diagnosis of *Oocyclus* the reader is referred to Clarkson and Short (2012).

Examined specimens are deposited in the following collections:

| | |
|---|---|
| **IZCAS** | Chinese Academy of Sciences, Institute of Zoology, Beijing, China |
| **SYSU** | Sun Yat-sen University, Guangzhou, China |

## Results

### Descriptions of new species

***Oocyclus extensus*** **sp. nov.**
https://zoobank.org/2A7B3F2F-10FB-4431-8C33-67ED91F49C00
Figs 1A–D, 4A–D, 6A, 7A, 8A

**Type material.** ***Holotype***: China • ♂; Xizang Autonomous Region, Xigazê, Dinggyê County, Zhêntang Town, on wet rock with a fine film of flowing water (西藏日喀则定结县陈塘镇流水岩壁表面); 27.8733°N, 87.4117°E; 2482 m elev.; 2023.VII.10; Zu-qi Mai, Cheng Liang & Yue-zheng Tu leg.; SYSU SYSBMZ2370001. ***Paratypes:*** 8 ♂♂, 8 ♀♀(SYSU SYSBMZ2370002 to 0017), 2 ♂♂, 2 ♀♀ (IZCAS COLMZD2370001 to 0004); same data as the holotype.

**Diagnosis.** Body large, length 5.3–6.2 mm, oblong-oval, and moderately convex. Dorsum black, with greenish luster under lateral illumination, slightly iridescent. Head, pronotum, and elytra with dense ground punctures consisting of extremely fine and moderately coarse punctures. Systematic punctures on labrum sparse and fine, not forming a continuous transverse row or groove. Posterolateral corners of pronotum angulate. Elytral suture slightly raised posteriorly; with 5 distinct rows of regular systematic punctures; lateral margins of elytra distinctly expanded outwards. Pseudepipleura wide from base to apex. Procoxae with sparse, spine-like setae scattered in fine pubescence. Meso- and metafemora without microsculpture on intervals of punctures. Abdominal ventrites with uniform pubescence over entire surface. Aedeagus (Fig. 1D) with parameres almost as long as median lobe; gradually narrowed from apical fourth to apex; apex of paramere slightly curved inwards and rounded. Median lobe slightly narrowed apically, gonopore situated apically, anterior margin of gonopore rounded.

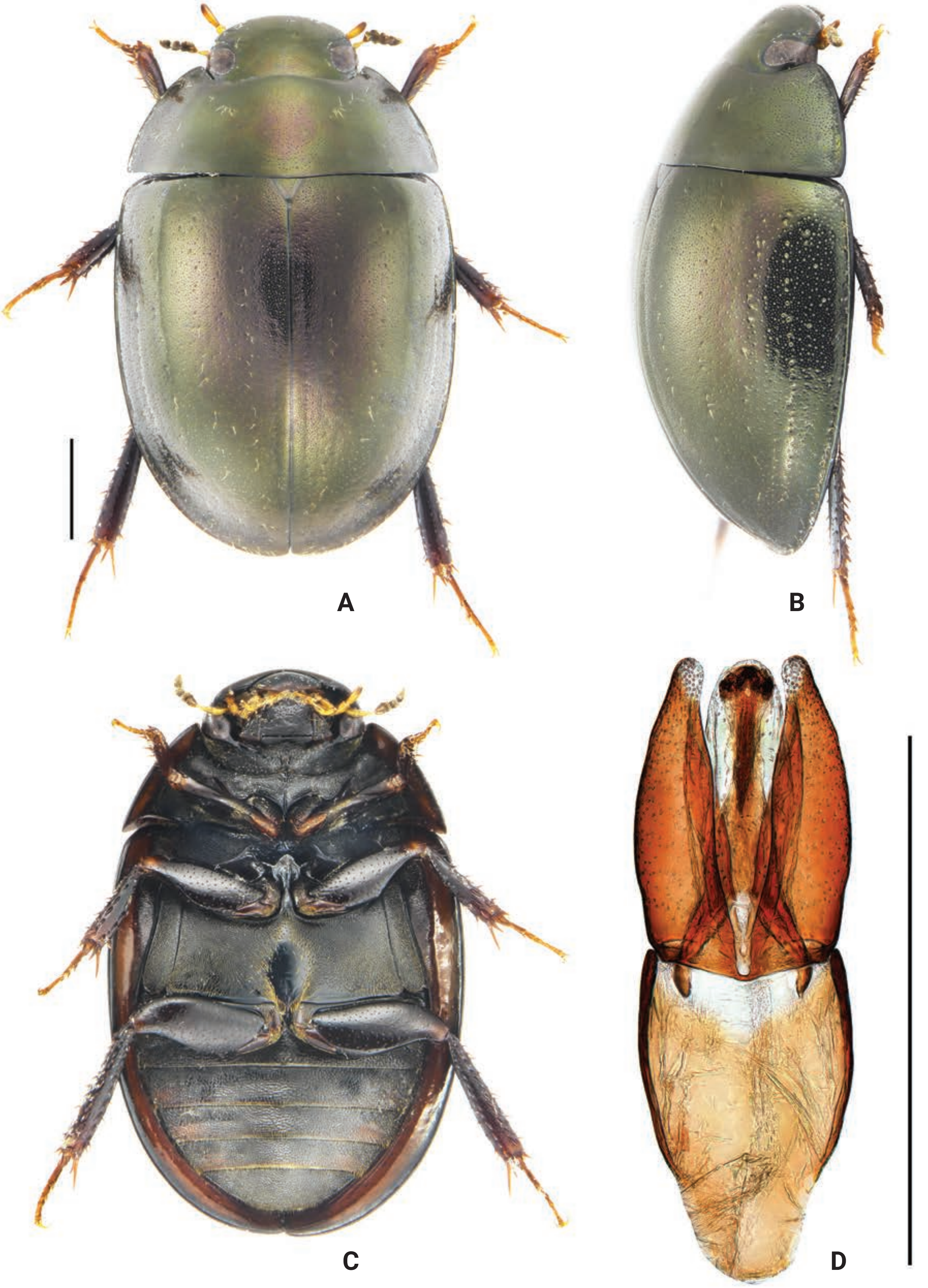

**Figure 1.** *Oocyclus extensus* sp. nov. **A** dorsal view **B** lateral view **C** ventral view **D** dorsal view of aedeagus. Scale bars: 1 mm.

**Description.** ***Form and color*** (Fig. 1A–C). Length 5.3–6.2 mm, width 3.4–4.0 mm; oblong-oval and moderately convex; elytra longer than wide. Dorsum black, with greenish luster under lateral illumination, slightly iridescent, more vividly colored when alive. Maxillary and labial palps yellowish brown, with last maxillary palpomere apically darkened. Antennae yellowish brown, with cupule (sixth antennomere) dark reddish brown or dark brown; club black. Ventral surface black. Epipleura, lateral margins of prosternum, and tarsomeres reddish brown; femora, tibiae, and sternites black or blackish brown. ***Head.*** Labrum, clypeus, and frons with both extremely fine and moderately coarse ground punctures; distance between punctures 0.2–3.0× width of 1 puncture. Systematic punctures on labrum sparse, not forming a continuous transverse row or groove, each systematic puncture with a long seta. Systematic punctures on clypeus almost undetectable. Frons with an irregular row of systematic punctures mesad of each eye, slightly larger than largest ground punctures and usually bearing long setae. Clypeus with a few very indistinct systematic punctures along anterolateral margins, slightly larger than surrounding ground punctures, and bearing short setae. Antennae with scape as long as antennomeres 2–5 combined, first 2 antennomeres of club subequal in length, and apical antennomeres slightly shorter than preceding 2 antennomeres combined. Maxillary palps short, subequal in length to the width of labrum, palpomere 2 slightly dilated, apical palpomeres ca 1.3× as long as penultimate. Labial palps ca 3/4× as the width of mentum. Mentum quadrate, anterior margin slightly convex; with coarse punctures on anterior and lateral portion, only with few punctures posteromedially. ***Thorax.*** Ground punctation on pronotum and elytra composed of extremely fine and moderately coarse punctures evenly mixed and distributed. Pronotal systematic punctures present, ca 1.5× the size of ground punctation and set with a fine seta, sometimes partially blending with coarser ground punctures; anterior and posterior series each forming an irregular row. Lateral margins of pronotum set with a few sparsely distributed setiferous punctures. Pronotum with anterior and lateral marginal rims, posterior marginal rim absent. Posterolateral corners of pronotum angulate. Prosternum moderately tectiform, with median carina along entire length, with a small blunt tooth anteriorly. Elytra with 5 distinct rows of punctures, diameter of systematic punctures ca 2× as wide as the coarse ground punctures; lateral margin of elytra distinctly expanded outwards, especially in posterior half; elytral suture slightly raised but easily detectable. Pseudepipleura wide throughout. Mesoventral process with lateral extensions sloping evenly downward. Metaventrite with an oval glabrous area posteromedially, slightly longer than wide, length of glabrous area as long as the total length of metaventrite. Pro- and mesocoxae densely pubescent; procoxae with sparse spine-like setae. Ventral surface of profemora densely pubescent at basal fifth, remainder scattered with fine punctures, interstices without microsculpture; meso- and metafemora glabrous, with coarse punctures and without microsculpture. Protibiae with several spines on dorsal face. Fifth tarsomere of pro- and mesotarsus subequal in length to the preceding 4 tarsomeres combined. Fifth metatarsomere equal in length to second tarsomere. ***Abdomen.*** Abdominal ventrites 1–5 with uniform pubescence, longest setae about as long as the setae around the metaventral glabrous area. Fifth ventrite entire. ***Aedeagus*** (Fig. 1D). Phallobase with basal 2/3 arcuate, manubrium gradually narrowed at posterior 1/3 and rounded posteriorly. Parameres almost as long as phallobase, widest at the base, arcuate medially outwards, gradually narrowed from apical fourth to apex; apex of paramere slightly curved inwards and rounded. Median lobe slightly narrowed apically, gonopore triangular, apically situated, and with rounded anterior margin.

**Remarks.** This species is similar to *Oocyclus rupicola* Minoshima, 2009 from Laos. It can be distinguished from *O. rupicola* by its on average larger body size (length 5.3–6.2 mm, width 3.4–4.0 mm vs length 4.93–5.85 mm, width 3.03–3.53 in *O. rupicola*), sparse, fine systematic punctures on labrum which do not form a continuous transverse row (vs forming a row of coarse punctures in *O. rupicola*), and rounded apex of the paramere of the aedeagus (vs narrowed and obliquely truncate inwards in *O. rupicola*) (Minoshima 2009).

**Etymology.** This species is named *extensus*, Latin, meaning "stretched out" and referring to the outwardly expanded elytra.

**Biology.** (Fig. 4A–D) The examined specimens were collected on exposed, seeping rock surfaces on the valley edge. They were together with other species of the family Hydrophilidae: *Oocyclus bhutanicus* Satô, 1979, *Agraphydrus nepalensis* Komarek, 2018, *Laccobius regalis* Knisch, 1924, and *Coelostoma gentilii* Jia, Aston & Fikáček, 2014. Adults hide in rock crevices during the day and are active at night.

**Distribution.** (Fig. 9) China (Xizang). Only known from type locality. Zhêntang Town is in a valley on the southern side of the central Himalayas and is a border town on the China–Nepal border and lies on the Pum Qu River.

### *Oocyclus latiorificialis* sp. nov.

https://zoobank.org/7793C4B1-3AAC-4664-9D8F-B8E4EE74BBDC
Figs 2A–D, 6E, 7E, 8E

**Type material.** ***Holotype***: China • ♂; Yunnan Province, Nujiang Lisu Autonomous Prefecture, Lushui County, Pianma Village, on wet rock with fine flowing water (怒江傈僳族自治州泸水市片马村流水岩壁); 26.014039°N, 98.650640°E; 2131 m elev.; 2021.V.17; Zhuo-yin Jiang, Zhen-ming Yang & Zu-qi Mai leg.; SYSU SYSBMZ2370018. ***Paratypes:*** 1 ♂; same data as the holotype; SYSU SYSBMZ2370019. • 16 unsexed spec.; Yunnan Prov., Lushui County, Yaojiaping (泸水县姚家坪); 26.1°N, 98.71°E; 2424 m elev.; 2016.V.17; Yu-dan Tang & Rui-juan Zhang leg.; SYSU SYSBMZ2370020 to 0035.

**Diagnosis.** Body medium-sized, length 4.1–4.3 mm, oval, and rather convex. Dorsum black, with distinct greenish luster under lateral illumination, slightly iridescent. Head, pronotum, and elytra with dense ground punctures consisting of extremely fine and moderately coarse punctures. Systematic punctures on labrum moderately dense, forming a nearly continuous transverse row. Posterolateral corners of pronotum evenly rounded. Elytral suture not raised; without distinct rows of systematic punctures; lateral margins of elytra not expanded outwards. Pseudepipleura narrowed posteriorly. Procoxae without distinct, spine-like setae in fine pubescence. Meso- and metafemora with fine microsculpture on intervals of punctures. Abdominal ventrites with uniform pubescence over entire surface. Aedeagus (Fig. 2D) with parameres almost as long as median lobe; inner margin of paramere sinuate in dorsal view and distinctly, subapically curved inward; apex of paramere broadly rounded. Median lobe parallel-sided medially, slightly widened at site of gonopore; gonopore situated apically; anterior margin of gonopore pointed.

**Description.** ***Form and color*** (Fig. 2A–C). Length 4.1–4.4 mm width 2.4–2.7mm, oval, rather convex; elytra longer than wide. Dorsum black, with distinct greenish luster under lateral illumination, slightly iridescent, more vividly colored when alive. Maxillary palps yellow, with apex black; labial palpi yellow. Mentum and stipes light to reddish brown, paler than ventral face of head. Legs, epipleura,

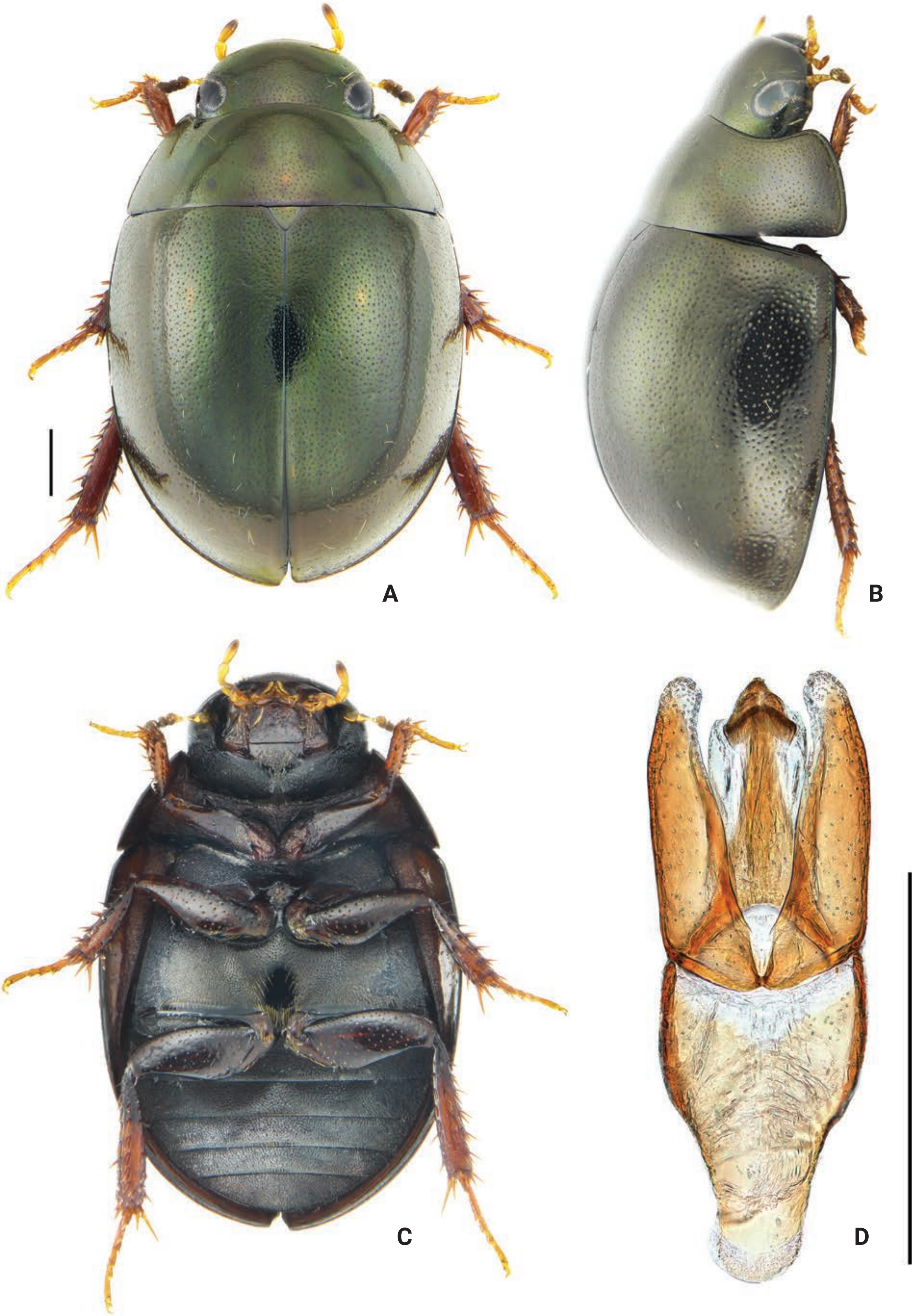

**Figure 2.** *Oocyclus latiorificialis* sp. nov. **A** dorsal view **B** lateral view **C** ventral view **D** dorsal view of aedeagus. Scale bars: 0.5 mm.

lateral margins of prosternum, and posterior margin of each ventrite light brown to dark reddish brown, with remainder of venter darker reddish brown. ***Head.*** Labrum, clypeus, and frons with both extremely fine and moderately coarse ground punctures, distance between punctures 0.5–4.0× as the width of 1 puncture. Systematic punctures on labrum moderately dense, forming a nearly continuous transverse row, with moderately long setae. Frons with an irregular row of systematic punctures mesad of each eye, bearing fine erect setae. Clypeus with a few very indistinct systematic punctures along anterolateral margins, slightly larger than surrounding ground punctures and bearing short setae. Antennae with scape subequal in length to antennomeres 2–5 combined; first two antennomeres of club subequal in length, and apical antennomere slightly longer than two preceding antennomeres combined. Maxillary palps short, subequal in length to the width of labrum; palpomere 2 slightly dilated, apical palpomere ca 1.3 as long as penultimate. Labial palpi ca 3/4 width of mentum. Mentum quadrate, anterior margin slightly convex, bearing very fine and scattered punctures. ***Thorax.*** Ground punctation on pronotum and elytra composed of extremely fine and moderately coarse punctures evenly mixed and distributed. Pronotal systematic punctures present, ca 1.5–2.0× size of ground punctation and set with a fine seta, sometimes partially blending with coarser ground punctures; anterior and posterior series each forming an irregular row. Lateral margins of pronotum set with a few sparsely distributed setiferous punctures. Pronotum with anterior and lateral marginal rims, posterior marginal rim absent. Posterolateral corners of pronotum evenly rounded. Prosternum moderately tectiform, with median carina along entire length but without distinct anteromedial tooth. Elytra without distinct rows of larger punctures, systematic punctures almost as coarse as coarser ground punctures, distinguished by the presence of fine, short setae; lateral margins of elytra not expanded outwards; elytra suture not raised. Pseudepipleura narrowed posteriorly. Mesoventral process with lateral extensions sloping evenly downward. Metaventrite posteromedially with an oval glabrous area, slightly longer than wide, length of glabrous area about 2/3 of the total length of metaventrite. Pro- and mesocoxae densely pubescent, without distinct spine-like setae. Ventral surface of profemora densely pubescent at basal 1/5, remainder scattered with fine punctures, interstices with fine microsculpture; meso- and metafemora glabrous, with coarse punctures and fine microsculpture. Protibiae with several spines on dorsal face. Fifth tarsomere of pro- and mesotarsus subequal in length to the preceding 4 tarsomeres combined. Fifth metatarsomere equal in length to second tarsomere. ***Abdomen.*** Abdominal ventrites 1–5 with uniform pubescence, longest setae about as long as the setae around the metaventral glabrous area. Fifth ventrite entire. ***Aedeagus*** (Fig. 2D). Phallobase parallel-sided to slightly arcuate at basal half, manubrium gradually narrowed at posterior 1/2 of phallobase and rounded posteriorly. Parameres slightly longer than phallobase, widest at the base and gradually narrowed, inner margin of paramere sinuate in dorsal view and distinctly curved subapically; apices broadly rounded. Median lobe almost as long as parameres, parallel-sided medially, and slightly widened at site of gonopore; gonopore triangular, situated apically, and with pointed anterior margin.

**Remarks.** This species is very similar to *O. bhutanicus* Satô, 1979, but can be easily distinguished by meso- and metafemora with fine microsculpture on intervals of punctures (vs lacking microsculpture in *O. bhutanicus*), aedeagus with median lobe as long as parameres and almost parallel-sided medially, slightly widened at level of gonopore (vs median lobe shorter than parameres and gradually narrowed from base to apex in *O. bhutanicus*), anterior margin of gonopore pointed (vs rounded in *O. bhutanicus*), and inner margin of paramere sinuate in dorsal view and distinctly curved subapically (vs inner margin of paramere almost straight in dorsal view in *O. bhutanicus*). This species also shares diagnostic features with *O. ximaensis* sp. nov., but it can be distinguished from the latter by dorsum with distinct greenish luster under lateral illumination (vs greenish luster weaker in *O. ximaensis*), meso- and metafemora with fine microsculpture (lacking microsculpture in *O. ximaensis*), and aedeagus with median lobe almost parallel-sided medially, slightly widened at level of gonopore (vs median lobe gradually narrowed from base to apex in *O. ximaensis*).

**Etymology.** Species name is combination of Latin *latus*, “wide”, and *orificialis*, “orifice”, referring to the widely open gonopore.

**Biology.** This species was founding living on wet rock surface at the margins of a waterfall.

**Distribution.** (Fig. 9) China (Yunnan). Only known from type locality.

### ***Oocyclus ximaensis* sp. nov.**

https://zoobank.org/2A925CD2-EC80-4A22-971E-7C0024471B48

Figs 3A–D, 5A–C, 6F, 7F, 8F

**Type material.** ***Holotype:*** CHINA • ♂; Yunnan Prov., Dehong Dai and Jingpo Autonomous Prefecture, Yingjiang County, Xima Town, Xingyun Secondary power stations (星云二级电站), at seepage rock wall by the river, 24.7854°N, 97.6472°E, 1021 m, 2022.VIII.19, Zu-qi Mai, Yu-chen Zheng & Yue-zheng Yu leg.; SYSU SYSBMZ2370036. ***Paratypes:*** 2 ♂♂, 5 ♀♀ (SYSU SYSBMZ2370037 to 0043), same data as the holotype.

**Diagnosis.** Body medium-sized, length 3.8–4.4 mm, oval, and rather convex. Dorsum black, with weak greenish luster, slightly iridescent. Head, pronotum, and elytra with dense ground punctures consisting of extremely fine, moderately coarse punctures. Systematic punctures on labrum moderately dense, forming a nearly continuous transverse row. Posterolateral corners of pronotum evenly rounded. Elytra suture not raised, without distinct rows of systematic punctures; lateral margins of elytra not expanded outwards. Pseudepipleura narrowed posteriorly. Procoxae without distinct, spine-like setae in fine pubescence. Meso- and metafemora without microsculpture on intervals of punctures. Abdominal ventrites with uniform pubescence over entire surface. Aedeagus (Fig. 3D) with parameres almost as long as median lobe; inner margin of paramere slightly sinuate in dorsal view and hardly curved subapically; apex of paramere rounded. Median lobe gradually narrowed from base to apex; gonopore situated apically; anterior margin of gonopore pointed.

**Description.** ***Form and color*** (Fig. 3A–C). Length 3.8–4.4 mm, width 2.3–2.7 mm, oval, rather convex; elytra longer than wide. Dorsum black with weak greenish luster under lateral illumination, slightly iridescent, more vividly colored when alive. Maxillary palps yellow with apex black, labial palpi yellow. Mentum and stipes yellowish brown, paler than ventral face of head. Legs, epipleura, lateral margins of prosternum, and posterior margin of each ventrite light brown

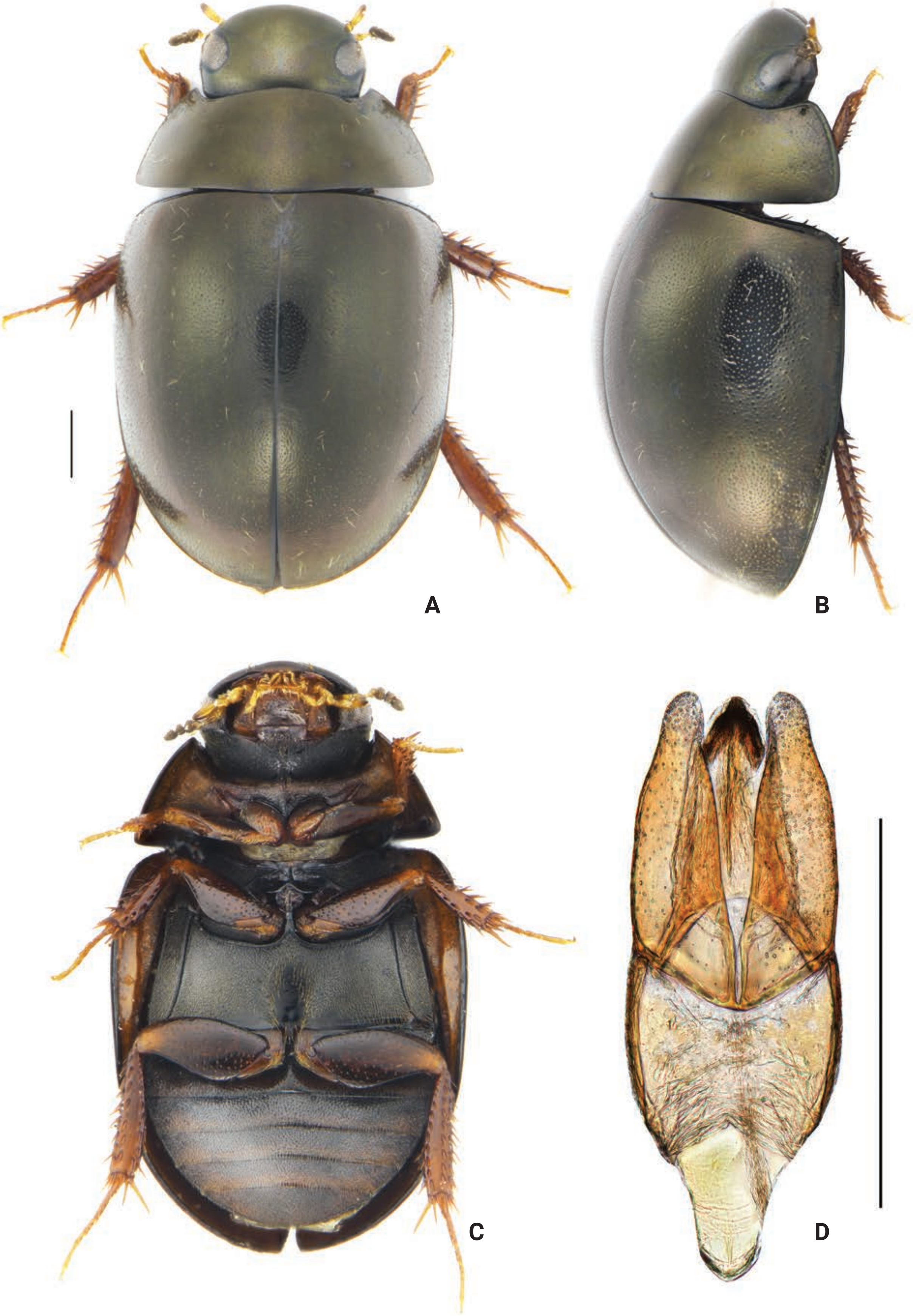

**Figure 3.** *Oocyclus ximaensis* sp. nov. **A** dorsal view **B** lateral view **C** ventral view **D** dorsal view of aedeagus. Scale bars: 0.5 mm.

to yellowish brown, with remainder of venter darker yellowish brown. ***Head.*** Labrum, clypeus, and frons with both extremely fine and moderately coarse ground punctures, distance between punctures 1.0–3.5× width of 1 puncture. Systematic punctures on labrum moderately dense, forming a nearly continuous transverse row setting with moderately long setae. Frons with an irregular row of systematic punctures mesad of each eye, bearing fine, erect setae. Clypeus with a few very indistinct systematic punctures along anterolateral margins, slightly larger than surrounding ground punctures, and bearing short setae. Antennae with scape subequal in length to antennomeres 2–5 combined, first 2 antennomeres of club subequal in length, and apical antennomere slightly longer than 2 preceding antennomeres combined. Maxillary palps short, subequal in length to the width of labrum, palpomere 2 slightly dilated, apical palpomeres ca 1.3 as long as penultimate. Labial palps ca 3/4 width of mentum. Mentum quadrate, anterior margin slightly convex, bearing very fine and scattered punctures. ***Thorax.*** Ground punctation on pronotum and elytra composed of extremely fine and moderately coarse punctures evenly mixed and distributed. Pronotal systematic punctures present, ca 1.5–2.0× size of ground punctation and set with a fine seta, sometimes partially blending with coarser ground punctures; anterior and posterior series each forming an irregular row. Lateral margins of pronotum set with a few sparsely distributed setiferous punctures. Pronotum with anterior and lateral marginal rims, posterior marginal rim absent. Posterolateral corners of pronotum evenly rounded. Prosternum moderately tectiform, with median carina along entire length but without distinct anteromedial tooth. Elytra without distinct rows of larger punctures, systematic punctures almost as coarse as coarser ground punctures, distinguished by the presence of fine and short setae; lateral margins of elytra not expanded outwards; elytra suture not raised. Pseudepipleura narrowed posteriorly. Mesoventral process with lateral extensions sloping evenly downward. Metaventrite posteromedially with an oval, glabrous area, slightly longer than wide, length of glabrous area ca 2/3 of total length of metaventrite. Pro- and mesocoxae densely pubescent; without distinct spine-like setae. Ventral surface of profemora densely pubescent at basal 1/5, remainder scattered with fine punctures, interstices smooth, without microsculpture; meso- and metafemora glabrous, with coarse punctures and without microsculpture. Protibiae with several spines on dorsal face. Fifth tarsomere of pro- and mesotarsus subequal in length to the preceding 4 tarsomeres combined. Fifth metatarsomere equal in length to second tarsomere. ***Abdomen.*** Abdominal ventrites 1–5 with uniform pubescence; longest setae about as long as setae around metaventral glabrous area. Fifth ventrite entire. ***Aedeagus*** (Fig. 3D). Phallobase slightly arcuate at basal 2/3; manubrium gradually narrowed at posterior 1/3 and rounded posteriorly. Parameres slightly longer than phallobase, widest at the base and gradually narrowed; inner margin of paramere slightly sinuate in dorsal view and hardly subapically curved; apex rounded. Median lobe almost as long as parameres, gradually narrowed from base to apex; gonopore triangular, apically situated; anterior margin of gonopore pointed.

**Remarks.** This species is very similar to *O. bhutanicus* Satô, 1979, but it can be distinguished from the latter by dorsum with weak greenish luster under lateral illumination (vs distinct greenish luster in *O. bhutanicus*), aedeagus with median lobe as long as parameres (vs shorter than parameres in *O. bhutanicus*), anterior margin of gonopore pointed (rounded in *O. bhutanicus*).

**Figure 4.** Habitats of *Oocyclus extensus* sp. nov. **A** valley at Zhêntang Town (Xizang), roadside with waterfalls **B** wet rock with fine flowing water **C, D** adults at night.

**Figure 5.** Habitat of *Oocyclus ximaensis* sp. nov. **A** river valley with forests on both sides in Xima Town (Yunnan); the red arrow indicates the rock wall with flowing water **B, C** adults at night.

**Etymology.** This species is named after Xima Town, where the type locality is located.

**Biology.** (Fig. 5A–C) This species was found on the surface of vertical stone walls with seepage on the side of the river valley.

**Distribution.** (Fig. 9) China (Yunnan). Only known from type locality.

## Additional faunistic records for China

***Oocyclus bhutanicus*** **Satô, 1979**
Figs 6D, 7D, 8D

**New material examined.** 5 ♂♂, 3 ♀♀; China• Xizang Autonomous Region, Xigazê, Dinggyê County, Zhêntang Town, on wet rock with fine flowing water

(西藏日喀则定结县陈塘镇流水岩壁表面), 2482 m, 27.8733°N, 87.4117°E, 2023.VII.10, Zu-qi Mai.; SYSU BJSB438001 • 1 ♂, 3 ♀♀ (SYSU), Xizang, Medog County, 80K, 1371 m, 27.8733N, 95.4673E, 2023.VI.15, Zu-qi Mai leg.; SYSU BJSB438002 to 005.

**Distribution.** (Fig. 9) China (Xizang), Bhutan, Nepal. **Newly recorded from Xizang.** Records from Thailand and China (Taiwan) by Hebauer and Wang (1998) need confirmation (Short and Swanson 2005).

### *Oocyclus dinghu* Short & Jia, 2011

Figs 6I, 7I, 8I

**New material examined.** 12 unsexed spec.; China• Guangdong Prov., Fengkai County, Heishiding Natural Reserve (广东省封开黑石顶自然保护区), 23.31°N, 111.52°E, 2014.IX.20–22, Ren-chao Lin, Feng-long Jia & Yu-dan Tang leg; SYSU BJSB439001. • 2 unsexed spec.; Guangdong, Dinghushan Natural Reserve (广东鼎湖山自然保护区), 1958, Cui-ying Li leg. (with label *Oocyclus latus*).; SYSU BJSB439002 to 003. • 1 ♂, 2 ♀♀; Guangxi Prov., Longsheng, Jiangdi (龙胜江底乡), 2013.IV.13–17, Hai-dong Chen leg.; SYSU BJSB4381006 to BJSB4381008.

**Distribution.** (Fig. 9) China (Guangdong, Guangxi). **Newly recorded from Guangxi**.

### *Oocyclus fikaceki* Short & Jia, 2011

Figs 6G, 7G, 8G

**New material examined.** China • **Zhejiang:** 2 ♂♂, 3 ♀♀, 14 unsexed spec.; Longquan, Fengyangshan Natural Reserve (龙泉凤阳山自然保护区), on wet rock, N.R. ca 1150m, 27°54'51"N, 119°11'56"E, 2018.IV.28, Yin & Miao.; SYSU. • **Hubei:** 2 ♂♂, 34 unsexed spec.; Dabieshan Mountian, Taohuachong mount (大别山脉桃花冲), 30°50.9'N, 116°1.7'E, 2014.VI.25, Zhen-hua Liu leg.; SYSU. • **Hunan:** 3 ♂♂, 6 ♀♀, 427 unsexed spec.; Zhuzhou Prefecture, Yanling County, Taoyuandong Natural Reserve, Zhulian waterfall (株洲市炎陵县桃源洞珠帘瀑布), 2014.V.26,Xiao-hua Chen, Ren-chao Lin & Chang Pan leg.; SYSU. • 168 unsexed spec.; Guidong County, Bamianshan Natural Reserve (桂东县八面山自然保护区),25°58'21"N, 113°42'37"E, 973m, 2015.VI.15, Ren-chao Lin & Yu-dan Tang leg.; SYSU. • 30 unsexed spec.; Guzhang County, Gaowangjie National Natural Reserve (古丈县高望界国家自然保护区), 28°29.898'N, 110°3.575'E, 1053m, 2017.VI.21, Feng-long Jia leg.; SYSU. • 23 unsexed spec.; Huaihua Prefecture, Mayang County, Lancun (怀化麻阳县兰村乡), 27°46'18"N, 109°51'51"E, 2017.VIII.14, Wei-cai Xie & Shi-shuai Wang leg.; SYSU. • **Jiangxi:** 32 unsexed spec.; Jing'an County, Daqishan forest farm (静安县大杞山林场), 28.67°N, 115.07°E, 350m, 2014.VII.16, Ren-chao Lin leg.; SYSU. • 1 ♂; Jing'an County, Sanzhaolun, Baishuidong scenic area (静安县三爪仑乡白水洞景区), 29.04°N, 115.11°E, 660m, 2014.VII.22, Ren-chao Lin leg.; SYSU. • 5 unsexed spec., Anfu County, Wugongshan (安福县武功山), 27.33°N, 114.23°E, 400m, 2014.VII.24; SYSU. • 1 unsexed spec.; Jing'an County, Guanyinyan (静安县观音岩), 29.04°N, 115.14°E, 690m, 2014.VII.20, Ren-chao Lin; SYSU.

**Distribution.** (Fig. 9) China (Fujian, Guangdong, Hubei, Hunan, Jiangxi, Zhejiang). **Newly recorded from Hubei, Hunan, and Zhenjiang**.

**Figure 6.** Dorsal view of Chinese *Oocyclus* spp. **A** *O. extensus* sp. nov. **B** *O. magnificus* Hebauer & Wang, 1998 **C** *O. sumatrensis* Orchymont, 1932 **D** *O. bhutanicus* Satô, 1979 **E** *O. latiorificialis* sp. nov. **F** *O. ximaensis* sp. nov. **G** *O. fikaceki* Short & Jia, 2011 **H** *O. shorti* Jia & Maté, 2012 **I** *O. dinghu* Short & Jia, 2011. Scale bars: 1 mm.

### ***Oocyclus magnificus*** **Hebauer & Wang, 1998**

Figs 6B 7B, 8B

**New material examined.** 3 ♂♂, 4 ♀♀; China • Taiwan, Taidong, Hairui, Lidao village (台东海瑞乡利稻), 1000m, 2017.V.13, Wen-yi Zhou leg.; SYSU. MZPC0050 to 0056. • 2 ♂♂, 1 ♀, 10 unsexed spec.; China • Taiwan, Lala Shan Mt. (between

**Figure 7.** Lateral view of Chinese *Oocyclus* spp. **A** *O. extensus* sp. nov. **B** *O. magnificus* Hebauer & Wang, 1998 **C** *O. sumatrensis* Orchymont, 1932 **D** *O. bhutanicus* Satô, 1979 **E** *O. latiorificialis* sp. nov. **F** *O. ximaensis* sp. nov. **G** *O. fikaceki* Short & Jia, 2011 **H** *O. shorti* Jia & Maté, 2012 **I** *O. dinghu* Short & Jia, 2011. Scale bars: 1 mm.

Fuxing town, Taoyuan County and Wulai town, Taibei County) (拉拉山,桃园县复兴镇和台北县乌来镇之间), 2006.IV.26, Living leg.; SYSU.

**Distribution.** (Fig. 9) China (Taiwan).

### *Oocyclus shorti* Jia & Maté, 2012

Figs 6H, 7H, 8H

**New material examined.** China • **Guangdong:** 3 ♂♂ 2 ♀♀, 47 unsexed spec.; Huizhou Prefecture, Longmen County, Nankunshan, Zhongpingwei Village (惠州龙门县南昆山中坪尾村), 23.6224°N, 113.8660°E, 639.0m, 2021.IX.26, Wei-cai

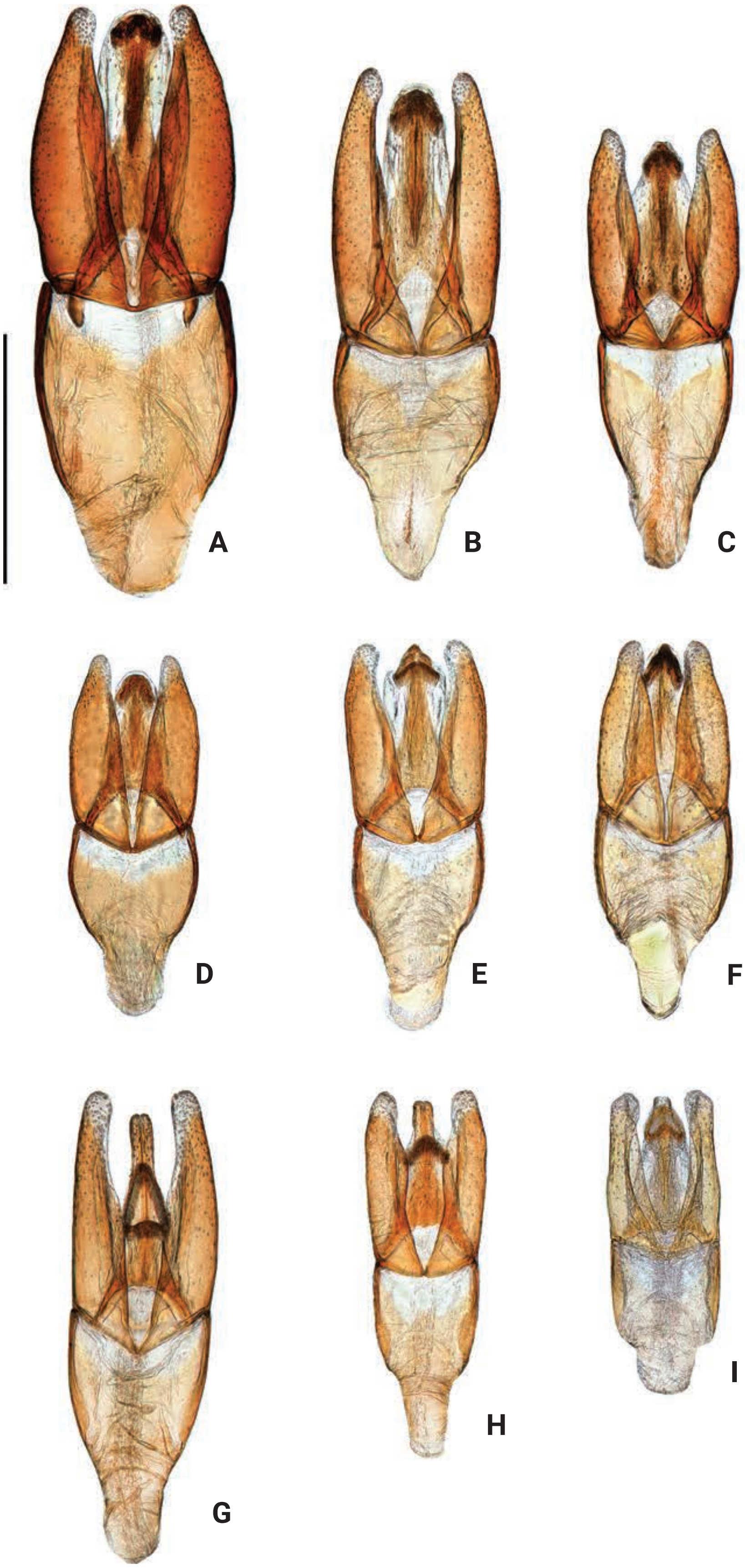

**Figure 8.** Aedeagus of Chinese *Oocyclus* spp. (dorsal view) **A** *O. extensus* sp. nov. **B** *O. magnificus* Hebauer & Wang, 1998 **C** *O. sumatrensis* Orchymont, 1932 **D** *O. bhutanicus* Satô, 1979 **E** *O. latiorificialis* sp. nov. **F** *O. ximaensis* sp. nov. **G** *O. fikaceki* Short & Jia, 2011 **H** *O. shorti* Jia & Maté, 2012 **I** *O. dinghu* Short & Jia, 2011. Scale bar: 0.5 mm.

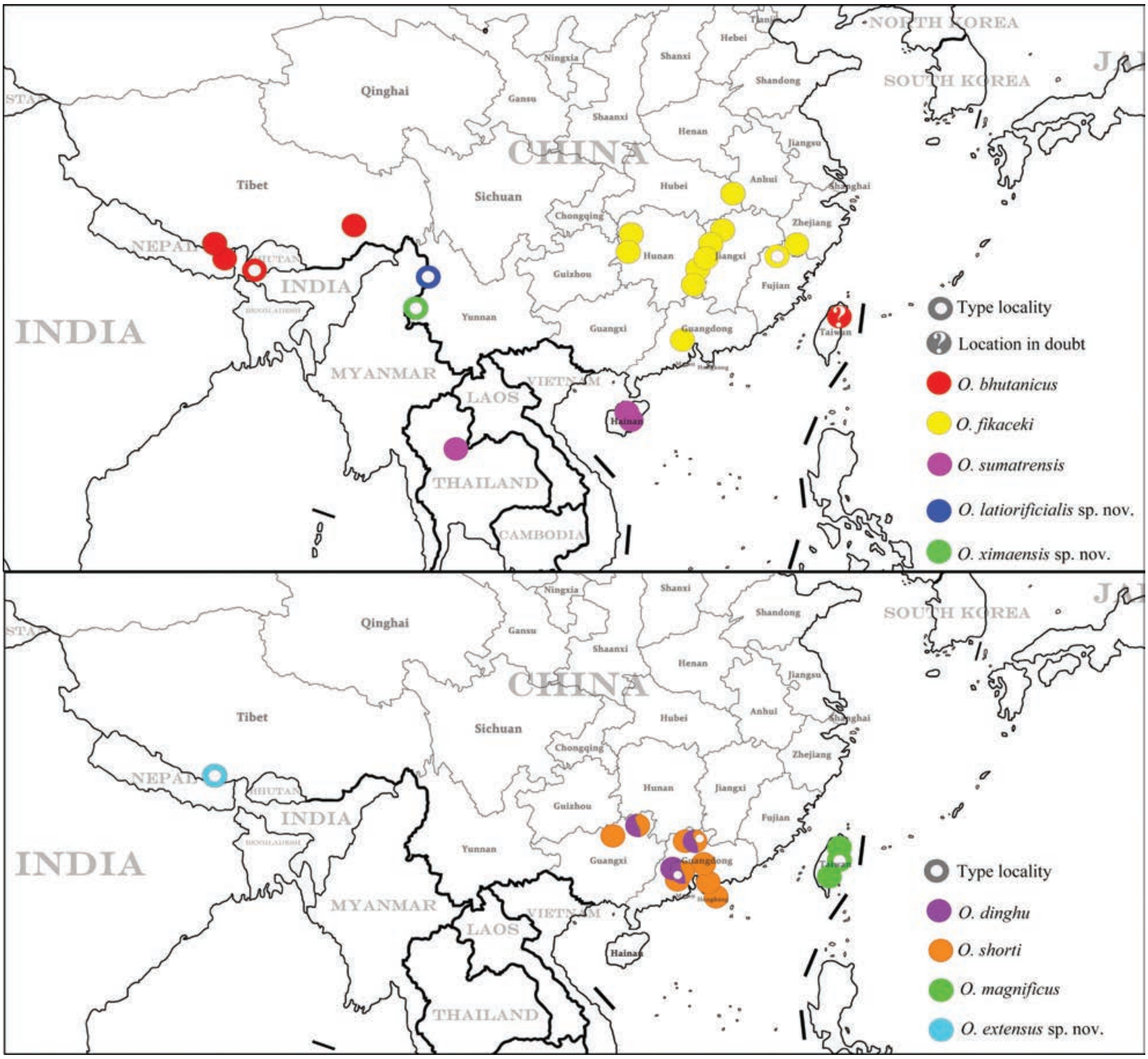

**Figure 9.** Distribution maps of Chinese *Oocyclus* spp.

Xie, Zhuo-yin Jiang & Zu-qi Mai leg.; SYSU. • 47 unsexed spec.; Fengkai County, Heishiding Natural Reserve (封开县黑石顶保护区), 23°31'N, 113°52'E, 2014.XI.20–22, Ren-chao Lin, Feng-long Jia & Yu-dan Tang et al. leg.; SYSU. • 8 unsexed spec.; Renhua County, Danxiashan, Zhanglaofeng (仁化县丹霞山长老峰), 2012.V.30, Feng-long Jia leg.; SYSU. • 3 unsexed spec.; Danxiashan, Jinshiyan (丹霞山锦石岩), 2021.VI.08, Feng-long Jia leg.; SYSU. • 1 ♂.; Danxiashan, Xianglong Lake (丹霞山翔龙湖), 2012.VIII.08, Feng-long Jia leg.; SYSU. • 45 unsexed spec.; Danxiashan, near Danxian Resort (丹霞山丹霞山庄), on wet rock, 2016.VI.08, Feng-long Jia leg.; SYSU. • 20 unsexed spec.; Shenzhen, Maluanshan Mt., (深圳马峦山), 2014.VI.13, Feng-long Jia & Wei-cai Xie leg.; SYSU. • 2 ♂♂, 1 ♀, 28 unsexed spec.; Shaoguan Prefecture, Chebaling National Natural Reserve (韶关车八岭国家自然保护区), 23°14'46"N, 113°33'56"E, 496m, 2017.V.28–29, Feng-long Jia, Shi-shuai Wang & Zu-long Liang leg.; SYSU. • 1 ♂; Foshan Prefecture, Gaoming County, Yangmei town (高明市杨梅镇),2006.IV.23–26, Feng-long Jia leg.; SYSU. • 16 unsexed spec.; Qingyuan Prefecture, on wet rock of roadside from Lianzhou city to

Tianlong Gorge, Datongshan Natural Reserve (连州至大东山自然保护区天龙峡路边潮湿石壁), 2013.IV.18, Feng-long Jia leg.; SYSU. • 3 ♂♂, 2 ♀♀, 40 unsexed spec.; Nanling, Dadongshan Natural Reserve (大东山自然保护区), 2013.IV.19–22, Feng-long Jia.; SYSU. • **Guangxi:** 2 ♂♂, 4 ♀♀, 64 unsexed spec.; Jiuwandashan, Yangmeiao village (九万大山杨梅坳), 25°11'42"N, 108°28'51"E, 1183m, 2015.VII.20, Ren-chao Lin & Yu-dan Tang; SYSU. • 2 ♂♂, 4 ♀♀, 28 unsexed spec.; Longsheng County, Jiangdi (龙胜江底乡), 2013.IV.13–17, Hai-dong Chen leg.; SYSU.

**Distribution.** (Fig. 9) China (Guangdong, Guangxi, Hongkong). **Newly recorded from Guangxi.**

### ***Oocyclus sumatrensis*** **Orchymont, 1932**

Figs 6C, 7C, 8C

**New material examined.** 2 ♂♂, 1 ♀, 11 unsexed spec.; China • Hainan Prov., Limushan Mt., Limu temple (黎母山黎母庙), 2011.V.5, Shuang Zhao leg.; SYSU.

**Distribution.** (Fig. 9) China (Hainan), Indonesia, Malaysia, Thailand (Short and Swanson 2005).

## A key to Chinese species

1 Elytra with distinct rows of systematic punctures. Pronotum with posterolateral corners angulate (Figs 6 A–C, 7A–C) .............................................. **2**

– Elytra without distinct rows of systematic punctures. Pronotum with posterolateral corners rounded (Figs 6 D–I, 7D–I) .......................................... **4**

2 Body length over 5.3 mm (Fig. 7A). Head, pronotum, and elytra with extremely fine and moderately coarse ground punctures. Lateral margins of elytra distinctly expanded (Fig. 6A). Pseudepipleura wide throughout ....... ........................................................................................ ***O. extensus*** **sp. nov.**

– Body length less than 5.2 mm (Fig. 7B, C). Head, pronotum, and elytra with fine ground punctures. Lateral margins of elytra not expanded (Fig. 6B, C). Pseudepipleura posteriorly narrowed ......................................................... **3**

3 Body length 5.0–5.2 mm. Elytra with 6 irregular rows of large punctures, a short scutellar row of punctures on elytra present (Figs 6B, 7B). Procoxae without spiniform setae ............................. ***O. magnificus*** **Hebauer & Wang**

– Body length less than 4.5 mm. Elytra with 5 distinct rows of punctures, without scutellar row of punctures (Figs 6C, 7C). Procoxae with distinct spiniform setae ................................................. ***O. sumatrensis*** **Orchymont**

4 Abdomen covered only with fine pubescence, without rows of long setae. Aedeagus with gonopore at apex of median lobe (Fig. 8D–F) ................... **5**

– Abdomen covered with fine pubescence and rows of long setae. Aedeagus with gonopore below apex of median lobe (Fig. 8G–I) ........................ **7**

5 Meso- and metafemora with fine microsculpture on intervals of punctures. Inner margin of paramere sinuate in dorsal view and distinctly subapically curved; median lobe almost parallel-sided medially, slightly widened at level of gonopore (Fig. 8E) ...................................... ***O. latiorificialis*** **sp. nov.**

– Meso- and metafemora without microsculpture on intervals of punctures. Inner margin of paramere straight or slightly sinuate in dorsal view, not subapically curved; median lobe gradually narrowed from base to apex .......... **6**

6 Dorsum with distinct greenish luster under lateral illumination. Aedeagus with median lobe shorter than parameres; anterior margin of gonopore rounded (Fig. 8D)........................................................... ***O. bhutanicus* Satô**

– Dorsum with weak greenish luster under lateral illumination. Aedeagus with median lobe as long as parameres; anterior margin of gonopore pointed (Fig. 8F) .........................................................***O. ximaensis* sp. nov.**

7 Maxillary palps with last palpomere not darkened, punctures on dorsal face finer and sparser. Aedeagus with parameres widely rounded and more or less expanded inwards apically. Median lobe with gonopore situated subapically (Fig. 8I)........................................... ***O. dinghu* Short & Jia**

– Maxillary palps with last palpomere darkened apically, punctures on dorsal face coarser and denser. Aedeagus with paramere narrowly rounded, not expanded inwards apically. Median lobe with gonopore situated at the middle or slightly above the middle ...........................................................**8**

8 Aedeagus with the outer margin of parameres distinctly curved inwards and clearly narrowed apically; median lobe abruptly narrowed at apical fourth, gonopore wider than long, situated 1.5× its length below apex (Fig. 8H)...................................................................................***O. shorti* Jia & Mate**

– Aedeagus with parameres not distinctly curved, and not narrowed apically; medial lobe slightly narrowed subapically, gonopore shaped as a long triangle, longer than wide, situated 1× its length below apex (Fig. 8G) ....... .....................................................................................***O. fikaceki* Short & Jia**

## Discussion

Three patterns of elytral punctures are known among known species from the Oriental region: 1) elytra with distinct rows of large punctures (including rows of systematic punctures), with ground punctures of almost uniform size, such as *O. sumatrensis* Orchymont, 1932, *O. magnificus* Hebauer & Wang, 1998, and *O. namtok* Short & Swanson, 2005; 2) elytra with a mixture of fine and coarse ground punctures, systematic punctures of almost the same size as coarse ground punctures and interspersed with coarse ground punctures, such as *O. bhutanicus* Satô, 1979, *O. dinghu* Short & Jia, 2011, *O. fikaceki* Short & Jia, 2011, *O. shorti* Jia & Mate, 2012, *O. latiorificialis* sp. nov., and *O. ximaensis* sp. nov.; 3) elytra with distinct rows of large punctures (including rows of systematic punctures), with fine punctures mixed with more coarse ground punctures, such as *O. sitesi* Short & Swanson, 2005, *O. rupicola* Minoshima, 2009 and *O. extensus* sp. nov.

Among Chinese species, two are assigned to pattern 1: *O. sumatrensis*, occurring on Hainan, and *O. magnificus*, endemic to Taiwan. Seven species are assigned to pattern 2: *O. dinghu*, *O. fikaceki*, *O. shorti*, *O. latiorificialis*, *O. bhutanicus*, and *O. ximaensis*, occurring on the Chinese mainland. Only one species, *O. extensus*, is assigned to pattern 3. As in South America, knowledge of the distribution of *Oocyclus* is still very incomplete (Clarkson and Short 2012). In South Asia and Southeast Asia, as well as southern China, many species remain undescribed. A distribution map of the genus in China is presented in Fig. 9. Some provinces in central and western-central China, such as Anhui, Hubei, Chongqing, and Sichuan, receive abundant rainfall and have a suitable climate. Therefore, it is very likely that some unknown species having pattern-2 elytral punctures occur in these regions.

Although *Oocyclus* species are similar in shape, some Neotropical and Oriental groups have evolved some special characters. All 24 Brazilian *Oocyclus* possess pale spots (or “taillights”) on the posterior quarter of the elytra (Clarkson and Short 2012; Jordão et al. 2018; Alencar et al. 2022), apart from the recently described *O. paraiso* from the Guiana Shield, which lacks these spots (Santana et al. 2023). This color feature is found in only two other species of the genus from Venezuela (Clarkson and Short 2012). None of the Oriental species have such a character. Ground punctures in most of the Oriental species vary in size, but only a few Neotropical species have such similar characters. These differences are probably the result of geographical isolation and microenvironment.

The distributions of most species show strong geographic patterns. The pattern of distributions of Venezuelan *Oocyclus* strongly corresponds to mountain ranges and rock outcrops (Short and Garcia 2010). In the fauna of the Neotropical and Oriental regions, only a few species are widely distributed, suggesting that species of *Oocyclus* species may be predominantly local endemics. In China *Oocyclus* species are known to co-occur with species of other genera of Hydrophilidae (*Enochrus*, *Coelostoma*, *Laccobius*), Hydraenidae (*Limnebius*), and Torridincolidae (*Satonius*) (Hájek et al. 2011). Species of these genera, which also inhabit wet rocks or margins of waterfalls, have been collected from Zhejiang Province, Hubei Province, and the Qingling Mountains. The areas in China north of the Yangtze River receive less rainfall and have fewer long-term waterfalls or wet-rock habitats. As a result, no species of *Enochrus*, *Coelostoma*, *Laccobius*, *Limnebius*, or *Satonius*, which inhabit wet rocks or the margins of waterfalls, have been collected there to date.

## Acknowledgements

We thank Dr Robert B. Angus, a specialist on Hydrophiloidea, the Natural History Museum, London, UK, who reviewed the manuscript. We are very grateful to Mr Wen-yi Zhou for collection and donation of the specimen of *O. magnificus* Hebauer & Wang. We thank Mr Cheng Liang (Chinese Academy of Sciences, Institute of Zoology), Mr Yu-chen Zheng and Mr Yue-zheng Tu (both from China Agricultural University) for helping Zu-qi Mai in the fieldwork. We are grateful to Dr. Bing-Lan Zhang, School of Life Sciences, Sun Yat-Sen University, for providing the equipment for macrophotography.

## Additional information

### Conflict of interest

The authors have declared that no competing interests exist.

### Ethical statement

No ethical statement was reported.

### Funding

This study was financially supported by “Science & Technology Fundamental Resources Investigation Program (grant no. 2022FY202100)”.

## Author contributions

Writing – original draft: F-l Jia, Z-q Mai. Writing – review and editing: Z-q Mai.

## Author ORCIDs

Feng-long Jia https://orcid.org/0000-0003-2391-5038
Zu-qi Mai https://orcid.org/0000-0003-3124-2021

## Data availability

All of the data that support the findings of this study are available in the main text.

## References

Alencar JBR, Short AEZ, Hamada N (2022) New species and new distributional records of the hygropetric water scavenger beetle genus *Oocyclus* Sharp (Coleoptera, Hydrophilidae) from the Brazilian Shield. Zootaxa 5087(2): 275–305. https://doi.org/10.11646/zootaxa.5087.2.3

Clarkson B, Short AEZ (2012) Revision of the *Oocyclus* Sharp of Brazil with description of ten new species (Coleoptera: Hydrophilidae: Laccobiini). Zootaxa 3183(1): 1–35. https://doi.org/10.11646/zootaxa.3183.1.1

Hájek J, Yoshitomi H, Fikáček M, Hayashi M, Jia F-L (2011) Two new species of *Satonius* Endrödy-Younga from China and notes on the wing polymorphism of *S. kurosawai* Satô (Coleoptera: Myxophaga: Torridincolidae). Zootaxa 3016(1): 51–62. https://doi.org/10.11646/zootaxa.3016.1.4

Hansen M (1991) The Hydrophiloid Beetles. Phylogeny, classification and a revision of the genera (Coleoptera, Hydrophiloidea). Biologiske Skrifter 40: 1–368.

Hebauer F, Wang J (1998) New dpecies of the genus *Oocyclus* Sharp, 1882 from India, Sri Lanka and Taiwan with a key to all known species (Coleoptera: Hydrophilidae). Acta Coleopterologica 14: 37–46.

Jia F-L, Mate JF (2012) A new species of *Oocyclus* Sharp from southeastern China (Coleoptera: Hydrophilidae). Zootaxa 3509(1): 81–84. https://doi.org/10.11646/zootaxa.3509.1.6

Jordão R, Clarkson B, Ferreira-Jr N (2018) A new species and new records of *Oocyclus* Sharp, 1882 (Coleoptera: Hydrophilidae) from Brazil. Zootaxa 4382(1): 195–200. https://doi.org/10.11646/zootaxa.4382.1.10

Minoshima Y (2009) First record of the hygropetric genus *Oocyclus* Sharp (Coleoptera: Hydrophilidae) from Laos, with description of a new species. Zootaxa 2192(1): 45–55. https://doi.org/10.11646/zootaxa.2192.1.2

Santana L, Short AEZ, Bentti CJ, Hamada N (2023) New species and new distributional records of the hygropetric water scavenger beetle genus *Oocyclus* Sharp (Coleoptera: Hydrophilidae) from the Guiana Shield. Zootaxa 5230(5): 567–594. https://doi.org/10.11646/zootaxa.5230.5.6

Satô M (1979) Ergebnisse der Bhutan-Expedition 1972 und Indien-Nepal-Expeditionen 1975–1977 des Naturhistorischen Museums in Basel. Coleoptera: Fam. Georissidae, Hydraenidae, Hydrophilidae und Ptilodactylidae. Entomologica Basiliensia 4: 43–67.

Short AEZ (2009) Two new species of the hygropetric genus *Oocyclus* Sharp from eastern India (Coleoptera: Hydrophilidae). Acta Entomologica Musei Nationalis Pragae 49: 625–630.

Short AEZ, Garcia M (2010) A review of the *Oocyclus* Sharp of Venezuela with description of twelve new species (Coleoptera: Hydrophilidae: Laccobiini). Zootaxa 2635(1): 1–31. https://doi.org/10.11646/zootaxa.2635.1.1

Short AEZ, Jia F-L (2011) Two new species of *Oocyclus* Sharp from China with a revised key to the genus for mainland Southeast Asia (Coleoptera: Hydrophilidae). Zootaxa 3012(1): 64–68. https://doi.org/10.11646/zootaxa.3012.1.6

Short AEZ, Perkins PD (2004) A revision of *Oocyclus* Sharp of Mexico and Central America (Coleoptera: Hydrophilidae). Zootaxa 783(1): 1–45. https://doi.org/10.11646/zootaxa.783.1.1

Short AEZ, Swanson A (2005) A revision of the *Oocyclus* Sharp of Thailand with description of six new species (Coleoptera: Hydrophilidae). Zootaxa 1078(1): 1–24. https://doi.org/10.11646/zootaxa.1078.1.1

Short AEZ, Greene L, Garcia M (2013) New species and new records of the hygropetric water beetle genus *Oocyclus* Sharp from South America (Coleoptera: Hydrophilidae). Zootaxa 3741(3): 349–358. https://doi.org/10.11646/zootaxa.3741.3.3

Toussaint EF, Short AEZ (2018) Transoceanic stepping-stones between Cretaceous waterfalls? The enigmatic biogeography of pantropical *Oocyclus* cascade beetles. Molecular Phylogenetics and Evolution 127: 416–428. https://doi.org/10.1016/j.ympev.2018.04.023

ZooKeys 1205: 39–50 (2024)
DOI: 10.3897/zookeys.1205.125164

Research Article

# Notes on the genus *Elegansovella* Hirschmann, 1989 (Acari, Mesostigmata, Urodinychidae)

Jenő Kontschán[1,2], Sergey G. Ermilov[3], Stefan Friedrich[4]

1 *Plant Protection Institute, HUN-REN Centre for Agricultural Research, Budapest, Hungary*
2 *Department of Plant Sciences, Albert Kázmér Faculty of Mosonmagyaróvár, Széchenyi István University, Mosonmagyaróvár, Hungary*
3 *Tyumen State University, Institute of Environmental and Agricultural Biology (X-BIO), Tyumen, Russia*
4 *Ludwig-Maximilians-University Munich, Faculty of Biology, Biocenter LMU, Planegg-Martinsried, Munich, Germany*
*Corresponding author: Jenő Kontschán (kontschan.jeno@atk.hun-ren.hu)*

## Abstract

The genus *Elegansovella* Hirschmann, 1989 (Mesostigmata: Uropodina: Urodinychidae) is resurrected for species of the *Uroobovella elegans*-group. This genus differs from the other taxa of *Uroobovella* Berlese, 1903 sensu lato based on the shape of the idiosoma and the caudal and dorsal setae. Three species from the *Uroobovella elegans*-group are transferred to the genus *Elegansovella*, as *E. pectintata* (Hirschmann, 1973), **comb. nov.**, *E. pectinatasimilis* (Hiramatsu, 1980), **comb. nov.** and *E. serangensis* (Hiramatsu, 1980), **comb. nov.** The other seven species from this species group are transferred to *Monstrobovella* **gen. nov.**, as *M. crustosa* (Vitzthum, 1926), **comb. nov.**, *M. enodis* (Hiramatsu, 1985), **comb. nov.**, *M. faceta* (Hiramatsu & Hirschmann, 1978), **comb. nov.**, *M. facetaoides* (Hiramatsu & Hirschmann, 1978), **comb. nov.**, *M. imadatei* (Hiramatsu, 1980), **comb. nov.**, *M. incerta* (Hiramatsu & Hirschmann, 1978), **comb. nov.** and *M. incertaoides* (Hiramatsu & Hirschmann, 1978), **comb. nov.** The new genus differs from *Elegansovella* by the shape of the idiosoma and the shape of marginal and dorsal setae. Six *Monstrobovella* species occur in the Oriental Realm and only one species is known from the Neotropical region. The present paper contains the description of a second Neotropical species of *Monstrobovella* (*M. mancocapaci* **sp. nov.**) which was found in Peru. The new species differs from its Neotropical congener in the dorsal and marginal setation.

**Key words:** Morphology, new combination, new genus, new species, Oriental and Neotropical regions, taxonomy, Uropodina

Academic editor: Farid Faraji
Received: 10 April 2024
Accepted: 21 May 2024
Published: 19 June 2024

ZooBank: https://zoobank.org/38EDC55B-C1E4-45AD-8978-7B0DE606BD2B

Citation: Kontschán J, Ermilov SG, Friedrich S (2024) Notes on the genus *Elegansovella* Hirschmann, 1989 (Acari, Mesostigmata, Urodinychidae). ZooKeys 1205: 39–50. https://doi.org/10.3897/zookeys.1205.125164

## Introduction

Giovanni Canestrini (1835–1900), the internationally noted acarologist, who also investigated the mites of the Bismarck Archipelago, discovered and described a new and unusual Uropodina mite: *Deraiophorus elegans* Canestrini, 1897. Werner Hirschmann, the noted Uropodina researcher, described a new species, *Deraiophorus pectinatus* Hirschmann, 1973 from New Guinea, which was later transferred (Hiramatsu and Hirschmann 1978) to the large catch-all genus *Uroobovella* Berlese, 1903, as *U. pectinatus* (Hirschmann 1973). Hirschmann (1973) synonymized *D. elegans* and *D. pectinatus*, and later he mentioned them only in terms of their synonymised name. Hirschmann (1989) revised this synonymy and presented both species again as two different taxa. Furthermore, Hirschmann and his co-worker Nabo Hiramatsu described seven new species from Indonesia and New Guinea (Hiramatsu and Hirschmann 1978; Hiramatsu 1980, 1985) and one new species from Ecuador (Hiramatsu and Hirschmann 1978). Additionally, *Trachyuropoda* (*Dinychura*) *crustosa* Vitzthum, 1926 was also transferred to *Uroobovella*. The systematic position of these species was not clear in Hirschmann's specific Gangsystematik system, therefore, he established a new species group for these eleven species (the *Uroobovella elegans*-group) and established in the same work a new genus, *Elegansovella* Hirschmann, 1989, for these species too (Hirschmann 1989).

An intensive acarological survey has been conducted on Peruvian mites for several years. Within this study, numerous species of Uropodina have also been discovered and described from Peru (Kontschán and Friedrich 2017, 2018, 2020a, 2020b; Błoszyk et al. 2019; Kontschán et al. 2023). In the current investigation of unidentified Uropodina species, a new species from the *Uroobovella elegans*-group was discovered in Peru. Therefore, we started studying this species group and recognised some problems as the *Uroobovella elegans*-group contains two species assemblages based on their morphology. The first corresponds to the genus *Elegansovella*, which has four species; the other seven belong to a new, previously undescribed genus.

## Materials and methods

Specimens of the herein presented species were found at ACP Panguana in the Peruvian Amazonia in Peru. All specimens investigated were cleared in lactic acid for a week and were then placed on half-covered well slides and examined using a Leica 1000 microscope with a drawing tube. All specimens are stored in ethanol and deposited in the Museo de Historia Natural, Universidad Nacional Mayor de San Marcos, Lima, Peru (MUSM) and SNSB-Zoologische Staatssammlung, Munich (ZSM).

Abbreviations: setae and pores: ***h*** = hypostomal seta, ***st*** = sternal seta. All measurements and the scales in the figures are given in micrometres (µm).

## Taxonomy

### Family Urodinychidae Berlese, 1917

**Remarks.** We provisionally retain the position of the genus *Elegansovella* in the family Urodinychidae on the basis of the following characters: setae *h1* long; chelicerae with internal sclerotized node and without mushroom- or flower-shaped sensory organ on fixed digit; corniculi smooth apically. However, all taxa of this family merit revision.

### Genus *Elegansovella* Hirschmann, 1989

*Elegansovella* Hirschmann, 1989: 102.
*Uroobovella elegans*-group Hirschmann, 1989: 97.
*Elegansovella*—Halliday 2015: 113.

**Type species.** *Deraiophorus elegans* Canestrini, 1897, by original designation.

**Diagnosis.** Idiosoma oval with vortex. One pair of anterolateral prolongations presented on idiosomal margin. Dorsal and marginal shields fused on anterior part of idiosoma. Dorsal setae tree-like, with a short stem and many long cross-bars. Three or four pairs of long and pilose setae situated close to posterior margin of dorsal shield. Marginal setae long and marginally pilose, situated on long marginal prolongations. Shape of female genital shield oval or scutiform, its surface smooth and situated between coxae II–IV. Male genital shield circular and situated between coxae IV. Ventral setae pilose. Tritosternum with vase-like base, its laciniae divided into three branches. Corniculi smooth, horn-like, internal malae serrate. Setae *h1* smooth and longer than other hypostomal setae, *h2*–*h4* serrate, but *h4* divided into two or three serrate branches. Pedofossae present, but without separated furrow for tarsi IV. Prestigmatid part of peritreme with five bends. Epistome serrate. Chelicerae with internal sclerotized node, fixed digit longer than movable digit. Movable digit with one or two large central teeth.

## List of the known species

### *Elegansovella elegans* (G. Canestrini, 1897)

*Deraiophorus elegans* G. Canestrini, 1897: 462.
*Uroobovella elegans*—Hiramatsu and Hirschmann 1978: 79.
*Deraiophorus pectinatus* Hirschmann, 1973: 77–78.
*Uroobovella pectinata*—Hiramatsu and Hirschmann 1978: 85.

**Occurrence and habitat.** This species was collected in Bismarck Archipelago and New Guinea (Hirschmann 1989).

**Note.** Hirschmann (1973) mentioned *D. elegans* as the synonym of *D. pectinata*. Later, he (Hirschmann 1989) separated these two species again based on the shape of the basis of the epistome and the width of the peritreme. In our opinion, these differences are too weak and not sufficient to separate the two species. Furthermore, both species were collected in the same region. Thus, we agree with Hirschmann's (1973) opinion that *D. elegans* is the junior synonym of *D. pectinata*.

### *Elegansovella pectinatasimilis* (Hiramatsu, 1980), comb. nov.

*Uroobovella pectinatasimilis* Hiramatsu, 1980: 49.

**Occurrence and habitat.** This species was found in a forest habitat, in Indonesia (Hiramatsu 1980).

### *Elegansovella serangensis* (Hiramatsu, 1980), comb. nov.

*Uroobovella serangensis* Hiramatsu, 1980: 49.

**Occurrence and habitat.** This species was also reported from a forest habitat, in Indonesia (Hiramatsu 1980).

## Key to species of the genus *Elegansovella*

1 Setae close to caudal margin of dorsal shield marginally serrate, vertex longer than wide .......... ***E. elegans***

– Setae close to caudal margin of dorsal shield marginally pilose, vertex shorter than wide .......... **2**

2 Genital shield of female oval, ventral setae with a short stem and many long cross-bars .......... ***E. pectinatasimilis***

– Genital shield of female scutiform, ventral setae wide and apically pilose. .......... ***E. serangensis***

## Genus *Monstrobovella* gen. nov.

https://zoobank.org/24822A35-6D59-444B-A7C4-ABDA2CBFE789

**Diagnosis.** Idiosoma pentagonal without vortex. Dorsal and marginal shields fused on anterior part of idiosoma. Dorsal setae T-shaped or setiform. Several longer or wider setae situated close to posterior margin of dorsal shield. Marginal setae very wide, phylliform and marginally serrate. Shape of female genital shield linguli- or scutiform, its surface smooth and situated between coxae II–IV. Male genital shield circular and situated between coxae IV. Ventral setae T-shaped, V-shaped or setiform. Pedofossae present, but without separated furrow for tarsi IV. Prestigmatid part of peritreme with two bends. Tritosternum with vase-like base, its laciniae divided into three branches. Corniculi smooth, horn-like, internal malae gently serrate. Setae h1 smooth and longer than other hypostomal setae, *h2* smooth or serrate, *h3* serrate, *h4* divided into two or three serrate branches. Epistome serrate. Chelicerae with internal sclerotized node, fixed digit longer than movable digit. Movable digit with one or two large central teeth.

**Type species.** *Uroobovella faceta* Hiramatsu & Hirschmann, 1978.

**Etymology.** The name of the new genus refers to a combination of the words monster (based on extreme morphology) and *Uroobovella*.

**Gender.** Feminine.

**Notes.** The new genus differs in many characters from *Elegansovella*. The distinguishing characteristics are summarized in Table 1 and a schematic illustration of the two genera is presented in Fig. 1.

**Table 1.** Most important differences between *Elegansovella* and *Monstrobovella* genera.

| | ***Elegansovella*** | ***Monstrobovella*** |
|---|---|---|
| Shape of idiosoma | oval | pentagonal |
| Vertex | present | absent |
| Marginal setae | long and pilose | phylliform and apically serrate |
| Setae on caudal part of dorsal shield | extremely long (four-six times longer than dorsal setae) | not very long (two times longer than dorsal setae) |
| Anterolateral prolognation | present | absent |
| Peritreme | with several bends | with two bends |

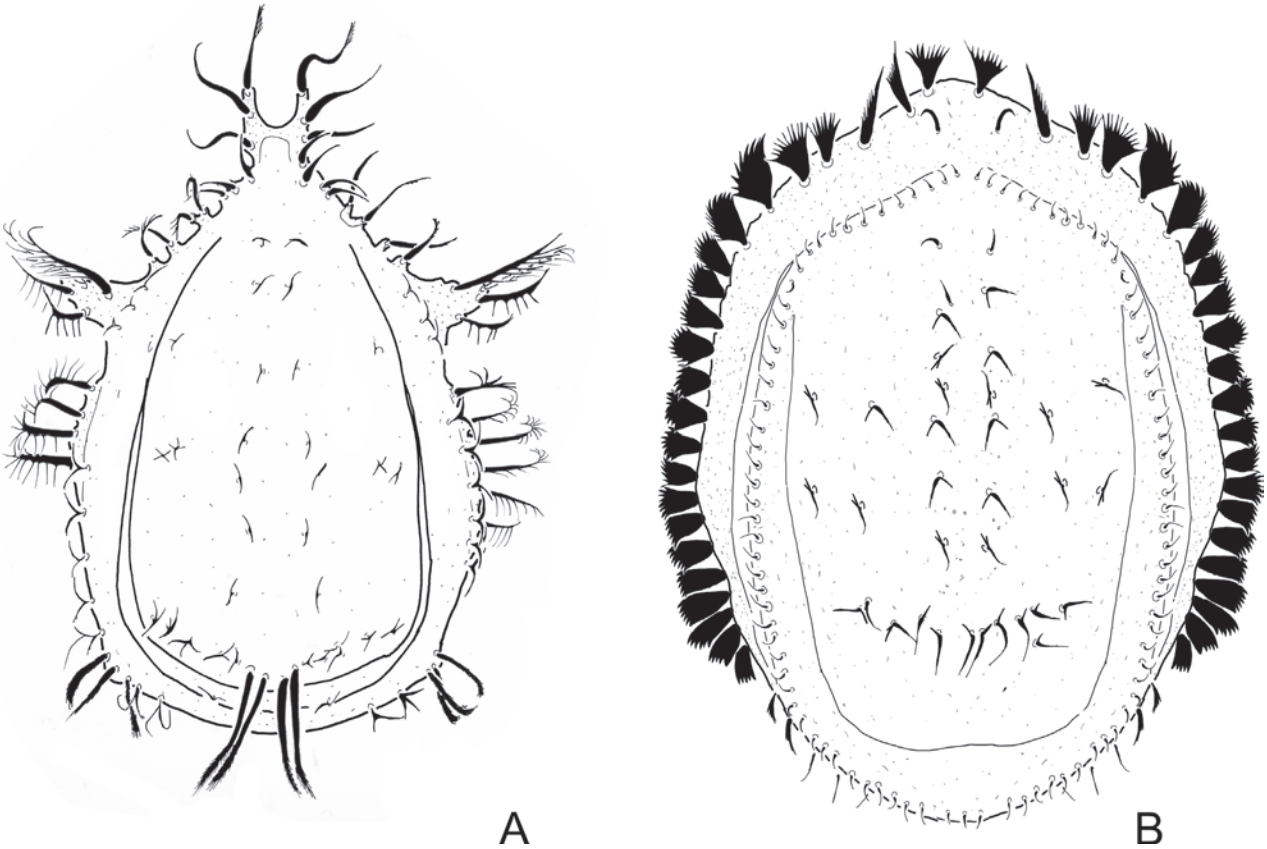

**Figure 1.** Schematic illustration of the genera *Elegansovella* (**A**) and *Monstrobovella* (**B**).

## List of the known species

***Monstrobovella crustosa* (Vitzthum, 1926), comb. nov.**

*Trachyuropoda* (*Dinychura*) *crustosa* Vitzthum, 1926: 112–117.
*Uroobovella crustosa*–Hirschmann and Zirngiebl-Nicol 1962: 59, 72.

**Occurrence and habitat.** This species was found in soil, in Malaysia (Vitzthum 1926).

***Monstrobovella enodis* (Hiramatsu, 1985), comb. nov.**

*Uroobovella enodis* Hiramatsu, 1985: 5–7.

**Occurrence and habitat.** This species was collected in soil, in Borneo (Malaysia) (Hiramatsu 1985).

***Monstrobovella faceta* (Hiramatsu & Hirschmann, 1978), comb. nov.**

*Uroobovella faceta* Hiramatsu & Hirschmann, 1978: 74–75.
*Uroobovella faceta*—Kontschán 2016: 95.

**Occurrence and habitat.** This species was collected in leaf litter in natural and agricultural areas, in Ecuador (Hiramatsu and Hirschmann 1978; Kontschán 2016).

### ***Monstrobovella facetaoides*** **(Hiramatsu & Hirschmann, 1978), comb. nov.**

*Uroobovella facetaoides* Hiramatsu & Hirschmann, 1978: 76.

**Occurrence and habitat.** This species was collected in New Guinea, its habitat is unknown. (Hiramatsu and Hirschmann 1978).

### ***Monstrobovella imadatei*** **(Hiramatsu, 1980), comb. nov.**

*Uroobovella imadatei* Hiramatsu, 1980: 48–49.

**Occurrence and habitat.** This species was collected in a forest, in Indonesia (Hiramatsu 1980).

### ***Monstrobovella incerta*** **(Hiramatsu & Hirschmann, 1978), comb. nov.**

*Uroobovella incerta* Hiramatsu & Hirschmann, 1978: 76–77.

**Occurrence and habitat.** This species was found in New Guinea, its habitat is unknown. (Hiramatsu and Hirschmann 1978).

### ***Monstrobovella incertaoides*** **(Hiramatsu & Hirschmann, 1978)**

*Uroobovella incertaoides* Hiramatsu & Hirschmann, 1978: 77.

**Occurrence and habitat.** This species was collected in New Guinea, its habitat is unknown. (Hiramatsu and Hirschmann 1978).

### ***Monstrobovella mancocapaci*** **sp. nov.**

https://zoobank.org/797AB257-D04B-4A76-BAF6-D7C20FA770D5
Figs 2–4

**Material examined.** ***Holotype*****.** Female. One female. Peru, Huánuco Department, Yuyapichis, ACP Panguana, 9°37'S, 74°56'W, 230 m a.s.l., Winkler extraction, 20 September to 07 October 2013, leg. S. Friedrich & F. Wachtel. ***Paratypes*****.** One female and one male. Locality and date same as for holotype. Holotype and two female and four male paratypes deposited in MUSM, other paratypes in the ZSM.

**Diagnosis.** Dorsal and ventral idiosoma without sculptural pattern, only some small oval pits situated on posterocentral area of dorsal shield. Dorsal setae smooth and robust, but several marginally pilose setae situated close

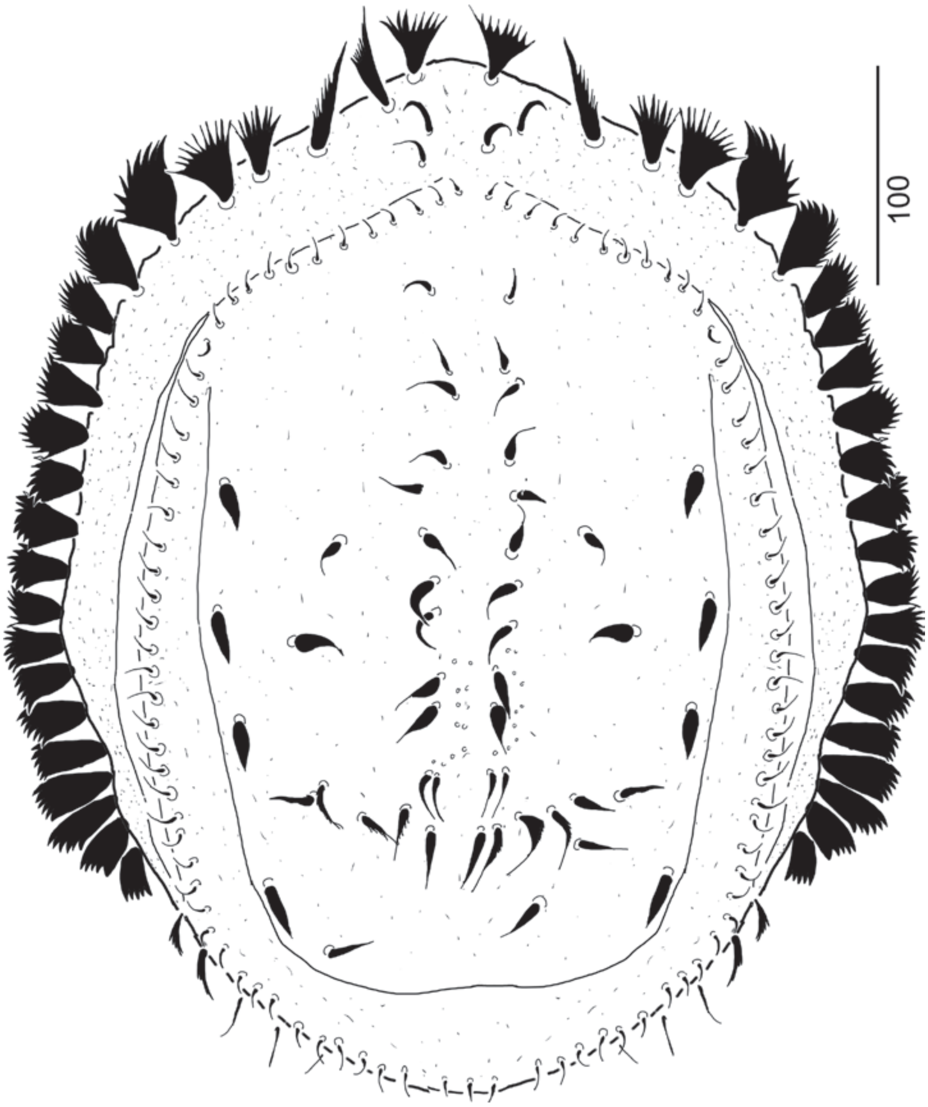

**Figure 2.** *Monstrobovella mancocapaci* sp. nov., holotype, female in dorsal view.

to posterior margin of dorsal shield. Marginal setae very wide, phylliform and marginally serrate. Ventral setae smooth and setiform. Shape of female genital shield linguliform. Male genital shield oval and situated between coxae IV.

**Description. Female** (*N* = 2). Shape of idiosoma pentagonal, colour yellowish brown, flat. Length of idiosoma 630, width at level of coxae IV 540.

***Dorsal idiosoma*** (Fig. 2). Marginal and dorsal shields fused anterolaterally. Surface of dorsal shield without sculptural pattern, only some oval pits (*ca* 2 × 3) situated on posterocentral area. Margin of dorsal shield bears more than 45 pairs of short (*ca* 8–9) smooth and needle-like setae. Majority of other dorsal (more than 21 pairs) setae smooth and robust (*ca* 15–24 long). Three pairs of robust and marginally serrate (*ca* 22–24 long) setae situated on posterior part of dorsal shield. Marginal shield wide with more than 25 pairs of wide, phylliform (*ca* 35–45 long) and marginally-serrate setae. Two pairs of smooth and needle-like (*ca* 20–22 long) setae situated on anterior area of marginal shield. Pores and lyriform fissures not visible on dorsal- and marginal shields.

***Ventral idiosoma*** (Fig. 3). Four pairs of sternal setae short (*ca* 7–9), needle-like and smooth. Setae *st1* inserted close to anterior margin of sternal

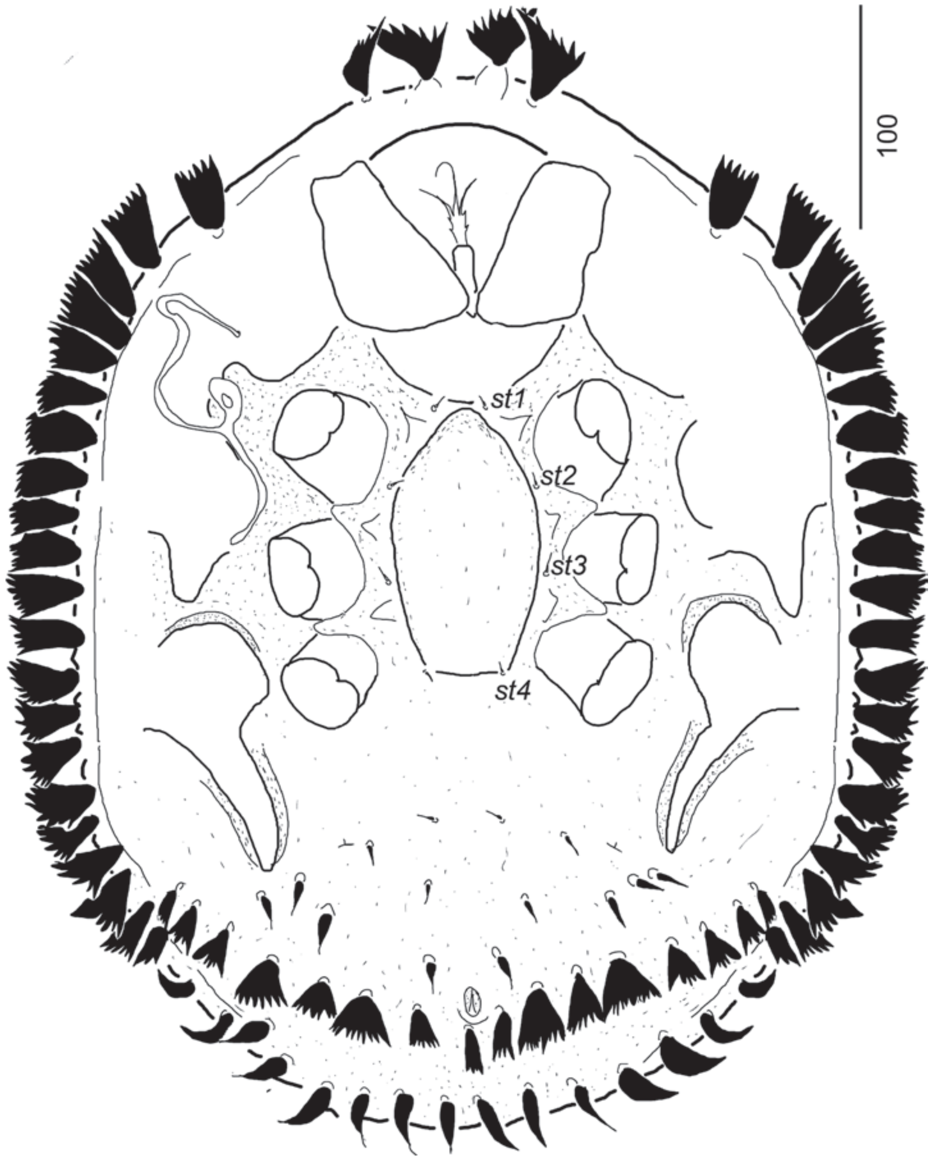

**Figure 3.** *Monstrobovella mancocapaci* sp. nov., holotype, female in ventral view.

shield, *st2* at mid-level of coxae II, *st3* at mid-level of coxae III, *st4* close to basal edge of genital shield. Sternal shield smooth, without any pores and lyrifissures. Three pairs of narrow and needle-like (*ca* 9–12 long) ventral setae situated between pedofossae IV. Three pairs of robust (*ca* 16–18 long) and spine-like ventral setae situated close to posterior end of pedofossae IV and one pair of robust and spine-like (*ca* 14–15) setae visible anterior to anal opening. Seven–eight pairs of wide, phylliform and marginally-serrate (*ca* 20–24 long) setae situated at level of anal opening and nine pairs of spine-like and very robust setae (*ca* 20–23 long) placed close to posterior margin of ventral idiosoma. One pair of lyriform fissure situated close to pedofossae IV. Ventral shield without ornamentation. Anal opening small and oval, *ca* 13–14 long and *ca* 7–8 wide.

Genital shield of female linguliform (*ca* 115–120 long and *ca* 60–65 wide) without sculptural pattern and without anterior process. Stigmata situated close to coxae II. Prestigmatid part of peritreme with two bends, poststigmatid part slightly curved. Pedofossae well developed, with smooth surface and separate furrow for tarsi IV.

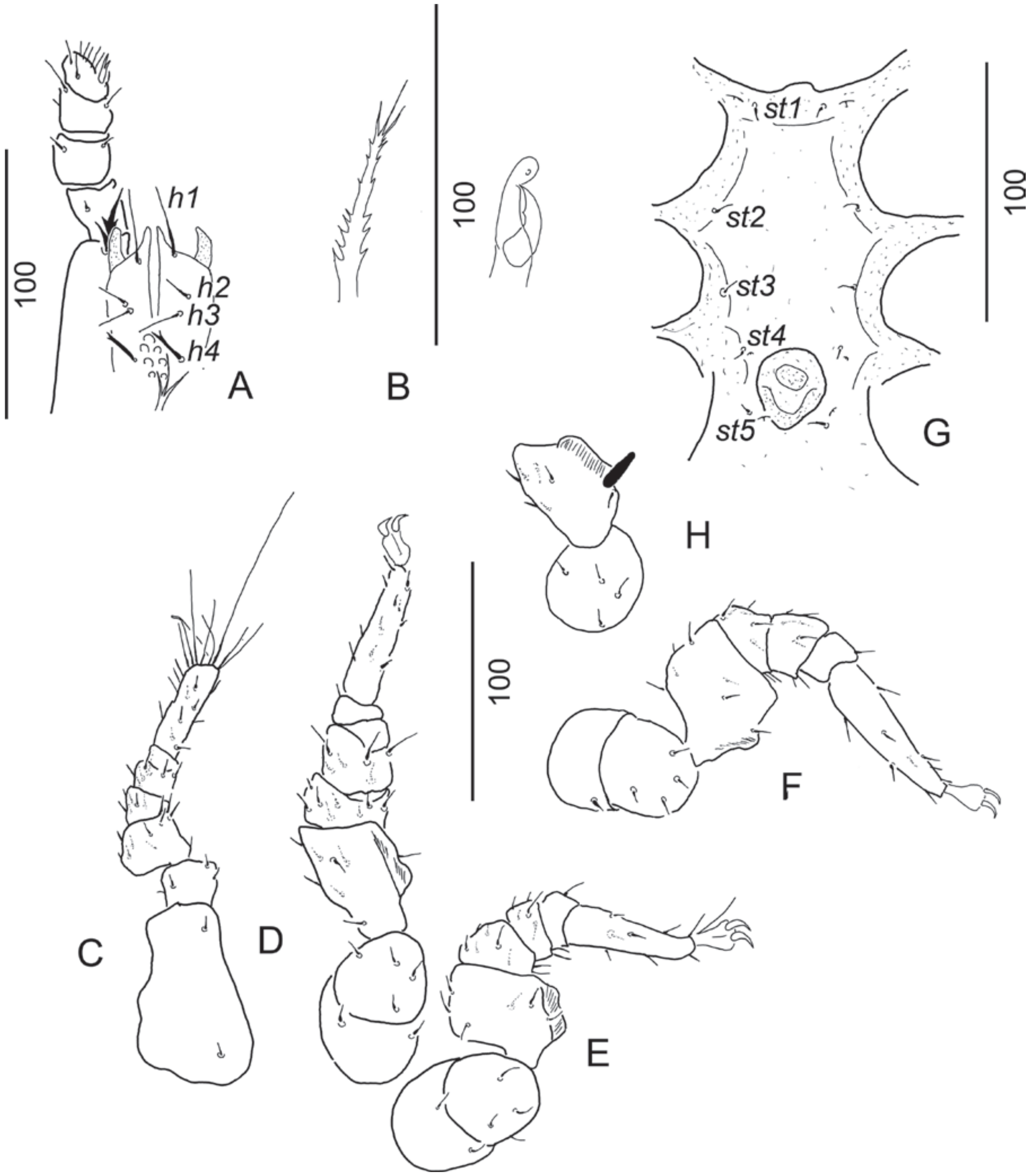

**Figure 4.** *Monstrobovella mancocapaci* sp. nov., holotype, female **A** gnathosoma and palp in ventral view **B** tritosternum in ventral view and chelicera in lateral view **C** leg I in ventrolateral view **D** leg II in ventrolateral view **E** leg III in ventrolateral view **F** leg IV in ventrolateral view **G** intercoxal area of male paratype **H** femur II of male paratype.

Tritosternum with narrow base, tritosternal laciniae divided three branches, its basal part with two pairs of lateral spines (Fig. 3).

***Gnathosoma*** (Fig. 4A). Corniculi smooth and horn-like, internal malae smooth, shorter than corniculi. Hypostomal setae *h1*, *h2* and *h3* smooth and needle-like, *h1* long (*ca* 27–28), *h2* and *h3* short (*ca* 11–13), *h4* apically bifurcated and *ca* 14–15 long. Some rounded denticles situated between setae *h4*. Chelicerae with internal sclerotized nodes, fixed digit of chelicerae (*ca* 26–27) slightly longer than movable digit (*ca* 20–22) (Fig. 4B), only one small tooth situated on central part of movable digit. Palp trochanter setae *v1* longer (*ca* 19–22) and trifurcated, *v2* shorter (*ca* 13–15) and spine-like. Other setae on palp segments smooth. Palp apotele bifurcate (Fig. 4A). Epistome marginally serrate (Fig. 4B).

***Legs.*** Length of legs (from base of coxae to apex of tarsi): **I** 185–190, **II** 220–225, **III** 170–175, **IV** 200–205. Leg **I** without ambulacral claws; all setae on legs smooth and needle-like (Fig. 4C–F).

**Male** (*N* = 1). Body 590–630 long and 490–540 wide.

***Dorsal idiosoma.*** As in female.

***Ventral idiosoma.*** Intercoxal area, with sternal setae and genital shield, as in Figure 4G. Sternal setae *ca* 7–9 long, smooth and needle-like. Setae *st1* inserted close to anterior margin of sternal shield, *st2* at level of posterior margin of coxae **II**, *st3* at mid-level of coxae **III**, *st4* close to anterior margin of genital shield, *st5* close to basal margin of genital shield. Surface of sternal shield without any sculptural pattern. One pair of lyriform fissures situated close to anterior margin of sternal shield, other two pairs situated close to setae *st4* and *st5*. Genital shield rounded, slightly longer than wide (*ca* 35 × 25) and situated between coxae IV (Fig. G).

***Legs.*** Femora of leg **II** each with a long (*ca* 18) and robust ventral setae (Fig. 4H). Other characters as in female.

**Developmental stages.** Unknown.

**Etymology.** The species name is dedicated to Manco Cápac (Manco Qhapaq or Manku Qhapaq) the first king of the Kingdom Cuzcó and the first emperor of the Inca dynasty.

**Remarks.** Only one *Monstrobovella* species (*M. faceta*) is known from the Neotropical region. *Monstrobovella faceta* has T-shaped dorsal setae whose cross-bar part is bifurcated. These setae are spine-like and smooth in the new species. The setae on the caudal region of the dorsal shield are numerous, very long and marginally serrate in the case of *M. faceta*, and there are only three short, marginally-serrate setae in the new species. Several long and T-shaped setae are situated posterior to coxae IV on the ventral idiosoma; these setae are missing in the new species. There are some small oval pits on posterocentral part of dorsal shield in the new species, which are missing in *M. faceta*.

## Key to the known *Monstrobovella* species based on females

1 Dorsal shield with some lateral furrows ........................................ **2**
– Dorsal shield without furrows........................................................ **3**
2 Six long furrows situated on posterior part of dorsal shield...... ***M. crustosa***
– Three long and three short furrows situated on posterior part of dorsal shield ........................................................................ ***M. imadatei***
3 Dorsal setae T-shaped...................................................................... 4
– Dorsal setae not T-shaped .............................................. ***M. mancocapaci***
4 End of cross-bar of T-shaped setae bifurcated ...................................... **5**
– End of cross-bar of T-shaped setae not bifurcated ................................ **6**
5 Ventral setae long, longer than distance between ventral setae.................. ............................................................................. ***M. facetaoides***
– Ventral setae short, distance between ventral setae longer than length of ventral setae ..................................................................... ***M. faceta***

6 Dorsal shield with one pair of strongly sclerotized round-like depression on anterior region ........................................................................ ***M. enodis***
– Dorsal shield without strongly sclerotized round-like depressions............**7**
7 All of ventral setae bifurcated, simple setae absent...........***M. incertaoides***
– Ventral setae bifurcated or simple ..............................................***M. incerta***

## Acknowledgements

We would like to thank Dr Juliane Diller and her husband Erich for inviting one of us (SF) to ACP Panguana, as well as Dr Diana Silva Dávila (Museo de Historia Natural, Universidad de San Marcos, Lima, Peru) for cooperation and the Dirección General Forestal y de Fauna Silvestre for issuing a collecting permit (# 0276-2013-AG-DGFFS-DGEFFS) and an export permit (# 000521-MINAGRI-DGFFS). Furthermore, we would like to thank Dr Jason Dunlop (Berlin, Germany) for his linguistic correction of the manuscript.

## Additional information

### Conflict of interest

The authors have declared that no competing interests exist.

### Ethical statement

No ethical statement was reported.

### Funding

No funding was reported.

### Author contributions

All authors have contributed equally.

### Author ORCIDs

Jenő Kontschán https://orcid.org/0000-0001-8274-4238
Stefan Friedrich https://orcid.org/0000-0002-1668-4633

### Data availability

All of the data that support the findings of this study are available in the main text.

## References

Berlese A (1903) Acari nuovi. Manipulus I.us. Redia (Firenze) 1: 235–252.

Berlese A (1917) Intorno agli Uropodidae. Redia (Firenze) 13: 7–16.

Błoszyk J, Friedrich S, Skoracki M (2019) *Rotundabaloghia dillerae*, a new species of soil mite (Parasitiformes: Uropodina: Rotundabaloghiidae) from Peru. International Journal of Acarology 46(1): 48–51. https://doi.org/10.1080/01647954.2019.1703810

Canestrini G (1897) Nuovi acaroidei della N. Guinea. Természetrajzi Füzetek 20: 461–474.

Halliday RB (2015) Catalogue of genera and their type species in the mite suborder Uropodina (Acari: Mesostigmata). Zootaxa 3972(2): 101–147. https://doi.org/10.11646/zootaxa.3972.2.1

Hiramatsu N (1980) Gangsystematik der Parasitiformes. Teil 373. Stadien von 3 neuen *Uroobovella*-Arten der *Pulchella*-Gruppe aus Indonesien. Acarologie. Schriftenreihe für Vergleichende Milbenkunde 27: 48–50.

Hiramatsu N (1985) Eine neue *Uroobovella*-Art (acarina: Uropodidae) aus Borneo. Acta Arachnologica 33(1): 5–8. https://doi.org/10.2476/asjaa.33.5

Hiramatsu N, Hirschmann W (1978) Gangsystematik der Parasitiformes. Teil 282. Teilgänge, Satdium von 4 neue *Uroobovella*-Arten und *Urobovella pectinata* (Hirschmann, 1973) der Pulchella-Gruppe aus Neue Guinea und Ekuador. Acarologie. Schriftenreihe fur Vergleichende Milbenkunde 24: 73–79.

Hirschmann W (1973) Gangsystematik der Parasitiformes. Teil 151. Gänge, Teilgänge, Stadien von 22 neuen Deriaophorus-Arten (Dinychini, Uropodinae). Acarologie. Schriftenreihe für Vergleichende Milbenkunde 19: 60–81.

Hirschmann W (1989) Gangsystematik der Parasitiformes. Teil 509. Die Ganggattung *Uroobovella* Berlese, 1903 – Artengruppen – Bestimmungstabellen – Diagnosen – (Dinychini, Uropodinae). Acarologie. Schriftenreihe für Vergleichende Milbenkunde 36: 84–196.

Hirschmann W, Zirngiebl-Nicol I (1962) Gangsystematik der Parasitiformes. Teil 6. Uropodiden. Die Gattung *Uroobovella* Berlese 1903 nov. comb. Teilgänge von Nenteria nov. comb. Acarologie. Schriftenreihe für Vergleichende Milbenkunde 5: 57–80.

Kontschán J (2016) Uropodina mites (Acari: Mesostigmata) from agricultural areas of Ecuador. Opuscula Zoologica Instituti Zoosystematici et Oecologici Universitatis Budapestinensis 47(1): 93–99. https://doi.org/10.18348/opzool.2016.1.93

Kontschán J, Friedrich S (2017) Contribution to the Uropodina mites of Peru (Acari: Mesostigmata). Zootaxa 4237(2): 359–370. https://doi.org/10.11646/zootaxa.4237.2.9

Kontschán J, Friedrich S (2018) First record of *Chelonuropoda* in Peru, with the description of a new species (Acari: Mesostigmata: Oplitidae). Ecologica Montenegrina 16: 124–129. https://doi.org/10.37828/em.2018.16.11

Kontschán J, Friedrich S (2020a) First record of the genus *Afrotrachytes* Kontschán (Acari: Uropodina) in Peru with the description of a new species. Acarological Studies 2(2): 77–82. https://doi.org/10.47121/acarolstud.713426

Kontschán J, Friedrich S (2020b) Resurrection of the genus *Formosaurella* Hirschmann (Uropodina: Discourellidae) with descriptions of a new species and a new subgenus. Systematic and Applied Acarology 25(8): 1508–1515. https://doi.org/10.11158/saa.25.8.12

Kontschán J, Ermilov SG, Friedrich S (2023) Contribution to the knowledge of the Neotropical Uropodina (Acari: Mesostigmata). Zootaxa 5360(2): 255–268. https://doi.org/10.11646/zootaxa.5360.2.5

Vitzthum H (1926) Acari als Commensalen von Ipiden. Zoologische Jahrbucher. Abteilung fur Systematik, Geographie und Biologie der Tiere 52: 407–503.

ZooKeys 1205: 51–88 (2024)
DOI: 10.3897/zookeys.1205.120300

Research Article

# Diversity of *Orbiniella* (Orbiniidae, Annelida) in the North Atlantic and the Arctic

Miguel A. Meca[1], Jon Anders Kongsrud[1], Katrine Kongshavn[1], Tom Alvestad[1], Karin Meißner[2], Nataliya Budaeva[1]

1 *Department of Natural History, University Museum of Bergen, University of Bergen, Bergen, Norway*
2 *Senckenberg Forschungsinstitute und Naturmuseun, German Centre for Marine Biodiversity Research, Hamburg, Germany*
*Corresponding author: Miguel A. Meca (Miguel.Meca@uib.no)*

Academic editor: Greg Rouse
Received: 8 February 2024
Accepted: 13 April 2024
Published: 20 June 2024

ZooBank: https://zoobank.org/A94034D3-8B98-461D-A58B-23654551B5D5

Citation: Meca MA, Kongsrud JA, Kongshavn K, Alvestad T, Meißner K, Budaeva N (2024) Diversity of *Orbiniella* (Orbiniidae, Annelida) in the North Atlantic and the Arctic. ZooKeys 1205: 51–88. https://doi.org/10.3897/zookeys.1205.120300

## Abstract

In this work, the diversity of the genus *Orbiniella* in the Nordic Seas and the North Atlantic waters south of Iceland is studied based on the analyses of molecular markers (mitochondrial COI, 16S rDNA and nuclear ITS2) and morphological characters. Our results showed the presence of at least five genetic lineages in the studied material which could also be morphologically identified by their segmental annulation patterns, the number and the shape of acicular spines, and the length and the shape of pygidial lobes. The species name *Orbiniella petersenae* is assigned to one of the lineages restricting its geographical and vertical distribution to the deep-sea areas north of Iceland and Jan Mayen, and three lineages are described as new species (i.e., *Orbiniella griegi* Meca & Budaeva, **sp. nov.**, *Orbiniella mayhemi* Meca & Budaeva, **sp. nov.**, and *Orbiniella parapari* Meca & Budaeva, **sp. nov.**) elevating the number of known species in the genus to 25. Three deep-sea species of *Orbiniella* in our study are reported only north of the Greenland-Iceland-Scotland Ridge, one deep-sea species found south of the ridge. A single shallow-water species is distributed along the ridge and on the Norwegian shelf.

**Key words:** Greenland-Iceland-Scotland Ridge, integrative taxonomy, molecular marker, new species, Nordic seas, SEM, species complex, species delimitation

## Introduction

The genus *Orbiniella* is the fifth most diverse genus in Orbiniidae with 22 valid species (Blake 2021). Most species (i.e., 13 of 22) occur in deep-water habitats exceeding 1000 m, with some of them inhabiting hypoxic biotopes, such as hydrothermal vents (e.g., *Orbiniella hobsonae* Blake & Hilbig, 1990) or the Clarion-Clipperton Fracture Zone in the abyssal Pacific Ocean (e.g., *Orbiniella abyssalis* Blake, 2020). Other *Orbiniella* are known from shallow waters, occurring in the soft bottoms from the intertidal to the continental shelf.

The genus is characterised by small size (up to 12 mm long in the largest species, *Orbiniella andeepia* Narayanaswamy & Blake, 2005), having a rounded prostomium, two achaetous segments followed by chaetigers without branchiae and, sometimes, also without parapodial lobes. The chaetae are represented by the crenulated capillary chaetae and also by the simple acicular spines. After the first described species of the genus, *Orbiniella minuta* Day, 1954, the number of species was increasing slowly with 11 species known until recently. The drastic increase in *Orbiniella* species number happened in the last seven years with 12 more species described (Blake 2017, 2020, 2021; Georgieva et al. 2023), with most coming from deep-sea habitats.

The only *Orbiniella* species reported from the NE Atlantic until now was *Orbiniella petersenae* Parapar, Moreira & Helgason, 2015. The species was described based on formalin-fixed material from Icelandic waters. Most of the specimens (including the holotype) were collected on the continental slope (1490 m to 1915 m depth) northeast of Iceland, in cold Arctic deep waters (-0.7 °C to -0.8 °C), whilst the other specimens were found on the shelf and upper slope (133 m to 1007 m depth) southwest of Iceland, in the warmer north-eastern Atlantic waters (4.8 °C to 7.4 °C). Despite limited geographical distribution, the reported depth and temperature ranges of *O. petersenae* are rather wide suggesting a possibility of a species complex. Numerous cases of cryptic speciation in the North Atlantic annelids were reported in the last decades based on the analyses of the combination of morphological and molecular data (e.g., Nygren and Pleijel 2011; Bogantes et al. 2018; Nygren et al. 2018; Grosse et al. 2020). The availability of the large material of *O. petersenae* recently collected during several Norwegian and German sampling programs allowed investigating genetic and morphological diversity of *Orbiniella* from various localities in the Nordic Seas (i.e., the Norwegian, Greenland, and the Iceland seas) and the adjacent waters of the North Atlantic.

The aim of the present study was to analyse morphological variation, genetic divergence, and phylogenetic relationships among several populations of *Orbiniella* inhabiting different depths and water masses in the NE Atlantic and the Nordic seas. As a result, five species were found in the studied material with the species name *O. petersenae* restricted to a particular molecular clade inhabiting bathyal depths north of Iceland and near Jan Mayen. Three of the other genetic lineages are herein described as new species.

## Material and methods

### Sampling

Specimens were collected between 1986 and 2016 during several expeditions and monitoring programs in the Nordic Seas and the NE Atlantic Ocean organised by the Department of Biological Sciences and the Centre for Deep Sea Research (University of Bergen, Norway), MAREANO (Marine Area database for Norwegian waters, Norway), and the IceAGE (Icelandic marine Animals: Genetics and Ecology, Germany) expedition organised by the “Deutsches Zentrum für Marine Biodiversitätsforschung” (DZMB), Hamburg. Some of the specimens were preserved directly in 96% ethanol for molecular analysis, whilst others were first fixed in 4% formalin and later stored in 70% ethanol (Suppl. material 1: table S1).

We analysed 964 specimens from 62 collecting sites, in the depth range 65–3892 m. The specimens are deposited in the Invertebrate collection of the

Department of Natural History, University Museum of Bergen, University of Bergen, Norway (**ZMBN**) and in the Senckenberg Museum of Frankfurt, Germany (**SMF**). In addition to the collected material, we also studied the holotype and 197 paratypes of *O. petersenae* sensu lato from the collections of the Icelandic Institute of Natural History, Reykjavik, Iceland (**IINH**) (see Parapar et al. 2015 and Suppl. material 1: table S1). Species distribution maps were generated in QGIS 3.28.1.

## Morphological characterisation

Specimens were studied under a stereomicroscope and a compound microscope using temporary slides of whole specimens mounted in 96% or 70% ethanol. For a better visualisation of the morphological characters, Scanning Electron Microscopy (SEM) and methylene blue stain diluted in distilled water were applied to the individuals. For SEM, specimens were dehydrated in a graded ethanol series, critical-point dried, sputter coated with gold/palladium alloy and photographed with a ZEISS Supra 55VP scanning electron microscope at the Electron Microscopy Laboratory (ELMILAB), University of Bergen. SEM photos were edited and combined to plates using Adobe Photoshop 2021 22.3.1. Aqueous solution of methylene blue was used to add contrast to external structures, such as parapodia or pygidium and to highlight segmental borders.

Nine morphological characters used in the previous studies on *Orbiniella* (Parapar et al. 2015; Blake 2020) were assessed in the studied specimens: (1) the shape of prostomium; (2) the relative length of peristomial segments; (3) the segmental annulation pattern along the body; (4) the shape of parapodia throughout the whole body; (5) the shape and length of notopodia; (6) the number and length of capillaries along the body; (7) the number and shape of the acicular spines; (8) the number of pre-pygidial segments, and (9) the length and shape of anal lobes.

The segments in *Orbiniella* species show secondary annulation with wide and narrow annuli interchanging each other in a particular pattern. Each segment can consist of one to four annuli, i.e. being uniannulate, biannulate, triannulate, or quadriannulate. Although the annulation pattern can be clearly seen on SEM images and in methylene blue stained specimens, the borders between the segments are often difficult to identify. However, the wide annuli are always associated with parapodia, and the narrow annuli are always located between the parapodia. Parapar et al. (2015) and Blake (2017, 2020, 2021) considered segmental annulation being an informative character in species identification. In the present study, we describe the annulation patters as the number of narrow rings between the parapodia.

## DNA Extraction, PCR amplification, and sequencing

We used two mitochondrial (COI and 16S rRNA) and one nuclear (ITS2 with a flanking region of 28S) marker. DNA was extracted using QuickExtract™ DNA Extraction Solution (Epicentre). A small piece of tissue, usually three or four segments, was placed into 70 µl QuickExtract™ solution, and incubated at 65 °C for 45 min followed by 2 min at 95 °C in a dry block thermostat. The sets of primers and amplification protocols used for each marker are summarised in

Suppl. material 1: table S2. The total volume of each PCR reaction was 25 µl containing: 17.35 µl of nuclease-free water, 2.5 µl of Buffer (10X), 2 µl of nucleotide mix (2.5 mM each dNTP), 1 µl of each primer (10 µM), 0.15 µl of TaKaRa Taq DNA polymerase (Clontech, concentration of 5 U/µl,), 1 µl of template DNA. Amplified PCR products were analysed by electrophoresis on a 1% agarose gel stained with GelRed Nucleic Acid Stain and then sent to Macrogen Inc. facilities (Amsterdam, the Netherlands) for purification and bidirectional sequencing. Consensus sequences were generated and edited in Geneious Prime 2020.1.2 (Biomatters Ltd., Auckland, New Zealand) (Kearse et al. 2012).

### Phylogenetic analyses and genetic distances

Molecular data were obtained for 54 specimens of *Orbiniella*. COI and 16S sequences of *Orbiniella plumisetosa* Buzhinskaya, 1993 (Bleidorn 2005; Bleidorn et al. 2009) as well as four 16S sequences of *Orbiniella* sp. 49 PB and *Orbiniella* sp. 279 PB (Bonifácio et al. 2020) were obtained from GenBank. Sequences of *Naineris quadricuspida* (Fabricius, 1780) and *Phylo norvegicus* (M. Sars in G. O. Sars, 1872) (Bleidorn et al. 2009) from GenBank were used as outgroups in COI, 16S and in the combined analysis (Suppl. material 1: table S1). ITS2 sequences were analysed without outgroups since the ITS2 sequences of other orbiniids available in GenBank were too dissimilar to align with our data. The dataset of each marker was aligned individually using MAFFT online service 7.475 (Katoh et al. 2019) under the L-INS-i strategy. Alignments were concatenated with Geneious Prime. Best-fit models for each partition were selected using the Akaike Information Criterion with small sample correction (AICc) (Sugiura 1978) in Partition Finder 2.1.1 (Lanfear et al. 2017). We applied the Symmetrical model with an estimated proportion of invariant sites and gamma distributed across sites (GTR+I+G) for the 16S, ITS2 and the first and second codon positions of COI, and the Hasegawa-Kishino-Yano model gamma distributed across sites (HKY+G) for the third codon position of COI. Phylogenetic analyses were done for individual markers and for the concatenated matrix composed of three markers in CIPRES Science Gateway 3.3 (Miller et al. 2012). Maximum Likelihood (ML) analyses were conducted in IQ-TREE 2.0.5 (Nguyen et al. 2015) with 1000 ultrafast bootstrap replicates. Bayesian Inference (BI) analyses were done in MrBayes 3.2.7 (Ronquist et al. 2012) with two independent runs (each performed for eight Markov Chain Monte Carlo simulations) for 40 million generations for the individual data sets and for 100 million for the combined data set, sampled every 1000 generations and 25% of the initial trees discarded as burn-in. We considered convergence of runs (Average Standard Deviation of Split Frequencies (ASDSF) < 0.03) and effective sample size of parameters (ESS > 200) calculated in Tracer 1.7.1 (Rambaut et al. 2018) to evaluate the runs and accept results of the analyses. The resulting ML and BI trees were visualised in Figtree 1.4.4 (http://tree.bio.ed.ac.uk/software/figtree/). The concatenated BI tree was edited in CorelDRAW X7, whilst the rest of the trees were edited with Inskape 1.1 (https://inkscape.org/). For the three genes individually, uncorrected p-distances with gaps treated as pairwise deletion were calculated in MEGAX 10.2.4 (Kumar et al. 2018).

### Species delimitation

To delineate putative species in our data sets, the Poisson Tree Processes model (PTP) (Zhang et al. 2013) and the Assemble Species by Automatic Partitioning (ASAP) (Puillandre et al. 2021) were used for individual markers. PTP was inferred through its webserver (https://species.h-its.org), using the obtained BI rooted trees for COI, 16S and unrooted tree for ITS2, 100000 generations and default settings. Outgroups were removed from the COI and 16S trees. The convergence of MCMC runs was checked in the maximum likelihood plot generated by the software. The ASAP was applied through its webserver (https://bioinfo.mnhn.fr/abi/public/asap/asapweb.html) using alignment files and a p-distance model.

## Results

### Phylogenetic analyses and genetic distances

The COI alignment was 662 bp long and comprised 38 sequences, 419 variables sites, and 404 parsimony-informative sites. The 16S alignment was 525 bp long and contained 51 sequences, 392 variables sites and 358 parsimony-informative sites, and the ITS2 alignment was 906 bp long and included 29 sequences, 478 variable sites, and 464 parsimony-informative sites. The final combined dataset consisted of 2093 bp and 61 sequences.

Both ML and BI trees for the combined dataset showed similar topologies, with specimens from the NE Atlantic and the Nordic seas grouping into four well-supported clades: Deep 1, Deep 2, Deep 3, and Shallow (BS between 95 and 100% and PP of 1) (Fig. 1, Suppl. material 2: fig. S1). The clade Deep 4 was represented by a single specimen. *Orbiniella* sp. 49 PB was sister to the clade combining all the NE Atlantic/Nordic specimens except Deep 1 (BS = 94%; PP = 1). *Orbiniella* sp. 279 PB was sister to the clade combining *Orbiniella* sp. 49 PB, Shallow, Deep 2, Deep 3, and Deep 4 (BS = 60%; PP = 0.82). The only difference between the ML and BI trees for the combined matrix was the position of the Deep 3 clade. In BI analysis, Deep 3 formed a poorly supported clade with Shallow (PP = 0.4; Fig. 1). In ML analysis, Deep 3 was sister to the poorly supported group including the clades Shallow, Deep 2, and Deep 4 (BS = 56%; Suppl. material 2: fig. S1). The topology of both ML and BI trees of the individual markers was the same for the three genes (Suppl. material 2: figs S2–S4), except for the BI of 16S in which Deep 3 was sister to the clade comprising Shallow and Deep 2 (PP = 0.5; Suppl. material 2: fig. S5). *Orbiniella plumisetosa* never fell within the ingroup (i.e., NE Atlantic and Nordic species, *Orbiniella* sp. 49 PB and *Orbiniella* sp. 279 PB), being sister with low support (BS < 75%; PP < 0.7) to *Phylo norvegicus* in all phylogenetic analyses except in the concatenated BI, in which was highly supported (PP = 0.99; Fig. 1).

The uncorrected p-distances within and between the NE Atlantic/Nordic clades and other *Orbiniella* sequences are summarised in Suppl. material 1: table S3. Apart from *O. plumisetosa*, *Orbiniella* sp. 49 PB, and *Orbiniella* sp. 279 PB, the within-clade average p-distances varied from 0 to 0.56%, and the between clade average p-distances varied from 17.86 to 29.68% in COI; 6.59–22.24% in 16S, and 2.05–30.6% in ITS2.

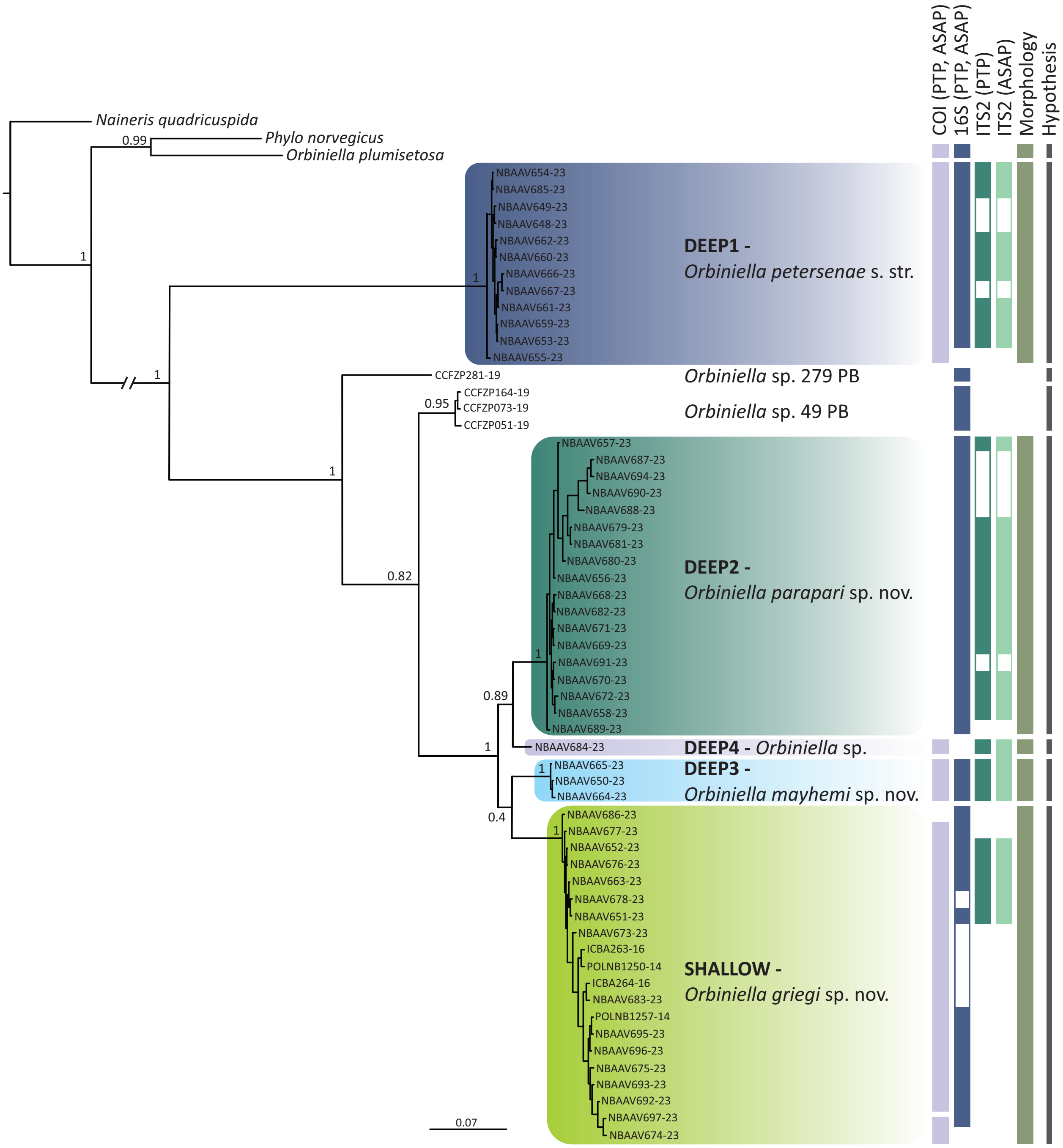

**Figure 1.** Bayesian inference (BI) based on the concatenated dataset of COI, 16S and ITS2. Bayesian posterior probabilities are shown on the nodes. Capital letters correspond with the clades discussed in the text. Species delimitation results inferred by DNA-based methods and morphology are indicated right to the BI tree along with the final species delimitation hypothesis. White bars indicate missing data.

## Species delimitation

Results of PTP based on COI returned six putative species with a support > 0.99 corresponding to four of the five NE Atlantic/Nordic clades, *Orbiniella plumisetosa*, and the specimens NBAAV674-23 and NBAAV697-23 delimited as a separate species (Suppl. material 2: File S1. A). The sequences of the Deep 2 clade, *Orbiniella* sp. 279 PB, and *Orbiniella* sp. 49 PB were absent in the COI dataset. The PTP for 16S resulted in seven putative species with a support

> 0.97 belonging to four of the five NE Atlantic/Nordic clades, *Orbiniella* sp. 279 PB, *Orbiniella* sp. 49 PB, and *O. plumisetosa* (Suppl. material 2: File S1. B). The sequences of the Deep 4 clade were absent in the 16S dataset. The PTP for ITS2 returned five putative species with a support > 0.99 corresponding to the five NE Atlantic/Nordic clades (Suppl. material 2: File S1. C).

The best ASAP partition (i.e., showing the lowest score) based on COI returned six groups corresponding to four of the five NE Atlantic/Nordic clades except Deep 2 since it was missing in the COI dataset (File S2. A). *Orbiniella plumisetosa*, and the specimens NBAAV674-23 and NBAAV697-23 were delimited as two separate species. The best ASAP partition for 16S included seven groups belonging to four of the five NE Atlantic/Nordic clades except Deep 4 since it was missing in the 16S dataset, *Orbiniella* sp. 279 PB, *Orbiniella* sp. 49 PB, and *O. plumisetosa* (File S2. B). The best ASAP partition for ITS2 gave four groups corresponding to the three of the NE Atlantic/Nordic clades, and Deep 3 together with Deep 4 merging in the same group (Suppl. material 2: File S2. C).

Combining the results of the phylogenetic analyses, genetic distances, and species delimitation, we consider five distinct species of *Orbiniella* present in the NE Atlantic/Nordic region (i.e., corresponding to the clades Deep 1, Deep 2, Deep 3, Deep 4, and Shallow).

## Morphological data

For the morphological analysis, all DNA vouchers belonging to a single genetic lineage were analysed in search of unambiguous characters for species delimitation. Once each species was morphologically defined, we also checked for intraspecific variation within the species using additional material.

From the nine selected characters, three were consistent and taxonomically informative among the species: the number of narrow annuli between parapodia and their pattern in the anterior body region, the number and shape of the acicular spines, and the length and shape of the anal lobes. The shape of the prostomium, peristomium and notopodia showed a great intraspecific variation within Deep 1 and Deep 2 clades. For Deep 3 and Shallow clades these characters were not variable among the specimens analysed. For the specimens from Deep 2 clade collected from the Loki’s Castle hydrothermal vent site, these characters showed less variation than from the other localities. The number of capillaries in each parapodial ramus, the length of capillary chaetae, and the position of acicular spines varied in the specimens from all genetic lineages (see species descriptions below). The number of capillary and acicular spines was variable throughout the body even within a single specimen. The length of capillaries varied from being equal to body width to longer than body width. Acicular spines were disposed as an anterior row in the upper side of the capillary bundle, as a posterior row in the lower side of the bundle or mixed with capillaries. If only a single spine was present per ramus, they were placed in vis-à-vis position in the parapodium (i.e., one spine in the notopodium directed towards the other spine in the neuropodium).

When using light microscopy, the segmental annulation was not always clear; however, they become more visible after applying methylene blue staining. Five different patterns in the number of narrow annuli between parapodia were recorded, one per species. The different segmental annulation patterns are illustrated in Fig. 2 and are explained as follows: **Deep 1**, one narrow annulus between parapodium 1 and 2, two narrow annuli between parapodia from parapodium 2 until 5–6, and three narrow annuli between parapodia from parapodium 5–6 until pygidium; **Deep 2**, one narrow annulus between parapodia from parapodium 1 until 5–6, two narrow annuli between parapodia from parapodium 5–6 until 10–14, and three narrow annuli between parapodia from parapodium 10–14 until pygidium; **Deep 3**, one narrow annulus between parapodia from parapodium 1 until 5–6 and two narrow annuli between parapodia from parapodium 5–6 until end of available fragment of the most complete specimen; **Deep 4**, two narrow annuli between parapodia from parapodium 1 until posterior body and three narrow annuli between parapodia in posterior-most body. **Shallow**, one narrow annulus between parapodia from parapodium 1 until 6, two narrow annuli between parapodia from parapodium 6 until 8, and three narrow annuli between parapodia from parapodium 8 until pygidium.

## Systematic account

The integrative analysis of the NE Atlantic/Nordic *Orbiniella* material resulted in assigning the species name *Orbiniella petersenae* to Deep 1 clade and in the description of Deep 2 clade as *Orbiniella parapari* Meca & Budaeva, sp. nov., Deep 3 clade as *Orbiniella mayhemi* Meca & Budaeva, sp. nov. and Shallow clade as *Orbiniella griegi* Meca & Budaeva, sp. nov. Deep 4 clade was represented by three incomplete specimens with genetic data available for only a single specimen. A similar morphotype to Deep 4 clade was found in formalin preserved

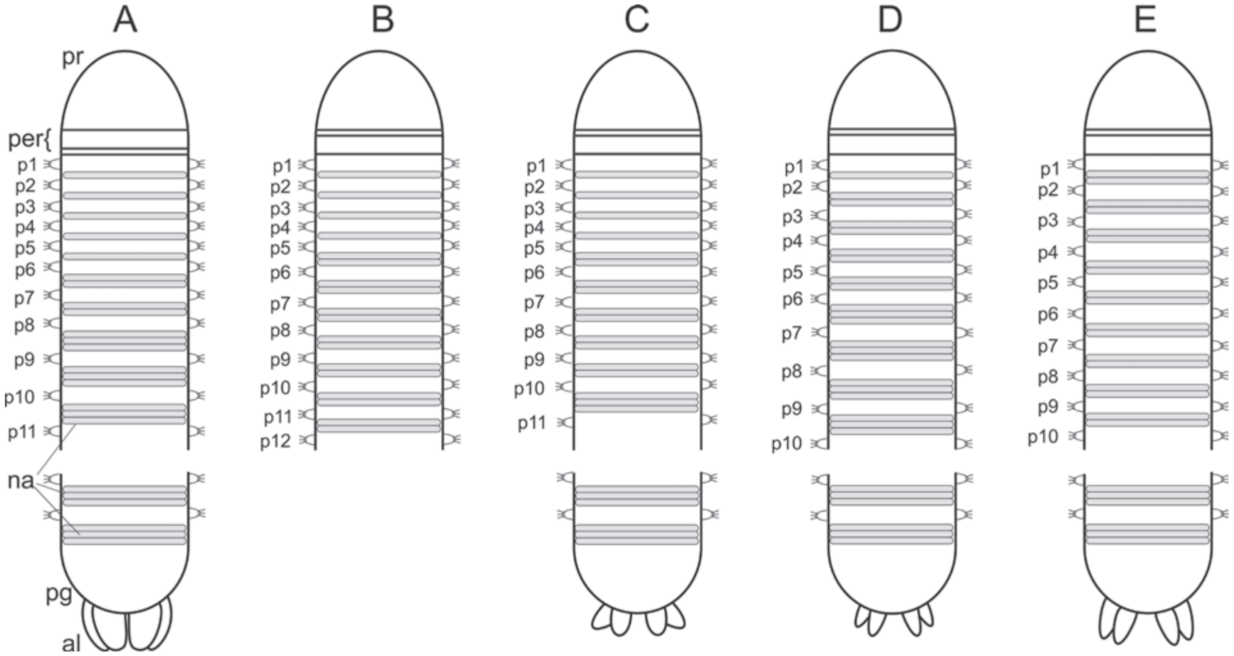

**Figure 2.** Schematic illustrations of the segmental annulation pattern and the shape of pygidial lobes in the studied *Orbiniella* species. Exact borders between the body segments are hard to define, the number of narrow annuli between parapodia that are used in species diagnoses are shown in grey colour **A** *Orbiniella griegi* Meca & Budaeva, sp. nov. (Shallow) **B** *Orbiniella mayhemi* Meca & Budaeva, sp. nov. (Deep 3) **C** *Orbiniella parapari* Meca & Budaeva, sp. nov. (Deep 2) **D** *Orbiniella petersenae* sensu stricto (Deep 1) **E** *Orbiniella* sp. (Deep 4). Abbreviations: al: anal lobes; na: narrow annuli; per: peristomium; pg: pygidium; pr: prostomium; p1–p12: parapodia number in the anterior body region.

specimens from the Norwegian and the Iceland Seas. We provide a detailed description of the morphology of the Deep 4 clade including morphologically similar formalin-fixed specimens, but do not name the species in the present study due to shortage of material.

## Orbiniidae Hartman, 1942

### *Orbiniella* Day, 1954

*Falklandiella* Hartman, 1967: 109. *Fide* Parapar et al. 2015: 333.
*Orbiniella* – Parapar et al. 2015: 333; Blake 2017: 109; Blake 2020: 38; Blake 2021: 99.

**Type species.** *Orbiniella minuta* Day, 1954, by monotypy.

**Diagnosis** (emended from Blake 2021). Body usually elongated, not divided into thorax and abdomen. In some species segmental size can change gradually between anterior and posterior body. Prostomium broad or elongate with rounded anterior margin. One pair of nuchal organs usually present, sometimes pigmented. Eyes present or absent. Peristomium usually bearing two segments. Secondary annulation present with segments being uniannulate, biannulate, triannulate, or quadriannulate. Parapodia biramous with only simple postchaetal lobes, or these entirely absent. Capillary noto- and neurochaetae always crenulated or weakly crenulated with pointed tips; prominent acicular spines present in neuropodia and, usually, also in notopodia; furcate chaetae absent. Branchiae absent. Pygidium with two or four anal lobes, with or without cirri.

**Remarks.** Blake reviewed *Orbiniella* in his monographs from 2017, 2020 and 2021, updating its generic diagnosis and the checklist of species. He reported segmental annulation pattern as a key character to separate *Orbiniella* species (Blake 2020), but this character was not included in the generic diagnosis. Similarly, Blake (2020) also reported and illustrated the anal lobes and cirri in the species descriptions without including them in the diagnosis. We consider these two characters, in combination with other characters discussed below, of high diagnostic value to separate *Orbiniella* from other orbiniid genera and here we include them in the generic diagnosis of *Orbiniella*.

The main diagnostic characters to identify *Orbiniella* species are absence of branchiae along with presence of acicular spines through the whole body, secondary annulation, and pygidium with or without anal cirri. *Microrbinia linea* Hartman, 1965, and some species of *Questa* also do not have branchiae; however, the former can be separated from *Orbiniella* by the presence of unusual long and serrated spines and the latter by the presence of bi- or tridentate crotchets. The other orbiniid having acicular spines through the whole body is *Methanoaricia dendrobranchiata* Blake, 2000. However, this species has very specialised morphology (i.e., elongate and narrow prostomium, long branched branchiae, long and cirriform parapodial lobes and pygidium with many anal cirri) and is easily distinguished. Secondary annulation has been reported also in some species of *Questa* and in *Microrbinia linea* Hartman, 1965, but they can be separated from *Orbiniella* by their unique chaetae mentioned before. Most orbiniids bear two or four (rarely many) anal cirri in the pygidium, and only some *Orbiniella* and *Questa* show no anal cirri, being a unique feature of both genera.

### ***Orbiniella griegi*** **Meca & Budaeva, sp. nov.**

https://zoobank.org/83E65E19-56DE-4A30-999F-0252BE24E7F7
Figs 3–5

*Orbiniella petersenae*: Parapar et al. 2015: 333–343, figs 3–9 (in part).

**Clade.** Shallow.

**Type material examined.** ***Holotype*** ZMBN 157444 (DNA voucher Orbi43). ***Paratypes*** ZMBN 157397 (1 paratype, DNA voucher Orbi32); ZMBN 157398 (1 paratype, DNA voucher Orbi33); ZMBN 157399 (1 paratype, DNA voucher Orbi30); ZMBN 157400 (1 paratype, DNA voucher Orbi31); ZMBN 157401 (3 paratypes); ZMBN 157402 (22 paratypes); ZMBN 157403 (1 paratype, DNA voucher Orbi28); ZMBN 157404 (1 paratype, DNA voucher Orbi27); ZMBN 157434 (1 paratype); ZMBN 157435 (1 paratype); ZMBN 157436 (1 paratype on SEM stub); ZMBN 157437 (1 paratype); ZMBN 157438 (1 paratype); ZMBN 157439 (1 paratype); ZMBN 157440 (1 paratype on SEM stub); ZMBN 157441 (1 paratype); ZMBN 157442 (5 paratypes); ZMBN 157443 (1 paratype); ZMBN 157445 (1 paratype, DNA voucher LC-57); ZMBN 157446 (1 paratype); ZMBN 157646 (1 paratype); SMF 32601 (1 paratype, DNA voucher Orbi4); SMF 32637 (1 paratype); SMF 32639 (1 paratype, DNA voucher Orbi17); SMF 32665 (1 paratype, DNA voucher Orbi5).

**Other material examined.** ZMBN 95697 (1 spm); ZMBN 95728 (E-voucher POLNB1250-14); ZMBN 95735 (E-voucher POLNB1257-14); ZMBN 157668 (E-voucher ICBA263-16); ZMBN 157669 (E-voucher ICBA264-16); ZMBN 157670 (E-voucher NBAAV696-23); ZMBN 157671 (E-voucher NBAAV686-23); ZMBN 157672 (E-voucher NBAAV697-23); ZMBN 157673 (E-voucher NBAAV692-23); ZMBN 157674 (E-voucher NBAAV693-23); 18 specimens from the *O. petersenae* sensu lato type series: IINH 34892 (2 spms); IINH 34894 (16 spms).

**Diagnosis.** An *Orbiniella* with segmental annulation pattern as follows: one narrow annulus between parapodium 1 and 6, two narrow annuli between parapodia from parapodium 6 until 8, and three narrow annuli between parapodia from parapodium 8 until pygidium. Acicular spines short and stout, up to two in both noto- and neuropodia. Pygidium with four long anal lobes assembled together.

**Type locality.** Basvika, Bergen area, Norwegian West coast, 60.3959, 5.1492, 172 m (Fig. 3).

**Description** (based on type specimens). Holotype complete with 32 chaetigers, 4.9 mm long and 0.4 mm wide at level of chaetiger 7. Body elongated and narrow, uniformly wide, slightly narrowing in pre-pygidial area. Pigmentation lacking in all analysed specimens.

Prostomium broad with rounded anterior margin, without eyespots (Fig. 4A). SEM micrographs showed two lateral, inconspicuous ciliary spots on both sides of prostomium, presumably nuchal organs (Fig. 4B). Peristomium with two prominent achaetous segments, second shorter than first, distinctly separated from each other and from first chaetiger by narrow annulus (Fig. 4A). From chaetiger 7–10 onwards segments becoming longer, more square-shaped. Segmental annulation in following pattern: one narrow annulus between parapodium 1 and 6, two narrow annuli between parapodia from parapodium 6 until 8, and three narrow annuli between parapodia from parapodium 8 until pygidium (Fig. 5A–C). Segmental annulation less defined in pre-pygidial region.

**Figure 3.** Distribution of *Orbiniella griegi* Meca & Budaeva, sp. nov. Black lines – Greenland-Scotland Ridge (GSR), star – type locality, coloured triangles – stations with examined morphology and molecular data, white triangles – stations with examined morphology.

Parapodia biramous, triangular-like, of similar size throughout body. Postchaetal neuropodial lobe absent. Digitate postchaetal notopodial lobes short and thick, from chaetiger 1 (Fig. 4C). Crenulated capillary chaetae and spines present in both rami from CH1. Capillaries equal in length to body width and numerous (6–8 per bundle) in anterior segments; shorter and reduced in number in posterior segments. Capillary chaetae with crenulation occurring on one side along whole chaeta or along half of its length (Fig. 4E). Spines short, stout, smooth, one or two per ramus (Fig. 4D). Last eight or nine chaetigers short and few achaetous (Fig. 5C). Pygidium with four long anal lobes assembled together (Fig. 5D).

**Variation.** The holotype and most of the paratypes shared the same morphology. However, some paratypes collected from the Norwegian shelf presented more numerous (7–10 per bundle) and longer (longer than body width) capillaries in anterior segments compared to specimens from the type locality

**Remarks.** *Orbiniella griegi* sp. nov. is morphologically nearly identical to the other three species described in this work: *O. mayhemi* sp. nov., *O. parapari* sp.

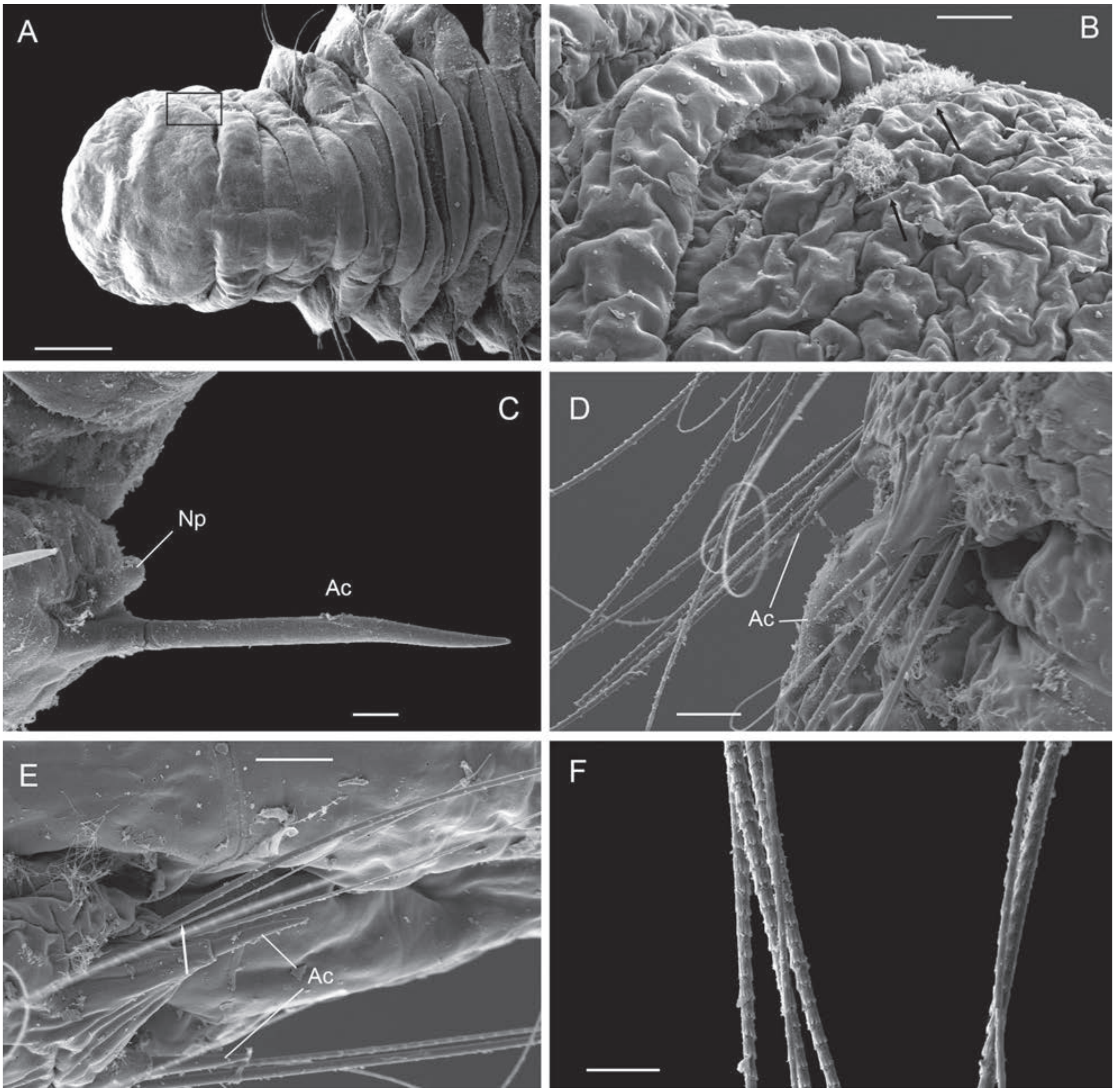

**Figure 4.** *Orbiniella griegi* Meca & Budaeva, sp. nov., SEM **A** paratype ZMBN 157440, anterior end, dorsal view **B** paratype ZMBN 157440, detail of right lateral side of prostomium showing presumable nuchal organ (insert of **A**) **C** paratype ZMBN 157440, notopodium of chaetiger 20 showing notopodial lobe and acicular spine **D** paratype ZMBN 157436, parapodium of chaetiger 7 showing acicular spines disposed in vis-à-vis position and capillaries **E** paratype ZMBN 157436, neuropodium of chaetiger 9 showing acicular spines and capillaries **F** paratype ZMBN 157440, capillary chaetae. Black arrows in **B**: Lateral ciliary spots; White arrow in **E**: Start of crenulation in capillary chaeta. Abbreviations: Ac: acicular spines; Np: notopodial lobe. Scale bars: 100 µm (**A**); 20 µm (**B, D, E**); 10 µm (**C, F**).

nov. and *O. petersenae* sensu stricto, which led to combining them into a single species by Parapar et al. (2015). However, the four species display differences in the segmental annulation pattern in the anterior body (i.e., an anterior-most region with one narrow annulus between parapodia followed by a short region with two narrow annuli between parapodia in *O. griegi* sp. nov., an anterior-most region with one narrow annulus between parapodia followed by a region bearing two narrow annuli between parapodia that extends to mid-posterior body in

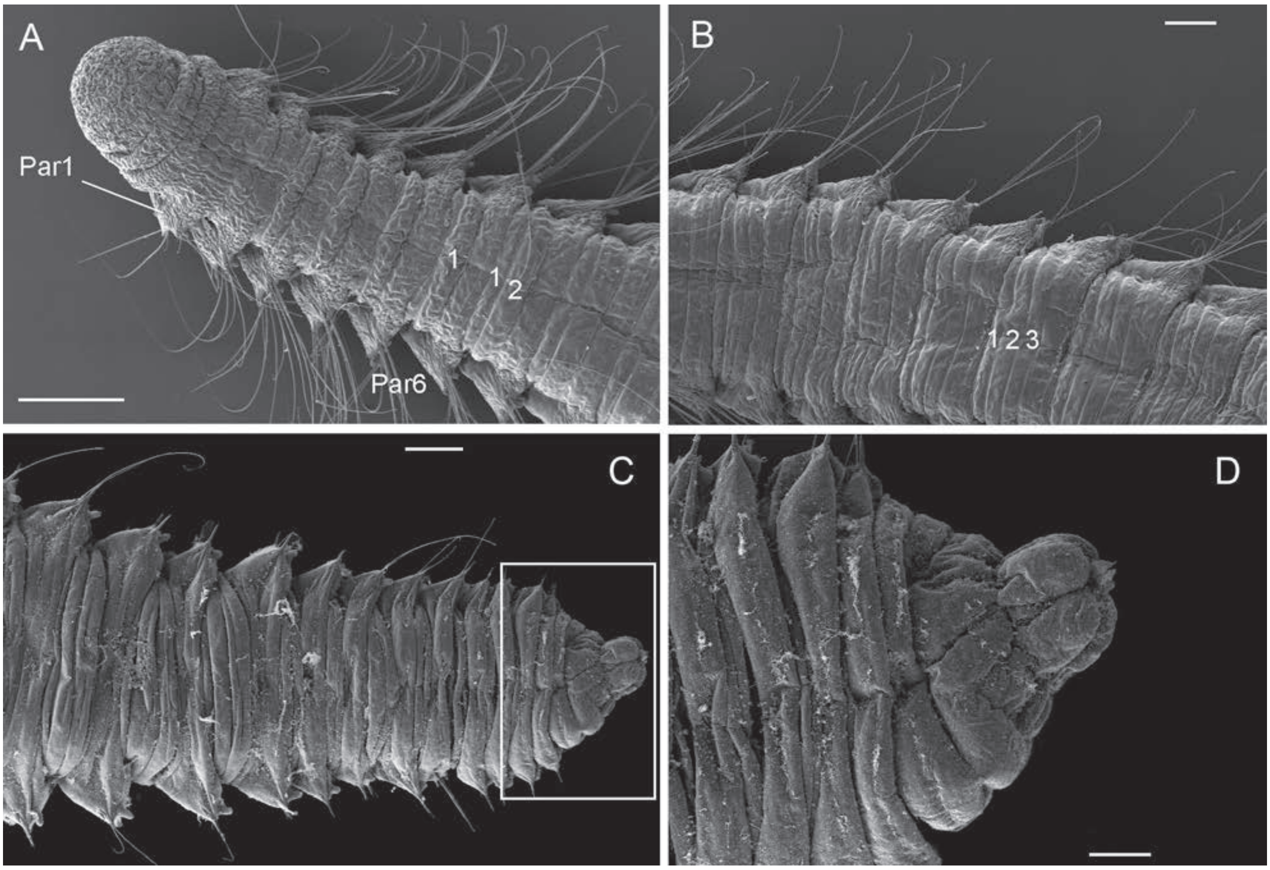

**Figure 5.** *Orbiniella griegi* Meca & Budaeva, sp. nov., SEM **A** paratype ZMBN 157436, anterior end, dorsal view showing narrow annuli between parapodia 1 and 8 **B** paratype ZMBN 157436, mid body, dorsal view showing narrow annuli between parapodia 9 and 16 **C** paratype ZMBN 157440, posterior end, dorsal view **D** paratype ZMBN 157440, detail of pygidium (insert of **C**). Numbers show the segmental annulation pattern. Abbreviations: Par1: first parapodium; Par6: sixth parapodium. Scale bars: 200 µm (**A**); 100 µm (**B–D**).

*O. mayhemi* sp. nov., an anterior-most region with one narrow annulus between parapodia followed by a region bearing two narrow annuli between parapodia that extends to mid-anterior body in *O. parapari* sp. nov., and an anterior-most region bearing one and two narrow annuli between parapodia followed by a region with three narrow annuli between parapodia in *O. petersenae* sensu stricto) (Fig. 2). *Orbiniella griegi* sp. nov. also differs from the other species by having one or two short and stout acicular spines while *O. mayhemi* sp. nov. has 1–3 short spines, *O. parapari* sp. nov. has 1–6 long and thin spines, and *O. petersenae* sensu stricto bears 1–5 short spines. It can further be distinguished by having long anal lobes assembled together while *O. parapari* sp. nov. and *O. petersenae* sensu stricto bear short lobes on their pygidia (Fig. 2). The shape of the lobes is unknown in *O. mayhemi* sp. nov. (see also Table 1 with comparison of the Nordic *Orbiniella* species). *Orbiniella griegi* sp. nov. also showed no intraspecific variation in the shape of prostomium, peristomium and notopodia. *Orbiniella griegi* sp. nov. resembles *O. mayhemi* sp. nov. in having a broad prostomium, but differs in the second peristomial segment being shorter than the first instead of the first segment being shorter than the second. Furthermore, both *O. griegi* sp. nov. and *O. mayhemi* sp. nov. bear digitate notopodial lobes, but showing slightly narrowing basal part in the latter.

**Table 1.** Discriminatory characters of the NE Atlantic *Orbiniella*. Abbreviations: Af, Available fragment; CH, Chaetiger; NA, Narrow annuli between parapodia; Par, Parapodium; Pg, Pygidium.

| Character | *Orbiniella griegi* sp. nov. | *Orbiniella mayhemi* sp. nov. | *Orbiniella parapari* sp. nov. | *Orbiniella petersenae sensu stricto* Parapar, Moreira & Helgason, 2015 |
|---|---|---|---|---|
| Prostomium | Broad | Broad | Broad or elongate | Broad or elongate |
| Nuchal organs | In patches | Not observed | One single congregation | One single congregation |
| Peristomial rings | First wider than second | first narrower than second | Both with same length or first narrower than second | Both with same length or first narrower than second |
| Segmental annulation pattern | One NA from Par 1 until 6, two NA from Par 6 until 8, and three NA from Par 8 until Pg | One NA from Par 1 until 5-6 and two NA from Par 5-6 until end of Af of the most complete specimen | One NA from Par 1 until 5-6, two NA from Par 5-6 until 10-14, and three NA from Par 10-14 until Pg | One NA between Par 1 and 2, two NA from Par 2 until 5-6, and three NA from Par 5-6 until Pg |
| Shape parapodia | Triangular | Rounded in the first chaetigers and triangular from CH7–CH10 | Triangular or rounded in the first chaetigers and triangular from CH7–CH10 | Triangular or rounded in the first chaetigers and triangular from CH7–CH10 |
| Shape notopodia | Digitate (short) | Digitate (short) with slightly narrowing basal part | Digitate (short or long) | Digitate (short or long) |
| Capillaries | 6-10 per bundle | 6-10 per bundle | 7-10 per bundle | 7-10 per bundle |
| Spines | 1-2 per ramus (short) | 1-3 per ramus (short) | 1-6 per ramus (long) | 1-5 per ramus (short) |
| Pygidium | Four long lobes assembled together | Not observed | Four short and thick lobes | Four short lobes |
| Distribution | Norwegian shelf, Faroe-Iceland Ridge and SW Iceland | SW and SE Iceland | Iceland Sea and Norwegian Sea | Iceland Sea, Norwegian Sea and southern Greenland Sea |
| Depth | 171-781 m | 913-2505 m | 1811-2832 m | 1053-2407 m |

*Orbiniella griegi* sp. nov., together with *O. marionensis* Gillet, 1999, are unique among the known shallow water *Orbiniella* species in having notopodial postchaetal lobes and in having acicular spines in both noto- and neuropodia, as in the seven deep-sea species: *O. andeepia* Narayanaswamy & Blake, 2005, from Antarctica, *O. longilobata* Blake, 2020, from South China Sea, *O. rugosa* Blake, 2020, from South China Sea, *O. tumida* Blake, 2020, from the California continental slope, *O. abyssalis* Blake, 2020, from the abyssal Pacific Ocean, *O. armata* Blake, 2021, from off South Carolina, and *O. mimica* Blake, 2021, from NW Atlantic. *Orbiniella griegi* sp. nov. differs from these species in having three narrow annuli between parapodia and a pygidium with four anal lobes assembled together and from *O. abyssalis*, additionally, in having two peristomial segments instead of a single peristomial segment.

**Distribution.** Norwegian coastal areas and shelf, Faroe-Island Ridge, and SW Iceland, 171–781 m (Fig. 3).

**Etymology.** This species is named in honour of Edvard Grieg, the Norwegian musician born and raised in Bergen, the city where the present study was conducted.

### *Orbiniella mayhemi* Meca & Budaeva, sp. nov.

https://zoobank.org/E68E6555-FA57-436A-BA90-C6EF1A4C2C32
Figs 6, 7

**Clade.** Deep 3.

**Type material examined.** ***Holotype*** SMF 32627 (DNA voucher Orbi19). ***Paratypes*** SMF 32588 (1 paratype); SMF 32628 (1 paratype on SEM stub); SMF 32630 (1 paratype); SMF 32640 (1 paratype on SEM stub, DNA voucher Orbi18); ZMBN 157433 (1 paratype, DNA voucher Orbi3).

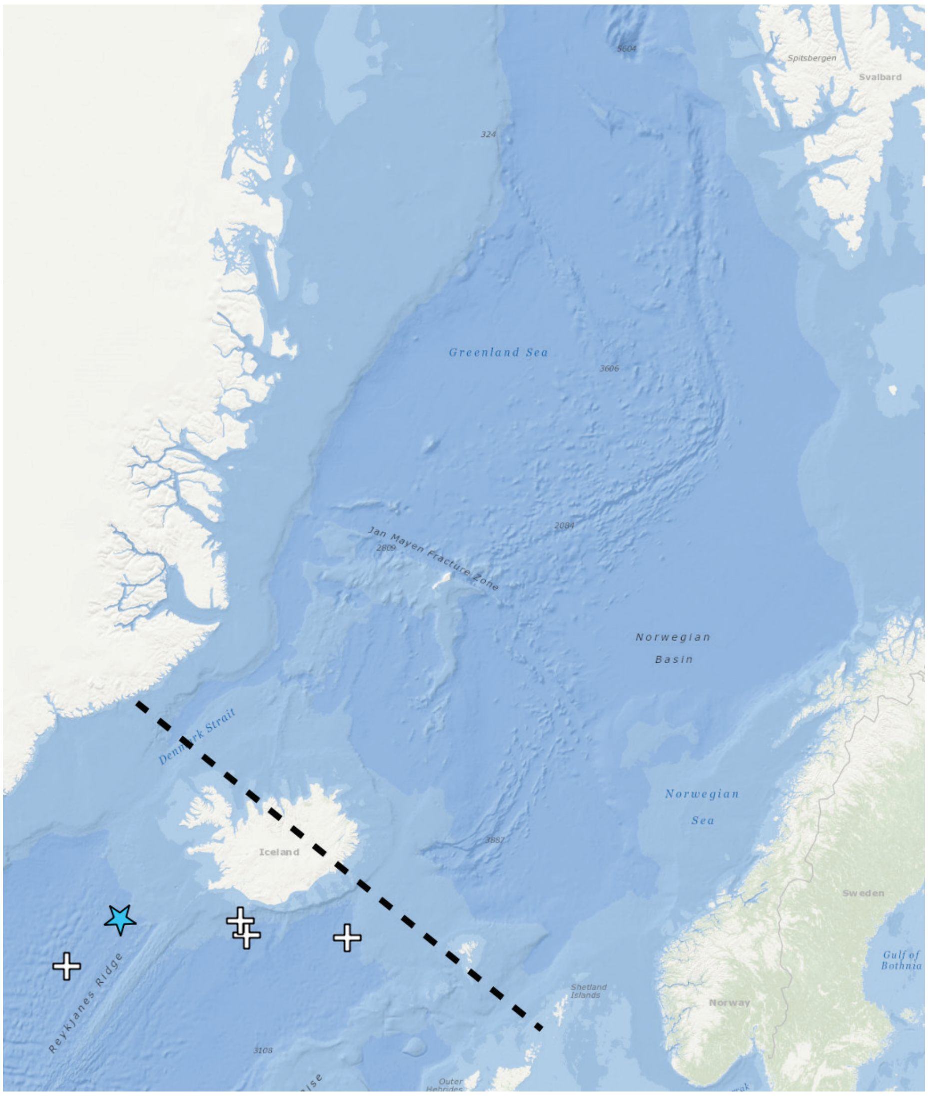

**Figure 6.** Distribution of *Orbiniella mayhemi* Meca & Budaeva, sp. nov. Black lines – Greenland-Scotland Ridge (GSR), star – type locality and the station with examined morphology and molecular data, white plusses – stations with examined morphology.

**Other material examined.** ZMBN 157432 (3 spms).

**Diagnosis.** An *Orbiniella* with segmental annulation pattern as follows: one narrow annulus between parapodia from parapodium 1 until 5 or 6 and two narrow annuli between parapodia from parapodium 5 or 6 until end of available fragment of the most complete specimen. Acicular spines short and stout, up to three in both noto- and neuropodia. Pygidium not observed.

**Type locality.** Irminger Basin, SW Iceland, NE Atlantic, 62.9888, -28.0950, 1588 m (Fig. 6).

**Description** (based on type specimens). Holotype incomplete with 14 chaetigers, 3.0 mm long and 0.36 mm wide at level of chaetiger 6. Body elongated and narrow, uniformly wide. Pigmentation lacking in all analysed specimens.

Prostomium broad with rounded anterior margin, without eyespots or nuchal organs (Fig. 7A). Peristomium with two prominent achaetous segments, first segment shorter than second segment, distinctly separated from each other and first chaetiger by a narrow annulus (Fig. 7A). Anterior chaetigers short,

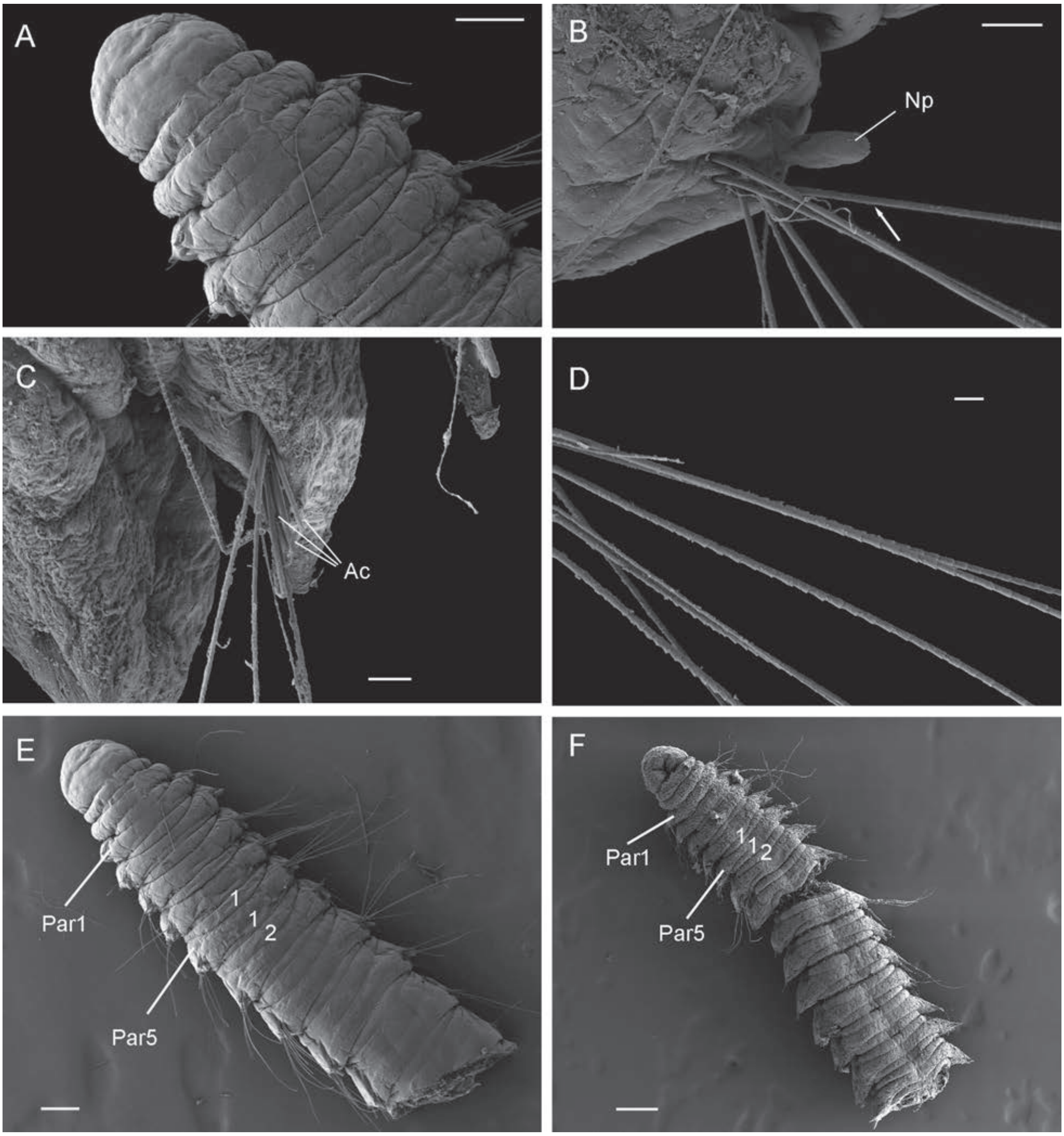

**Figure 7.** *Orbiniella mayhemi* Meca & Budaeva, sp. nov. SEM **A** paratype SMF 32640, anterior end, dorsal view **B** paratype SMF 32640, notopodium of chaetiger 7 showing notopodial lobe and capillaries **C** paratype SMF 32628, neuropodium of chaetiger 5 showing acicular spines and capillaries **D** paratype SMF 32640, capillary chaetae **E** paratype SMF 32640, anterior fragment showing narrow annuli between parapodia 1 and 10, dorsal view **F** paratype SMF 32628, anterior fragment showing narrow annuli between parapodia 1 and 14, ventral view. White arrow in **B**: Start of crenulation in capillary chaeta. Abbreviations: Ac: acicular spines; Np: notopodial lobe; Par1: first parapodium; Par5: fifth parapodium. Scale bars: 100 µm (**A, E**); 20 µm (**B, C**); 10 µm (**D**); 200 µm (**F**).

becoming longer and more square-shaped from chaetiger 7–10 onwards. Segmental annulation pattern: one narrow annulus between parapodia from parapodium 1 until 5 or 6 and two narrow annuli between parapodia from parapodium 5 or 6 until end of available fragment of most complete specimen (Fig. 7E, F). Posterior part and pygidium not observed.

Parapodia biramous, wider than long, with postchaetal notopodial lobes short, digitate with slightly narrowing basal part, from chaetiger 1 (Fig. 7B). Postchaetal neuropodial lobes absent. Crenulated capillary chaetae and acicular spines present in both rami from chaetiger 1. Capillaries equal in length to body width and numerous (6–8 per bundle) in anterior segments; shorter and reduced in number in posterior segments. Capillary chaetae with crenulation occurring on one side along whole chaeta or along half of its length (Fig. 7D). Acicular spines short, stout, and smooth, up to three per ramus (Fig. 7C).

**Variation.** The holotype and most of the paratypes shared the same morphology. However, some paratypes presented more numerous (7–10 per bundle) and longer (longer than body width) capillaries in anterior segments.

**Remarks.** *Orbiniella mayhemi* sp. nov. differs from the other three species described in this work (i.e., *O. griegi* sp. nov., *O. parapari* sp. nov., and *O. petersenae* sensu stricto) in having a body region bearing two narrow annuli between parapodia more extensive than in the other three species. *Orbiniella mayhemi* sp. nov. also bears short, stout, and smooth spines as *O. griegi* sp. nov. and *O. petersenae* sensu stricto, but differing in number (i.e., 1–3 per ramus in *O. mayhemi* sp. nov.; 1 or 2 in *O. griegi* sp. nov., and 1–5 in *O. petersenae* sensu stricto).

Similarly to *O. griegi* sp. nov., *Orbiniella mayhemi* sp. nov. resembles the seven deep-sea congeners *O. andeepia*, *O. longilobata*, *O. rugosa*, *O. tumida*, *O. abyssalis*, *O. armata*, and *O. mimica* in having notopodial postchaetal lobe and in having acicular spines in both noto- and neuropodia. However, *O. mayhemi* sp. nov. differs from *O. abyssalis* in having two peristomial segments instead of a single peristomial segment. Among these seven deep-sea species, *O. mimica* is the closest geographically with *O. mayhemi* sp. nov. (NW vs NE Atlantic, respectively), being similar in having one or two narrow annuli between parapodia and up to three acicular spines. *Orbiniella mimica* differs, however, in presenting a papillated dorsal surface on the prostomium and numerous glands in the parapodia and chaetal segments instead of a smooth surface and a uniform digitate notopodial postchaetal lobe instead of a lobe narrowing basally.

**Distribution.** From SW to SE Iceland, 913–2505 m (Fig. 6).

**Etymology.** The species is named in honour to the Norwegian Black Metal band from Oslo, Mayhem, one of the bands that most contributed to the development of the Norwegian Black Metal in the 90-s. MAM was listening to their music to endure the darkest hours in the lab.

### ***Orbiniella parapari* Meca & Budaeva, sp. nov.**

https://zoobank.org/CD7DFB4F-57FD-46C4-A575-1135877C7B91
Figs 8–10

*Orbiniella petersenae*: Parapar et al. (2015): 333–343, figs 3–9 (in part).

**Clade.** Deep 2.

**Type material examined.** ***Holotype*** ZMBN 157405 (DNA voucher Orbi40). ***Paratypes*** ZMBN 157406 (8 paratypes); ZMBN 157407 (1 paratype on SEM stub); ZMBN 157408 (9 paratypes); ZMBN 157409 (2 paratypes on SEM stub); ZMBN 157410 (1 paratype on SEM stub); ZMBN 157411 (1 paratype, DNA voucher Orbi37); ZMBN 157412 (1 paratype on SEM stub, DNA voucher Orbi38); ZMBN 157413 (1 paratype on SEM stub, DNA voucher Orbi38); ZMBN 157414 (3 paratypes); ZMBN 157415 (4 paratypes); ZMBN 157416 (1 paratype); ZMBN 157417 (1 paratype); ZMBN 157418 (2 paratypes); ZMBN 157424 (3 paratypes); ZMBN 157425 (8 paratypes); ZMBN 157426 (2 paratypes); ZMBN 157429 (2 paratypes on SEM stub); SMF 32659 (3 paratypes); SMF 32662 (5 paratypes); SMF 32644 (1 paratype); SMF 32653 (4 paratypes); SMF 32655 (5 paratypes); SMF 32664 (1 paratype, DNA voucher Orbi26); SMF 32666 (4 paratypes); SMF 32667 (1 paratype, DNA voucher Orbi10); SMF 32668 (1 paratype on SEM stub, DNA voucher Orbi11); SMF 32669 (1 paratype on SEM stub, DNA voucher Orbi12); SMF 32680 (1 paratype).

**Other material examined.** ZMBN 157427 (4 spms); ZMBN 157428 (45 spms); ZMBN 157430 (30 spms); ZMBN 157431 (4 spms); ZMBN 157675 (E-voucher NBAAV687-23); ZMBN 157676 (E-voucher NBAAV689-23); ZMBN 157677 (E-voucher NBAAV691-23); ZMBN 157678 (E-voucher NBAAV690-23); ZMBN 157679 (E-voucher NBAAV694-23); ZMBN 157680 (E-voucher NBAAV688-23); SMF 32652 (8 spms); SMF 32654 (2 spms); SMF 32657 (39 spms); IceAGE sample DZMB-HH 33669 (E-voucher NBAAV668-23); IceAGE sample DZMB-HH 49578 (E-voucher NBAAV671-23); IceAGE sample DZMB-HH 49614 (E-voucher NBAAV669-23); IceAGE sample DZMB-HH 49614 (E-voucher NBAAV670-23); 56 specimens from the *O. petersenae* sensu lato type series: IINH 43199 (40 spms), IINH 43197 (16 spms).

**Diagnosis.** An *Orbiniella* with segmental annulation pattern as follows: one narrow annulus between parapodia from parapodium 1 until 5 or 6, two narrow annuli between parapodia from parapodium 5 or 6 until 10–14, and three narrow annuli between parapodia from parapodium 10–14 until pygidium. Acicular spines long and thin, up to six in both noto- and neuropodia. Pygidium with four short and thick anal lobes.

**Type locality.** Loki's Castle, Arctic Mid-Ocean Ridge, 73.5663, 8.1610, 2450 m (Fig. 8).

**Description** (based on type specimens). Holotype complete with 29 chaetigers, 4.3 mm long and 0.5 mm wide at level of chaetiger 6. Body short and thick, uniformly wide, narrowing in preanal area. Pigmentation lacking. Prostomium broad with rounded anterior margin, without eyespots (Fig. 9A). Peristomium with two prominent achaetous segments, first peristomial segment shorter than second, distinctly separated from each other and first chaetiger by narrow annulus (Fig. 9A). No conspicuous nuchal organs observed. Anterior segments short, becoming longer, more square-shaped from chaetiger 8 onwards. Segmental annulation of following pattern: one narrow annulus between parapodia from parapodium 1 until 5 or 6, two narrow annuli between parapodia from parapodium 5 or 6 until 10–14, and three narrow annuli between parapodia from parapodium 10–14 until pygidium (Fig. 10A, B). Segmental annulation less defined in pre-pygidial region.

Parapodia biramous, wider than long (Fig. 9C), with postchaetal notopodial lobe digitate, short, and thick from chaetiger 1. Postchaetal neuropodial lobe absent. Crenulated capillary chaetae and acicular spines present in both rami from chaetiger 1. Capillaries in anterior segments longer than body width and numerous (7–10 per bundle), in posterior segments shorter and reduced in number. Acicular spines long, thin, and smooth, up to six per ramus (Fig. 9E).

Last five or six posterior segments slightly shorter and last two achaetous (Fig. 10C). Pygidium with four short and thick anal lobes (Fig. 10D).

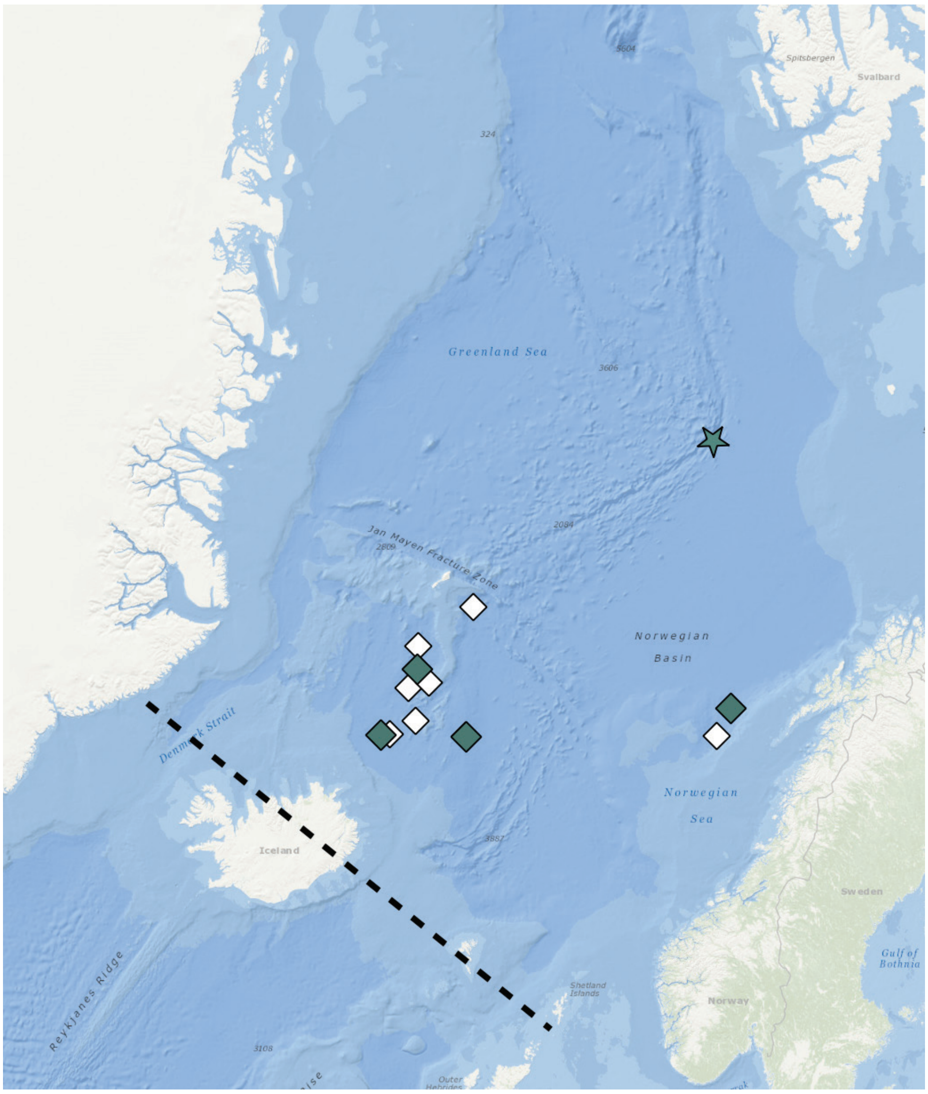

**Figure 8.** Distribution of *Orbiniella parapari* Meca & Budaeva, sp. nov. Black lines – Greenland-Scotland Ridge (GSR), star – type locality, coloured rhombuses – stations with examined morphology and molecular data, white rhombuses – stations with examined morphology.

**Variation.** The holotype and all paratypes collected from the Loki's Castle vent field shared the same morphology. Other paratypes collected from the Iceland Sea and the Norwegian Sea showed variation in the shape of prostomium, peristomium and notopodia.

Some of the specimens collected in the IceAGE project displayed three different patterns of dorsal segmental pigmentation: lateral patches from chaetiger 3 to the rest of the body; transversal bands through all the segment in chaetigers 3, 4, and 5 and in patches in the remaining chaetigers; bands in chaetiger 3, 4, and 5 without pigmentation in the rest of the body. The remaining pigmentation might be due to more recent collection date of the IceAGE specimens comparable to the type material.

The shape of prostomium varied between being broad (Figs 9A, 10A) or elongate, with a rounded anterior margin. Poorly defined brownish eyespots were observed in some of the specimens from the *O. petersenae* sensu lato type series material. Most of the paratypes had the first segment of the peristomium

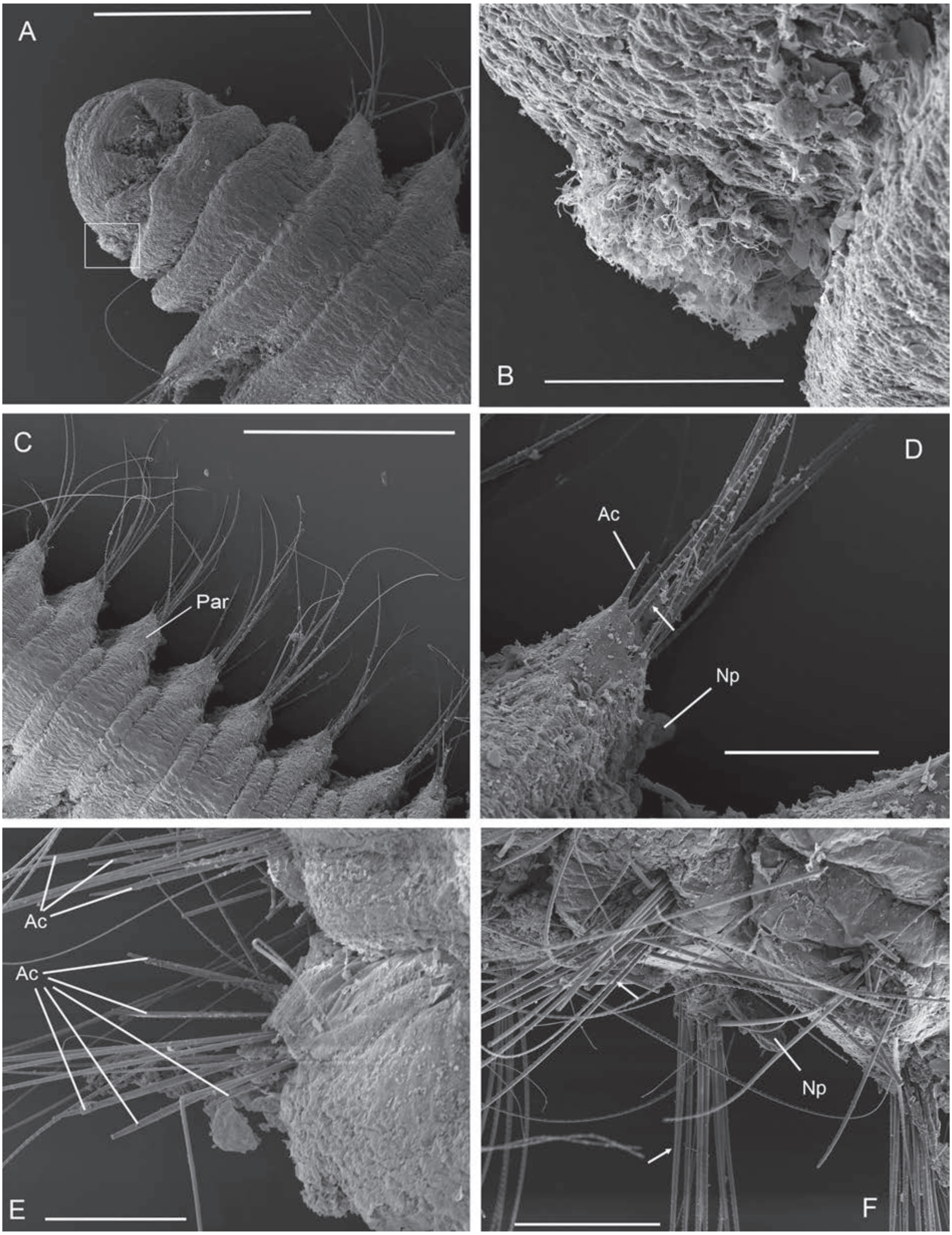

**Figure 9.** *Orbiniella parapari* Meca & Budaeva, sp. nov., SEM **A** paratype ZMBN 157429, anterior end, ventral view **B** paratype ZMBN 157429, detail of right lateral side of prostomium showing presumed nuchal organ (insert of A) **C** paratype ZMBN 157429, first eight anterior parapodia **D** paratype ZMBN 157429, neuropodium of chaetiger 3 showing acicular spines, capillaries, and notopodial lobe from dorsal ramus **E** paratype ZMBN 157410, neuropodium of chaetiger 17 showing acicular spines **F** paratype ZMBN 157412, notopodium of chaetiger 7 showing notopodial lobe and capillaries. White arrows in **D** and **F**: Start of crenulation in capillary chaeta. Abbreviations: Ac: acicular spines; Np: notopodial lobe; Par: parapodia. Scale bars: 200 µm (**A**); 30 µm (**B**); 300 µm (**C**); 50 µm (**D**); 100 µm (**E, F**).

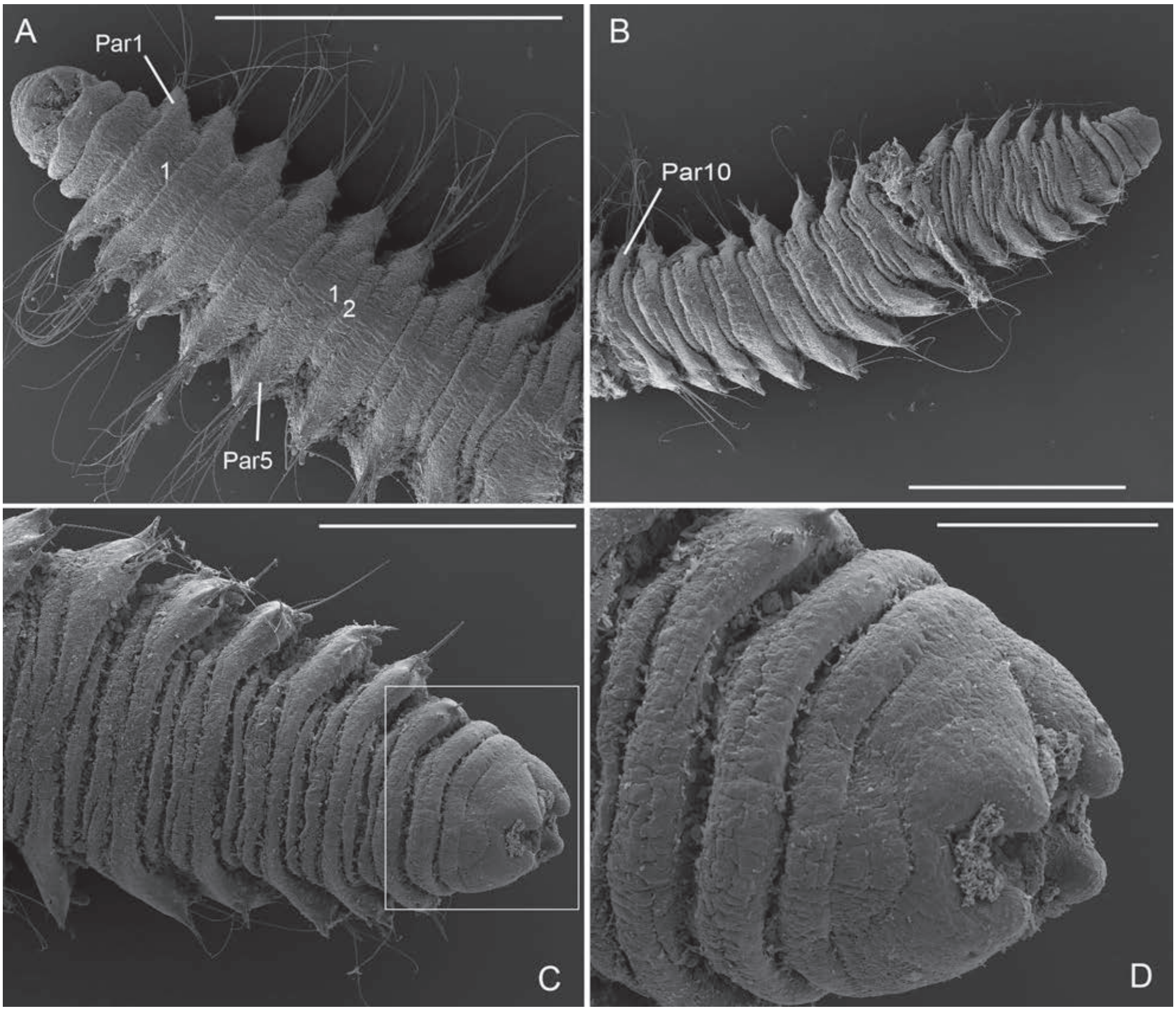

**Figure 10.** *Orbiniella parapari* Meca & Budaeva, sp. nov., SEM of paratypes ZMBN 157429 **A** anterior end showing narrow annuli between parapodia 1 and 9, ventral view **B** mid body and posterior end, ventral view **C** posterior end, ventral view **D** detail of pygidium (insert of C). Numbers show the segmental annulation pattern. Abbreviations: Par1: first parapodium; Par5: fifth parapodium; Par10: tenth parapodium. Scale bars: 500 µm (**A, B**); 300 µm (**C**); 100 µm (**D**).

shorter than the second, as in the holotype, but a few paratypes were with both segments equal in length. Notopodia varied between being digitate, long, and thin or digitate, short, and thick (Fig. 9D, F; Table 1).

SEM micrographs of several paratypes showed one single prominent lateral ciliary congregation at each side of the prostomium, which we interpreted as nuchal organs (Fig. 9B). Capillary chaetae with crenulation occurring on one side along the whole chaeta (Fig. 9D) or along half of its length (Fig. 9F). Crenulation can be clear along the whole chaeta or become more obvious distally. The specimens from the *O. petersenae* sensu lato type series and the holotype showed capillaries longer than body width in anterior segments as Parapar et al. (2015) stated. However, other specimens from the material collected in this study presented shorter capillaries equal to body width.

**Remarks.** Among the Nordic *Orbiniella* species described here, *O. parapari* sp. nov. closely resembles *O. petersenae* sensu stricto, with which it has overlapping geographical ranges (i.e., Iceland Sea and Norwegian Sea). Both species are similar in bearing high number of acicular spines (i.e., 1–5 per ramus in the former and 1–6 in the latter), which, however, appear longer and thinner in *O. parapari* sp. nov. Also, both species share a pygidium with four short, thick anal lobes, although the lobes are slightly shorter and thicker in *O. parapari* sp. nov. Both species also have one, two, and three narrow annuli between parapodia; however, their pattern of progression along the body differs: an anterior-most region with one narrow annulus between parapodia followed by a region bearing two narrow annuli between parapodia that extends to mid-anterior body, and continuing with three narrow annuli between parapodia in *O. parapari* sp. nov.; and an anterior-most region bearing one and two narrow annuli between parapodia followed by an extensive region with three narrow annuli between parapodia in *O. petersenae* sensu stricto. *Orbiniella griegi* sp. nov. also shows one to three narrow annuli between parapodia (with a different pattern, see the description of *O. griegi*), but has fewer (1 or 2) acicular spines and a pygidium with four long anal lobes assembled together.

As in the case of the other Nordic *Orbiniella* species described here, *O. parapari* sp. nov. shares a number of morphological characters with the seven deep-sea congeners: *O. andeepia*, *O. longilobata*, *O. rugosa*, *O. tumida*, *O. abyssalis*, *O. armata*, and *O. mimica* (see details on similarities and dissimilarities of these species with respect to *O. mayhemi* sp. nov.). However, *O. parapari* sp. nov. differs from these seven species in having three intersegmental rings, and with the exception of *O. mimica*, a pygidium bearing four short anal lobes. *Orbiniella mimica* also bears four lobes in the pygidium, but they are much shorter than in *O. parapari* sp. nov. and each of them is accompanied by a long, thin anal cirrus. Moreover, *O. mimica* presents a unique papillated dorsal surface and a smaller number (up to 3) of acicular spines than in *O. parapari* sp. nov. (up to 6 spines).

**Distribution.** Iceland Sea and Norwegian Sea, 1811–2832 m (Fig. 8).

**Etymology.** This species is dedicated to the Spanish polychaetologist Dr. Julio Parapar, who described the first *Orbiniella* species in the North Atlantic waters, *Orbiniella petersenae* Parapar, Moreira & Helgason, 2015.

### ***Orbiniella petersenae*** **Parapar, Moreira & Helgason, 2015, sensu stricto**

Figs 11–13

*Orbiniella petersenae*: Parapar et al. 2015: 333–343, figs 3–9 (in part).

**Clade.** Deep 1.

**Type material examined.** ***Holotype*** IINH 35670. ***Paratypes*** IINH 29822 (27 paratypes), IINH 34897 (1 posterior end of a paratype on SEM stub), IINH 34899 (9 paratypes), IINH 35671 (36 paratypes), IINH 35672 (1 posterior end of a paratype), IINH 35673 (3 paratypes), IINH 35699 (6 paratypes on SEM stub).

**Other material examined.** ZMBN 157647 (35 spms); ZMBN 157648 (1 spms); ZMBN 157649 (1 spm on SEM stub); ZMBN 157650 (2 spms on SEM stub); ZMBN 157651 (1 spm); ZMBN 157652 (60 spms); ZMBN 157653 (3 spms); ZMBN 157654 (12 spms); ZMBN 157655 (10 spms); ZMBN 157656 (1 spm); ZMBN 157657 (28 spms); ZMBN 157658 (1 spm); ZMBN 157659 (11 spms); ZMBN 157660 (7 spms); ZMBN 157661 (38 spms); ZMBN 157662 (322 spms); ZMBN 157663 (2 spms on SEM stub); SMF 32584 (2 spms); SMF 32589 (4 spms); SMF 32629 (6 spms);

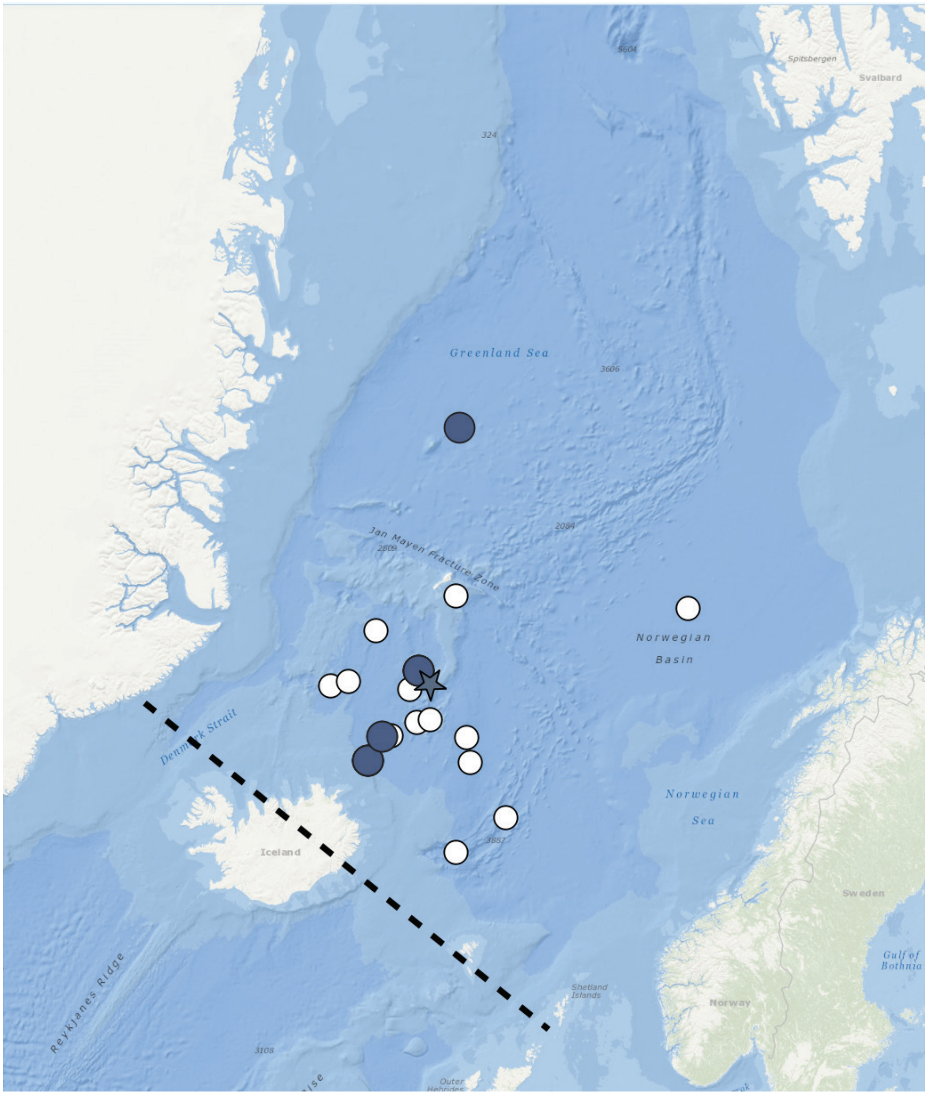

**Figure 11.** Distribution of *Orbiniella petersenae* sensu stricto. Black lines – Greenland-Scotland Ridge (GSR), star – type locality, coloured circles – stations with examined morphology and molecular data, white circles – stations with examined morphology.

SMF 32632 (23 spms); SMF 32633 (4 spms); SMF 32634 (3 spms); SMF 32635 (3 spms); SMF 32636 (52 spms); SMF 32646 (17 spms); SMF 32647 (41 spms); SMF 32648 (2 spms); SMF 32670 (DNA voucher Orbi2 on SEM stub); SMF 32671 (DNA voucher Orbi7); SMF 32672 (DNA voucher Orbi8); SMF 32673 (DNA voucher Orbi9); SMF 32675 (DNA voucher Orbi1); SMF 32676 (DNA voucher Orbi13); SMF 32677 (DNA voucher Orbi14); SMF 32678 (DNA voucher Orbi15 on SEM stub); SMF 32679 (DNA voucher Orbi16 on SEM stub); SMF 32660 (DNA voucher Orbi20); IceAGE sample DZMB-HH 33669 (E-voucher NBAAV667-23).

**Diagnosis.** An *Orbiniella* with segmental annulation pattern as follows: one narrow annulus between parapodium 1 and 2, two narrow annuli between parapodia from parapodium 2 until 5 or 6, and three narrow annuli between parapodia from parapodium 5 or 6 until pygidium. Acicular spines short and stout, up to five in both noto- and neuropodia. Pygidium with four short anal lobes.

**Type locality.** Jan Mayen microcontinent, Iceland Sea, 68.8285, -9.2403, 1849 m (Fig. 11).

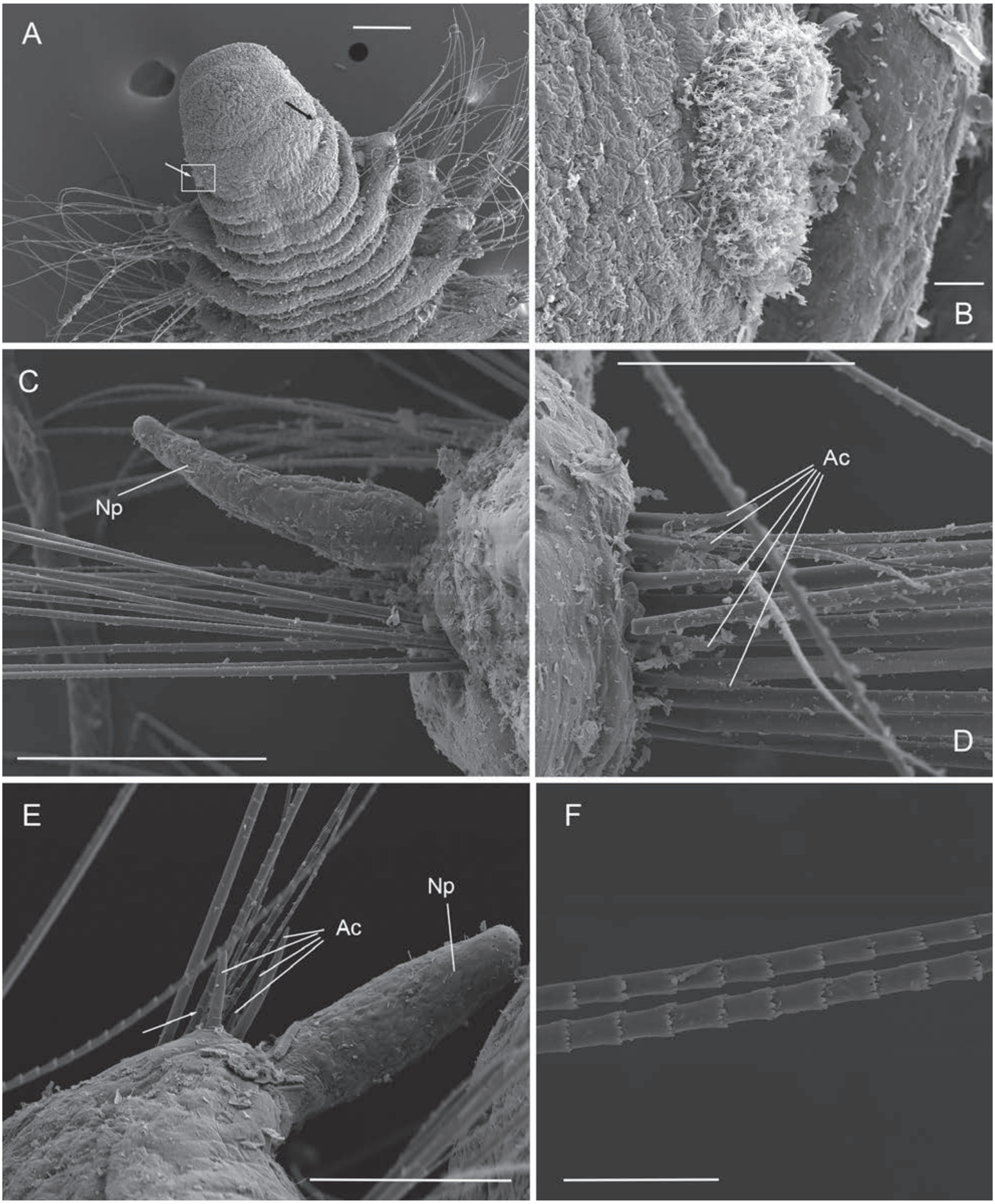

**Figure 12.** *Orbiniella petersenae* sensu stricto, SEM **A** paratype ZMBN 157649, anterior end, dorsal view **B** paratype ZMBN 157649, detail of left lateral side of prostomium showing presumed nuchal organs (insert of A) **C** paratype SMF 32678, notopodium of chaetiger 3 showing notopodial lobe and capillaries **D** paratype SMF 32678, neuropodim of chaetiger 7 showing acicular spines and capillaries **E** paratype ZMBN 157663, notopodium of chaetiger 10 showing notopodial lobe, acicular spines, and capillaries **F** paratype SMF 32678, detail of capillary chaetae. White and black arrows in A: Lateral ciliary spots; White arrow in E: Start of crenulation in capillary chaeta. Abbreviations: Ac: acicular spines; Np: notopodial lobe. Scale bars: 100 µm (**A – C**); 40 µm (**D**); 50 µm (**E**); 10 µm (**F**).

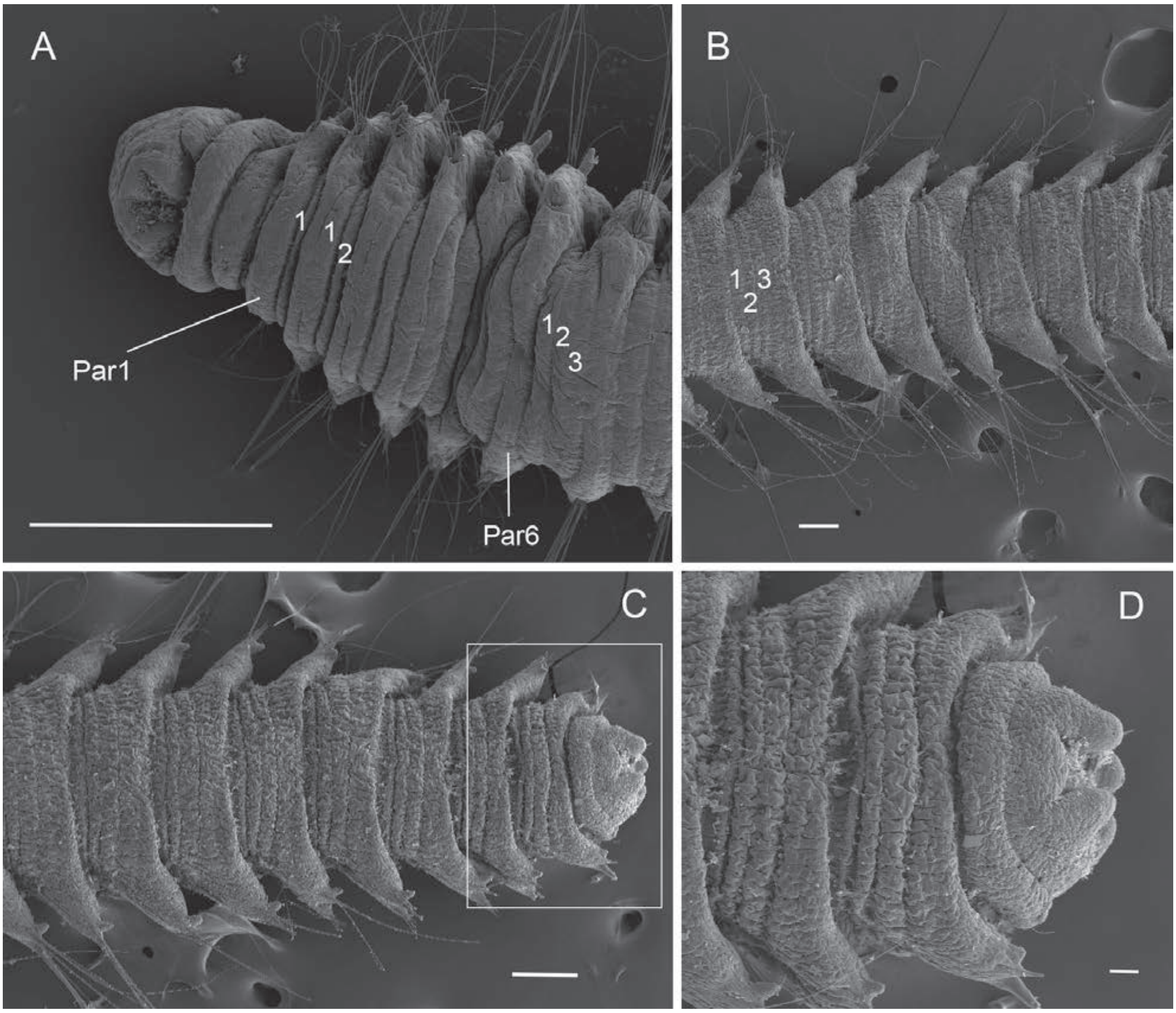

**Figure 13.** *Orbiniella petersenae* sensu stricto, SEM **A** paratype ZMBN 157663, anterior end, ventral view showing narrow annuli between parapodia 1 and 7 **B** paratype ZMBN 157650, midbody, ventral view showing narrow annuli between parapodia 17 and 24 **C** paratype ZMBN 157650, posterior end, ventral view **D** paratype ZMBN 157650, detail of last two chaetigers together with pygidium (insert of C). Numbers indicate narrow annuli between parapodia. Abbreviations: Par1: first parapodium; Par6: sixth parapodium. Scale bars: 500 µm (**A**); 100 µm (**B, C**); 20 µm (**D**).

**Remarks.** The morphology of the holotype fully agrees with the original description. The analysis of the IINH paratypes and the new material in this study under a light microscope and SEM allowed elucidating the degree of variability in some morphological characters not discussed by Parapar et al. (2015).

The prostomium shape varied between elongate (Fig. 12A) and broad (Fig. 13A), both with a rounded anterior margin (Table 1). In some specimens from the *O. petersenae* sensu lato type series material, brownish eyespots with poorly defined borders were observed. Most of the paratypes showed the same type of peristomium as in the holotype (i.e., the first ring shorter than the second one), but a few paratypes were with equal rings. Notopodia varied from digitate, long, and thin (Fig. 12C) to digitate, short and thick (Fig. 12E). Some of the IceAGE specimens presented the same three patterns of dorsal segmental pigmentation observed in *O. parapari*, possibly due to better preservation conditions.

SEM micrographs showed one single prominent lateral ciliary congregation at each side of the prostomium, which we interpret as nuchal organs (Fig. 12B). Capillary chaetae with crenulation occurring on one side along the whole chaeta or along half of its length (Fig. 12D, E). The holotype and the paratypes showed capillaries longer than body width in anterior segments as stated by Parapar et al. (2015). However, some specimens from the material collected in this study presented shorter capillaries equal to body width. Acicular spines were up to five per ramus, instead of up to three reported in Parapar et al. (2015) (Fig. 12D).

As mentioned above, among the NE Atlantic/Nordic *Orbiniella* species, *Orbiniella petersenae* sensu stricto is most similar to *O. parapari* sp. nov., furthermore, these two species have an overlapping distribution. As in the case of *O. parapari* sp. nov., *O. petersenae* sensu stricto shares a number of morphological characters with the seven deep-sea congeners: *O. andeepia*, *O. longilobata*, *O. rugosa*, *O. tumida*, *O. abyssalis*, *O. armata*, and *O. mimica* (see remarks section of *O. parapari* sp. nov. for comparison of the two species). One sample from a station near Jan Mayen (1243 m) contained an outstanding number of *O. petersenae* sensu stricto (i.e., 322 specimens).

**Distribution.** Iceland Sea and southern Greenland Sea, 1053–2407 m. Possibly Norwegian Sea, 2525–3892 m (Fig. 11).

### ***Orbiniella* sp.**

Figs 14–16

*Orbiniella petersenae*: Parapar et al. 2015: 333–343, figs 3–9 (in part).

**Clade.** Deep 4.

**Material examined.** ZMBN 130943 (1 spm); ZMBN 157696 (1 spm on SEM stub); ZMBN 157665 (5 spms); ZMBN 157666 (2 spms on SEM stub); ZMBN 157667 (1 spm on SEM stub, DNA voucher Orbi47). 16 specimens from the *O. petersenae* sensu lato type series: IINH 43198 (5 spms). IINH 43231 (11 spms).

**Description of ethanol preserved specimens.** DNA voucher Orbi47 (ZMBN 157667) incomplete with 15 chaetigers, 1.7 mm long and 0.3 mm wide at level of chaetiger 6. Body short and thick, with uniform width. Two more specimens from the same sample as the DNA voucher (ZMBN 130943 and ZMBN 157696) in poor condition (i.e., anterior fragments of fewer than ten segments and destroyed chaetae). Pigmentation lacking in all analysed specimens.

Prostomium broad with rounded anterior margin, without eyespots (Fig. 14A). SEM micrographs showed no cilia on prostomium. Peristomium with two prominent achaetous segments, first segment shorter than second segment, distinctly separated from each other and first chaetiger by narrow annulus (Fig. 14B). Segmental annulation consisted of two narrow annuli between parapodia from parapodium 1 until end of available fragment (Fig. 14A). Posterior part and pygidium not observed.

Parapodia biramous, triangular-like, of similar size throughout fragment. Posterior notopodial lobes from chaetiger 1, digitate, short, and thick (Fig. 14C). Posterior neuropodial lobes absent. Crenulated capillary chaetae and acicular spines in both rami from chaetiger 1. Capillaries in anterior segments longer

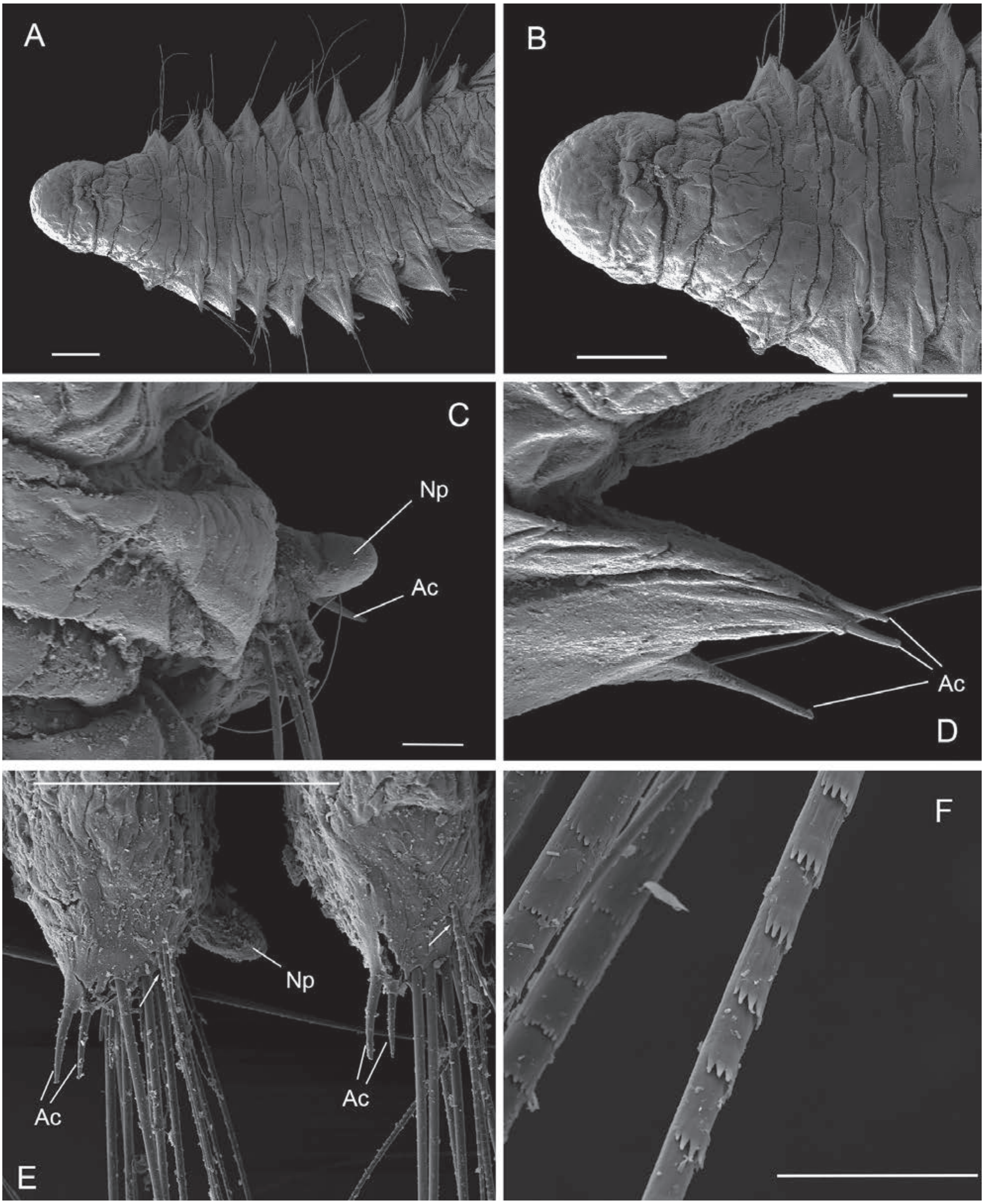

**Figure 14.** *Orbiniella* sp. SEM **A** specimen ZMBN 157696, anterior end, ventral view **B** specimen ZMBN 157696, detail of prostomium and peristomium **C** specimen ZMBN 157667, notopodium of chaetiger 6 showing notopodial lobe, acicular spine, and capillaries **D** specimen ZMBN 157696 Neuropodium of chaetiger 10 showing acicular spines **E** specimen ZMBN 157666, notopodia of chaetigers 5 and 6 showing notopodial lobe, acicular spines, and capillaries **F** specimen ZMBN 157666, detail of capillary chaetae. White arrows in E: Start of crenulation in capillary chaeta. Abbreviations: Ac: acicular spines; Np: notopodial lobe. Scales: 100 μm (**A, B, E**); 20 μm (**C, D**); 10 μm (**F**).

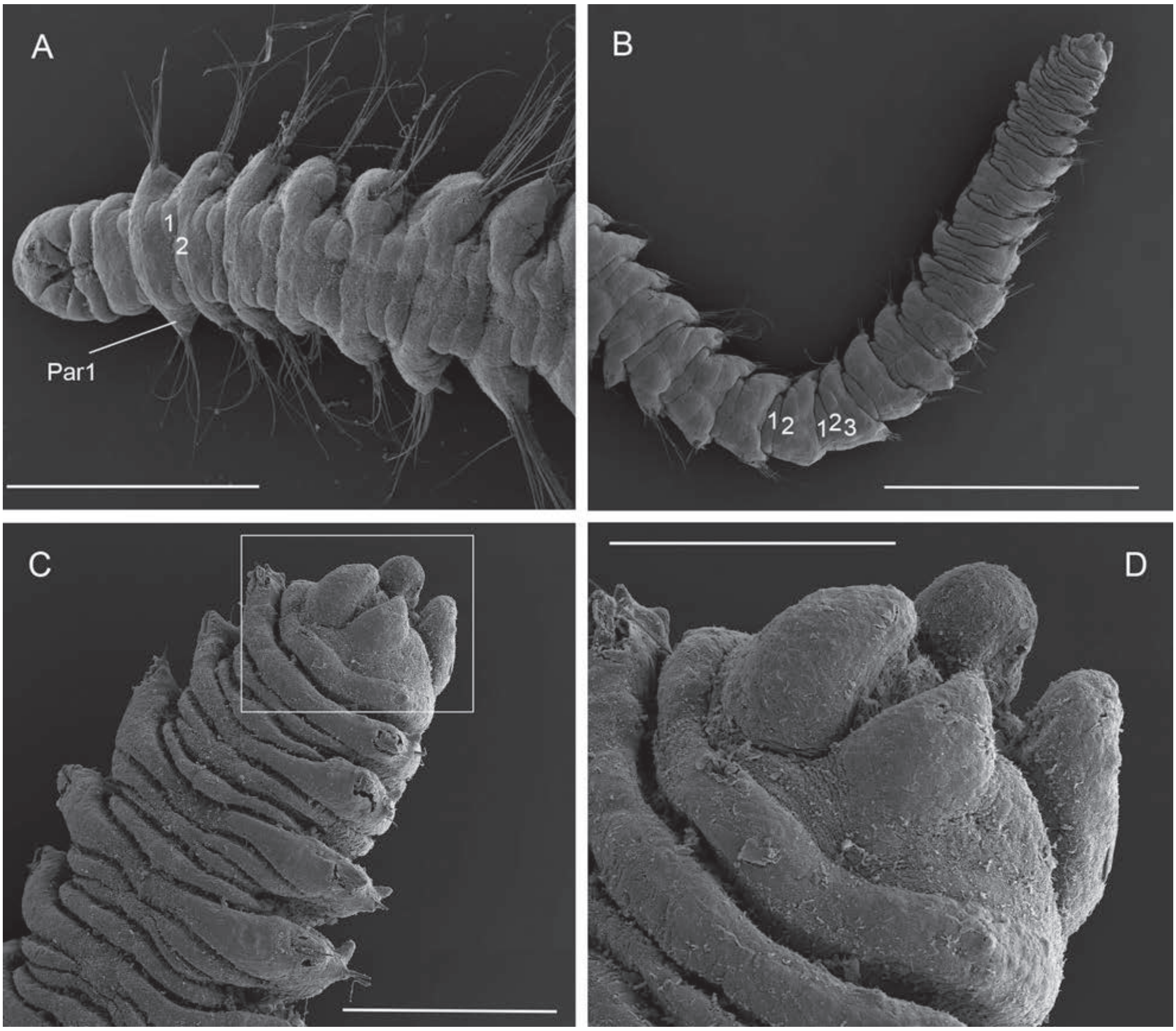

**Figure 15.** *Orbiniella* sp. SEM of ZMBN 157666 **A** anterior end, ventral view showing narrow annuli between parapodia 1 and 8 **B** midbody and posterior end, ventral view showing narrow annuli between parapodia 9 and 29 **C** posterior end, dorsal view **D** Detail of pygidium (insert of C). Numbers indicate narrow annuli between parapodia. Abbreviation: Par1: first parapodium. Scale bars: 500 µm (**A**); 1000 µm (**B**); 200 µm (**C**); 100 µm (**D**).

than body width and numerous (7–10 per bundle), shorter and reduced in number in posterior segments. Acicular spines short, stout, and smooth, up to three per ramus (Fig. 14C, D).

**Description of formalin preserved specimens.** Five well preserved specimens originally fixed in formalin collected in the Norwegian Sea (ZMBN 157665) as well as 16 specimens from *O. petersenae* sensu lato type series from the Iceland Sea shared similar morphology with the DNA voucher from Deep 4 clade (i.e., same segmental annulation pattern and chaetal distribution type). A morphological description of these specimens is provided below, although the affinity of them to Deep 4 clade remains unconfirmed with molecular data.

Shape of prostomium varies between broad and elongate, with rounded anterior margin (Fig. 15A). Eyespots absent. Peristomium with two prominent achaetous segments, first segment shorter than second segment, distinctly separated from each other and first chaetiger by narrow annulus.

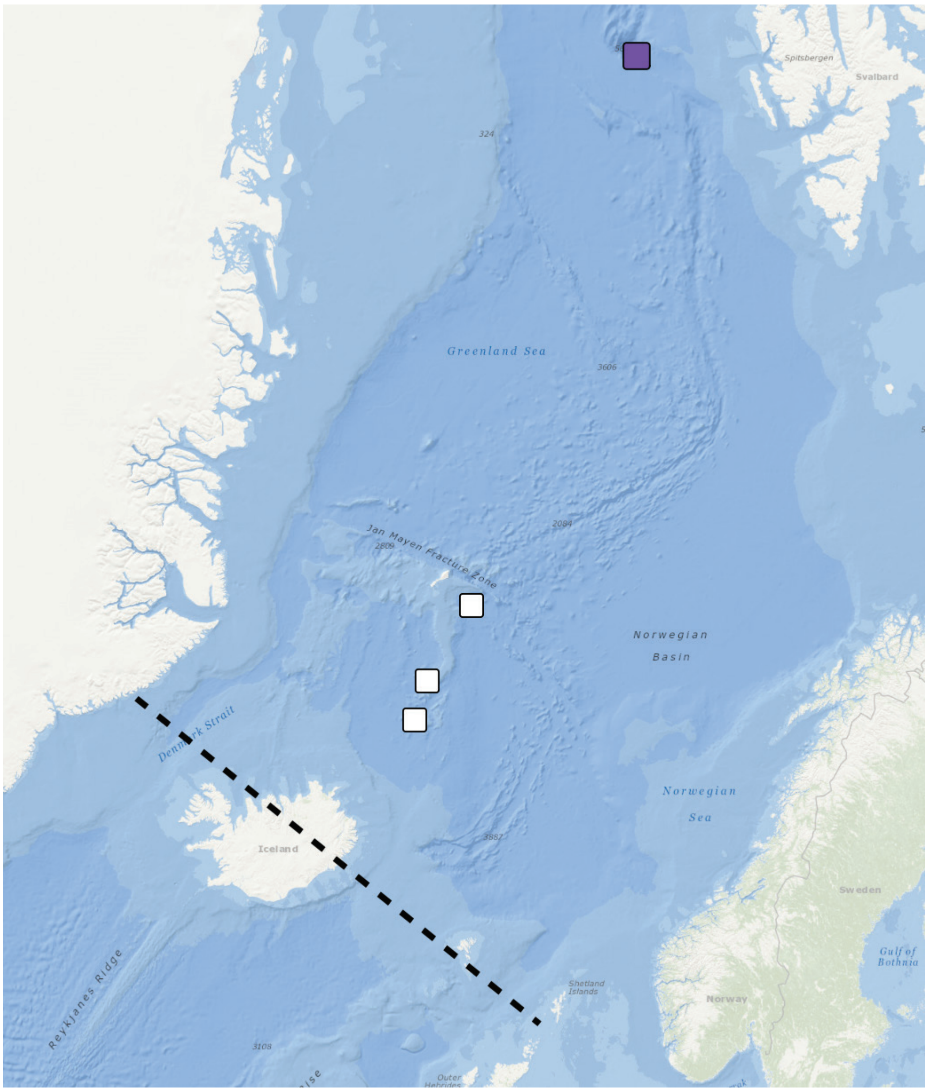

**Figure 16.** Distribution of *Orbiniella* sp. Black lines – Greenland-Scotland Ridge (GSR), coloured square – station with examined morphology and molecular data, white squares – stations with examined morphology.

Segmental annulation pattern as follows: two narrow annuli between parapodia from parapodium 1 until posterior body and three narrow annuli between parapodia in posterior-most body (Fig. 15A, B). Annulation well defined in pre-pygidial region (Fig. 15C). From chaetiger 7–10 onwards segments becoming longer, more square-shaped.

Parapodia biramous, triangular-like, of similar size throughout body. Postchaetal notopodial lobes from chaetiger 1, digitate, short, and thick (Fig. 14C, E). Postchaetal neuropodial lobes absent. Crenulated capillary chaetae and acicular spines in both rami from chaetiger 1. Notopodia and neuropodia bearing each 7–10 long crenulated capillaries, being longer than body width in anterior segments and shorter and less numerous in posterior segments. Capillary chaetae with crenulation occurring on one side along whole chaeta or along half of its length (Fig. 14E). Last five or six posterior segments slightly shorter and last two achaetous (Fig. 15C). Pygidium with four long and wide anal lobes (Fig. 15D).

**Distribution.** Northern Greenland Sea, 3356 m. Possibly Iceland Sea and Norwegian Sea, 1844–2525 m (Fig. 16).

# Discussion

## Systematics and species delimitation

*Orbiniella petersenae*, the only species of *Orbiniella* known up to date from the North Atlantic, was recorded from a great diversity of bottom water temperatures and depths between different localities. Due to this environmental plasticity and a limited number of morphological characters used in *Orbiniella* diagnoses, we assessed if more than one species is present in the area using molecular tools. In the present study, we report four *Orbiniella* species from the Nordic Seas and one more species from the deep waters south of Iceland based on the combination of molecular and morphological data utilised in the phylogenetic and species delimitation analyses. We restrict the species name *Orbiniella petersenae* to one of the genetic lineages limiting its geographical and vertical ranges to the deep-sea areas of the Iceland Sea and the southern Greenland Sea. Three more species, *O. griegi* sp. nov. (shallow habitats along the Greenland-Scotland Ridge and along the Norwegian coast), *O. parapari* sp. nov. (deep Nordic Seas), and *O. mayhemi* sp. nov. (deep NE Atlantic, south of Iceland), are here formally described as new taxa. One more species, reported in the northern deep Greenland Sea and possibly also in the deep Iceland Sea and the Norwegian Sea, is described here but not formally named due to lack of specimens allowing more detailed morphological studies and further molecular information

*Orbiniella petersenae* sensu stricto, *O. parapari* sp. nov., and *O. griegi* sp. nov. show a unique segmental annulation pattern in the genus, combining one, two, and three narrow annuli between parapodia. Moreover, the former two species display the highest number of acicular spines (up to five in *O. petersenae* sensu stricto and up to six in *O. parapari* sp. nov.) in the parapodia within the whole genus. *Orbiniella griegi* sp. nov. has a unique pygidium with four anal lobes assembled together (Fig. 2).

Up to date, the only available genetic data on *Orbiniella* were the four 16S sequences belonging to *Orbiniella sp.* 49 and *Orbiniella sp.* 279 from the NE Pacific in Bonifácio et al. (2020) and the Nad4, COI, 16S and 18S sequences of *O. plumisetosa* in Bleidorn (2005) and Bleidorn et al. (2009). Georgieva et al. (2023) reported two new *Orbiniella* species (i.e., *Orbiniella jamesi* Georgieva, Wiklund, Ramos, Neal, Glasby & Gunton, 2023 and *Orbiniella* sp.) from the New South Wales (Australia) based on COI, 16S and 18S sequences. These species were not included in the present analysis. We do not consider them belonging to *Orbiniella* due to the presence of branchiae, a character not reported in any other *Orbiniella* species (Blake 2017, 2020, 2021). Furthermore, both species were placed within the *Scoloplos*/*Leitoscoloplos* clade in our preliminary analysis of orbiniid phylogeny based on mitochondrial genome and nuclear data (in preparation) and their generic affinity requires further clarification. Our data include sequences of three molecular markers (COI, 16S and ITS2) of five *Orbiniella* species from the NE Atlantic and the Nordic seas considerably expanding the taxon and marker coverage in this poorly studied orbiniid genus.

*Orbiniella* was not recovered as monophyletic in our phylogenetic analyses based on the combined dataset. *Orbiniella plumisetosa* was sister to *Phylo norvegicus*, with high support only in the concatenated BI, while all other *Orbiniella* species were combined into another highly supported clade. This can be due to the amount of missing data in the analysis both in taxon and sequence data coverage. Nevertheless, the Orbiniidae systematics remains unresolved and the boundaries of most of the genera are poorly understood (Bleidorn et al. 2009; Zhadan et al. 2015; Meca et al. 2021). Further investigation of the composition and the placement of *Orbiniella* within the orbiniid tree can clarify the monophyletic status of the genus.

Five well supported clades within *Orbiniella* and three more species present as single individuals were recovered in our phylogenetic analyses. The species delimitation analyses recovered eight putative species. Although COI data were absent in *O. parapari* sp. nov. and 16S data were absent in *Orbiniella* sp., all five species had at least one mitochondrial and one nuclear marker in the combined dataset, supporting robust phylogeny and species delimitation results. Two delimitation conflicts were reported in the analyses. For the COI dataset, both PTP and ASAP analyses supported splitting *O. griegi* sp. nov. into two putative species. For the ITS2 dataset, the ASAP analyses supported combining *O. mayhemi* and *Orbiniella* sp. into a single putative species. All other analyses delimited the five North Atlantic/Nordic clades as separate species. Additionally, we found several consistent morphological characters in each of the putative species supporting the overall proposed delimitation scheme (Table 1).

The four new species of *Orbiniella* described in this study formed a highly supported clade in the combined and in the individual marker datasets. The uncorrected p-distances between the four species in this clade ranged from 17.9 to 29.7% in COI, from 6.6 to 22.2% in 16S, and from 2.1 to 30.6% in ITS2. *Orbiniella petersenae* sensu stricto was genetically the most distant species form the rest of the species found in the NE Atlantic and the Nordic seas differing by more than 20% in p-distance in COI, 16S and ITS2 markers.

## Morphological diagnostic characters

Blake (2020) reviewed all the morphological characters used for species description in the deep-water *Orbiniella* and listed seven key characters required to separate them. Among those, the ones which better discriminated the NE Atlantic/Nordic *Orbiniella* species were: (1) the segmental annulation pattern, (2) number and shape of the acicular spines and (3) shape and length of the anal lobes. The shape of the prostomium, relative length of the peristomial segments and shape and length of the notopodia showed a great intraspecific variation within *O. petersenae* sensu stricto and *O. parapari* sp. nov. (see species descriptions and Table 1). Parapar et al. (2015) questioned the taxonomic value of the intersegmental ring pattern since the annulation was more conspicuous under SEM and thus could be an artefact of the critical point drying. We evaluated the appropriateness of SEM procedures for the analysis of the narrow annuli between parapodia in the NE Atlantic/Nordic *Orbiniella* through applying methylene blue staining in the studied material, and we could confirm the annulation pattern being identical in the stained wet specimens and the specimens studied for SEM. Therefore, we reaffirm the use of the segmental annulation pattern for species discrimination in *Orbiniella* and the application of both SEM and light microscopy in combination with methylene blue staining for the analysis of this character.

We also explored the taxonomic utility of the dorsal segmental pigmentation, characteristics of the crenulation in the capillaries, the presence of the nuchal organs and the eyes. Dorsal segmental pigmentation was discovered in two species: *O. petersenae* sensu stricto and *O. parapari* sp. nov.; however, it was not specific for either of them nor was it present in every examined specimen. Therefore, we do not consider dorsal segmental pigmentation to be a character useful for species discrimination. We suggest variation in pigmentation might be an artefact of fixation and conservation procedures, and observations of pigmentation in live specimens should help to clarify the use of it in species diagnoses. SEM observations allowed evaluating the variation in (1) the start of the crenulation and (2) the pronunciation of this crenulation in the capillaries of some specimens. The crenulation can start from the base or from the middle of a capillary chaeta, and it can be pronounced from the start or be weak basally and more obvious distally. All kind of capillaries were present in the five NE Atlantic/Nordic *Orbiniella* species and, therefore, it does not appear to be a useful character for species differentiation. SEM micrographs allowed us to elucidate some differences in the nuchal organs in *Orbiniella* species. *Orbiniella griegi* sp. nov. presented two lateral, not very prominent ciliary spots, whilst *O. petersenae* sensu stricto and *O. parapari* sp. nov. showed one single prominent lateral ciliary congregation on each side of the prostomium. Although no nuchal organs were found in *O. mayhemi* sp. nov. or in *Orbiniella* sp., more observations of specimens are needed to confirm the absence of the nuchal organs in these species. The fact that just a small portion of all the observed specimens of *O. petersenae* sensu stricto and *O. parapari* sp. nov. showed eyespots, indicates that their absence might be due to fading during long-term storage in ethanol. We consider the presence of eyes a character not reliable for species discrimination. We cannot discard the presence of eyespots in *O. griegi* sp. nov., *O. mayhemi* sp. nov. and *Orbiniella* sp., as well as in other *Orbiniella* species seemingly lacking eyes. Similar to the dorsal pigmentation, observations of live specimens should help in clarifying the use of eyes in species diagnoses.

## Species distribution

Our data suggest that the species of *Orbiniella* in the NE Atlantic and adjacent Nordic Seas have restricted vertical distribution either in the shelf and upper slope habitats as in *O. griegi* sp. nov. distributed across the Norwegian shelf and the Greenland-Scotland Ridge (GSR) between 171–781 m, or at the depths below 1000 m as in *O. petersenae* sensu stricto, *O. parapari*, *O. mayhemi*, and *Orbiniella* sp. Notably, all deep-sea *Orbiniella* species reported in this study occur on either side of the GSR only: *O. petersenae* sensu stricto and *O. parapari* sp. nov. were reported in the Iceland Sea and Norwegian Sea, and also in the southern Greenland Sea, *Orbiniella* sp. in the northern Greenland Sea and possibly also in the Iceland Sea and Norwegian Sea, whilst *O. mayhemi* inhabits the waters south-west of Iceland. Despite low number of species analysed here, the GSR with its maximum depth at ca. 900 m appears to act as a barrier for the deep-sea *Orbiniella* species dispersal. This corroborates the preliminary results on other annelid genera (Budaeva et al. 2019), on isopods (Brix and Svavarsson 2010; Schnurr et al. 2018) and on cumaceans (Uhlir et al. 2021). Notably, GSR coincides with the biogeographical border drawn for the shelf fauna separating the Arctic and the Boreal regions (Mironov 2013). In the eastern part of the

North Atlantic this border extends along the Norwegian shelf up to the Barents Sea with coastal Norwegian shelf areas warmed by the Gulf Stream and inholding Atlantic fauna. The significance of this border for the deep-sea species distribution has not been clearly demonstrated using comprehensive data. Our data on *Orbiniella* species distribution support the presence of the border in both the upper and lower bathyal areas.

## Conclusions

Diversity of *Orbiniella* in the NE Atlantic and the adjacent Nordic Seas constitutes at least five species, four of which are new to science. Three species, *Orbiniella parapari* Meca & Budaeva, sp. nov., *Orbiniella griegi* Meca & Budaeva, sp. nov., and *Orbiniella mayhemi* Meca & Budaeva, sp. nov., are formally described and the fourth species is left unnamed due to the scarcity of the available material. The diagnosis and distribution of *Orbiniella petersenae*, the only species previously known from the region, are clarified. All five species are morphologically very similar but can be separated by subtle differences in their pattern of segmental annulation, number and shape of the acicular spines, and length and shape of the four anal lobes in the pygidium, highlighting the taxonomic value of these characters for species discrimination in *Orbiniella*.

The Greenland-Iceland-Scotland Ridge acts as a barrier for the deep-sea *Orbiniella* species distribution in the North Atlantic and the Nordic Seas, with three of the deep-water species (i.e., *O. petersenae* sensu stricto, *O. parapari* sp. nov., and *Orbiniella* sp. reported exclusively north of the ridge in the cold Arctic waters, and *O. mayhemi* sp. nov. reported south of Iceland in warmer Atlantic waters. The shallow water *O. griegi* sp. nov. is distributed along the biogeographical border between the North Atlantic and the Arctic regions.

## Acknowledgements

We would like to thank all participants of the IceAGE expeditions and in particular Saskia Brix for organisation and acting as cruise leader. We are also grateful for the support of the entire benthos team of the DZMB Hamburg who sorted the samples in the lab and took care of the sample management for the different cruises around Iceland. We thank the KG Jebsen Center for Deep Sea Research and the MAREANO program for the access to specimens collected from the Norwegian Sea.

We are grateful to Louise Lindblom and Kenneth Meland (DNA lab, UiB) for assisting during molecular laboratory work, and to Irene Heggstad (ELMILAB, UiB) for helping with SEM. We would like to thank Arne Nygren for his advice on PCR protocols regarding the ITS2 marker, and Dimitar Dimitrov for helping with species delimitation methods and for discussing the results of the molecular analyses. Manuel Malaquias and Torsten Struck gave useful feedback on MAM's presentation on preliminary results at the ForBio annual meeting 2020. Oscar Díaz-Díaz gave useful comments on orbiniid taxonomical characters after MAM's presentation during SILPOLY 2022, which highly improved the quality of the manuscript. We are grateful to Javier Sánchez-Almazán and to the Museo Nacional de Ciencias Naturales de Madrid (MNCN, Spain) for providing space and equipment to analyse the specimens from the *Orbiniella petersenae* sensu lato type series. Special thanks to Julio Parapar, who helped with returning the specimens to IINH once the taxonomic work was done and to Guðmundur Guðmundsson for accepting the materials at IINH and providing the registration numbers. We are grateful to Antje Fischer, Marie-Louise Tritz, and Ekin Tilic for help with registering *Orbiniella* from the IceAGE materials in the collection of the Senckenberg Natural History Museum, Germany (SMF). We would also like to thank Anna Zhadan and an anonymous reviewer for their valuable comments and suggestions, which significantly contributed to improving the quality of the paper.

## Additional information

### Conflict of interest

The authors have declared that no competing interests exist.

### Ethical statement

No ethical statement was reported.

### Funding

The study was supported by the Norwegian Biodiversity Information Centre funded projects: Annelids from the deep Norwegian waters – AnDeepNor (project number 25-17-70184238) and Fauna of hydrothermal vents and cold seeps in Norwegian waters (project number 3-20-70184243).

### Author contributions

Conceptualization: JAK, MAM, NB. Data curation: TA, JAK, KM, MAM. Formal analysis: MAM, NB, KK. Investigation: NB, MAM. Methodology: MAM. Resources: JAK, NB, KM, KK, TA. Software: NB, MAM. Supervision: JAK, NB. Visualization: MAM. Writing - original draft: MAM. Writing - review and editing: NB, JAK, KM.

### Author ORCIDs

Miguel A. Meca https://orcid.org/0000-0002-3798-6809
Katrine Kongshavn https://orcid.org/0000-0002-4265-0912
Nataliya Budaeva https://orcid.org/0000-0001-9748-2285

### Data availability

All of the data that support the findings of this study are available in the main text or Supplementary Information.

## References

Blake JA (2017) Polychaeta Orbiniidae from antarctica, the Southern Ocean, the Abyssal pacific Ocean, and off South America. Zootaxa 4218(1): 1–145. https://doi.org/10.11646/zootaxa.4218.1.1

Blake JA (2020) New species and records of deep-water Orbiniidae (Annelida, Polychaeta) from the Eastern Pacific continental slope, abyssal Pacific Ocean, and the South China Sea. Zootaxa 4730(1): 1–61. https://doi.org/10.11646/zootaxa.4730.1.1

Blake JA (2021) New species and records of Orbiniidae (Annelida, Polychaeta) from continental shelf and slope depths of the Western North Atlantic Ocean. Zootaxa 4930(1): 1–123. https://doi.org/10.11646/zootaxa.4930.1.1

Blake JA, Hilbig B (1990) Polychaeta from the vicinity of deep-sea hydrothermal vents in the eastern Pacific II: New species and records from the Juan de Fuca and Explorer Ridge systems. Pacific Science 44(3): 219–253.

Bleidorn C (2005) Phylogenetic relationships and evolution of Orbiniidae (Annelida, Polychaeta) based on molecular data. Zoological Journal of the Linnean Society 144(1): 59–73. https://doi.org/10.1111/j.1096-3642.2005.00160.x

Bleidorn C, Hill N, Erséus C, Tiedemann R (2009) On the role of character loss in orbiniid phylogeny (Annelida): Molecules vs morphology. Molecular Phylogenetics and Evolution 52(1): 57–69. https://doi.org/10.1016/j.ympev.2009.03.022

Bogantes VE, Halanych KM, Meißner K (2018) Diversity and phylogenetic relationships of North Atlantic Laonice Malmgren, 1867 (Spionidae, Annelida) including the description of a novel species. Marine Biodiversity 48(2): 737–749. https://doi.org/10.1007/s12526-018-0859-8

Bonifácio P, Martínez Arbizu P, Menot L (2020) Alpha and beta diversity patterns of polychaete assemblages across the nodule province of the eastern Clarion-Clipperton Fracture Zone (equatorial Pacific). Biogeosciences 17(4): 865–886. https://doi.org/10.5194/bg-17-865-2020

Brix S, Svavarsson J (2010) Distribution and diversity of desmosomatid and nannoniscid isopods (Crustacea) on the Greenland–Iceland–Faeroe Ridge. Polar Biology 33(4): 515–530. https://doi.org/10.1007/s00300-009-0729-8

Budaeva N, Alvestad T, Bakken T, Capa M, Meißner K, Nygren A, Oug E, Kongsrud J (2019) DNA barcoding reveals cryptic diversity and genetic connectivity in the deep-sea annelids across the Greenland–Scotland Ridge. In: Adamowicz SJ, Ekrem T, Stur E, Bakken T, Martin MD (Eds) Scientific abstracts from the 8th International Barcode of Life Conference. Eight International Barcode of Life Conference, Trondheim (Norway), June 2019. https://cdnsciencepub.com/doi/pdf/10.1139/gen-2019-0083

Buzhinskaya GA (1993) Occurrence of *Orbiniella plumisetosa* sp. n. (Polychaeta: Orbiniidae) in the north-western Pacific Ocean and a key to species of the genus *Orbiniella*. Explorations of the Fauna of the Seas 43(51): 76–81.

Day JH (1954) The Polychaeta of Tristan da Cunha 1937–1938. Results of the Norwegian Expedition to Tristan da Cunha 1937–1938(29): 1–35.

Fabricius O (1780) Fauna Groenlandica, systematice sistens animalia groenlandiae occidentalis hactenus indagata, quoad nomen specificium, triviale, vernaculumque, synonyma auctorum plurimum, descriptionem, locum, victum, generationem, mores, usum capturamque singuli, pro ut detegendi occasio fuit, maximaque parte secundum proprias observationes. Hafniae Lipsiae xvi: 1–452. https://doi.org/10.5962/bhl.title.13489

Georgieva MN, Wiklund H, Ramos DA, Neal L, Glasby CJ, Gunton LM (2023) The annelid community of a natural deep-sea whale fall off eastern Australia. Records of the Australian Museum 75(3): 167–213. https://doi.org/10.3853/j.2201-4349.75.2023.1800

Gillet P (1999) A new species of *Orbiniella* (Orbiniidae: Polychaeta) from Marion Island, Indian Ocean. Proceedings of the Biological Society of Washington 112(3): 592–597.

Grosse M, Bakken T, Nygren A, Kongsrud JA, Capa M (2020) Species delimitation analyses of NE Atlantic *Chaetozone* (Annelida, Cirratulidae) reveals hidden diversity among a common and abundant marine annelid. Molecular Phylogenetics and Evolution 149: 106852. https://doi.org/10.1016/j.ympev.2020.106852

Hartman O (1967) Polychaetous annelids collected by the USNS Eltanin and Staten Island cruises, chiefly from Antarctic seas. Allan Hancock Monographs in Marine Biology 2: 1–387.

Katoh K, Rozewicki J, Yamada KD (2019) MAFFT online service: Multiple sequence alignment, interactive sequence choice and visualization. Briefings in Bioinformatics 20(4): 1160–1166. https://doi.org/10.1093/bib/bbx108

Kearse M, Moir R, Wilson A, Stones-Havas S, Cheung M, Sturrock S, Buxton S, Cooper A, Markowitz S, Duran C, Thierer T, Ashton B, Meintjes P, Drummond A (2012) Geneious Basic: An integrated and extendable desktop software platform for the organization and analysis of sequence data. Bioinformatics (Oxford, England) 28(12): 1647–1649. https://doi.org/10.1093/bioinformatics/bts199

Kumar S, Stecher G, Li M, Knyaz C, Tamura K (2018) MEGA X: Molecular evolutionary genetics analysis across computing platforms. Molecular Biology and Evolution 35(6): 1547–1549. https://doi.org/10.1093/molbev/msy096

Lanfear R, Frandsen PB, Wright AM, Senfeld T, Calcott B (2017) PartitionFinder 2: New methods for selecting partitioned models of evolution for molecular and morphological phylogenetic analyses. Molecular Biology and Evolution 34(3): 772–773. https://doi.org/10.1093/molbev/msw260

Meca MA, Zhadan A, Struck TH (2021) The Early Branching Group of Orbiniida Sensu Struck et al., 2015: Parergodrilidae and Orbiniidae. Diversity 13(1): 29. https://doi.org/10.3390/d13010029

Miller MA, Pfeiffer W, Schwartz T (2012) The CIPRES science gateway: enabling high-impact science for phylogenetics researchers with limited resources. In: Proceedings of the 1st Conference of the Extreme Science and Engineering Discovery Environment: Bridging from the extreme to the campus and beyond, Chicago Illinois (USA), July 2012. Association for Computing Machinery, New York, 1–8. https://doi.org/10.1145/2335755.2335836

Mironov AN (2013) Biotic complexes of the Arctic Ocean. Invertebrate Zoology 10(1): 3–48. https://doi.org/10.15298/invertzool.10.1.02

Narayanaswamy BE, Blake JA (2005) A new species of *Orbiniella* (Polychaeta: Orbiniidae) from deep basins of Antarctica. Journal of the Marine Biological Association of the United Kingdom 85(4): 843–846. https://doi.org/10.1017/S0025315405011793

Nguyen LT, Schmidt HA, Von Haeseler A, Minh BQ (2015) IQ-TREE: A fast and effective stochastic algorithm for estimating maximum-likelihood phylogenies. Molecular Biology and Evolution 32(1): 268–274. https://doi.org/10.1093/molbev/msu300

Nygren A, Pleijel F (2011) From one to ten in a single stroke-resolving the European Eumida sanguinea (Phyllodocidae, Annelida) species complex. Molecular Phylogenetics and Evolution 58(1): 132–141. https://doi.org/10.1016/j.ympev.2010.10.010

Nygren A, Parapar J, Pons J, Meißner K, Bakken T, Kongsrud JA, Oug E, Gaeva D, Sikorski A, Johansen RA, Hutchings PA, Lavesque N, Capa M (2018) A mega-cryptic species complex hidden among one of the most common annelids in the North East Atlantic. PLoS ONE 13(6): e0198356. https://doi.org/10.1371/journal.pone.0198356

Parapar J, Moreira J, Helgason GV (2015) First record of genus *Orbiniella* Day, 1954 (Polychaeta: Orbiniidae) in North Atlantic Ocean with the description of a new species. Zootaxa 4006(2): 330–346. https://doi.org/10.11646/zootaxa.4006.2.5

Puillandre N, Brouillet S, Achaz G (2021) ASAP: Assemble species by automatic partitioning. Molecular Ecology Resources 21(2): 609–620. https://doi.org/10.1111/1755-0998.13281

Rambaut A, Drummond AJ, Xie D, Baele G, Suchard MA (2018) Posterior summarization in Bayesian phylogenetics using Tracer 1.7. Systematic Biology 67(5): 901–904. https://doi.org/10.1093/sysbio/syy032

Ronquist F, Teslenko M, Van Der Mark P, Ayres DL, Darling A, Höhna S, Larget B, Liu L, Suchard MA, Huelsenbeck JP (2012) MrBayes 3.2: Efficient Bayesian phylogenetic inference and model choice across a large model space. Systematic Biology 61(3): 539–542. https://doi.org/10.1093/sysbio/sys029

Sars GO (1872) Diagnoser af nye Annelider fra Christianiaforden, efter Professor M. Sar’s efterladte Manuskripter. Forhandlinger i Videnskabs-Selskabet i Christiania 1871: 406–417.

Schnurr S, Osborn KJ, Malyutina M, Jennings R, Brix S, Driskell A, Svavarsson J, Martinez Arbizu P (2018) Hidden diversity in two species complexes of munnopsid isopods (Crustacea) at the transition between the northernmost North Atlantic and the Nordic Seas. Marine Biodiversity 48(2): 813–843. https://doi.org/10.1007/s12526-018-0877-6

Sugiura N (1978) Further analysis of the data by Akaike’s information criterion and the finite corrections: Further analysis of the data by Akaike’s. Communications in Statistics. Theory and Methods 7(1): 13–26. https://doi.org/10.1080/03610927808827599

Uhlir C, Schwentner M, Meland K, Kongsrud JA, Glenner H, Brandt A, Thiel R, Svavarsson J, Lörz AN, Brix S (2021) Adding pieces to the puzzle: insights into diversity and distribution patterns of Cumacea (Crustacea: Peracarida) from the deep North Atlantic to the Arctic Ocean. PeerJ 9: e12379. https://doi.org/10.7717/peerj.12379

Zhadan A, Stupnikova A, Neretina T (2015) Orbiniidae (Annelida: Errantia) from Lizard Island, Great Barrier Reef, Australia with notes on orbiniid phylogeny. Zootaxa 4019(1): 773–801. https://doi.org/10.11646/zootaxa.4019.1.27

Zhang J, Kapli P, Pavlidis P, Stamatakis A (2013) A general species delimitation method with applications to phylogenetic placements. Bioinformatics (Oxford, England) 29(22): 2869–2876. https://doi.org/10.1093/bioinformatics/btt499

## Supplementary material 1

### Sampling data, PCR protocol and genetic distances

Authors: Miguel A. Meca, Jon Anders Kongsrud, Katrine Kongshavn, Tom Alvestad, Karin Meißner, Nataliya Budaeva

Data type: xlsx

Explanation note: **table S1.** List of material used in this study with sampling information, museum numbers, voucher numbers, GenBank accession. **table S2.** Primers and PCR settings for COI, 16S rDNA and ITS2. **table S3.** Pairwise genetic distances within and between the NE Atlantic/Nordic clades and public *Orbiniella* sequences.

Link: https://doi.org/10.3897/zookeys.1205.120300.suppl1

## Supplementary material 2

### Phylogenetic trees regarding COI, 16 and ITS2 markers, and species delimitation results

Authors: Miguel A. Meca, Jon Anders Kongsrud, Katrine Kongshavn, Tom Alvestad, Karin Meißner, Nataliya Budaeva

Data type: docx

Explanation note: **fig. S1.** Maximum likelihood (ML) analysis based on the concatenated dataset of COI, 16S and ITS2. Bootstrap values are shown on the nodes. Capital letters correspond with the clades discussed in the text. **fig. S2.** Bayesian inference (BI) and Maximum likelihood (ML) analysis based on COI gene. Node support is indicated on the nodes (PP/BS). Capital letters correspond with the clades discussed in the text. **fig. S3.** Bayesian inference (BI) and Maximum Likelihood (ML) analysis based on ITS2 gene. Node support is indicated on the nodes (PP/BS). Capital letters correspond with the clades discussed in the text. **fig. S4.** Maximum likelihood (ML) analysis based on 16S gene. Bootstrap values are shown on the nodes. Capital letters correspond with the clades discussed in the text. **fig. S5.** Bayesian inference (BI) based on 16S gene. Bayesian posterior probabilities are shown on the nodes. Capital letters correspond with the clades discussed in the text. **File S1.** PTP species delimitation. A. COI. B. 16S. C. ITS2. **A.** Species delimitation – COI fragment: PTP results; **B.** Species delimitation – 16S fragment: PTP results; **C.** Species delimitation – ITS2 fragment: PTP results; **File S2.** ASAP species delimitation. A. COI. B. COI. C. ITS2. **A.** Species delimitation – COI fragment: ASAP results; **B.** Species delimitation – 16S fragment: ASAP results; **C.** Species delimitation – ITS2 fragment: ASAP results

Link: https://doi.org/10.3897/zookeys.1205.120300.suppl2

ZooKeys 1205: 89–99 (2024)
DOI: 10.3897/zookeys.1205.114394

Short Communication

# A new Mexican species of the *Cryptopygus* complex (Collembola, Isotomidae) associated with the hermit crab *Coenobita clypeatus* (Crustacea, Coenobitidae)

José G. Palacios-Vargas[1]

1 *Laboratorio de Ecología y Sistemática de Microartrópodos, Departamento de Ecología y Recursos Naturales, Facultad de Ciencias, Universidad Nacional Autónoma de México, 04510 México, D.F., Mexico*

*Corresponding author: José G. Palacios-Vargas (troglolaphysa@hotmail.com)*

## Abstract

A new species of *Cryptopygus* Willem, 1901 associated with hermit crabs living on seashores of Quintana Roo State, Mexico, is described and illustrated. It is blind, with 9–11 postlabial setae, unguis with a pair of lateral teeth, empodial appendix lanceolate and almost as long as unguis, tenaculum with 4 + 4 teeth and 3–4 setae on corpus, manubrium with 11–14 pairs of manubrial setae on anterior surface and 17–18 pairs on posterior surface, and mucro bidentate. An updated key for the identification of 29 American species of *Cryptopygus* complex is included.

**Key words:** Sand, seashore, taxonomy, Xcacel

**Academic editor:** Louis Deharveng
**Received:** 18 October 2023
**Accepted:** 30 April 2024
**Published:** 20 June 2024

**ZooBank:** https://zoobank.org/8447F80F-36AE-4EAB-9BE2-6D868D47A6B7

**Citation:** Palacios-Vargas JG (2024) A new Mexican species of the *Cryptopygus* complex (Collembola, Isotomidae) associated with the hermit crab *Coenobita clypeatus* (Crustacea, Coenobitidae). ZooKeys 1205: 89–99. https://doi.org/10.3897/zookeys.1205.114394

## Introduction

This contribution is a part of the project aimed at the microarthropods associated with hermit crabs, in which the male of *Coenaletes caribaeus* Bellinger, 1985 (Coenaletidae) has been redescribed (Palacios-Vargas et al. 2000) and other Collembola and some Acari recorded from this crab (Maldonado-Vargas and Palacios-Vargas 1999).

The genus *Cryptopygus* Willem, 1901 *sensu lato* represents a complex of genera (Potapov 2001; Potapov et al. 2013). The species of this complex live in a wide variety of environments such as soil, litter, caves, and sandy beaches. Here, I use the name *Cryptopygus* in its broad sense. There are altogether 76 valid species involved in the genus (Bellinger et al.1996–2023), which has a global distribution. The purpose of this paper is to describe a new species of *Cryptopygus* found in hermit crabs collected in marine waters of Quintana Roo State, Mexico. As shown by Palacios-Vargas (1997), there are several *Cryptopygus* species known from Mexico, namely *C. benhami* Christiansen & Bellinger, 1980 found in caves from Guerrero and Mexico States and *C. exilis* from Veracruz State. Later, Palacios-Vargas and Thibaud (2001) described an additional species, *Cryptopygus axacayacatl* Vargas & Thibaud, 2001, which lives on sandy beaches from Guerrero State. Moreover, *Pauropygus caussaneli* (Thibaud, 1996), which belongs to the same complex, was cited from Guerrero state by Potapov et al. (2013).

## Materials and methods

The material of the new species comes from Xcacel beach, Quintana Roo State. It was found while examining the hermit crab *Coenobita clypeatus* (Fabricius, 1787) living in *Cittarium pica* (Linnaeus, 1758) shells. Hermit crabs were put in a bucket with fresh water and springtails floating on the surface were collected. The specimens were fixed in ethanol 96% and later cleared with KOH 10% and mounted on slides using Hoyer solution. To harden the solution, the slides were dried in a slide warmer at 45–50 °C for 1 week. Finally, each specimen was labeled with its collecting data. Specimens were examined with a Carl Zeiss Primo Star phase-contrast microscope. The drawings were made with the aid of a drawing tube.

Abbreviations:

| | |
|---|---|
| **Abd** | abdominal segment; |
| **Ant** | antennal segment; |
| **PAO** | postantennal organ; |
| **S** | sensillum; |
| **Tita** | tibiotarsus; |
| **Th** | thoracic segment. |

## Taxonomy

**Entomobryomorpha**
**Isotomidae**
**Anurophorinae**

***Cryptopygus* Willem, 1901**

**Diagnosis (modified from Potapov 2001).** Anurophorinae with fused Abd V and VI, well-developed furcula and bidentate or tridentate mucro. Slender body shape, from small to median size. Eyes from 0+0 to 8+8. Color usually pale. Integument smooth, with rare exceptions. Furcula present, mucro separated from dens, bi- or tridentate. Manubrium with 1–8 pairs of anterior setae. Dens slender, smooth or crenulated, continuously narrowing towards its apex. Abd V and VI fused. PAO and empodium present; anal spines absent, apical bulb usually absent on antenna. Clavate tibiotarsal hairs absent or present. Body setae usually short, macrosetae differentiated at least on last abdominal segments.

***Cryptopygus coenobitus* sp. nov.**
https://zoobank.org/41349B8A-6C87-41D9-B1E3-169668996F9A
Figs 1–16

**Type material.** ***Holotype*.** Female on slide. ***Paratype*:** male on slide. Type material kept at Facultad de Ciencias, UNAM. Slides numbered: FC-UNAM:LESM-AC: 22863 and FC-UNAM:LESM-AC: 22864.

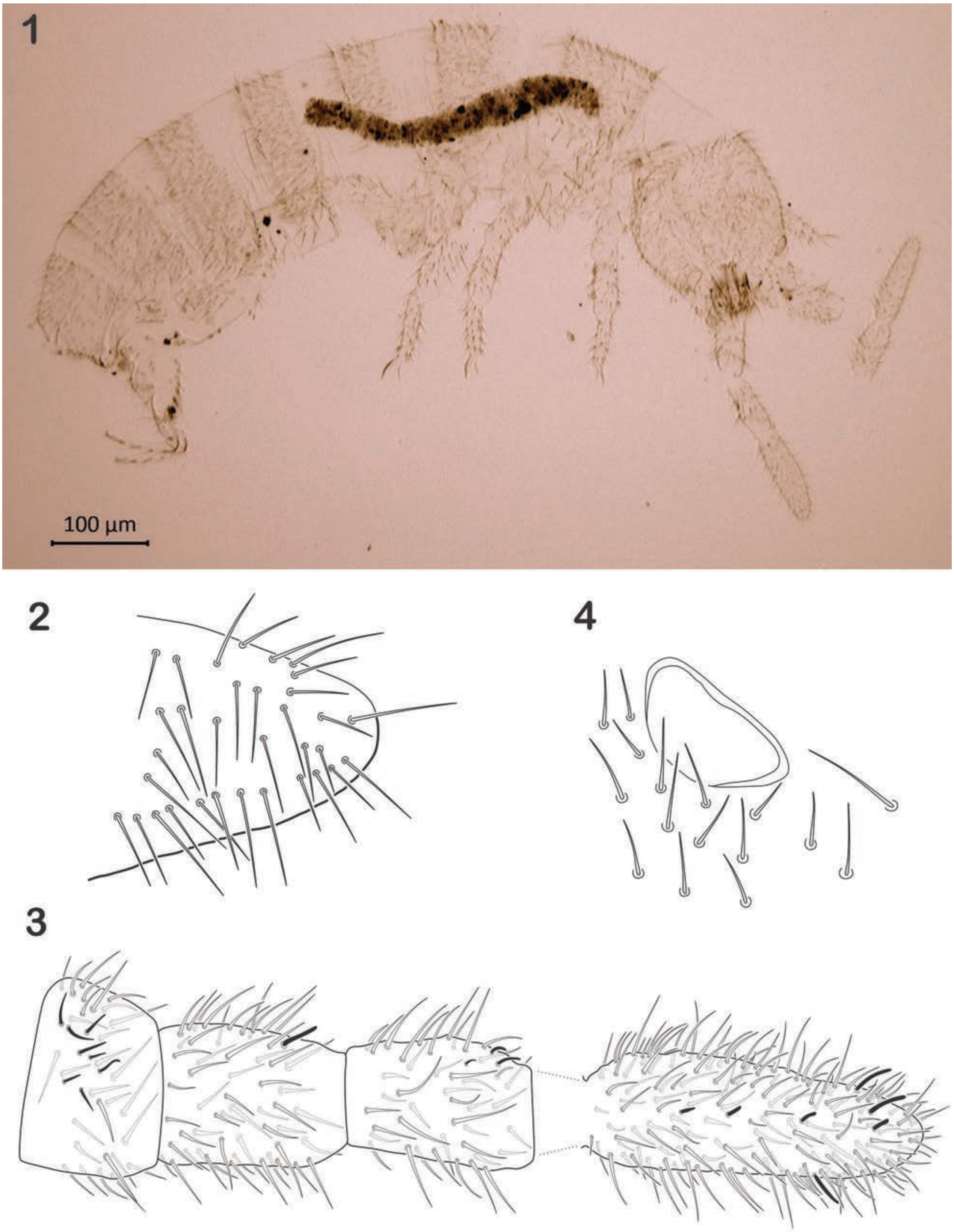

**Figures 1–4.** *Cryptopygus coenobitus* sp. nov. **1** habitus, image from phase-contrast microscope, lateral view **2** Abd II, lateral partial view **3** antenna I–IV, from I to III in ventral view, IV dorsal view **4** PAO.

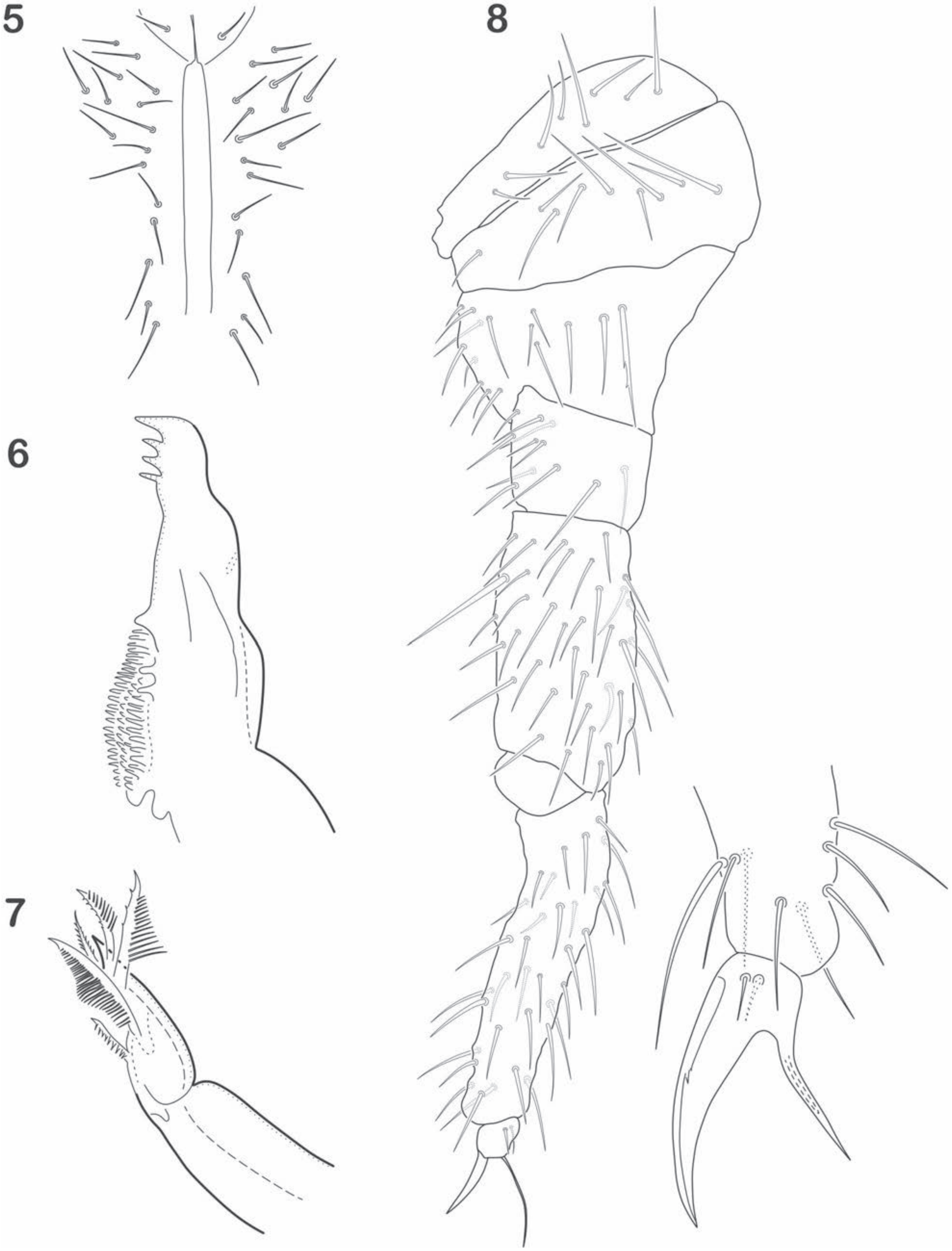

**Figures 5–8.** *Cryptopygus coenobitus* sp. nov. **5** postlabial setae **6** mandible **7** maxilla **8** tita III and magnification of foot complex.

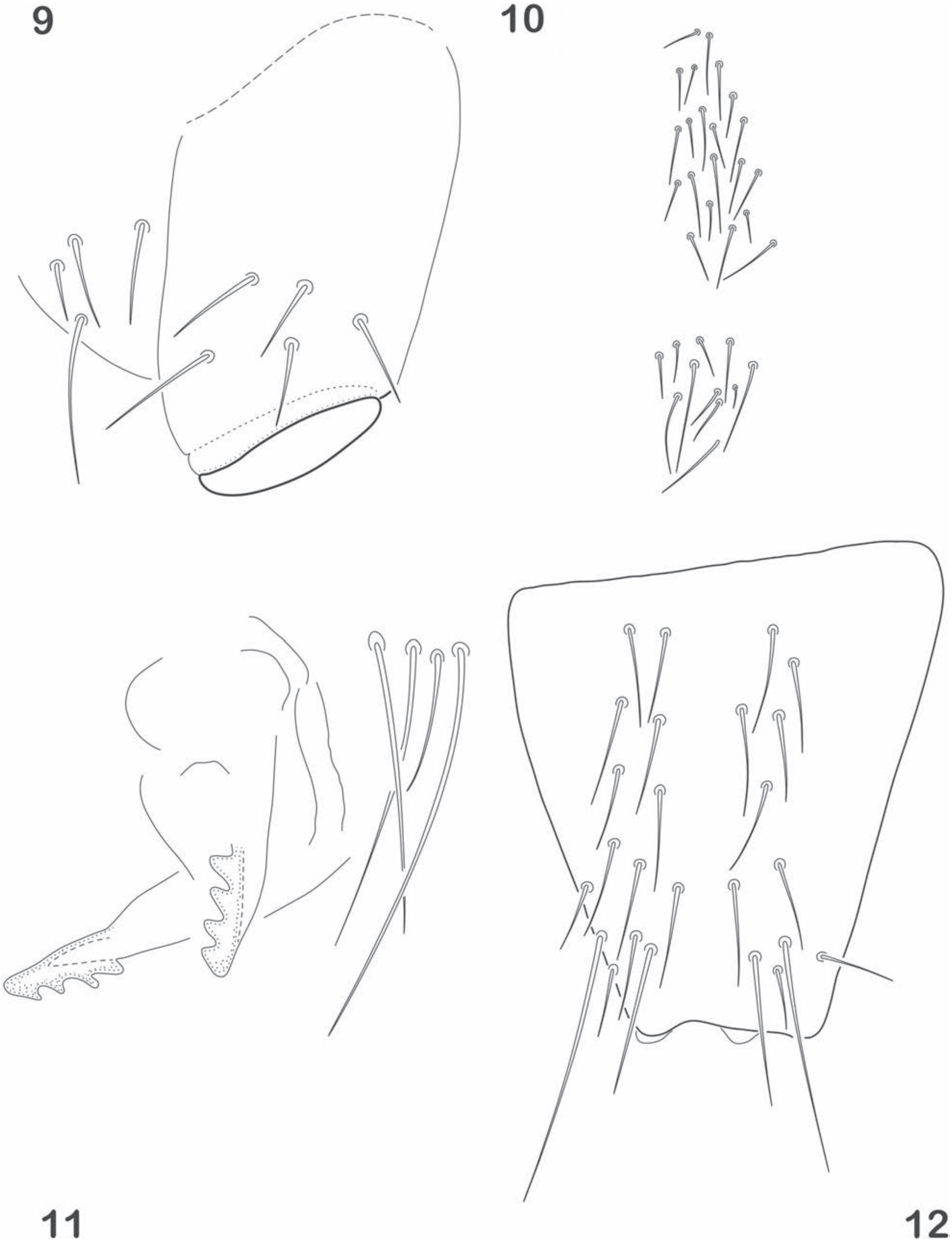

**Figures 9–12.** *Cryptopygus coenobitus* sp. nov. **9** ventral tube, lateral view **10** coxae furcalis anterior and posterior **11** tenaculum **12** manubrium, anterior view.

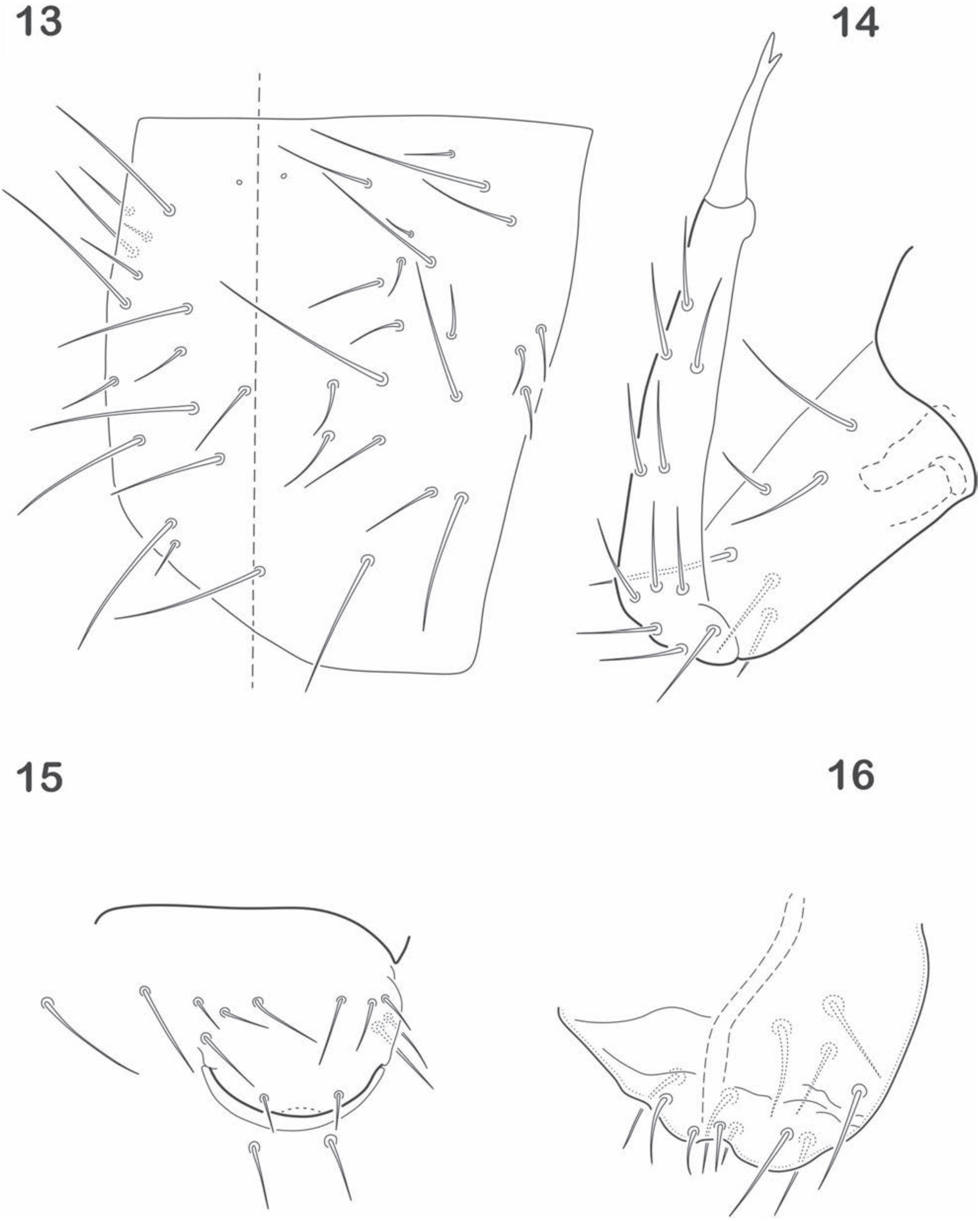

**Figures 13–16.** *Cryptopygus coenobitus* sp. nov. **13** manubrium latero-posterior view, line shows midline **14** dens and mucro **15** female genital plate **16** male genital plate.

**Type locality.** Mexico – Quintana Roo • Municipality of Solidaridad; Xcacel; ex. *Coenobita clypeatus*; 20°20'13"N, 87°20'45"W; 6 June 2022; J.G. Palacios-Vargas, M. Ojeda & A. Arango leg.

**Diagnosis.** White and eyeless *Cryptopygus*, with 9+9 to 11+11 postlabial setae, 1 pair of lateral teeth on unguis; retinaculum with 4 + 4 teeth and 3–4 setae on corpus, 11–14 pairs of manubrial setae on anterior surface, and 17–18 pairs on posterior surface, dens smooth, 4 setae on posterior basal part and 11–13 on anterior side, mucro bidentate.

**Description.** Setae smooth, acuminate, mostly short, some micro- and few slightly barbulated macrosetae (40–50 µm). Sensilla on terga in posterior row of setae, only slightly differentiated from ordinary setae, thinner and hyaline (Figs 1, 2). Microsensillum on Th. II normal. Abd. V and VI completely fused. Dorsal setation from Th I to Abd IV, 15,8/4,4,5,8 irregular lines (Fig. 1). Thorax without ventral setae. Abd VI without foil setae. Sensillar formula from Th II to Abd V: 3,3/2,2,2,3,2.

Length of head 140–150 µm, length of body 750–1000 µm. Antennae 250 µm, longer than head (ratio = 1:1.75). Ratio Ant. I–IV as 1:1.5; 1.5; 2.5. Ant. I with 33–36 setae, 9 thin and short ventral sensilla; Ant. II with 54 setae with few microsensilla and one thick, long sensillum on ventral–distal position (Fig. 3). Ant. III with 44 setae, antennal organ III with 2 microsensilla, 2 fine guard sensilla and 1 ventro-external microsensillum. Ant IV with about 70 setae, and 8 long and fine sensilla. Apex of the segment with a microsensillum and a small organite, apical bulb absent. Eyes absent, postantennal organ oval (25 × 12 µm), surrounded by 5 setae (Fig. 4). Labrum with 4 short, thin prelabral setae; 4 long setae in anterior row, 5 spiniform setae in median row, and 4 spiniform setae in posterior row, formula 4/4,5,4. With 4 sublobal hairs on outer maxillary lobe; labium with full set of guards on papillae A–E, and 3 proximal and 4 baso-median setae. Postlabial setae 9+9-11+11 (Fig. 5). Mandibles with 3–4 apical teeth and molar surface well developed (Fig. 6). Maxilla with 6 lamellae, with some plumose (Fig. 7).

Thorax without ventral setae. All femora with 1 ventral acuminate tenent hair. Tita with 2,3,3 acuminate tenent hairs and without a distal subsegment (Fig. 8). Tita I = 60 µm, Tita = 80 µm. Unguis I = 13 µm, unguiculus I = 11 µm. Unguis with 1 pair of lateral teeth in the median part. Unguiculus lanceolate, acuminate, not lamellate, almost as long as unguis. Ventral tube with 4 + 4 basal setae and 5 + 5 latero-distal setae (Fig. 9). Abd. IV on ventral surface with 4+5 setae by side; anterior subcoxa furcalis with 19–20 setae; posterior subcoxa furcalis with 10 setae, 4 of them longer than others (Fig. 10).

Tenaculum with 4+4 teeth, corpus with 3–4 setae (Fig. 11). Furcula well developed, manubrium with 11–14 pairs of anterior setae (Fig. 12), 3 small lateral setae and 18 pairs of setae on posterior side. (Fig. 13). Dens smooth, only 4 setae of different size on posterior basal part and 10–14 subequal setae on anterior surface (Fig. 14). Manubrium 80 µm, dens 100 µm, mucro 25 µm. Ratio 1:1.25; 0.3. Mucro bidentate. Genital plate of female with 2 eugenital setae and 5 pairs of pregenital setae (Fig. 15). Male with 4 pairs of eugenital setae and a few circumgenital setae (Fig. 16).

**Etymology.** This species is a noun in apposition after the genus of the hermit crab in which it was found.

**Distribution.** *Cryptopygus coenobitus* sp. nov. is only known from Xcacel, Quintana Roo State, Mexico.

## Key to *Cryptopygus* complex s. l. from the Americas

(some genera are excluded; they are not common, or descriptions are too brief)

1 Mucro quinquedentate (3 teeth and 2 basales spines), blind and colorless, body length 0.7 mm .......................................................................................... ***Mucrosomia caeca* Wahlgren, 1906** (South Georgia, Argentina, Chile, Peru, Venezuela; general distribution: widely in Antarctic and Subantarctic)
– Mucro bi- or tridentate, eyes and color present or absent..........................**2**
2 Foil setae on the end of fused tergite V+VI present...........**3 (*Hemisotoma*)**
– Foil setae on the end of fused tergite V+VI absent....................................**4**
3 Body length 1.0–1.2 mm, 8–7 eyes per side, ungual tooth present ........... ......................................... ***H. thermophila* (Axelson, 1900)** (cosmopolitan)
– Body length 0.9 mm, 5 eyes per side, ungual tooth absent......................... ............................................................... ***H. similis* (James, 1933)** (Canada)
4 Mandible reduced and elongated, molar plate with 2 strong basal teeth, antenna set together on frontal part of head, PAO large and wide ............. ......................................... ***Pauropygus caussaneli* (Thibaud, 1996)** (Mauritania, Mexico Pacific cost; sandy seashores of the tropics and subtropics)
– Mandible normal, not elongated, molar plate without strong basal teeth, antenna set separate on head, PAO elongated and narrow .......................**5**
5 Conspicuous flattened sensilla on fused abdominal tergite V+VI .............. ..........................................................................................**6 (*Proisotomodes*)**
– Flattened sensilla on fused abdominal tergite V+VI absent.......................**7**
6 Eyes absent, Ant I with 1 thick sensillum....................................................... ...... ***P. axayacatl* Palacios-Vargas & Thibaud, 2001** (Mexico Pacific coast)
– 1+1 eyes, Ant II with 2 thick sensilla.................................................................. ***P. bipunctatus* (Axelson, 1903)** (USA, Europe; general distribution: Holarctic)
7 Eyes and pigment present ..........................................................................**11**
– Eyes and pigment absent.............................................................................**8**
8 Manubrium with 11–14 pairs of anterior setae, unguis with 2 lateral teeth .................................................. ***Cryptopygus coenobitus* sp. nov.** (Mexico)
– Manubrium with 1–2 pairs of anterior setae, unguis without lateral teeth...**9**
9 Unguis with 1 tooth .......................................................................................... .......................... ***C. benhami* Christiansen & Belinger, 1980** (USA, Mexico)
– Unguis without any tooth...........................................................................**10**
10 Manubrium with 2 anterior and 8 posterior pairs of setae .......................... ...................................... ***C. elegans* (Rapoport & Izarra, 1962)** (Argentina)
– Manubrium with 1 anterior pair of setae ..................................................**13**
11 8+8 eyes.......................................................................................................**20**
– 6+6 or fewer eyes .........................................................................................**12**
12 2+2 eyes.......................................................................................................**13**
– 3+3 to 6+6 eyes ...........................................................................................**15**
13 Body length about 2 mm, ventral tube with 7 basal and 8+8 distal setae... ..................................................***C. arcticus* Christiansen & Bellinger, 1980**
– Body length 1 mm, ventral tube with 1 basal seta and 4+4 distal setae .. ..........................................................................................................**14**
14 Mucro with 3 teeth ..........................***C. parallelus* (Wahlgren, 1901)** (Chile)
– Mucro with 2 teeth ...........***C. quadrioculatus* (Rapoport, 1963)** (Argentina)

15 3+3 eyes per side .......... **16**

– With more eyes per side.......... **17**

16 Body 1.7 mm, PAO very long, 5–6 times longer than 1 eye ` .......... ***C. insignis*** **Massoud & Rapoport, 1968** (Chile, Argentina)

– Body 0.6 mm, PAO short, 3 times longer than 1 eye .......... ***C. trioculatus*** **Izarra, 1972** (Argentina)

17 5+5 eyes per side .......... **18**

– 6+6 eyes per side .......... **24**

18 Mucro with 3 teeth, unguis without teeth, length up to 1.25 mm.......... ***C. patagonicus*** **Izarra, 1972** (Argentina)

– Mucro with 2 teeth, unguis with or without teeth, length less than 1 mm.......... **19**

19 Dens with many anterior and posterior setae .......... ***C. decemoculatus*** **Folsom, 1937** (USA)

– Dens with only 5 anterior and 4 posterior setae.......... ***C. quinqueoculatus*** **Izarra, 1970** (Argentina)

20 Body length less than 1 mm, Ant III with 9 sensilla.......... ***C. indecisus*** **Massoud & Rapoport, 1968** (Argentina, Chile)

– Body length more than 1.4 mm, Ant III with only 5 sensilla.......... **21**

21 Unguis without teeth .......... **22**

– Unguis with teeth.......... **23**

22 Manubrium with 2–3 pairs of ventral setae; dens with 4 anterior and 9 posterior setae.......... ***C. ambus*** **Christiansen & Bellinger, 1980** (USA)

– Manubrium with 1 pair of ventral setae; dens with 0 anterior and 18 posterior pairs of setae .......... ***C. pentatomus*** **(Börner, 1906)** (Brazil)

23 Unguis with 1 median tooth.......... ***C. aquae*** **(Bacon, 1914)** (USA, Canada, Pacific coast)

– Unguis with 1 median and 2 lateral teeth .......... ***C. araucanus*** **Massoud & Rapoport, 1968** (Argentina, Chile)

24 Body length 2 mm .......... **25**

– Body length less than 2 mm .......... **26**

25 Unguis with 2 lateral teeth .......... ***C. antarcticus*** **Willem, 1901** (Antarctic, Argentina)

– Unguis without lateral teeth..***C. cinctus*** **Wahlgren, 1906** (Argentina, Chile)

26 Body length about 1.5 mm.......... **27**

– Body length less than 1 mm .......... **28**

27 Ventral tube with 2 basal and 4+4 distal setae; dens with 20 anterior and 19 posterior setae .......... ***C. separatus*** **Denis, 1931** (Costa Rica)

– Ventral tube with 6 basal and 4+4 distal setae; dens with 5 anterior and 6 posterior setae.......... ***C. ulrikeae*** **(Najt & Thibaud, 1987)** (Ecuador)

28 Dens with 6 anterior and 13 pairs of setae.......... ***C. andinus*** **Díaz & Najt, 1995** (Venezuela)

– Dens with 6 anterior and 4 pairs of setae.......... ***C. hirsutus*** **(Denis, 1931)** (Costa Rica, Peru)

29 Dens with 7 anterior and 2 posterior setae, mucro with 2 teeth .......... ***C. exilis*** **(Gisin, 1960)** (USA, Mexico, Europe)

– Manubrium with 4 pairs of anterior and 3 posterior setae, mucro with 3 teeth .......... ***Cryptopygus yosiii*** **Izarra, 1965** (Argentina)

## Discussion

*Cryptopygus coenobitus* sp. nov. is similar to *Proisotomodes axayacatl*, *Mucrosomia caeca*, *Cryptopygus benhami*, *C. elegans*, *C. exilis*, *C. yosiii*, and *Pauropygus caussaneli* in lacking eyes and pigment, but these species have four basal setae and 4+4 setae on ventral tube (vs 8 basal and 5+5 in the new species) and four teeth on the ramus of the tenaculum and one seta on the corpus (vs 3–4 on corpus in the new species). Most species have one or two pairs of setae on the anterior side of the manubrium, in contrast to 18 pairs in the new species. Moreover, the new species has many postlabial setae (9–11 pairs), an unguis with a pair of lateral teeth but without an internal tooth, a lanceolate empodium that is almost as long as the unguis, a manubrium with 8+8 anterior setae, and a tridentate mucro with two basal spines.

When *C. coenobitus* sp. nov. is compared with *Isotominella laterochaeta* from South Africa, there are some characters common, such as the lack of eyes and pigment and the presence of numerous setae on ventral side of head, mainly along the ventral line. The furcula is also very similar in shape, there are four setae on posterior basal part and 11–13 on anterior surface, and the mucro is bidentate. The main differences are that *C. coenobitus* lacks ventral setae on thorax III, and the ventral tube has 5 + 5 laterodistal and 4 + 4 posterior setae (vs 5–8+5–8 laterodistal and 6–9 posterior in *I. laterochaeta*). The tenaculum has 4+4 teeth, and the corpus bears three or four setae (vs 4+4 teeth and 2 setae on corpus).

There are some important characters that have been omitted in the descriptions of many species of the *Cryptopygus* complex, such as (1) postlabial chaetotaxy, which usually represents four or five pairs of setae, (2) the shape of maxillary lamellae, which can be modified depending on food preferences, and (3) the setation of coxae furcalis, but this last charactive might have important diagnostic value.

*Cryptopygus coenobitus* sp. nov. seems to be psammobiotic, and its morphology does not appear modified for living in association with hermit crabs. The maxillae are plumose, as an adaptation for filtration of food particles from the water, and the mandibles are normal, not modified, as in *Coenaletes* spp. (Coenaletidae) which live between the *Cittarium pica* shell and the hermit crab occupant. The new *Cryptopygus* species has been found in the sand but is able to enter to the shells occupied by hermit crabs, as in other Collembola genera such as *Cyphoderus* and additional microarthropods as found by Maldonado-Vargas and Palacios-Vargas (1999).

## Acknowledgements

This research is part of the author's sabbatical leave, approved by Dr Víctor Velázquez Aguilar, principal of the Faculty of Sciences, UNAM. Angela Arango, Eduardo Pacheco, and Margarita Ojeda assisted at field and laboratory work, and the latter also photographed the habitus of the new species. Figures were prepared by Jair Páez. The author expresses his gratitude to Dr Ľubomír Kováč and Dr Mikhail Potapov for their constructive criticism that improved the manuscript.

## Additional information

### Conflict of interest

The authors have declared that no competing interests exist.

### Ethical statement

No ethical statement was reported.

### Funding

No funding was reported.

### Author contributions

The author solely contributed to this work.

### Author ORCIDs

José G. Palacios-Vargas https://orcid.org/0000-0001-9097-6813

### Data availability

All of the data that support the findings of this study are available in the main text.

## References

Bellinger PF, Christiansen KA, Janssens F (1996–2023) Checklist of the Collembola of the World. http://www.collembola.org [Accessed on: 2023-09-29]

Maldonado-Vargas C, Palacios-Vargas JG (1999) Microartrópodos asociados con el cangrejo ermitaño *Coenobita clypeatus*. XXXIV Congreso Nacional de Entomología (México): 57–61.

Palacios-Vargas JG (1997) Catálogo de los Collembola de México. Servicios Editoriales, Facultad de Ciencias, UNAM. México, D. F. 102 pp.

Palacios-Vargas JG, Thibaud JM (2001) Three new species of Mexican littoral Collembola of genera *Willemia*, *Cryptogygus* and *Isotogastrura* (Hypogastruridae, Isotomidae, Isotogastruridae). Reviue Françoise Entomologie 23: 161–168. https://doi.org/10.4039/Ent130195-2

Palacios-Vargas JG, Cutz LQ, Maldonado C (2000) Redescription of the male of *Coenaletes caribaeus* (Collembola: Coenaletidae) associated with hermit crabs. Annals of the Entomological Society of America 93(2): 194–197. https://doi.org/10.1603/0013-8746(2000)093[0194:ROTMOC]2.0.CO;2

Potapov M (2001) Synopses on Palearctic Collembola, Vol. 3. Isotomidae. Abhandlungen und Berichte des Naturkundemuseums Görlitz 73(2): 1–603.

Potapov M, Gao Y, Dehaveng L (2013) Taxonomy of the *Cryptopygus* complex. I. *Pauropygus*—a new worldwide littoral genus (Collembola, Isotomidae). ZooKeys 304: 1–16. https://doi.org/10.3897/zookeys.304.4083

ZooKeys 1205: 101–113 (2024)
DOI: 10.3897/zookeys.1205.118358

Research Article

# *Ooceraea hainingensis* sp. nov.: A new Chinese *Ooceraea* (Hymenoptera, Formicidae, Dorylinae) species with a dealate queen, closely allied to the queenless clonal raider ant *O. biroi*

Qionghua Gao[1], Jiliang Long[1], Chengyuan Liu[2], Haoyu Liu[3], Hao Ran[4], Kip D. Lacy[5], Daniel J. C. Kronauer[5,6]

1 *Guangxi Key Laboratory of Agri-Environmental and Agri-Products Safety/National Demonstration Center for Experimental Plant Science Education, College of Agriculture, Guangxi University, Nanning, 530004, China*
2 *Center for Evolutionary and Organismal Biology, Zhejiang University School of Medicine, Hangzhou, 310058, China*
3 *Haining Ziwei Senior High School, Haining, 314400, China*
4 *State Key Laboratory of Genetic Resources and Evolution, Kunming Institute of Zoology, Chinese Academy of Sciences, Kunming, Yunnan, 650223, China*
5 *Laboratory of Social Evolution and Behavior, The Rockefeller University, 1230 York Avenue, New York, NY, 10065, USA*
6 *Howard Hughes Medical Institute, The Rockefeller University, 1230 York Avenue, New York, NY, 10065, USA*
*Corresponding author: Qionghua Gao (gaoqionghua123@163.com)*

## Abstract

The clonal raider ant, *Ooceraea biroi*, is a queenless species that reproduces asexually, and these traits make it an attractive model system for laboratory research. However, it is unclear where on the ant phylogeny these traits evolved, partly because few closely related species have been described and studied. Here, we describe a new raider ant species, *Ooceraea hainingensis* **sp. nov.**, from Zhejiang, China. This species is closely related to *O. biroi* but can be distinguished by the following features: 1) workers of *O. hainingensis* **sp. nov.** have an obvious promesonotal suture and a metanotal groove, whereas these characters are ambiguous in *O. biroi*; and 2) the subpetiolar process of *O. hainingensis* is prominent and anteroventrally directed like a thumb with sublinear posteroventral margin, while in *O. biroi*, it is anteroventrally directed but slightly backward-bent. Molecular phylogenetic analyses confirm that *O. hainingensis* is genetically distinct from *O. biroi*. Importantly, unlike *O. biroi*, *O. hainingensis* has a queen caste with wings and well-developed eyes. This suggests that the loss of the queen caste and transition to asexual reproduction by workers is specific to *O. biroi* and occurred after that species diverged from closely related congeneric species.

**Key words:** Caste, evolution, Formicidae, identification key, systematics, taxonomy

Academic editor: Sebastian Salata
Received: 17 January 2024
Accepted: 9 May 2024
Published: 20 June 2024

ZooBank: https://zoobank.org/E2DDD355-7A36-44D3-B896-40E39F44A6CD

Citation: Gao Q, Long J, Liu C, Liu H, Ran H, Lacy KD, Kronauer DJC (2024) *Ooceraea hainingensis* sp. nov.: A new Chinese *Ooceraea* (Hymenoptera, Formicidae, Dorylinae) species with a dealate queen, closely allied to the queenless clonal raider ant *O. biroi*. ZooKeys 1205: 101–113. https://doi.org/10.3897/zookeys.1205.118358

## Introduction

Most ant species live in colonies with two anatomically distinct female castes: queens and workers. Division of reproductive labor between castes has contributed to ants' ecological success, but some species have lost the ability to produce one of these castes. One example is the clonal raider ant, *Ooceraea biroi* (Forel, 1907), which has lost the ancestral capacity to produce queens. In this species, colonies are composed entirely of anatomical workers that all reproduce asexually via thelytokous (female-producing) parthenogenesis (development from an egg without fertilization by sperm) (Tsuji and Yamauchi 1995; Ravary and Jaisson 2004; Kronauer et al. 2012; Oxley et al. 2014). These unusual reproductive traits have made *O. biroi* a useful laboratory model species by providing control over genotype in experiments and facilitating genome engineering for functional studies of their social biology (Trible et al. 2017; Hart et al. 2023; Ivasyk et al. 2023; Li et al. 2023). In addition, these traits offer opportunities for comparative study. For example, genomic comparisons between closely related species that retain the capacity to produce queens and species that have lost this capacity might yield insight into the mechanistic basis of caste development.

However, comparative study is currently limited by the lack of knowledge across the genus *Ooceraea* Roger, 1862. Little is known about the biology of *Ooceraea* species other than *O. biroi*, apart from taxonomic species descriptions based on field-collected specimens. This is partly because *Ooceraea* are subterranean and have relatively small colonies, and are therefore rarely encountered. Members of the genus are found throughout tropical and subtropical regions of East Asia and Oceania (Borowiec 2016, 2019; Janicki et al. 2016; Guénard et al. 2017; AntCat 2024; AntWeb 2024), except for *O. biroi*, which has a wide global tropical and subtropical invasive range (Wetterer et al. 2012; Trible et al. 2020). The phylogeny of the 16 described *Ooceraea* species has yet to be resolved (AntCat 2024, AntWeb 2024), and we know little about the reproductive biology of most of these species. Queens have been documented from colony series of five species, including typical dealate queens found in *O. octoantenna* Zhou & Chen, 2020 (see Zhou et al. 2020) and *O. siamensis* Jaitrong et al., 2021, and ergatoid queens found in *O. besucheti* (Brown, 1975), *O. crypta* (Mann, 1921) and *O. quadridentata* Yamada et al., 2018. Queens have not been documented from any other *Ooceraea* species, but this should not necessarily be taken to mean that these species lack queens. Indeed, some species were described only from leaf litter samples [*O. alii* (Bharti & Akbar, 2013)] or single workers [*O. pawa* (Mann, 1919)], rather than from entire colony series. Therefore, it remains unclear where on the *Ooceraea* phylogeny the queen caste was lost.

Here, we expand the knowledge of *Ooceraea* reproductive biology and caste systems by describing workers and a queen of a novel species of this genus from southeastern China. Molecular phylogenetic analysis revealed that this new species is a close relative of *O. biroi*, suggesting that the loss of the queen caste occurred since the common ancestor of these two species.

## Material and methods

A colony (colony ID: GXU220610) consisting of 17 workers and a dealate queen was collected from the soil of a bamboo forest located at the foot of Yuemiao Mountain, Qianjiang village, Yuanhua Town, Haining County, Jiaxing City, Zhejiang Province, China. The holotype is a pinned worker specimen (individual ID: GXU220610-W-01), preserved in the Insect Collection of Guangxi University (**GXU**), Nanning, Guangxi, China. The paratypes are five workers (individual ID: GXU220610-W-02~06) stored in 75% ethanol at the same institution. These specimens were briefly removed from the ethanol, point mounted, photographed, and then returned to 75% ethanol for preservation. We flash-froze tissue from the queen specimen (individual ID: GXU220610-Q-01) and several worker specimens (individual ID: GXU220610-W-07~17) and stored them at -80 °C before DNA extraction and sequencing.

The *O. biroi* colony (colony ID: GXU230727) used for species comparison was collected from Binqiao Town, Longzhou County, Chongzuo City, Guangxi Province, China. Species identification was based on both morphological characters and *COI* and *COII* genetic information.

We extracted genomic DNA using Qiagen's QIAmp DNA Micro Kit (California, USA) following the manufacturer's instructions. PCR amplifications were conducted using the universal primers LCO1490 (5'-GGTCAACAAATCATAAAGATATTGG-3') and HCO2198 (5'-TAAACTTCAGGGTGACCAAAAAATCA-3') for *COI* (Folmer et al. 1994), as well as the primers AntLeu (5'- AATATGGCAGATTAGTGCAATGAA-3') (Kronauer et al. 2012) and Barbara(5'-CCACAAATTTCTGAACATTGACCA-3') (Simon et al. 1994) for *COII*. The PCR products were then run on agarose gels and Sanger sequenced by Sangon Biotech (Shanghai, China). The resulting sequences were assembled in ContigExpress and aligned with additional, publicly available *Ooceraea* sequences for phylogenetic analysis (see Table 1 for details). The mitochondrial *COI* and *COII* sequences of *Ooceraea* sp. MY08 were obtained from the raw sequence data (BioSample: SAMEA12364593; SRA: ERS9971404) reported in Romiguier et al. (2022). We assembled the complete mitochondrial genome using GetOrganelle (v.1.7.7.0) and annotated it with MITOS. Sequence alignment was performed using the MUSCLE algorithm implemented in MEGA 11 (Tamura et al. 2021). A *COI* + *COII* supermatrix was then constructed using the phylotools package (Zhang et al. 2017) in RStudio. Based on the number of parameters, we selected the "GTR+G+I" model as the best fit for the alignment. Maximum likelihood analysis was then conducted using the GTR+G+I substitution model to estimate the tree topology, and branch support was calculated using the bootstrap method with 1000 replicates.

**Table 1.** Samples used in the phylogenetic analysis.

| Samples | Locality | GenBank accession | | References |
|---|---|---|---|---|
| | | ***COI*** **600bp** | ***COII*** **536bp** | |
| Line A *Ooceraea biroi* isolate C13 | Okinawa, Japan | JX157194 | JX157205 | Kronauer et al. 2012 |
| Line B *Ooceraea biroi* isolate STC1 | Jolly Hill, St. Croix | JX157211 | JX157226 | Kronauer et al. 2012 |
| Line C *Ooceraea biroi* isolate C11 | Okinawa, Japan | JX157193 | JX157204 | Kronauer et al. 2012 |
| Line D *Ooceraea biroi* isolate Cbi48 | Tutuila, Am. Samoa | JX157201 | JX157212 | Kronauer et al. 2012 |
| Line E *Ooceraea biroi* isolate Cbi25 | Uttarakhand, India | JX157196 | JX157207 | Kronauer et al. 2012 |
| Line F *Ooceraea biroi* isolate Cbi26 | Jammu, India | JX157197 | JX157208 | Kronauer et al. 2012 |
| Line G *Ooceraea* sp. isolate Cbi6 | Nghệ An, Vietnam | JX157195 | JX157206 | Kronauer et al. 2012 |
| Line H *Ooceraea* sp. isolate Cbi27 | Guangdong, China | JX157198 | JX157209 | Kronauer et al. 2012 |
| Line I *Ooceraea biroi* isolate BG2 | Khulna, Bangladesh | MT086805 | MT086822 | Trible et al. 2020 |
| Line J *Ooceraea biroi* isolate BG3 | Khulna, Bangladesh | MT086806 | MT086823 | Trible et al. 2020 |
| Line K *Ooceraea biroi* isolate BG12 | Dhaka, Bangladesh | MT086814 | - | Trible et al. 2020 |
| Line L *Ooceraea biroi* isolate BG13 | Lawachara, Bangladesh | MT086815 | MT086829 | Trible et al. 2020 |
| Line M *Ooceraea biroi* isolate BG14 | Lawachara, Bangladesh | MT086816 | MT086830 | Trible et al. 2020 |
| ***Ooceraea hainingensis*** **sp. nov.** | Zhejiang, China | PP110965 | PP134994 | This study |
| *Ooceraea australis* | Cape York, Australia | JX157199 | JX157210 | Kronauer et al. 2012 |
| *Ooceraea fragosa* | Sinharaja Forest Reserve, Sri Lanka | MT267599 | – | Longino and Branstetter 2021 |
| *Ooceraea quadridentata* | Dak Lak, Vietnam | LC611729 | – | Yamada 2021 |
| *Ooceraea* sp. MY08 | Maliau Basin Centre, Malaysia | SAMEA12364593 | SAMEA12364593 | Romiguier et al. 2022 |
| *Syscia augustae* (outgroup) | Honduras | BK012238 | BK012238 | Allio et al. 2020 |

We examined the point-mounted specimens using a Nikon 745T stereomicroscope, and took high-quality multi-focused montage images using a Keyence VHX 6000 digital microscope under 200X magnification. We removed artefacts and unnecessary parts of the images and assembled images into figures using Adobe Photoshop CC 2019. The morphological terminology follows Borowiec (2016). We used ImageJ to make morphometric measurements of the following body parts. All measurements are in millimeters.

| | |
|---|---|
| **HL** | Head length: the maximum length of the cranium in full-face view, measured by the straight-line distance from the clypeus' foremost point, extending to the central point of the cranial posterior margin; |
| **HW** | Head width: the greatest width of the cranium (full-face view, excluding the eyes); |
| **SL** | Scape length: the maximum length of the antennal scape excluding the basal condylar bulb; |
| **MW** | Mesosomal width: the maximum width of the promesonotum in dorsal view; |
| **ML** | Mesosomal or Weber's length: the maximum diagonal length of the mesosoma in lateral view, measured from the posterodorsal border of the pronotal flange to the posterior basal angle of the metapleuron; |
| **PL** | Petiolar length: maximum length of petiole in lateral view (excluding helcium); |
| **PH** | Petiolar height: maximum height of petiole in lateral view (including subpetiolar process); |
| **PW** | Petiolar width: maximum width of petiole in dorsal view; |
| **PPL** | Postpetiolar length: maximum length of postpetiole in lateral view (excluding helcium); |
| **PPH** | Postpetiolar height: maximum height of postpetiole in lateral view; |
| **PPW** | Postpetiolar width: maximum width of postpetiole in dorsal view; |
| **CI** | Cephalic index: HW/HL × 100; |
| **SI** | Scape index: SL/HW × 100; |
| **PI1** | Petiolar index 1: PL/PH × 100; |
| **PI2** | Petiolar index 2: PW/PL × 100; |
| **PPI1** | Postpetiolar index 1: PPL/PPH × 100; |
| **PPI2** | Postpetiolar index 2: PPW/PPL × 100; |
| **WI** | Waist index: PPW/PW × 100. |

## Results

### Taxonomy

***Ooceraea hainingensis* sp. nov.**
https://zoobank.org/B6AB9D4B-57F8-4758-8903-7DD969206A60
Figs 1–3

**Etymology.** The species epithet *hainingensis* refers to the type locality.

**Type material.** ***Holotype*:** one worker ant; point mounted. Original label: "China, Zhejiang, Haining, Qianjiang village, Yuemiao Mountain, 30.372187°N, 120.810766°E, nesting in the subterranean zone, 10.VI.2022, Haoyu Liu leg.". ***Paratypes*:** five workers from the same colony as the holotype. These type

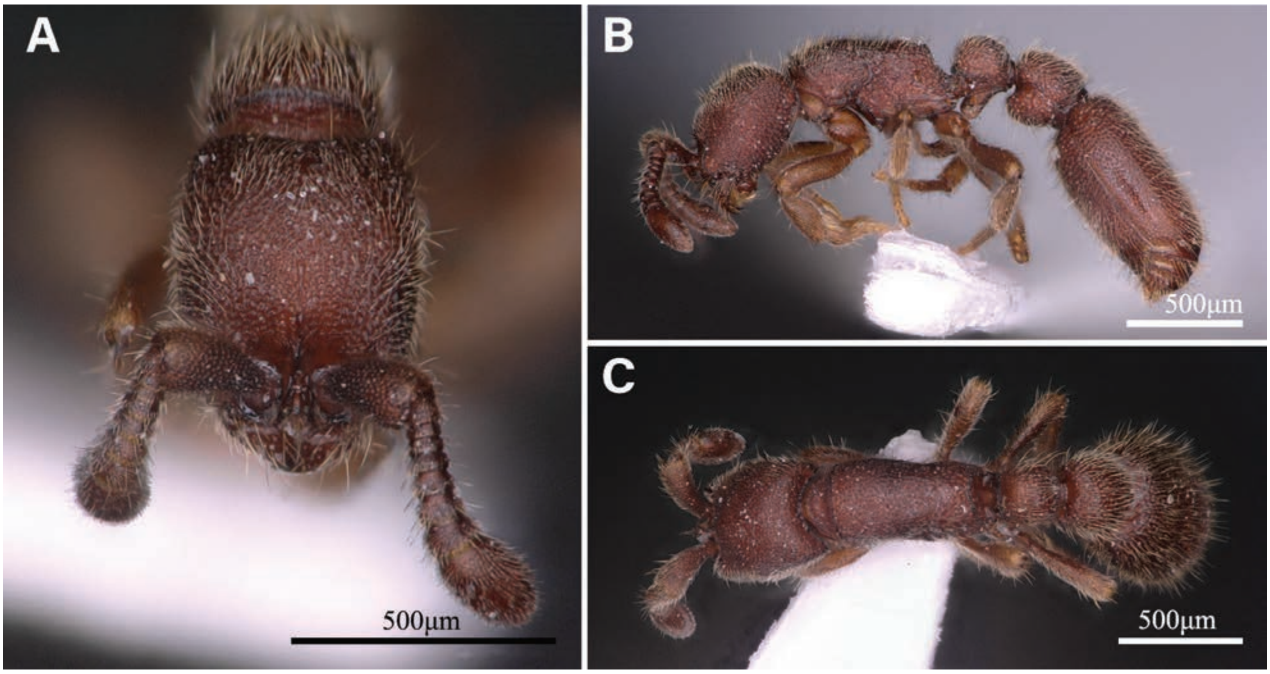

**Figure 1.** *Ooceraea hainingensis* sp. nov., holotype worker **A** head in full-face view **B** body in lateral view **C** body in dorsal view.

specimens are deposited in the Insect Collection of Guangxi University (GXU), Nanning, Guangxi, China.

**Description of the workers.** ***Measurements and indices***: Holotype: HL 0.53, HW 0.46, SL 0.19, MW 0.32, ML 0.74, PL 0. 0.22, PH 0.36, PW 0.22, PPL 0.25, PPH 0.33, PPW 0.30, CI 87, SI 42, PI1 59, PI2 104, PPI1 75, PPI2 123, WI 135. Paratypes (*N* = 5): HL 0.50–0.56, HW 0.43–0.47, SL 0.18–0.26, MW 0.32, ML 0.66–0.73, PL 0.19–0.22, PH 0.33–0.37, PW 0.22–0.26, PPL 0.22–0.26, PPH 0.30–0.34, PPW 0.27–0.32, CI 82–88, SI 42–57, PI1 52–63, PI2 110–133, PPI1 68–78, PPI2 117–145, WI 117–131.

***Head*:** In full-face view (Fig. 1A), the cranium subrectangular, distinctly longer than broad; lateral sides weakly/very slightly convex; posterior margin weakly concave medially; posterolateral corners rounded. Mandibles subtriangular, and the masticatory margin lacks distinct denticles. Antennae 9-segmented; scape short and clavate, reaching up to the mid-length of the cranium in full-face view. Antennal sockets fully exposed. Compound eyes and ocelli absent.

***Mesosoma***: Dorsum of mesosoma slightly convex in lateral view (Fig. 1B). Pronotum in dorsal view (Fig. 1C) with anterior margin rounded. Promesonotal suture and metanotal groove present (Fig. 2A). Propodeum in dorsal view with posterior margin concave; propodeal lobe is well formed and roundly shaped (Fig. 2B).

***Metasoma*:** Petiole (abdominal segment II) in lateral view (Fig. 1B) much higher than long when including subpetiolar process (PI1, 52–66), with dorsal margin weakly convex. Petiole in dorsal view subrectangular (Fig. 1C), slightly wider than long (PI2, 104–132), with lateral sides weakly convex. Subpetiolar process in lateral view prominent and anteroventrally directed like a thumb, with posteroventral margin sublinear (Fig. 1B, 2B). Postpetiole (abdominal segment III) in lateral view subrectangular, much higher than long (PPI1, 68–78), with dorsal and ventral margin weakly convex. Postpetiole in dorsal view almost trapezoidal, wider posteriorly, broader than long (PPI2, 117–127), and wider

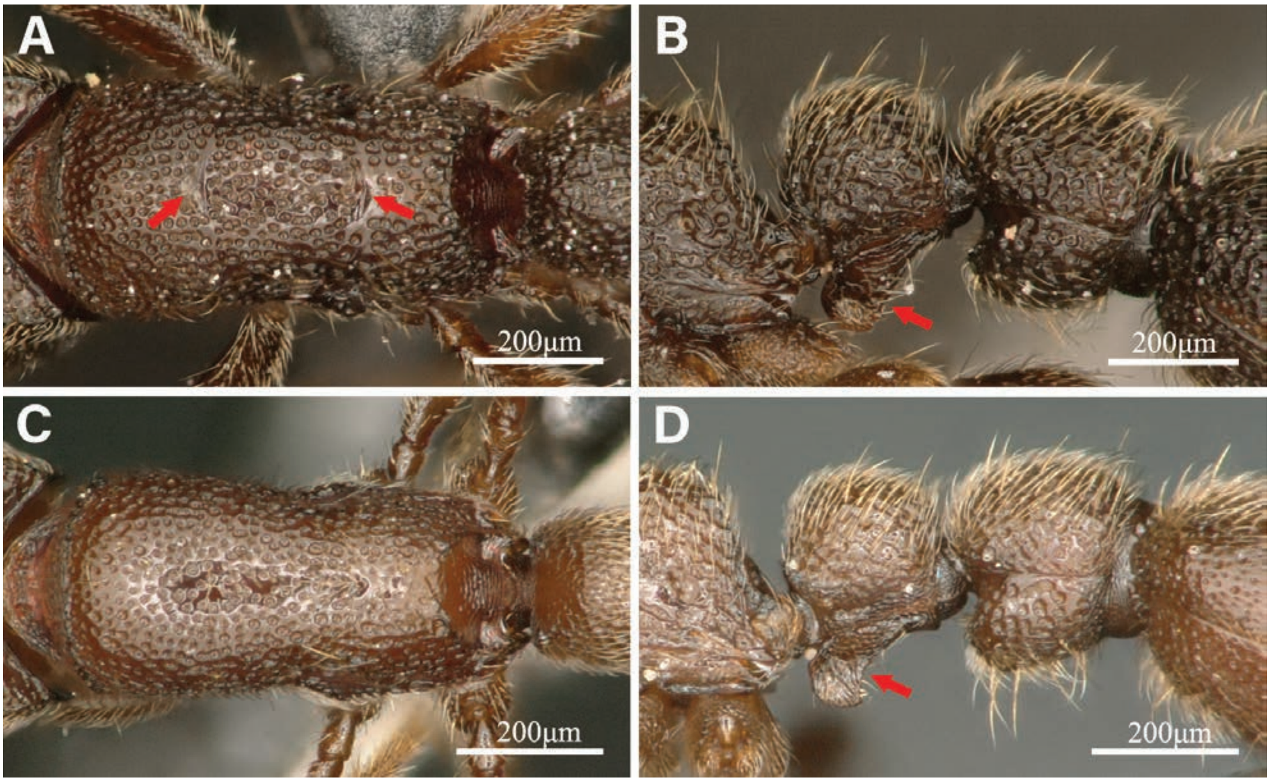

**Figure 2.** Differences between *Ooceraea hainingensis* sp. nov. and *O. biroi* workers **A** *O. hainingensis* mesosoma in dorsal view **B** *O. hainingensis* petiole and postpetiole in lateral view **C** *O. biroi* mesosoma in dorsal view **D** *O. biroi* petiole and postpetiole in lateral view. The red arrows indicate the significant differences between the two species.

than petiole (WI, 117–135), with lateral margins slightly convex. Postpetiolar tergite in lateral view consists of a convex dorsum that is larger than the sternite. The first gastral tergite (abdominal tergite IV) elongated elliptically in dorsal view, with its anterior margin concave and the lateral margin convex.

***Sculpture*:** The head, mesosoma, petiole, and postpetiole with dense foveae, with foveae in mesosoma, petiole, and postpetiole slightly larger than in the head in lateral view. Posterior face of propodeum smooth. The first segment of the gaster (abdominal tergite and sternite IV) densely foveolate; with foveae somewhat smaller than those of cranium and mesosoma. Antennal scape and legs micropunctate. Legs roughly shagreened.

***Pilosity*:** Body entirely densely covered with decumbent or standing hairs.

***Color*:** Body light brown to dark reddish-brown; legs paler.

**Recognition.** *Ooceraea hainingensis* sp. nov. is readily distinguishable from other described *Ooceraea* species by the following characteristics: 9-segmented antenna; eyes absent in the worker caste; the promesonotum slightly convex; the promesonotal suture and metanotal groove obvious; and the subpetiolar process prominent and anteroventrally directed like a thumb with sublinear posteroventral margin.

*Ooceraea hainingensis* sp. nov. is generally similar to *O. biroi*, but these species differ in the shape of the subpetiolar process, promesonotal suture, and metanotal groove (Fig. 2).

**Description of the dealate queen. *Measurement and indices*:** Dealate queen (*N* = 1). HL 0.55, HW 0.48, SL 0.25, EL 0.08, MW 0.41, ML 0.81, PL 0.22, PH 0.37, PW 0.22, PPL 0.28, PPH 0.36, PPW 0.25, CI 87, SI 51, PI1 58, PI2 104, PPI1 77, PPI2 92, WI 113.

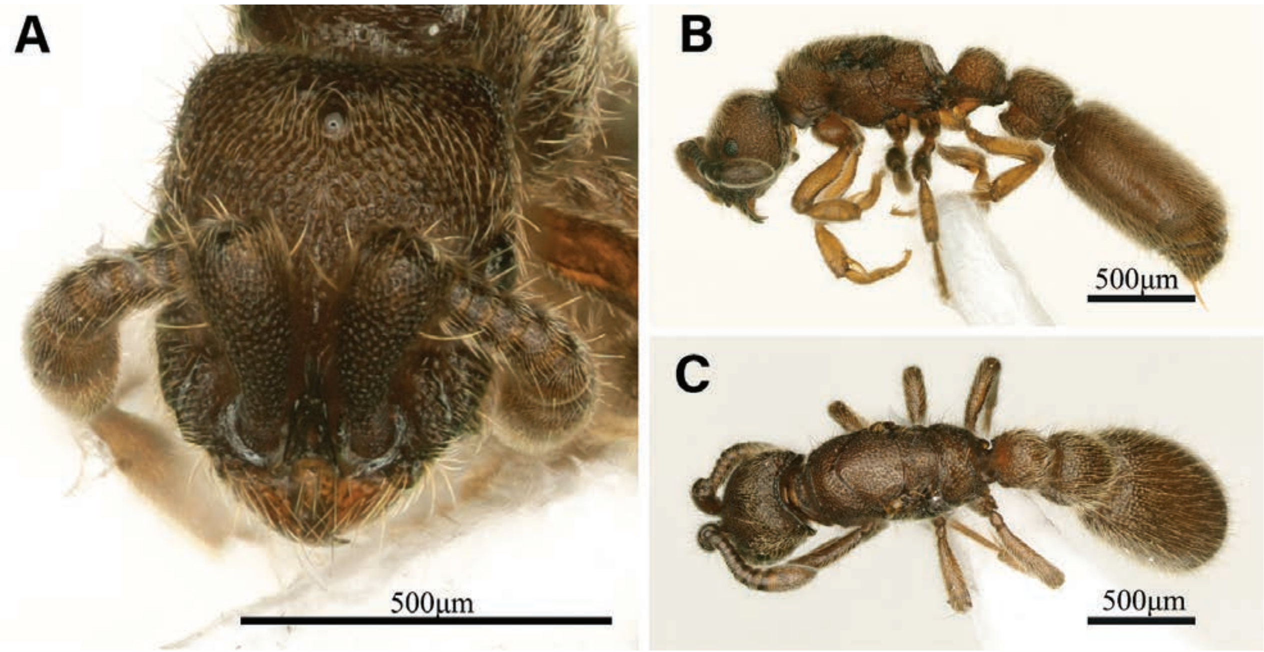

**Figure 3.** *Ooceraea hainingensis* sp. nov. dealate queen, non-type specimen **A** head in full-face view **B** body in lateral view **C** body in dorsal view.

***Queen description*:** Similar to worker in structure, sculpture, coloration and pilosity, but differs from the worker by the following modifications: the body size slightly larger (HW 0.48 in dealate queen, 0.43–0.47 mm in workers; HL 0.55 in dealate queen, 0.50–0.56 mm in workers); compound eyes present approximately at mid-length of the head side; ocelli present and closely approximated (Fig. 3A); mesosoma with unfused flight sclerites.

In lateral view (Fig. 3B), the mesosoma dorsum slightly convex. In dorsal view, the mesoscutum subpentagonal (Fig. 3C), with its lateral sides enclosed by the V-shaped posterior margin of the pronotum; notauli and parapsidal lines absent. The metanotum is narrow. The propodea dorsum with posterior margin concave.

**Male.** Unknown.

**Habitat.** The type specimens are from a colony collected from the Yuemiao Mountain, Haining City of Zhejiang Province in China (30.372187°N, 120.810766°E). The collection site has relatively high canopy cover with low light penetration (Fig. 4A). The temperature at the time of collection was 20 °C. One queen and seventeen worker specimens were collected from the soil in a bamboo forest (Fig. 4B).

**Distribution.** Only known from the type locality.

## Phylogenetic analysis

The maximum likelihood phylogeny indicates that *O. hainingensis* sp. nov. forms a well-supported clade with Line G and Line H, which represent potentially undescribed *Ooceraea* species that were collected in Nghệ An (Vietnam) and Guangdong (China) (Fig. 5, Table 1). In our analysis, this clade is sister to, and genetically distinct from the *O. biroi* clade, which includes representative sequences of isolates of *O. biroi* from its native range in Bangladesh, more

**Figure 4.** The ecology of *Ooceraea hainingensis* sp. nov. **A** habitat at the type locality of *O. hainingensis* from Haining, Zhejiang Province in China **B** live colony of *O. hainingensis* reared in the lab. The red arrow indicates the dealate queen.

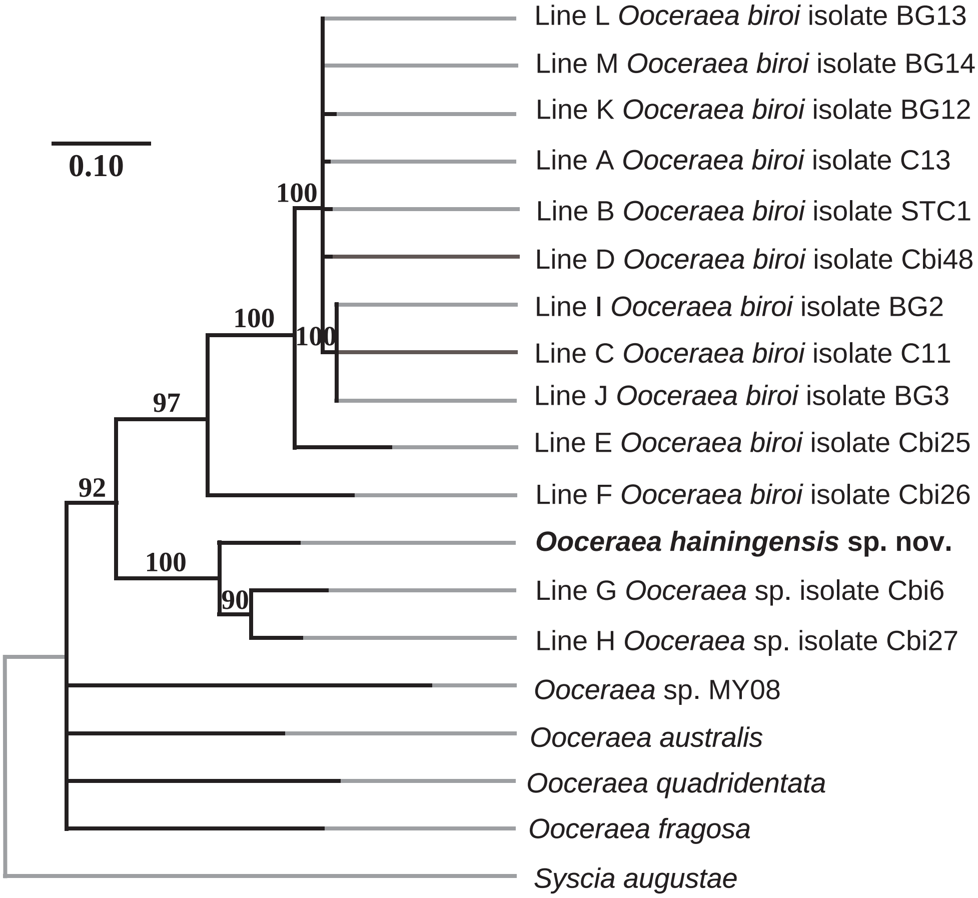

**Figure 5.** Maximum likelihood (ML) phylogenetic tree of *Ooceraea* species based on *COI* + *COII* sequences, with *Syscia augustae* as the outgroup. Numbers above branches indicate bootstrap values, and nodes with bootstrap support < 75 have been collapsed. Phylogenetic branch lengths (black) measured as the number of substitutions per site (see scale bar). The focal species *Ooceraea hainingensis* sp. nov. is highlighted in bold.

distantly related samples from India, and its invasive range globally. The new species of *O. hainingensis* was further supported by the large percentage of sequence differences, i.e., p-distances, calculated in MEGA (Suppl. material 1).

### Key to *Ooceraea* of China

1 Antennae 8-segmented ............................ ***O. octoantenna*** **Zhou et al., 2020**
– Antennae 9-segmented ............................ **2**
2 Promesonotal suture and metanotal groove ambiguous; subpetiolar process prominent and ventrally directed ............................ ***O. biroi*** **Forel, 1907**
– Promesonotal suture and metanotal groove obvious; subpetiolar process prominent and anteroventrally directed like a thumb with sublinear posteroventral margin ............................ ***O. hainingensis*** **sp. nov.**

Note: Although the type locality (Shanghai, China) of previously described *Cerapachys sinensis* Wheeler, 1928 (one of the invalid synonyms of *O. biroi*) is very close to the collecting site of *O. hainingensis* sp. nov., they can be easily distinguished by the shape of the subpetiolar process.

## Discussion

In this study, we describe the worker and queen of *Ooceraea hainingensis* sp. nov., a novel species of *Ooceraea* from southeastern China. Molecular phylogenetic analysis demonstrates that *O. hainingensis* sp. nov. is a close relative of *O. biroi*, an emerging model species that lacks the queen caste and reproduces asexually via thelytokous parthenogenesis. The presence of queens in *O. hainingensis* sp. nov. suggests that the loss of the queen caste occurred in the lineage leading to *O. biroi* after the divergence of these two species. This improves our knowledge of caste evolution within the genus *Ooceraea*, but a comprehensive understanding will require a more complete taxonomic and molecular phylogenetic study.

It remains unclear when asexual reproduction evolved in *Ooceraea*. Because successful lab rearing or genotyping studies have yet to be conducted on any *Ooceraea* species other than *O. biroi*, it is not known whether other *Ooceraea* species reproduce sexually or asexually. Such studies will shed light on whether asexual reproduction is an ancient trait within *Ooceraea* or whether it evolved concurrently with the loss of the queen caste in the lineage leading to *O. biroi*.

We have only scratched the surface of the diversity of reproductive strategies within *Ooceraea*. First, more species likely remain to be described, meaning that continued collecting efforts in the known range of *Ooceraea* may be worthwhile. Indeed, this study marks the second new *Ooceraea* species discovered in China in recent years, including *O. octoantenna* (see Zhou et al. 2020). Counting *O. biroi* means that three *Ooceraea* species can be found in China, and these can be readily distinguished based on the obvious promesonotal suture and metanotal groove and the morphology of the subpetiolar process. Second, more information is needed about the biology of described species. Apart from *O. biroi*, very few collections of *Ooceraea* are recorded in the literature, meaning that we know almost nothing about within-species variation in reproductive strategies. The recent discovery of a queen-like mutant lineage of *O. biroi* highlighted such within-species variation in caste phenotypes, and revealed candidate molecular mechanisms for caste evolution in *Ooceraea* (see Trible et al. 2023). Comparative genomic studies across and within *Ooceraea* species with diverse reproductive biology might help identify mechanisms of caste evolution in ants. Moving forward, the thorough study of the reproductive biology of this genus will be a goldmine for understanding the evolution and mechanistic basis of caste development and thelytokous parthenogenesis.

## Acknowledgments

We would like to express our gratitude to Zhilin Chen for sharing images of a *Syscia guizhouensis* (Zhou, 2006) specimen while we were drafting our manuscript. Special thanks to reviewers Marek Borowiec and Aiki Yamada, and the subject editor Sebastian Salata for their valuable feedback on the manuscript.

## Additional information

### Conflict of interest

The authors have declared that no competing interests exist.

### Ethical statement

No ethical statement was reported.

### Funding

This study was supported by the Specific Research Project of Guangxi for Research Bases and Talents (AD22035916), the Youth Science Foundation of the Natural Science Foundation of Guangxi Province (2024GXNSFBA010431), and the Project of Bama County for Talents in Science and Technology (No. 20210025).

### Author contributions

Formal analysis: QG. Funding acquisition: QG. Investigation: JL, QG. Methodology: JL. Resources: HL, CL. Writing - original draft: QG. Writing - review and editing: DJCK, QG, CL, JL, KDL, HR.

### Author ORCIDs

Qionghua Gao https://orcid.org/0000-0003-2365-1431
Kip D. Lacy https://orcid.org/0000-0002-3149-8927

### Data availability

All of the data that support the findings of this study are available in the main text or Supplementary Information.

## References

Allio R, Schomaker-Bastos A, Romiguier J, Prosdocimi F, Nabholz B, Delsuc F (2020) MitoFinder: Efficient automated large-scale extraction of mitogenomic data in target enrichment phylogenomics. Molecular Ecology Resources 20(4): 892–905. https://doi.org/10.1111/1755-0998.13160

AntCat (2024) An Online Catalog of the Ants of the World by Barry Bolton. https://www.antcat.org [Accessed 10th April, 2024]

AntWeb (2024) AntWeb. https://www.antweb.org [Accessed 10th April, 2024]

Bharti H, Akbar SA (2013) Taxonomic studies on the ant genus *Cerapachys* Smith (Hymenoptera, Formicidae) from India. ZooKeys 336: 79–103. https://doi.org/10.3897/zookeys.336.5719

Borowiec ML (2016) Generic revision of the ant subfamily Dorylinae (Hymenoptera, Formicidae). ZooKeys 608: 1–280. https://doi.org/10.3897/zookeys.608.9427

Borowiec ML (2019) Convergent evolution of the army ant syndrome and congruence in big-data phylogenetics. Systematic Biology 68(4): 642–656. https://doi.org/10.1093/sysbio/syy088

Brown WL (1975) Contributions toward a reclassification of the Formicidae. v. Ponerinae, tribes Platythyreini, Cerapachyini, Cylindromyrmecini, Acanthostichini, and Aenictogitini. Search: Agriculture; Cornell University Agricultural Experiment Station 15: 1–115.

Folmer O, Black M, Hoeh W, Lutz R, Vrijenhoek R (1994) DNA primers for amplification of mitochondrial cytochrome c oxidase subunit I from diverse metazoan invertebrates. Molecular Marine Biology and Biotechnology 3: 294–299.

Forel A (1907) The Percy Sladen Trust Expedition to the Indian Ocean in 1905, under the leadership of Mr. J. Stanley Gardiner, M.A. Fourmis des Seychelles, Amirantes, Farquhar et Chagos. Transactions of the Linnean Society of London 12: 91–94. https://doi.org/10.1111/j.1096-3642.1907.tb00512.x

Guénard B, Weiser MD, Gomez K, Narula N, Economo EP (2017) The Global Ant Biodiversity Informatics (GABI) database: synthesizing data on the geographic distribution of ant species (Hymenoptera: Formicidae). Myrmecological News 24: 83–89.

Hart T, Frank DD, Lopes LE, Olivos-Cisneros L, Lacy KD, Trible W, Ritger A, Valdés-Rodríguez S, Kronauer DJC (2023) Sparse and stereotyped encoding implicates a core glomerulus for ant alarm behavior. Cell 186(14): 3079–3094. https://doi.org/10.1016/j.cell.2023.05.025

Ivasyk I, Olivos-Cisneros L, Valdés-Rodríguez S, Droual M, Jang H, Schmitz RJ, Kronauer DJC (2023) DNMT1 mutant ants develop normally but have disrupted oogenesis. Nature Communications 14(1): 2201. https://doi.org/10.1038/s41467-023-37945-4

Jaitrong W, Yamane S, Wiwatwitaya D (2021) A new species and a new record of the ant genus *Ooceraea* Roger, 1862 (Hymenoptera: Formicidae: Dorylinae) from Thailand. Far Eastern Entomologist = Dal’nevostochnyi Entomolog 441: 1–10. https://doi.org/10.25221/fee.441.1

Janicki J, Narula N, Ziegler M, Guénard B, Economo EP (2016) Visualizing and interacting with large-volume biodiversity data using client-server web-mapping applications: The design and implementation of antmaps. org. Ecological Informatics 32: 185–193. https://doi.org/10.1016/j.ecoinf.2016.02.006

Kronauer DJ, Pierce NE, Keller L (2012) Asexual reproduction in introduced and native populations of the ant *Cerapachys biroi*. Molecular Ecology 21(21): 5221–5235. https://doi.org/10.1111/mec.12041

Li Z, Bhat B, Frank ET, Oliveira-Honorato T, Azuma F, Bachmann V, Parker DJ, Schmitt T, Economo EP, Ulrich Y (2023) Behavioural individuality determines infection risk in clonal ant colonies. Nature Communications 14(1): 5233. https://doi.org/10.1038/s41467-023-40983-7

Longino JT, Branstetter MG (2021) Integrating UCE phylogenomics with traditional taxonomy reveals a trove of New World *Syscia* species (Formicidae: Dorylinae). Insect Systematics and Diversity 5(2): 1–51. https://doi.org/10.1093/isd/ixab001

Mann WM (1919) The ants of the British Solomon Islands. Bulletin of the Museum of Comparative Zoology at Harvard College 63: 273–391.

Mann WM (1921) The ants of the Fiji Islands. Bulletin of the Museum of Comparative Zoology at Harvard College 64: 401–499.

Oxley PR, Ji L, Fetter-Pruneda I, McKenzie SK, Li C, Hu H, Zhang G, Kronauer DJC (2014) The genome of the clonal raider ant *Cerapachys biroi*. Current Biology 24(4): 451–458. https://doi.org/10.1016/j.cub.2014.01.018

Ravary F, Jaisson P (2004) Absence of individual sterility in thelytokous colonies of the ant *Cerapachys biroi* Forel (Formicidae, Cerapachyinae). Insectes Sociaux 51(1): 67–73. https://doi.org/10.1007/s00040-003-0724-y

Romiguier J, Borowiec ML, Weyna A, Helleu Q, Loire E, Mendola CL, Rabeling C, Fisher BL, Ward PS, Keller L (2022) Ant phylogenomics reveals a natural selection hotspot preceding the origin of complex eusociality. Current Biology 32(13): 2942–2947. https://doi.org/10.1016/j.cub.2022.05.001

Simon C, Frati F, Beckenbach A, Crespi B, Liu H, Flook P (1994) Evolution, weighting, and phylogenetic utility of mitochondrial gene sequences and a compilation of conserved polymerase chain reaction primers. Annals of the Entomological Society of America 87(6): 651–701. https://doi.org/10.1093/aesa/87.6.651

Tamura K, Stecher G, Kumar S (2021) MEGA11: Molecular evolutionary genetics analysis version 11. Molecular Biology and Evolution 38(7): 3022–3027. https://doi.org/10.1093/molbev/msab120

Trible W, Olivos-Cisneros L, McKenzie SK, Saragosti J, Chang NC, Matthews BJ, Oxley PR, Kronauer DJC (2017) *Orco* mutagenesis causes loss of antennal lobe glomeruli and impaired social behavior in ants. Cell 170(4): 727–735. https://doi.org/10.1016/j.cell.2017.07.001

Trible W, McKenzie SK, Kronauer DJC (2020) Globally invasive populations of the clonal raider ant are derived from Bangladesh. Biology Letters 16(6): 20200105. https://doi.org/10.1098/rsbl.2020.0105

Trible W, Chandra V, Lacy KD, Limón G, McKenzie SK, Olivos-Cisneros L, Arsenault SV, Kronauer DJC (2023) A caste differentiation mutant elucidates the evolution of socially parasitic ants. Current Biology 33(6): 1047–1058. https://doi.org/10.1016/j.cub.2023.01.067

Tsuji K, Yamauchi K (1995) Production of females by parthenogenesis in the ant, *Cerapachys biroi*. Insectes Sociaux 42(3): 333–336. https://doi.org/10.1007/BF01240430

Wetterer JK, Kronauer DJC, Borowiec ML (2012) Worldwide spread of *Cerapachys biroi* (Hymenoptera: Formicidae: Cerapachyinae). Myrmecological News 17: 1–4.

Yamada A (2021) *Ooceraea quadridentata* AIK20180302-2 mitochondrial COX1 gene for cytochrome c oxidase subunit I, partial cds. https://www.ncbi.nlm.nih.gov/nuccore/LC611729

Yamada A, Phung THL, Eguchi K (2018) Description of a new species of the ant genus *Ooceraea* Roger, 1862 (Hymenoptera: Formicidae; Dorylinae) from the Vietnam's Central Highlands. Journal of Insect Biodiversity 7(1): 17–23. https://doi.org/10.12976/jib/2018.07.1.2

Zhang J, Pei N, Mi X, Zhang MJ (2017) Package 'phylotools'. dimension, 12. https://github.com/helixcn/phylotools

Zhou S, Chen D, Chen Z (2020) Discovery of novel *Ooceraea* (Hymenoptera: Formicidae: Dorylinae) species with 8-segmented antennae from China. Sociobiology 67(2): 139–143. https://doi.org/10.13102/sociobiology.v67i2.3740

## Supplementary material 1

### Estimates of Evolutionary Divergence between Sequences

Authors: Qionghua Gao, Jiliang Long, Chengyuan Liu, Haoyu Liu, Hao Ran, Kip D. Lacy, Daniel J. C. Kronauer

Data type: xlsx

Explanation note: The number of base differences per site from between sequences are shown. The rate variation among sites was modeled with a gamma distribution (shape parameter = 1.25). This analysis involved 19 nucleotide sequences. Codon positions included were 1st+2nd+3rd+Noncoding. All positions with less than 95% site coverage were eliminated, i.e., fewer than 5% alignment gaps, missing data, and ambiguous bases were allowed at any position (partial deletion option). There were a total of 600 positions in the final dataset. Evolutionary analyses were conducted in MEGA11.

Link: https://doi.org/10.3897/zookeys.1205.118358.suppl1

ZooKeys 1205: 115–167 (2024)
DOI: 10.3897/zookeys.1205.125014

Research Article

# Revision of *Trigastrotheca* Cameron (Hymenoptera, Braconidae, Braconinae) with descriptions of 13 new species

Donald L. J. Quicke[1], Simon Van Noort[2,3], Avunjikkattu Parambil Ranjith[1], Ariel L. L. Friedman[4], Hans Mejlon[5], Buntika A. Butcher[1,2]

1 *Integrative Insect Ecology Research Unit, Department of Biology, Faculty of Science, Chulalongkorn University, Pathumwan, Thailand*
2 *Research and Exhibitions Department, South African Museum, Iziko Museums of South Africa, P.O. Box 61, Cape Town, 8000, South Africa*
3 *Department of Biological Sciences, University of Cape Town, Private Bag, Rondebosch, 7701, South Africa*
4 *The Steinhardt Museum of Natural History, Tel Aviv University, Tel Aviv 69978, Israel*
5 *Museum of Evolution, Zoology, Uppsala University, Norbyvägen 16, SE-752 36 Uppsala, Sweden*
*Corresponding author: Buntika A. Butcher (Buntika.A@chula.ac.th)*

Academic editor: Kees van Achterberg
Received: 9 April 2024
Accepted: 10 May 2024
Published: 21 June 2024

ZooBank: https://zoobank.org/CB5CEA6F-6527-4F21-9957-5A32B7179AB5

Citation: Quicke DLJ, Van Noort S, Ranjith AP, Friedman ALL, Mejlon H, Butcher BA (2024) Revision of *Trigastrotheca* Cameron (Hymenoptera, Braconidae, Braconinae) with descriptions of 13 new species. ZooKeys 1205: 115–167. https://doi.org/10.3897/zookeys.1205.125014

## Abstract

The Old World braconine wasp genus *Trigastrotheca* Cameron is revised. The genus is recorded from the island of Madagascar for the first time based on two new species, *T. christianhenrichi* Quicke & Butcher, **sp. nov.** and *T. formosa* Quicke & Friedman, **sp. nov.** *Trigastrotheca griffini* Quicke, **sp. nov.** is described from Australia; *T. aethiopica* Quicke & Friedman, **sp. nov.** is described from Ethiopia; *T. braeti* Quicke & Butcher, **sp. nov.** is described from Congo; *T. simba* van Noort, **sp. nov.** is described from Tanzania; *T. freidbergi* Quicke & Friedman, **sp. nov.**, *T. carinata* Ranjith, **sp. nov.**, *T. flava* Ranjith, **sp. nov.** and *T. similidentata* Ranjith, **sp. nov.** are described from India; *T. khaoyaiensis* Quicke & Butcher, **sp. nov.**, *T. naniensis* Quicke & Butcher, **sp. nov.**, and *T. sublobata* Quicke & Butcher, **sp. nov.** are described from Thailand. *Trigastrotheca tridentata* is recorded from Thailand for the first time. A putative female of *T. sureeratae* is described for the first time. *Acrocerilia tricolor* Quicke & Ingram, 1993 is transferred into *Trigastrotheca*, as *T. acroceropsis* **nom. nov.** A key is provided for the identification of species.

**Key words:** Identification key, molecular phylogeny, morphology, parasitoid, taxonomy

## Introduction

*Trigastrotheca* Cameron is a small genus of highly distinctive parasitoid wasps known mainly from the Indo-Australian region (Enderlein 1920; Quicke et al. 2017; Raweearamwong et al. 2020) but also occurring in Africa and Australia (Quicke and Ingram 1993). The unique morphological characteristic of *Trigastrotheca* is the modified posterior margin of the fifth metasomal tergite with strong submedial posterior emarginations giving rise to a medial and pair of sublateral points in the female (Quicke 1987). The otherwise similar males lack these modifications and have rather long and posteriorly weakly convex T5. The latter led van Achterberg (1983) to describe a male of a species from west Africa (Sierra Leone) in a separate genus, *Kenema* van Achterberg. Quicke (1987), having seen series comprising both sexes, considered *Kenema* to be a junior subjective synonym of *Trigastrotheca*. However, van Achterberg and Sigwalt (1987) did not follow this and described a second species under the generic name *Kenema*, from Senegal based only on a male and provided a key to separate the two genera. We reject this, as did Samartsev (2023) as the characters employed are either sexually dimorphic or weak, and further, the two species placed in *Kenema* both being from West Africa, could well just display characters of a local species complex.

Until recently, the only species described from tropical Asia was *T. tridentata* (Enderlein, 1920) from Indonesia (Sumatra), the type species of Enderlein's genus *Odontopygia* Enderlein, 1920. *Odontopygia* was synonymised with *Trigastrotheca* by Quicke (1987), although the combination of *T. tridentata* was not actually published until Quicke and van Achterberg (1990). Quicke et al. (2017) considered a specimen of *T. tridentata*, from India to represent a range extension; however, careful re-examination has revealed several further differences and we herein describe it as another new species. *Trigastrotheca costator* Thunberg, 1822, from South Africa, was originally described in the genus *Ichneumon* and later made the type species of *Coelodontus* Roman, 1912, and this was also synonymised with *Trigastrotheca* by Quicke (1987). *Trigastrotheca costator* was later renamed *T. romani* Quicke, 2005, due to homonymy within the genus *Ichneumon* (Quicke and Stanton 2005).

Raweearamwong et al. (2020) provided a checklist to the 15 species recognised at the time, which included eight from the Afrotropical region. Of these *Mesobracon inermis* (Guérin-Meneville, 1848), originally described in the Rogadinae genus *Spinaria*, was transferred to *Trigastrotheca* by Quicke and Stanton (2005) based on the short original description which mentions a dentate posterior metasomal margin of T5 but which lacked illustrations. The species was subsequently listed as such by Yu et al. (2016) and by Raweearamwong et al. (2020). One of us (DLJQ) had overlooked that in his revision of Afrotropical rogadine braconid genera, van Achterberg (1991) who had examined the type specimen, which is deposited in Zoologische Staatssammlung München, Germany and transferred *S. inermis* to the braconine genus *Mesobracon* Szépligeti. Therefore, we do not consider this species further here.

Quicke and Koch (1990) transferred *Habrobracon rugosus* Szépligeti, 1914, from Tanzania to *Kenema*. and to *Trigastrotheca* (Quicke and Stanton 2005), and recently, Samartsev (2023) transferred *Habrobracon notata* Szépligeti, 1914, from Equatorial Guinea, to *Trigastrotheca*. Both species, are based only on their male holotypes in the MNB, and are therefore excluded from the present study.

The only known host record is for the East African *T. laikipiensis* Quicke which is an idiobiont brood parasite attacking eggs, larvae, and pupae of acacia-ants, predominantly *Crematogaster* Lund, 1831, species (Quicke and Stanton 2005; Stanton et al. 2005). However, since acacia ants do not occur in Asia or Australia, their hosts there must belong to other groups. One possibility might be ant plants such as *Myrmecodia* species (Rubiaceae).

Here we consider the world fauna as a whole and recognise a total of 26 described and valid species of which we describe and illustrate 13 as new and transfer one species from *Acrocerilia* van Achterberg, 1989, to the genus. We present a key to the world species although excluding Afrotropical members known only from males which were described under the generic name *Kenema* since we are currently unable confidently to integrate into the taxonomy either by associating with similarly colored species described from females or confirming that they are indeed separate species. Additionally, notes are provided on *T. acroceropsis* nom. nov., *T. trilobata*, and *T. romani*, and their holotypes illustrated photographically. The female specimen of *T. sureeratae* is described for the first time.

## Materials and methods

Terminology follows van Achterberg (1988) except for wing venation nomenclature which follows Sharkey and Wharton (1997); see also fig. 2.2 in Quicke (2015) for comparison of wing venation naming systems. Femur lengths were measured excluding the trochantellus. Metasomal tergite/tergites are abbreviated as **T/TT**.

Specimens were imaged by a variety of different systems. Those of *T. christianhenrichi* sp. nov. and *T. aethiopica* sp. nov. were taken with a Leica DFC295 digital camera mounted on a Leica M205C microscope; image stacks were processed with Leica Application Suite 4.2.0 and Helicon Focus 5.3. The holotype of *T. trilobata* and types of *T. simba* sp. nov. were imaged at SAMC with a Leica LAS 4.9 imaging system, comprising a Leica® Z16 microscope with a Leica DFC450 Camera and 0.63 × video objective attached. The imaging process, using an automated Z-stepper, was managed using the Leica Application Suite V 4.9 software installed on a desktop computer. Diffused lighting was achieved using a Leica LED 5000 Dome. Specimens of *T. griffini* sp. nov. were imaged using a Keyence VHX-7000 Digital microscope and Keyence image stitching software. Images of *T. carinata* sp. nov., *T. flava* sp. nov. and *T. similidentata* sp. nov.were taken with Keyence VHX-6000 digital microscope. The specimen of *T. sublobata* sp. nov. was imaged using an Olympus SXZ16 microscope with an Olympus DP72 camera and images combined using the Cell^D image processing system.

Collections holding specimens are abbreviated as follows:

| | |
|---|---|
| **AIMB** | ATREE Insect Museum, Bengaluru, India; |
| **CUMZ** | Insect Museum, Chulalongkorn University Museum of Natural History, Bangkok, Thailand; |
| **CNCO** | Canadian National Collection of Insects, Ottawa; |
| **DZUC** | Department of Zoology, University of Calicut, Kerala, India; |
| **NHMUK** | Natural History Museum, London, U.K.; |
| **HNHM** | Hungarian Natural History Museum, Budapest, Hungary; |
| **SMNHTAU** | The Steinhardt Museum of Natural History, Tel Aviv University, Tel Aviv, Israel; |
| **MNB** | Museum für Naturkunde, Humboldt Universität, Berlin, Germany; |
| **SAMC** | Iziko South African Museum, Cape Town, South Africa. |

### Molecular methods

Sequences for the barcoding region of cytochrome oxidase *c* subunit 1 (COI) and for the D2-D3 expansion region of 28S rDNA (28S) were generated from wasp legs by the Centre for Biodiversity Genomics, University of Guelph, based on standard protocols as described in Hebert et al. (2003), Park et al. (2010), and Quicke et al. (2023a) respectively. Alignment of COI was trivial as there were no indels. The length-variable 28S sequences were aligned according to the secondary structure model of Gillespie et al. (2005) as in other studies

(Butcher et al. 2014; Quicke et al. 2016). The concatenated data set was analysed using the maximum likelihood programme RAxML-NG (Kozlov et al. 2019) with full bootstrap (100 replicates). Outgroups were selected from the clade that was recovered as immediate sister group to *Trigastrotheca* in the four gene maximum likelihood (IQ-TREE) analysis of the Braconinae by Quicke et al. (2023a), together with a representative of *Physaraia* Shenefelt, from the next closest clade.

Gene sequences are deposited in GenBank and accession numbers are given in Table 1.

**Table 1.** *Trigastrotheca* specimens used for molecular analyses with their provenances and GenBank accession numbers for sequence analysed.

| Taxon | Provenance | Sample Process ID | GenBank Accessions Nos. | |
|---|---|---|---|---|
| | | | COI | 28S |
| *T. braeti* sp. nov. | Republic of Congo | BBTH4962-22 | PP782008 | – |
| *T. doiphukhaensis* | Thailand | BBTH1811-19 | ON325092 | OQ848751 |
| *T. doiphukhaensis* | Thailand | BBTH3135-22 | PP782009 | – |
| *T. formosa* sp. nov. | Madagascar | BBTH744-17 | PP782007 | – |
| *T. formosa* sp. nov. | Madagascar | BBTH743-17 | MH260662 | MH234981 |
| *T. griffini* sp. nov. | Australia | NSWHP2575-19 | OQ928290 | OQ924399 |
| *T. khaoyaiensis* sp. nov. | Thailand | BBTH3133-22 | PP782011 | – |
| *T. khaoyaiensis* sp. nov. | Thailand | BBTH3134-22 | OQ928234 | – |
| *T. laikipiensis* | Kenya | BBTH1634-18 | ON324918 | ON128915 |
| *T. sureeratae* | Thailand | BBTH569-16 | MH260659 | MH234978 |
| *T. sureeratae* | Thailand | BBTH714-17 | PP782010 | PP782168 |
| *T. sureeratae* | Thailand | BBTH3136-22 | PP782012 | – |
| *T. tridentata* | Thailand | BBTH2668-21 | ON324922 | ON128916 |
| *T. tridentata* | Thailand | ASQSQ481-09 | HM435195 | ON128916 |
| *T. aethiopica* sp. nov. | Ethiopia | BBTH740-17 | MH260693 | MH235015 |
| *Philomacroploea* sp. | Thailand | BBTH2780-21 | MH260667, ON325042 | MH234988 |
| *Crinibracon chromusae* | India | DQHYM079-17 | MH260687 | MH235009 |
| *Physaraia* sp. | South Africa | ETKII915-12 | ON324968 | ON128926 |
| *Simplicibracon* sp. | South Africa | GMSAQ502-13 | OQ928236 | OQ922158 |
| *Testudobracon longicaudis* | Japan | GBAH22892-19 | LC020125 | – |

## Results

### Molecular analysis

The most likely phylogenetic tree obtained by analysis of the concatenated data set is shown in Fig. 1 with bootstrap support value ranges ≥ 75% indicated. The genus *Trigastrotheca* had 100% bootstrap support. *Trigastrotheca tridentata* was strongly supported (100% bootstrap) as sister group to *T. sureeratae* Quicke & Butcher, 2017, and three other Thai species (*T. doiphukhaensis* Raweearamwong, Quicke & Butcher, *T. khaoyaiensis* sp. nov. and *T. naniensis* sp. nov.) formed a clade with 96% bootstrap support, which, in turn, formed the sister group to the Australian *T. griffini* sp. nov. with 87% support.

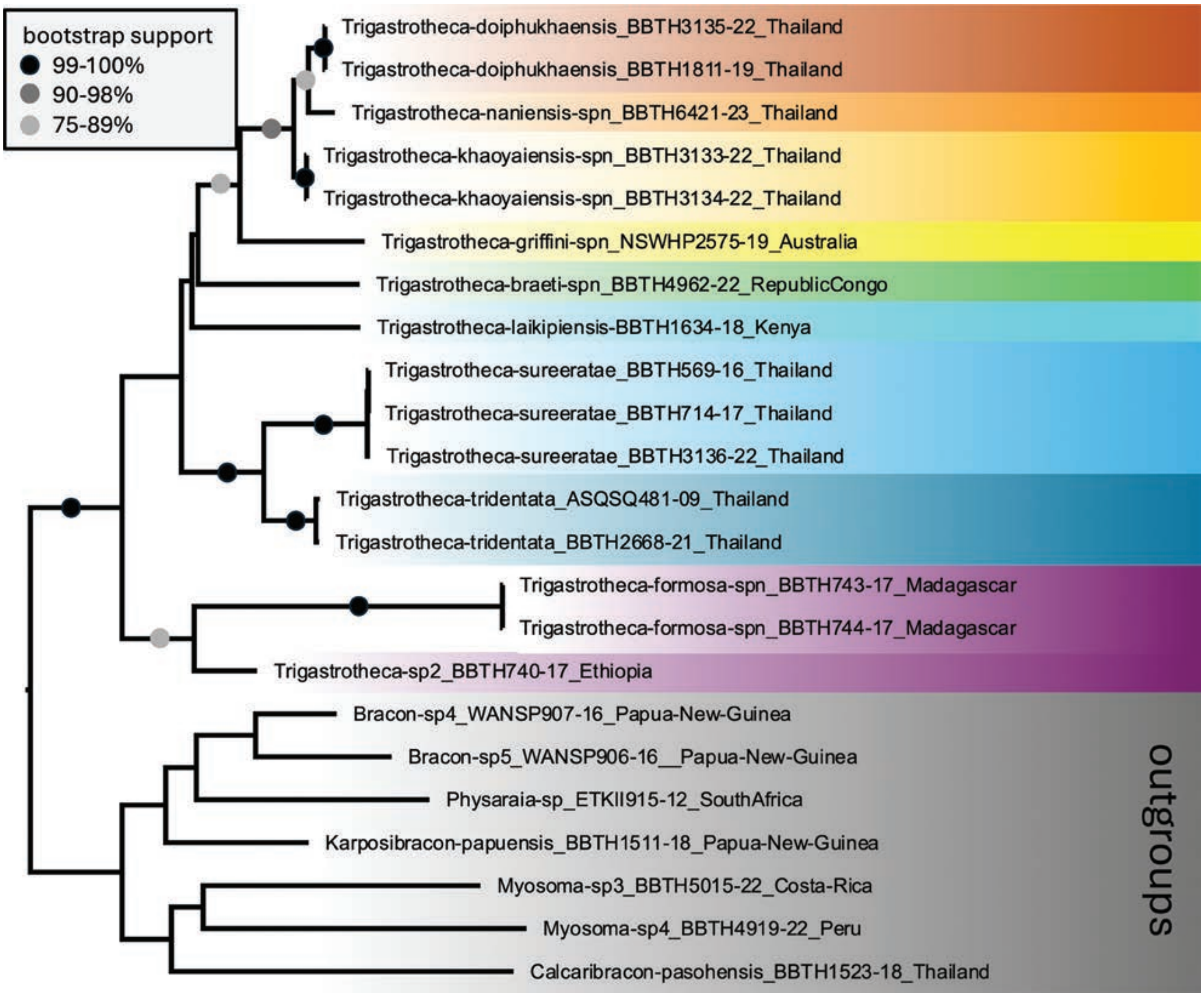

**Figure 1.** Maximum likelihood bootstrap tree of all available *Trigastrotheca* sequences rooted with a representative of the putatively closely related genera, based on analysis of concatenated cytochrome oxidase (COI) and 28S rDNA sequences.

## Key to the species of *Trigastrotheca* – not including males of Afrotropical species with entirely ochreous-yellow meso- and metasomas; for these see van Achterberg and Sigwalt (1987)

1 Body unicolourous, mostly ochraceous yellow (Figs 2, 3, 5, 10, 14, 24, 33, 37) .......... **2**

– Body bicolorous or at least metasoma bicolourous or tricolourous (combinations of black, red-brown, ochreous yellow and ivory white/cream) (Figs 7, 12, 17, 19, 21, 25, 27, 29) .......... **9**

2 (1) Stemmaticum entirely yellow (Figs 3C, 5C) .......... **3**

– Stemmaticum largely or entirely piceous or black (Figs 2A, 10C, 14C, 23E, 33D, 36D) .......... **4**

3 (2) Fore wing vein C+SC+R black (Figs 3A, 4C, D) postero-lateral margin of T5 finely denticulate along lateral 0.75 (Fig. 4A); medial lobe of T5 forming obtuse angle (Fig. 4B); eye 2.5 × as long as temple in dorsal view. (Fig. 3C) .......... ***T. braeti* Quicke & Butcher, sp. nov.**

– Fore wing vein C+SC+R brown-yellow (Fig. 6A, B); postero-lateral margin of T5 distinctly more strongly denticulate on lateral 0.6 (Fig. 6A); medial lobe of T5 forming acute angle (Fig. 6C); eye 2.1 × as long as temple in dorsal view (Fig. 5C) ........................................ ***T. carinata*** **Ranjith, sp. nov.**

4 (2) T5 with medial lobe shorter than lateral lobes (Fig. 11B, C); postero-lateral margin of T5 unevenly serrate, denticles more developed laterally (Figs 11A, 24E) ........................................ **5**

– T5 with medial lobe as long as lateral lobes; postero-lateral margin of T5 evenly serrate (Figs 4A, 33E, 37A, D) ........................................ **7**

5 (4) Fore wing vein C+SC+R black (Fig. 24A, F); fore wing vein 3RSa > 1.4 × longer than r-rs (Fig. 24F) ........................................ ***T. simba*** **van Noort, sp. nov.**

– Fore wing vein C+SC+R brown-yellow (Figs 11D, 14A, 16B); fore wing vein 3RSa < 1.2 × longer than r-rs (Figs 11D, 16B) ........................................ **6**

6 (5) OOL 2.0 × POL (Fig. 10C); propodeum without longitudinal striae posteriorly (Fig. 10F); fore wing vein 2RS 1.0 × as long as r-rs (Fig. 11D)... ........................................ ***T. flava*** **Ranjith, sp. nov.**

– OOL > 2.0 × POL (Fig. 14C); propodeum with distinct longitudinal striae posteriorly (Fig. 15C); fore wing vein 2RS > 1.0 × longer than r-rs (Fig. 15B) ........................................ ***T. freidbergi*** **Quicke & Friedman, sp. nov.**

7 (4) Frons and vertex granulate (Fig. 32D); area of frons anterolateral to median ocellus with weakly diverging striae........... ***T. trilobata*** **Cameron, 1906**

– Frons and vertex rugose (Figs 2C, 33D); area of frons anterolateral to median ocellus without striae ........................................ **8**

8 (7) Second metasomal suture evenly wide and crenulated and weakly arched (Fig. 33F); lateral lobes of T5 rounded apically (Fig. 33E) ......... ........................................ ***T. romani*** **Quicke, 2005**

– Second metasomal suture wider and more coarsely crenulated medially and distinctly arched (Fig. 2G); lateral lobes of T5 distinctly acute, spine like (Fig. 2E) ........................................ ***T. aethiopica*** **Quicke & Friedman, sp. nov.**

9 (1) Occiput yellow ........................................ **10**

– Occiput piceous or black ........................................ **15**

10 (9) T2 yellow ........................................ **11**

– T2 dark brown or black medially surrounded by paler marks or at least black medially ........................................ **13**

11 (10) Mesoscutum yellow without dark patches; TT1 and 2 with sublateral brownish patches; semicircular emargination of T5 yellow posteriorly ........................................ ***T. luzonensis*** **Quicke & Butcher, 2017**

– Mesoscutum yellow with dark patches; TT1 and 2 yellow or ivory white; semicircular emargination of T5 ivory white posteriorly ......... **12**

12 (11) Antenna with 41 flagellomeres; notauli distinct, impressed; fore wing veins r-rs and 2RS straight; frons ivory white laterally........................... ........................................ ***T. tricolor*** **Quicke & Ingram, 1993**

– Antenna with at least 51 flagellomeres; notauli virtually absent; fore wing veins r-rs and 2RS wavy; frons yellow laterally.............................. ........................................ ***T. pariyanonthae*** **Quicke & Butcher, 2017**

13 (10) Propodeum black; mesopleuron largely black; scutellum medially black with lateral yellowish spots; T2 with inverted T-shaped blackish patch ........................................ ........ ***T. doiphukhaensis*** **Raweearamwong, Quicke & Butcher, 2020**

– Propodeum yellow; mesopleuron yellow; scutellum yellow; T2 almost completely blackish ........................................ **14**

14 (13) Median area of metanotum with a distinct mid-longitudinal carina; base of hind wing with a well-developed glabrous area distal to vein cu-a; antenna with 49–53 flagellomeres; fore wing length > 4.5 [4.9–5.1] mm...................................... ***T. sureeratae* Quicke & Butcher, 2017**

– Median area of metanotum without mid-longitudinal carina; base of hind wing with reduced setosity but this extending to vein cu-a anteriorly and with only a small glabrous area posteriorly; antennae with 45–47 flagellomeres; fore wing length < 4.0 [3.6] mm ........................................ ................................................................***T. maetoi* Quicke & Butcher, 2017**

15 (9) Mesoscutum reddish yellow or dark chestnut red; without black patches on lateral lobes and on anterior of medial lobe (Figs 8B, 17E, 29D)......**16**

– Mesoscutum with three large black patches on lateral lobes and anterior 1/2 of medial lobe (Figs 19D, 21E, 34E).......................................**19**

16 (15) Hind femur and tibia reddish yellow (Figs 8E, 12E); face uniformly yellow or cream colored without black triangular mark above clypeus (Fig. 12B) ...................................................................................**17**

– Hind femur and tibia reddish black (Figs 17A, 29A); face with black triangular mark above clypeus (Figs 17B, 29B) .................................**18**

17 (16) Flagellum brown-yellow with apical 10 segments black (Fig. 7A); mesoscutum entirely dark chestnut red; scutellum medially black with whitish spots antero-laterally (Fig. 8B); postero-lateral emarginations of T5 shallow (Fig. 8D); mesopleuron with 2 black spots; occiput broadly black on upper 1/2 (Fig. 7C) ....................................................... ......................................***T. christianhenrichi* Quicke & Butcher, sp. nov.**

– Flagellum entirely black (Fig. 12A); mesoscutum with posterior 1/2 of middle lobe cream colored (Fig. 12E); scutellum completely yellow (Fig. 12E); postero-lateral emarginations of T5 deeply curved (Fig. 13A); mesopleuron with 1 black spot (Fig. 12D); occiput yellow (Fig. 12C) ................................***T. formosa* Quicke & Friedman, sp. nov.**

18 (16) Metanotum with mid-longitudinal carina on anterior 1/2, bifurcated forming a large triangular area on posterior 1/2 (Fig. 30A); T2 with large black area medially (Fig. 30B); frons entirely black except with yellow spots antero-laterally (Fig. 29A).......... ***T. acroceropsis* Ranjith & Quicke, nom. nov.**

– Metanotum with complete mid-longitudinal carina (Fig. 17E); T2 with narrow mid-longitudinal black stripe (Fig. 18B); frons black only medially (Fig. 17C) ................................................ ***T. griffini* Quicke, sp. nov.**

19 (15) Scutellum completely yellow without black patches (Fig. 27C); longitudinal black patch on middle lobe of mesoscutum present at anterior 1/2; antenna with 26–28 flagellomeres .............................................**20**

– Scutellum medially black, lateral margins yellow; longitudinal black patch on middle lobe of mesoscutum extending to posterior 1/2; antenna with > 30 flagellomeres.............................................................**22**

20 (19) T5 of female with shallow sub-median semicircular emarginations and medial protuberance weak and very broad and not protruding beyond lateral lobes (Fig. 27E); frons without mid-longitudinal carina ........................................................... ***T. sublobata* Quicke, sp. nov.**

– T5 of female with deep sub-median semicircular emarginations creating strong medial point that protrudes beyond lateral lobes (Fig. 35A); frons with mid-longitudinal carina ......................................................**21**

21 (20) Mesopleuron with black patches; antenna with 26 or 27 flagellomeres; POL 1.2 × OOL ............................................ ***T. laikipiensis*** **Quicke, 2005**

– Mesopleuron without black patches; antenna with 38 flagellomeres; POL 0.4 × OOL ........................... ***T. sureeratae*** **Quicke & Butcher, 2017**

22 (19) Face brownish ventrally and laterally (Fig. 25B); pronotum brownish laterally (Fig. 25D); occiput black laterally (Fig. 25C, D) ..................... **23**

– Face completely yellow (Fig. 19B); pronotum yellow except for at most a small blackish spot (Figs 19E, 21D); occiput yellow laterally (Figs 19C, 21C)........................................................................................ **24**

23 (22) T2 with broad brown patch medially; postero-lateral margin of T5 concave laterally forming sharp angulation with lateral margin; T5 brown antero-laterally ....................................... ***T. tridentata*** **(Enderlein, 1920)**

– T2 with narrow piceous patch medially (Fig. 26C); postero-lateral margin of T5 weakly convex merging the lateral margin as smoothly in a curve (Fig. 26B); T5 yellow antero-laterally (Fig. 26D) ........................... ............................................................ ***T. similidentata*** **Ranjith, sp. nov.**

24 (22) T4 thin and pale posteriorly (Fig. 20B); propodeum anterolaterally with cream-colored mark (Fig. 19E); median posterior lobe of T5 narrow, sides converging at an acute angle (Fig. 20B); OOL 2.1 × POL (Fig. 19C) ........................... ***T. khaoyaiensis*** **Quicke & Butcher, sp. nov.**

– T4 black; posteriorly; propodeum entirely black (Fig. 21D); median posterior lobe of T5 broadly rounded, sides converging at an obtuse angle (Fig. 22D); OOL 1.7 × POL (Fig. 21C) ............................................ .................................................. ***T. naniensis*** **Quicke & Butcher, sp. nov.**

## Descriptive taxonomy

### *Trigastrotheca aethiopica* Quicke & Friedman, sp. nov.

https://zoobank.org/DA6BED39-C1C9-467E-9C6C-0CFE555CC2B0
Fig. 2

**Type material.** ***Holotype*** ♀, Ethiopia, Erer River, Rt.4, 20 km E. Harar, 9°14.5'N, 42°14.8'E, 11.ix.2007, 1330 m, coll. L. Friedman (SMNHTAU).

**Diagnosis.** Body ochreous yellow except for piceous stemmaticum. Similar to *T. trilobata* and *T. romani*. Differs from *T. trilobata* in having the anterior of the pterostigma yellow (Fig. 2A). Differs from *T. romani* in having the anterior of pterostigma yellow and the second metasomal suture more strongly arched and distinctly wider medially (Fig. 2G cf. Fig. 33F).

**Description.** Holotype female. Length of body 4.9 mm, fore wing 4.6 mm. ***Head*.** Antenna incomplete with 39 flagellomeres. Terminal flagellomere lost. First flagellomere 1.2 × longer than 2$^{nd}$ and 3$^{rd}$, the latter 1.8 × longer than wide. Width of head: width of face: height of eye = 2.5: 1.5: 1.0. Face with fine transverse striations laterally; with weak mid-longitudinal ridge. Inter-tentorial distance 1.5 × longer than tentorio-ocular distance. Malar suture impressed. Malar space 1.3 × as long as basal width of mandible. Frons strongly impressed with a complete mid-longitudinal carina. Shortest distance between posterior ocelli: transverse diameter of posterior ocellus: shortest distance between posterior ocellus and eye = 1.0: 1.0: 2.5. ***Mesosoma*** 1.4 × longer than high. Mesoscutum rugose; notauli not impressed except very short anterior part with few weak

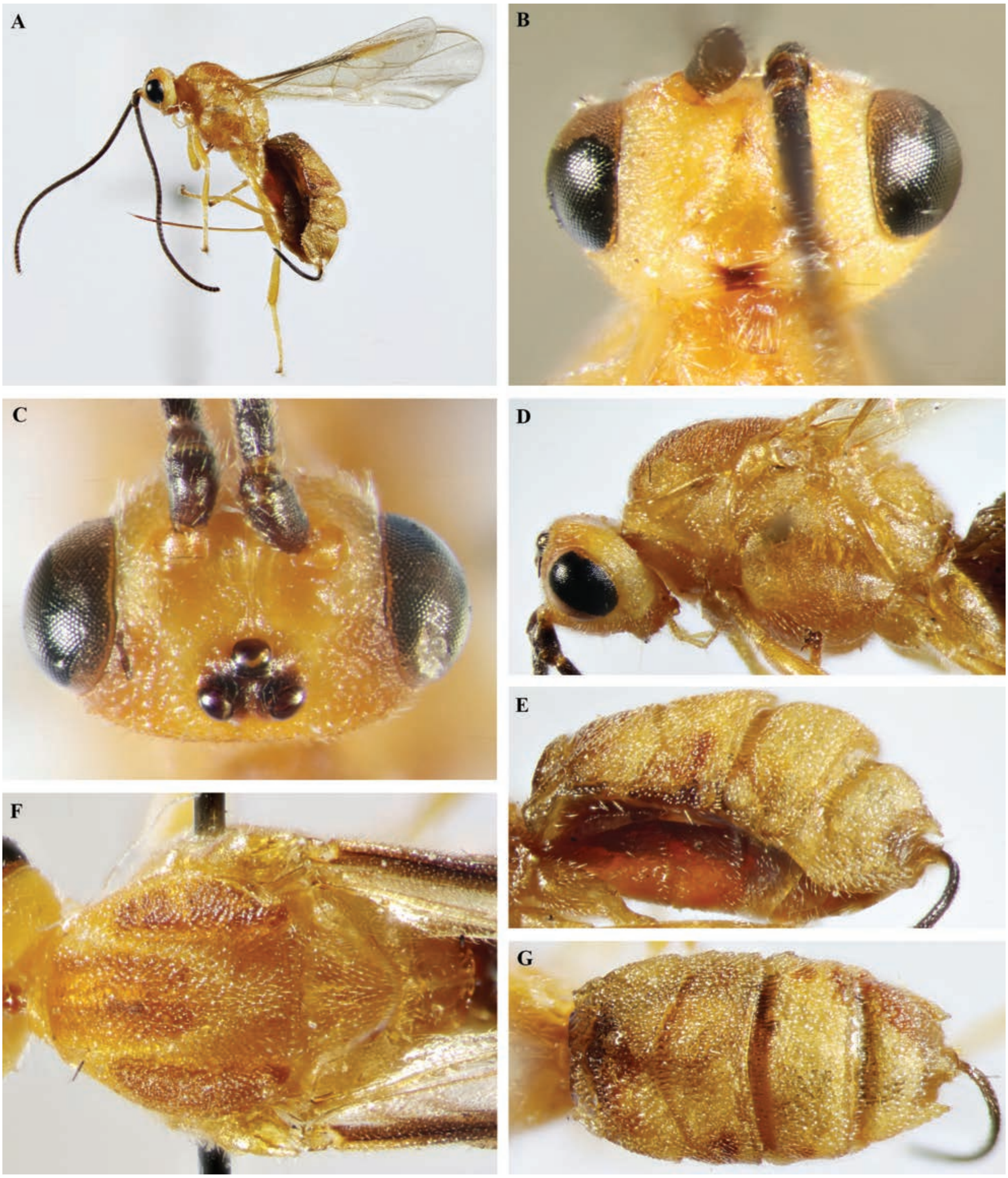

**Figure 2.** *Trigastrotheca aethiopica* sp. nov. ♀, holotype **A** habitus, lateral view **B** head, anterior view **C** head, dorsal view **D** head and mesosoma, lateral view **E** metasoma, lateral view **F** mesosoma, dorsal view **G** metasoma, dorsal view.

crenulations, very shallow posteriorly. Scutellar sulcus shallow, narrow, finely crenulate. Scutellum smooth, setose without small pit medially behind sulcus. Median area of metanotum with complete mid-longitudinal carina. Propodeum largely smooth and shiny; mid-longitudinal carina complete, lamelliform, bordered narrowly by fine crenulations; posteriorly propodeum with short longitudinal carinae associated with longitudinal wrinkles. ***Wings.*** Fore wing. Lengths of fore wing veins r-rs: 3RSa: 3RSb = 1.0: 1.5: 4.7. Lengths of vein 2RS: 3RSa: rs-m = 1.5: 1.5: 1.0. Base of hind wing glabrous. ***Legs.*** Lengths of fore femur: fore tibia: fore tarsus = 1.0: 1.3: 1.3. Lengths of hind femur: hind tibia: hind tarsus = 1.0: 1.2: 1.3. Claws with small acutely pointed basal lobe. ***Metasoma.*** T1 1.6 × wider than long. T2 0.8 × as long as T3. T1 coriaceous. TT1–5 with coarse reticulate sculpture. Second metasomal suture and basal grooves of TT4 and 5 deep, strigose. T5 with postero-lateral margin of convex, distinctly and evenly denticulate; medial protuberance acutely rounded. ***Coloration.*** Body mostly yellow except antenna, eye and tarsi black, and stemmaticum which is dark brown.

**Male.** Unknown.

**Distribution.** Afrotropical (Ethiopia).

**Host.** Unknown.

**Etymology.** Specific name refers to Ethiopia, the provenance of the holotype.

### ***Trigastrotheca braeti*** Quicke & Butcher, sp. nov.

https://zoobank.org/0D16308C-DF02-42B2-A85E-8F46DDF6064E
Figs 3, 4

**Type material. *Holotype*** ♀, The Republic of the Congo, Pool, Abio Lesio-Louna N.P., 1.vi–18.vii.2008, 3.099125°S, 15.27157°W, 330 m, Malaise trap in forest-savanna transition zone, coll. Yves Braet, DNA voucher P.I.D. BBTH4962-22 (CUMZ). ***Paratypes*:** 1 ♀, same data as holotype except 23.x.2008, coll. Y. Braet & M.J. Sharkey, DNA voucher P.I.D. BBTH1561-18 (failed); 1 ♂, same data as holotype except 3°16.1965'S, 15°28.267'E, 23.x.2008, coll. coll. Y. Braet & M.J. Sharkey, DNA voucher P.I.D. BBTH1557-18 (failed) (CUMZ).

**Diagnosis.** Similar to *T. carinata* sp. nov. from India, in having the body including stemmaticum entirely ochreous yellow, but differs in the shape of the head with the eye 2.5 × as long as temple in dorsal view. In addition, fore wing vein C+SC+R black, fore wing veins r-rs and rs-m wavy, and the T5 is relatively more elongate but with the posterior emarginations being shallower and medio-posterior projection being less acute.

**Description.** Holotype female. Length of body 5.0 mm, fore wing 4.3 mm. ***Head.*** Antenna with 41 flagellomeres. Terminal flagellomere, short, sub-triangular, acuminate. First flagellomere 1.0 × longer than 2nd and 3rd, the latter 1.4 × longer than wide. Width of head: width of face: height of eye = 2.5: 1.5: 1.0. Face granulate rugose, transversely striate antero-medially with weak mid-longitudinal ridge. Inter-tentorial distance 1.3 × longer than tentorio-ocular distance. Malar suture impressed. Malar space 1.7 × as long as basal width of mandible. Antennal sockets strongly produced. Frons rugose with a mid-longitudinal groove, strongly moderately behind antennal socket. Shortest distance between posterior ocelli: transverse diameter of posterior ocellus: shortest distance between posterior ocellus and eye = 1.3: 1.0: 2.8. ***Mesosoma*** 1.3 × longer than high. Mesoscutum rugose; notauli not impressed except very short anterior part with few weak crenulations. Scutellar sulcus shallow, narrow, finely crenulate. Scutellum granulate with a small pit medially behind sulcus. Median area of metanotum with complete mid-longitudinal carina. Propodeum rugose; mid-longitudinal carina complete, lamelliform, bordered narrowly by fine crenulations; posteriorly propodeum with short longitudinal carinae associated with longitudinal

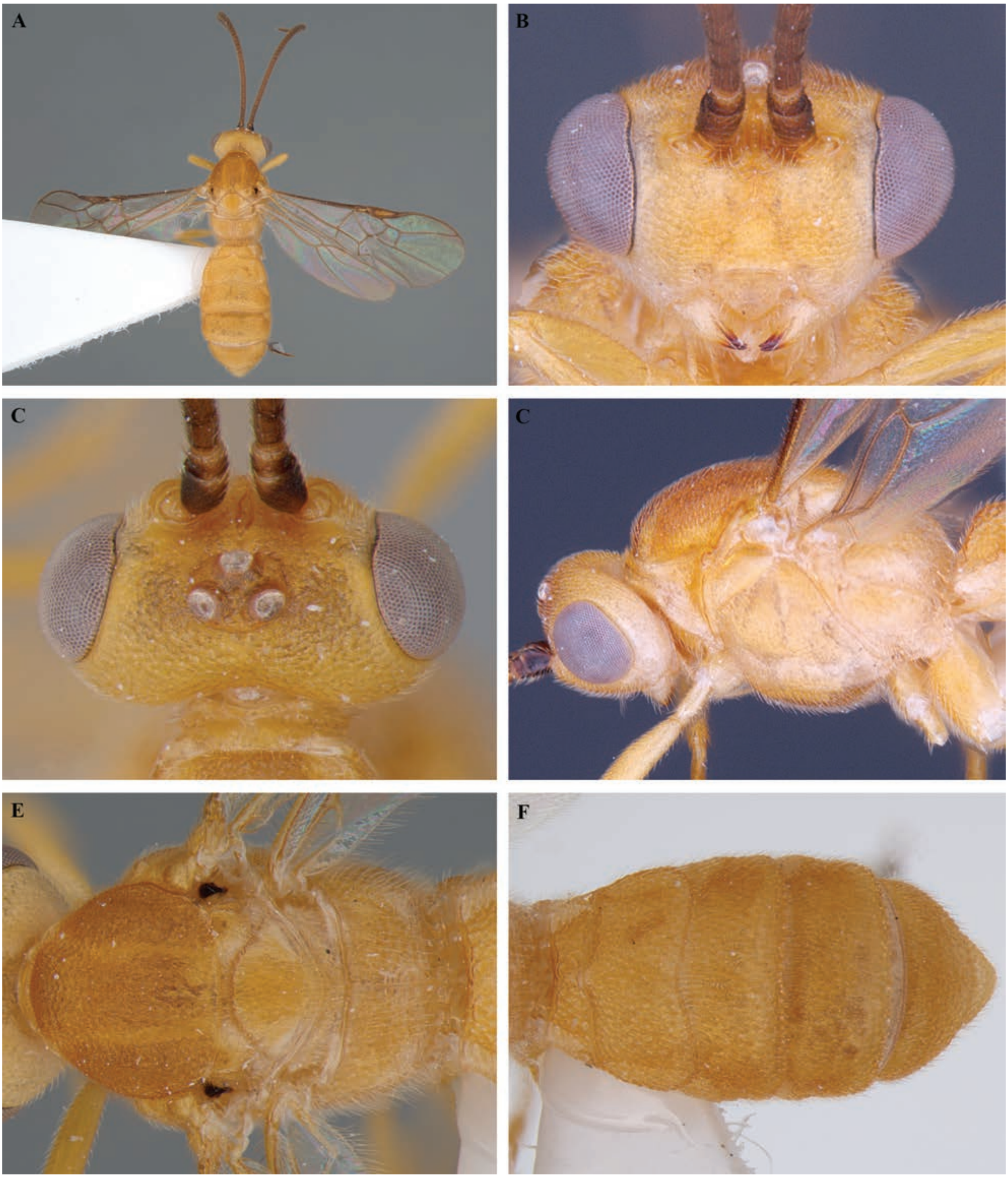

**Figure 3.** *Trigastrotheca braeti* sp. nov. ♀, holotype **A** habitus, dorsal view **B** head, anterior view **C** head, dorsal view **D** head and mesosoma, lateral view **E** mesosoma, dorsal view **F** metasoma, dorsal view.

wrinkles. ***Wings.*** Fore wing. Lengths of fore wing veins r-rs: 3RSa: 3RSb = 1.0: 1.2: 4.7. Lengths of vein 2RS: 3RSa: rs-m = 1.1: 1.0: 1.1. Base of hind wing with short glabrous area. ***Legs.*** Lengths of fore femur: fore tibia: fore tarsus = 1.0: 1.0: 1.1. Lengths of hind femur: hind tibia: hind tarsus = 1.0: 1.3: 1.2. Claws with basal lobe rather small, distally angulate but hardly protruding. ***Metasoma.*** T1 1.5 × wider than long. T2 0.9 × as long as T3. T1 coriaceous. TT1–5 with coarse

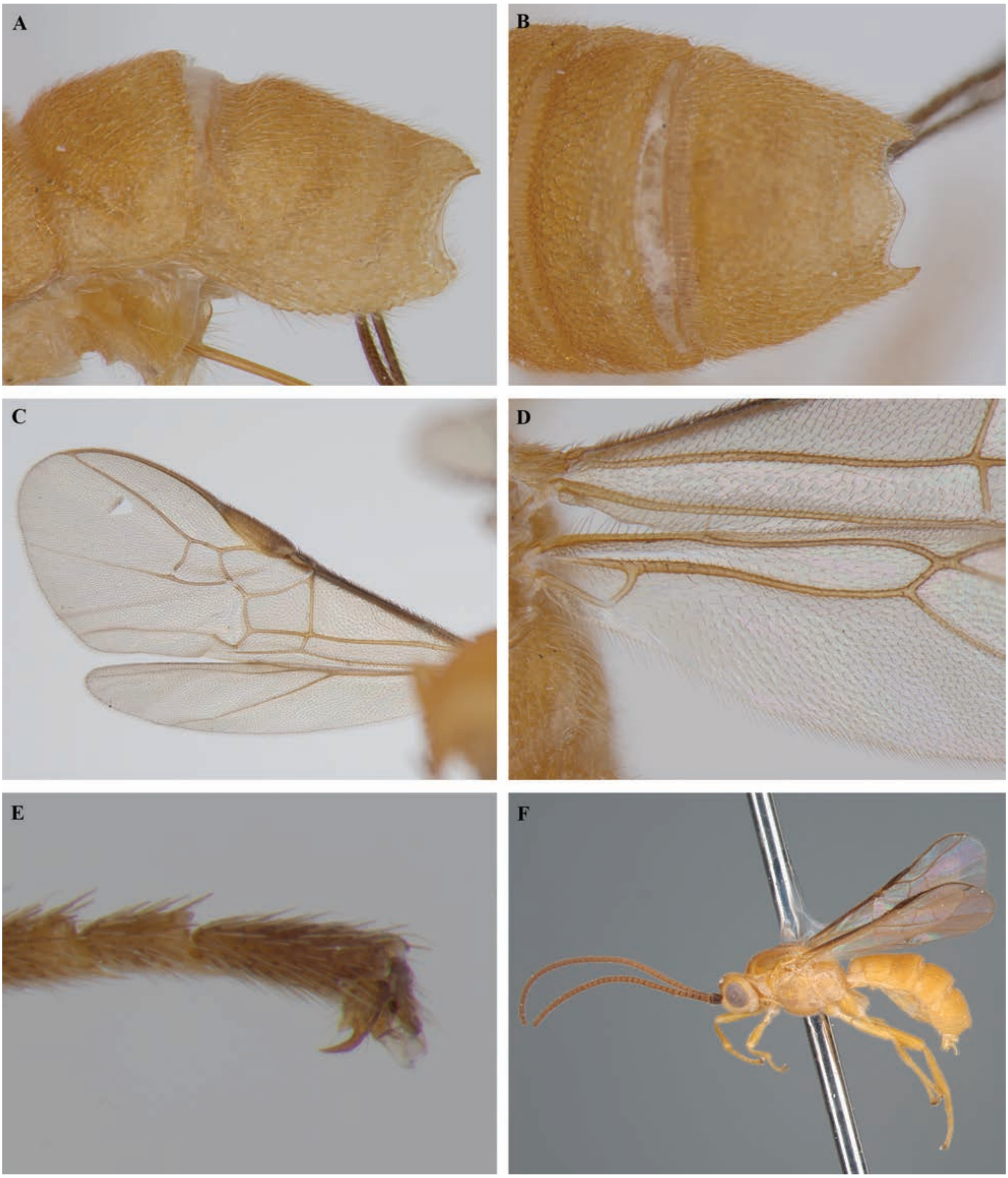

**Figure 4.** *Trigastrotheca braeti* sp. nov. ♀, holotype **A** TT4 and 5, lateral view **B** TT4 and 5, dorsal view **C** wings **D** base of hind wing, detail **E** apex of hind tarsus and claw; Paratype ♂ **F** habitus, lateral view.

reticulate sculpture Second metasomal suture and basal grooves of TT4 and 5 deep, strigose. T5 with postero-lateral margin of convex, indistinctly denticulate; medial protuberance broadly rounded. ***Coloration*.** Body yellow except scape, pedicel, pterostigma, tarsi brown, flagellomere yellowish brown.

**Variation**. Body length 4.6 mm paratype female, 4.4 mm paratype male. Posterior margin of male T5 virtually straight with a weak medial emargination.

**Male.** Same as female.

**Distribution.** Afrotropical (Republic of Congo).

**Host.** Unknown.

**Etymology.** Named after Dr Yves Braet, collector and friend of the senior author.

### *Trigastrotheca carinata* Ranjith, sp. nov.

https://zoobank.org/F747A595-E9F5-4EE3-A958-CE3EBD047B2A
Figs 5, 6

**Type material.** ***Holotype*** ♀, India: Kerala, Palakkad, Silent Valley, 17.iv.2018, Malaise trap, coll. Sinu P.A. (AIMB).

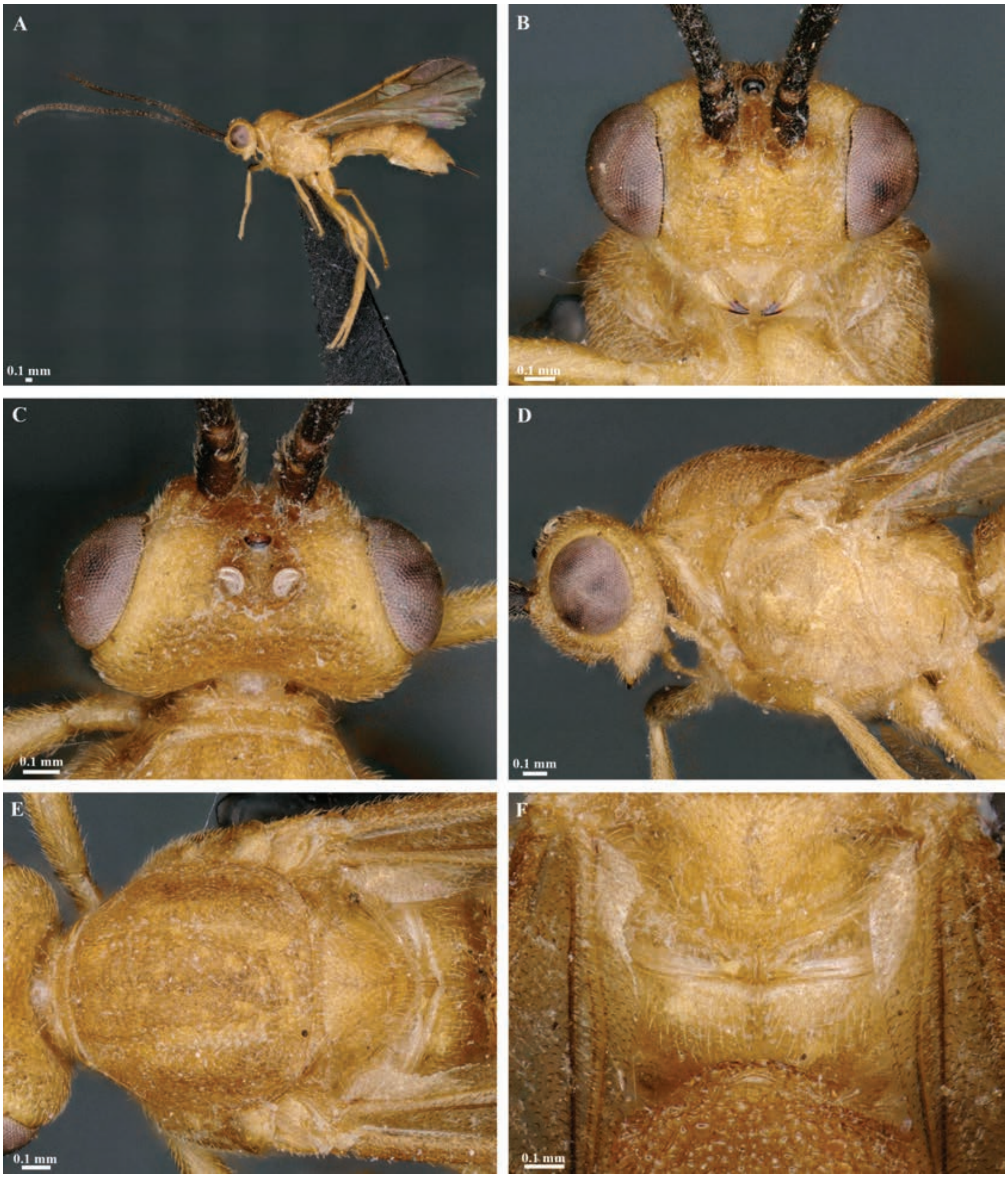

**Figure 5.** *Trigastrotheca carinata* Ranjith, sp. nov. ♀ holotype **A** habitus, lateral view **B** head, anterior view **C** head, dorsal view **D** head and mesosoma, lateral view **E** mesosoma, dorsal view **F** scutellum, metanotum and propodeum, dorsal view.

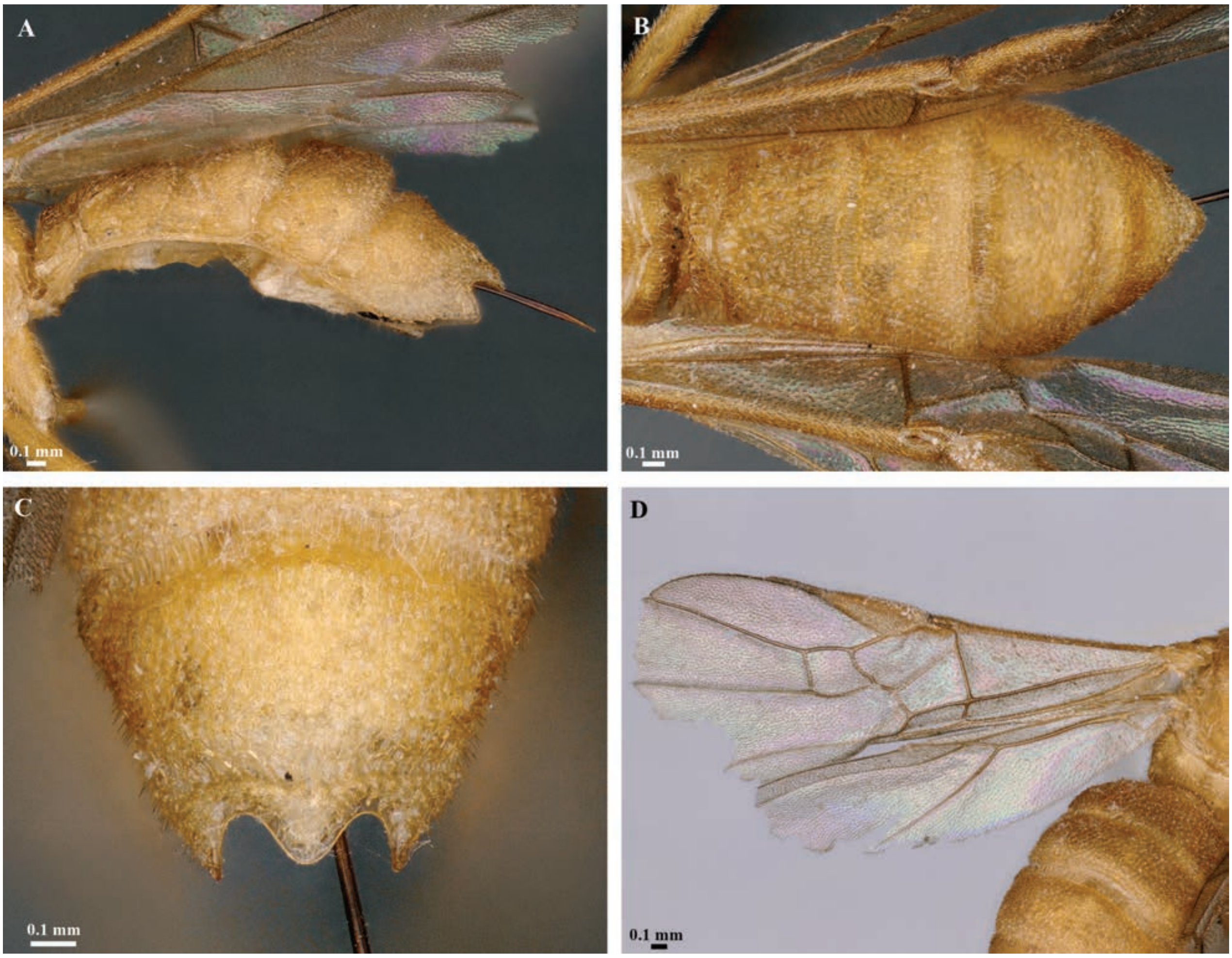

**Figure 6.** *Trigastrotheca carinata* Ranjith, sp. nov. ♀ holotype **A** metasoma, lateral view **B** mesosoma, dorsal view **C** T5, dorsal view **D** wings.

**Diagnosis.** Similar to *T. braeti* sp. nov. from Africa, in having the body including stemmaticum entirely ochreous yellow, but differs in the shape of the head with the eye only 2.1 × as long as temple in dorsal view. In addition, fore wing vein C+SC+R brown-yellow, fore wing veins r-rs and rs-m are not wavy, and the T5 is relatively broader with deeper posterior emarginations and a more acute medio-posterior projection. Similar also to *T. freidbergi* sp. nov. but stemmaticum yellow and T5 relatively far longer (Fig. 6C cf. Fig. 16A).

**Description.** Holotype female. Length of body 4.0 mm, fore wing 3.0 mm. ***Head.*** Antenna with 42 flagellomeres. Terminal flagellomere, short, sub-triangular, acuminate. First flagellomere 1.0 × longer than 2nd and 3rd, the latter 1.3 × longer than wide. Width of head: width of face: height of eye = 2.5: 1.4: 1.0. Face transversely striate-rugose; with weak mid-longitudinal ridge. Inter-tentorial distance 1.4 × longer than tentorio-ocular distance. Malar suture impressed. Malar space 2.1 × as long as basal width of mandible. Antennal sockets strongly produced. Frons strongly impressed behind antennal sockets, with mid-longitudinal carina. Shortest distance between posterior ocelli: transverse diameter of posterior ocellus: shortest distance between posterior ocellus and eye = 1.0: 1.0: 2.1. ***Mesosoma*** 1.4 × longer than high. Mesoscutum rugose; notauli not impressed except very short anterior part with few weak crenulations. Scutellar sulcus shallow, narrow, finely crenulate, very shallow posteriorly. Scutellum sparsely punctate, setose without small pit medially behind sulcus. Median area of metanotum with complete mid-longitudinal carina. Propodeum faintly rugose; mid-longitudinal carina complete, lamelliform, bordered narrowly by fine crenulations; posteriorly propodeum with short longitudinal carinae associated with longitudinal wrinkles. ***Wings*.** Fore wing. Lengths of fore wing veins r-rs: 3RSa: 3RSb = 1.0: 1.3: 4.5. Lengths of vein 2RS: 3RSa: rs-m = 1.0: 1.1: 1.0. Base of hind wing with sparse setae. ***Legs*.** Lengths of fore femur: fore tibia: fore tarsus = 1.1: 1.2: 1.0. Lengths of hind femur: hind tibia: hind tarsus = 2.0: 2.3: 1.0. Claws with small acutely pointed basal lobe. ***Metasoma*.** T1 2.8 × wider than long. T2 1.1 × as long as T3. T1 coriaceous. TT1–5 with coarse reticulate sculpture. Second metasomal suture and basal grooves of TT4 and 5 deep, strigose. T5 with postero-lateral margin of convex, unevenly denticulate; medial protuberance acutely rounded posteriorly. ***Coloration*.** Body mostly yellow except antenna, apex of mandible, tarsi, ovipositor sheath brown.

**Male.** Unknown.

**Distribution.** Oriental (India).

**Host.** Unknown.

**Etymology.** The species is named after the presence of mid-longitudinal carina of frons which will separate the species from other Indian species.

### *Trigastrotheca christianhenrichi* Quicke & Butcher, sp. nov.

https://zoobank.org/1BD13FD7-E056-4E2F-B254-C25074FEC1C8
Figs 7–9

**Type material.** ***Holotype*** ♀, Madagascar, Fianarantsoa Province, Parc National Ranomafana, Malaise trap in mixed tropical forest, radio tower at forest edge, 21°15.05'S, 47°24.43'E, 1130 m, 21–28.i.2002, col. R. Harin'Hala, (CALACAD).

**Diagnosis.** This is the only species with bicolorous antennal flagellum, mostly orange-yellow but with approximately apical 10 black (Fig. 7A). Otherwise with a largely similar color pattern to *T. formosa* sp. nov. though darker red-brown (chestnut), both having a largely red mesoscutum. Unlike in the latter, the back of the head has a wide black mark and the mesoscutum is uniformly red-brown.

**Description.** Length of body 5.0 mm, fore wing 5.3 mm. ***Head*.** Antenna with 50 flagellomeres. Terminal flagellomere, short, sub-triangular, acuminate. First flagellomere 1.1 × longer than 2nd and 3rd, the latter 1.2 × longer than wide. Width of head: width of face: height of eye = 2.1: 1.1: 1.0. Face granulate; with weak mid-longitudinal ridge. Inter-tentorial distance 1.7 × longer than tentorio-ocular distance. Malar suture impressed. Malar space 1.5 × as long as basal width of mandible. Antennal sockets strongly produced, laterally, lamelliform, giving rise posteriorly to a longitudinal carina that divides the anterior frons into four depressed pits, two laterally and two on the sides of carina; lateral to these carinae frons strongly impressed, pit like. Frons, vertex, and occiput granulate. Shortest distance between posterior ocelli: transverse diameter of posterior ocellus: shortest distance between posterior ocellus and eye = 1.5: 1.0: 3.0. ***Mesosoma*** 1.5 × longer than high. Mesoscutum smooth, sparsely punctate; notauli not impressed except very short anterior part with

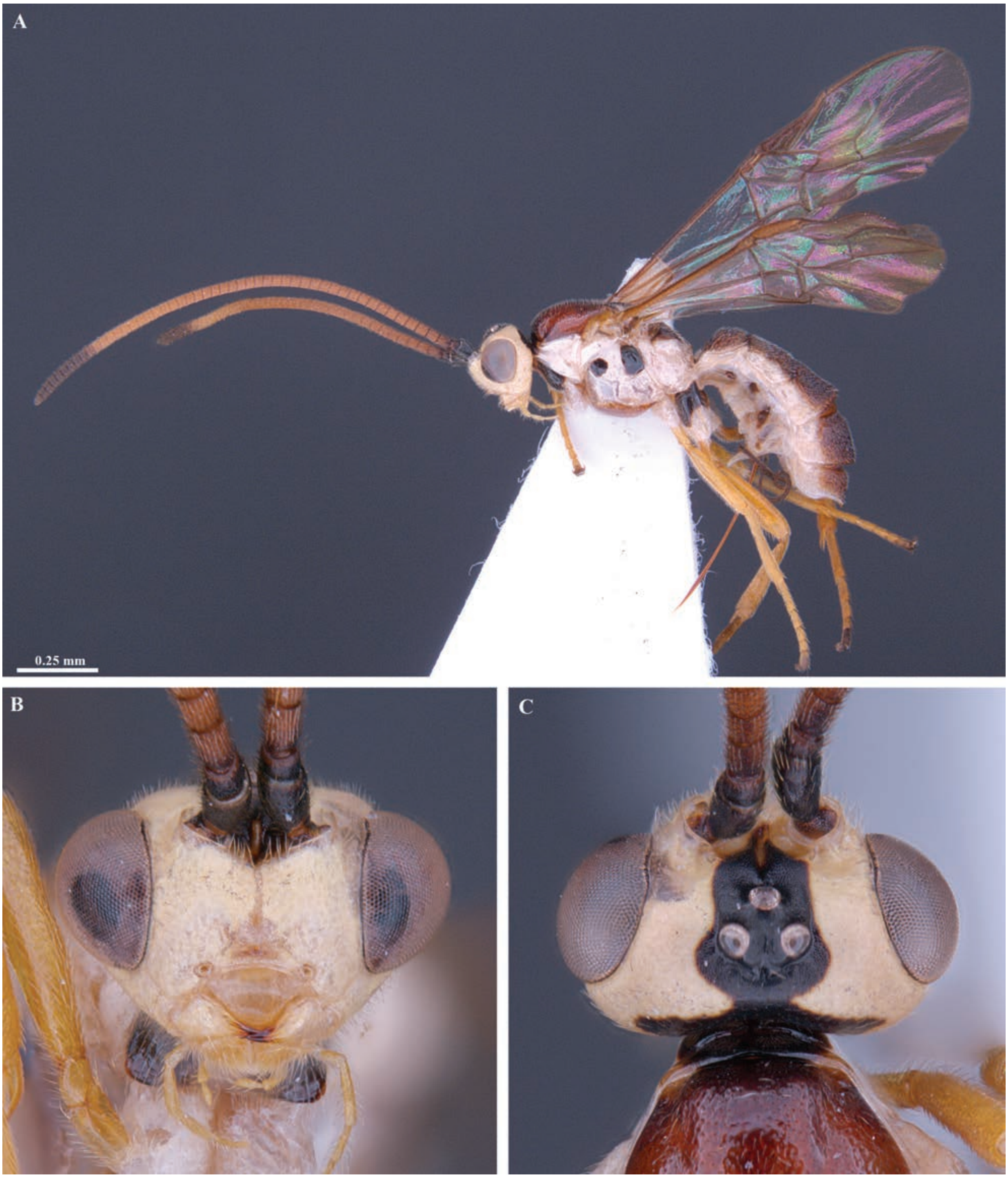

**Figure 7.** *Trigastrotheca christianhenrichi* sp. nov. ♀ holotype **A** habitus, lateral view **B** head, anterior view **C** head, dorsal view.

few weak crenulations, very shallow posteriorly. Scutellar sulcus shallow, narrow, finely crenulate. Scutellum smooth, sparsely setose with a small pit medially behind sulcus. Median area of metanotum with complete mid-longitudinal carina. Propodeum largely smooth and shiny, faintly granulate near mid-longitudinal carina; mid-longitudinal carina complete, lamelliform, bordered narrowly by fine crenulations; posteriorly propodeum with short longitudinal carinae associated with longitudinal wrinkles. ***Wings.*** Fore wing. Lengths of fore wing

**Figure 8.** *Trigastrotheca christianhenrichi* sp. nov. ♀ holotype **A** habitus, except posterior metasoma, lateral view **B** mesosoma, dorsal view **C** metanotum and propodeum, dorsal view **D** metasoma, lateral view **E** mesosoma, dorsal view.

veins r-rs: 3RSa: 3RSb = 1.0: 1.1: 4.3. Lengths of vein 2RS: 3RSa: rs-m = 1.3: 1.5: 1.0. Base of hind wing with large glabrous area distal to vein 1CU. ***Legs.*** Lengths of fore femur: fore tibia: fore tarsus = 1.3: 1.0: 1.2. Lengths of hind femur: hind tibia: hind tarsus = 1.0: 1.1: 1.2. Claws with small acutely pointed basal lobe. ***Metasoma.*** T1 coriaceous, 3.3 × wider than long with a pair of posteriorly narrowing dorsal carina. T2 1.1 × as long as T3. TT1–5 with

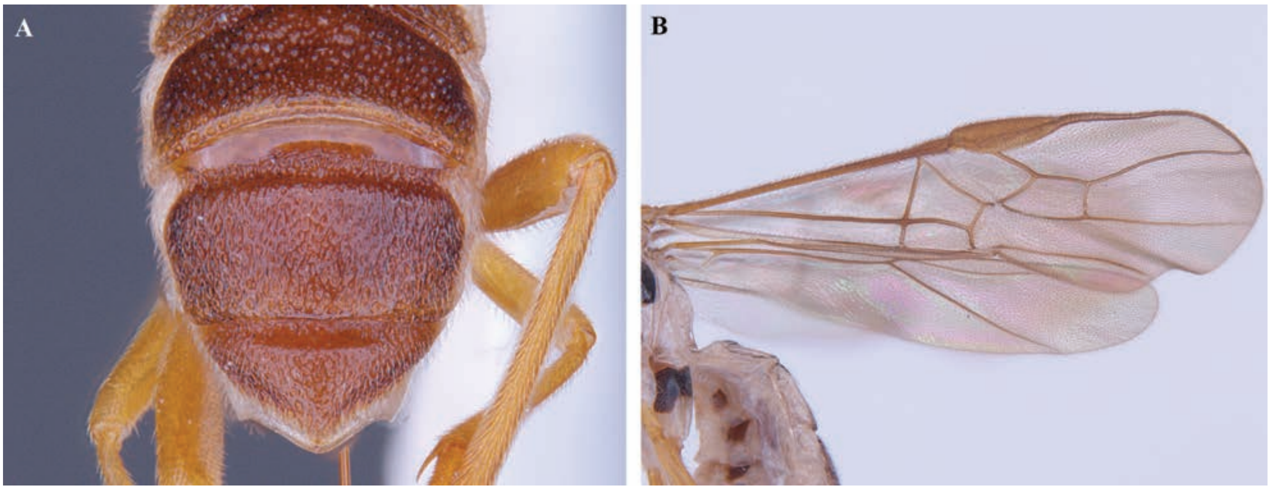

**Figure 9.** *Trigastrotheca christianhenrichi* sp. nov. ♀ holotype **A** TT3–5, dorsal view **B** wings.

coarse reticulate sculpture. Second metasomal suture and basal grooves of TT4 and 5 deep, strigose. T5 with postero-lateral margin of convex, not denticulate; medial protuberance rounded posteriorly; postero-lateral emarginations not defined. ***Coloration.*** Antenna largely reddish brown, scape and pedicel, terminal 10 flagellomeres black. Head ochraceous yellow except for large black, T-shaped mark around stemmaticum and back of head. Mesoscutum reddish brown except blackish anteriorly, pronotum dorsally, propleuron black, pronotum laterally, scutellum antero-laterally and posteriorly, mesopleuron except a pair of black patches, metapleuron, posterior 1/2 of propodeum, fore, mid, and distal 1/2 of hind coxa, metasoma laterally, posterior margin of T5 ivory white, propodeum anterior 1/2, metasoma except laterally reddish brown.

**Male.** Unknown.

**Distribution.** Afrotropical (Madagascar).

**Host.** Unknown.

**Etymology.** Named after the senior author's friend Christian Henrich.

### ***Trigastrotheca flava*** **Ranjith, sp. nov.**

https://zoobank.org/6E22C497-8E35-40FE-AC81-2284C644C3EF

Figs 10, 11

**Type material.** ***Holotype*** ♀, India: Karnataka, Chintamani, 26.v.2010, coll. Somraj Gunda (AIMB). ***Paratypes.*** 4 ♀ with the same data as holotype (AIMB).

**Diagnosis.** Similar to *Trigastrotheca freidbergi* Quicke & Friedman, sp. nov. in being entirely ochraceous with piceous/black stemmaticum and brown-yellow fore wing vein C+SC+R and fore wing with a short 2nd submarginal cell (vein 3RSa being < 1.2 × longer than r-rs and shorter than 2RS).

**Description.** Holotype ♀. Length of body 4.3 mm, fore wing 3.4 mm. ***Head.*** Antenna with 39 flagellomeres. Terminal flagellomere, short, sub-triangular, acuminate. First flagellomere 1.0 × longer than 2nd and 3rd, the latter 1.2 × longer than wide. Width of head: width of face: height of eye = 2.8: 1.5: 1.0. Face finely rugose-punctate with weak mid-longitudinal ridge. Inter-tentorial distance 1.8 × longer than tentorio-ocular distance. Malar suture impressed. Malar space 1.3 × as long as basal width of mandible. Antennal sockets not strongly produced.

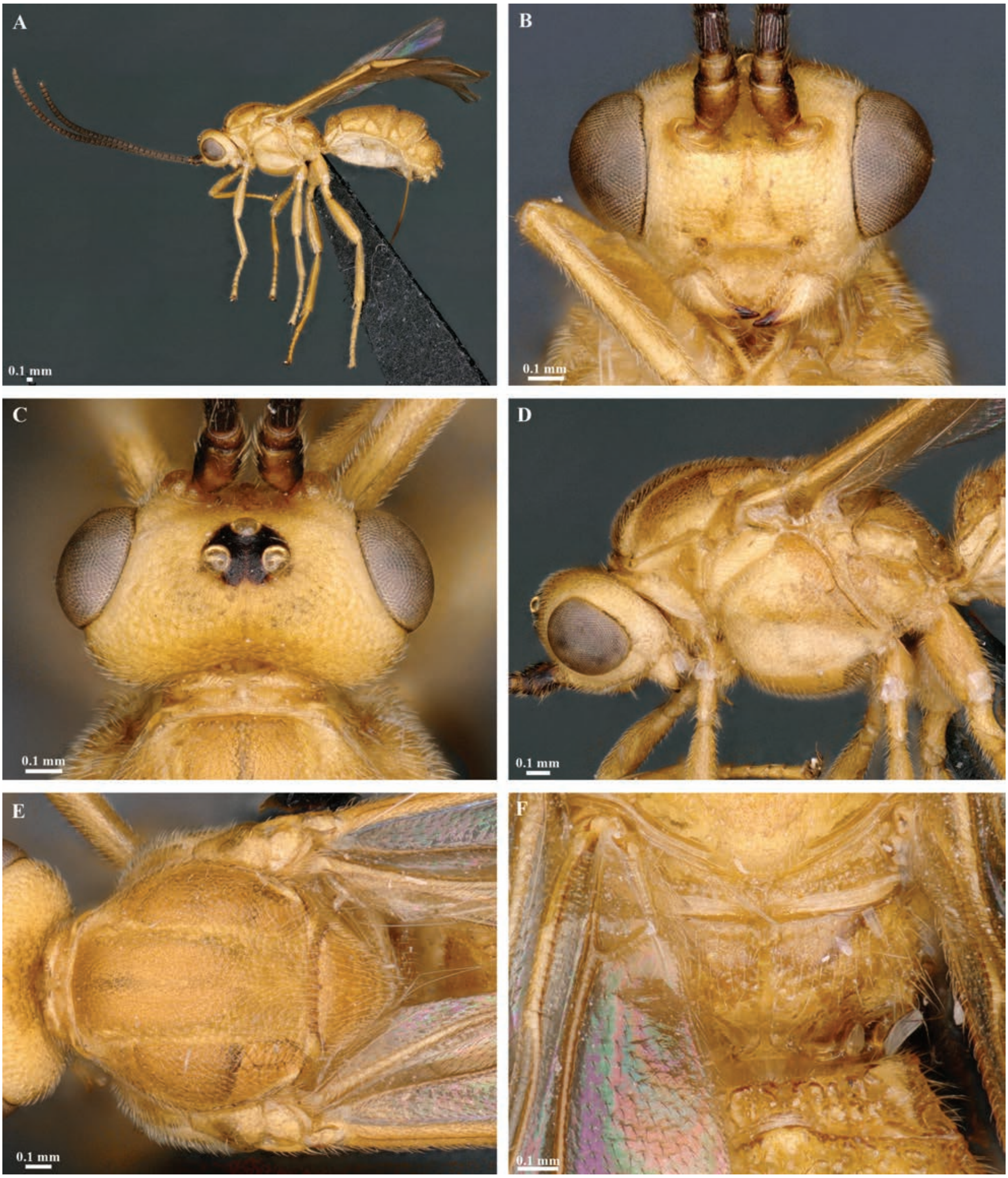

**Figure 10.** *Trigastrotheca flava* sp. nov. ♀ holotype **A** habitus, lateral view **B** head, anterior view **C** head, dorsal view **D** head and mesosoma, lateral view **E** mesosoma, dorsal view **F** metanotum and propodeum, dorsal view.

Frons moderately impressed without mid-longitudinal carina. Shortest distance between posterior ocelli: transverse diameter of posterior ocellus: shortest distance between posterior ocellus and eye = 1.1: 1.0: 2.7. ***Mesosoma*** 1.4 × longer than high. Mesoscutum rugose; notauli not impressed except very short anterior part with few weak crenulations. Scutellar sulcus shallow, narrow, finely crenulate. Scutellum finely punctate without small pit medially behind sulcus.

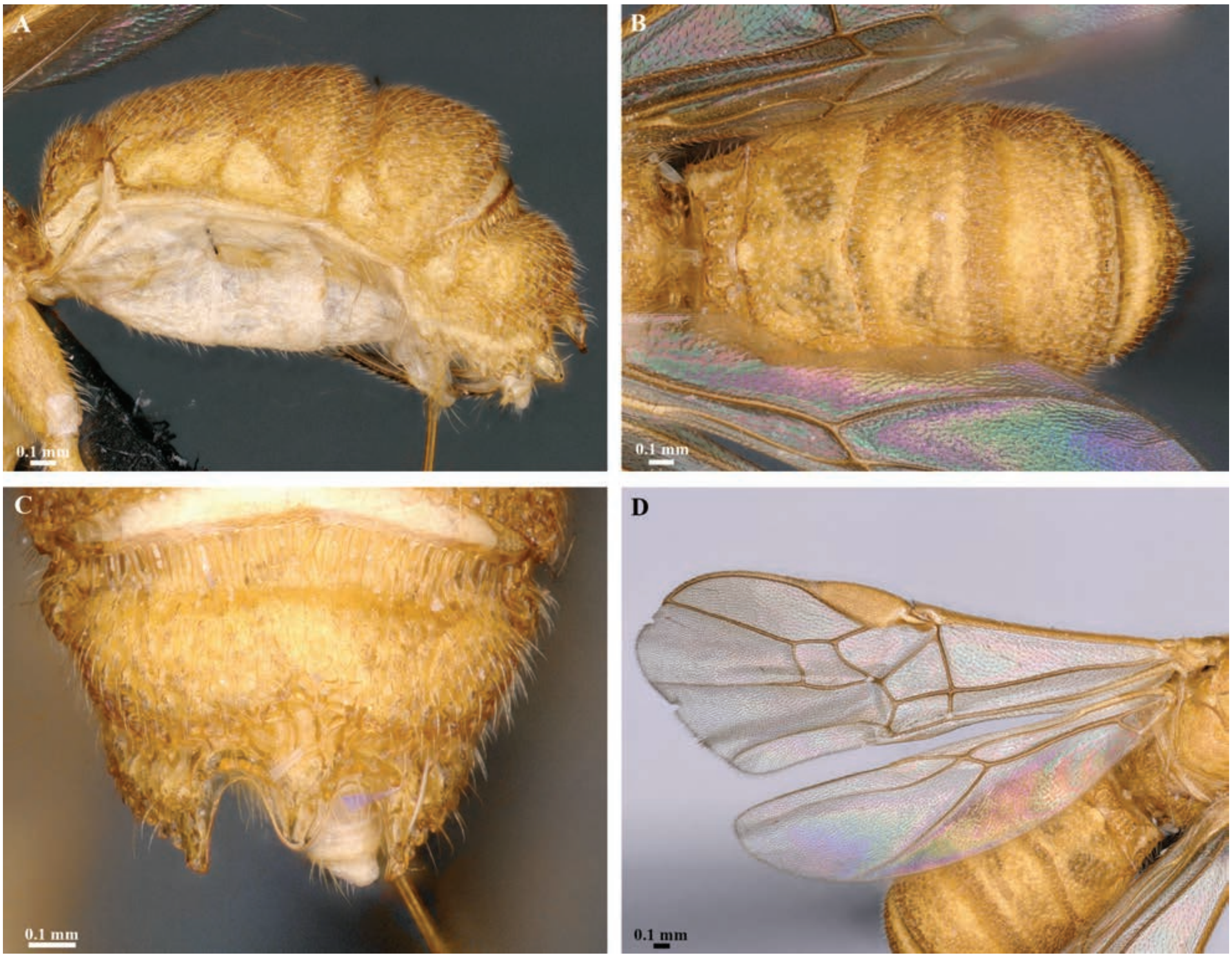

**Figure 11.** *Trigastrotheca flava* sp. nov. ♀ holotype **A** metasoma, lateral view **B** metasoma, dorsal view **C** T5, dorsal view **D** wings.

Median area of metanotum with complete mid-longitudinal carina. Propodeum finely granulate-rugose; mid-longitudinal carina complete, faintly lamelliform, bordered narrowly by fine crenulations; posteriorly propodeum with short longitudinal carinae associated with longitudinal wrinkles. ***Wings.*** Fore wing. Lengths of fore wing veins r-rs: 3RSa: 3RSb = 1.0: 1.2: 3.9. Lengths of vein 2RS: 3RSa: rs-m = 1.3: 1.0: 1.0. Base of hind wing with at least a pair of setae. ***Legs.*** Lengths of fore femur: fore tibia: fore tarsus = 1.0: 1.1: 1.1. Lengths of hind femur: hind tibia: hind tarsus = 2.1: 2.3: 1.0. Claws with small acutely pointed basal lobe. ***Metasoma.*** T1 2.1 × wider than long. T2 0.9 × as long as T3. T1 coriaceous. TT1–5 with coarse reticulate sculpture. Second metasomal suture and basal grooves of TT4 and 5 deep, strigose. T5 with postero-lateral margin of convex, unevenly denticulate; medial protuberance acutely rounded posteriorly. ***Coloration.*** Body mostly yellow except antenna, apex of mandible, ovipositor sheath brown.

**Male.** Unknown.

**Distribution.** Oriental (India).

**Host.** Unknown.

**Etymology.** The species is named after the yellow-colored body, *flava* meaning yellow in Latin.

### ***Trigastrotheca formosa*** **Quicke & Friedman, sp. nov.**

https://zoobank.org/91E3C3CA-0334-47CD-8F8C-7E5EF5A66BF5
Figs 12, 13

**Type material.** ***Holotype*** ♀, Madagascar, Analamatsaky, 47 km W Tolanaro, spiny forest, 25°1.0'S, 46°37.0'E, 21.x.2007, L. Friedman, DNA voucher P.I.D. BBTH744-17 (SMNHTAU). ***Paratypes*****:** 2 ♀, same data as holotype; one DNA voucher P.I.D. BBTH743-17 (SMNHTAU).

**Diagnosis.** Similar to *T. christianhenrichi* sp. nov., also from Madagascar, but differing in having entirely dark flagellum, the black mark on the stemmaticum only extending to a point on the vertex and anterior occiput, the mesoscutum with posterior 1/2 of middle lobe cream-colored, and the scutellum reddish yellow.

**Description.** Length of body 4.1 mm, fore wing 4.2 mm. ***Head*****.** Antenna incomplete with 38 flagellomeres. Terminal flagellomere lost. First flagellomere 1.1 × longer than 2nd and 3rd, the latter 1.5 × longer than wide. Width of head: width of face: height of eye = 2.4: 1.3: 1.0. Face granulate with weak mid-longitudinal ridge. Inter-tentorial distance 1.8 × longer than tentorio-ocular distance. Malar suture impressed. Malar space 1.5 × as long as basal width of mandible. Antennal sockets strongly produced. Frons strongly impressed only behind antennal sockets without mid-longitudinal carina. Frons, vertex, and occiput granulate. Shortest distance between posterior ocelli: transverse diameter of posterior ocellus: shortest distance between posterior ocellus and eye = 1.0: 1.0: 1.7. ***Mesosoma*** 1.5 × longer than high. Mesoscutum smooth, sparsely punctate; notauli crenulated, impressed on anterior 1/2 shallow posteriorly. Scutellar sulcus shallow, narrow, finely crenulate. Scutellum smooth, sparsely setose with a small pit medially behind sulcus. Median area of metanotum with complete mid-longitudinal carina. Propodeum largely smooth and shiny, faintly transversely striate near mid-longitudinal carina; mid-longitudinal carina complete, lamelliform, bordered narrowly by fine crenulations; posteriorly propodeum with short longitudinal carinae associated with longitudinal wrinkles. ***Wings*****.** Fore wing. Lengths of fore wing veins r-rs: 3RSa: 3RSb = 1.0: 1.2: 4.0. Lengths of vein 2RS: 3RSa: rs-m = 1.3: 1.3: 1.0. Base of hind wing with large glabrous area distal to vein 1CU. ***Legs*****.** Lengths of fore femur: fore tibia: fore tarsus = 1.0: 1.0: 1.1. Lengths of hind femur: hind tibia: hind tarsus = 1.0: 1.1: 1.1. Claws with small acutely pointed basal lobe. ***Metasoma*****.** T1 coriaceous, 1.8 × wider than long, with pair of posteriorly uniting dorsal carina. T2 0.8 × as long as T3. TT1–5 with coarse reticulate sculpture. Second metasomal suture and basal grooves of TT4 and 5 deep, strigose. T5 with postero-lateral margin slightly concave, not denticulate; medial protuberance acutely rounded posteriorly; postero-lateral emarginations concave. ***Coloration*****.** Body mostly reddish brown except scape, pedicel, eye, ocellar area, occiput medially, mesoscutum antero-laterally, propleuron, mesopleuron with posterior black patch, T1 medially, ovipositor sheath black, face, clypeus, maxillary and labial palps, frons, vertex and occiput laterally, pronotum dorsally, legs yellow, pronotum laterally, middle lobe of mesoscutum posteriorly, mesopleuron anteriorly, metasoma laterally ivory white.

**Male.** Unknown.

**Distribution.** Afrotropical (Madagascar).

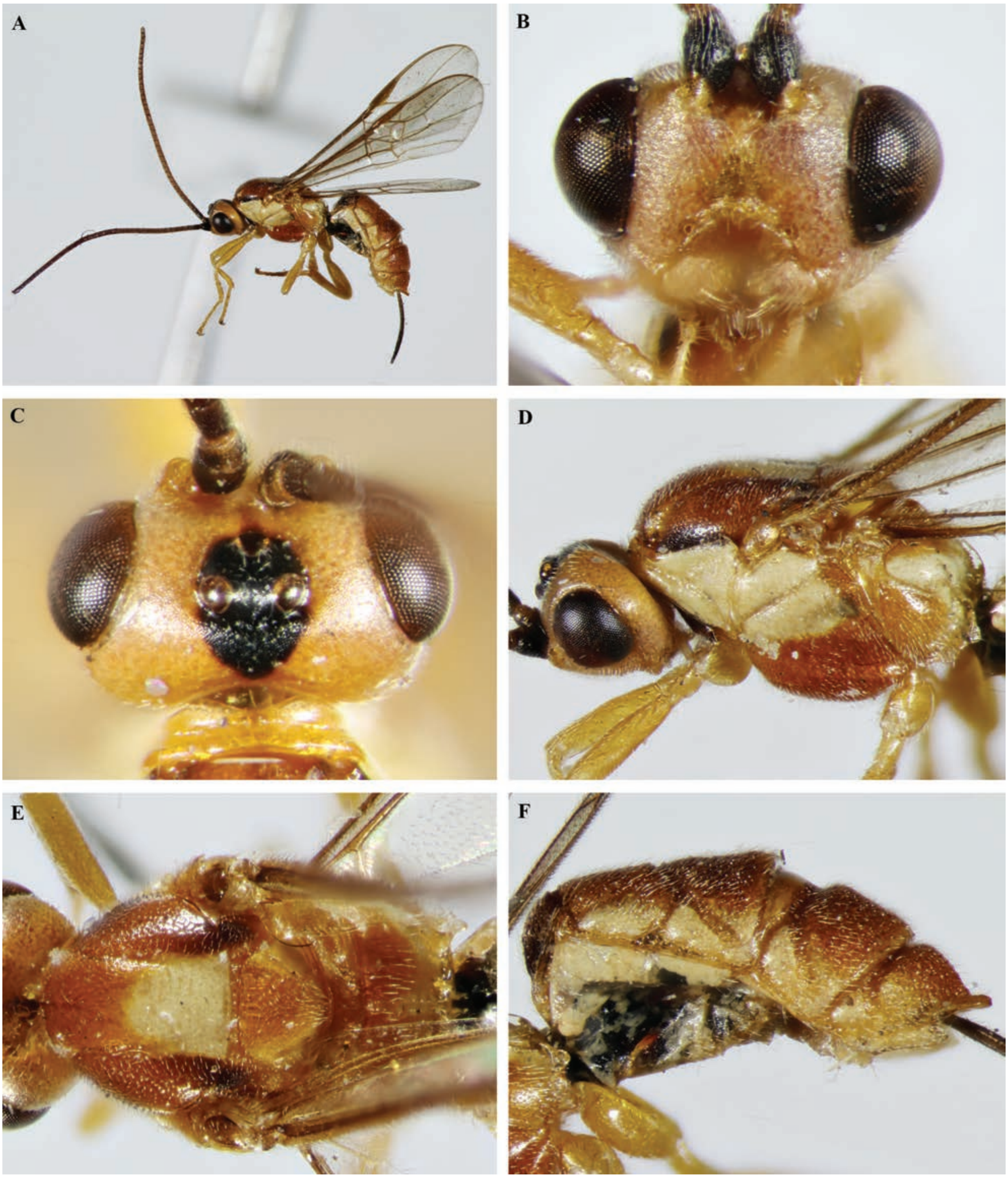

**Figure 12.** *Trigastrotheca formosa* sp. nov. ♀ holotype **A** habitus, lateral view **B** head, anterior view **C** head, dorsal view **D** head and mesosoma, lateral view **E** mesosoma, dorsal view **F** metasoma, lateral view.

**Host.** Unknown.

**Etymology.** Latin, *formosa*, meaning beautiful.

**Notes.** Excluded from the type series is a female with same data as the holotype but with the head entirely black but otherwise extremely similar. This seems to be a particularly unusual color variant for intraspecific variability, but it seems most probable, in the absence of additional data, that this is conspecific.

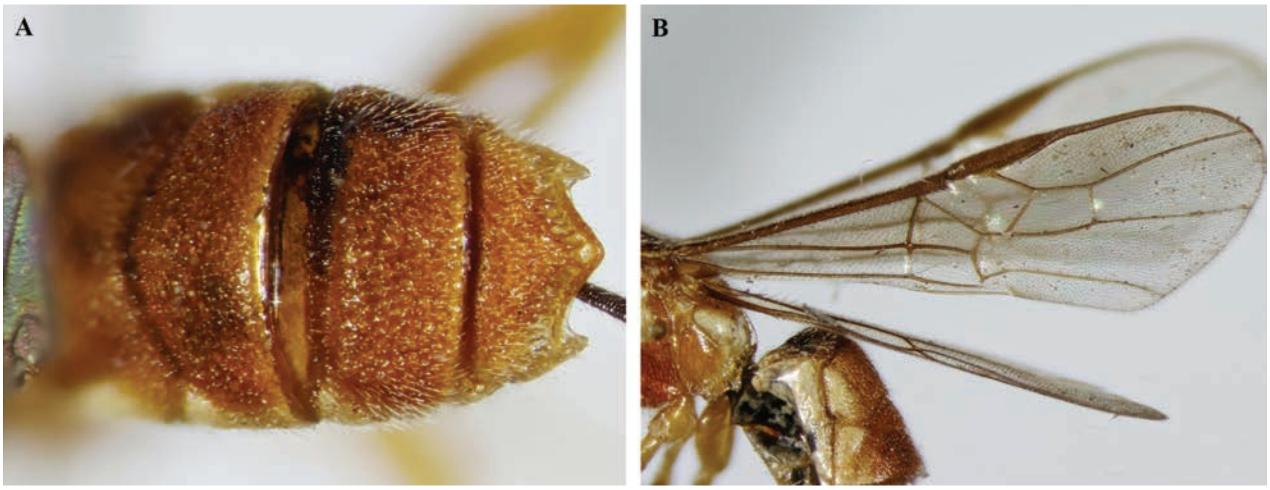

**Figure 13.** *Trigastrotheca formosa* sp. nov. ♀ holotype **A** TT3–5, dorsal view **B** wings.

### *Trigastrotheca freidbergi* Quicke & Friedman, sp. nov.

https://zoobank.org/BD2AD2C4-25E9-4C21-B355-F45AACA98F54

Figs 14–16

**Type material.** ***Holotype*** ♀, India: Rajasthan, Nagda Temple, 25 km N Udaipur Lake, 22.xi.2002, A. Freidberg (CUMZ). ***Paratype*.** 4 ♀, same data as holotype (2 in SMNHTAU, 2 in MNB).

**Diagnosis.** Uniformly brownish yellow but with stemmaticum and fore wing vein C+SC+R and pterostigma pale brown-yellow, second submarginal cell short with vein 3RSa shorter that 2RS (Fig. 16B). Similar to *Trigastrotheca carinata* Ranjith, sp. nov. but stemmaticum black and T5 relatively far shorter (Fig. 16A cf. Fig. 6C).

**Description.** Holotype female. Length of body 5.5 mm, fore wing 3.9 mm. ***Head*.** Antenna with 38 flagellomeres. Terminal flagellomere acuminate. First flagellomere 1.2 × longer than 2nd and 3rd, the latter 1.5 × longer than wide. Width of head: width of face: height of eye = 2.5: 1.3: 1.0. Face with fine transverse striations laterally; with weak mid-longitudinal ridge. Inter-tentorial distance 1.8 × longer than tentorio-ocular distance. Malar suture impressed. Malar space 1.2 × as long as basal width of mandible. Antennal sockets strongly produced. Frons strongly impressed with a complete mid-longitudinal carina. Shortest distance between posterior ocelli: transverse diameter of posterior ocellus: shortest distance between posterior ocellus and eye = 1.0: 1.0: 2.0. ***Mesosoma*** 1.4 × longer than high. Mesoscutum rugose; notauli not impressed except very short anterior part with few weak crenulations. Scutellar sulcus shallow, narrow, finely crenulate. Scutellum sparsely punctate without small pit medially behind sulcus. Median area of metanotum with complete mid-longitudinal carina. Propodeum largely smooth and shiny, faintly rugose antero-laterally; mid-longitudinal carina complete, not lamelliform, bordered narrowly by fine crenulations; posteriorly propodeum with short longitudinal carinae. ***Wings*.** Fore wing. Lengths of fore wing veins r-rs: 3RSa: 3RSb = 1.0: 1.2: 4.5. Lengths of vein 2RS: 3RSa: rs-m = 1.1: 1.0: 1.1. Base of hind wing glabrous. ***Legs*.** Lengths of fore femur: fore tibia: fore tarsus = 1.0: 1.1: 1.1. Lengths of hind femur: hind tibia: hind tarsus = 1.0: 1.2: 1.1. Claws with small acutely

**Figure 14.** *Trigastrotheca freidbergi* sp. nov. ♀ holotype **A** habitus, lateral view **B** head, anterior view **C** head, dorsal view.

pointed basal lobe. ***Metasoma.*** T1 1.7 × wider than long. T2 0.9 × as long as T3. T1 coriaceous. TT1–5 with coarse reticulate sculpture Second metasomal suture and basal grooves of TT4 and 5 deep, strigose. T5 with postero-lateral margin of convex, unevenly denticulate; medial protuberance acutely rounded. ***Coloration.*** Body mostly yellow except antenna, eye, stemmaticum, tarsi, ovipositor sheath black.

**Figure 15.** *Trigastrotheca freidbergi* sp. nov. ♀ holotype **A** head and mesosoma, lateral view **B** mesosoma, dorsal view **C** metanotum and propodeum, dorsal view **D** metasoma, lateral view **E** metasoma, dorsal view **F** T5, lateral view.

**Male.** Unknown.

**Distribution.** Oriental (India).

**Host.** Unknown.

**Etymology.** Named after the late Dr Amnon Freidberg of Tel Aviv University, collector and prolific dipterist.

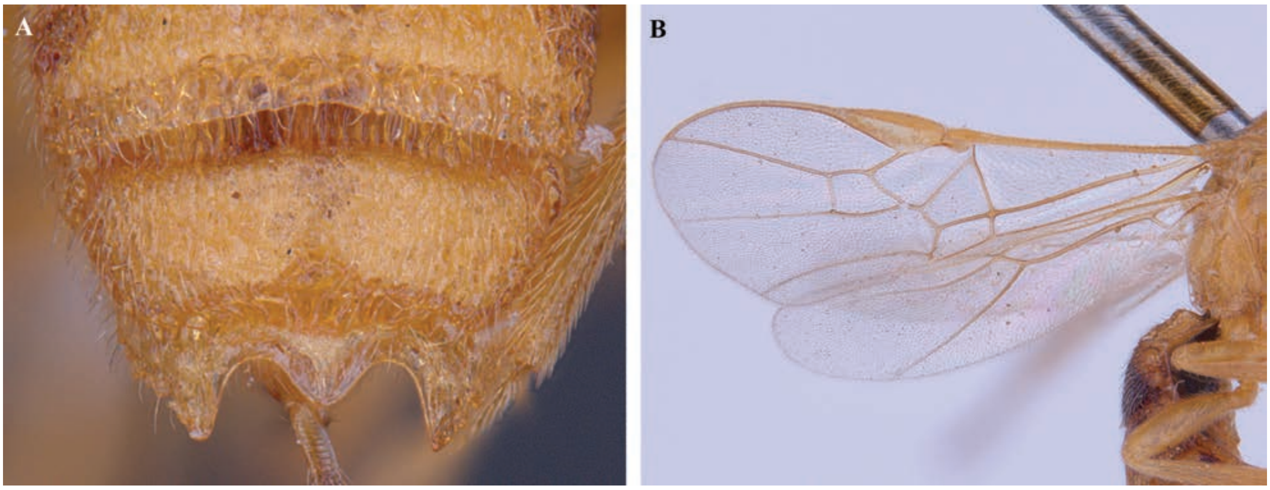

**Figure 16.** *Trigastrotheca freidbergi* sp. nov. ♀ holotype **A** T5, dorsal view **B** wings.

**_Trigastrotheca griffini_ Quicke, sp. nov.**
https://zoobank.org/2011896B-33F1-4DAC-80FE-7EF3663901D9
Figs 17, 18

**Type material.** ***Holotype*** ♂, Australia, New South Wales, Hat Head, 22.ii.2019, 31.0626°S, 153.052°E, 36.58 m, coll. P.D.N. Hebert, U.V. light sheet, DNA voucher P.I.D. NSWHP2575-19 (CNCO).

**Diagnosis.** Tricolourous, largely orange-red with cream and piceous/black markings. Black mark on stemmaticum extending to form a point on vertex. Mesoscutum, orange-red except for posterior 1/2 of middle lobe which is cream, and bordered postero-laterally by piceous markings.

**Description.** Length of body 5.5 mm, fore wing 4.1 mm. ***Head*.** Antenna with 44 flagellomeres. Terminal flagellomere acuminate. First flagellomere 1.0 × longer than 2nd and 3rd, the latter 1.3 × longer than wide. Width of head: width of face: height of eye = 2.3: 1.1: 1.0. Face granulate with interrupted weak mid-longitudinal ridge. Inter-tentorial distance 1.4 × longer than tentorio-ocular distance. Malar suture impressed. Malar space 1.6 × as long as basal width of mandible. Antennal sockets strongly produced. Frons strongly impressed medially and behind antennal sockets with mid-longitudinal carina. Frons, vertex, and occiput granulate. Shortest distance between posterior ocelli: transverse diameter of posterior ocellus: shortest distance between posterior ocellus and eye = 1.0: 1.2: 2.2. ***Mesosoma*** 1.5 × longer than high. Mesoscutum smooth, granulate medio-posteriorly, sparsely punctate; notauli impressed anterior 1/2, crenulated, shallow posteriorly. Scutellar sulcus shallow, narrow, finely crenulate. Scutellum smooth, sparsely setose without small pit medially behind sulcus. Median area of metanotum with complete mid-longitudinal carina. Propodeum largely smooth and shiny, coarsely rugose posteriorly, distinctly transversely striate near mid-longitudinal carina; mid-longitudinal carina complete, lamelliform, bordered narrowly by fine crenulations; posteriorly propodeum with short longitudinal carinae associated with longitudinal wrinkles. ***Wings*.** Fore wing. Lengths of fore wing veins r-rs: 3RSa: 3RSb = 1.0: 1.6: 4.7. Lengths of vein 2RS: 3RSa: rs-m = 1.3: 1.3: 1.0. Base of hind wing with large glabrous area distal to vein 1CU. ***Legs*.** Lengths of fore femur: fore tibia: fore tarsus = 1.0: 1.1: 1.1. Lengths of hind femur: hind tibia: hind tarsus = 1.0: 1.1: 1.3. Claws with small acutely

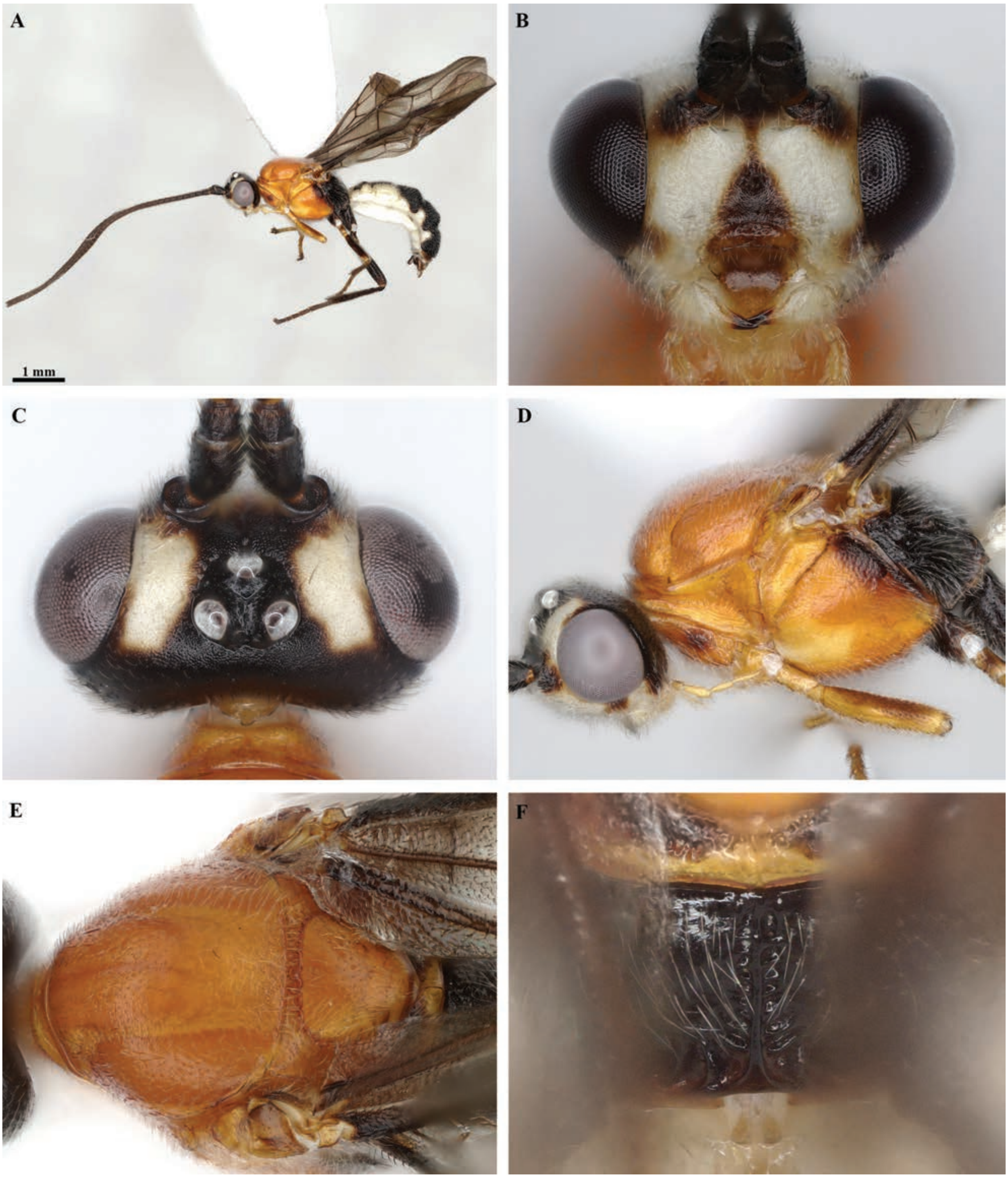

**Figure 17.** *Trigastrotheca griffini* sp. nov. ♂ holotype **A** habitus, lateral view **B** head, anterior view **C** head, dorsal view **D** head and mesosoma, lateral view **E** mesosoma, dorsal view **F** metanotum and propodeum, dorsal view.

pointed basal lobe. ***Metasoma.*** T1 coriaceous, 1.8 × wider than long, with pair of posteriorly uniting dorsal carina. T2 1.1 × as long as T3. TT1–5 with coarse reticulate sculpture. Second metasomal suture and basal grooves of TT4 and 5 deep, strigose. T5 with postero-lateral margin convex, without emarginations. ***Coloration.*** Body mostly black except face laterally, malar space, mandible except apically, frons, and vertex laterally, T1 except medially, T2 except medially,

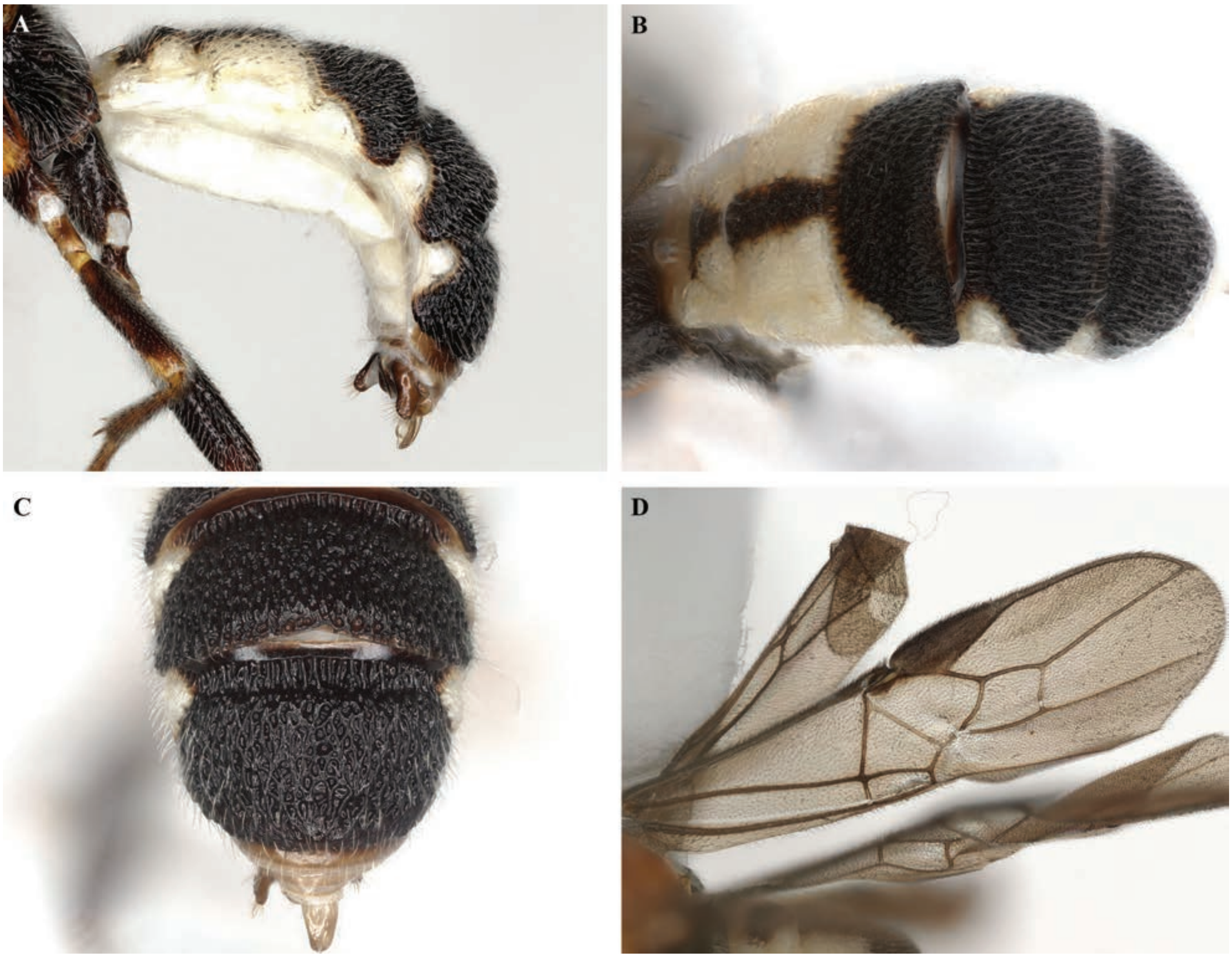

**Figure 18.** *Trigastrotheca griffini* sp. nov. ♂ holotype **A** metasoma, lateral view **B** metasoma, dorsal view **C** TT4 and 5, dorsal view **D** fore wing.

TT3–5 antero-laterally ivory white, maxillary and labial palps, pronotum, mesoscutum, scutellum, mesopleuron, metanotum except anteriorly yellow.

**Female.** Unknown.

**Distribution.** Australian (Australia).

**Host.** Unknown.

**Etymology.** Named after Griffin Hebert who provided much assistance in the deployment of Australian Malaise traps during the fieldwork that resulted in collection of the holotype.

### ***Trigastrotheca khaoyaiensis* Quicke & Butcher, sp. nov.**

https://zoobank.org/D3EE1FC5-DA9C-49B9-B3F8-EAC8D29B0598
Figs 19, 20

**Type material.** ***Holotype*** ♀, Thailand, Nakhon Ratchasima, Khao Yai National Park, 17.vi.2022, 14°26.016'N, 101°22.153'E, Malaise trap 3, coll. B. Butcher (CUMZ). ***Paratype***. 1 ♀, same data as holotype except 27.iv.2022 (CUMZ).

**Diagnosis.** Tricolourous black, yellow, and white, with the face entirely yellow except for dark spot on outer margin of antennal socket. Similar to *T. khaoyaiensis* sp. nov. but differing in having the median lobe of T5 far more acute

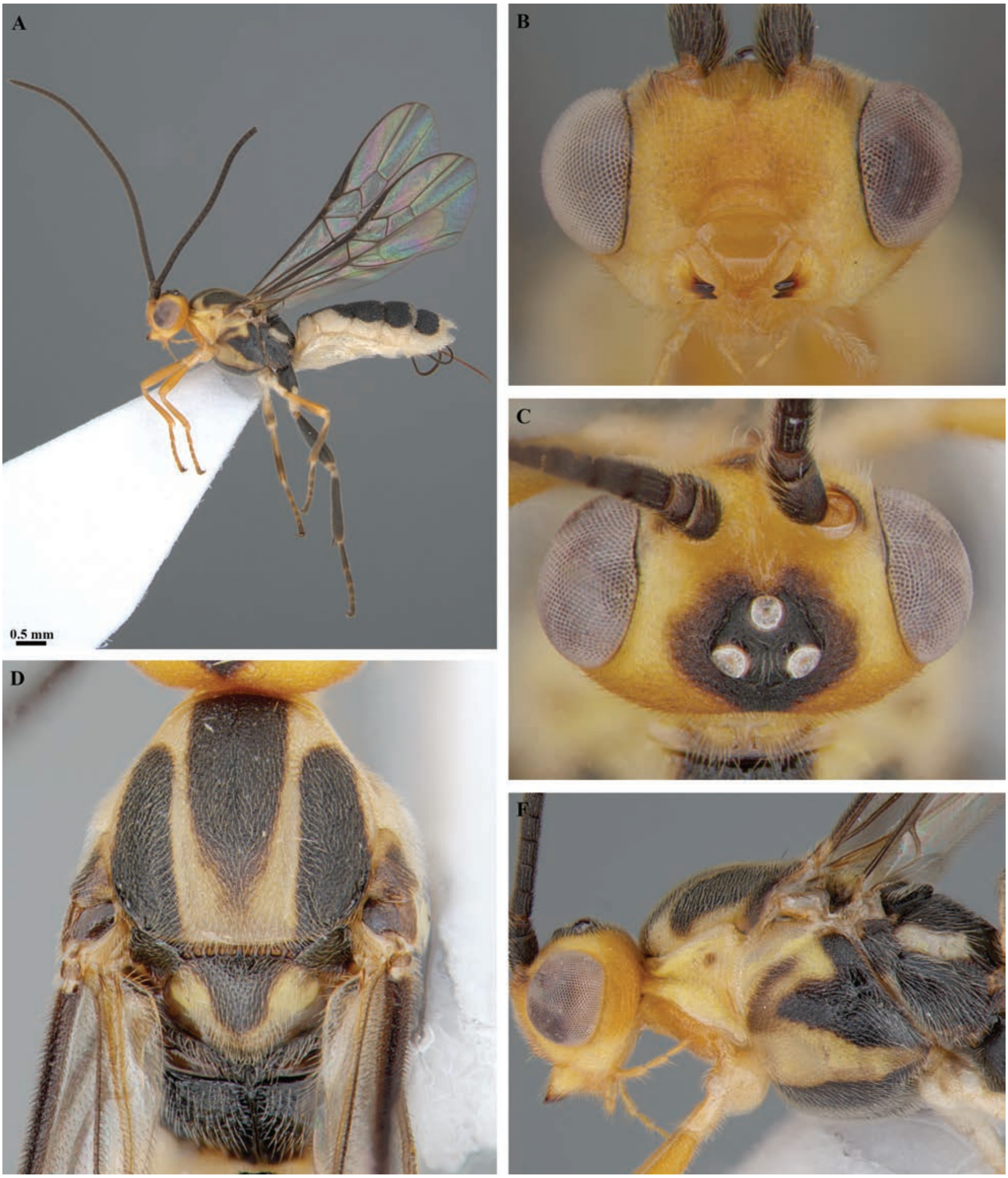

**Figure 19.** *Trigastrotheca khaoyaiensis* sp. nov. ♀ holotype **A** habitus, lateral view **B** head, anterior view **C** head, dorsal view **D** mesosoma dorsal view **E** head and mesosoma, lateral view.

(Fig. 20B cf. Fig. 22D), the black raised median part of the T5 being shorter and wider with the posterior white margin relatively larger.

**Description.** Holotype female. Length of body 6.1 mm, fore wing 4.5 mm. ***Head*.** Antenna with 44 flagellomeres. Terminal flagellomere acuminate. First flagellomere 1.1 × longer than 2nd and 3rd, the latter 1.2 × longer than wide. Width of head: width of face: height of eye = 2.4: 1.3: 1.0. Face transversely

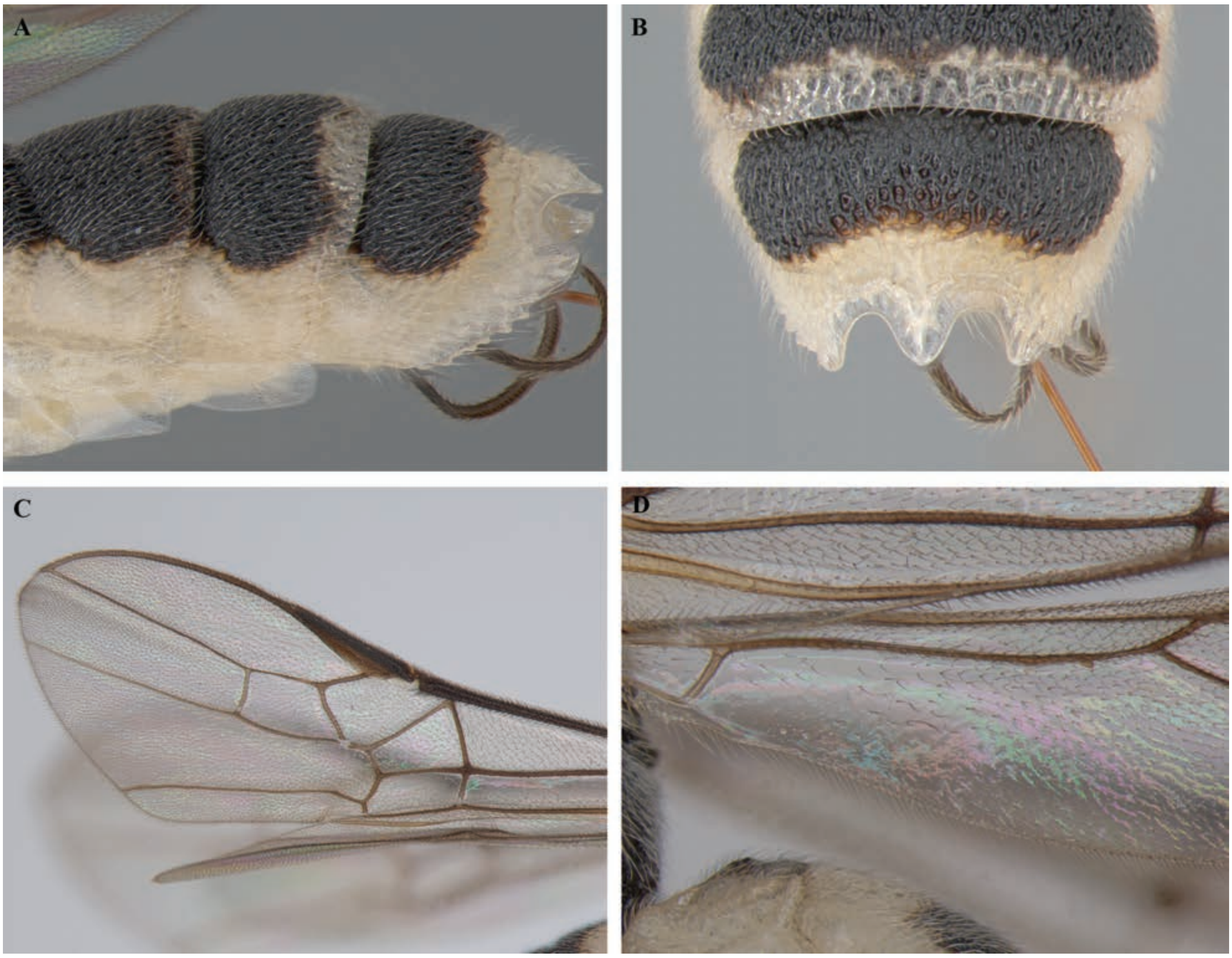

**Figure 20.** *Trigastrotheca khaoyaiensis* sp. nov. ♀ holotype **A** TT3–5, lateral view **B** TT4 and 5, dorsal view **C** fore wing **D** hind wing, basal part.

striate-rugose; with distinct mid-longitudinal ridge. Inter-tentorial distance 1.6 × longer than tentorio-ocular distance. Malar suture impressed. Malar space 1.5 × as long as basal width of mandible. Antennal sockets strongly produced. Frons faintly rugose, strongly impressed behind antennal sockets, with mid-longitudinal carina. Shortest distance between posterior ocelli: transverse diameter of posterior ocellus: shortest distance between posterior ocellus and eye = 1.0: 1.0: 2.2. ***Mesosoma*** 1.5 × longer than high. Mesoscutum granulate-rugose; notauli not impressed except very short anterior part with few weak crenulations, very shallow posteriorly. Scutellar sulcus shallow, narrow, finely crenulate. Scutellum granulate without small pit medially behind sulcus. Median area of metanotum with complete mid-longitudinal carina. Propodeum granulate; mid-longitudinal carina complete, lamelliform, bordered narrowly by fine crenulations; posteriorly propodeum with short longitudinal carinae associated with longitudinal wrinkles. ***Wings.*** Fore wing. Lengths of fore wing veins r-rs: 3RSa: 3RSb = 1.0: 1.5: 4.5. Lengths of vein 2RS: 3RSa: rs-m = 1.2: 1.5: 1.0. Base of hind wing glabrous. ***Legs.*** Lengths of fore femur: fore tibia: fore tarsus = 1.0: 1.1: 1.1. Lengths of hind femur: hind tibia: hind tarsus = 1.0: 1.2: 1.3. Claws with small acutely pointed basal lobe. ***Metasoma.*** T1 1.5 × wider than long. T2 0.9 × as long as T3. T1 coriaceous. TT1–5 with coarse reticulate sculpture. Second metasomal suture and basal grooves of TT4 and 5 deep, strigose. T5 with postero-lateral margin of convex, distinctly, evenly denticulate; medial protuberance acutely rounded posteriorly; postero-lateral emarginations defined. ***Coloration*.** Body black except face, clypeus, malar space, mandible except apex, maxillary and labial palps, temple, frons and vertex laterally, occiput ventrally, pronotum, propleuron, mesoscutum antero-laterally, submedially and posteriorly, scutellum laterally and posteriorly, mesopleuron anteriorly and posteriorly, metapleuron anteriorly, fore leg, mid coxa ventrally, mid femur except ventrally, mid tibia basally, hind trochanter, hind tibia basally yellow, T1 except medially, T2 except medially and posteriorly, metasoma laterally, T5 posterior 1/2 ivory white.

**Male.** Unknown.

**Distribution.** Oriental (Thailand).

**Host.** Unknown.

**Etymology.** Named after Khao Yai National Park Thailand where the type material was collected.

### ***Trigastrotheca naniensis*** **Quicke & Butcher, sp. nov.**

https://zoobank.org/12F783D1-0387-4A82-AB52-111D0110B99B
Figs 21, 22

**Type material.** ***Holotype*** ♀, Thailand, Nan Province, Doi Phu Kha National Park, 16.xii.2022, 19°12.157'N, 101°04.388'E, 1327 m, Global Malaise Trap project trap 2, coll. Butcher, B.A. (DNA voucher CCDB47579-E11) (CUMZ).

**Diagnosis.** Tricolourous, black, yellow, ivory white, with the face entirely yellow except for dark patch on outer side of antennal socket. Similar to *T. khaoyaiensis* sp. nov. in having a yellow face without black marks but differs in having T4 completely black all the way to posterior margin.

**Description.** Holotype female. Length of body 4.5 mm, fore wing 3.9 mm. ***Head*.** Antenna with 37 flagellomeres. Terminal flagellomere, short, sub-triangular, acuminate. First flagellomere 1.0 × longer than 2nd and 3rd, the latter 1.5 × longer than wide. Width of head: width of face: height of eye = 2.3: 1.2: 1.0. Face transversely striate-rugose with weak mid-longitudinal ridge. Inter-tentorial distance 1.5 × longer than tentorio-ocular distance. Malar suture impressed. Malar space 1.3 × as long as basal width of mandible. Antennal sockets strongly produced. Frons strongly impressed behind antennal socket with mid-longitudinal carina. Shortest distance between posterior ocelli: transverse diameter of posterior ocellus: shortest distance between posterior ocellus and eye = 1.2: 1.0: 2.3. ***Mesosoma*** 1.5 × longer than high. Mesoscutum rugulose; notauli not impressed except very short anterior part with few weak crenulations. Scutellar sulcus shallow, narrow, finely crenulate. Scutellum faintly granulate without small pit medially behind sulcus. Median area of metanotum with complete mid-longitudinal carina. Propodeum rugose; mid-longitudinal carina complete, lamelliform, bordered narrowly by fine crenulations; posteriorly propodeum with short longitudinal carinae associated with longitudinal wrinkles. ***Wings*.** Fore wing. Lengths of fore wing veins r-rs: 3RSa: 3RSb = 1.0: 1.4: 5.3. Lengths of vein 2RS: 3RSa: rs-m = 1.2: 1.5: 1.0. Base of hind wing with large glabrous area. ***Legs*.** Lengths of fore femur: fore tibia: fore tarsus = 1.0: 1.0: 1.2. Lengths of hind femur: hind tibia: hind tarsus

**Figure 21.** *Trigastrotheca naniensis* sp. nov. ♀ holotype **A** habitus, lateral view **B** head, anterior view **C** head, dorsal view **D** head and mesosoma, lateral view **E** mesosoma, dorsal view **F** metanotum and propodeum, dorsal view.

= 1.0: 1.3: 1.2. Claws with small acutely pointed basal lobe. ***Metasoma.*** T1 1.3 × wider than long. T2 1.1 × as long as T3. T1 coriaceous. TT1–5 with coarse reticulate sculpture. Second metasomal suture and basal grooves of TT4 and 5 deep, strigose. T5 with postero-lateral margin of convex, evenly denticulate; medial protuberance broadly rounded posteriorly. ***Coloration.*** Body black except face, clypeus, malar space, mandible except apex, maxillary and labial

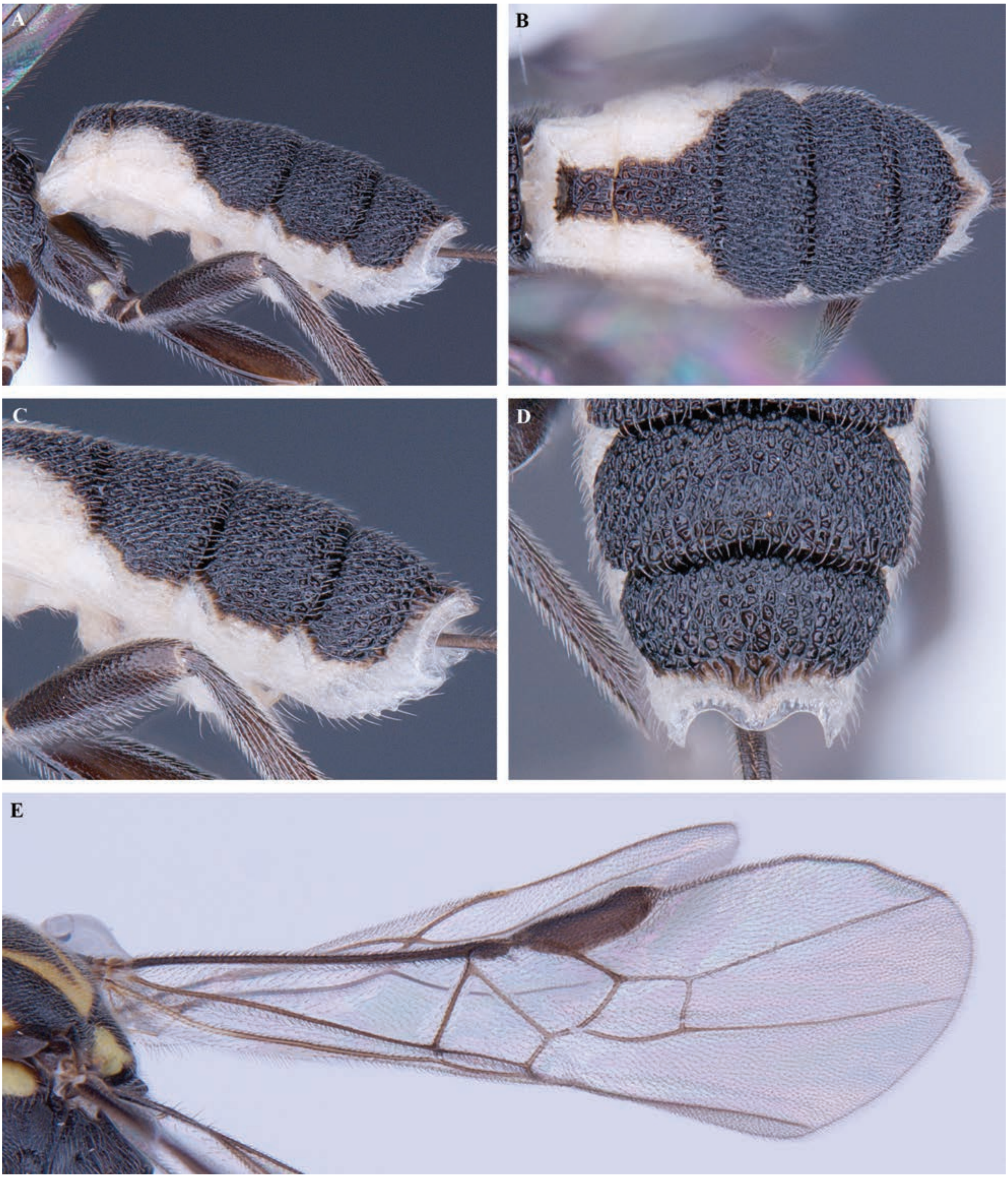

**Figure 22.** *Trigastrotheca naniensis* sp. nov. ♀ holotype **A** metasoma, lateral view **B** metasoma, dorsal view **C** TT3–5, lateral view **D** TT4 and 5, dorsal view **E** wings.

palps, temple, frons, and vertex laterally, occiput except medially, pronotum, propleuron, mesoscutum antero-laterally, submedially, and posteriorly, scutellum laterally and posteriorly, mesopleuron anteriorly and posteriorly, fore leg yellow, T1 except medially, T2 except medially and posteriorly, metasoma laterally, T5 posteriorly ivory white.

**Male.** Unknown.

**Distribution.** Oriental (Thailand).

**Host.** Unknown.

**Etymology.** Named after the province of Nan in north Thailand where the holotype was collected.

### *Trigastrotheca simba* van Noort, sp. nov.

https://zoobank.org/C0B3DA61-2120-4065-AA70-18618CDBD032
Figs 23, 24

**Type material.** ***Holotype*** ♀, Tanzania, Mkomazi Game Reserve, Kamakota Hill, 4.14°S, 28.24°E, 4 Dec 1995, S. van Noort, on *Ficus ingens* (Miq.) Miq. With ripe fig crop (SAMC). ***Paratypes*:** 1 ♂, same data as holotype (SAMC).

**Diagnosis.** Similar to *T. trilobata* but tarsal claw with a smaller, bidentate, and more rounded basal lobe compared to a larger, more foliaceous, and acutely triangular basal lobe in *T. trilobata*. The postero-lateral margin of T5 has more prominent teeth (~ 8 or 9) compared to *T. trilobata* which has only 5 or fewer obvious teeth (Fig. 33D). Postero-medial protuberance of T5 acutely rounded, shorter than lateral lobes, with concavities lateral of medial protuberance acutely invaginated, whereas in *T. trilobata* the medial protuberance is of equivalent length to the lateral lobes; and the concavities lateral of medial protuberance are broadly invaginated.

**Description.** Holotype female. Length of body 5.16 mm, fore wing 4.14 mm. ***Head*.** Antenna with 36 flagellomeres. Terminal flagellomere with a spicule. First flagellomere equivalent in length to the 2nd and 3rd, the latter 1.25 × longer than wide. Width of head: width of face: height of eye = 2.5: 1.3: 1.0. Face with fine transverse striations laterally; with mid-longitudinal ridge dissipating ventrally. Inter-tentorial distance 2.3 × longer than tentorio-ocular distance. Malar suture impressed. Malar space equivalent to basal width of mandible. Frons strongly impressed with a complete mid-longitudinal carina. Shortest distance between posterior ocelli: transverse diameter of posterior ocellus: shortest distance between posterior ocellus and eye = 1.0: 1.0: 2.3. ***Mesosoma*** 1.5 × longer than high. Mesoscutum rugose; notauli weakly impressed for entire length with weak crenulations. Scutellar sulcus shallow, narrow, finely crenulate. Scutellum weakly rugose, setose without small pit medially behind sulcus. Median area of metanotum with complete mid-longitudinal carina. Propodeum weakly rugose; mid-longitudinal carina complete, lamelliform, with ~ 9 transverse, curved striae radiating laterally for short distance before grading into rugulosity; posteriorly propodeum with short longitudinal carinae. ***Wings*.** Fore wing. Lengths of fore wing veins r-rs: 3RSa: 3RSb = 1.0: 1.5: 4.6. Lengths of vein 2RS: 3RSa: rs-m = 1.0: 1.3: 1.8. Base of hind wing glabrous. ***Legs*.** Lengths of fore femur: fore tibia: fore tarsus = 1.0: 1.2: 1.2. Lengths of hind femur: hind tibia: hind tarsus = 1.0: 1.1: 1.0. Claws with small rounded weakly bilobate basal lobe. ***Metasoma*.** T1 2.0 × wider than long. T2 0.7 × as long as T3. TT1–5 with coarse reticulate sculpture. Second metasomal suture weakly strigose, basal grooves of TT4 and 5 deep, strigose. T5 with postero-lateral margin convex, distinctly denticulate (~ 8 or 9 uneven teeth) along anterior 3/4 of margin; medial protuberance acutely rounded,

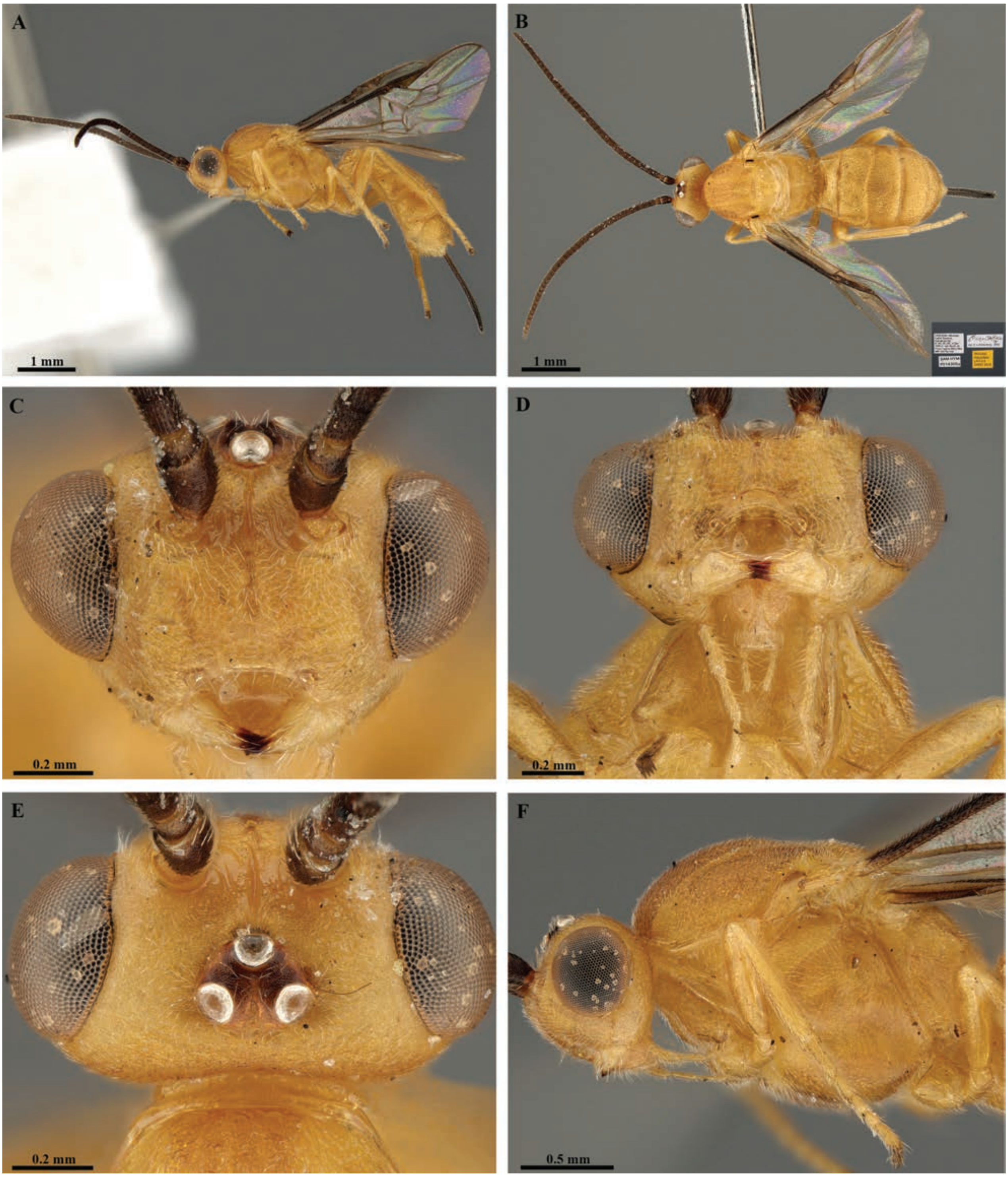

**Figure 23.** *Trigastrotheca simba* sp. nov. ♀ holotype **A** habitus, lateral view **B** habitus, dorsal view with labels inset **C** head, anterior view **D** head, antero-ventral view **E** head, dorsal view **F** head and mesosoma, lateral view.

shorter than lateral lobes, concavities lateral of medial protuberance acutely invaginated. ***Coloration.*** Body mostly yellow except antenna, eyes, and tarsi black, and stemmaticum which is dark brown with orange margins.

**Male.** Same as female.

**Distribution.** Afrotropical (Tanzania).

**Figure 24.** *Trigastrotheca simba* sp. nov. ♀ holotype **A** head and mesosoma, dorsal view **B** scutellum, metanotum and propodeum, dorsal view **C** T1, dorsal view **D** T5, dorsal view **E** metasoma, lateral view **F** fore wing.

**Host.** Unknown, but both the female and male were hand collected from a *Ficus ingens* tree with a ripe fig crop, and they may have been locating or recently emerged from arboreal nesting *Crematogaster* on the tree.

**Etymology.** Specific name refers to the presence alongside wild lions of this uniformly pale colored species in the East African savanna (Mkomazi Game Reserve, now a National Park), the provenance of the holotype. Simba is Kiswahili for lion. Noun in apposition.

## ***Trigastrotheca similidentata*** **Ranjith, sp. nov.**

https://zoobank.org/0FF021B2-B86C-40A7-8103-0977CD70B1F4
Figs 25, 26

**Type material.** ***Holotype*** ♀, INDIA: Karnataka, Chamarajanagar, Biligiri Rangaswamy Temple Tiger Reserve, scrub jungle, 12°01'41.4"N, 77°06'55.1"E;

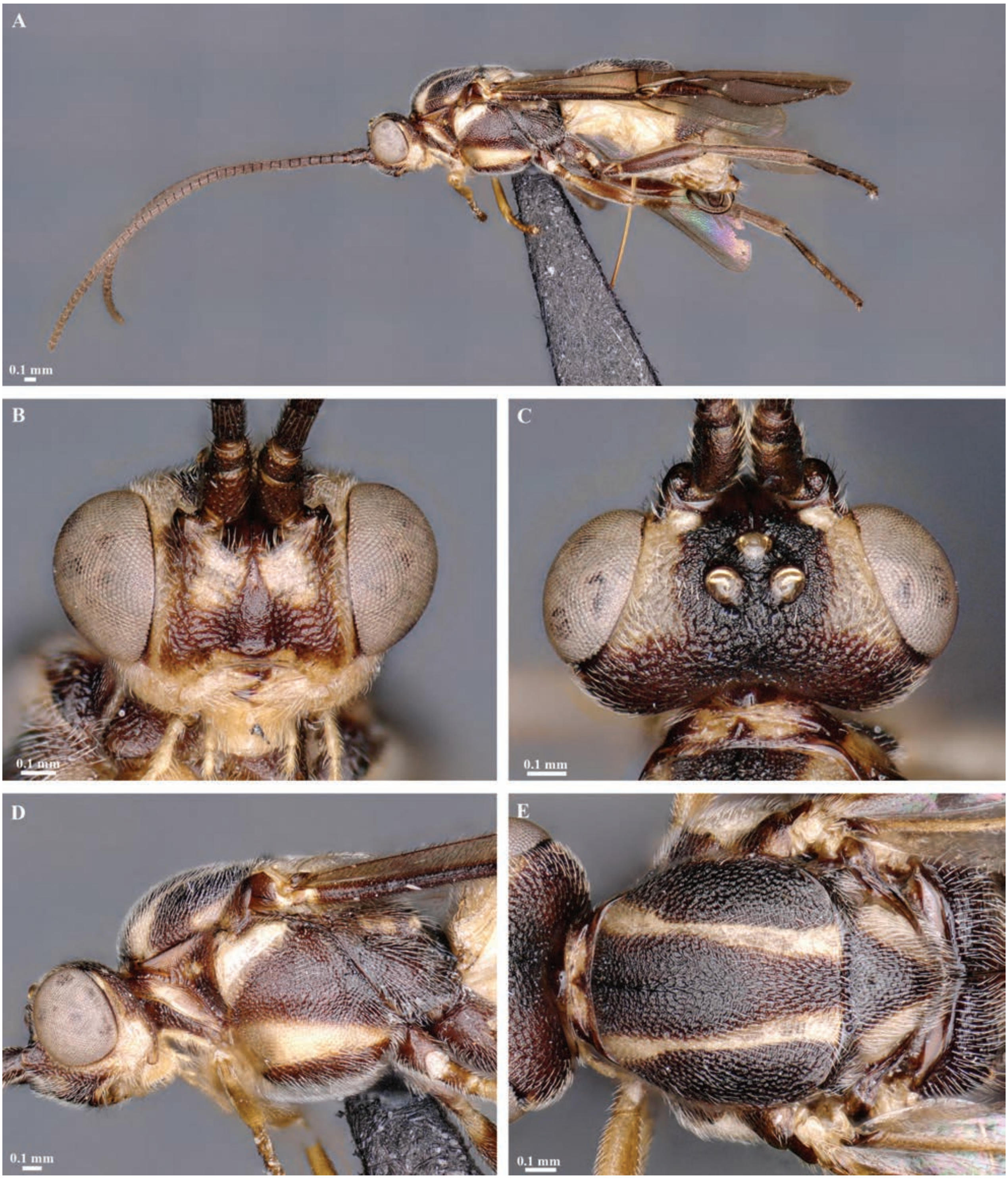

**Figure 25.** *Trigastrotheca similidentata* sp. nov. ♀ holotype **A** habitus, lateral view **B** head, anterior view **C** head, dorsal view **D** head and mesosoma, lateral view **E** mesosoma, dorsal view.

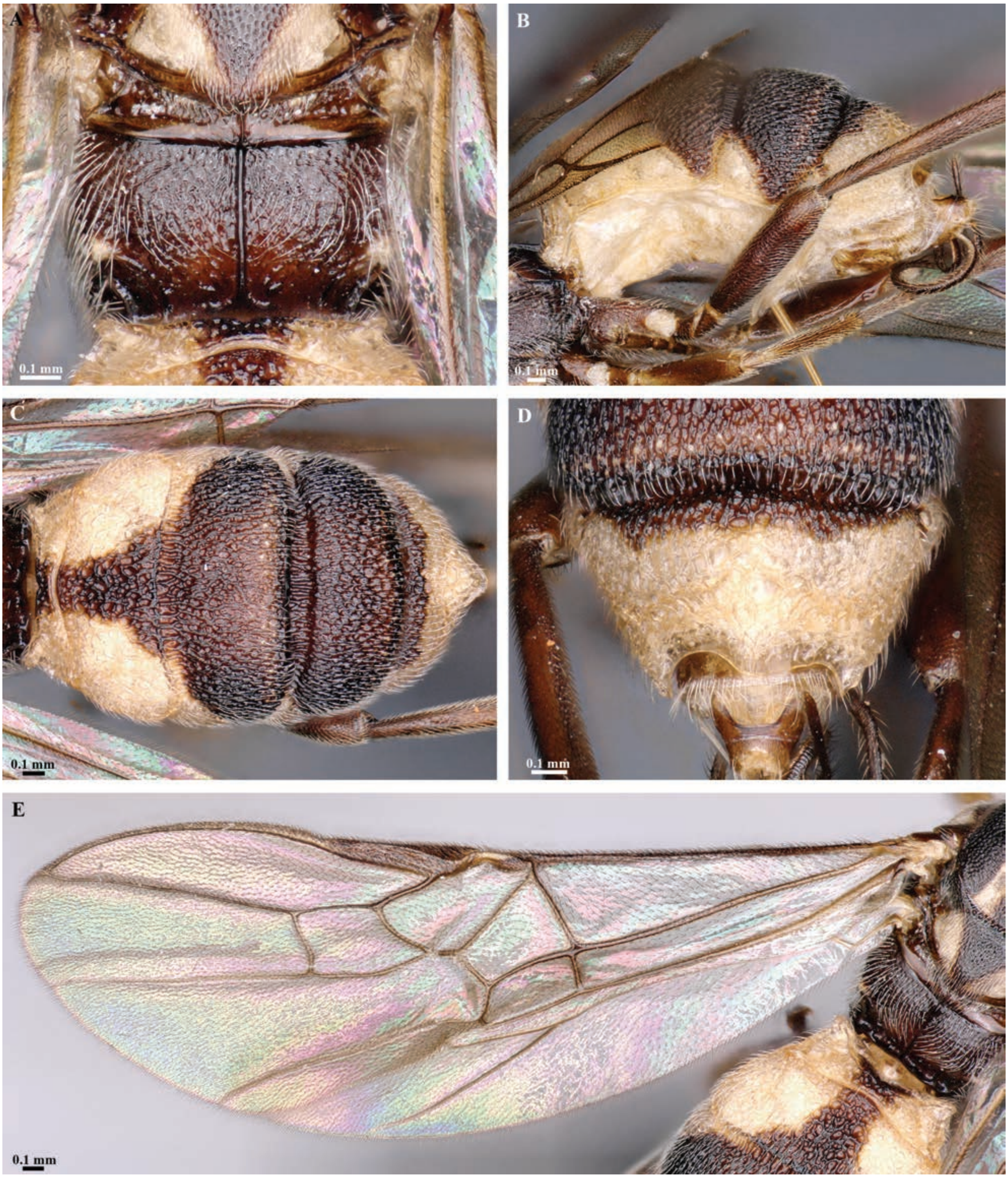

**Figure 26.** *Trigastrotheca similidentata* sp. nov. ♀ holotype **A** metanotum and propodeum, dorsal view **B** metasoma, lateral view **C** metasoma, dorsal view **D** T5, dorsal view **E** wings.

31.v–15.vi.2005, Malaise trap, coll. D.R. Priyadarsanan (AIMB). ***Paratype***, 1 ♀, India: Karnataka, Kadnur, Malaise Trap, 14.xi.2005, coll. D.R. Priyadarsanan (DZUC).

**Diagnosis.** Similar to *T. tridentata* in having an entirely black mesoscutum except for yellow notauli in having the medio-posterior lobe of T5 broadly rounded (Fig. 26D) (far more acutely pointed in *T. tridentata*) and in the posterolateral parts of the T5 not concave laterally. In addition, the black mark at the base of

T5 does not extend to the lateral margins whereas in *T. tridentata* the black is produced reaching the side and posterior margins.

**Description.** Length of body 3.6 mm, fore wing 3.1 mm. ***Head*.** Antenna incomplete with 42 flagellomeres. Terminal flagellomere acuminate. First flagellomere 1.1 × longer than 2nd and 3rd, the latter 1.3 × longer than wide. Width of head: width of face: height of eye = 2.2: 1.1: 1.0. Face transversely striate-rugose with long mid-longitudinal ridge. Inter-tentorial distance 1.8 × longer than tentorio-ocular distance. Malar suture impressed. Malar space 1.5 × as long as basal width of mandible. Antennal sockets strongly produced. Frons strongly impressed only behind antennal sockets with mid-longitudinal carina. Frons, vertex, and occiput granulate-rugose. Shortest distance between posterior ocelli: transverse diameter of posterior ocellus: shortest distance between posterior ocellus and eye = 1.0: 1.4: 2.4. ***Mesosoma*** 1.5 × longer than high. Mesoscutum transversely rugose-striate with a weak mid-longitudinal carina medio-anteriorly; notauli impressed anterior 1/2, crenulated, shallow posteriorly. Scutellar sulcus deep, narrow, finely crenulate. Scutellum distinctly punctate, setose with a small pit medially behind sulcus. Median area of metanotum with complete mid-longitudinal carina. Propodeum faintly rugose, mid-longitudinal carina complete, lamelliform posteriorly, bordered narrowly by fine crenulations; posteriorly propodeum with short longitudinal carinae associated with longitudinal wrinkles. ***Wings*.** Fore wing. Lengths of fore wing veins r-rs: 3RSa: 3RSb = 1.0: 1.1: 3.7. Lengths of vein 2RS: 3RSa: rs-m = 1.0: 1.1: 1.0. Base of hind wing with large glabrous area distal to vein 1CU. ***Legs*.** Lengths of fore femur: fore tibia: fore tarsus = 1.0: 1.2: 1.2. Lengths of hind femur: hind tibia: hind tarsus = 1.0: 1.2: 1.4. Claws with small acutely pointed basal lobe. ***Metasoma*.** T1 coarsely reticulate, 1.7 × wider than long, with pair of posteriorly uniting dorsal carina. T2 0.7 × as long as T3. TT1–5 with coarse reticulate sculpture. Second metasomal suture and basal grooves of TT4 and 5 deep, strigose. T5 with postero-lateral margin slightly concave, denticulate; medial protuberance broadly rounded posteriorly; postero-lateral emarginations concave. ***Coloration*.** Body mostly reddish brown except scape, pedicel, eye, ocellar area, occiput medially, mesoscutum antero-laterally, propleuron, mesopleuron with posterior black patch, T1 medially, ovipositor sheath black, face, clypeus, maxillary and labial palps, frons, vertex, and occiput laterally, pronotum dorsally, legs yellow, pronotum laterally, middle lobe of mesoscutum posteriorly, mesopleuron anteriorly, metasoma laterally ivory white.

**Male.** Unknown.

**Distribution.** Oriental (India).

**Host.** Unknown.

**Etymology.** From Latin, *similis* and *dentata*, in reference to its likeness to *T. tridentata*.

### *Trigastrotheca sublobata* Quicke, sp. nov.

https://zoobank.org/3C2251FF-3194-47AB-9CC1-34407BFE2E0E
Fig. 27

**Type material. *Holotype*** ♀, Thailand: Nan Province, Phasing, 2018–2019, light trap, coll. Chansri, K. (CUMZ).

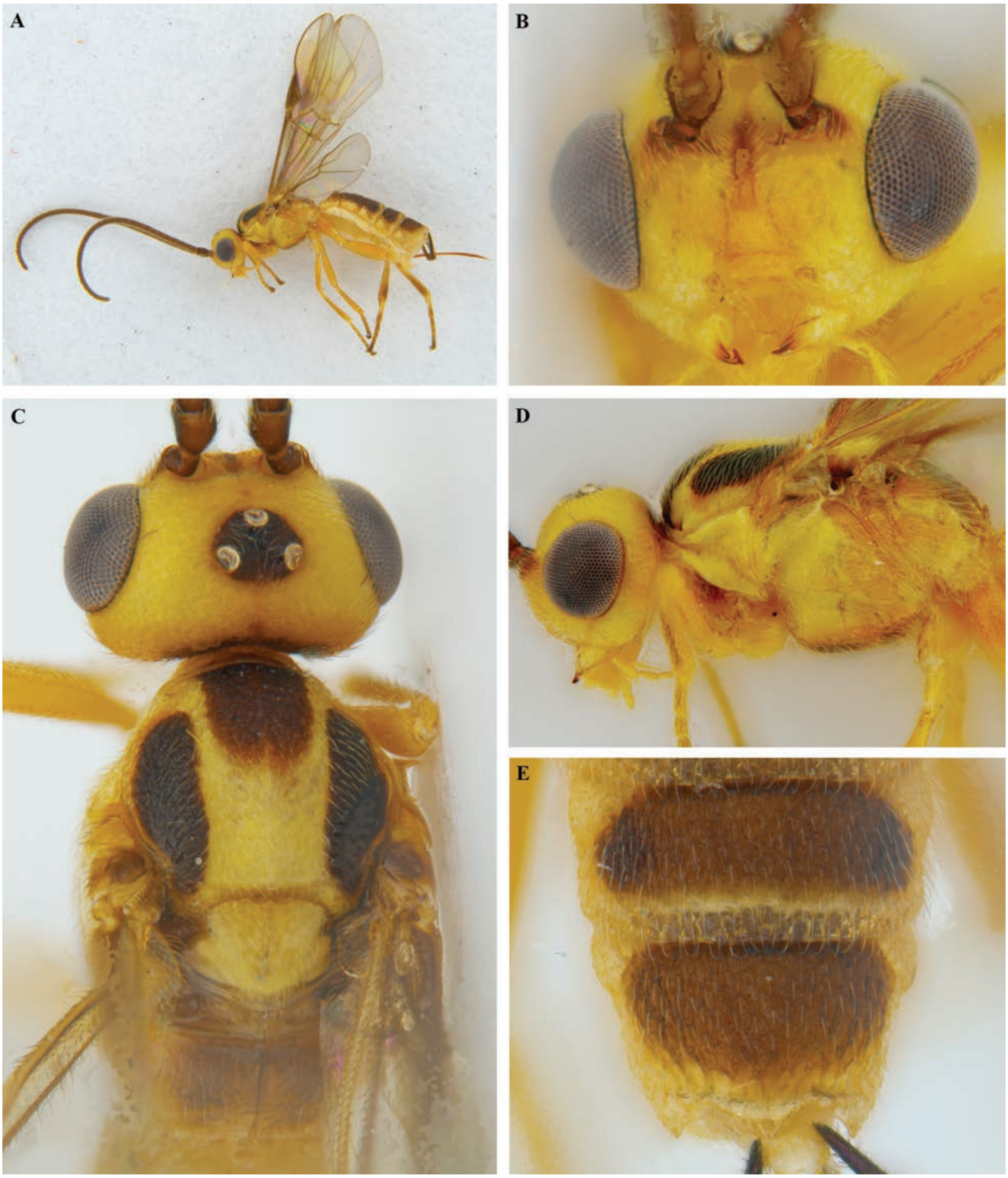

**Figure 27.** *Trigastrotheca sublobata* sp. nov. ♀ holotype **A** habitus, lateral view **B** head, anterior view **C** head and mesosoma, dorsal view **D** head and mesosoma, lateral view **E** TT4 and 5, dorsal view.

**Diagnosis.** May be distinguished from the other Oriental species with three black patches on the mesoscutum and medial black patches on most of the metasomal tergites by its only weakly produced and very wide middle lobe of T5 (Fig. 27E).

**Description.** Holotype female. Length of body 3.1 mm, fore wing 2.7 mm. ***Head*.** Antenna with 28 flagellomeres. Terminal flagellomere, short, sub-triangular, acuminate. First flagellomere 1.0 × longer than 2nd and 3rd, the latter 1.7 × longer than wide. Width of head: width of face: height of eye = 2.5: 1.3: 1.0. Face with fine transverse striations radiating towards middle from eye margin; with weak mid-longitudinal ridge. Inter-tentorial distance 1.1 × longer than tentorio-ocular distance. Malar suture impressed. Malar space 1.6 × as long as basal width of mandible. Antennal sockets strongly produced. Frons hardly impressed behind antennal socket with shallow mid-longitudinal groove. Shortest distance between posterior ocelli: transverse diameter of posterior ocellus: shortest distance between posterior ocellus and eye = 1.5: 1.0: 2.8. ***Mesosoma*** 1.5 × longer than high. Mesoscutum granulate; notauli not impressed except very short anterior part with few weak crenulations. Scutellar sulcus shallow, narrow, finely crenulate. Scutellum finely granulate without small pit medially behind sulcus. Median area of metanotum with complete mid-longitudinal carina. Propodeum granulate; mid-longitudinal carina complete, not lamelliform, not bordered narrowly by fine crenulations; posteriorly propodeum with short longitudinal carinae associated with few longitudinal wrinkles. ***Wings*.** Fore wing. Lengths of fore wing veins r-rs: 3RSa: 3RSb = 1.0: 1.0: 4.1. Lengths of vein 2RS: 3RSa: rs-m = 1.3: 1.2: 1.0. Base of hind wing distinctly setose. ***Legs*.** Lengths of fore femur: fore tibia: fore tarsus = 1.0: 1.0: 1.2. Lengths of hind femur: hind tibia: hind tarsus = 1.0: 1.3: 1.2. Claws with small acutely pointed basal lobe. ***Metasoma*.** T1 1.6 × wider than long. T2 1.1 × as long as T3. T1 coriaceous. TT1–5 with coarse reticulate sculpture. Second metasomal suture and basal grooves of TT4 and 5 deep, strigose. T5 with postero-lateral margin of convex, unevenly denticulate; medial protuberance broadly rounded posteriorly. ***Coloration*.** Body yellow except mandible apically, stemmaticum, occiput ventrally, middle lobe of mesoscutum anterior 1/2, lateral lobe of mesoscutum, tegula, propleuron posteriorly, mesopleuron ventrally, propodeum anterior 1/2, hind tibia apical 1/2, hind tarsus, T1 postero-medially, T2 except laterally, TT3–5 except laterally and posteriorly, ovipositor sheath brown.

**Male.** Unknown.

**Distribution.** Oriental (Thailand).

**Host.** Unknown.

**Etymology.** Name refers to the relatively short medial and lateral lobes of the T5.

## Notes on described species

### ***Trigastrotheca acroceropsis*** Ranjith & Quicke, nom. nov.

Figs 27, 28

*Acrocerilia tricolor* Quicke & Ingram, 1993: 302, 306.

**Diagnosis.** Tricolourous, orange-red, black, and ivory white. Mesoscutum orange-red without dark marks as in *T. griffini* Quicke, sp. nov. but differs in the black central area of T2 being far larger and widening posteriorly. Basal lobe of claw largely rounded with small distal tooth (Fig. 28D). In addition, see Quicke and Ingram (1993: 304, 306).

**Figure 28.** *Trigastrotheca sublobata* sp. nov. ♀ holotype **A** metasoma, lateral view **B** fore wing.

**Notes.** After re-examining images of the male holotype *Acrocerilia tricolor*, we found that it is not conspecific with the type species of *Acrocerilia*, viz. *A. pachynervis* van Achterberg, 1989, also based on a male specimen, and we hereby formally transfer it to *Trigastrotheca*. The species name *tricolor* is preoccupied in the genus *Trigastrotheca* (*T. tricolor* Quicke & Ingram, 1993). *Trigastrotheca tricolor* is therefore a secondary homonym. Here we propose *T. acroceropsis* Ranjith & Quicke as a replacement name.

### ***Trigastrotheca nigricornis*** **Cameron, [1909] 1910**

Figs 29, 30

**Notes.** The holotype female from South Africa (Cape Colony) is in the MFN but is too badly eaten by dermestids (Shenefelt 1978) to permit species-level identification, and it is therefore not included in the key. However, the original description is fairly complete for the time and includes the following diagnosis for distinguishing it from *T. trilobata*: “May be known from the type species of the genus, *T. trilobata*, Cam. (Ann. S. Afr. Mus., V, 32), by the shorter ovipositor (4 mm with a body length of 5 mm in the latter), by the middle lobe on the apex of the abdomen being hardly developed and by the 1st abscissa of the radius being longer, not shorter, than the 2nd.”

**Figure 29.** *Trigastrotheca acroceropsis* nom. nov. ♂ holotype **A** habitus, dorsal view with labels inset **B** head, anterior view **C** head, dorsal view **D** mesosoma, anterior metasoma and wings, dorsal view **E** head and mesosoma, lateral view.

### *Trigastrotheca romani* Quicke, 2005
Fig. 31

**Diagnosis.** Similar to *T. trilobata* but differs in the frons anterolateral to median ocellus without diverging striae, the second metasomal suture being less strongly arched medially (Fig. 33F cf. Fig. 37B) and the posteromedial lobe of T5 being less sharp and protruding.

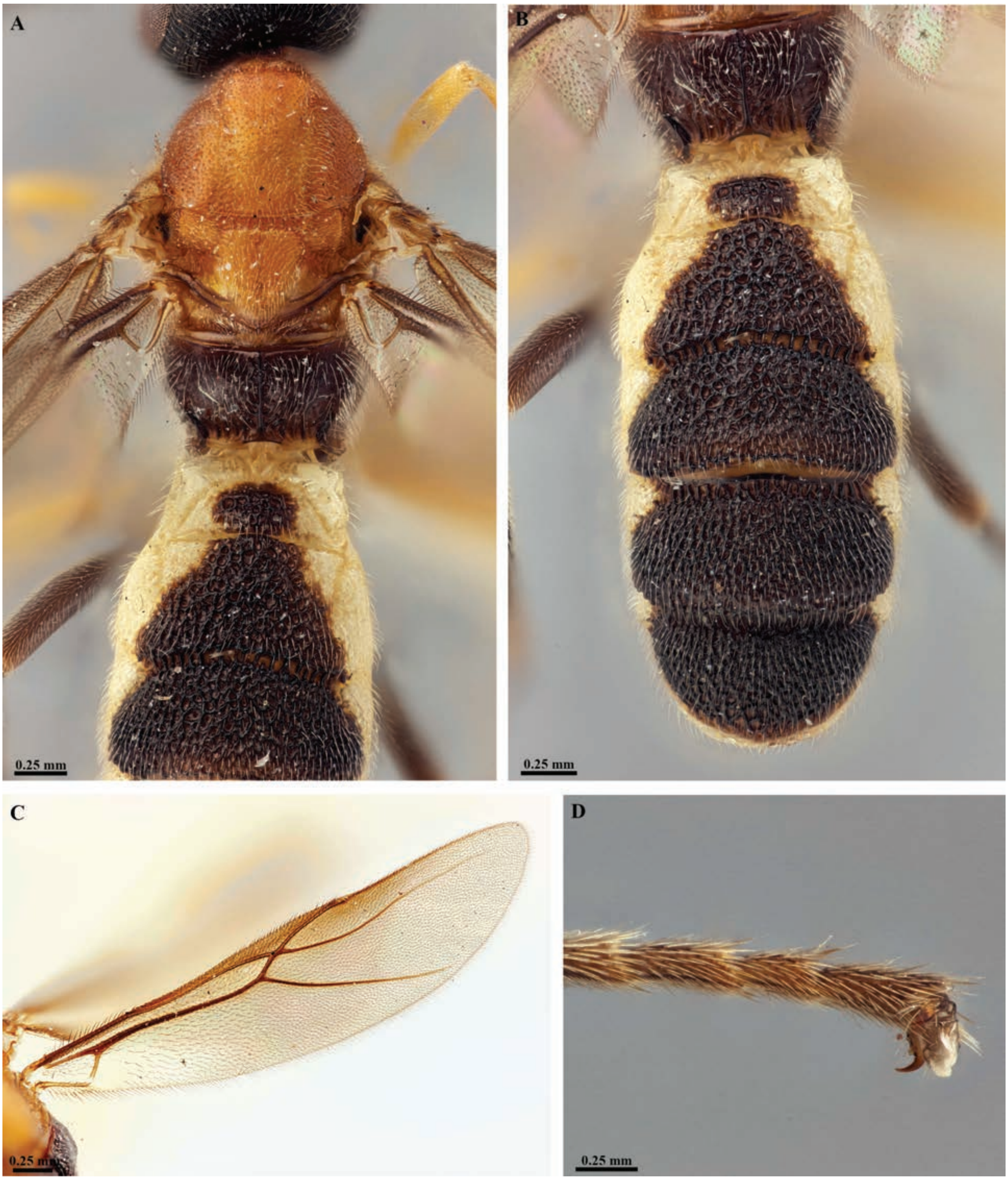

**Figure 30.** *Trigastrotheca acroceropsis* nom. nov. ♂ holotype **A** mesosoma and anterior metasoma, dorsal view **B** propodeum and metasoma, dorsal view **C** hind wing **D** distal hind tarsomeres and claw.

### *Trigastrotheca sureeratae* Quicke & Butcher, 2017

Figs 32, 33

**Material examined.** 1 ♀, Thailand, Nan Province, Sakaerat, 22.iv.2022 (CUMZ). DNA voucher P.I.D. BBTH3136-22.

**Diagnosis, female.** Similar to male except body length 5.0 mm. Antenna with 38 flagellomeres. Median flagellomeres as long as wide. First flagellomere 1.0 ×

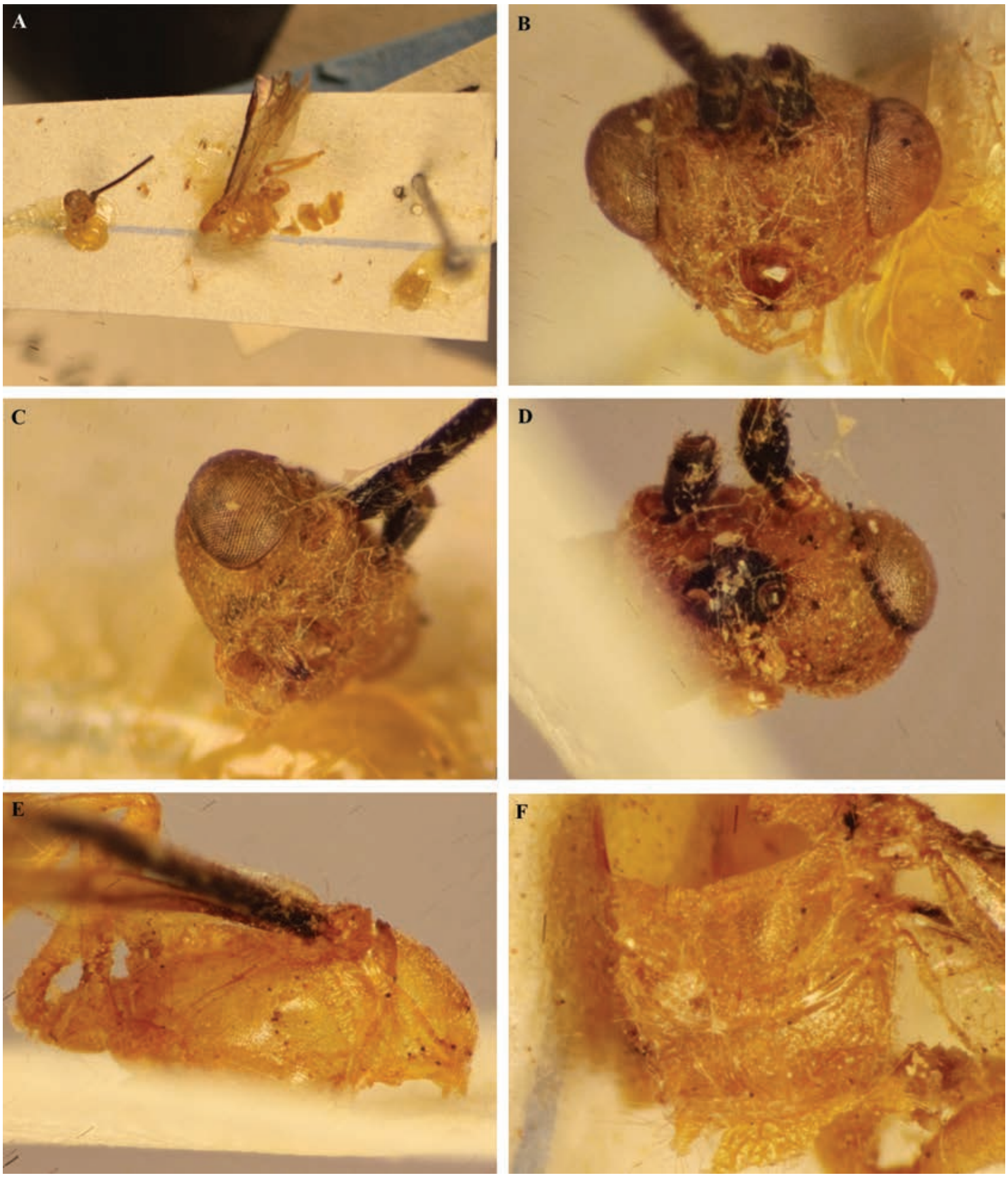

**Figure 31.** *Trigastrotheca nigricornis* ♀ holotype **A** remains on card rectangle **B** head, anterior view **C** head, oblique anterior view **D** head, dorsal view **E** mesosoma, lateral view **F** scutellum and propodeum, dorsal view.

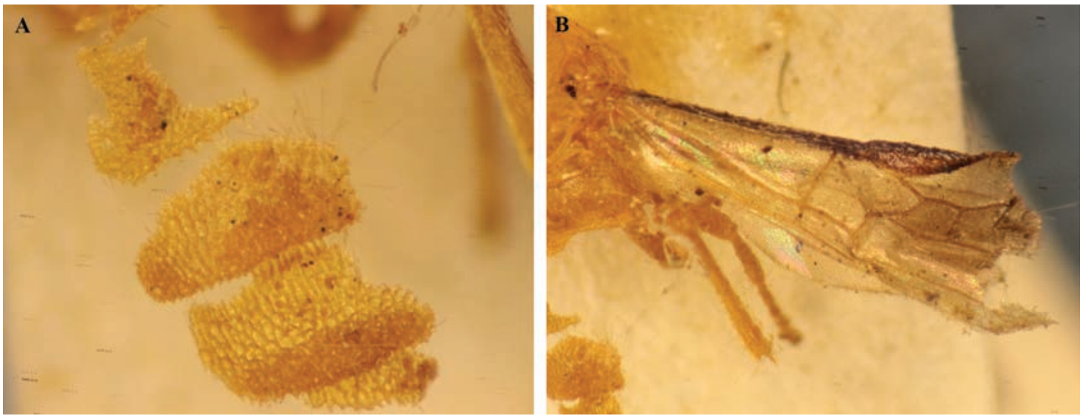

**Figure 32.** *Trigastrotheca nigricornis* ♀ holotype **A** remains of tergites, dorsal view **B** remains of wings.

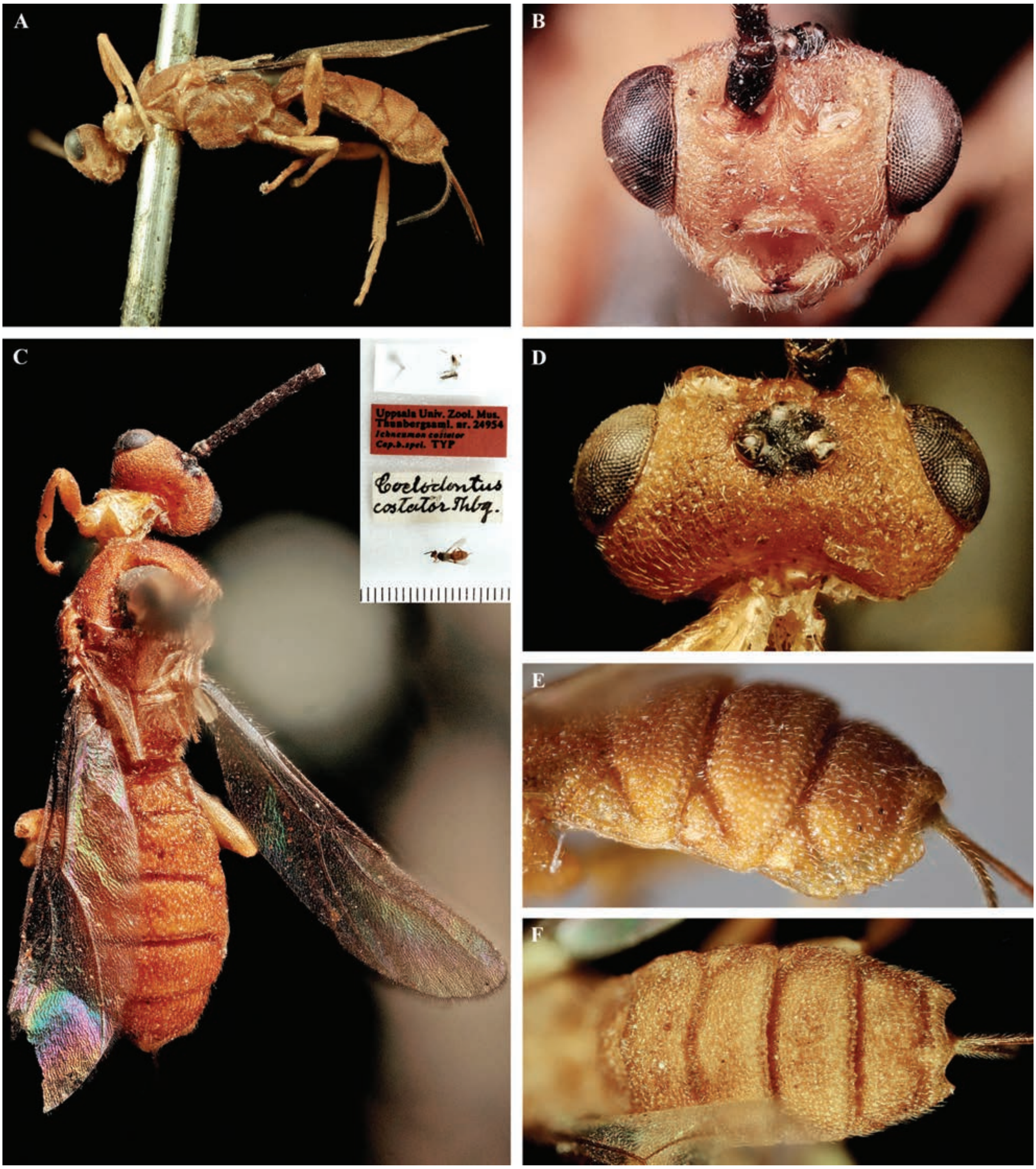

**Figure 33.** *Trigastrotheca romani* ♀ holotype **A** habitus, lateral view **B** head, anterior view **C** habitus dorsal view [notes: color is artefactually redder than in reality; labels inset] **D** head, dorsal view **E** TT2–5, lateral view **F** metasoma, dorsal view.

longer than 2nd and 3rd, respectively, 1.6 × longer than wide. Width of head: width of face: height of eye = 2.4: 1.3: 1.0. Inter tentorial distance: tentorio-ocular distance = 1.5: 1.0. Frons with strong mid-longitudinal carina. Shortest distance between posterior ocelli: transverse diameter of posterior ocellus: shortest distance between posterior ocellus and eye = 1.3: 1.0: 3.0. Lengths of veins r-rs: 3RSa: 3RSb = 1.0: 1.3: 4.6. Lengths of veins 2RS: 3RSa: rs-m = 1.2: 1.2: 1.0. Base of hind wing without large glabrous area. Lengths of fore femur: fore tibia: fore tarsus = 1.0: 1.0: 1.3. Lengths of hind femur: hind tibia: hind tarsus = 1.0: 1.4: 1.3.

T2 with parallel sided sublateral grooves. Second metasomal suture straight. Median length of T3 1.1 × T2. Mesoscutum with three longitudinal black patches. Propodeum black anterior 2/3. T2 with narrow black longitudinal patch.

**Notes.** The female specimen of *T. sureeratae* is comes close to *T. laikipiensis* and the differences are mentioned in the taxonomic key.

### ***Trigastrotheca tricolor*** **Quicke & Ingram, 1993**

**Diagnosis.** The color pattern is unique in the genus, viz. largely ochraceous yellow but head piceous with pair large, sub-rectangular areas laterally on the frons; the notauli, posterior 1/2 of middle lobe of mesoscutum and scutellum paler; metasomal tergites bicolorous, ochraceous except TT1 and 2 and anterolateral corners of T3 and posterior margin of T5 which are ivory-white. In addition, see Quicke and Ingram (1993: 331–332, figs 3, 87, 112, 113).

### ***Trigastrotheca tridentata*** **Enderlein, [1918] 1920**

**Diagnosis.** Tricolourous, black, cream, sulphur-yellow. This is the only known species which has the postero-lateral margin of the T5 concave with an abrupt lateral angulation (see Raweearamwong et al. 2020: 183, fig. 3F).

### ***Trigastrotheca trilobata*** **Cameron, 1906**

Figs 34, 35

**Diagnosis.** Similar to *T. aethiopica* sp. nov. and *T. romani* in being ochraceous except for black stemmaticum. Differs from *T. aethiopica* sp. nov. in having the pterostigma largely black, especially on the anterior 1/2, and from *T. romani* in that it has the frons anterolateral to median ocellus with distinct weakly diverging striae which is similar to the condition found in the male of *T. serrata* (van Achterberg & Sigwalt, 1987).

**Notes.** The type species of *Trigastrotheca* is *T. trilobata* Cameron, 1906 from South Africa or Zimbabwe [Rhodesia] (Cameron 1906). The type label in Cameron's handwriting states "Cape" (Fig. 32A), but on the underside of the card that the specimen is micro-pinned to with a minute pin "Rhodesia" and an illegible word is written (see http://www.waspweb.org/ichneumonoidea/Braconidae/Braconinae/Trigastrotheca/Trigastrotheca_trilobata.htm).

## Discussion

There were previously seven valid described species of *Trigastrotheca* described from mainland Africa (including two based on males described under the generic name *Kenema* but excluding *M. inermis*), six from Asia, and one from Australia (Raweearamwong et al. 2020). The additional species described here extend its known distribution to Madagascar, and collectively result from the work of individual collectors and more recently by large Malaise trapping initiatives (e.g. Quicke et al. 2023b).

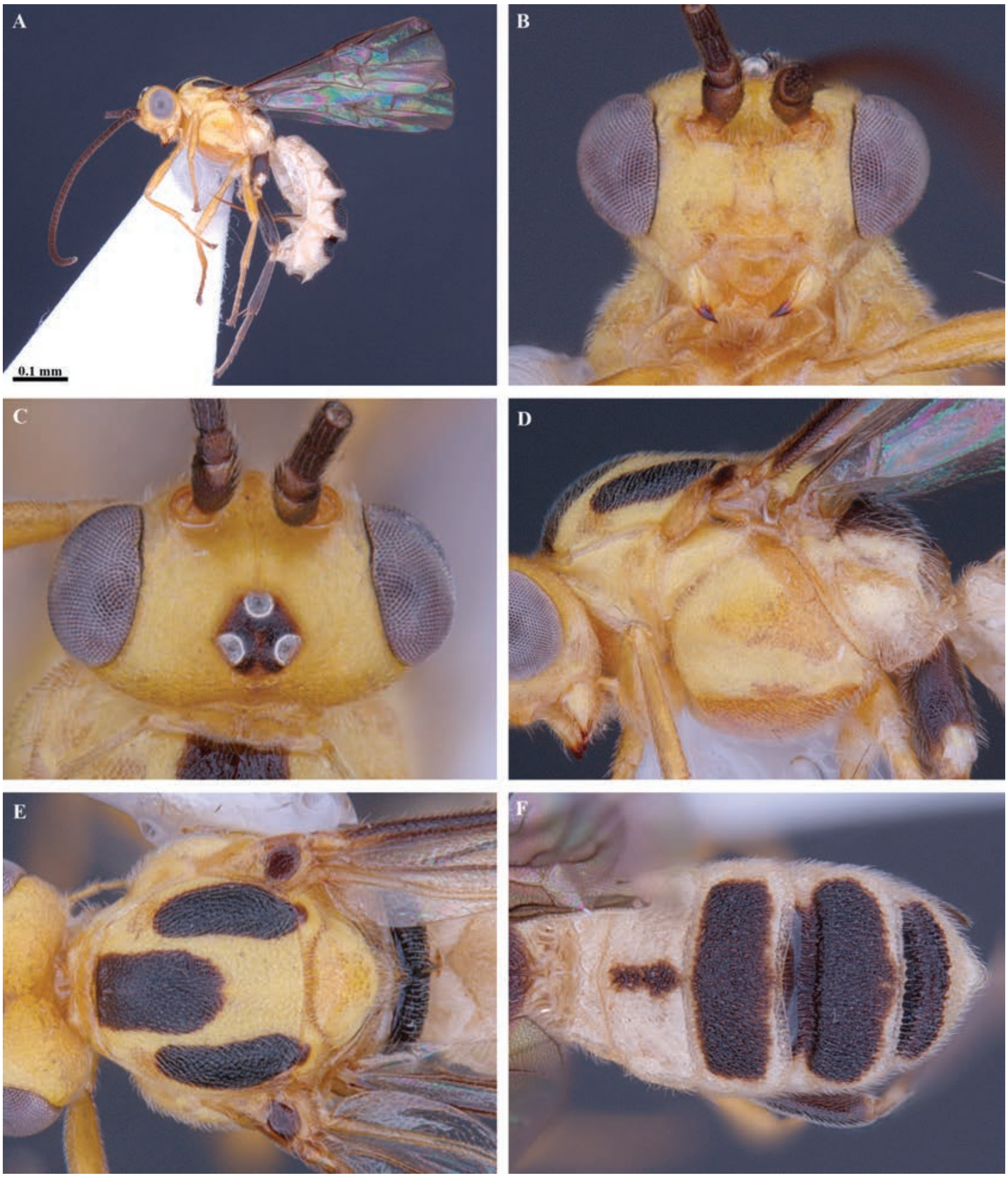

**Figure 34.** *Trigastrotheca sureeratae* ♀ A. habitus, lateral view **B** head, anterior view **C** head, dorsal view **D** mesosoma, lateral view **E** mesosoma, dorsal view **F** metasoma, dorsal view.

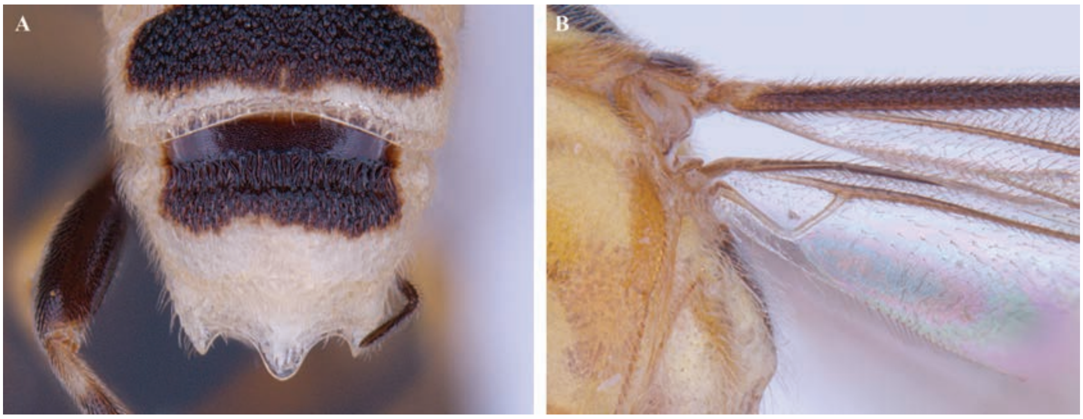

**Figure 35.** *Trigastrotheca sureeratae* ♀ **A** T5, dorsal view **B** base of hind wing

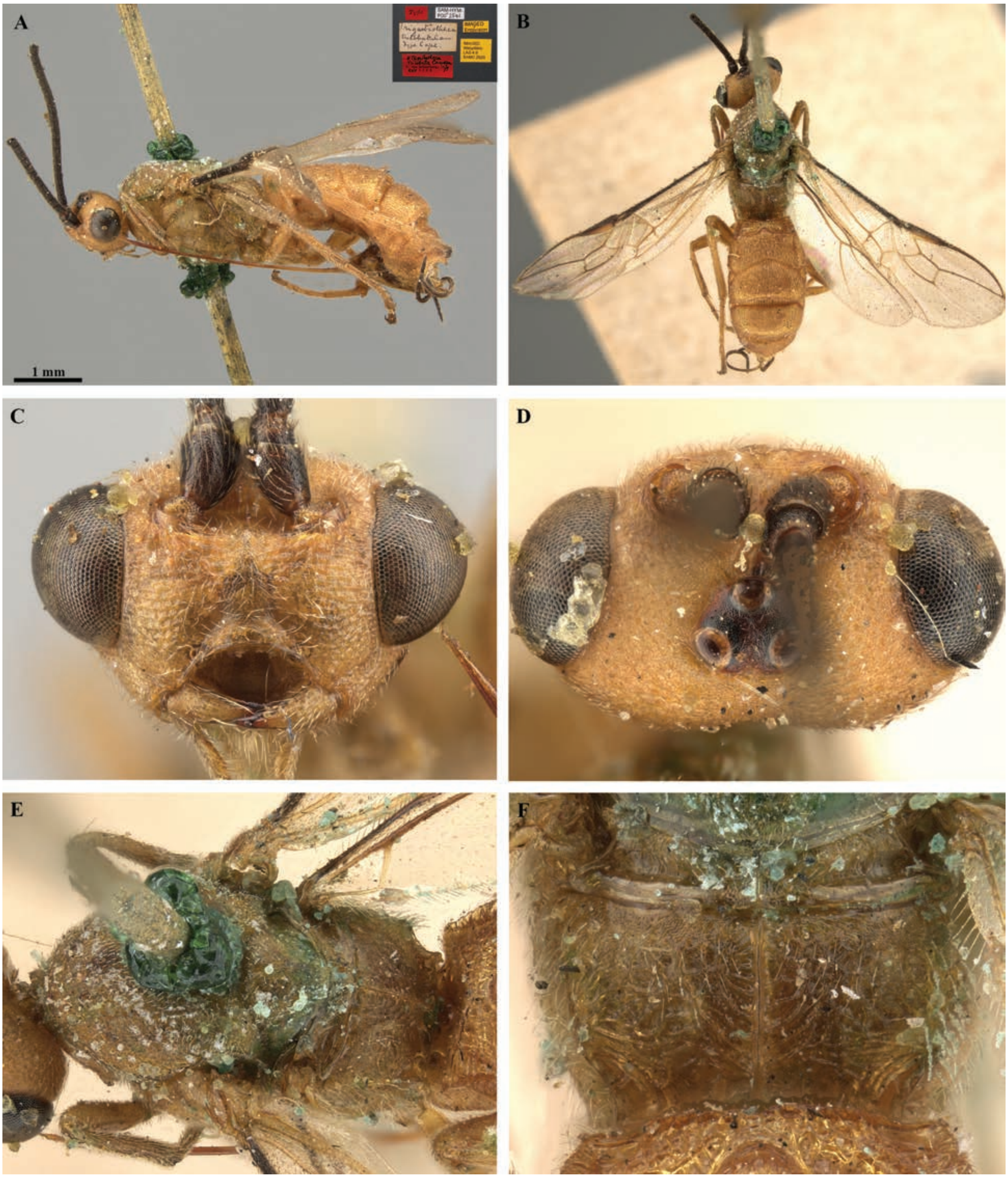

**Figure 36.** *Trigastrotheca trilobata* ♀ holotype **A** habitus, lateral view with labels inset **B** habitus, dorsal view **C** head, anterior view **D** head, dorsal view, E, mesosoma, slightly oblique dorsal view **F** metanotum and propodeum, dorsal view.

The molecular phylogenetic tree presented (Fig. 1) lacks strong support for most of the deeper nodes but some small groups of species are well supported. The sequenced species from Thailand comprise two separate clades, one containing three species that share the very similar (black, yellow, and white) color patterns to *T. tridentata*; however, the latter is recovered separately being strongly (99% bootstrap) as sister group to *T. sureeratae* Quicke & Butcher, 2017, which has a rather different, predominantly yellow brown pattern, though

**Figure 37.** *Trigastrotheca trilobata* ♀ holotype **A** metasoma, lateral view **B** metasoma, dorsal view **C** T1, dorsal view **D** TT4 and 5, lateral view **E** T5, dorsal view **F** wings.

still with a black and white metasoma. Unfortunately, *T. sureeratae* is known only from males so it is not currently possible to compare potentially more informative characters of the posterior metasomal tergite.

As regards the Afrotropical species known only from males and have virtually entirely ochreous yellow bodies (van Achterberg and Sigwalt 1987), we consider that there is insufficient material and, in particular, species for which members of both sexes are known, that it would be imprudent to attempt to incorporate them into the identification key with females. We believe that it will only be possible to integrate the species based only on a single male holotype into the study when fresh material (with correct identification) and ideally also molecular data, are available. In the case of other species, we have found that qualitative differences in color pattern adequate for correct identification in most cases. Regarding *Trigastrotheca quickei* van Achterberg, 1983, from Sierra Leone, the original description does not mention the color of the stemmaticum, but there is no indication that it is darker that the rest of the head from the figure, in which case it would run in our key to *T. carinata* sp. nov. which comes from India. *Trigastrotheca serrata* van Achterberg & Sigwalt, 1987, from Senegal, would run to couplet 4, but cannot be taken further since the serration of the T5 is probably not comparable between males and females.

## Acknowledgements

We are very grateful to Dr Julia Stigenberg for arranging the image of the type of *Ichneumon costator*. Kees van Achterberg (Naturalis Biodiversity Center, Leiden) kindly confirmed some generic placements. Susan Wright (Queensland Museum, Brisbane), Jaclyn McKeown (University of Guelph), and Konstantin Samartsev took and provided the images of *T. acroceropsis* nom. nov., *T. griffini* sp. nov., and *T. nigricornis*, respectively. APR thanks Dr Priyadarsanan D.R. and Dr Sinu P.A. for the specimens. We thank the subject editor and reviewers for their helpful comments and suggestions.

## Additional information

### Conflict of interest

The authors have declared that no competing interests exist.

### Ethical statement

No ethical statement was reported.

### Funding

This research was funded by National Research Council of Thailand (NRCT) (N42A650262) and Chulalongkorn University; Rachadaphiseksomphot Fund (RU66_008_2300_002); RSPG-Chula to BAB. APR and DLJQ were supported by postdoctoral fellowships from the Rachadaphiseksomphot Fund, Graduate School, Chulalongkorn University.

### Author contributions

Conceptualization: DLJLJQ, BAAB. Data curation: APR, SVN, ALLF, HM. Formal analysis: DLJLJQ. Funding acquisition: BAAB. Investigation: DLJLJQ, APR, SVN, ALLF, HM. Methodology: BAAB, DLJLJQ. Project administration: BAAB. Resources: BAAB, ALLF, SVN, APR. Supervision: BAAB. Validation: HM, BAAB. Visualization: HM, DLJLJQ, APR. Writing – original draft: DLJLJQ. Writing – review and editing: SVN, HM, BAAB, ALLF, APR.

### Author ORCIDs

Donald L. J. Quicke https://orcid.org/0000-0003-4471-6775
Simon Van Noort https://orcid.org/0000-0001-6930-9741

Avunjikkattu Parambil Ranjith https://orcid.org/0000-0001-7061-9659
Ariel L. L. Friedman https://orcid.org/0000-0003-4389-6858
Hans Mejlon https://orcid.org/0000-0003-0815-4656
Buntika A. Butcher https://orcid.org/0000-0002-0541-0709

## Data availability

All of the data that support the findings of this study are available in the main text.

## References

Butcher BA, Zaldivar-Riverón A, Van de Kamp T, Dos Santos Rolo T, Baumbach T, Quicke DLJ (2014) Extension of historical range of Betylobraconinae (Hymenoptera: Braconidae) into Palaearctic region based on a Baltic amber fossil, and description of a new species of *Mesocentrus* Szépligeti from Papua New Guinea. Zootaxa 3860(5): 449–463. https://doi.org/10.11646/zootaxa.3860.5.4

Cameron P (1906) Descriptions of new species of parasitic Hymenoptera chiefly in the collection of the South African Museum, Cape Town. Annals of the South African Museum 5: 17–186.

Cameron P (1909) [1910] On some African species of the subfamilies Exothecinae, Aphrastobraconinae, Cheloninae, Doryctinae, Cardiochilinae and Microgasterinae in the Royal Berlin Zoological Museum. Zeitschrift für Naturwissenschaft 81: 433–450.

Enderlein G (1920) [1918] Zur Kenntnis aussereuropäischer Braconiden. Archiv für Naturgeschichte 84 (A): 51–224. https://doi.org/10.5962/bhl.part.13627

Gillespie JJ, Yoder MJ, Wharton RA (2005) Predicted secondary structure for 28S and 18S rRNA from Ichneumonoidea (Insecta: Hymenoptera: Apocrita): impact on sequence alignment and phylogeny estimation. Journal of Molecular Evolution 61(1): 114–137. https://doi.org/10.1007/s00239-004-0246-x

Guérin-Méneville FE (1848) Ordre des Hymenopteres. In: Voyage en Abyssinie exécuté pendant les anneées 1839–1843 (von Mr. Lefebvre). Bertrand, Paris, 346–348.

Hebert PDN, Cywinska A, Ball SL, de Waard JR (2003) Biological identification through DNA barcodes. Proceedings of the Royal Society of London Series A: Biological Sciences 270: 96–99. https://doi.org/10.1098/rspb.2002.2218

Kozlov AM, Darriba D, Flouri T, Morel B, Stamatakis A (2019) RAxML-NG: A fast, scalable, and user-friendly tool for maximum likelihood phylogenetic inference. Bioinformatics (Oxford, England) 35(21): 4453–4455. https://doi.org/10.1093/bioinformatics/btz305

Park DS, Suh SJ, Oh HW, Hebert PDN (2010) Recovery of the mitochondrial COI barcode region in diverse Hexapoda through tRNA-based primers. BMC Genomics 11(1): 1–7. https://doi.org/10.1186/1471-2164-11-423

Quicke DLJ (1987) The Old World genera of braconine wasps (Hymenoptera: Braconidae). Journal of Natural History 21(1): 43–157. https://doi.org/10.1080/00222938700770031

Quicke DLJ (2015) The Braconid and Ichneumonid Parasitic Wasps: Biology, Systematics, Evolution and Ecology. Wiley Blackwell, Oxford, 688 pp. https://doi.org/10.1002/9781118907085

Quicke DLJ, Ingram SN (1993) Braconine wasps of Australia. Memoirs of the Queensland Museum 31: 299–336.

Quicke DLJ, Koch F (1990) Die Braconinae-Typen der beiden bedeutendsten Hymenopteren Sammlungen der DDR. Deutsche Entomologische Zeitschrift 37(4–5): 213–227. https://doi.org/10.1002/mmnd.19900370403

Quicke DLJ, Stanton ML (2005) *Trigastrotheca laikipiensis* sp. nov. (Hymenoptera: Braconidae): a new species of brood parasitic wasp that attacks foundress queens of three coexisting Acacia-ant species in Kenya. Journal of Hymenoptera Research 14: 182–190.

Quicke DLJ, van Achterberg C (1990) The type specimens of Enderlein's Braconinae (Hymenoptera: Braconidae) housed in Warsaw. Tijdschrift voor Entomologie 133: 251–264.

Quicke DLJ, Belokobylskij SA, Smith MA, Rota J, Hrcek J, Butcher BA (2016) A new genus of rhysipoline wasp (Hymenoptera: Braconidae) with modified wing venation from Africa and Papua New Guinea, parasitoid on Choreutidae (Lepidoptera). Annales Zoologici 66(2): 173–192. https://doi.org/10.3161/00034541ANZ2016.66.2.003

Quicke DLJ, Butcher BA, Ranjith AP, Belokobylskij SA (2017) Revision of the non-Afrotropical species of *Trigastrotheca* Cameron (Hymenoptera: Braconidae: Braconinae) with descriptions of four new species. Zootaxa 4242(1): 95–110. https://doi.org/10.11646/zootaxa.4242.1.5

Quicke DLJ, Jasso-Martínez JM, Ranjith AP, Sharkey MJ, Manjunath R, Naik S, Hebert PDN, Priyadarsanan DR, Thurman J, Butcher BA (2023a) Phylogeny of the Braconinae (Hymenoptera: Braconidae): a new tribal order! Systematic Entomology 49(1): 84–109. https://doi.org/10.1111/syen.12608

Quicke DLJ, Hebert PDN, Pentinsaari M, Butcher BA (2023b) Barcoding Hymenoptera: 11 Malaise traps in three Thai forests: the first 68 trap weeks and 15,338 parasitoid wasp sequences. Forests 14(10): 1991. https://doi.org/10.3390/f14101991

Raweearamwong M, Quicke DLJ, Butcher BA (2020) A new species of *Trigastrotheca* Cameron (Hymenoptera: Braconidae: Braconinae) from Thailand. Zootaxa 4801(1): 179–184. https://doi.org/10.11646/zootaxa.4801.1.10

Samartsev KG (2023) Review of the genus *Cassidibracon* Quicke, 1987 and related taxa of the *Plesiobracon* group of genera (Hymenoptera: Braconidae: Braconinae). Caucasian Entomological Bulletin 19: 353–398. https://doi.org/10.5281/zenodo.10435707

Sharkey MJ, Wharton RA (1997) Morphology and terminology. In: Wharton RA, Marsh PM, Sharkey MJ (Eds) Identification manual to the New World genera of Braconidae. Special Publication of the International Society of Hymenopterists 1: 19–37.

Shenefelt RD (1978) Hymenopterorum Catalogus (nov. editio). Part 15. Braconidae 10. Junk, The Hague, 1425–1825.

Stanton ML, Palmer TM, Young TP (2005) Ecological barriers to early colony establishment in three coexisting acacia-ant species in Kenya. Insectes Sociaux 55(4): 393–401. https://doi.org/10.1007/s00040-005-0826-9

Szépligeti GV (1914) Afrikanische Braconiden des Königl. zoologischen Museums in Berlin. Mitteilungen aus dem Zoologischen Museum in Berlin 7: 154–230.

Thunberg CP (1822) Ichneumonidea, Insecta Hymenoptera illustrata. Mémoires de l'Académie Imperiale des Sciences de Saint Petersbourg 8: 249–281.

van Achterberg C (1983) Six new genera of Braconinae from the Afrotropical region (Hymenoptera, Braconidae). Tijdschrift voor Entomologie 126: 175–202.

van Achterberg C (1988) Revision of the subfamily Blacinae Foerster (Hymenoptera: Braconidae). Zoölogische Verhandelingen 249: 1–324.

van Achterberg C (1991) Revision of the genera of the Afrotropical and W. Palearctic Rogadinae Foerster (Hymenoptera: Braconidae). Zoologische Verhandelingen Leiden 273: 1–102.

van Achterberg C, Sigwalt B (1987) Three new genera of Braconinae from the Afrotropical region (Hymenoptera: Braconidae). Zoologische Mededelingen Leiden 6: 443–458.

Yu DS, van Achterberg C, Horstman K (2016) Taxapad 2016, Ichneumonoidea 2015. Database on flash drive. Ottawa, Ontario, Canada.

ZooKeys 1205: 169–189 (2024)
DOI: 10.3897/zookeys.1205.115506

Research Article

# To what extent are ephippia of Mexican Anomopoda (Crustacea, Cladocera) identifiable?

Gerardo Guerrero-Jiménez[1], Frida S. Álvarez-Solis[1], Elaine Aguilar-Nazare[1], Araceli Adabache-Ortiz[1], Aleksandra Baquero-Mariaca[1], Robert L. Wallace[2], Marcelo Silva-Briano[1]

1 *Universidad Autónoma de Aguascalientes, Centro de Ciencias Básicas, Departamento de Biología. Avenida Universidad 940, C.P. 20131, Aguascalientes, Ags. Mexico*
2 *Department of Biology, Ripon College, Ripon, WI 54971, USA*
*Corresponding authors: Marcelo Silva-Briano (msilva@correo.uaa.mx); Robert L. Wallace (wallacer@ripon.edu)*

## Abstract

Diapausing embryos encased within cladoceran ephippia result from sexual reproduction and increase genetic diversity. They are also important means by which species bypass harsh environmental conditions and disperse in space and time. Once released, ephippia usually sink to the benthos and remain there until hatching. Using the Sars' method (incubating sediments to identify cladoceran hatchlings), ephippial egg bank biodiversity can be evaluated. Yet, even when samples are incubated under a variety of conditions, it is not possible to warrant that all have hatched. Few keys are available that facilitate the identification of cladocerans by using only ephippial morphology. Our goal was to analyze some cladoceran ephippia from Mexico, to develop a means to identify them using easily recognizable characteristics. Ephippia of 23 cladoceran species from waters in Aguascalientes (México) in 11 genera (*Alona*, *Biapertura*, *Ceriodaphnia*, *Chydorus*, *Daphnia*, *Dunhevedia*, *Ilyocryptus*, *Macrothrix*, *Moina*, *Pleuroxus*, and *Simocephalus*) were analyzed. In our analysis six morphological features were selected that permitted the identification of ephippia to species(-group) level. The results demonstrate that with a proper catalog of features, some ephippia can be identified.

**Key words:** Diapausing embryos, dormancy, ephippia, sediment, SEM, taxonomy, ultrastructure

OPEN ACCESS

**Academic editor:** Kay Van Damme
**Received:** 8 November 2023
**Accepted:** 30 March 2024
**Published:** 24 June 2024

**ZooBank:** https://zoobank.org/8562273E-9958-4E51-AC34-758E15A931D6

**Citation:** Guerrero-Jiménez G, Álvarez-Solís FS, Aguilar-Nazare E, Adabache-Ortiz A, Baquero-Mariaca A, Wallace RL, Silva-Briano M (2024)To what extent are ephippia of Mexican Anomopoda (Crustacea, Cladocera) identifiable? ZooKeys 1205: 169–189. https://doi.org/10.3897/zookeys.1205.115506

## Introduction

Many aquatic micrometazoans produce diapausing embryos (DEs) that permit them to bypass adverse conditions in their habitat, including drought (Schröder et al. 2007), inadequate food conditions (Drillet et al. 2011), and the presence of predators (Hairston and Munns 1984; Slusarczyk 1995; Pijanowska and Stolpe 1996). Taxa capable of producing DEs or other dormant stages include protists (Perrigo et al. 2012), bryozoans (Figuerola et al. 2003), cladocerans (Kokkinn and Williams 1987), copepods (Uye 1985), gastrotrichs (Ricci and Balsamo 2000), nematodes (Ptatscheck and Traunspurger 2020), rotifers (Walsh et al. 2017), and tardigrades (Altiero et al. 2009). The resulting dormant stages in Cladocera usually sink to the bottom, although in some macrothricids, ephippia may be attached to macrophyte leaves (Fryer 1972) or algae (see appendix in Guerrero-Jiménez et al. 2020). Thus, DEs constitute a genetically diverse egg-bank for future generations and they may disperse passively by anemochory (Rivas Jr et al. 2018, 2019), anthropochory (Bailey et al. 2003; Panov et al. 2004; Perrigo et al. 2012), hydrochory (Ricci and Balsamo 2000), and zoochory (Moreno et al. 2019; Vanschoenwinkel et al. 2011). When conditions are favorable, these dormant stages may hatch and replenish the previous population or establish a new one elsewhere (Montero-Pau et al. 2017; Vargas et al. 2019; Odriozola et al. 2020; García-Zamorano and Jiménez-Contreras 2023).

Water fleas (Crustacea, Cladocera) are important components of freshwater ecosystems, passing energy and nutrients on to higher trophic levels (Gulati and DeMott 1998). Most cladocerans reproduce by cyclic parthenogenesis with gamogenetic reproduction happening occasionally. Gamogenetic females of the order Anomopoda Sars, 1865 produce diapausing embryos (resting eggs) covered by a protective, saddle-shaped structure called the ephippium (G., *epi*, on + *hippos*, horse), which usually contains one or two embryos (Fryer 1972); in some macrothricids more than two are observed (Scourfield 1902; Smyly 1956), as well as in Eurycercidae and some other lineages. Some taxa may reproduce dormant stages asexually (Decaestecker et al. 2009), such as an entire population of *Daphnia pulex* Leydig, 1860 from North America (Hebert and Crease 1983). Knowledge of the conditions that permit hatching of DEs from sediment samples allows researchers to incubate sediments and identify the hatchlings; from such studies one can develop species lists of the cladocerans in a habitat (Vandekerkhove et al. 2005b). This method is called “the Sars’ Method” (Van Damme and Dumont 2010). Nevertheless, one can never be certain that the DEs from all species present in a sediment sample have hatched, even when the samples have been incubated under a variety of settings that otherwise appear to mimic favorable natural conditions. In addition, hatching is not possible when sediments have been preserved in a fixative. Considering these obstacles, developing comprehensive species lists of a cladoceran community would be improved if researchers were able to identify unhatched ephippia based solely on their morphology. This method is already very widely used in paleolimnology, where cladoceran ephippial identification is one of the pillars of reconstructing past conditions of lakes; entire identification books exist on only remains of cladocerans and ephippia from Europe (Szeroczyfiska and Sarmaja-Korjonen 2007). One of the first advancements in the identification of unhatched ephippia came from drawings of different ornamentations in species of *Bosmina longirostris* complex O.F. Müller, 1785 by Scourfield (1901). Later, Scourfield (1902) expanded on this by illustrating the ephippia of what he called at the time the “Lynceid Entomostraca” (chydorids). Goulden (1966) further improved our knowledge of ephippial morphology by illustrating variation in four *Moina* species. Subsequently, Vanderkerkhove et al. (2004) recognized 29 ephippial morphotypes and Mergeay et al. (2005) observed clear differences in several *Daphnia* species from Kenya. Subfossil records are also a widely used tool for the identification of cladocerans in the field of paleolimnology. In particular, Szeroczyfiska and Sarmaja-Korjonen (2007) provide detailed descriptions of morphological traits of ephippia belonging to several species of Daphniidae and Chydoridae in particular in their ‘Atlas of Subfossil Cladocera from Central and Northern Europe’. More detailed studies were accomplished using SEM technology to illustrate ephippia ornamentations in fossil records, and in ephippia that were still attached to the female (Kotov 2013). Kotov et al. (2018) also demonstrated differences in six *Ceriodaphnia* species from central, northern European Russia, predominantly for their practical use in paleolimnological settings. More recently Guerrero-Jiménez et al. (2020) presented 11 morphotypes extracted from sediments from Spain and Mexico, of different species of water fleas.

Yet, despite the excellent progress that has been made in our ability to differentiate ephippia of different species, we still lack useful diagnostic features. Thus, the aim of our research was to revisit an old – yet important – and largely unstudied question posed more than 30 years ago by Kokkinn and Williams (1987): "is ephippial morphology a useful taxonomic descriptor in the Cladocera?" Studies like Kotov et al. (2018) have shown that it can indeed be useful even between close species, to some extent, yet sometimes large detail is needed. There are at least two major problems to the development of a key to cladoceran ephippia: (1) the information on their taxonomic characters is scattered in the literature and (2) we have insufficient information on their features as a standardized nomenclature of ephippial characters is largely lacking. This knowledge gap is acerbated by the fact that there are at least 620 described cladoceran species (Forró et al. 2007), and most ephippia are studied in Palearctic settings. Thus, we still lack sufficient information so that ephippial morphology can become a useful tool for researchers studying the contemporary ephippial egg bank.

Here we report our results in producing a first database that will hopefully improve our ability to identify cladoceran ephippia of some Mexican taxa based only on their morphology. This information could be an important tool to estimate cladoceran diversity in freshwaters in the region (Vandekerkhove et al. 2005a, b) and subsequently to appreciate their adaptation to the environment within an evolutionary context (Brendonck and De Meester 2003; Gueriau et al. 2016).

## Materials and methods

### Study sites and species examined

Sixteen water ponds were analyzed from Aguascalientes, México: 1. El Niagara 2. Tanque de los Jiménez 3. El Tepetate de Abajo, Mal Paso 4. Sierra Fría, Bordo 1: 5. Sierra Fría, Bordo 4; 6. Sierra Fría, Bordo 5: 7. Boca de Túnel; 8. Bordo Siglo XXI; 9. Tapias Viejas 1; 10. El Cedazo Park: 11. Rodolfo Landeros Park: 12. Pulgas Pandas; 13. UAA; 14. Los Gavilanes: 15. El Ocote: 16. Villa Hidalgo. We provide additional details of the study sites in Suppl. material 1: appendix A. We examined ephippia of 23 taxa (Table 1).

### Diapausing eggs collection

Using an acrylic tube (2 m × 7.5 cm), we randomly collected sediment samples (cores) from three different points at each study site. We used only the upper 3 cm of cores to extract potentially vital ephippia (Pérez-Martínez et al. 2013). Samples were stored in the dark in a plastic bag at 4 °C. To extract ephippia from sediments we used the sugar flotation method of Onbé (1978) modified by Marcus (1990). For some species, ephippia were collected from the littoral zone and in other cases from algal mats. Additionally, ephippia of *Simocephalus mixtus* (Sars, 1903) were obtained from a laboratory culture (see details in Suppl. material 1: appendix B).

**Table 1.** List of the cladoceran taxa examined in this study.

| | |
|---|---|
| 1 | *Alona aguascalientensis* Sinev & Silva-Briano, 2012 |
| 2 | *Alona* sp. |
| 3 | *Biapertura ossiani* Leydig, 1860 |
| 4 | *Ceriodaphnia cornuta* Sars, 1886 |
| 5 | *Ceriodaphnia dubia* Richard, 1894 |
| 6 | *Ceriodaphnia laticaudata* P.E. Müller, 1867 |
| 7 | *Ceriodaphnia reticulata* Jurine, 1820 |
| 8 | *Chydorus sphaericus* s.l. O.F. Müller, 1776 |
| 9 | *Daphnia* (*Ctenodaphnia*) *exilis* Herrick, 1895 |
| 10 | *Daphnia leavis* Birge, 1879 |
| 11 | *Daphnia parvula* Fordyce, 1901 |
| 12 | *Daphnia pulex* Leydig, 1860 |
| 13 | *Dunhevedia crassa* King, 1853 |
| 14 | *Ilyocryptus agilis* Kurz, 1878 |
| 15 | *Macrothrix mexicanus* Ciros-Pérez, Silva-Briano & Elías-Gutiérrez, 1996 |
| 16 | *Macrothrix rosea* (Jurine, 1820) – *M. triserialis* Brady, 1886 (see Dumont et al. 2002) |
| 17 | *Macrothrix smirnovi* Ciros-Pérez & Elías-Gutiérrez, 1997 |
| 18 | *Moina macrocopa* Straus, 1820 |
| 19 | *Moina micrura* Kurz, 1875 |
| 20 | *Picripleuroxus denticulatus* Birge, 1879 |
| 21 | *Simocephalus mixtus* Sars, 1903 |
| 22 | *Simocephalus vetulus* O.F. Müller, 1776 |
| 23 | *Simocephalus* sp. |

## Organism identification and documentation

We recorded a photomicrograph of the ephippia using a Nikon Eclipse light microscope (LM) with a digital camera DS-Fi2 under 4×, 10×, or 20× magnification. To initiate hatching, individual ephippia were placed in wells of a 96-well, polyethylene microplate (CELLTREAT® Scientific Products, 20 Mill St Ste 130, Pepperell, MA 01463) and incubated in a bioclimatic chamber in commercial water (Ciel®, Coca Cola®) under the conditions of 16:8 light/dark period, 20 °C temperature, and white light with an intensity of 345.50 ± 20.54 μmol $s^{-1}$ $m^{-2}$). Once hatched, the females were cultured until they matured, at which time they were identified using the key of Elías-Gutiérrez et al. (2008).

## SEM analysis

To analyze their ornamentation, ephippia were isolated and fixed in 4% formalin. For SEM study, specimens were dehydrated using a graded ethanol series (60, 70, 80, 90, 96%), after which a critical point drying was performed. Ephippia were attached to a SEM stub (1 cm high × 1.2 cm in diameter) and sputter coated with gold. All samples were observed under a SEM JEOL 5900 LV®, photomicrographs were taken to document ephippial characteristics.

*Characterization of ephippia*. To identify ephippia to species level we used six characteristics that we could see using LM and SEM: size, shape, color (including transparency), number of resting eggs, presence of ornamentation and/or accessory structure, and type of ornamentation or accessory structures.

1. Size. Ephippia were categorized into three groups: small (< 400 µm), medium (≥ 400–800 µm) and large (> 800 µm).
2. Shape. Ephippia were classified in geometrical categories: triangular, half oval, square, rectangular, and irregular. In determining the shape of ephippia, accessory structures were not considered.
3. Color. We categorized the color of ephippia when observed under LM.
4. Number of diapausing embryos in an ephippium. The number of diapausing embryos observed inside of the chamber of the ephippium were counted.
5. Type of ornamentation. We recorded features observable by SEM on the surface of ephippia; these included depressions ("craters"), verrucae, striae ("grooves"), pores, reticulations, and scales. "None" indicates the absence of ornamentation and/or accessory structure. **Craters/depressions** defined as small concave holes on the surface of the ephippia with oval or irregular shape present on the surface were categorized as craters (see Fig. 1A). **Verrucae** are identified as small, spherical structures present on some parts

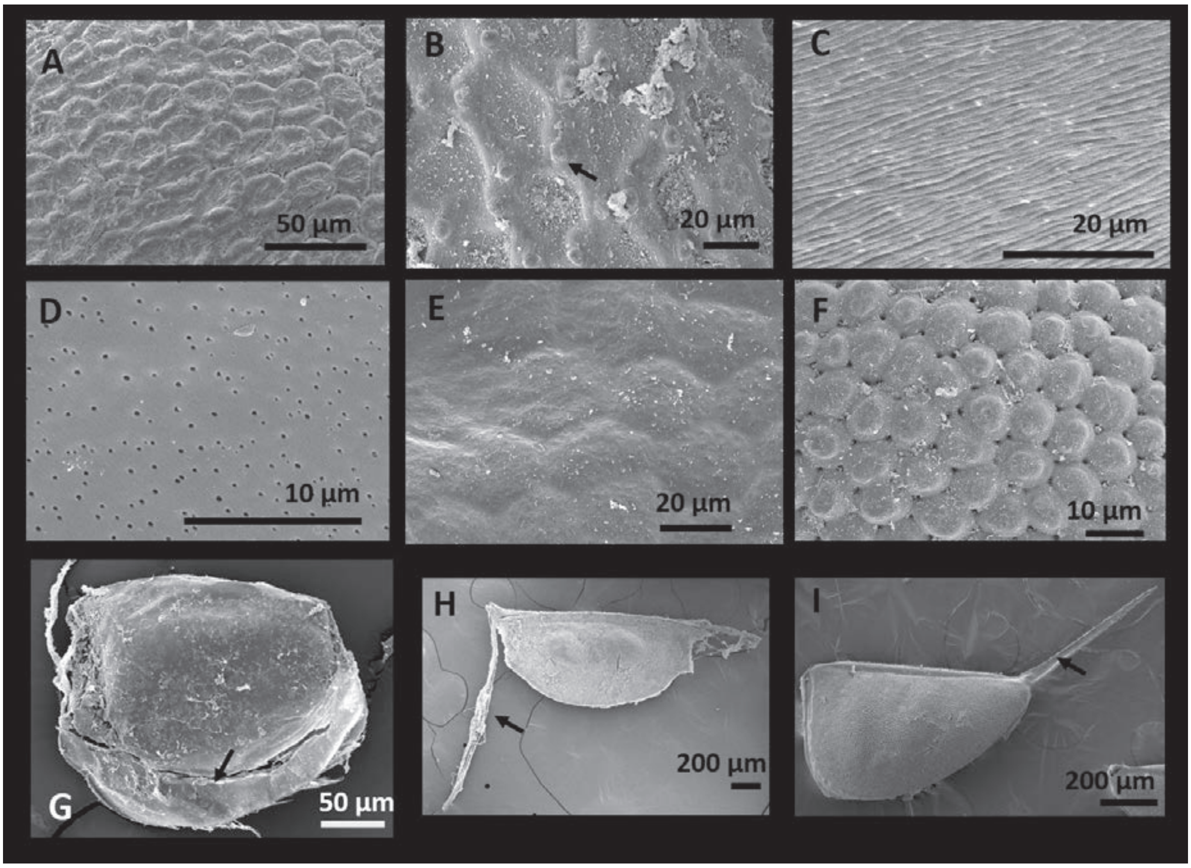

**Figure 1.** Micrographs of the ornamentation and accessory structure within species studied taken by SEM **A** Depressions ("craters") in *Moina macrocopa* Straus, 1820 **B** Verrucae in *Macrothrix mexicanus* Ciros-Pérez, Silva-Briano & Elías-Gutiérrez, 1996, see arrow **C** Striae in *Biapertura ossiani* Leydig, 1860 **D** Pores in *Dunhevedia crassa*; King, 1853 **E** Faint hexagonal reticulation in *Pleuroxus denticulatus* Birge, 1879 **F** "Scales" with depressions in between in *Macrotrix rosea* Jurine, 1820 **G** Filamentous membrane in *Alona aguascalientensis* Sinev & Silva-Briano, 2012, see arrow **H** Ventral appendices in *Daphnia* (*Ctenodaphnia*) *exilis* Herrick, 1895, see arrow **I** Spinules on the main posterodorsal spine in *Daphnia pulex* Leydig, 1860, see arrow.

of the surface of ephippia as verrucae (see Fig. 1B). **Striae** are pronounced marks in the surface of the ephippia visible by LM (see Fig. 1C). **Pores** have different sizes, but sometimes they were too small to be observed using only LM; in those cases, high resolution SEM was needed (see Fig. 1D). **Reticulations** are smooth marks in the surface of the ephippium with specific patterns that included lines, hexagonal, oval, or irregular shape. Usually, we were not able to observe these by LM; in that case we used the SEM (see Fig. 1E). **Scales** are small, membrane-like structures on the surface of ephippia as scales. These resembled laminar structures, usually covering the entire surface of the ephippium, they could be oval, rounded, or irregular in shape (see Fig. 1F). **Filamentous membranes** are remnants of the membrane that attached it to the ventral portion of the female carapace (see Fig. 1G).

6. Accessory structures. Accessory features were considered to be any extra structures in the basic morphology of the ephippia; these included membranes, peduncles, and spinules. “None” is used when they are absent. Ventral appendices are peduncle-like structure defined as the thin margin attached to the posterior ventral portion of the ephippium (see Fig. 1H). Spinules are labeled as pointed structures present at the posterior portion of ephippia. These varied in size with some being small lying in the margin of the egg (see Fig. 1I).

## Results

A total of 4017 ephippia belong to 23 cladoceran species in 11 genera: *Alona* Baird, 1843, *Biapertura* Smirnov, 1971, *Ceriodaphnia* Dana, 1853, *Chydorus* Leach, 1816, *Daphnia* O.F. Müller, 1785, *Dunhevedia* King, 1853, *Ilyocryptus* G.O. Sars, 1861, *Macrothrix* Baird, 1843, *Moina* Baird, 1850, *Pleuroxus* Baird, 1843, and *Simocephalus* Schoedler, 1858 were analyzed (see Figs 2–7, Suppl. material 1: appendix B).

1. Size. Within each genus, most species had ephippia of similar size; therefore, while size was useful in identification of the genus, it could not be used for species-level diagnosis (Table 1).
2. Shape. The shape of cladoceran ephippia varied among the genera we examined. Ephippial shape in some genera was consistent: all species of *Simocephalus* had a triangular shape (Fig. 7(21, 22, 23)), while a half oval shape was seen in *Ceriodaphnia* (Figs 2(4), 3(5, 6, 7)). On the other hand, ephippial shape varied in different *Macrothrix* species (Figs 5(15, 16), 6(17)). Another important feature was the margin of the ephippium. The margin of ephippia in *Alona* and *Daphnia* were similar in shape; but in some species the margins were rounded, while in others they were sharp. These differences are enough to distinguish between some species within a genus (Figs 2(1, 2, 3), 4(10, 11, 12)).
3. Color. The most common colors seen in the species studied were brown and dark (Gerrish and Cáceres 2003; Vandekerkhove et al. 2004); however, most ephippia were at least partially transparent. Thus, color was just used in cases that present patterns used to identify ephippia to the level of species: e.g., *Simocephalus vetulus* O.F. Müller, 1776 and *Simocephalus* sp. Within the ephippia, some embryos were orange in color (Fig. 7(22, 23)).

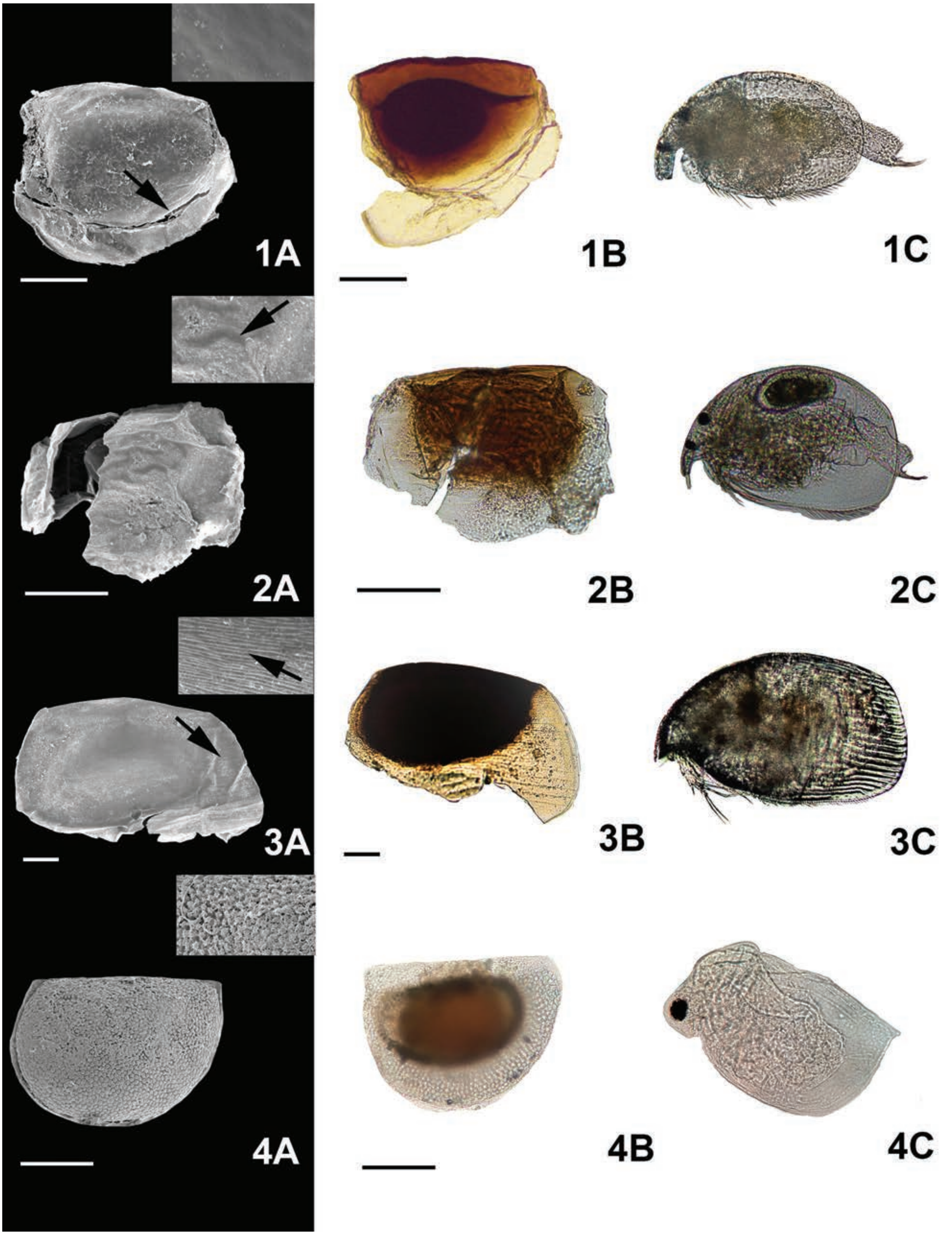

**Figure 2.** Micrographs of the ephippial ornamentation taken by **A** SEM **B** light microscope, and **C** the organisms hatched from the dormant embryos. 1. *A. aguascalientensis* Sinev & Silva-Briano, 2012 (immature individual in 1C), 2. *Alona* sp., 3. *Biapertura ossiani* Leydig, 1860, 4. *Ceriodaphnia cornuta* Sars, 1886. Arrows show the zoom of the specific ornamentation. Scale bars: 100 µm.

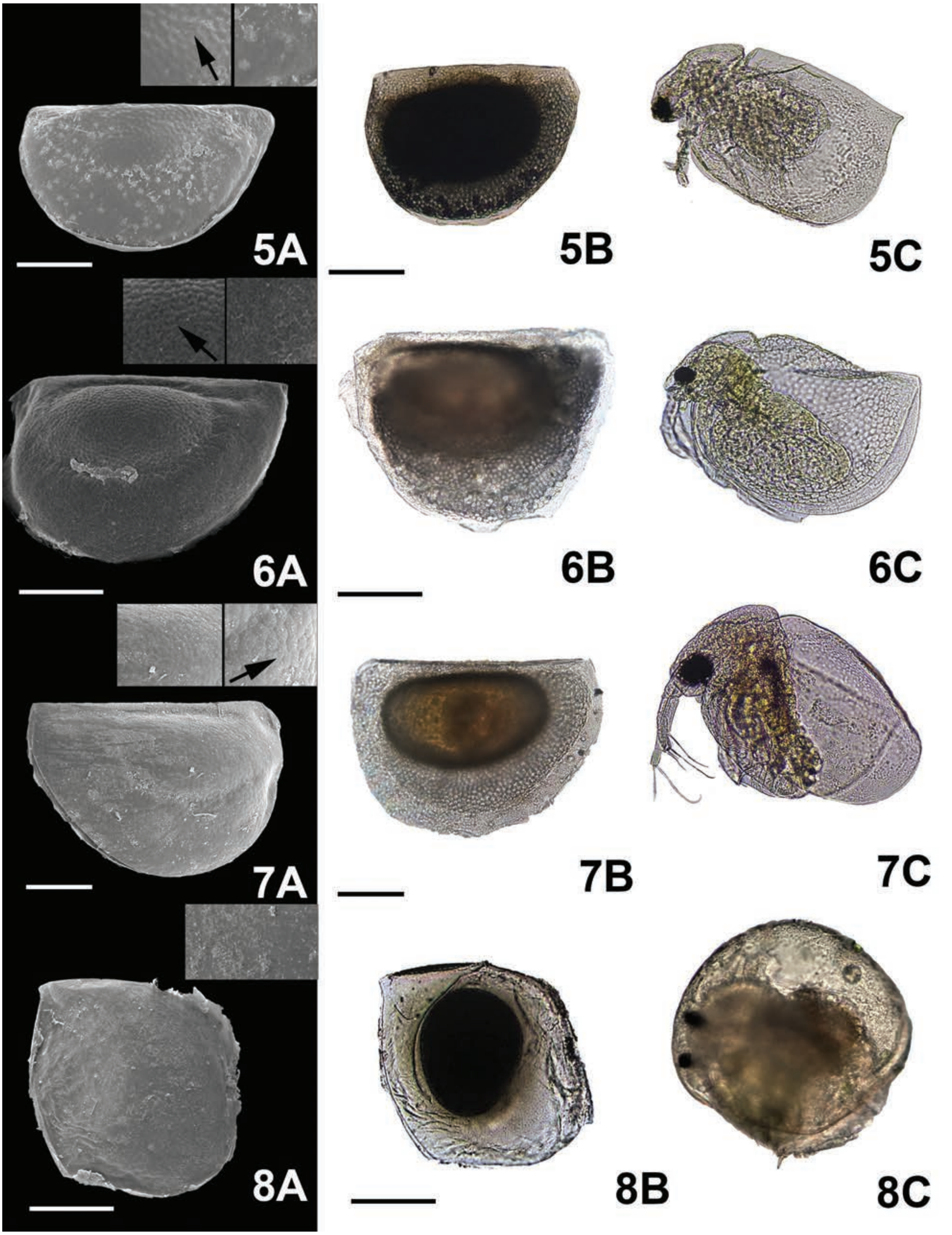

**Figure 3.** Micrographs of the ephippial ornamentation taken by SEM (**A**) light microscope (**B**) and organism hatched from the egg (**C**). 5. *C. dubia* Richard, 1894, 6. *C. laticaudata* P.E. Müller, 1867, 7. *C. reticulata* Jurine, 1820, 8. *Chydorus sphaericus* complex O.F. Müller, 1776. Arrows show the zoomed in image of the ornamentation. Scale bars: 100 μm.

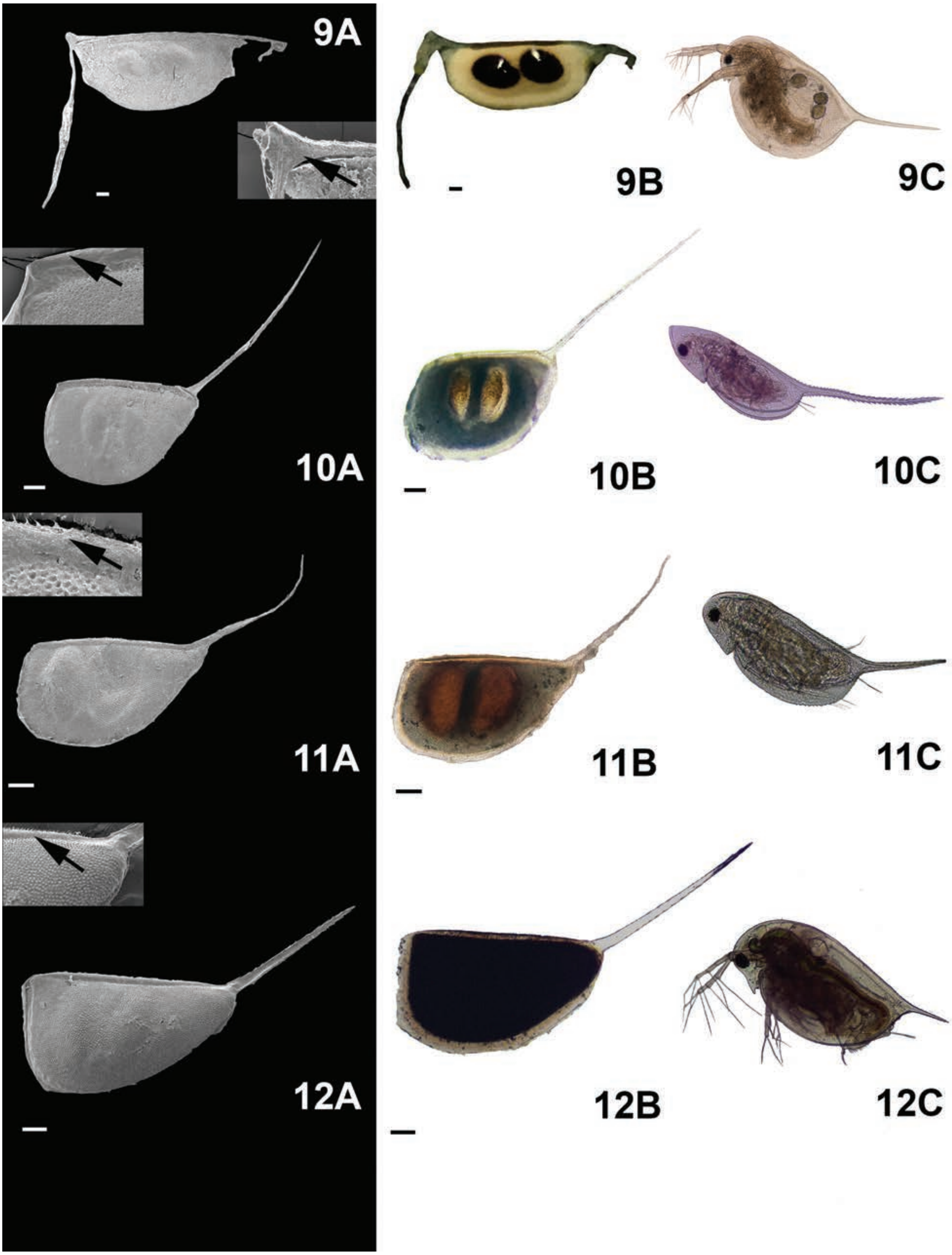

**Figure 4.** Micrographs of the ephippial ornamentation of some *Daphnia* taxa, taken by SEM (**A**) and light microscope (**B**) and organism hatched from the dormant embryo (some immature) (**C**). 9. *Daphnia* (*Ctenodaphnia*) *exilis* Herrick, 1895, 10. *D. leavis* Birge, 1879, 11. *D. parvula* Fordyce, 1901, 12. *D. pulex* Leydig, 1860. Arrows show the zoomed in image of the ornamentation and some spinules or serrations. Scale bars: 100 µm.

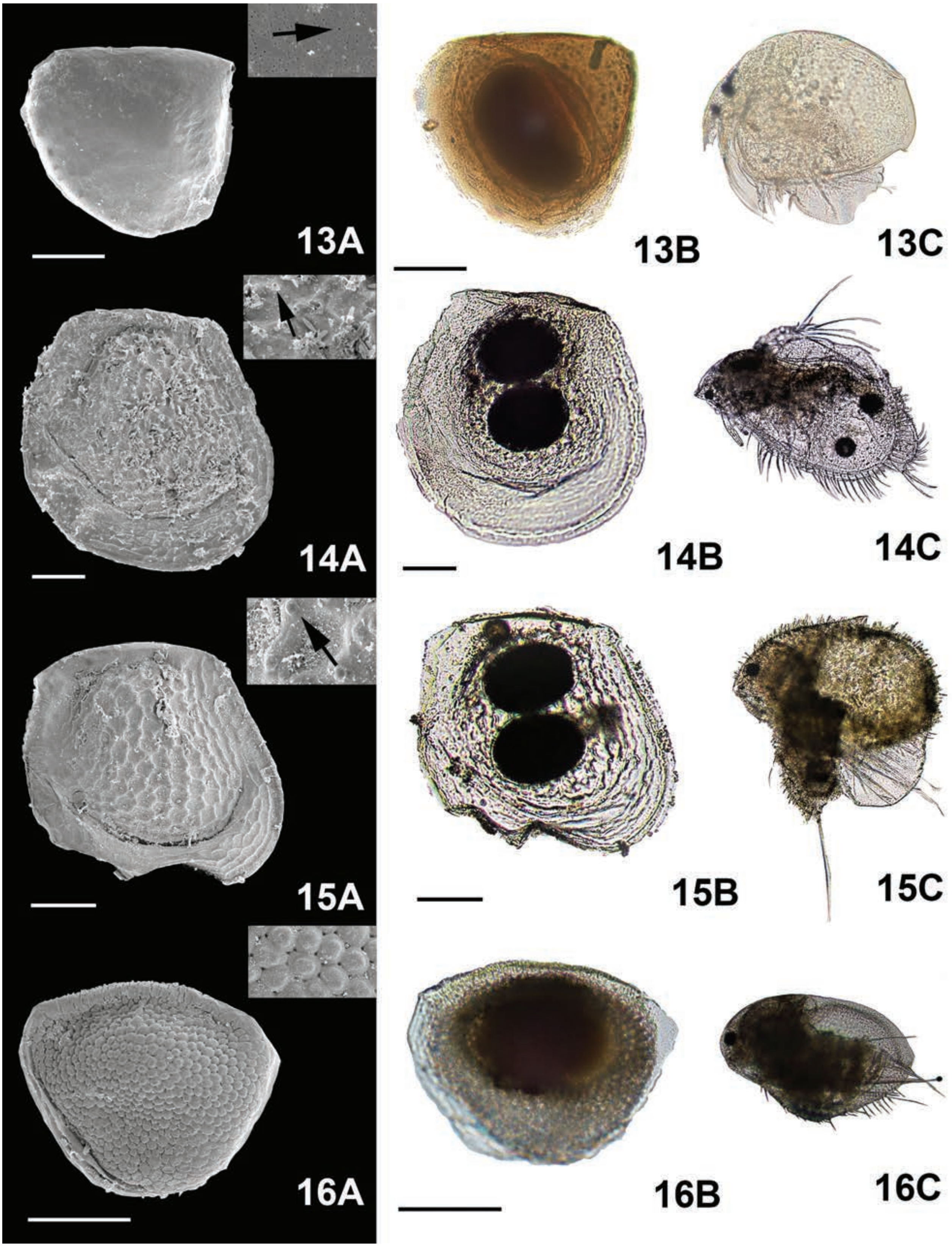

**Figure 5.** Micrographs of the ephippial ornamentation taken by SEM (**A**) light microscope (**B**) and organism hatched from the egg (some immature) (**C**). 13. *Dunhevedia crassa* King, 1853, 14. *Ilyocryptus agilis* Kurz, 1878, 15. *Macrothrix mexicanus* Ciros-Pérez, Silva-Briano & Elías-Gutiérrez, 1996, 16. *M. rosea* Jurine, 1820. Arrows show the zoomed in image of the ornamentation. Scale bars: 100 µm.

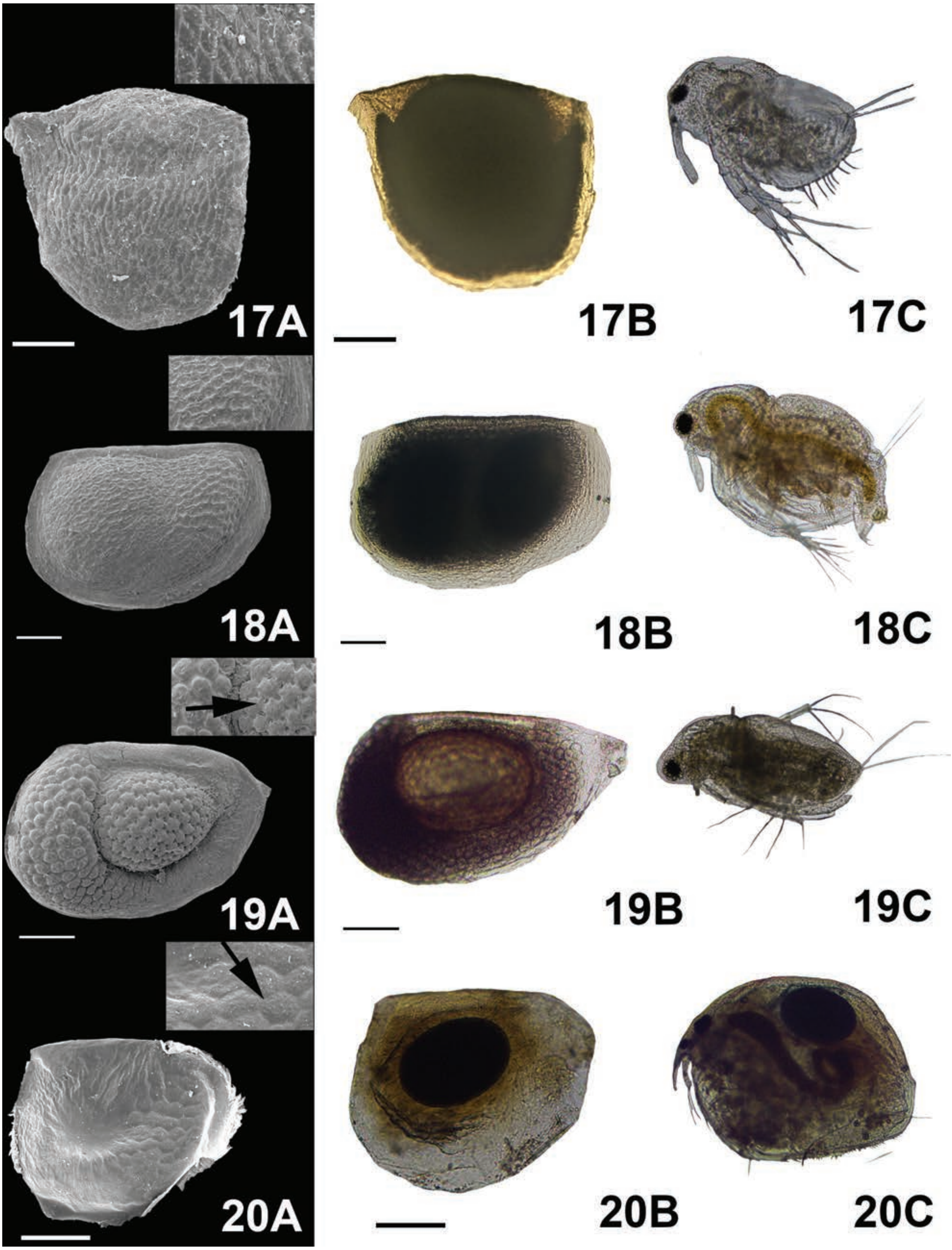

**Figure 6.** Micrographs of the ephippial ornamentation taken by SEM (**A**) light microscope (**B**) and organism hatched from the egg (**C**). 17. *Macrothrix smirnovi* Ciros-Pérez & Elías-Gutiérrez, 1997, 18. *M. macrocopa* Straus, 1820, 19. *M. micrura* Kurz, 1875, 20. *Pleuroxus denticulatus* Birge, 1879. Arrows show the zoomed in image of the ornamentation. Scale bars: 100 µm.

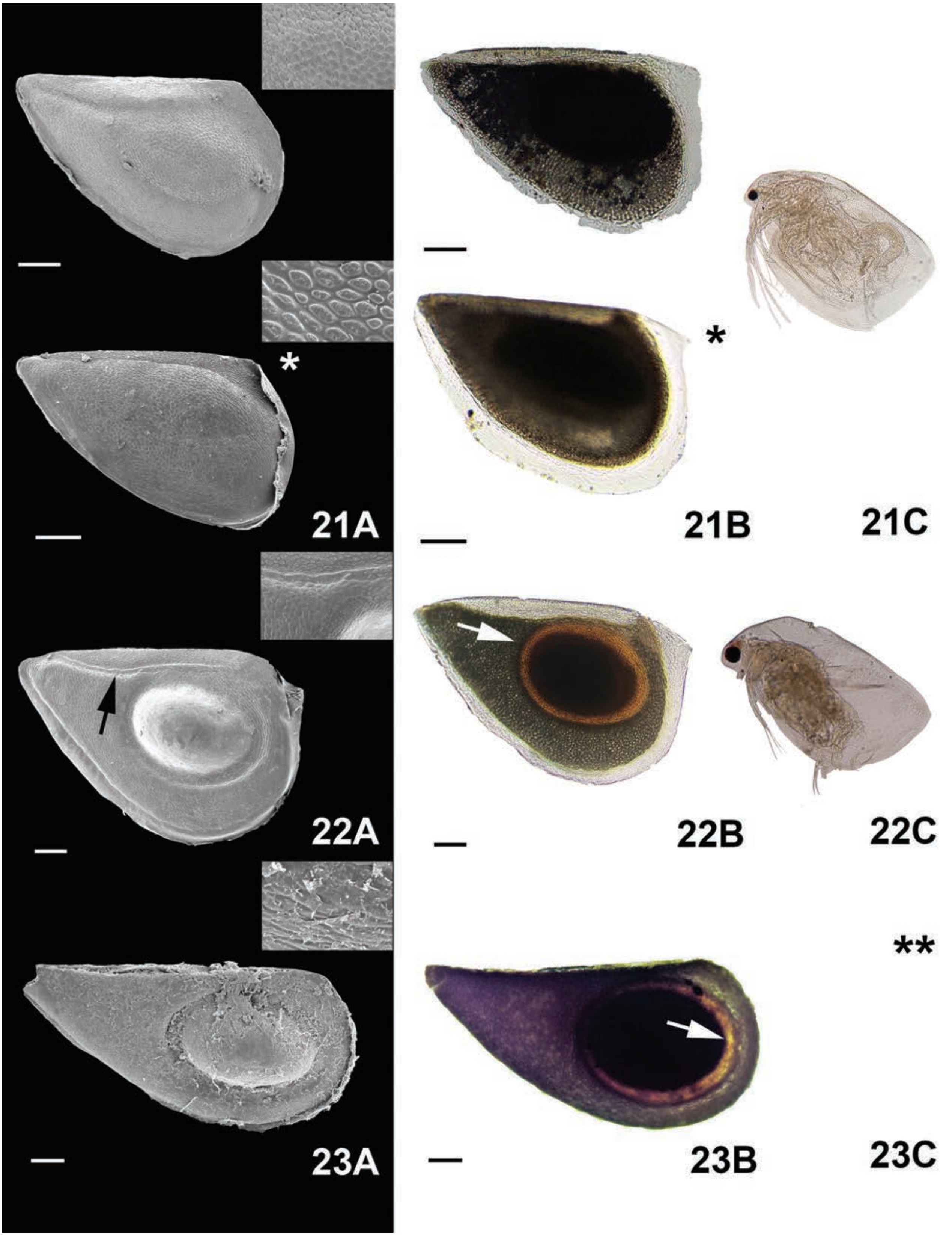

**Figure 7.** Micrographs of the ephippial ornamentation of *Simocephalus*, taken by SEM (**A**) light microscope (**B**) and organism hatched from the egg (**C**). 21. *Simocephalus mixtus* Sars, 1903, 22. *Simocephalus vetulus* O.F. Müller, 1776, 23. *Simocephalus* sp. (embryo/adult absent). Scale bars: 100 µm. (*) Ephippium extracted from laboratory cultures without males being present; (**) no hatched organism.

4. "Resting egg" (dormant embryo) number. The number of DEs within the ephippia of the species we studied is reported in Table 2.
5. Type of ornamentation. Five types of ornamentation were observed. (i) ***Depressions ("craters"):*** These were commonly observed in *Daphnia* sp. and *Moina macrocopa* Straus, 1820. These structures were observed only under SEM (Fig. 6(18A, arrow)). (ii) ***Verrucae:*** Small spherical structures were observed only in *Macrothrix mexicanus* Ciros-Pérez et al. 1996 (Fig. 5(15A, arrow)). (iii) ***Striae:*** Pronounced marks in the surface of the ephippia were identified; these were linear in *Biapertura ossiani* Leydig, 1860 (Fig. 2(1A, arrow)), smooth and rounded in *Ceriodaphnia dubia* Richard, 1894 (Fig. 3(5A, arrow)), pronouncedly rounded in *M. mexicanus* (Fig. 5(15A), and small, interlocking linear in *Simocephalus* sp. (Fig. 7(23A)), no link or patterns between all these species were observed. (iv) ***Pores:*** Very small pores were detected on the surface of the ephippia of *Dunhevedia crassa* King, 1853 (Fig. 5(13A, arrow)). (v) ***Reticulation***: Reticulations were seen in some genera. In *Alona* and *Biapertura* species, linear reticulations were evident (Fig. 2(1, 2, 3)); in *Ceriodaphnia*, the reticulation cells were oval (Figs 2(4), 3(5, 6, 7)); in *Pleuroxus* they were hexagonal in shape (Fig. 6(20A)). (vi) ***Scales:*** Different types of scales were observed. Small and irregular ones were present in *Ceriodaphnia cornuta* Sars, 1886 (Fig. 2(4A)); rounded scales were seen in the *Macrothrix rosea* Jurine, 1820 (see Dumont et al. 2002) (Fig. 5(16A)); oval scales were present in *S. mixtus* and *S. vetulus* (Fig. 7(21A, 22A)). Finally, in *Moina micrura* Kurz, 1875, two different types of scales were detected: rounded scales in the anterior portion of the ephippium and scales with irregular shape covering the section where the DE was located (Fig. 3(5A)).
6. Accessory structures. Only five species: *Alona aguascalientensis* Sinev and Silva-Briano, 2012, *Daphnia* (*Ctenodaphnia*) *exilis* Herrick, 1895, *Daphnia leavis* Birge, 1879, *D. parvula* Fordyce, 1901, and *D. pulex* Leydig, 1860 have accessory structures. Most of those were seen in *Daphnia* (Table 2, Fig. 4). (vii) ***Filamentous membranes:*** Filamentous membranes were observed only in *A. aguascalientensis* (Fig. 3(5A)). (viii) ***Ventral appendices:*** These were only observed in *C. exilis* (Fig. 3(5A)). (ix) ***Spinules:*** Spinules were specific to *Daphnia*, but they were also observed in *C. exilis*. In *Daphnia*, a long caudal spinule is present (Fig. 3(5A)), while in *C. exilis*, both caudal spinule and anterior projection were observed. In the posterior portion, a small spinule was attached to the ventral appendix while a longer spinule is observed in the anterior part of the ephippium (Fig. 3(5A)).

## Discussion

### Taxon-specificity in ephippial morphology

Here we provide data of six morphological characteristics on ephippial morphology on 23 taxa (Figs 2–7). Most of our results provide evidence of taxon-specificity in ephippial morphology among the studied species, but there were several challenges. For example, identification of *Ceriodaphnia* species was problematic. When using light microscopy, Vanderkerkhove et al. (2004) also reported difficulty in identifying *Ceriodaphnia laticaudata* P.E. Müller, 1867,

**Table 2.** Taxonomic standardization with six categories to identify ephippia in 11 genera of cladocerans.

| Genus | Egg size (µm) | Egg shape | Color | RE | Type of ornamentation | Accessory structure | Species |
|---|---|---|---|---|---|---|---|
| *Alona* | Small (< 400) | Rectangular | Brown and dark in the resting egg chamber | 1 | None | Width filamentous membrane in the base of the egg | *A. aguascalientensis* |
| | | Rectangular | Light brown | 1 | Striae | None | *A.* sp. |
| *Biapertura* | Medium (≥ 400–800) | Rectangular | Black and transparent membrane | 1 | Thin linear reticulations and soft parallel striae | None | *B. ossiani* |
| *Ceriodaphnia* | Small (< 400) | Semi-circular | Transparent and brown in the resting egg chamber | 1 | Irregular and small scales in all egg | None | *C. cornuta* |
| | Small (< 400) | Semi-circular | Transparent and dark in the resting egg chamber | 1 | Soft rounded striae in the resting egg portion | None | *C. dubia* |
| | Small (< 400) | Semi-circle | Transparent and brow in the resting egg chamber | 1 | Very soft oval reticulations in the margin of the egg but more visible in the resting egg portion | None | *C. laticaudata* |
| | Small (< 400) | Semi-circle | Transparent and brown in the resting egg chamber | 1 | Very soft oval reticulations | None | *C. reticulata* |
| *Chydorus* | Small (< 400) | Square | Light brown and dark in the resting egg chamber | 1 | None | None | *C. sphaericus* |
| *Daphnia* | Large (> 800) | Rectangular | White and dark in the resting egg chamber | 2 | Small irregular reticulations | Spinule and ventral appendix | *D.* (*Ctenodaphnia*) *exilis* |
| | Large (> 800) | Rectangular | Dark and surrounded by transparent membrane | 2 | small craters | Large and thin spinule | *D. laevis* |
| | Medium (≥ 400–800) | Triangular | Transparent grey and dark in the resting egg chamber | 2 | small craters | Large and thin spinule, but wider in the base | *D. parvula* |
| | Medium (≥ 400–800) | Triangular | Dark and surrounded by transparent membrane | 2 | small craters | Large spinule and width | *D. pulex* |
| *Dunhevedia* | Small (<400) | Half oval | Brown and dark brown in the resting egg chamber | 1 | Several small pores | None | *D. crassa* |
| *Ilyocryptus* | Medium (≥ 400–800) | Oval | Transparent | 2 | Oval striae with apical small verrucae | None | *I. agilis* |
| *Macrothrix* | Medium (≥ 400–800) | Irregular | Transparent and dark resting eggs | 2 | Oval striae with apical verrucae | None | *M. mexicanus* |
| | Small (< 400) | Half oval | Transparent brown and Dark in the resting egg chamber | 1 | Rounded scales | None | *M. rosea* |
| | | Square | Dark and surrounded by transparent membrane | 2 | None | None | *M. smirnovi* |
| *Moina* | Medium (≥ 400–800) | Rectangular | Dark rounded by transparent membrane | 2 | Craters | None | *M. macrocopa* |
| | Medium (≥ 400–800) | Oval | Brownish orange and dark in the resting egg chamber | 1 | Rounded and irregular scales | None | *M. micrura* |

| Genus | Egg size (µm) | Egg shape | Color | RE | Type of ornamentation | Accessory structure | Species |
|---|---|---|---|---|---|---|---|
| *Pleuroxus* | Medium (≥ 400–800) | Rectangular | Light brown and resting eggs dark | 1 | Hexagonal reticulation in the posterior portion | None | *P. denticulatus* |
| *Simocephalus* | Medium (≥ 400–800) | Triangular | Dark surrounded by transparent membrane | 1 | Oval scales | None | *S. mixtus* |
|  | Large (> 800) | Triangular | Different gray tonalities and the resting egg chamber orange | 1 | Scales and a margin that round the egg | None | *S. vetulus* |
|  | Large (> 800) | Triangular | Dark surrounded by transparent membrane and resting egg chamber orange | 1 | Interlocking linear small striae | None | *S.* sp. |

**RE =** resting egg

*Ceriodaphnia pulchella* (Sars, 1862), *Ceriodaphnia quadrangula* O.F. Müller, 1785, and *Ceriodaphnia reticulata* (Jurine, 1820). On the other hand, Kotov et al. (2018) were able to differentiate among four species. Berner (1985) in a study on the *Ceriodaphnia cornuta* complex, found high variability between species and proposed the separation of *C. cornuta* and *C. rigaudi* by comparing different details of the ephippia. In SEM studies, we also found that *C. cornuta* differed from other species in the genus. However, the smooth surface of ephippia in *C. dubia*, *C. laticaudata*, and *C. reticulata* made taxonomical distinctions difficult. Another example is seen in ephippia of *S. mixtus*: those from cultures showed clear ornamentation, while those from sediments did not. We also note that in some *Daphnia* species ephippia from sediment samples did not always retain their posterior spinulae. Although differences between some external ornamentations in cladocerans are linked to plasticity, the latter ephippial structure may degrade while in the sediment. Thus, ornamentations or appendages can be present when ephippia are formed in cultures, but may be absent in specimens collected from sediments, as seen in many of our *Daphnia* samples.

Does form follow function (Gould 1971) in cladoceran ephippia or is their morphology simply the residue of their formation while part of the female? This is a difficult question to answer. For example, ornamentation in the ephippium of *Chydorus sphaericus* complex is the same as the shell ornamentation in the female adult (see Fig. 2(8A–8C)). Despite the difficulty in coming to specific conclusions about the diversity of *Chydorus sphaericus* group (Kotov et al. 2016), ephippial eggs were still useful to identify the species group. In *Daphnia* species, spinules in the resting eggs are also present in the female (see Fig. 3(9–12A, B, C)). On the other hand, *Moina micrura*, *Ilyocryptus agilis*, *Macrothrix mexicanus*, and *Simocephalus vetulus* are clear examples of different ornamentations in diapausing eggs in comparison to the female. These examples could suggest that these structures possess a specific function during dormancy. However, we must remember that selection pressures do not operate on a single trait, they work on the entire animal within its environment: this is referred to as the Pareto optimality (Tendler et al. 2015). Thus, any research on ephippia must consider the importance of ephippial characteristics in the ephippial female, as well as while it resides in the sediment. For instance, the peduncle presents in *Daphnia pulicaria* Forbes, 1893 from Sierra Nevada (Spain) might be used for dispersion or to remain in the surface of the lake, as was observed by Guerrero-Jiménez et al. (2020). In *S. vetulus*, the margin of the ephippia is ornamented and the chamber in which the DE resides is orange eggs were mostly floating (see Suppl. material 1: appendix B). Different levels of carotenoids produce the orange pigmentation present in ephippia of cladoceran species permitting greater light absorption, which could improve hatching (Stross, 1966). On the other hand, spinules on ephippia of *Daphnia* spp. are probably a residual of the structures that protect adult females from predators.

In Mexico, approximately 150 cladoceran species have been reported (Elías-Gutiérrez et al. 2008), so our study has only covered a small proportion (15%) of the total diversity. This number is likely to increase simply because only 1% of watersheds in the area have been explored (Elías-Gutiérrez et al. (1999). While our work analyzed 23 morphotypes this represents the beginning of the studies in ephippia structures from subtropical areas. We urge that more work should be done on this subject, including paleolimnological research, such as an adaptation to a (sub) tropical context of the 'Atlas of Subfossil Cladocera from Central and Northern Europe' by Szeroczyfiska and Sarmaja-Korjonen (2007). Additionally, by combining light microscopy and SEM techniques, useful results could be obtained. An example of this is the remarkable work of Kotov (2013), who demonstrated that even in subfossil samples, good ultrastructure of the ornamentation could be obtained, leading to positive identifications at detailed levels.

In this work, we could identify some useful diagnostic traits for different morphotypes, even for some where high plasticity is well known, such as the *Chydorus sphaericus* complex, *Daphnia*, and *Alona*. However, we keep in mind that this condition will surely change when research of species increases. We recommend studying the ornamentations of ephippial structures to detect the boundaries for each taxon or complex of species, and ultimately, contribute to understand the evolution and biodiversity of water fleas in contemporary and past lakes. Our efforts augment current information which could shed light on cryptic speciation in cladocerans as several complex groups have been reported by Petrusek et al. (2003), Elías-Gutiérrez and Valdez-Moreno (2008), Quiroz-Vázquez and Elías-Gutiérrez (2009), and Bekker et al. (2016). While identification of cladoceran ephippia by itself has proven difficult (Murat and Sevil 2014), improving our ability to identify them to species level, will extend our knowledge of cladoceran distribution, especially to habitats that cannot be sampled throughout the year: i.e., those that are too remote and ephemeral ponds.

## Conclusions

We found that ephippial morphology was relatively consistent and contained useful diagnostic features. Our results show useful differences in the morphology of ephippia in the taxa encountered, except in *Ceriodaphnia*; thus, morphological differences of ephippia in that genus remain a challenge. Because the six features we used in this study allowed us to achieve a useful identification of the ephippia we examined, we conclude that morphological characterization of ephippia is a sufficiently robust tool for the identification of ephippia, for certain taxa. Nevertheless, we recognize that a serious knowledge gap remains. Our analysis and the database we provide needs to be expanded to include many more species and additional stable characteristics. When this is achieved, ephippial morphology will be a convenient and practical means for cladoceran morphological identification.

## Acknowledgements

We thank Biol. Roberto Viscalla who provided some samples used in the study and Ekaterina Retes Pruneda for identifying some species. We thank also the anonymous reviewers for their constructive remarks and comments on an earlier draft of the manuscript.

## Additional information

### Conflict of interest

The authors have declared that no competing interests exist.

### Ethical statement

No ethical statement was reported.

### Funding

The first author thanks Mexico´s National Council for Science and Technology (CONACYT) for providing the postdoctoral grant I1200/224/2021 MOD.ORD. 01/10/2022 – BECAS DE CONSOLIDACION. RLW was funded in part by the NSF DEB 2051710.

### Author contributions

Investigation: FSÁS, ABM. Methodology: AAO. Supervision: MSB. Writing – original draft: EAN. Writing – review and editing: GGJ, RLLW.

### Author ORCIDs

Gerardo Guerrero-Jiménez https://orcid.org/0000-0002-1788-8099
Frida S. Álvarez-Solís https://orcid.org/0009-0003-2188-0078
Elaine Aguilar-Nazare https://orcid.org/0009-0002-7090-6038
Araceli Adabache-Ortiz https://orcid.org/0000-0003-4332-9650
Aleksandra Baquero-Mariaca https://orcid.org/0009-0005-3765-7414
Robert L. Wallace https://orcid.org/0000-0001-6305-4776
Marcelo Silva-Briano https://orcid.org/0000-0002-5372-2408

### Data availability

All of the data that support the findings of this study are available in the main text or Supplementary Information.

## References

Altiero T, Bertolani R, Rebecchi L (2009) Hatching phenology and resting eggs in tardigrades. Journal of Zoology (London, England) 280(3): 290–296. https://doi.org/10.1111/j.1469-7998.2009.00664.x

Bailey SA, Duggan IC, van Overdijk CDA, Jenkins PT, MacIsaac HJ (2003) Viability of invertebrate diapausing eggs collected from residual ballast sediment. Limnology and Oceanography 48(4): 1701–1710. https://doi.org/10.4319/lo.2003.48.4.1701

Bekker EI, Karabanov DP, Galimov YR, Kotov AA (2016) DNA barcoding reveals high cryptic diversity in the North Eurasian *Moina* species (Crustacea: Cladocera). PLoS One 11(8): e0161737. https://doi.org/10.1371/journal.pone.0161737

Berner DB (1985) Morphological differentiation among species in the *Ceriodaphnia cornuta* complex (Crustacea, Cladocera) With 2 figures in the text. Internationale Vereinigung für theoretische und angewandte Limnologie. Verhandlungen – Internationale Vereinigung für Theoretische und Angewandte Limnologie 22(5): 3099–3103. https://doi.org/10.1080/03680770.1983.11897839

Brendonck L, De Meester L (2003) Egg banks in freshwater zooplankton: Evolutionary and ecological archives in the sediment. Hydrobiologia 491(1–3): 65–84. https://doi.org/10.1023/A:1024454905119

Decaestecker E, De Meester L, Mergeay J (2009) Cyclical parthenogenesis in *Daphnia*: sexual versus asexual reproduction. In: Schön I, K Martens & P Dijk (Eds) Lost Sex: The evolutionary biology of parthenogenesis. Springer, Dordrecht, 295–316. https://doi.org/10.1007/978-90-481-2770-2_15

Drillet G, Hansen BW, Kiørboe T (2011) Resting egg production induced by food limitation in the calanoid copepod *Acartia tonsa*. Limnology and Oceanography 56(6): 2064–2070. https://doi.org/10.4319/lo.2011.56.6.2064

Dumont HJ, Silva-Briano M, Subhash Babu KK (2002) A re-evaluation of the *Macrothrix rosea-triserialis* group, with the description of two new species (Crustacea Anomopoda: Macrothricidae). Hydrobiologia 467(1/3): 1–44. https://doi.org/10.1023/A:1014933227259

Elías-Gutiérrez M, Valdez-Moreno M (2008) A new cryptic species of *Leberis* Smirnov, 1989 (Crustacea, Cladocera, Chydoridae) from the Mexican semi-desert region, highlighted by DNA barcoding. Hidrobiológica 18: 63–74.

Elías-Gutiérrez M, Ciros-Pérez J, Suárez-Morales E, Silva-Briano M (1999) The freshwater Cladocera (Orders Ctenopoda & Anomopoda) of México, with comments on selected taxa. Crustaceana 72(2): 171–186. https://doi.org/10.1163/156854099503267

Elías-Gutiérrez M, Suárez-Morales E, Gutiérrez Aguirre MA, Silva-Briano M, Granados Ramírez JG, Garfias-Espejo T (2008) Cladócera y Copépoda de las aguas continentales de México, Guía Ilustrada. Universidad Autónoma de México y El Colegio de la Frontera Sur, México, 322 pp.

Figuerola J, Green AJ, Santamaría L (2003) Passive internal transport of aquatic organisms by waterfowl in Donana, south-west Spain. Global Ecology and Biogeography 12(5): 427–436. https://doi.org/10.1046/j.1466-822X.2003.00043.x

Forró L, Korovchinsky NM, Kotov AA, Petrusek A (2007) Global diversity of cladocerans (Cladocera; Crustacea) in freshwater. Hydrobiologia 595(1): 177–184. https://doi.org/10.1007/s10750-007-9013-5

Fryer G (1972) Observations on the ephippia of certain macrothricid cladocerans. Zoological Journal of the Linnean Society 51(1): 79–96. https://doi.org/10.1111/j.1096-3642.1972.tb00774.x

García-Zamorano J, Jiménez-Contreras J (2023) Zooplankton egg bank: Characterization and effect of biotic factors on hatching. International Journal of Limnology 59: 3. https://doi.org/10.1051/limn/2023002

Gerrish GA, Cáceres CE (2003) Genetic versus environmental influence on pigment variation in the ephippia of *Daphnia pulicaria*. Freshwater Biology 48(11): 1971–1982. https://doi.org/10.1046/j.1365-2427.2003.01136.x

Gould SJ (1971) D'Arcy Thompson and the science of form. New Literary History 2(2): 229–258. https://doi.org/10.2307/468601

Goulden CE (1966) Co-Occurrence of Moinid Cladocera and Possible Isolating Mechanisms, Internationale Vereinigung für theoretische und angewandte Limnologie 16: 1669–1672. https://doi.org/10.1080/03680770.1965.11899491

Gueriau P, Rabet N, Clement G, Lagebro L, Vannier J, Briggs DE, Charbonnier S, Olive S, Bethoux O (2016) A 365-Million-Year-Old Freshwater Community Reveals Morphological and Ecological Stasis in Branchiopod Crustaceans. Current Biology 26(3): 383–390. https://doi.org/10.1016/j.cub.2015.12.039

Guerrero-Jiménez G, Ramos-Rodríguez E, Silva-Briano M, Adabache-Ortiz A, Conde-Porcuna JM (2020) Analysis of the morphological structure of diapausing propagules as a potential tool for the identification of rotifer and cladoceran species. Hydrobiologia 847(1): 243–266. https://doi.org/10.1007/s10750-019-04085-0

Gulati RD, DeMott WR (1998) The role of food quality for zooplankton: Remarks on the state-of-the-art, perspectives and priorities. Freshwater Biology 39(3): 753–768. https://doi.org/10.1046/j.1365-2427.1997.00275.x

Hairston Jr NG, Munns Jr WR (1984) The timing of copepod diapause as an evolutionarily stable strategy. American Naturalist 123(6): 733–751. https://doi.org/10.1086/284236

Hebert PD, Crease T (1983) Clonal diversity in populations of *Daphnia pulex* reproducing by obligate parthenogenesis. Heredity 51(1): 353–369. https://doi.org/10.1038/hdy.1983.40

Kokkinn MJ, Williams WD (1987) Is ephippial morphology a useful taxonomic descriptor in the Cladocera? An examination based on a study of *Daphniopsis* (Daphniidae) from Australian salt lakes. In: Forro L, Frey DG (Eds) Cladocera: Proceedings of the Cladocera Symposium, Budapest 1985. Springer Netherlands, Dordrecht, 67–73. https://doi.org/10.1007/978-94-009-4039-0_8

Kotov AA (2013) Morphology and phylogeny of the Anomopoda (Crustacea: Cladocera). KMK, Moscow, 638 pp.

Kotov AA, Karabanov DP, Bekker EI, Neretina TV, Taylor DJ (2016) Phylogeography of the *Chydorus sphaericus* Group (Cladocera: Chydoridae) in the Northern Palearctic. PLoS ONE 11(12): e0168711. https://doi.org/10.1371/journal.pone.0168711

Kotov AA, Ibragimova AG, Neretina AN (2018) Identification of *Ceriodaphnia* Dana, 1853 (Crustacea: Cladocera) taxa from European Russia based on ephippial morphology. Zootaxa 4527(1): 105–123. https://doi.org/10.11646/zootaxa.4527.1.9

Marcus NH (1990) Calanoid copepod, cladoceran, and rotifer eggs in sea-bottom sediments of northern Californian coastal waters: Identification, occurrence and hatching. Marine Biology 105(3): 413–418. https://doi.org/10.1007/BF01316312

Mergeay J, Verschuren D, Meester LD (2005) *Daphnia* species diversity in Kenya, and a key to the identification of their ephippia. Hydrobiologia 542(1): 261–274. https://doi.org/10.1007/s10750-004-4952-6

Montero-Pau J, Serra M, Gómez A (2017) Diapausing egg banks, lake size, and genetic diversity in the rotifer *Brachionus plicatilis* Müller (Rotifera, Monogononta). Hydrobiologia 796(1): 77–91. https://doi.org/10.1007/s10750-016-2833-4

Moreno E, Pérez-Martínez C, Conde-Porcuna JM (2019) Dispersal of rotifers and cladocerans by waterbirds: Seasonal changes and hatching success. Hydrobiologia 834(1): 145–162. https://doi.org/10.1007/s10750-019-3919-6

Murat K, Sevil E (2014) Morphological examination of the resting egg structure of 3 cladoceran species. Turkish Journal of Zoology 38: 2. https://doi.org/10.3906/zoo-1302-47 [*Ceriodaphnia quadrangula* (O.F. Müller, 1785), *Daphnia longispina* (O.F. Müller, 1776), and *D. magna* Straus, 1820]

Odriozola M, Zagarese HE, Diovisalvi N (2020) Zooplankton hatching from dormant eggs in a large Pampean shallow lake. Hydrobiologia 847(9): 2097–2111. https://doi.org/10.1007/s10750-020-04233-x

Onbé T (1978) Sugar flotation method for sorting the resting eggs of marine cladocerans and copepods from sea-bottom sediment. Nippon Suisan Gakkaishi 44(12): 1411. https://doi.org/10.2331/suisan.44.1411

Panov VE, Krylov PI, Riccardi N (2004) Role of diapause in dispersal and invasion success by aquatic invertebrates. Journal of Limnology 63(1s): 56–69. https://doi.org/10.4081/jlimnol.2004.s1.56

Pérez-Martínez C, Jiménez L, Moreno E, Conde-Porcuna JM (2013) Emergence pattern and hatching cues of *Daphnia pulicaria* (Crustacea, Cladocera) in an alpine lake. Hydrobiologia 707(1): 47–57. https://doi.org/10.1007/s10750-012-1404-6

Perrigo AL, Romeralo M, Baldauf SL (2012) What's on your boots: An investigation into the role we play in protist dispersal. Journal of Biogeography 39(5): 998–1003. https://doi.org/10.1111/j.1365-2699.2012.02691.x

Petrusek A, Korinek M, Cerny M (2003) Analysis of Cladoceran cryptic species: What approaches can we take? Acta Facultatis Ecologiae 10: 105–107.

Pijanowska J, Stolpe G (1996) Summer diapause in *Daphnia* as a reaction to the presence of fish. Journal of Plankton Research 18(8): 1407–1412. https://doi.org/10.1093/plankt/18.8.1407

Ptatscheck C, Traunspurger W (2020) The ability to get everywhere: Dispersal modes of free-living, aquatic nematodes. Hydrobiologia 847(17): 3519–3547. https://doi.org/10.1007/s10750-020-04373-0

Quiroz-Vázquez P, Elías-Gutiérrez M (2009) A new species of the freshwater cladoceran genus *Scapholeberis* Schoedler, 1858 (Cladocera: Anomopoda) from the semidesert Northern Mexico, highlighted by DNA barcoding. Zootaxa 2236(1): 50–64. https://doi.org/10.11646/zootaxa.2236.1.4

Ricci C, Balsamo M (2000) The biology and ecology of lotic rotifers and gastrotrichs. Freshwater Biology 44(1): 15–28. https://doi.org/10.1046/j.1365-2427.2000.00584.x

Rivas Jr JA, Mohl J, Van Pelt RS, Leung MY, Wallace RL, Gill TE, Walsh EJ (2018) Evidence for regional aeolian transport of freshwater biota in an arid region. Limnology and Oceanography Letters 3(4): 320–330. https://doi.org/10.1002/lol2.10072

Rivas Jr JA, Schröder T, Gill TE, Wallace RL, Walsh EJ (2019) Anemochory of diapausing stages of microinvertebrates in North American drylands. Freshwater Biology 64(7): 1303–1314. https://doi.org/10.1111/fwb.13306

Schröder T, Howard S, Arroyo L, Walsh EJ (2007) Sexual reproduction and diapause of *Hexarthra* sp. (Rotifera) in short-lived Chihuahuan Desert ponds. Freshwater Biology 52(6): 1033–1042. https://doi.org/10.1111/j.1365-2427.2007.01751.x

Scourfield DJ (1901) The ephippium of *Bosmina*. In: Scourfield DJ (Ed.) Journal of the Quekett Microscopical Club 8: 51–56.

Scourfield DJ (1902) The ephippia of the Lynceid Entomostraca. In: Scourfield DJ (Ed.) Journal of the Quekett Microscopical Club 8: 217–244.

Slusarczyk M (1995) Predator-induced diapause in *Daphnia*. Ecology 76(3): 1008–1013. https://doi.org/10.2307/1939364

Smyly WJP (1956) A note on the number of eggs in the ephippium of *Acantholeberis curvirostris* (O.F. Müller), (Cladocera, Macrothricidae). Journal of the Quekett Microscopical Club ser. 4 4: 315–316.

Stross RG (1966) Light and temperature requirements for diapause development and release in *Daphnia*. Ecology 47(3): 368–374. https://doi.org/10.2307/1932977

Szeroczyfiska K, Sarmaja-Korjonen K (2007) Atlas of subfossil Cladocera from central and northern Europe. Friends of the Lower Vistula Society, Swiecie, 83 pp.

Tendler A, Mayo A, Alon U (2015) Evolutionary tradeoffs, Pareto optimality and the morphology of ammonite shells. BMC Systems Biology 9(1): 12. https://doi.org/10.1186/s12918-015-0149-z

Uye S-i (1985) Resting egg production as a life history strategy. Bulletin of Marine Science 37: 440–449.

Van Damme K, Dumont HJ (2010) Cladocera of the Lençóis Maranhenses (NE-Brazil): Faunal composition and a reappraisal of Sars' Method. Brazilian Journal of Biology 70(3 suppl): 755–779. https://doi.org/10.1590/S1519-69842010000400008

Vandekerkhove J, Declerck S, Brendonck L, Conde-Porcuna JM, Jeppesen E, Johansson LS, De Meester L (2005a) Uncovering hidden species: Hatching diapausing eggs for the analysis of cladoceran species richness. Limnology and Oceanography: Methods 3(9): 399–407. https://doi.org/10.4319/lom.2005.3.399

Vandekerkhove J, Declerck S, Jeppesen E, Conde-Porcuna JM, Brendonck L, De Meester L (2005b) Dormant propagule banks integrate spatio-temporal heterogeneity in cladoceran communities. Oecologia 142(1): 109–116. https://doi.org/10.1007/s00442-004-1711-3

Vanderkerkhove J, Declerck S, Vanhove M, Brendonck L, Jeppesen E, Conde-Porcuna JM, De Meester L (2004) Use of ephippial morphology to assess richness of anomopods: Potentials and pitfalls. Journal of Limnology 63(1s): 75–84. https://doi.org/10.4081/jlimnol.2004.s1.75

Vanschoenwinkel B, Waterkeyn A, Nhiwatiwa T, Pinceel T, Spooren E, Geerts A, Clegg B, Brendonck L (2011) Passive external transport of freshwater invertebrates by elephant and other mud-wallowing mammals in an African savannah habitat. Freshwater Biology 56(8): 1606–1619. https://doi.org/10.1111/j.1365-2427.2011.02600.x

Vargas AL, Santangelo JM, Bozelli RL (2019) Recovery from drought: Viability and hatching patterns of hydrated and desiccated zooplankton resting eggs. International Review of Hydrobiology 104(1–2): 26–33. https://doi.org/10.1002/iroh.201801977

Walsh EJ, May L, Wallace RL (2017) A metadata approach to documenting sex in phylum Rotifera: Diapausing embryos, males, and hatchlings from sediments. Hydrobiologia 796(1): 265–276. https://doi.org/10.1007/s10750-016-2712-z

## Supplementary material 1

### Supplemetary data

Authors: Gerardo Guerrero-Jiménez, Frida S. Álvarez-Solis, Elaine Aguilar-Nazare, Araceli Adabache-Ortiz, Aleksandra Baquero-Mariaca, Robert L. Wallace, Marcelo Silva-Briano

Data type: docx

Explanation note: map with coordinates of all locations where samples were collected; table with the distribution and the number of the ephippia morphotypes found. In addition, a figure with all morphotypes identified and used for experiments; picture of a small wood piece with several ephippia of *Simocephalus mixtus*.

Link: https://doi.org/10.3897/zookeys.1205.115506.suppl1

ZooKeys 1205: 191–204 (2024)
DOI: 10.3897/zookeys.1205.117807

Research Article

# An updated review of the genus *Toxorhina* Loew, 1850 (Diptera, Limoniidae) from Yunnan, China with a description of a new species

Hanhuiying Lv[1,2], Yuanyuan Xu[2,3], Shulin Liu[2], Linghui Li[2], Kejian Lin[1], Xiao Zhang[2]

1 *Key Laboratory of Biohazard Monitoring and Green Prevention and Control in Artificial Grassland, Ministry of Agriculture and Rural Affairs, Institute of Grassland Research, Chinese Academy of Agricultural Sciences, Hohhot 010010, China*
2 *Shandong Engineering Research Center for Environment-Friendly Agricultural Pest Management, College of Plant Health and Medicine, Qingdao Agricultural University, Qingdao 266109, China*
3 *Guangxi Key Laboratory of Agric-Environment and Agric-Products Safety, National Demonstration Center for Experimental Plant Science Education, Agricultural College, Guangxi University, Nanning 530004, China*
*Corresponding authors: Kejian Lin (linkejian@caas.cn); Xiao Zhang (xzhang_cn@163.com)*

## Abstract

Seven species of the genus *Toxorhina* Loew, 1850 have been recorded from China, of which three are known to occur in Yunnan Province. Herein, all known species from Yunnan, China are reviewed with more detailed descriptions and illustrations of the male hypopygium. A species of *Toxorhina* belonging to the subgenus *Ceratocheilus* Wesché, 1910 from Yunnan, *T.* (*C.*) *pianmica* **sp. nov.**, is described and illustrated as new to science.

**Key words:** *Ceratocheilus*, crane flies, Elephantomyiini, Limoniinae, male hypopygia, taxonomy

Academic editor: Pavel Starkevic
Received: 25 December 2023
Accepted: 15 April 2024
Published: 24 June 2024

ZooBank: https://zoobank.org/31CA30DA-E778-4046-B479-5F1705D4FC9A

Citation: Lv H, Xu Y, Liu S, Li L, Lin K, Zhang X (2024) An updated review of the genus *Toxorhina* Loew, 1850 (Diptera, Limoniidae) from Yunnan, China with a description of a new species. ZooKeys 1205: 191–204. https://doi.org/10.3897/zookeys.1205.117807

## Introduction

*Toxorhina* Loew, 1850 is a genus in the family Limoniidae (Diptera) with 152 extant species and subspecies, of which 79 species and two subspecies belong to the subgenus *Ceratocheilus* Wesché, 1910, 68 species belong to the subgenus *Toxorhina* and three species belong to the subgenus *Eutoxorhina* Alexander, 1934 (Oosterbroek 2023). Members of *Toxorhina* differ from most limoniid crane flies in their particularly elongate rostrum and are often recorded as feeding on flowers (e.g., Alexander and McAtee 1920; Alexander 1937; Lehnebach and Robertson 2004; Oosterbroek and Lukashevich 2021). The genera *Elephantomyia* Osten Sacken, 1860 and *Helius* Lepeletier & Serville, 1828 (in Latreille et al. 1828) have a similar elongate rostrum to *Toxorhina*, and these three genera, together with another limoniid genus without an elongate rostrum (i.e., *Protohelius* Alexander, 1928), form the tribe Elephantomyiini (Alexander 1920; Savchenko et al. 1992; Hynes 1997; Podenas and Gelhaus 2007; Kang et al. 2023).

Seven species of *Toxorhina* have been recorded from China, of which four (three new species and one newly-recorded species) were published in Zhang et al. (2015), in which all Chinese species were revised. After that, we had the opportunity to examine more specimens of Elephantomyiini collected from Yunnan Province, China, deposited in the Entomological Museum of China Agricultural University, Beijing, China (CAU). Yunnan is a part of the Yunnan-Guizhou Plateau and has a diverse environment and high species diversity; three species of *Toxorhina* are known to occur in the province (Zhang et al. 2015; Oosterbroek 2023). In this study, we obtain more specimens for all three known species of *Toxorhina* in Yunnan and provide more detailed descriptions and illustrations of the male hypopygium. In addition, a new species of *Toxorhina* from Yunnan, *T.* (*C.*) *pianmica* sp. nov., is also described and illustrated.

## Material and methods

The specimens of this study were collected through light trapping at different locations in Yunnan, China (Fig. 1) and deposited in the CAU. Preparations of the male hypopygium were made by soaking dissected tip of abdomen in cold 10% hydroxide (NaOH) for 10 hours. Details of body coloration were examined in specimens immersed in 75% ethanol ($C_2H_5OH$). Prepared specimens were examined using a ZEISS Stemi 2000-C stereomicroscope. Photographs were captured using a Canon EOS 5D Mark IV digital camera through a Canon EF100 mm f/2.8L Macro IS USM lens, and the details of the male hypopygium were captured by that camera attached to a Phenix PH100-3B41L-IPL biomicroscope.

The morphological terminology mainly follows Cumming and Wood (2017) and de Jong (2017). The following abbreviations in figures are used: **aed** = aedeagus, **ea** = ejaculatory apodeme, **goncx** = gonocoxite, **gonst** = gonostylus, **i gonst** = inner gonostylus, **interb** = interbase, **o gonst** = outer gonostylus, **pm** = paramere, **st** = sternite, **tg** = tergite.

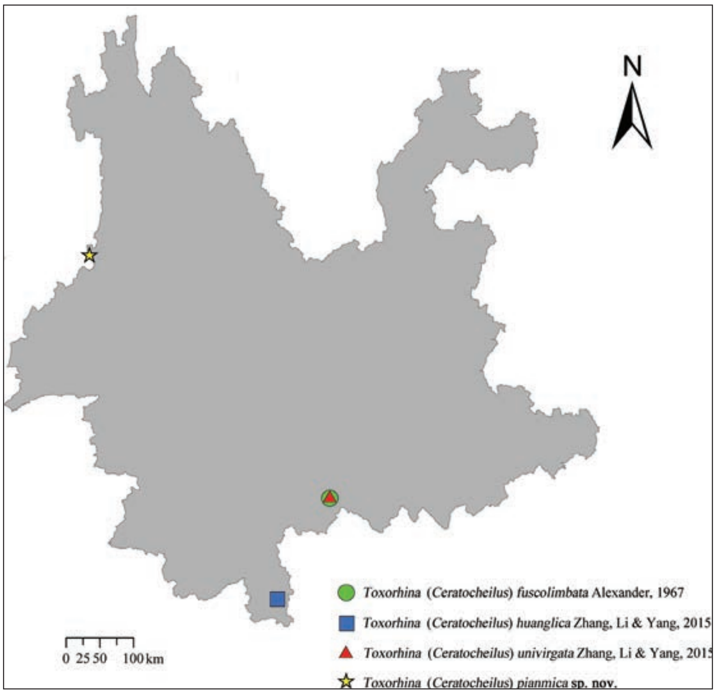

**Figure 1.** Collecting sites of *Toxorhina* species from Yunnan, China in this study. *Toxorhina* (*Ceratocheilus*) *fuscolimbata* and *T.* (*C.*) *univirgata*, Huanglianshan National Nature Reserve; *T.* (*C.*) *huanglica*, Xishuangbanna Tropical Rainforest Nature Reserve; *T.* (*C.*) *pianmica*, Pianma Town.

## Taxonomy

### Key to species of the genus *Toxorhina* from Yunnan

1 Wing with black seams along cord and m-m (Zhang et al. 2015: fig. 3d). Gonocoxite with 2 gonostyli (Fig. 2A, B) .......................................................... ........................... ***Toxorhina* (*Ceratocheilus*) *fuscolimbata* Alexander, 1967**

– Wing without conspicuous seams along cord or m-m (Figs 4D, 6B, C; Zhang et al. 2015: figs 5d, 13d). Gonocoxite with 1 gonostylus (Figs 3A, B, 5A, B, 7A, B)........................................................................................**2**

2 Pleuron without longitudinal stripe (Fig. 4A). Wing with cell d open by absence of m-m, $R_4$ ending slightly before end of basal section of $R_5$ (Fig. 4D). Gonocoxite dorsally with three brownish-black, stout preapical setae (Fig. 5A, F)..............................***Toxorhina* (*Ceratocheilus*) *pianmica* sp. nov.**

– Pleuron with one or two longitudinal stripes (Fig. 6A; Zhang et al. 2015: figs 3a, 5a, 13a). Wing with cell d closed, $R_4$ ending beyond r-m (Fig. 6B, C; Zhang et al. 2015: figs 3d, 5d, 13d). Gonocoxite dorsally without stout preapical setae (Figs 2A, 3A, 7A) .................................................................**3**

3 Pleuron dark yellow with two black longitudinal stripes (Zhang et al. 2015: fig. 5a). Wing with $R_4$ ending slightly beyond end of basal section of $R_5$ (Zhang et al. 2015: fig. 5d). Gonocoxite dorsally with a blunt, basal lobe; lobe provided with numerous stout setae (Fig. 3A, G). Interbase elongated, rod-shaped, about 10 times as long as wide (Fig. 3A, B, C, E). Tip of aedeagus bifid with arms short (Fig. 3A, B, C, E, I) .................................................. ..................... ***Toxorhina* (*Ceratocheilus*) *huanglica* Zhang, Li & Yang, 2015**

– Pleuron yellow with one dark brown longitudinal stripe (Fig. 6A; Zhang et al. 2015: fig. 13a). Wing with $R_4$ ending beyond end of basal section of $R_5$ by 1/3–2/5 of its own length (Fig. 6B, C; Zhang et al. 2015: fig. 13d). Gonocoxite dorsally without basal lobe (Fig. 7A). Interbase as a short and flattened plate, about 3 times as long as wide (Fig. 7A–D). Tip of aedeagus bifid, arms very long, filiform (Fig. 7A–D, H)........................................... .....................***Toxorhina* (*Ceratocheilus*) *univirgata* Zhang, Li & Yang, 2015**

### ***Toxorhina* (*Ceratocheilus*) *fuscolimbata* Alexander, 1967**
Fig. 2

*Toxorhina* (*Ceratocheilus*) *fuscolimbata* Alexander, 1967 in Alexander 1967: 185. Type locality: India, Assam, Manipur, Hkayam Boum.
*Toxorhina* (*Ceratocheilus*) *fuscolimbata* in Zhang et al. 2015: 64.

**Specimens examined.** CHINA • 2 ♂♂; Yunnan Province, Lvchun County, Huanglianshan National Nature Reserve, Yakou Protection Station; 1931 m a.s.l.; 22.8956°N, 102.3008°E; 7 July 2016; Qilemoge leg.; light trap; CAU.

**Diagnosis.** Prescutum and presutural scutum brownish-yellow with three broad and nearly confluent brownish-black longitudinal stripes. Pleuron yellow with two black longitudinal stripes. Wing with black seams along cord and m-m and paler seam over base of CuA. Cell d closed. $R_4$ ending beyond end of basal section of $R_5$ by half of its own length, m-cu beyond fork of M by 1/4–1/2 of its own length. Gonocoxite with 2 gonostyli. Gonocoxite dorsally without stout

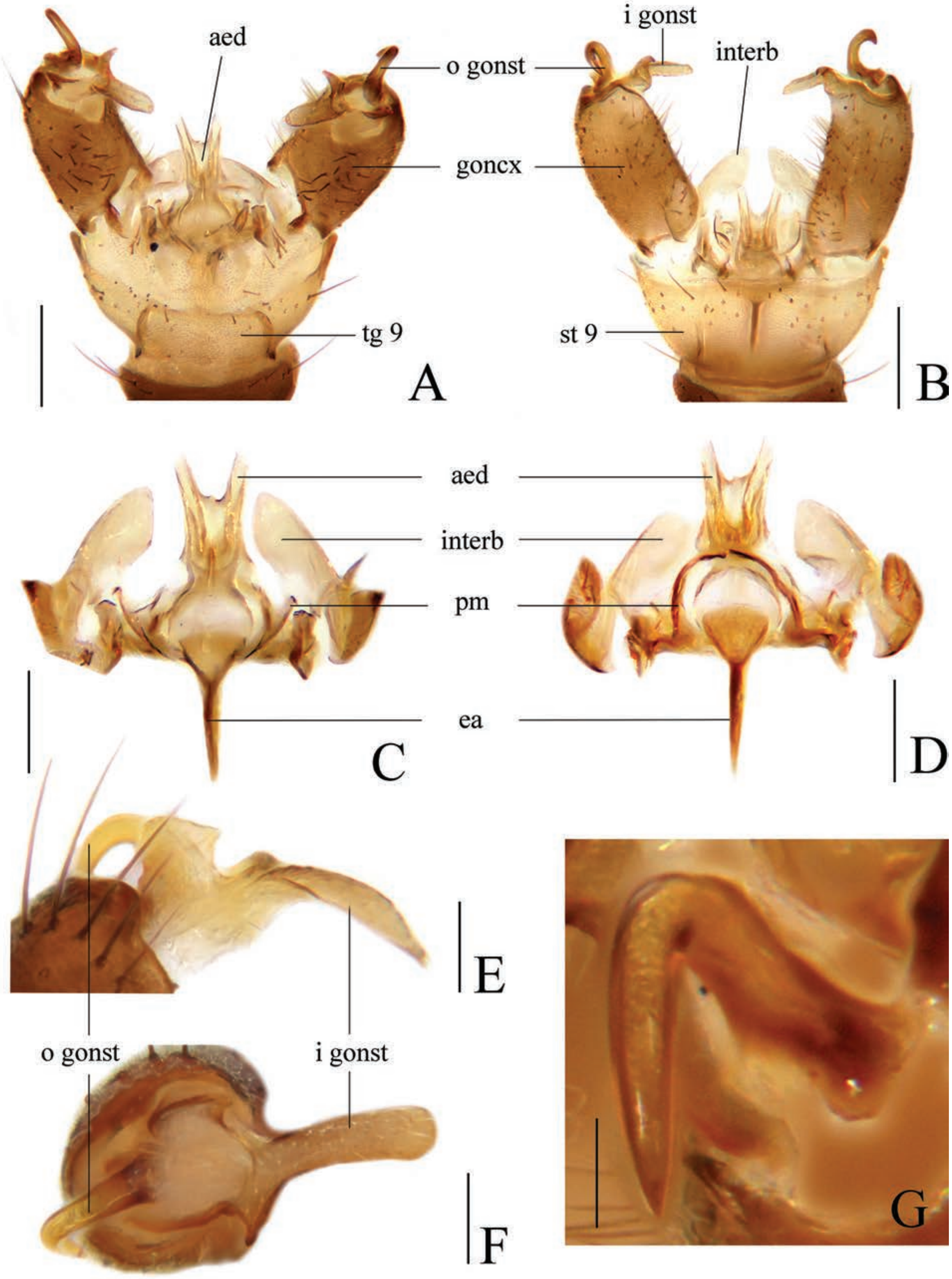

**Figure 2.** *Toxorhina* (*Ceratocheilus*) *fuscolimbata* **A** male hypopygium, dorsal view **B** male hypopygium, ventral view **C** aedeagal complex, dorsal view **D** aedeagal complex, ventral view **E** gonostyli, dorsal view **F** gonostyli, posterior view **G** outer gonostylus, posterior view. Scale bars: 0.2 mm (**A, B**); 0.1 mm (**C, D**); 0.05 mm (**E, F**); 0.02 mm (**G**).

preapical setae. Interbase as a short and flattened plate. Tip of aedeagus bifid with arms short and divergent.

**Description. Male.** Hypopygium (Fig. 2). Tergite 9 brownish-yellow with dark brown setae, posterior margin with a broad and nearly rounded emargination (Fig. 2A). Gonocoxite dark brown, cylindrical, with dark brown setae; setae on dorsal side darker and stronger (Fig. 2A, B). Outer gonostylus dark brown, slender and rod-shaped, about 10 times as long as wide, strongly curved ventrally and inwards at middle; tip acute (Fig. 2A, B, E–G). Inner gonostylus brownish-yellow, about 4 times as long as wide, with rounded tip, basally provided with additional, ventral horn-like process (Fig. 2A, B, E, F). Interbase brownish-yellow, as a short and flattened plate, about 3 times as long as wide; tip blunt (Fig. 2A–D). Parameres dark brown, arched and medially fused, distally connecting to base of interbase (Fig. 2C, D). Ejaculatory apodeme dark brown, rod-shaped and straight, about 7 times as long as wide (Fig. 2C, D). Aedeagus brownish-yellow, stout at base, tip bifid with arms short and divergent (Fig. 2A–D).

**Distribution.** China (Guangxi, Tibet, Yunnan), India (Oosterbroek 2023).

**Behavior.** The species can be attracted by light.

**Remarks.** Alexander (1967) first described this species based on one male and two female specimens collected in India, and later added figures of the wing and male hypopygium for this species (Alexander 1970). Zhang et al. (2015) reported this species as a new record from China and redescribed and illustrated it. A more detailed description and illustration of the male hypopygium of this species are provided in this study.

### ***Toxorhina* (*Ceratocheilus*) *huanglica* Zhang, Li & Yang, 2015**

Fig. 3

*Toxorhina* (*Ceratocheilus*) *huanglica* Zhang, Li & Yang, 2015 in Zhang et al. 2015: 67. Type locality: China, Yunnan, Lvchun, Huanglianshan, Qimaba.

**Specimens examined.** CHINA • 1 ♂; Yunnan Province, Mengla County, Xishuangbanna Tropical Rainforest Nature Reserve, Wangtianshu Scenic Spot; 661 m a.s.l.; 21.5090°N, 101.6003°E; 9 July 2016; Qingxia Zhou leg.; light trap; CAU.

**Diagnosis.** Prescutum and presutural scutum brownish-yellow with three broad dark brown longitudinal stripes. Pleuron dark yellow with two black longitudinal stripes. Wing with cell d closed. $R_4$ ending slightly beyond end of basal section of $R_5$, m-cu at or slightly before fork of M. Gonocoxite with 1 gonostylus. Gonocoxite dorsally with a blunt, basal lobe covered with numerous setae. Interbase elongated, rod-shaped. Tip of aedeagus bifid with arms short and divergent.

**Description. Male.** Hypopygium (Fig. 3). Tergite 9 brown with dark brown setae, posterior margin medially with U-shaped deep incision and two translucent areas on both sides (Fig. 3A, F). Gonocoxite dark brown, conical with tip round; dorsal face with a blunt, basal lobe covered with numerous stout setae (Fig. 3A, G); setae on gonocoxite brownish-black (Fig. 3A, B). Gonostylus brown, curved inwards at middle, basal half stout with a longitudinal groove, distal half slender with tip round; outer side of middle with outwardly curved spine (Fig. 3A, B, H). Interbase dark brown, elongated, rod-shaped, about

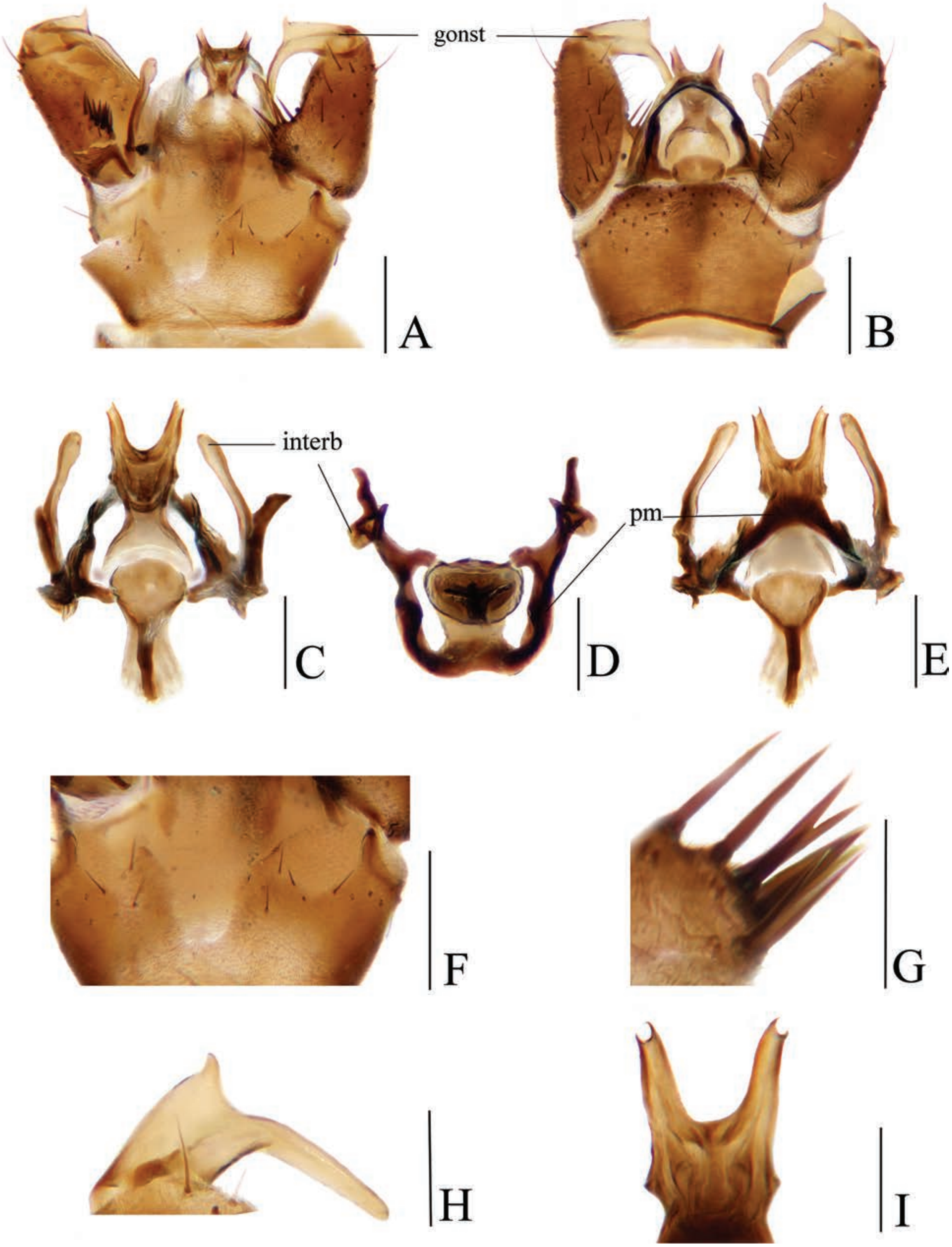

**Figure 3.** *Toxorhina* (*Ceratocheilus*) *huanglica* **A** male hypopygium, dorsal view **B** male hypopygium, ventral view **C** aedeagal complex, dorsal view **D** aedeagal complex, posterior view **E** aedeagal complex, ventral view **F** posterior margin of tergite 9, dorsal view **G** setae at base of gonocoxite, dorsal view **H** gonostylus, dorsal view **I** tip of aedeagus, ventral view. Scale bars: 0.2 mm (**A, B**); 0.1 mm (**C–F, H**); 0.05 mm (**G, I**).

10 times as long as wide; tip inflated and round (Fig. 3A–C, E). Parameres brownish-black, medially arched fused, distal connecting to base of interbase (Fig. 3C–E). Ejaculatory apodeme brown with middle brownish-black, sheet-like, base narrow (Fig. 3C–E). Aedeagus dark brown, stout at base, tip bifid with arms short and divergent (Fig. 3A–C, E, I).

**Distribution.** China (Yunnan) (Oosterbroek 2023).

**Behavior.** The species can be attracted by light.

**Remarks.** The species was originally described and illustrated by Zhang et al. (2015) based on material collected in China. A more detailed description and illustration of the male hypopygium of this species are provided in this study.

### ***Toxorhina* (*Ceratocheilus*) *pianmica* Xu, Lv & Zhang, sp. nov.**

https://zoobank.org/C4EF4120-18B3-44FF-8398-0745D97927D3
Figs 4, 5

**Type material.** ***Holotype***. China • ♂; Yunnan Province, Lushui County, Pianma Town; 2123 m a.s.l.; 26.0142°N, 98.6272°E; 6 July 2013; Xuankun Li leg.; light trap; CAU. ***Paratypes***. China • 3 ♂♂; same data as for holotype; CAU.

**Diagnosis.** Prescutum and presutural scutum dark brown with edges of prescutal suture and both sides of caudal edge darker (Fig. 4C). Pleuron dark brown. Wing with cell d open by absence of m-m. $R_4$ ending slightly before end of basal section of $R_5$, m-cu before fork of M by about 1/3 of its own length. Gonocoxite with 1 gonostylus. Gonocoxite dorsally with three brownish-black, stout preapical setae, and a blunt lobe at inside of base; the lobe with nine stout setae. Interbase elongated, rod-shaped. Tip of aedeagus bifid with arms short and divergent.

**Description. Male** (Fig. 4A). Body length 4.4–4.9 mm (excluding rostrum), wing length 4.5–5.0 mm, rostrum length 2.7–3.0 mm, halter length 0.6–0.7 mm.

Head (Fig. 4B). Dark brown. Setae on head dark brown. Antenna with scape pale brown, pedicel and first flagellomere brown, remaining flagellomeres pale brown. Scape short cylindrical, with dark brown setae. Pedicel globular, with dark brown setae. First flagellomere oval, remaining flagellomeres cylindrical; terminal two flagellomeres longest with pale brown verticils. Rostrum about 3/5 of length of wing, brown with dark brown setae.

Thorax (Fig. 4C). Pronotum brown. Prescutum and presutural scutum dark brown, with edges of prescutal suture and both sides of caudal edge darker. Postsutural scutum dark brown, paler in middle area. Scutellum dark brown with side and caudal edges black, paler in middle area. Mediotergite brown with side edges brownish-black. Pleuron dark brown (Fig. 4A). Coxae yellow with bases brown; trochanters yellow; femora brown with bases paler; tibiae brown; base of fore tarsus brown, remaining tarsi missing. Setae on legs brown. Wing (Fig. 4D) pale brown, without stigma. Veins brown. Venation: Sc ending slightly beyond origin of Rs; sc-r a great distance before tip of Sc; $R_4$ ending slightly before end of basal section of $R_5$; distal section of $R_5$ approach $M_{1+2}$ toward tip; CuP curved suddenly at middle; cell d open by absence of m-m; m-cu before fork of M by about 1/3 its own length. Halter yellow.

Abdomen (Fig. 4A). Segments 1–6 brown with caudal edges darker, segments 7–8 dark brown.

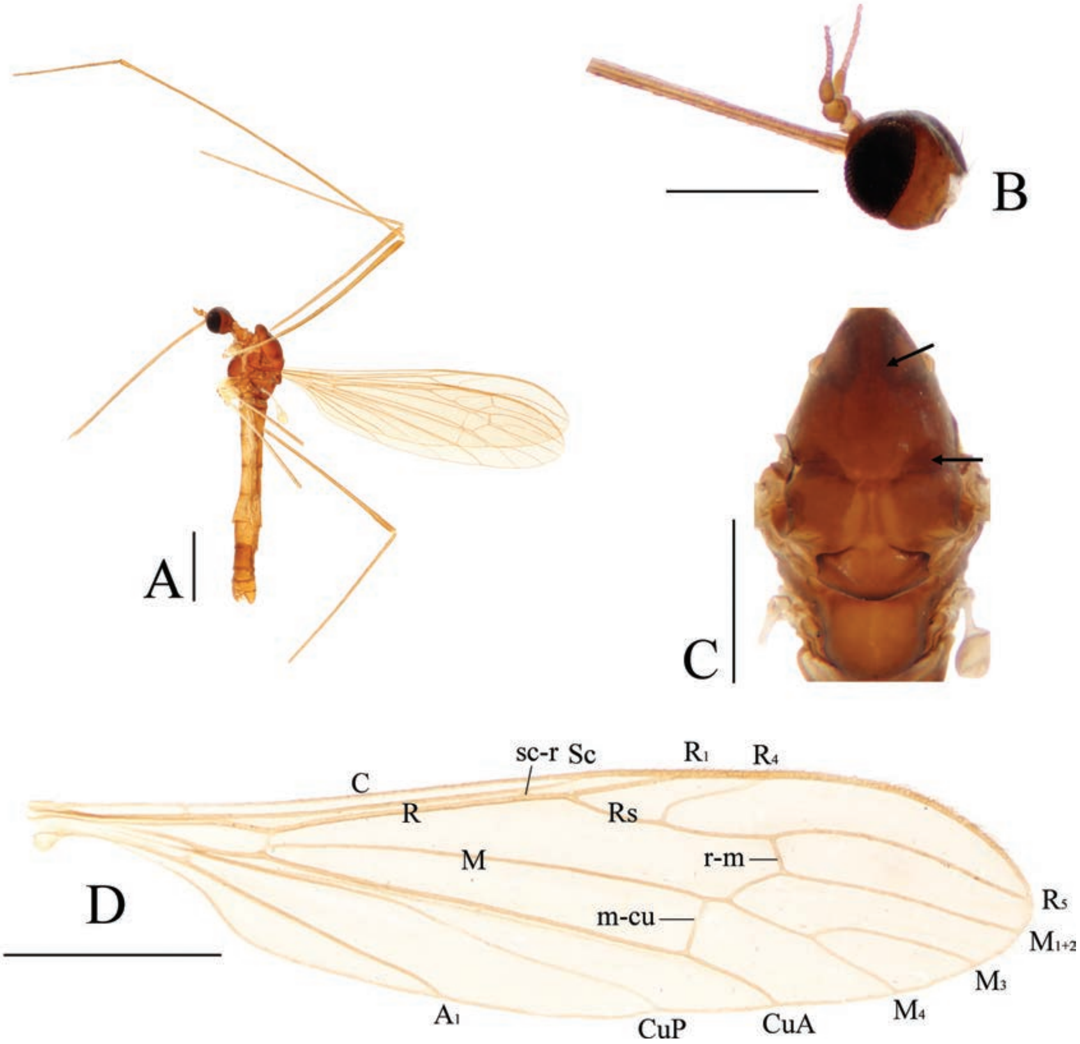

**Figure 4.** *Toxorhina* (*Ceratocheilus*) *pianmica* sp. nov. **A** habitus of male, lateral view **B** head, lateral view **C** thorax, dorsal view (the arrows refer to the dark areas on prescutum and presutural scutum) **D** wing. Scale bars: 1.0 mm (**A, D**); 0.5 mm (**B, C**).

Hypopygium (Fig. 5). Tergite 9 dark brown with dark brown setae, posterior margin with two large translucent areas on both sides (Fig. 5A, E). Gonocoxite brown, conical with tip round (Fig. 5A, B); dorsal face with a few sparse brown setae at outside, three brownish-black, stout preapical setae (Fig. 5A, F), and a blunt lobe at inside of base, this lobe with nine stout setae (Fig. 5A, G); ventral face with numerous brown setae at inside (Fig. 5B). Gonostylus brownish-yellow, curved inwards at basal 1/3; the basal 1/3 stout with a longitudinal groove, distal 2/3 slender with tip round; outer side of basal 1/3 with outwardly curved spine (Fig. 5A, B, H). Interbase pale brownish-yellow, elongated, rod-shaped, about 10 times as long as wide; tip inflated and round (Fig. 5A–D). Parameres dark brown, medially arched fused, distally connecting to base of interbase (Fig. 5C, D). Ejaculatory apodeme dark brown except pale base, rod-shaped (Fig. 5C, D). Aedeagus dark brown, stout at base, tip bifid with arms short and divergent (Fig. 5A–D, I).

**Female.** Unknown.

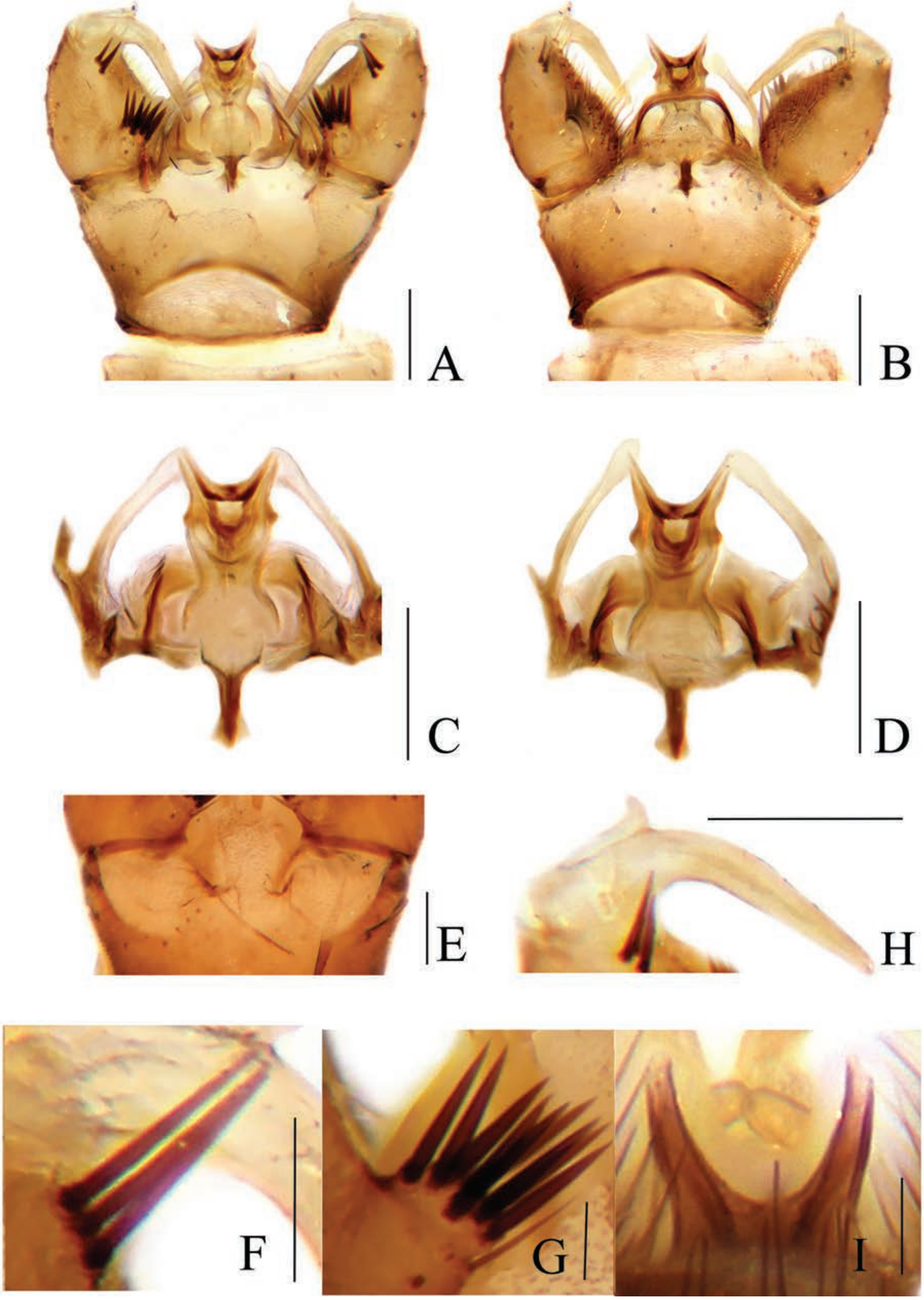

**Figure 5.** *Toxorhina* (*Ceratocheilus*) *pianmica* sp. nov. **A** male hypopygium, dorsal view **B** male hypopygium, ventral view **C** aedeagal complex, dorsal view **D** aedeagal complex, ventral view **E** posterior margin of tergite 9, dorsal view **F** preapical setae gonocoxite, dorsal view **G** setae at base of gonocoxite, dorsal view **H** gonostylus, dorsal view **I** tip of aedeagus, ventral view. Scale bars: 0.1 mm (**A–E, H**); 0.02 mm (**F, G, I**).

**Etymology.** The species is named after the type locality, Pianma Town.

**Distribution.** China (Yunnan).

**Behavior.** The species can be attracted by light.

**Remarks.** The new species is similar to *T.* (*C.*) *simplicistyla* Alexander, 1967 from India in having similar wing venation, but can be separated by the brown abdomen with segments 7–8 darker (Fig. 4A), the gonostylus conspicuously curved with a spine at the basal 1/3 (Fig. 5A, B, H), and the interbase with the tip inflated (Fig. 5A–D). In *T.* (*C.*) *simplicistyla*, the abdomen is brownish-black, the gonostylus is very gently curved with a spine near the middle, and the tip of the interbase is not inflated (Alexander 1967).

### ***Toxorhina* (*Ceratocheilus*) *univirgata* Zhang, Li & Yang, 2015**

Figs 6, 7

*Toxorhina* (*Ceratocheilus*) *univirgata* Zhang, Li & Yang, 2015 in Zhang et al. 2015: 76. Type locality: China, Yunnan, Lvchun, Huanglianshan.

**Specimens examined.** China • 4 ♂♂; Yunnan Province, Lvchun County, Huanglianshan National Nature Reserve, Yakou Protection Station; 1931 m a.s.l.; 22.8956°N, 102.3008°E; 7 July 2016; Qilemoge leg.; light trap; CAU.

**Diagnosis.** Prescutum and presutural scutum brownish-yellow with three broad brown longitudinal stripes. Pleuron yellow with one dark brown longitudinal stripe. Wing with cell d closed. $R_4$ ending beyond end of basal section of $R_5$ by 1/3–2/5 of its own length, m-cu from a distance before to at fork of M. Gonocoxite with 1 gonostylus. Gonocoxite dorsally without stout setae. Interbase as a short and flattened plate. Tip of aedeagus bifid with arms very long.

**Description. Male** (Fig. 6A). Body length 5.3–5.8 mm (excluding rostrum), wing length 5.0–5.5 mm, rostrum length 4.8–5.3 mm, halter length 0.6–0.7 mm.

Head (Fig. 6A). Rostrum slightly shorter than wing, dark brown with dark brown setae.

Thorax (Fig. 6A). Coxae pale yellow, fore coxa slightly darker; trochanters yellow with tips black; femora brown with bases paler; tibiae brown; tarsi brown with tips slightly paler (Fig. 6A). Wing with position of m-cu unstable, ranging from a distance before fork of M to at fork of M (Fig. 6B, C).

Hypopygium (Fig. 7). Tergite 9 brownish-yellow with dark brown setae, posterior margin with two nearly triangular lobes, separated by V-shaped incision, laterally with two translucent areas on both sides (Fig. 7A, E). Gonocoxite brownish-yellow, long conical with tip round; setae on gonocoxite dark brown, outside of ventral face without setae (Fig. 7A, B). Gonostylus brown with distal half paler, curved inwards at middle, basal half stout with numerous small spines at outer side, distal half slender with tip round; outer side of middle with a spine; the spine curved outwards (Fig. 7A, B, F, G). Interbase brownish-yellow, as a short and flattened plate, about 3 times as long as wide; tip blunt (Fig. 7A–D). Parameres pale brownish-yellow with edges brown, sheet-like, distally connecting to base of interbase (Fig. 7C,

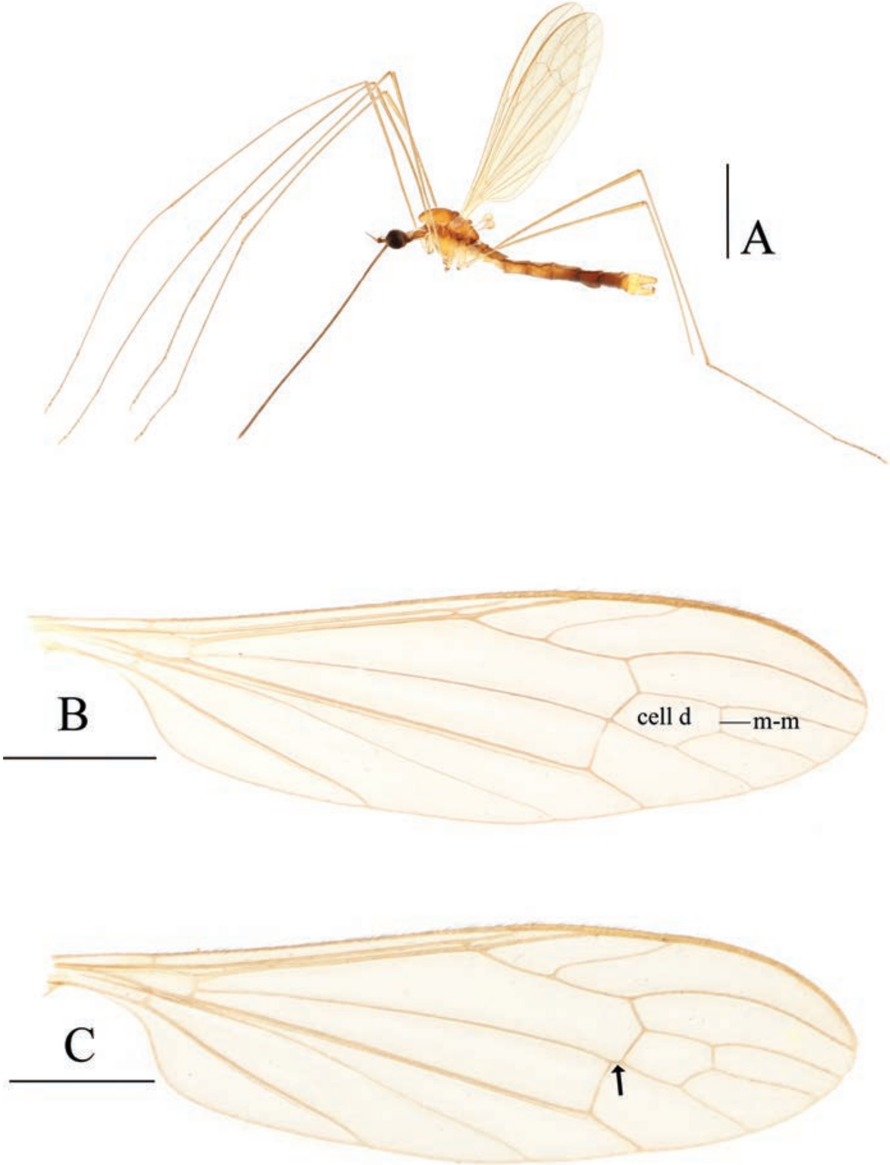

**Figure 6.** *Toxorhina* (*Ceratocheilus*) *univirgata* **A** habitus of male, lateral view **B** wing **C** variation of wing (the arrow refers to the positional variation of m-cu). Scale bars: 2.0 mm (**A**); 1.0 mm (**B, C**).

D). Ejaculatory apodeme pale brownish-yellow with middle brown, sheet-like, base narrow (Fig. 7C, D). Aedeagus pale brownish-yellow with brown, stout base; tip bifid, arms filiform and very long, bent dorsally with tip bent outward (Fig. 7A–D, H–J).

**Distribution.** China (Yunnan) (Oosterbroek 2023).

**Behavior.** The species can be attracted by light.

**Remarks.** Zhang et al. (2015) described and illustrated this species as a new species from China. This study supplements the description of the legs, wing, and rostrum. In addition, a more detailed description and illustrations of the male hypopygium of this species are also provided.

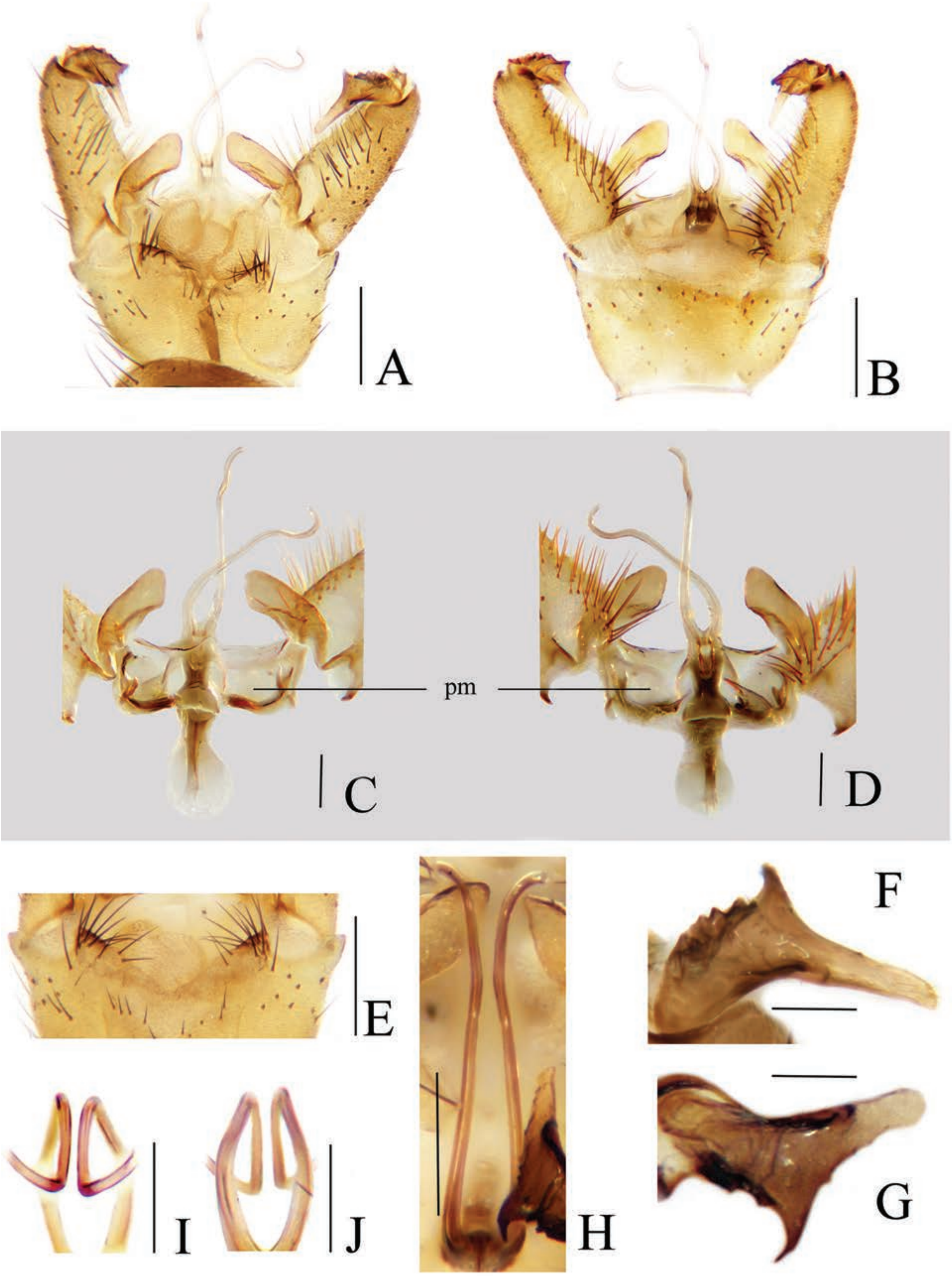

**Figure 7.** *Toxorhina* (*Ceratocheilus*) *univirgata* **A** male hypopygium, dorsal view **B** male hypopygium, ventral view **C** aedeagal complex, dorsal view **D** aedeagal complex, ventral view **E** posterior margin of tergite 9, dorsal view **F** gonostylus, dorsal view **G** gonostylus, posterior view **H** aedeagus, posterior view **I** tip of aedeagus, dorsal view **J** tip of aedeagus, ventral view. Scale bars: 0.2 mm (**A, B, E**); 0.1 mm (**C, D, H–J**); 0.05 mm (**F, G**).

## Acknowledgements

We express our sincere thanks to Ding Yang for his great help during the study of specimens from the CAU. We are also very grateful to Xuankun Li, Qilemoge and Qingxia Zhou for collecting the specimens.

## Additional information

### Conflict of interest

The authors have declared that no competing interests exist.

### Ethical statement

No ethical statement was reported.

### Funding

This work was supported by the National Natural Science Foundation of China (32100356), the National Science & Technology Fundamental Resources Investigation Program of China (Grant No. 2019FY100400) and the National Animal Collection Resource Center, China.

### Author contributions

Conceptualization, X.Z. and K.L.; methodology, X.Z.; resources, X.Z.; data collection, S.L. and L.L.; taxonomic study, H.L., Y.X. and X.Z.; writing–original draft preparation, H.L., Y.X., S.L. and L.L.; writing–review and editing, X.Z. and K.L.; visualization, H.L., Y.X., S.L. and L.L.; supervision, X.Z. and K.L.; project administration, X.Z. and K.L; funding acquisition, X.Z. and K.L.

### Author ORCIDs

Hanhuiying Lv https://orcid.org/0009-0007-2912-5893
Yuanyuan Xu https://orcid.org/0009-0005-2118-0391
Shulin Liu https://orcid.org/0009-0008-6858-6972
Linghui Li https://orcid.org/0009-0003-7432-9482
Kejian Lin https://orcid.org/0000-0002-8531-8506
Xiao Zhang https://orcid.org/0000-0002-8054-0968

### Data availability

All of the data that support the findings of this study are available in the main text.

## References

Alexander CP (1920) The crane-flies of New York. Part II. Biology and phylogeny. Memoirs. Cornell University Agricultural Experiment Station 38: 691–1133. https://doi.org/10.5962/bhl.title.33641

Alexander CP (1928) New or little-known Tipulidae from eastern Asia (Diptera). II. Philippine Journal of Science 35: 455–489.

Alexander CP (1934) New or little-known Tipulidae from eastern Asia (Diptera). XVIII. Philippine Journal of Science 53: 267–300.

Alexander CP (1937) Undescribed species of African Tipulidae (Order Diptera). Part I. Occasional Papers of the National Museum of Southern Rhodesia 6: 1–11.

Alexander CP (1967) Undescribed species of crane flies from the Himalaya mountains (Diptera: Tipulidae). XV. Journal of the New York Entomological Society 75: 183–187.

Alexander CP (1970) New and little-known Indian craneflies (Diptera: Tipulidae). III. Oriental Insects 4(1): 77–88. https://doi.org/10.1080/00305316.1970.10433943

Alexander CP, McAtee WL (1920) Diptera of the superfamily Tipuloidea found in the District of Columbia. Proceedings of the United States National Museum 58(2344): 385–435. https://doi.org/10.5479/si.00963801.58-2344.385

Cumming JM, Wood DM (2017) Adult morphology and terminology. In: Kirk-Spriggs AH, Sinclair BJ (Eds) Manual of Afrotropical Diptera, Volume 1: Introductory Chapters and Keys to Diptera Families. Suricata 4. South African National Biodiversity Institute, Pretoria, 89–133.

de Jong H (2017) Limoniidae and Tipulidae (Crane Flies). In: Kirk-Spriggs AH, Sinclair BJ (Eds) Manual of Afrotropical Diptera, Volume 2: Nematocerous Diptera and lower Brachycera. Suricata 5. South African National Biodiversity Institute, Pretoria, 427–477.

Hynes CD (1997) The immature stages and biology of the craneflies *Toxorhina caledonica* and *Elephantomyia garrigouana* (Diptera: Limoniidae). The Pan-Pacific Entomologist 73: 93–99.

Kang Z, Xu Y, Wang G, Yang D, Zhang X (2023) First mitochondrial genomes of the crane fly tribe Elephantomyiini (Diptera, Tipuloidea, Limoniidae): Comparative analysis and phylogenetic implications. Arthropod Systematics & Phylogeny 81: 731–746. https://doi.org/10.3897/asp.81.e97946

Latreille PA, Lepeletier ALM, Serville JGA, Guérin-Méneville FÉ (1828) Entomologie, ou histoire naturelle des crustacés, des crachnides et des insectes. Encyclopédie méthodique. Histoire naturelle. Vol. 10(2). Société de Gens de Lettres, de Savans et d'Artistes, Paris, 489 pp. [345–832 + errata]

Lehnebach CA, Robertson AW (2004) Pollination ecology of four epiphytic orchids of New Zealand. Annals of Botany 93(6): 773–781. https://doi.org/10.1093/aob/mch097

Loew H (1850) Uber den Bernstein und die Bernsteinfauna. Programm Koniglichen Realschule zu Meseritz 1850: 3–44. https://doi.org/10.5962/bhl.title.98386

Oosterbroek P (2023) Catalogue of the Craneflies of the World (CCW). https://ccw.naturalis.nl/index.php [Accessed 18 December 2023]

Oosterbroek P, Lukashevich ED (2021) Flower-visiting by long-proboscid limoniid crane flies (Diptera, Limoniidae). Fly Times 67: 1–12.

Osten Sacken CR (1860) New genera and species of North American Tipulidae with short palpi, with an attempt at a new classification of the tribe. Proceedings. Academy of Natural Sciences of Philadelphia 11: 197–254.

Podenas S, Gelhaus JK (2007) Identification keys for Limoniinae (Diptera, Limoniidae) of Mongolia and adjacent territories. Vilnius, Lithuania, 1–85.

Savchenko EN, Oosterbroek P, Stary J (1992) Family Limoniidae. Catalogue of Palaearctic Diptera 1: 183–369.

Wesché W (1910) On the new Tipulid Subfamily Ceratocheilinae. Journal of the Linnean Society of London, Zoology 30(201): 355–360. https://doi.org/10.1111/j.1096-3642.1910.tb02141.x

Zhang X, Li Y, Yang D (2015) A review of the genus *Toxorhina* Loew from China, with descriptions of three new species (Diptera, Limoniidae). ZooKeys 480: 59–80. https://doi.org/10.3897/zookeys.480.7526

ZooKeys 1205: 205–222 (2024)
DOI: 10.3897/zookeys.1205.121507

Research Article

# *Paragoniastrea variabilis* Kishi, Nomura & Fukami, sp. nov. (Cnidaria, Anthozoa, Scleractinia), a new coral species previously considered as a variant of *Paragoniastrea deformis*, from Japan and northern Taiwan

Daigo Kishi[1], Keiichi Nomura[2], Yoko Nozawa[3,4,5], Seiji Arakaki[6], Hironobu Fukami[7]

1 *Graduate School of Agriculture, University of Miyazaki, Miyazaki 889-2155, Japan*
2 *Sabiura Marine Park Research Station, Kushimoto, Wakayama 649-3514, Japan*
3 *Biodiversity Research Center, Academia Sinica, Taipei 115, Taiwan*
4 *Tropical Biosphere Research Center, University of the Ryukyus, Okinawa 905-0227, Japan*
5 *Department of Marine Science, Faculty of Fisheries and Marine Science, Universitas Diponegoro, Semarang, Indonesia*
6 *Amakusa Marine Biological Laboratory, Kyushu University, Kumamoto 863-2507, Japan*
7 *Department of Marine Biology and Environmental Sciences, Faculty of Agriculture, Miyazaki University, Miyazaki 889-2155, Japan*
*Corresponding author: Hironobu Fukami (hirofukami@cc.miyazaki-u.ac.jp)*

**Academic editor:** James Reimer
**Received:** 23 February 2024
**Accepted:** 21 May 2024
**Published:** 24 June 2024

**ZooBank:** https://zoobank.org/FC13D3F7-BDB8-4ED0-AB72-9F19B9FCCA50

**Citation:** Kishi D, Nomura K, Nozawa Y, Arakaki S, Fukami H (2024) *Paragoniastrea variabilis* Kishi, Nomura & Fukami, sp. nov. (Cnidaria, Anthozoa, Scleractinia), a new coral species previously considered as a variant of *Paragoniastrea deformis*, from Japan and northern Taiwan. ZooKeys 1205: 205–222. https://doi.org/10.3897/zookeys.1205.121507

## Abstract

A new zooxanthellate scleractinian coral, *Paragoniastrea variabilis* Kishi, Nomura & Fukami, **sp. nov.** (Scleractinia, Merulinidae), is described from non-coral reef regions of Japan and northern Taiwan. This new species was previously recognized as a morphological variant of *Paragoniastrea deformis* (Veron, 1990) and can be morphologically distinguished from that species by lacking groove-and-tube structures on corallite wall joints, and by having larger calices, numerous septa, and up to three corallites in one valley. The new species also formed an independent clade from its congeners, *P. australensis* (Milne Edwards & Haime, 1857), *P. deformis* and *P. russelli* (Wells, 1954), in the molecular phylogeny based on the mitochondrial intergenic region and nuclear ribosomal internal transcribed spacers.

**Key words:** Merulinidae, molecular phylogeny, taxonomy, temperate region, zooxanthellate scleractinian corals

## Introduction

The zooxanthellate scleractinian coral genus *Paragoniastrea* Huang, Benzoni & Budd, 2014, which belongs to the family Merulinidae Verrill, 1865, inhabits the Indo-Pacific region (Huang et al. 2014). Currently, this genus contains three species, namely, *P. australensis* (Milne Edwards & Haime, 1857), *P. deformis* (Veron, 1990), and *P. russelli* (Wells, 1954), which were transferred from other merulinid genera, *Favites* or *Goniastrea*, to this genus based on molecular phylogenetic and morphological data (Huang et al. 2014). *Paragoniastrea* is characterized by encrusting or massive colony morphology, plocoid, cerioid or meandroid in corallite arrangements, and developed paliform lobes. These characteristics are similar to those of *Favites* and *Goniastrea*, but *Paragoniastrea* is distinguished from these genera by its distinct phylogenetic affinities (Huang et al. 2014; Quek et al. 2023) and several morphological differences in corallite characteristics, such as the height of calice relief, septa (number, tooth height, and spacing), and theca structure (Huang et al. 2014).

*Paragoniastrea deformis*, described from Kushimoto, Wakayama, mainland Japan, is mainly distributed around the warm-temperate, non-coral reef region of Japan (Veron 1990, Nishihira and Veron 1995). Although *P. deformis* has also been reported from the Philippines (Wilfredo and Emmi 2003), whether it is the same species or not remains unknown because the specimen (P1L01316) shown by Wilfredo and Emmi (2003) has corallites approximately twice as large as the holotype and has up to three distinct corallites in a valley between corallite walls. *Paragoniastrea deformis* is known to have groove-and-tube structures (groove-and-tubercle structure *sensu* Rosen 1968) on corallite wall joints. Groove-and-tube structure is defined as a feature of vertical and horizontal intercommunicating holes between adjacent corallites, some of which are formed around corallites by parasitic worms (Rosen 1968; Randall and Eldredge 1976). This character has been used as a specific morphological characteristic in some species, including *P. deformis* and *Favites valenciennesii* (Milne Edwards & Haime, 1849) (Veron 1990). However, some colonies of *P. deformis* do not have any groove-and-tube structures, and they are considered to be intraspecific morphological variations of *P. deformis* (Nishihira 1991; Uchida and Soyama 1994; Nishihira and Veron 1995; Veron 2000; Veron et al. 2016). Huang et al. (2014) reported that two specimens of *P. deformis* (*Paragoniastrea* sp.) with a non-groove-and-tube type were separated from typical *P. deformis* with groove-and-tube structures by molecular phylogenetic analysis. To date, morphological and molecular phylogenetic analyses for the non-groove-and-tube type of *P. deformis* remain insufficient to define it as a species different from typical *P. deformis*. Groove-and-tube structure is recognized as one of the key species-specific morphological characters in *Favites valenciennesii*. Thus, this structure might be a good key character to define species in this genus.

This study has shown that the non-groove-and-tube type of *P. deformis* is distinct from *P. deformis* in both morphology and phylogeny, and describes a new species, *Paragoniastrea variabilis* sp. nov. In addition, three specimens without groove-and-tube structures but distinguished from *P. variabilis* sp. nov. by their distinct phylogenetic affinities and slight morphological differences were tentatively designated as *P.* aff. *deformis* as it is not yet clear if they represent a different species or not from *P. deformis*.

## Materials and methods

### Materials

Sampling of materials was conducted at seven sites (Shirahama and Kushimoto, Wakayama; Fukashima Island, Oita; Takashima Island, Nagasaki; Shimanourashima Island and Oshima Island, Miyazaki; Amakusa, Kumamoto) in Japan and at one location (Yehliu, New Taipei) in northern Taiwan (Fig. 1, Suppl. material 1). For comparison with the new species, we examined the holotype of *P. deformis* (MTQ G61876) and the photographic images of holotypes of

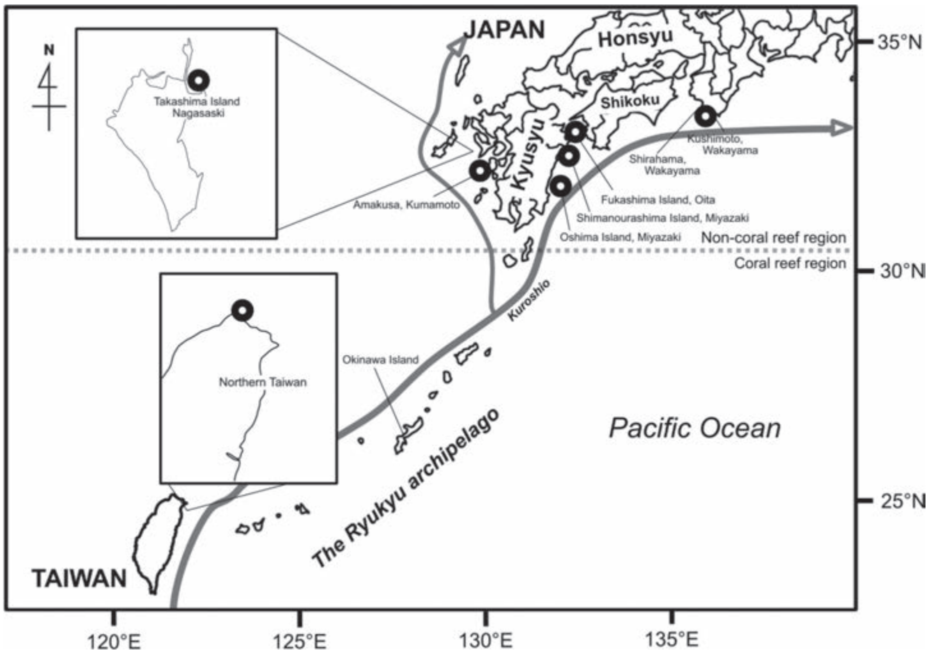

**Figure 1.** Sampling sites (black circles) where we collected skeletal and genetic samples in this study.

*P. australensis* (MNHN IK-2010-409) and *P. russelli* (USNM 45004). Specimens of other *Paragoniastrea* species collected at the same sites were also used (Suppl. material 1). Samples were collected by a hammer and chisel to break only the necessary size (around 10 cm$^3$) for morphological analysis.

A small piece (<1 cm$^3$) was also cut from each collected sample with nippers for molecular phylogenetic analysis and was mixed with a guanidine solution (4M guanidine thiocyanate, 0.1% sodium N-laurylsarcosine, 10 mM Tris-HCl pH 8.0, 0.1M 2-mercaptoethanol; Fukami et al. 2004) to dissolve tissues. The remaining samples were bleached and labeled with numbers associated with the collection sites, and they were stored as skeletal specimens for use in morphological analysis.

The holotype and two paratypes of *Paragoniastrea variabilis* sp. nov. have been deposited in the Department of Marine Biology and Environmental Sciences, University of Miyazaki (MUFS) in Miyazaki, Japan. The other specimens were deposited in the following institutions: Seto Marine Biological Laboratory (SMBL), Wakayama, Japan; Sabiura Marine Park Research Station (SMP), Wakayama, Japan, and Zoological Collection, Biodiversity Research Museum, Academia Sinica (ASIZC), Taipei, Taiwan. Museum abbreviations for type materials are as follows: Muséum national d'Histoire naturelle de Paris (MNHN, France), Museum of Tropical Queensland (MTQ, Australia), and National Museum of Natural History, Smithsonian Institution (USNM, USA).

## Morphological analysis

Measurements and observations of the skeletal specimens from Japan were made using a digital microscope (Keyence VHS-1000; WRAYMER WRAYCAM-NOA630 + Leica MZ16) and a scanning electron microscope (Hitachi High-Tech TM-1000). Taiwan specimens were photographed by a digital camera

(OM system Tough TG-6) and the skeletal image was measured by Image J (version 1.5.3, https://imagej.net/ij/index.html).

To analyze the morphological differences between *P. variabilis* sp. nov. and *P. deformis*, morphological characteristics were compared using the Brunner-Munzel test or the Welch t-test, after confirming normality and homogeneity. In addition, principal component analysis (PCA) was performed on morphological data of *P. variabilis* sp. nov., *P. deformis* and *P.* aff. *deformis*, which were measured and standardized in this study. PCA was performed using the prcomp function in R version 4.3.1 (The R Foundation for Statistical Computing http://www.R-project.org). The PCA result was plotted using the R packages *devtools* and *ggbiplot*. The specimens shown in Suppl. material 1 were used in these analyses.

## Molecular phylogenetic analysis

Total genomic DNA was extracted from each guanidine sample by the conventional phenol-chloroform extraction method. Using the extracted DNA, mitochondrial intergenic region (IGR) and nuclear ribosomal internal transcribed spacers (ITS) were amplified by the PCR method. Primers used for each marker were MCOIF3 (5’- CCA AGA CGA TAT TTC GGA CTT -3’) and tRNAmetR (5’- GTG AGA CTC GAA CTC ACT TTT TT -3’) for IGR (Mitsuki et al. 2021), 1S (5’- GGG TAC CCT TTG TAC ACA CAC CGC CCG TCG CT -3’) and 2SS (5’- GCT TTG G GC GGC AGT CCC AAG CAA CCC GAC TC -3’) for ITS (Wei et al. 2006). PCR was performed in each sample using 11.32 μL of sterile distilled water, 2 μL of 10×buffer, 2 μL of forward primer, 2 μL of reverse primer, 1.6 μL of dNTPs, 0.08 μL of exTaq and 1 μL of DNA of each sample. PCR conditions for ITS and IGR markers were 94 °C for 60 s followed by 35 cycles at 94 °C for 30 s, 55 °C for 45 s, and 72 °C for 90 s, and 72 °C for 5 mins for the final extension. However, for some samples with unsuccessful amplification, we used the following PCR conditions: 94 °C for 60 s, 94 °C for 30 s, 48 °C for 45 s, and 72 °C for 90 s, repeated 5 times, followed by 94 °C for 30 s, 55 °C for 45 s, and 72 °C for 90 s, repeated 30 times, and 72 °C for 5 mins for the final extension. The amplified PCR products were treated with shrimp alkaline phosphatase and exonuclease I at 37 °C for 40 mins and 80 °C for 20 mins.

DNA sequences were determined by direct sequencing using ABI3730 sequencers by a contracted research service (FASMAC Co. Ltd., Kanagawa, Japan). Alignments of IGR and ITS sequences were carried out using the E-INS-i option in MAFFT 7 online (https://mafft.cbrc.jp/alignment/server/) (Kuraku et al. 2013; Katoh et al. 2019) under default parameters. Molecular phylogenetic trees were reconstructed using the neighbor-joining (NJ) and maximum-likelihood (ML) methods after all indels were deleted in MEGA ver. 11.0 (Tamura et al. 2021). MEGA was also used to estimate a model of nucleotide evolution for each marker (HKY+G for IGR, T92+G for ITS markers) and to conduct a bootstrap analysis (with 1000 replicates). All DNA sequences obtained in this study were submitted to the DNA Data Bank of Japan (DDBJ) (accession numbers LC804981–LC804999 for IGR, LC801365–LC801368, LC801370–LC801379 for ITS; Suppl. material 1).

The published DNA sequences of *Paragoniastrea* species used by Huang et al. (2014) for IGR and ITS were used to compare with our data (Suppl. material

2). There were many multi-peaks in the DNA sequences of ITS for two samples (sample numbers: JP009, JP065) used by Huang et al. (2014). Therefore, we newly extracted genomic DNA from one guanidine sample (JP065), which is stored at the University of Miyazaki and used in the analysis for ITS. For both the IGR and ITS trees, DNA sequences (accession numbers KJ666508 and KJ666509 for IGR, KJ666394 and KJ666396 for ITS) of *Merulina ampliata* from Huang et al. (2014) were used as outgroups.

## Taxonomy account

**Family Merulinidae Milne Edwards & Haime, 1857**
**Genus *Paragoniastrea* Huang, Benzoni & Budd, 2014**

***Paragoniastrea variabilis* Kishi, Nomura & Fukami, sp. nov.**
https://zoobank.org/CD11CAA7-81EA-4241-8DAE-BB1F80F5E406
Figs 2–5
Japanese name: henge-kamenoko-kikumeishi

G*oniastrea deformis*: Nishihira 1991: 254, 1 unnumbered fig.; Uchida and Soyama 1994: 65, figs 13, 14; Nishihira and Veron 1995: 345 (part), 3 unnumbered color figs; Veron 2000: 167 (part), 6; Nomura and Mezaki 2005: 35, pl. 1, fig. 28; Veron et al. 2016: part, unnumbered figs 4th, 6th in the 1st row, 3rd, 5th in 2nd row.
*Paragoniastrea* sp.: Sugihara et al. 2015: 153, 4 unnumbered figs; Huang et al. 2014: fig. 6I.
*Paragoniastrea* sp. HENGE *sensu* Nomura et al. 2016: 11; Nomura 2016: 44, figs A–F, 45 (part), figs A, D, E (B, C, F = *P. australensis*); Nomura et al. 2020: 40, fig. 20, G–I.

**Type material. *Holotype*:** MUFS C588 (size 74 × 49 mm), sample MO417, Oshima Island, Nichinan, Miyazaki, Japan (31.527593°N, 131.401469°E), depth 9 m, 14 November 2021, coll. H. Fukami. ***Paratypes*:** MUFS C78 (size 102 × 88 mm), sample number JP065, Sabiura, Kushimoto, Wakayama, Japan (33.464375°N, 135.785721°E), depth 5 m, 22 October 2012, coll. H. Fukami; MUFS C586 (size 90 × 66 mm), sample AM19-24, Satsuki, Amakusa, Kumamoto, Japan (32.457516°N, 130.207903°E), depth 4 m, 25 July 2019, coll. H. Fukami.

**Other material. Japan.** SMP-HC 894, Takatomi Bay, Kushimoto, Wakayama, depth 10 m, 12 May 2003, coll. K. Nomura; SMP-HC 1038, Tosaki, Kushimoto, depth 6 m, 14 Dec 2003, coll. K. Nomura; SMP-HC 1203, 1205, 1208, Sabiura, Kushimoto, depth 3 m, 23 June 2005, coll. K. Nomura; SMP-HC 1749, Tanami, Kushimoto, depth 3 m, 24 Apr 2009, coll. K. Nomura; SMP-HC 1799, Takatomi Bay, Kushimoto, depth 6 m, 14 July 2009, coll. K. Nomura; SMP-HC 2957, Sabiura, Kushimoto, Wakayama, depth 9 m, 13 Dec 2015, coll. K. Nomura; SMP-HC 3049, Sabiura, Kushimoto, Wakayama, depth 10 m, 4 Feb 2016, coll. K. Nomura; MUFS C585, sample AM19-14, Satsuki, Amakusa, Kumamoto, depth 4 m, 25 July 2019, coll. H. Fukami; MUFS C587, sample NB92, Shimanourashima Island, Miyazaki, depth 13 m, 15 May 2015, coll. H. Fukami; MUFS C589, sample TK89, Takashima Island, Nagasaki, depth 3 m, 24 September 2021, coll. H. Fukami. **Taiwan.** ASIZC0001666, sample TWN45, Yehliu, New Taipei, depth 11 m, 4 July 2019, coll. H. Fukami (Suppl. material 1).

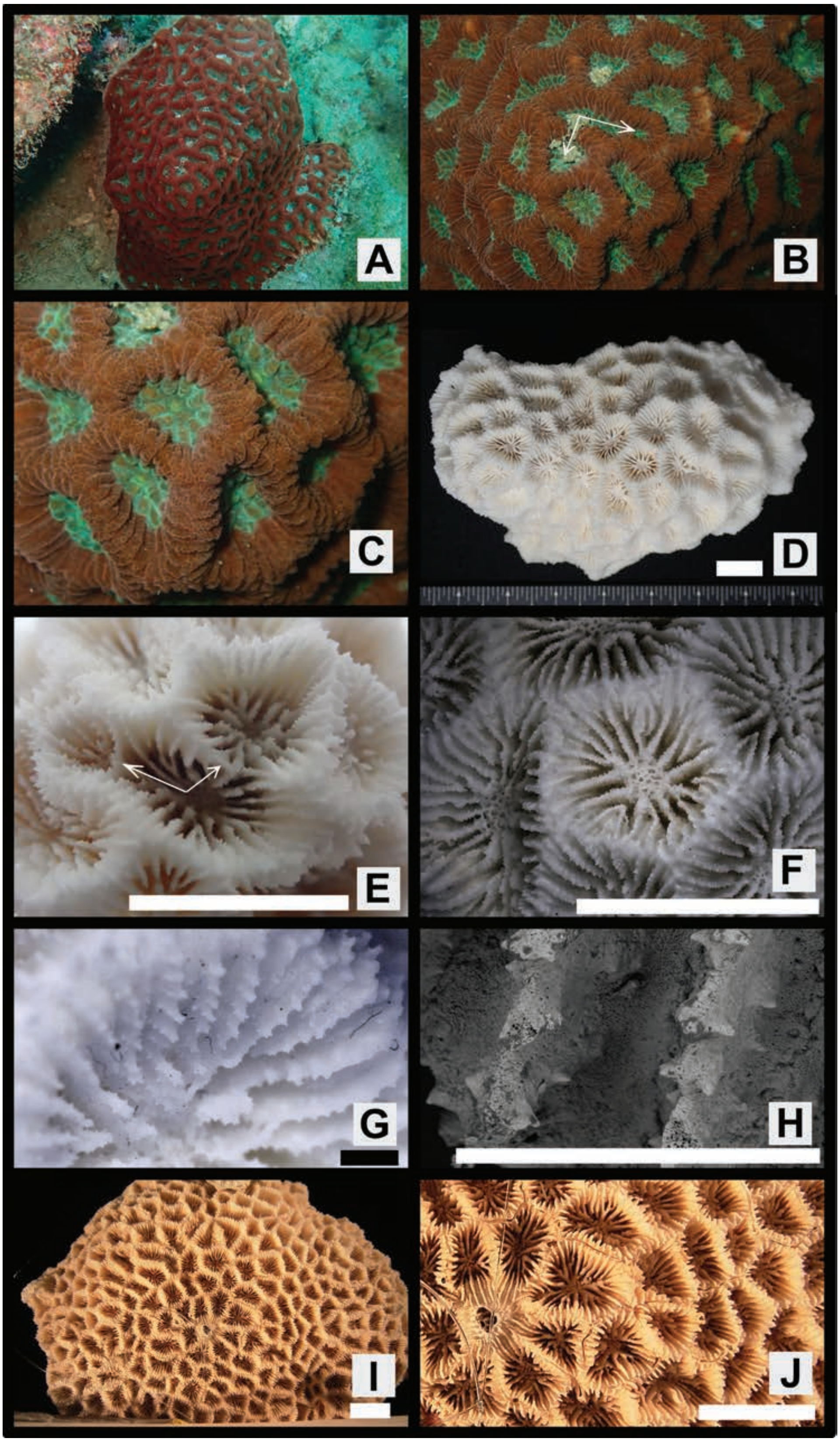

**Figure 2.** *Paragoniastrea variabilis* sp. nov. (Holotype: MUFS C588) and *Paragoniastrea deformis* (Holotype: MTQ G32487) **A–H** *P. variabilis* **A** colony *in situ* **B** close up of corallite division in two directions **C** close up the colony *in situ* **D** full scale of the skeletal specimen **E** corallite division in two directions from the skeletal specimen **F** corallites of the skeletal specimen **G** close up of one corallite of the skeletal specimen **H** septal teeth of the skeletal specimen **I–J** *P. deformis* **I** full scale of the skeletal specimen, **J** corallites of the skeletal specimen. Scale bar: 10 mm (**D, E, F, I, J**); 1 mm (**G, H**).

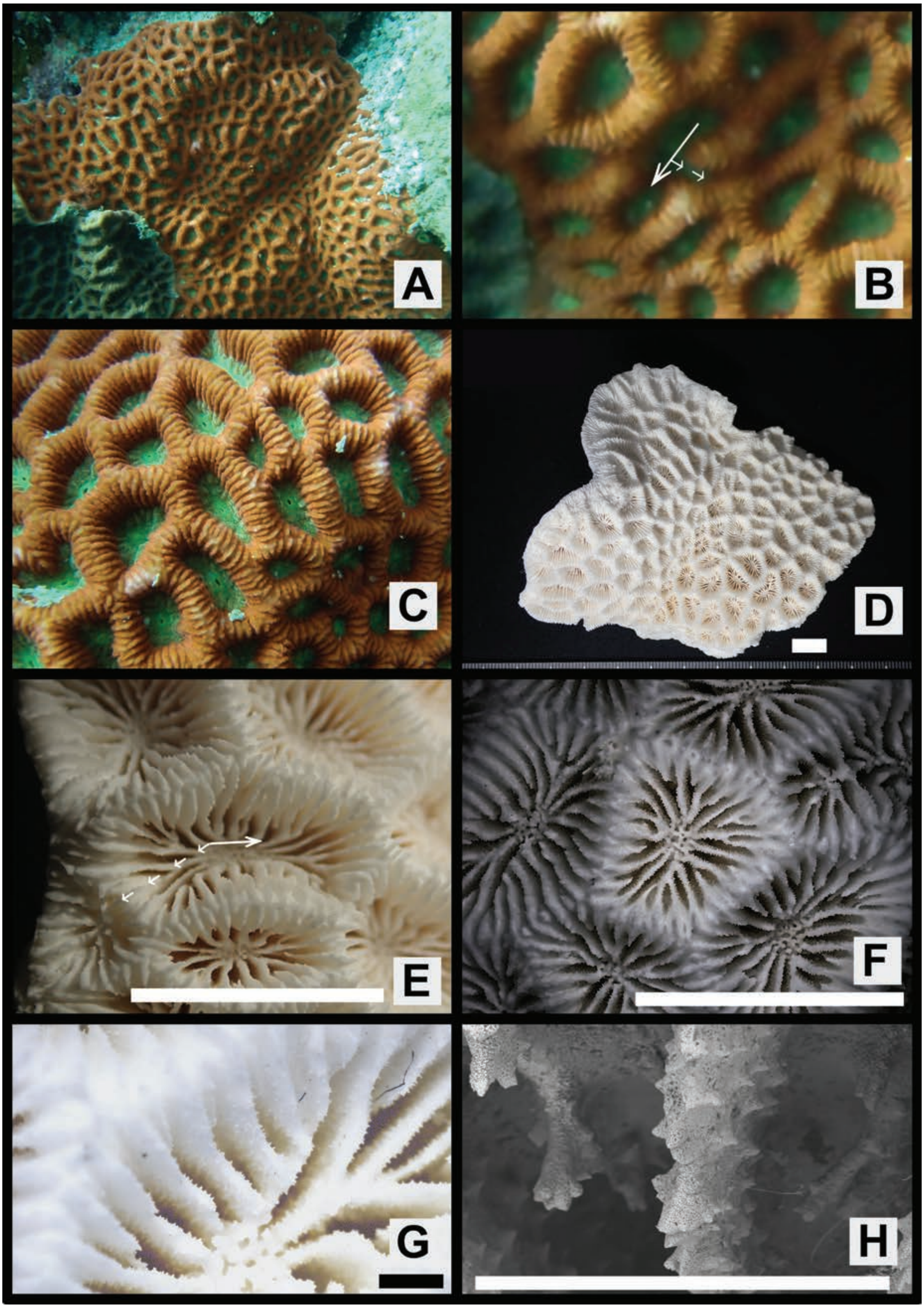

**Figure 3.** *Paragoniastrea variabilis* sp. nov. (Paratype: MUFS C78). **A** colony *in situ* **B** close up of corallite division in two directions **C** close up the colony *in situ* **D** full scale of the skeletal specimen **E** corallite division in two directions from the skeletal specimen **F** corallites of the skeletal specimen **G** close up of one corallite of the skeletal specimen **H** septal teeth of the skeletal specimen. Scale bar: 10 mm (**D, E**, **F**); 1 mm (**G**, **H**).

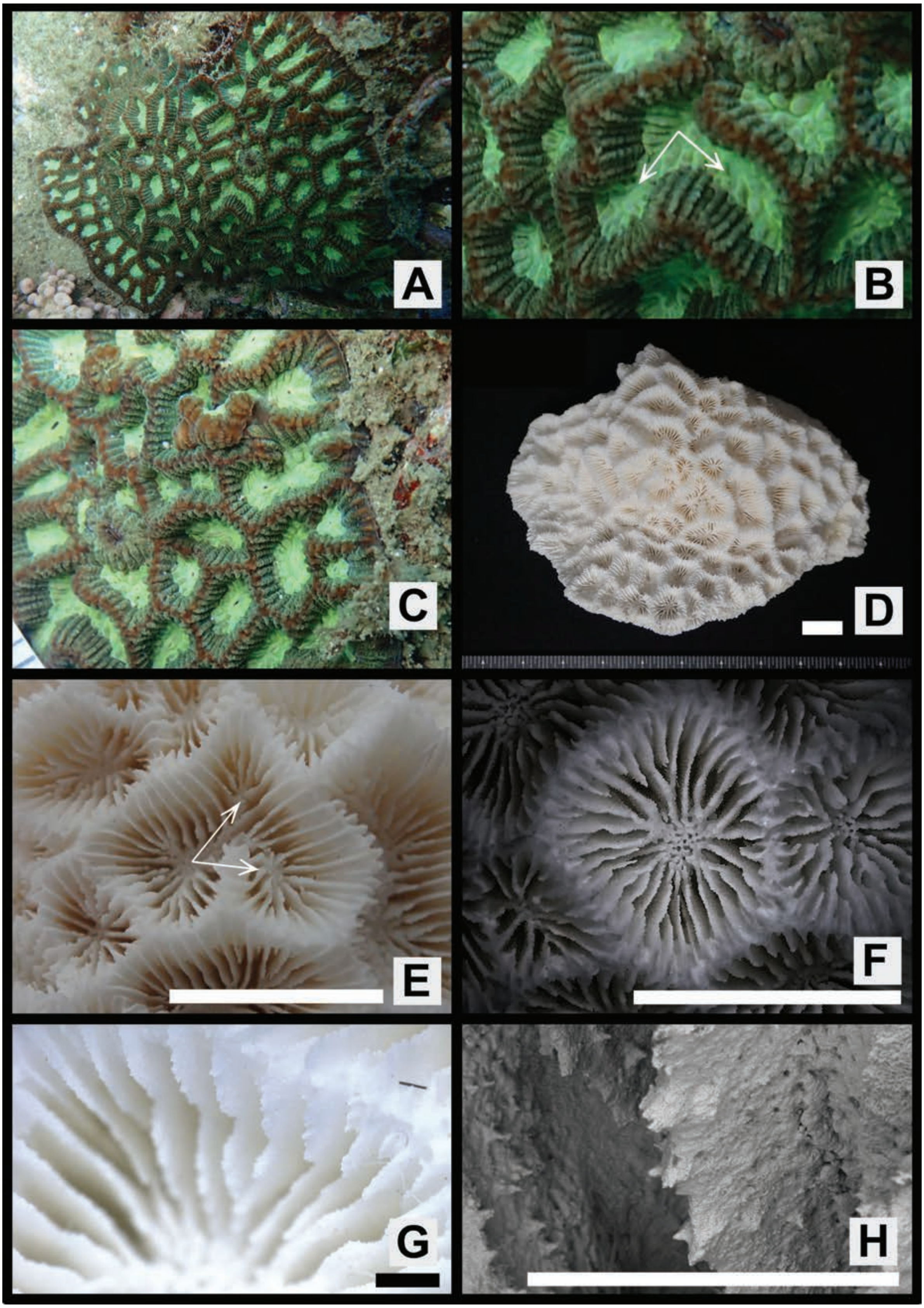

**Figure 4.** *Paragoniastrea variabilis* sp. nov. (Paratype: MUFS C585) **A** colony *in situ* **B** close up of corallite division in two directions **C** close up the colony *in situ* **D** full scale of the skeletal specimen **E** corallite division in two directions from the skeletal specimen **F** corallites of the skeletal specimen **G** close up of one corallite of the skeletal specimen **H** septal teeth of the skeletal specimen. Scale bar: 10 mm (**D, E, F**); 1 mm (**G, H**).

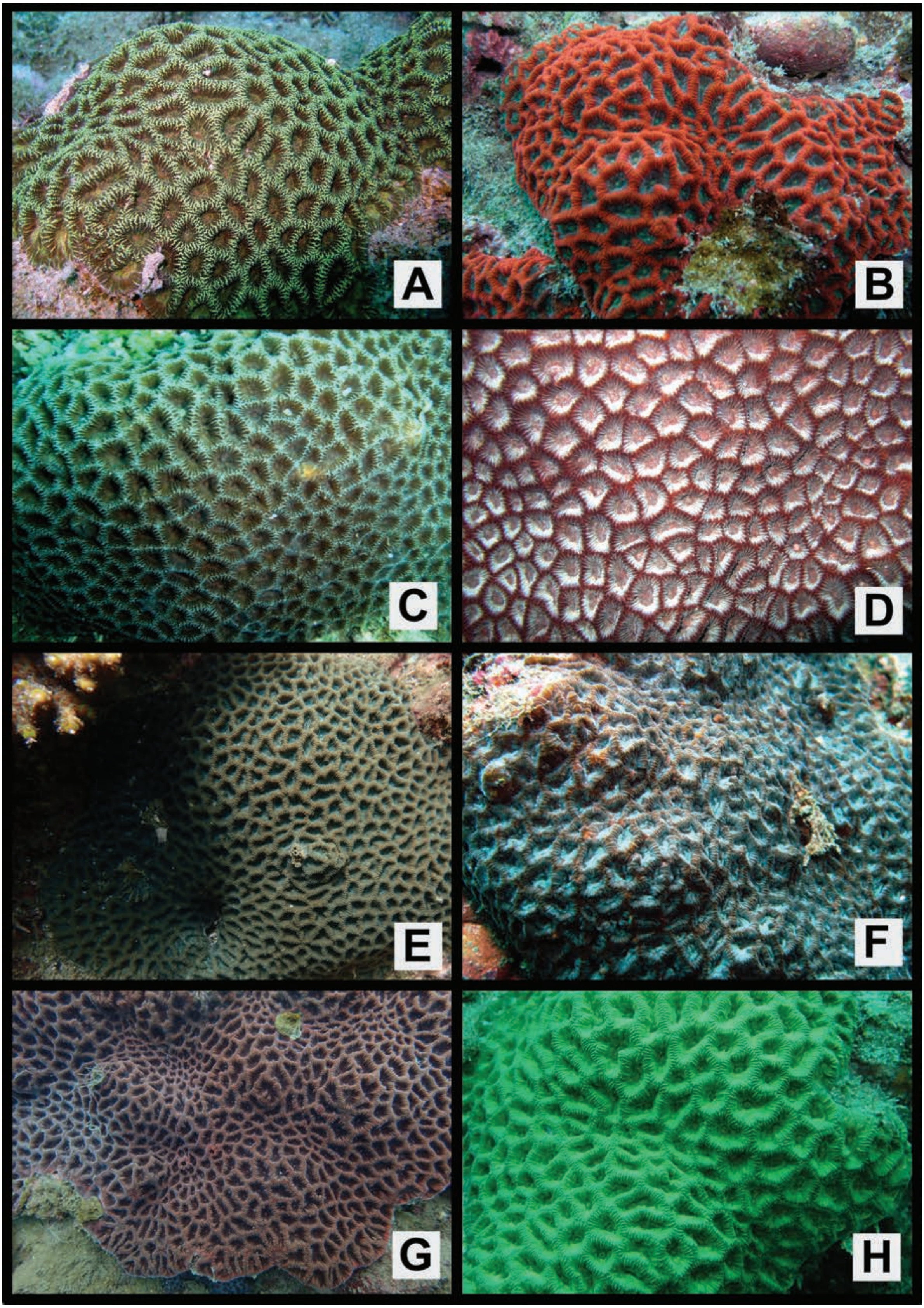

**Figure 5.** Color variation in life of *Paragoniastrea variabilis* sp. nov. **A** SMP-HC 894, Kushimoto, Wakayama, Japan **B** SMP-HC 1205, Kushimoto, Wakayama, Japan **C** SMP-HC 1749, Amakusa, Kumamoto, Japan **D** SMP-HC 1038, Kushimoto, Wakayama, Japan **E** MUFS C585, Amakusa, Kumamoto, Japan **F** SMP-HC 1208, Kushimoto, Wakayama, Japan **G** ASIZC0001666, Yehliu, New Taipei, Taiwan **H** SMP-HC 1203, Kushimoto, Wakayama, Japan.

**Comparative specimens.** *Paragoniastrea australensis*. MUFS C571, sample AM19-3, Amakusa, Kumamoto, Japan; MUFS C572, sample AM19-38, Amakusa, Kumamoto, Japan; MUFS C573, sample MO451, Oshima Island, Miyazaki, Japan; MUFS C574, sample MO457, Oshima Island, Miyazaki, Japan; MUFS C575, sample MO461, Oshima Island, Miyazaki, Japan; MUFS C576, sample NB96, Shimanourashima Island, Miyazaki, Japan; MUFS C577, sample NB148, Shimanourashima Island, Miyazaki, Japan; MUFS C578, sample OI10, Fukashima Island, Oita, Japan.

*Paragoniastrea deformis*. Holotype (MTQ G32487), Kushimoto, Wakayama, Japan; MUFS C579, sample AM19-18, Amakusa, Kumamoto, Japan; MUFS C580, sample AM19-21, Amakusa, Kumamoto, Japan; MUFS C581, sample AM19-26, Amakusa, Kumamoto, Japan; MUFS C582, sample AM19-36, Amakusa, Kumamoto, Japan; MUFS C583, sample MO450, Oshima Island, Miyazaki, Japan; MUFS C584, sample MO452, Oshima Island, Miyazaki, Japan; ASIZC0001667, sample TWN46, Yehliu, New Taipei, Taiwan; ASIZC0001669, sample TWN48, Yehliu, New Taipei, Taiwan.

*Paragoniastrea* aff. *deformis*. MUFS C590, sample AM19-19, Amakusa, Kumamoto, Japan; SMBL Cni-10321, sample JPO30, Shirahama, Wakayama, Japan; ASIZC0001691, sample TWN79, Yehliu, New Taipei, Taiwan.

**Description.** Colonies massive or encrusting, surface smooth or rather uneven (Figs 2A, 3A, 4A, 5A–H).

Corallites intratentacular budding, arrangement mainly cerioid, rarely meandroid, 1–3 corallites lined up in one valley between corallite walls, percentage of having two corallites 2–19 (average ± SD: 8.2 ± 6.0) % and three corallites 0–8 (3.3 ± 3.3) %. Outline distorted quadrangular or pentagonal, usually compressed, calices 6.1–11.8 (average ± SD: 9.0 ± 1.6) mm in long diameter, moderately deep, height of calice relief (vertical distance from upper margin of corallite walls to columella) 2.0–4.3 (average 3.0 ± 0.7) mm (Figs 2B–F, 3B–F, 4B–F, Table 1).

Septa formed by usually straight plates, steeply sloped along the corallite walls, numerous, present up to 4th cycles, range of number 28–62 (average ± SD: 44.7 ± 7.8), length uneven, 2.7–5.1 (3.7 ± 0.7) mm length, width of primary septa thin, 0.19–0.26 (0.21 ± 0.02) mm wide, secondary and tertiary septa almost same width as primaries, quaternary septa usually faint. Primary and secondary septa connected to each other, and sometimes tertiary septa connected as well. Primary and secondary, and sometimes part of tertiary septa reaching columella (total number of septa reaching columella 9–21, average ± SD: 13.5 ± 2.4). Dorsal margin of septa with 4–9 (average ± SD: 5.6 ± 0.9) teeth. Teeth arranged vertically in single row, and surface covered with multiple spiny-like granules, sometimes with one short ridge on center of lateral faces. Distance between septal teeth is 0.1–0.6 (average ± SD: 0.31 ± 0.08) mm. Lateral faces of septa with sparsely distributed granules same as septal teeth (Figs 2E–G, 3E–G, 4E–G, Table 1).

Primary and secondary, and partial or all tertiary septa with rather distinct paliform lobes. Paliform lobes 0.68–1.37 (average ± SD: 1.18 ± 0.15) mm long vertically, uneven in shape and size, with 1–4 (2.1 ± 0.8) teeth on dorsal margin (Figs 2E–G, 3E–G, 4E–G, Table 1).

Columella rather large, spongy, formed by many entangled trabeculae, 0.9–2.8 (average ± SD: 1.6 ± 0.5) mm in long diameter (Figs 2F, 3F, 4F, Table 1).

Corallite walls joined between adjacent corallites, rather steeply sloped but standing upright even near the center of corallum, rather thin, groove-and-tube structure absent on walls joint (Figs 2D–F, 3D–F, 4D–F).

**Table 1.** Morphological characteristics of *Paragoniastrea* spp. Left half is average (standard deviation), right half is value range (minimum to maximum). The measurements for each of the characteristics were taken from five corallites per specimen. For characteristics marked with an asterisk, three characters were measured from one corallite and the average of the three characters was treated as data from one corallite. Measurement in mm.

| **Characteristics** | ***P. variabilis* sp. nov.** | ***P. deformis*** | ***P.* aff. *deformis*** | |
|---|---|---|---|---|
| | **n=16** | **n=8** | **n=2 (AM19-19, JP030)** | **n=1 (TWN79)** |
| Groove-and-tube structure | absent | present | absent | absent |
| Long diameter of calice | 9.0 (1.6), 6.1–11.8 | 5.4 (0.8), 4.5–7.7 | 8.6 (1.0), 7.2–10.2 | 8.2 (0.4), 7.6–8.9 |
| Long diameter of columella | 1.6 (0.5), 0.9–2.8 | 1.5 (0.4), 1.24–2.3 | 1.9 (0.3), 1.4–2.4 | 1.8 (0.3), 1.3–2.1 |
| height of calice relief | 3.0 (0.7), 2.0–4.3 | 2.2 (0.6), 1.2–3.6 | 3.1 (0.7), 2.2–4.6 | no data |
| Width of primary septa* | 0.21 (0.02), 0.19–0.26 | 0.30 (0.02), 0.28–0.34 | 0.24 (0.02), 0.20–0.30 | 0.23 (0.02), 0.19–0.26 |
| No. of septa per calice | 44.7 (7.8), 28–62 | 33.1 (3.7), 29–44 | 66.5 (5.2), 59–76 | 36.6 (4.1), 32–44 |
| No. of septa reaching collemulla | 13.5 (2.4), 9–21 | 10.8 (1.7), 6–12 | 21.1 (1.4), 19–24 | 18.0 (2.1), 16–21 |
| Length of septa* | 3.7 (0.7), 2.7–5.1 | 3.5 (0.8), 1.4–4.1 | 3.8 (0.7), 2.8–5.1 | 3.2 (0.7), 2.1–4.4 |
| No. of teeth on septa* | 5.6 (0.9), 4–9 | 5.5 (0.6), 4–8 | 6.5 (0.5), 5–8 | 6.9 (0.5), 6–8 |
| Distance between septal teeth* | 0.31 (0.08), 0.1–0.6 | 0.34 (0.09), 0.2–0.6 | 0.29 (0.06), 0.2–0.4 | 0.20 (0.03), 0.1–0.3 |
| Hight of paliform lobe* | 1.18 (0.15), 0.68–1.37 | 1.14 (0.17), 0.87–1.37 | 1.12 (0.13), 0.86–1.27 | no data |
| No. of teeth on paliform lobe* | 2.1 (0.8), 1–4 | 2.3 (0.5), 1–4 | 3.0 (0.6), 2–4 | 1.4 (0.3), 1–2 |
| No. of corallites in one valley | up to three, corallites | up to two, corallites | up to two, corallites | up to two, corallites |
| Percentage of two corallites in a valley | 8.2 (6.0), 2–19 | 4.4 (2.3), 3–8 | 6.5 (0.8), 6–7 | 7 |
| Percentage of three corallites in a valley | 3.3 (3.3), 0–8 | 0 | 0 | 0 |

**Color in life.** Colors are highly variable, usually soft bodies of corallite walls and calices are different. Corallite walls brown, greenish-brown, light greenish-brown, red or reddish-brown; calices brown, light brown, green, greenish-brown or light green (Figs 2A–C, 3A–C, 4A–C, 5A–H).

**Distribution and habitat.** *Paragoniastrea variabilis* sp. nov. is known from warm-temperate, non-coral reef region in Japan (Wakayama, Kochi, Oita, Nagasaki, Kumamoto, Miyazaki and Kagoshima) and northern Taiwan (Fig. 1), found in shallow water at depths of 3–15 m, and is sympatric with all other species of the *Paragoniastrea* from Japan, namely *P. australensis*, *P. deformis* and *P.* aff. *deformis*.

**Etymology.** The species is named from Latin *variabilis* (variable), in reference to the considerable color variations.

## Remarks

### Differences between species of *Paragoniastrea* based on morphological analysis

*Paragoniastrea* previously included three species, namely, *P. australensis*, *P. deformis* and *P. russelli* (Huang et al. 2014; Hoeksema and Cairns 2024). This study adds the new species *P. variabilis* sp. nov. (see Key to the species of *Paragoniastrea* below), which is separated from its congeners by following a combination of several characters: (1) The arrangement of corallites is dominantly cerioid, rarely meandroid; (2) Primary septa are not clearly thicker than secondary septa; and (3) the groove-and-tube structure is absent on corallite wall joint.

The new species most closely resembles *P. deformis* in *Paragoniastrea* (Figs 2, 7). Both species have significant differences not only in the presence or absence of groove-and-tube structure but also in the following characteristics. *Paragoniastrea variabilis* sp. nov. has a larger average calice diameter ($p < 0.001$), average number of septa per calice ($p < 0.001$), and average number of septa reaching columella ($p < 0.001$) than *P. deformis*. In addition, *P. deformis* has wider primary septa than *P. variabilis* sp. nov. ($p < 0.001$) and up to two corallites in one valley between corallite walls, whereas *P. variabilis* sp. nov. has up to three corallites (Figs 2, 6, 7, Table 1).

Identifying the species, two specimens of sample AM19-19 (MUFS C590) from Kumamoto and JP030 (SMBL Cni-10321) from Wakayama, which were identified as *P. deformis* by Huang et al. (2014), had more septa per calice and more septa reaching columella than *P. deformis* and *P. variabilis* sp. nov. Although these specimens are morphologically different from known species, sufficient molecular phylogenetic evidence has not been obtained. Therefore, these specimens were tentatively treated as *Paragoniastrea* aff. *deformis*. In addition, one specimen, TWN79 (ASIZC0001691) from Taiwan, has similar morphological characteristics to *P. variabilis* sp. nov., but phylogenetic analysis showed this sample was included in the *P. deformis* clade in the IGR tree but formed an independent clade with specimen JP030 identified as *P.* aff. *deformis*, apart from *P. deformis* and *P. variabilis* sp. nov. in the ITS tree (see below molecular phylogenetic analysis). Thus, this specimen was treated as *P.* aff. *deformis*.

Principal component analysis using long diameter of columella, width of primary septa, number of teeth on septa, long diameter of columella, number of septa per calice, and number of septa reaching columella divided our samples into three groups. Among them, *P. variabilis* sp. nov. and *P. deformis* were separated along the PC1 axis, with PC1 explaining 47.9% of the morphological multivariate variance. *Paragoniastrea* aff. *deformis* was also distinct from *P. deformis* along the PC1 axis, but it partially overlapped with *P. variabilis* sp. nov. (Fig. 8).

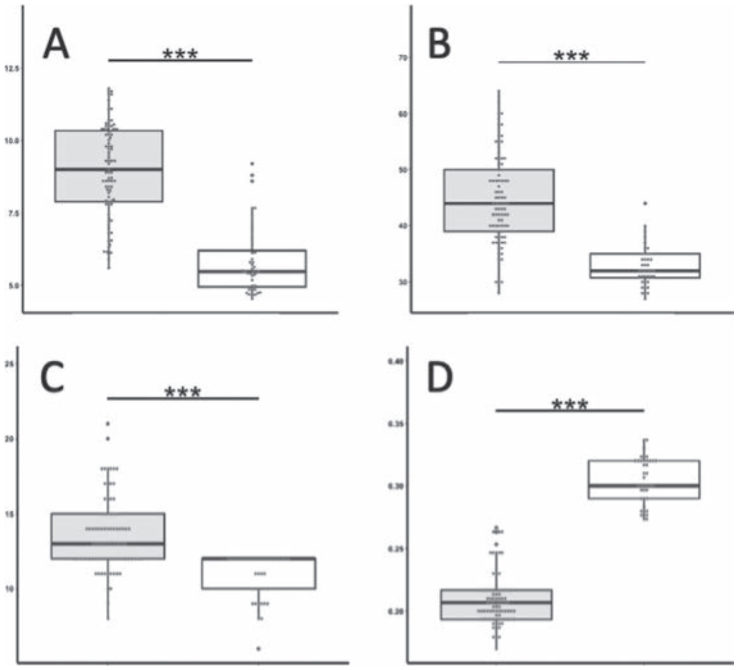

**Figure 6.** Morphological comparison between *P. variabilis* sp. nov. (left) and *P. deformis* (right) **A** long diameter of calice **B** number of septa per calice **C** number of septal reaching to columella **D** width of primary septa. Vertical bars indicate standard deviations, and the black horizontal line in the box-and-whisker chart indicates the median. ***: $p<0.001$.

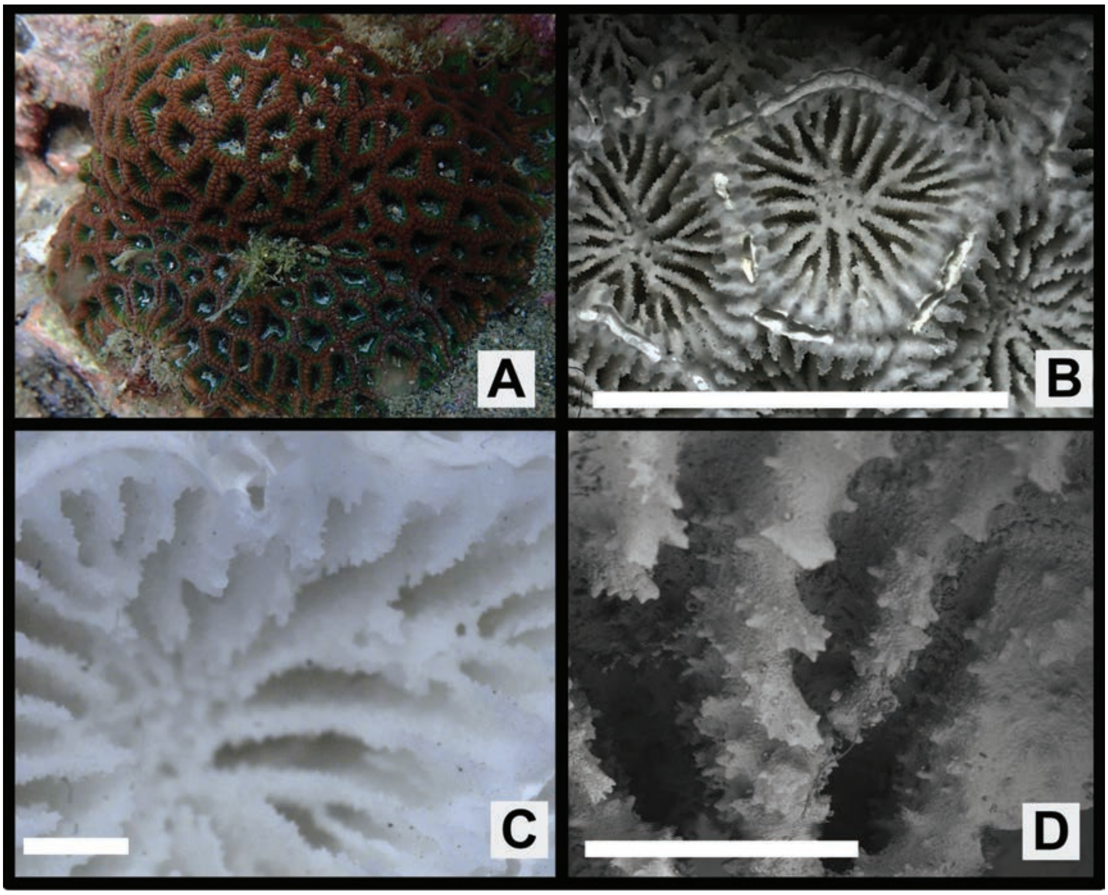

**Figure 7.** *Paragoniastrea deformis* (MUFS C580) **A** colony *in situ* **B** corallites of the skeletal specimen **C** close up of one corallite of the skeletal specimen **D** septa and septal teeth. Scale bars: 10 mm (**B**); 1 mm (**C, D**).

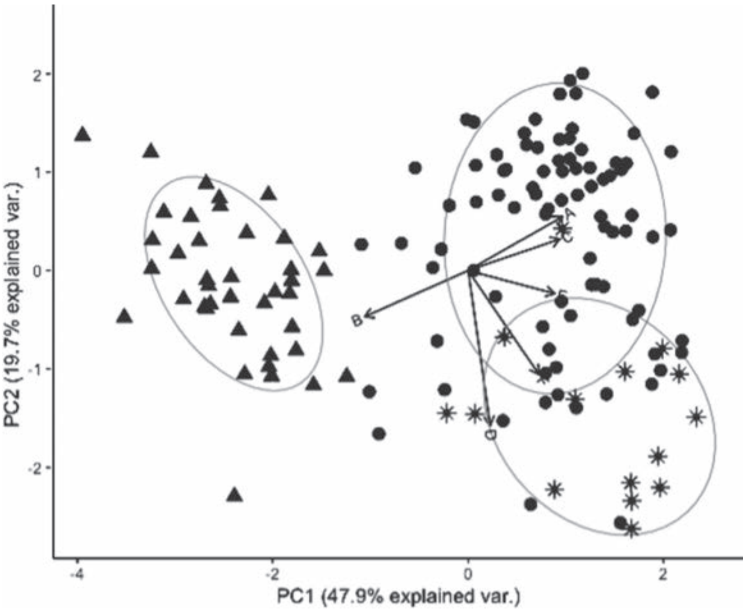

**Figure 8.** Principal component analysis on morphological characteristics of specimens in *P. variabilis* sp. nov. (black circle), *P. deformis* (black triangle) and *P.* aff. *deformis* (black asterisk). Arrows indicate long diameter of calice (**A**), width of primary septa (**B**), number of teeth on septa (**C**), long diameter of columella (**D**), number of septa per calice (**E**), number of septa reaching columella (**F**).

## Key to the species of *Paragoniastrea*

1 Corallites arrangement procoid, cerioid or meandroid, width of primary septa clearly thicker than secondary septa .................................. ***P. russelli***

– Corallites arrangement cerioid or meandroid, width of primary septa not clearly thicker than secondary septa .......................................................... **2**

2 Corallites arrangement of meandroid dominant ................... ***P. australensis***

– Corallites arrangement cerioid dominant, meandroid rare ......................... **3**

3 Groove-and-tube structure present on joint of corallite walls...... ***P. deformis***

– Groove-and-tube structure absent on joint of corallite walls....................... ........................................................................................ ***P. variabilis* sp. nov.**

## Differences between species of *Paragoniastrea* based on molecular phylogenetic analysis

For the IGR marker, the overall sequence length was 894 nucleotides with 102 polymorphic sites. The molecular phylogenetic tree of IGR showed that *P. variabilis* sp. nov. formed an independent clade from the other clades, including *P. deformis*, *P. australensis* and *P. russelli*. All three samples, AM19-19 (MUFS C590), TWN79 (ASTZC0001691), and JP030 (SMBL Cni-10321) of *P.* aff. *deformis* were included within the clade of *P. deformis* (Fig. 9).

For the ITS marker, the overall sequence length was 774 nucleotides with 69 polymorphic sites. The ITS tree showed that *P. deformis* and *P. variabilis* sp. nov. were also clearly separated into different clades (Fig. 9). Two samples (TWN79

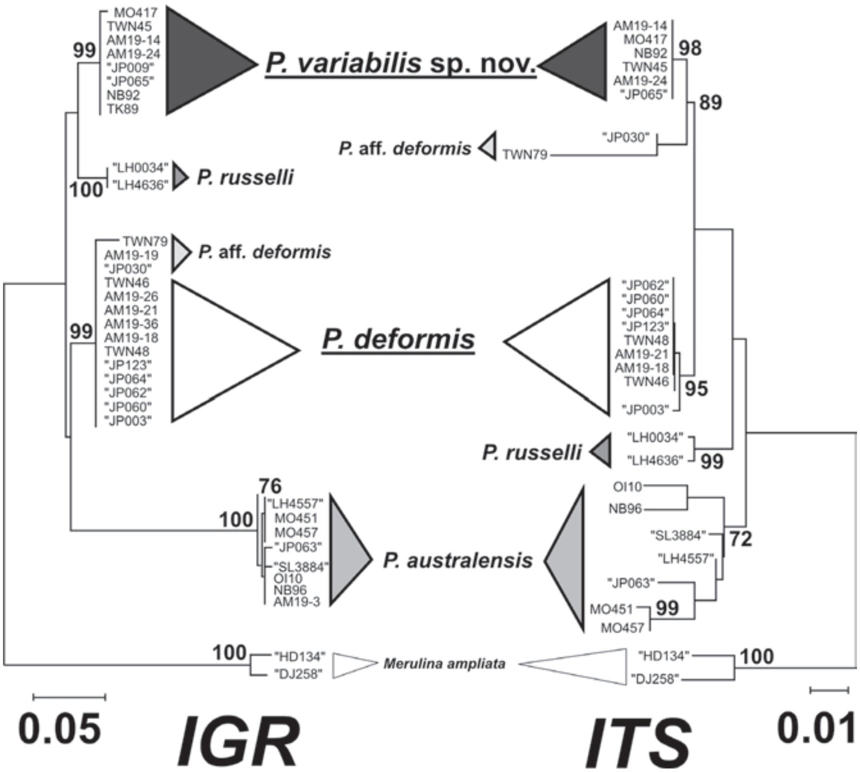

**Figure 9.** Molecular phylogenetic tree based on IGR (left) and ITS (right) for *Paragoniastrea* species. DNA sequences obtained from DDBJ were shown with double quotation marks with the specimen number.

and JP030) of *P.* aff. *deformis* formed an independent clade. The third sample (AM19-19) of *P.* aff. *deformis* could not be used for this analysis because of PCR amplification failure.

## Conclusion

*Paragoniastrea variabilis* sp. nov. had been considered an intraspecific morphological variant of *P. deformis* because of their sympatric distributions and similar morphology (see synonymy). In this study, the results of morphological and molecular phylogenetic analyses showed that *P. variabilis* sp. nov. and *P. deformis* are clearly distinct from each other. Thus, we describe *P. variabilis* sp. nov. as a new species of *Paragoniastrea*.

Finally, the taxonomic position of *P.* aff. *deformis* (Fig. 10) remains unclear because of insufficient morphological and phylogenetic studies, so better sampling and analyses will be needed to clarify its species status.

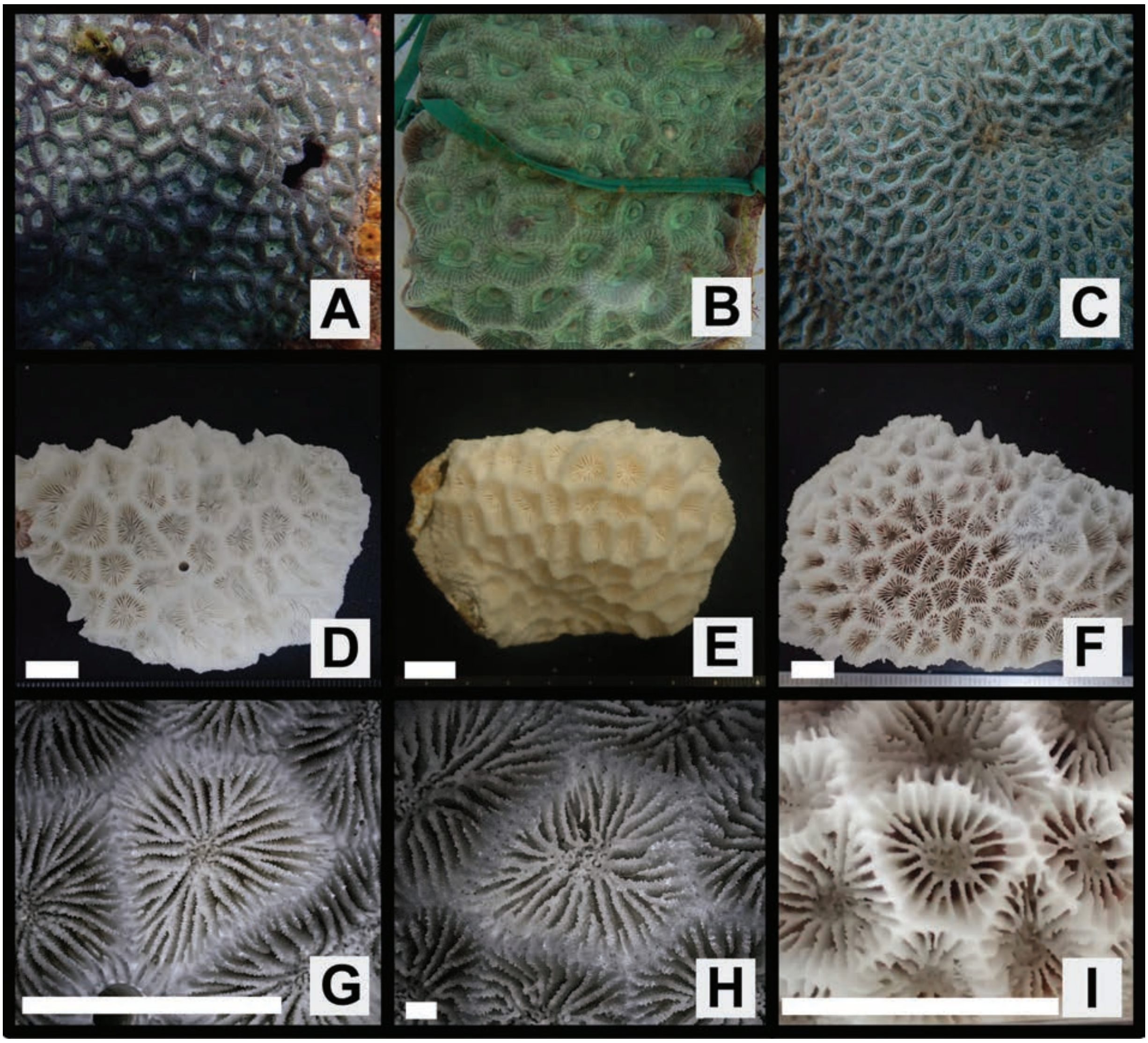

**Figure 10.** *Paragoniastrea.* aff. *deformis* **A–C** colonies *in situ* **D–F** full scale of the skeletal specimens **G–I** corallites of the skeletal specimens **A, D, G** MUFS C590 (AM19-19), Amakusa, Kumamoto Japan **B, E, H** ASIZC0001691 (TWN79), Yehliu, New Taipei, Taiwan **C, F, I** SMBL Cni-10321 (JP030), Kushimoto, Wakayama, Japan. Scale bar: 10 mm (**D–G, I**); 1 mm (**H**).

## Acknowledgements

We thank Shinta Kato, and members of Coral Lab. of University of Miyazaki for their assistance with sampling and analysis. We also thank Bert Hoeksema and Danwei Huang for suggestions that helped improve the manuscript. K. Nomura would like to express gratitude to Kushimoto Marine Park Center for providing various facilities during the research activities. Permission for collecting specimens to undertake the research was obtained from the applicable local governments in Japan and Taiwan.

## Additional information

### Conflict of interest

The authors have declared that no competing interests exist.

### Ethical statement

No ethical statement was reported.

### Funding

This study was funded by JSPS KAKENHI (No.18K06423, 23H00529) to H. Fukami.

### Author contributions

Data curation: DK, HF, SA, YN, KN. Formal analysis: DK. Investigation: HF. Project administration: HF. Writing - original draft: KN, DK, HF. Writing - review and editing: YN, SA.

### Author ORCIDs

Hironobu Fukami https://orcid.org/0000-0002-7647-6668

### Data availability

All of the data that support the findings of this study are available in the main text or Supplementary Information.

## References

Fukami H, Budd AF, Levitan DR, Jara J, Kersanach R, Knowlton N (2004) Geographic differences in species boundaries among members of the *Montastraea annularis* complex based on molecular and morphological markers. Evolution 58: 324–337. https://doi.org/10.1111/j.0014-3820.2004.tb01648.x

Hoeksema BW, Cairns S (2024) World List of Scleractinia. *Paragoniastrea* Huang, Benzoni and Budd, 2014. [World Register of Marine Species] https://www.marinespecies.org/aphia.php?p=taxdetails&id=817176 [on 2024-01-25]

Huang D, Benzoni F, Arrigoni R, Baird AH, Berumen ML, Bouwmeester J, Chou LM, Fukami H, Licuanan WY, Lovell ER, Meier R, Todd PA, Budd AF (2014) Towards a Phylogenetic classification of reef corals: The Indo-Pacific genera *Merulina*, *Goniastrea* and *Scapophyllia* (Scleractinia, Merulinidae). Zoologica Scripta 43(5): 531–548. https://doi.org/10.1111/zsc.12061

Katoh K, Rozewicki J, Yamada DY (2019) MAFFT online service: Multiple sequence alignment, interactive sequence choice and visualization. Briefings in Bioinformatics 20(4): 1160–1166. https://doi.org/10.1093/bib/bbx108

Kuraku S, Zmasek CM, Nishimura O, Katoh K (2013) aLeaves facilitates on-demand exploration of metazoan gene family trees on MAFFT sequence alignment server with enhanced interactivity. Nucleic Acids Research 41(W1): W22–W28. https://doi.org/10.1093/nar/gkt389

Mitsuki Y, Isomura N, Nozawa Y, Tachikawa H, Huang D, Fukami H (2021) Distinct species hidden in the widely distributed coral *Coelastrea aspera* (Cnidaria, Anthozoa, Scleractinia). Invertebrate Systematics 35(8): 876–891. https://doi.org/10.1071/IS21025

Nishihira M (1991) Field guide to hermatypic corals of Jama. First enlarged edition. Tokai University Press, Tokyo, 264 pp. [In Japanese]

Nishihira M, Veron JEN (1995) Hermatypic corals of Japan. Kaiyusya, Tokyo, 439 pp. [In Japanese]

Nomura K (2016) Zooxanthellate scleractinian corals of Kushimoto II, Vacatina. Marine Pavilion, supplement 6, 69 pp. [In Japanese] http://www.kushimoto.co.jp/marinepavilion/data/sup6.pdf

Nomura K, Mezaki T (2005) Reef building corals from Ostuki, Kochi Prefecture, Japan. Kuroshio Biosphere 2: 29–41. [In Japanese] https://kuroshio.or.jp/wp-content/uploads/2019/06/KuroshioBiosphere_02_29-41_NomuraMezaki.pdf

Nomura K, Fukami H, Zayasu Y, Shimada G, Kitano Y, Yokochi H, Shimoike K, Tachikawa H, Oku Y, Suzuki G, Kajiwara K (2016) Revision of Zooxanthellate scleractinian corals of Kushimoto. Marine Pavilion, supplement 4, 20 pp. [In Japanese] http://www.kushimoto.co.jp/marinepavilion/data/sup4.pdf

Nomura K, Yokochi H, Kimura T, Kajiwara K, Nojima S, Arakaki S (2020) Zooxanthellate scleractinian corals collected from the Amakusa Islands, Kumamoto, western Kyushu, Japan. Coastal Ecosystems 7: 1–52.

Quek ZBR, Jain SS, Richards ZT, Arrigoni R, Benzoni F, Hoeksema BW, Carvajal JI, Wilson NG, Baird AH, Kitahara MV, Seiblitz IGL, Vaga CF, Huang D (2023) A hybrid-capture approach to reconstruct the phylogeny of Scleractinia (Cnidaria: Hexacorallia). Molecular Phylogenetics and Evolution 186: 107867. https://doi.org/10.1016/j.ympev.2023.107867

Randall RH, Eldredge LG (1976) Skeletal modification by a polychaete annelid in some scleractinian corals. Coelenterate Ecology and Behavior. Springer, 453–465. https://doi.org/10.1007/978-1-4757-9724-4_48

Rosen BR (1968) An account of a pathologic structure in the Faviidae (Anthozoa): A revision of *Favia valenciennesii* (Edwards & Haime) and its allies (Pis.1–8). Bulletin of the British Museum (Natural History). Zoology 16: 323–352. https://doi.org/10.5962/p.314176

Sugihara K, Nomura K, Yokochi H, Shimoike K, Kajiwara K, Suzuki G, Zayasu Y, Dewa N, Fukami H, Kitano Y, Matsumoto H, Mezaki T, Nagata S, Tachikaw H, Kimura T (2015) Zooxanthellate scleractinian corals of Tanegashima Island. Center for Environmental Biology and Ecosystem Studies, National Institute for Environmental Studies, Japan, 197 pp. [In Japanese]

Tamura K, Stecher G, Kumar S (2021) MEGA11: Molecular Evolutionary Genetics Analysis Version 11. Molecular Biology and Evolution 38(7): 3022–3027. https://doi.org/10.1093/molbev/msab120

Uchida H, Soyama I (1994) Rochy reef animals. In: Okutani T (Ed.) Yama-kei, Tokyo, 367 pp. [In Japanese]

Veron JEN (1990) New Scleractinia from Japan and other Indo-West Pacific countries. Galaxea 9: 95–173.

Veron JEN (2000) Corals of the World, Vol. 3. Australian Institute of Marine Science, Townsville, 490 pp.

Veron JEN, Stafford-Smith MG, Turak E, DeVantier LM (2016) Corals of the World. http://www.coralsoftheworld.org/species_factsheets/species_factsheet_summary/goniastrea-deformis/ [Accessed 18 Feb 2024]

Wei NWV, Wallace CC, Dai CF, Pillay KM, Chen CA (2006) Analyses of the ribosomal internal transcribed Spacers (ITS) and 5.8 S gene indicate that extremely high rDNA heterogeneity is a unique feature in the scleractinian coral genus *Acropora* (Scleractinia; Acroporidae). Zoological Studies 45: 404–418. http://zoolstud.sinica.edu.tw/Journals/45.3/404.pdf

Wilfredo YL, Emmi BC (2003) Range extensions of Japanese Scleractinia to the Philippines. Galaxea. Journal of the Coral Reef Studies 5: 63–67. https://doi.org/10.3755/jcrs.2003.63

## Supplementary material 1

### List of specimens that we collected or used in this study

Authors: Daigo Kishi, Keiichi Nomura, Yoko Nozawa, Seiji Arakaki, Hironobu Fukami
Data type: xlsx
Explanation note: Sample information including sampling sites and DNA sequences.

Link: https://doi.org/10.3897/zookeys.1205.121507.suppl1

## Supplementary material 2

### List of species of *Paragoniastrea* referred from Huang et al. (2014) and used in molecular phylogenetic analysis

Authors: Daigo Kishi, Keiichi Nomura, Yoko Nozawa, Seiji Arakaki, Hironobu Fukami
Data type: xlsx
Explanation note: Sample list of referred DNA sequences.

Link: https://doi.org/10.3897/zookeys.1205.121507.suppl2

ZooKeys 1205: 223–238 (2024)
DOI: 10.3897/zookeys.1205.123911

Research Article

# Genetic identification, morphology and distribution of *Natrix helvetica* subspecies in southern and western Switzerland (Reptilia, Squamata, Serpentes)

Andreas Schild[1], Hannes Baur[1,2], Stefan T. Hertwig[1,2], Uwe Fritz[3], Sylvain Ursenbacher[4,5,6]

1 *Institute of Ecology and Evolution, University of Bern, Baltzerstrasse 6, 3012 Bern, Switzerland*
2 *Naturhistorisches Museum Bern, Bernastrasse 15, 3005 Bern, Switzerland*
3 *Museum of Zoology (Museum für Tierkunde), Senckenberg Dresden, A. B. Meyer Building, 01109 Dresden, Germany*
4 *Department of Environmental Sciences, Section of Conservation Biology, University of Basel, Bernoullistrasse 32, 4056 Basel, Switzerland*
5 *info fauna – karch, University of Neuchâtel, Avenue de Bellevaux 51, 2000 Neuchâtel, Switzerland*
6 *Balaton Limnological Research Institute, 8237 Tihany, Klebelsberg Kuno u. 3, Hungary*
*Corresponding authors: Uwe Fritz (uwe.fritz@senckenberg.de); Sylvain Ursenbacher (sylvain.ursenbacher@infofauna.ch)*

## Abstract

Most of Switzerland is inhabited by the nominotypical subspecies of the barred grass snake (*Natrix helvetica helvetica*), which is characterized by mitochondrial DNA lineage E. Only in the northeast of the country, the common grass snake (*N. natrix*) occurs and hybridizes with *N. h. helvetica* in a narrow contact zone. However, we discovered that in southern and western Switzerland barred grass snakes representing another mtDNA lineage (lineage C) are widely distributed. Lineage C is typical for Alpine populations of the southern subspecies *N. h. sicula*. Our microsatellite analyses of the Swiss samples revealed differences between the two subspecies and also a substructure with two clusters in each subspecies. Furthermore, we discovered a contact and hybrid zone of *N. h. helvetica* and *N. h. sicula* along the northern shore of Lake Geneva and also confirm that interbreeding with alien common grass snakes (*N. n. moreotica*, mtDNA lineage 7) occurs there. This finding is of concern for nature conservation and measures should be taken to prevent further genetic pollution. Using morphometrics, we found no differences between the two subspecies of *N. helvetica*, while *N. natrix* was slightly distinct from *N. helvetica*.

**Key words:** Microsatellites, mitochondrial DNA, morphometrics, nuclear DNA, taxonomy

OPEN ACCESS

**Academic editor:** Robert Jadin
**Received:** 25 March 2024
**Accepted:** 21 May 2024
**Published:** 26 June 2024

**ZooBank:** https://zoobank.org/A60403D8-E057-44B6-9E48-3FF7D9F951A1

**Citation:** Schild A, Baur H, Hertwig ST, Fritz U, Ursenbacher S (2024) Genetic identification, morphology and distribution of *Natrix helvetica* subspecies in southern and western Switzerland (Reptilia, Squamata, Serpentes). ZooKeys 1205: 223–238. https://doi.org/10.3897/zookeys.1205.123911

## Introduction

Grass snakes constitute a complex of three species which were regarded as conspecific for many decades (Kabisch 1999; Pokrant et al. 2016; Kindler et al. 2017). *Natrix astreptophora* (Seoane, 1884) occurs in the North African Maghreb region, the Iberian Peninsula and adjacent France. *Natrix helvetica* (Lacepède, 1789) lives in Western Europe north of the Pyrenees and in Britain and Italy. In Central Europe *N. helvetica* ranges eastward approximately to the Rhine region. *Natrix natrix* (Linnaeus, 1758) occupies the largest distribution range of the three species, from east of the Rhine region across Fennoscandia, the Balkan Peninsula and large parts of the Near East to Lake Baikal in Central Asia. Traditionally, many grass snake subspecies have been recognized, based on often somewhat fuzzy morphological features such as body proportions, coloration and size (see reviews in Kabisch 1999; Kindler et al. 2013; Fritz and Schmidtler 2020). Most of these subspecies are currently no longer recognized (Kindler et al. 2018a; Schultze et al. 2020; Asztalos et al. 2021b). According to the current view (Asztalos et al. 2021b), two subspecies of *N. natrix* occur in Central Europe, the nominotypical subspecies *N. n. natrix* and *N. n. vulgaris* Laurenti, 1768. However, the two subspecies hybridize in large parts of southern and southeastern Central Europe, while the populations in northeastern Switzerland represent *N. n. vulgaris* with introgressed mitochondria of *N. n. natrix* (Asztalos et al. 2021a, 2021b). For *N. helvetica*, four subspecies are currently distinguished. *Natrix helvetica helvetica* is distributed north of the Alps, while *N. h. sicula* (Cuvier, 1829) occurs south of the Alps, i.e., on the Italian Peninsula and on Sicily. Two further subspecies live in Corsica (*N. h. corsa* [Hecht, 1930]) and Sardinia (*N. h. cetti* Gené, 1839; Schultze et al. 2020). *Natrix helvetica sicula* crossed the Alps at least twice and occurs in the Inn River drainage of Austria and southernmost Bavaria (Glaw et al. 2019; Asztalos et al. 2021a). In addition, in Switzerland one record is known from beyond the Simplon Pass in the canton Valais (Kindler and Fritz 2018). *Natrix helvetica sicula* harbours several deeply divergent mtDNA lineages, reflecting ancient divergence processes on the Italian Peninsula and Sicily that began approximately 6.8 million years ago (Kindler et al. 2018a; Schultze et al. 2020). The populations of *N. h. sicula* relevant for the present study possess mtDNA lineage C (Schultze et al. 2020).

There are many regions across the distribution range of grass snakes where non-native individuals were introduced (France: Asztalos et al. 2020; Germany and Great Britain: Kindler et al. 2017; Italy: Schultze et al. 2020; Netherlands: van Riemsdijk et al. 2020; Asztalos et al. 2021c). Within the scope of a study in Switzerland, Dubey et al. (2017) genetically uncovered alien grass snakes (*N. natrix*) allegedly originating from Rijeka, western Croatia, which escaped in the 1970s from an outdoor reptile park in Lausanne (46.5427°, 6.6423°). However, the mtDNA lineage detected there (lineage 7 of Kindler et al. 2017, corresponding to *N. n. moreotica* [Bedriaga, 1882]) does not occur in the putative source region, but distinctly further southeast in the Balkans, western Anatolia and Cyprus (Asztalos et al. 2021b). Additionally, Dubey et al. (2017) found grass snakes yielding mtDNA lineage C at the same site in Lausanne. In contrast, Chèvre (2015) and Kindler and Fritz (2018) detected this lineage only in the cantons of Valais and Ticino, raising the question of whether these records also refer to non-native snakes or whether clade C, i.e., *N. h. sicula*, might have a wider distribution in Switzerland.

Dubey et al. (2017) assumed that grass snakes with lineage C also escaped from the reptile park and established in the region. However, it is also possible that *N. h. sicula* had passed the Alps in the Holocene and naturally occurs in western Switzerland. As grass snakes of clades C (*N. h. sicula*) and 7 (*N. n. moreotica*) have potentially hybridized at Lausanne with the native *N. h. helvetica* (clade E), it is of utmost importance for nature conservation to find out whether clade C is also native in western Switzerland or has been introduced.

The aim of the present study is to determine the natural distribution of *N. h. sicula* in Switzerland. To do so, we collected DNA samples from wild snakes and museum specimens to determine their mtDNA lineage. In addition, we used nuclear DNA markers (microsatellites) for Bayesian cluster analyses to estimate the amount of admixture between snakes corresponding to different mitochondrial lineages. In accordance with the concept of integrative taxonomy, we also used various characters of pholidosis and colour pattern as well as morphometric measurements to identify possible external morphological differences in our sample.

## Materials and methods

### Study area and sampling

The immediate study area was limited to southern and western Switzerland. It comprised the cantons of Vaud, Valais and Ticino (Fig. 1) as lineage C has been detected there before (database of info fauna – karch; https://www.infofauna.ch/). The sampling scheme was habitat-specific, i.e., we focused on preferred habitats of grass snakes, like ponds, rivers, lakes and spots with previous sightings. Snakes were caught by hand, measured on site, and released directly afterwards at the exact location of capture. DNA samples were taken with buccal swabs (dried and stored at -20 °C) or scale clipping (one to four ventral scales stored in 70% alcohol). Following Thorpe (1979) and Chèvre (2015), individuals with a total length of less than 50 cm were classified as juveniles. To reduce handling time, all necessary body parts of adult snakes were photographed for later morphological analyses. Furthermore, museum specimens from Vaud, Valais and Ticino were studied; a few additional individuals from the adjacent cantons were also included. From museum specimens, liver or muscle tissue was sampled. A list of samples is provided in Suppl. material 1: table S1.

### DNA extraction and purification

Samples were incubated with ATL buffer and proteinase K (Qiagen) in a heat block for 16–20 h at 56 °C. Scales were previously placed in water for 24 h to remove alcohol. After digestion, liquid from swab tips was extracted using a centrifuge. The DNA was purified following the protocol "Purification of total DNA from Animal Tissues (Spin-Column Protocol)" of the DNeasy Blood and Tissue Kit (Qiagen) using a Qiagen robot.

### mtDNA sequencing

To determine the mtDNA lineage, the cytochrome *b* gene (cyt *b*) and the NADH dehydrogenase subunit 4 gene with adjacent regions coding for tRNAs (ND4) were used, as in previous studies on grass snakes (e.g., Kindler et al. 2013, 2017; Chèvre 2015; Pokrant et al. 2016; Glaw et al. 2019; Schultze et al. 2020; Asztalos et al. 2021a, 2021b). Amplification followed Kindler et al. (2013) and Chèvre (2015). PCR products were sequenced by LGC Genomics GmbH (Berlin, Germany). Sequences were processed with CodonCode Aligner (https://www.codoncode.com) and compared with GenBank sequences to determine the mitochondrial lineage.

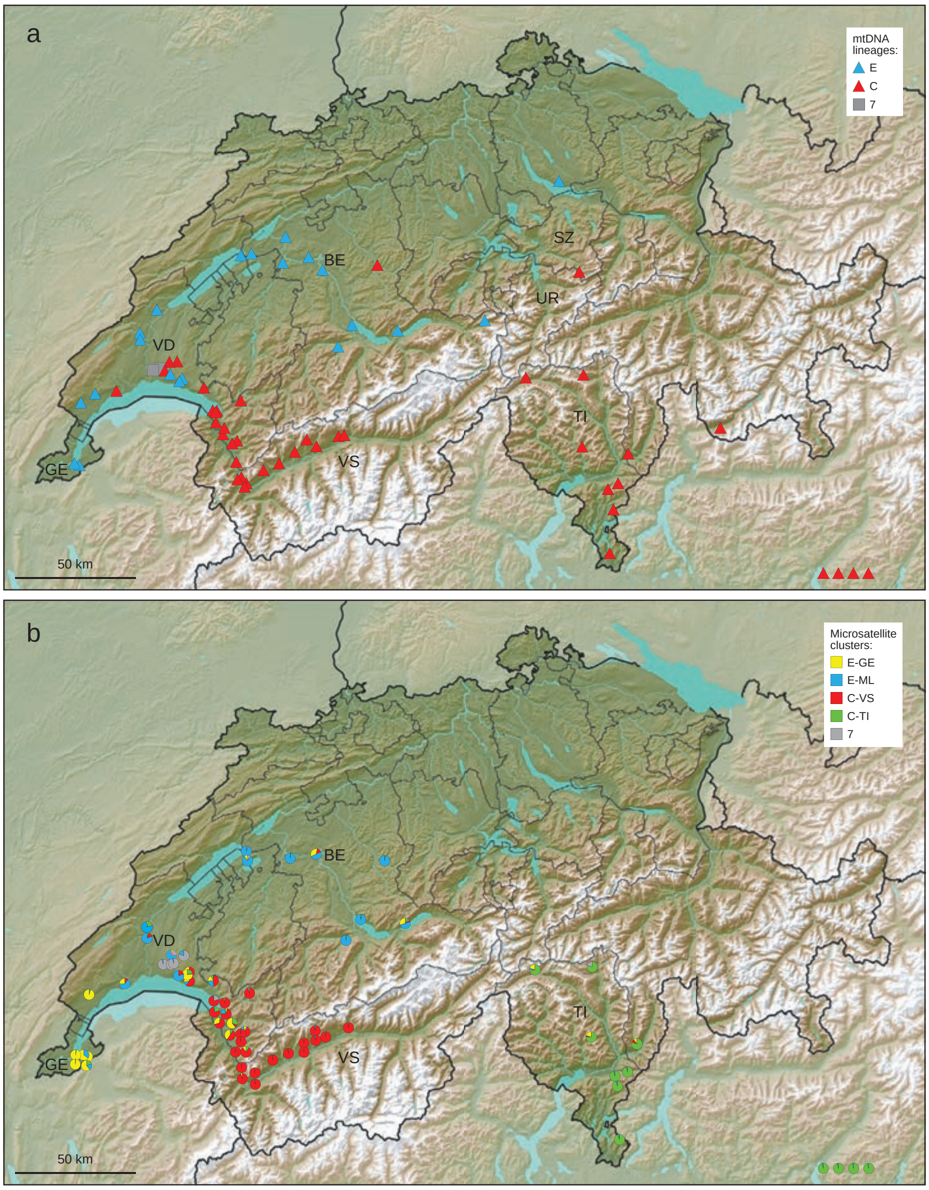

**Figure 1.** Distribution of mitochondrial lineages of grass snakes in southern and western Switzerland (**a**) and microsatellite clusters according to our STRUCTURE analyses (**b**). Symbols and colours of mitochondrial lineages correspond to Kindler et al. (2013). Some symbols are slightly shifted from the sampling location, enhancing readability. The four samples in the bottom right corner originate from northern Italy beyond the map sector. Borders within Switzerland denote cantons. Abbreviations for cantons mentioned in the text: BE – Bern, GE – Geneva, SZ – Schwyz, TI – Ticino, UR – Uri, VD – Vaud, VS – Valais. Lake Geneva, mentioned in the text, is located in the southwesternmost part of Switzerland (cantons of Geneva and Vaud) and adjacent France. The maps were created by modifying a Wikimedia map (https://commons.wikimedia.org/wiki/File:Reliefkarte_Schweiz2.png).

## Microsatellite analyses

The same thirteen microsatellite loci were used as in Chèvre (2015) and Kindler et al. (2017) and genotyped according to their protocols. PCR products were analysed on an ABI 3130xl Genetic Analyser (Applied Biosystems) at the Zoological Institute of the University of Basel. The Microsatellite Plugin in GENEIOUS PRIME 2020.0.3 (https://www.geneious.com) was used to visualize peaks and determine allele lengths.

For inferring the nuclear genomic identity of the 73 successfully processed samples, the Bayesian clustering approach based on the Monte Carlo Markov chain (MCMC) algorithm implemented in the software STRUCTURE ver. 2.3.4 (Pritchard et al. 2000; Pritchard and Wen 2002) was used. STRUCTURE assumes unlinked microsatellite loci at linkage equilibrium and divides the dataset into partitions (*K*) optimized for the presence of Hardy-Weinberg equilibrium. After a burn-in of 100,000 generations, MCMCs were run for 200,000 iterations, ten times per *K* between one and ten. The optimal number of *K* was determined using both the Δ*K* method (Evanno et al. 2005) in STRUCTURE HARVESTER software (Earl and vonHoldt 2012) and the L(*K*) approach of Pritchard and Wen (2002). The best STRUCTURE run (highest likelihood) with the optimal *K* was used both to determine genotypic identity and to assess admixture. Snakes with an assignment ≥ 80% to a specific cluster were treated as pure. $F_{ST}$ values between clusters were calculated with FSTAT ver. 2.9.3 (Goudet 1995) using only genotypically non-admixed individuals.

## Morphological analyses

Only snakes exceeding 50 cm in total length and with a genotypic cluster assignment ≥ 80% were used for morphological examinations. Following Chèvre (2015), morphological variables with strong geographic variation were selected (Suppl. material 1: table S2) and analysed along with landmark data to examine for possible morphological differences between microsatellite clusters. The dataset was enriched with additional data from photographs provided by M. Chèvre (21 genotyped *N. h. helvetica*, mtDNA lineage E; 20 genotyped *N. n. vulgaris*, mtDNA lineage 3 from northeastern Switzerland), so that 31 males, 38 females and three sex-undetermined grass snakes were available for morphology.

## Geometric morphometrics of landmark data

To obtain landmark data, standardized pictures were used showing the right and dorsal sides of the head of adult snakes. Fixing the focal length and manual focus of the camera ensured that the scale of the pictures was identical, which was double-checked using a ruler in the pictures. Photographs were taken twice to calculate mean landmark coordinates, which reduces potential inaccuracies due to slight shifts in photographing and placing landmarks. M. Chèvre provided only a single photograph per snake, for which landmark coordinates were produced twice to account for imprecise landmark placing. Mostly easily identifiable junctions of scales were chosen as landmarks to facilitate the workflow (Suppl. material 1: fig. S1).

Some landmarks were removed for analysis because the sample size was too small for 27×2 coordinate variables. Landmark 8 was removed because the temporal scale was sometimes divided and/or small, so it did not reach the 7th supralabial scale. Landmarks 12, 14, 16 and 18 were excluded as they all have other landmarks in close proximity. Lastly, landmarks 21, 24 and 27 were removed because they are located at the edge and might already be influenced by the curvature of the head. Therefore, only nineteen landmarks (1–7, 9–11, 13, 15, 17, 19, 20, 22, 23, 25, 26) were finally used (Suppl. material 1: figs S3, S4).

Landmarks were placed in the software TPSDIG2 ver. 2.30 (Rohlf 2017) and its coordinates were saved in tps files created by the software TPSUTIL32 ver. 1.74 (Rohlf 2013). In the statistical software R ver. 3.4.1 (R Core Team 2017), the function *estimate.missing*() from the package GEOMORPH (Adams et al. 2019) was used to interpolate missing landmarks with the thin-plate spline method. Then, mean values were calculated for each landmark per specimen and side.

All analyses of the mean landmark coordinates were performed in MORPHOJ ver. 1.07a (Klingenberg 2011), similar to the procedure described in Sidlauskas et al. (2011). First, a least-square Procrustes Fit was calculated. Allometric correction was then performed using a linear regression with the log centroid size as explanatory variable and the Procrustes coordinates as the response variable. The regression included a permutation test with 10,000 rounds and pooled regression within clusters. To examine shape changes, the regression residuals were included in a Canonical Variate Analysis (CVA) with a permutation test for pairwise distances of 10,000 iterations. Scatterplots of CV scores were checked for clustering of groups and wireframe graphs were used to visualize shape changes. The starting and target shape of wireframe graphs were placed next to each other, as suggested by Klingenberg (2013), to be able to objectively examine shape changes. Besides visually plotting the shape differences, the CVA also runs both Mahalanobis and Procrustes permutation tests (10,000 iterations) to check for the significance of shape differences.

## Analysis of distance measurements

Distance measurements (SVL, TL, HL and HW; Suppl. material 1: table S2) were taken in the field and analysed using Multivariate Ratio Analysis (Baur and Leuenberger 2011; Baur 2024). The 'shape PCA' enables the examination of shape changes depending on size. The 'PCA ratio spectrum' then allows the interpretation of principal components (PCs) in terms of ratios and shows the most discriminating ratio with respect to a particular shape PC. This approach has been used in several studies to find morphological differences among taxa (László et al. 2013; Baur et al. 2014; Huber and Baur 2016; Gebiola et al. 2017; Waser et al. 2017). The package MICE (van Buuren and Groothuis-Oudshoorn 2011) was used to replace missing values through multiple imputation within variable groups after excluding individuals with > 25% missing data.

## Analysis of scale counts and colour markings

Scale counts (VS, SCS, PTS and GS; Suppl. material 1: table S2) taken in the field or from photographs were analysed using a standard PCA on the correlation matrix of the data. Colour markings (LBS, LBL, LBW, NMS, NMW, NMUC, NMLC and NMPS; Suppl. material 1: table S2) were quantified with the number of coloured scales as the unit and analysed using a standard PCA on the correlation matrix of the data.

## Linear discriminant analysis

Distance measurements, scale counts, measures for colour markings and three additional variables (RelRedPos, TPOS and BW; Suppl. material 1: table S2) were compared in a linear discriminant analysis to check whether microsatellite clusters are distinguishable. The function *lda*() from the package MASS (Venables and Ripley 2002) was used with equal priors and CV=TRUE. This was repeated for samples of *N. helvetica* only to test whether the discrimination could be improved.

## Results

### Distribution of mtDNA lineages

The distribution of mtDNA lineages in southern Switzerland is shown in Fig. 1a (for details of each sample, see Suppl. material 1: table S1). The cantons of Ticino and Valais are solely inhabited by *Natrix helvetica* with lineage C, typical for Alpine *N. h. sicula*. In contrast, the snakes in the cantons north of the Alps harbour mainly lineage E, typical for *N. h. helvetica*. However, north of the Alps a few lineage C individuals were recorded as well (cantons of Bern, Schwyz and Vaud). The northern shore of Lake Geneva seems to be a broad contact zone of lineages C and E. In addition, in this region, in Lausanne, some *N. n. moreotica* (mtDNA lineage 7) were caught, as already described by Dubey et al. (2017).

### Microsatellite clusters

According to Pritchard and Wen (2002), the optimal number of clusters $K$ has the highest likelihood L($K$) value, which is here $K$=5 (Suppl. material 1: fig. S2, top left). In contrast, the Δ$K$ method (Evanno et al. 2005) revealed $K$=2 as the best solution but also inferred a second pronounced peak for $K$=5 (Suppl. material 1: fig. S2, bottom right). The Δ$K$ method reliably identifies the uppermost hierarchical level of genetic partitioning (Evanno et al. 2005); in our case, this corresponds to samples representing the two species of grass snake, *N. helvetica* and *N. natrix*. For inferring genotypic partitions (clusters) within *N. helvetica* and *N. natrix*, either subsets corresponding to each species can be examined separately in STRUCTURE or the STRUCTURE runs using the highest L($K$) value can be inspected. Considering the highest L($K$) value and the second peak of the Δ$K$ approach, we present here the results for STRUCTURE runs using $K$=5. These five clusters correspond in our dataset to one cluster for *N. natrix* (i.e., genotypes of *N. n. moreotica* from Lausanne plus *N. n. vulgaris* from northeastern Switzerland) and four clusters within *N. helvetica* (for details, see Suppl. material 1: table S1).

Fig. 1b shows the geographic distribution of the five microsatellite clusters for western and southern Switzerland. One cluster (grey in Fig. 1b) represents the alien *N. n. moreotica* with mtDNA lineage 7 from Lausanne. *Natrix helvetica sicula* (mtDNA lineage C) is divided into two clusters, one in Valais (C-VS, red in Fig. 1b) and another one in Ticino (C-TI, green in Fig. 1b). Translated into the hydrographic net, the green cluster is found in river valleys connected to the great pre-Alpine Italian lakes and the Po drainage, and the red cluster is confined to the eastern (i.e., Alpine) Rhone drainage, from eastern Lake Geneva upstream. *Natrix helvetica helvetica* (mtDNA lineage E) is also divided into two clusters, one in the Swiss Plateau (Mittelland; E-ML, blue in Fig. 1b) and another cluster along Lake Geneva (E-GE, yellow in Fig. 1b). Admixture between clusters is evident in particular, but not only, in geographic contact zones, mainly the Lake Geneva region and the adjacent Rhone valley near Montreux. Most of these admixed snakes are *N. helvetica* (admixture among the four respective microsatellite clusters; 16 individuals from the cantons Geneva, Bern, Vaud and Ticino; Suppl. material 1: table S1). Another *N. helvetica* from the canton Bern (Langnau im Emmental) shows mito-nuclear discordance. This snake harbours a mitochondrial haplotype of lineage C combined with a microsatellite assignment to cluster E-ML. However, there are two further snakes with mito-nuclear discordance resulting from hybridization of *N. helvetica* with the alien *N. n. moreotica* in the region of Lausanne. These two snakes are having predominantly *N. natrix* genotypes combined with mitochondrial haplotypes of *N. helvetica* (lineage C; Suppl. material 1: table S1).

Genetic differentiation ($F_{ST}$) values are similar between clusters, except for the slightly lower values for E-GE/E-ML and for E-ML/*natrix*, whereas the highest value was observed between C-VS/E-GE (Suppl. material 1: table S3).

## Morphology

For morphological and landmark analyses, snakes representing the clusters E-ML and E-GE were merged in one cluster E, while C-VS and C-TI were kept separate. C-VS and C-TI are geographically divided by mountainous regions difficult to cross for grass snakes, whereas E-ML and E-GE are in contact and admixing. Additionally, the number of samples for E-GE is very limited.

Mahalanobis and Procrustes permutation tests revealed significant morphological differences between all clusters (Table 1). However, Fig. 2 shows that there is always some overlap among all clusters, except for the lateral landmarks, where *N. natrix* was distinct. Also, there are no obvious shape differences visible in the wireframe graphs (Suppl. material 1: figs S3, S4).

Shape PCA and standard PCAs show no differentiation of mtDNA lineages E, C-VS and C-TI of *N. helvetica* (Fig. 3). Only *N. natrix* is slightly distinct because

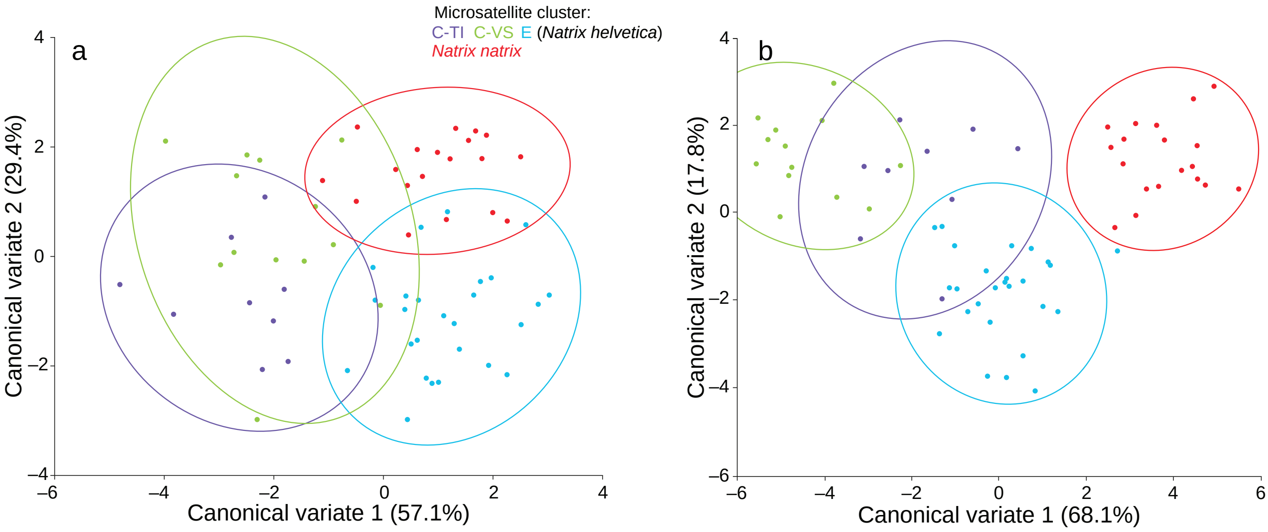

**Figure 2.** Canonical Variate Analysis (CVA) of dorsal (**a**) and lateral (**b**) landmark coordinates for grass snakes assigned to the microsatellite clusters of *Natrix helvetica* (E, C-VS, C-TI) and *N. natrix* (*N. n. vulgaris*, mtDNA lineage 3, from northeastern Switzerland). Only individuals with a genotypic cluster assignment ≥ 80% are included; circles represent 95% confidence ellipses.

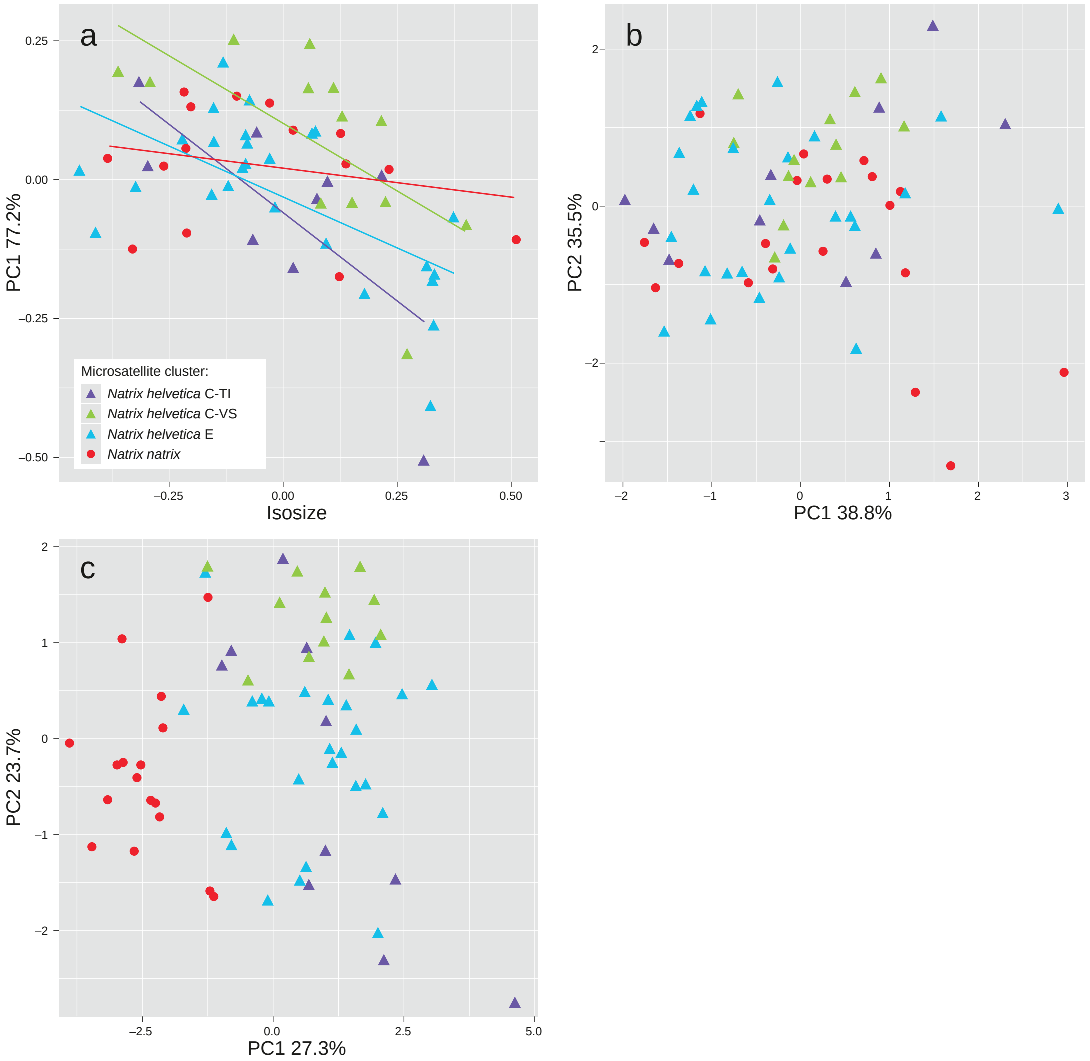

**Figure 3.** Shape PCA of distance measurements (**a**), standard PCA of scale counts (**b**) and standard PCA of colour marking measurements (**c**) for grass snakes assigned to the microsatellite clusters of *Natrix helvetica* (C-TI, C-VS, E) and *N. natrix* (*N. n. vulgaris*, mtDNA lineage 3, from northeastern Switzerland). Only individuals with a genotypic cluster assignment ≥ 80% are included.

of smaller and differently shaped markings. Similar results are obtained for the linear discriminant analysis. *Natrix natrix* also represents here the most distinct cluster with a percentage of 86.7% of correctly allocated individuals. For all other clusters, the percentages are below 70% (Suppl. material 1: table S4). Mean values and standard deviations of each morphological trait are summarized for the two *N. helvetica* subspecies in Suppl. material 1: table S5.

## Discussion

After the discovery of two putatively alien mtDNA lineages of grass snake around Lausanne (lineages C and 7 of Kindler et al. 2013), concerns were raised about genetic pollution of native populations of *Natrix helvetica* (Dubey et al. 2017). It was clear that the common grass snakes harbouring mtDNA lineage 7, now identified with the subspecies *N. natrix moreotica* (see Asztalos et al. 2021b), are allochthonous and originate from the former Vivarium at Lausanne. However, for the other mitochondrial lineage (C), typical for

**Table 1.** Statistical test results of Canonical Variate Analysis (CVA) of lateral and dorsal landmarks (Fig. 2) using 10,000 permutations for each test. E, C-VS and C-TI represent *Natrix helvetica* clusters derived from microsatellite analyses (Fig. 1); *natrix* refers to samples from northeastern Switzerland (*N. n. vulgaris*, mtDNA lineage 3).

| **Lateral landmarks** | | | | | | | |
|---|---|---|---|---|---|---|---|
| **Mahalanobis distances among groups** | | | | **Procrustes distances among groups** | | | |
| | *natrix* | E | C-VS | | *natrix* | E | C-VS |
| E | 4.8305 | | | E | 0.0308 | | |
| C-VS | 8.2776 | 5.6166 | | C-VS | 0.0380 | 0.0285 | |
| C-TI | 6.5247 | 4.5882 | 5.2595 | C-TI | 0.0431 | 0.0324 | 0.0237 |
| **P values from permutation tests** | | | | **P values from permutation tests** | | | |
| | *natrix* | E | C-VS | | *natrix* | E | C-VS |
| E | < 0.001 | | | E | < 0.001 | | |
| C-VS | < 0.001 | < 0.001 | | C-VS | < 0.001 | < 0.001 | |
| C-TI | < 0.001 | < 0.001 | < 0.001 | C-TI | < 0.001 | < 0.001 | 0.0783 |
| **Dorsal landmarks** | | | | | | | |
| **Mahalanobis distances among groups** | | | | **Procrustes distances among groups** | | | |
| | *natrix* | E | C-VS | | *natrix* | E | C-VS |
| E | 2.7561 | | | E | 0.0232 | | |
| C-VS | 3.5488 | 3.7053 | | C-VS | 0.0236 | 0.0268 | |
| C-TI | 4.4217 | 4.1624 | 2.9620 | C-TI | 0.0375 | 0.0389 | 0.0264 |
| **P values from permutation tests** | | | | **P values from permutation tests** | | | |
| | *natrix* | E | C-VS | | *natrix* | E | C-VS |
| E | < 0.001 | | | E | < 0.001 | | |
| C-VS | < 0.001 | < 0.001 | | C-VS | < 0.001 | < 0.001 | |
| C-TI | < 0.001 | < 0.001 | < 0.001 | C-TI | < 0.001 | < 0.05 | < 0.001 |

Alpine representatives of *N. helvetica sicula* (Schultze et al. 2020; Asztalos et al. 2021a), there remained the possibility of a natural occurrence. Dubey et al. (2017) also assumed that grass snakes with clade C had escaped from the Vivarium in the 1970s, together with the ancestors of what is now called *N. n. moreotica* (in Dubey et al. 2017, the inappropriate name *N. n. persa* is still used; see Asztalos et al. 2021b). However, the Alpine lineage of *N. n. sicula* is widely distributed in northern Italy, including the Alps, and its range extends northwards across the Alps to Tyrol and southernmost Bavaria (Glaw et al. 2019; Schultze et al. 2020; Asztalos et al. 2021a; Neumann et al. 2024). Until recently, only two records for *N. n. sicula* from Switzerland were published, one from Ticino and the other from beyond the Simplon Pass (Niedergesteln, Valais; Kindler and Fritz 2018; Schultze et al. 2020). Yet, these records and the wide Alpine distribution of *N. h. sicula* suggest that this subspecies could not only occur naturally in Switzerland, but that it has a much wider distribution than previously thought. This is supported by our present investigation.

Our study shows that *N. h. sicula* is widely distributed in the cantons of Ticino and Valais and ranges to the canton of Vaud, along Lake Geneva, where it hybridizes with *N. h. helvetica*, as evidenced by microsatellite genotypes. Therefore, *N. h. sicula* should no longer be considered as non-native around Lausanne, as supposed by Dubey et al. (2017) for the records of mtDNA lineage C there.

The two microsatellite clusters of *N. h. helvetica* and *N. h. sicula* correspond to local population structure. It is possible that our cluster E-GE (Fig. 1b) matches the southern cluster revealed by Asztalos et al. (2020), who also identified two distinct clusters for *N. h. helvetica*. Their southern cluster from France could reach upstream in the Rhone Valley to Lake Geneva, whereas our cluster E-ML could match the northern cluster of Asztalos et al. (2020). However, the sample from Geneva in Asztalos et al. (2020) was also assigned to the northern group and the differentiation of the cluster E-GE could instead also be related to a local effect (isolation by distance) and the tendency of STRUCTURE to cluster samples with similar ancestry. In contrast, until now, no substructure has been described for Alpine *N. h. sicula*, but the distribution pattern of our two clusters C-VS and C-TI makes sense biogeographically. Each cluster matches another drainage system (Alpine Rhone Valley vs. Po drainage).

North of Lake Geneva, we were not only able to detect the natural contact and hybridization zone of the two subspecies of *N. helvetica*. Our microsatellite data (Fig. 1b; Suppl. material 1: table S1) also confirm genetic pollution of *N. helvetica* from alien *N. n. moreotica*. Nature conservation should take action to prevent wider introgression of alien genes in this region. Non-native snakes and their hybrids should be removed before they further compromise the genetic identity of the native populations of *N. helvetica*, which is currently classified as “endangered” in the most recent Swiss Red List of Reptiles (BAFU & info fauna 2023).

The distribution and hybrid zone of *N. h. helvetica* and *N. h. sicula* in Switzerland can be explained in a biogeographical context. Kindler et al. (2018b) suggested that the nominotypical subspecies survived the last glaciation in southern France, from where it expanded its range to more northern regions during the Holocene warming. *Natrix helvetica sicula*, on the other hand, was inferred to have survived the last glaciation in a distinct ‘microrefugium’ in northeastern Italy (Kindler et al. 2013; Schultze et al. 2020), but it was impossible to endure in the Alpine Rhone Valley, which was completely covered by ice during the Late Glacial Maximum (Seguinot et al. 2018). As a consequence of the Holocene warming, *N. h. sicula* crossed the main Alpine chain not only in the east to Tyrol and southern Bavaria (Glaw et al. 2019; Asztalos et al. 2021a), but also in the west, as we know now. There, it established a secondary contact and hybrid zone with *N. h. helvetica* along Lake Geneva. This scenario implies transalpine dispersal at altitudes of about 2000–2200 m a.s.l., i.e., at altitudes that were only very recently colonized by the species (database of info fauna – karch, which hosts more than 25,000 records for grass snakes in Switzerland and is the national reference centre for Swiss amphibians and reptiles). Thus, it can be speculated that *N. h. sicula* crossed the western Alps during a Holocene period, which was at least as warm as present, probably via the Simplon Pass (approx. 2000 m a.s.l.).

In this context, two other northern records of grass snakes with lineage C are difficult to interpret (Langnau im Emmental, canton Bern, and Muotathal, canton Schwyz, directly at the border to canton Uri). For the snake from Muotathal no genotype is available, but the snake from Langnau im Emmental is, according to its microsatellite genotype, a pure representative of the cluster E-ML. Also, two other snakes from the canton Bern have an admixed genotype (Fig. 1; Suppl. material 1: table S1), suggesting that some *N. h. sicula* left indeed their genetic footprint there. It is well known that grass snakes are spread with building material, etc. or have been voluntarily moved (e.g., Ahnelt et al. 2021; Asztalos et al. 2021c), so these northern records are not necessarily evidence for wide-reaching natural dispersal and introgression across the Alps.

In contrast to genetic data, our morphological analyses revealed only a weak differentiation among the studied grass snakes. Only the two species *N. helvetica* and *N. natrix* could be morphologically discriminated with some confidence, while the used traits were not helpful in discriminating the two subspecies of individual genetic clusters within *N. helvetica*. This does not contradict the validity of the involved two subspecies because morphological traits that can be distinguished by humans are neither necessarily biologically relevant nor a prerequisite for taxonomic distinctness (compare, for instance, Kindler and Fritz 2018; Dufresnes et al. 2023, 2024). Also, we could have missed some relevant traits in coloration and pattern that were only recently highlighted (Fritz et al. 2023). According to these authors, some individuals of *N. h. sicula* show a "spotted" colour pattern that never occurs in the nominotypical subspecies. It cannot be excluded that further traits exist that help to identify the different subspecies even in the field, but it remains a challenge to disentangle this situation.

## Acknowledgements

We thank M. Chèvre for advice, data, photos and his lab protocols and V. Zwahlen for assistance with processing microsatellites. Special thanks go to all researchers and institutions that provided samples: M. Chèvre, S. Dubey, E. Gallice, T. Gil, G. Meier, B. Meister, D. Muri, the Musée de la nature Sion (S. Gerber), the Museo cantonale di storia naturale Lugano (N. Zambelli), and the Naturhistorisches Museum Bern (R. Hagmann). We thank all authorities of the cantons of Vaud, Valais and Ticino for the necessary permits. The figures were enhanced by M. H. Fischer. An anonymous reviewer, P. Mikulíček and the editor R. Jadin provided helpful comments on the manuscript.

## Additional information

### Conflict of interest

The authors have declared that no competing interests exist.

### Ethical statement

Captures in the wild were conducted according to the local authorities' requirements (veterinary authorisation number GR_2013_15kü).

### Funding

This study was funded by the Swiss Bundesamt für Umwelt (BAFU).

### Author contributions

Conceptualization: SU. Data curation: AS, SU. Formal analysis: AS, HB. Funding acquisition: SU. Investigation: AS. Methodology: SU. Project administration: SU. Resources: HB, STH. Supervision: SU. Visualization: AS, UF. Writing – original draft: AS, UF. Writing – review and editing: AS, HB, STH, SU, UF.

## Author ORCIDs

Hannes Baur https://orcid.org/0000-0003-1360-3487
Stefan T. Hertwig https://orcid.org/0000-0003-1617-8180
Uwe Fritz https://orcid.org/0000-0002-6740-7214
Sylvain Ursenbacher https://orcid.org/0000-0001-5093-6403

## Data availability

All data that support the findings of this study are available in the main text or the Suppl. material. No new haplotypes were identified in the present study, which is why no sequences were uploaded to the European Nucleotide Archive (ENA).

## References

Adams DC, Collyer ML, Kaliontzopoulou A (2019) Geomorph: Software for geometric morphometric analyses. R package version 3.1.0. https://cran.r-project.org/package=geomorph

Ahnelt H, Romanova T, Klinge A, Böhme W, Fritz U, Asztalos M (2021) The common grass snake (*Natrix natrix*) on Sylt: Human-mediated colonization of a North Sea island. Salamandra 57: 285–290.

Asztalos M, Ayaz D, Bayrakcı Y, Afsar M, Tok CV, Kindler C, Jablonski D, Fritz U (2021b) It takes two to tango – Phylogeography, taxonomy and hybridization in grass snakes and dice snakes (Serpentes: Natricidae: *Natrix natrix*, *N. tessellata*). Vertebrate Zoology 71: 813–834. https://doi.org/10.3897/vz.71.e76453

Asztalos M, Glaw F, Franzen M, Kindler C, Fritz U (2021a) Transalpine dispersal: Italian barred grass snakes in southernmost Bavaria – This far but no further! Journal of Zoological Systematics and Evolutionary Research 59: 1136–1148. https://doi.org/10.1111/jzs.12471

Asztalos M, Schultze N, Ihlow F, Geniez P, Berroneau M, Delmas C, Guiller G, Legentilhomme J, Kindler C, Fritz U (2020) How often do they do it? An in-depth analysis of the hybrid zone of two grass snake species (*Natrix astreptophora* and *Natrix helvetica*). Biological Journal of the Linnean Society 131: 756–773. https://doi.org/10.1093/biolinnean/blaa152

Asztalos M, Wielstra B, Struijk RPJH, Ayaz D, Fritz U (2021c) Aliens in the Netherlands: Local genetic pollution of barred grass snakes (Squamata: Serpentes: Natricidae). Salamandra 57: 173–179.

BAFU & info fauna (2023) Rote Liste der Reptilien. Gefährdete Arten der Schweiz. Bundesamt für Umwelt BAFU, Bern, 32 pp.

Baur H (2024) Morphometric methods for species recognition. In: Heraty JM, Woolley JB (Eds) Chalcidoidea of the World. CABI Press, Oxford, in press.

Baur H, Kranz-Baltensperger Y, Cruaud A, Rasplus J-Y, Timokhov AV, Gokhman VE (2014) Morphometric analysis and taxonomic revision of *Anisopteromalus ruschka* (Hymenoptera: Chalcidoidea: Pteromalidae) – An integrative approach. Systematic Entomology 39: 691–709. https://doi.org/10.1111/syen.12081

Baur H, Leuenberger C (2011) Analysis of ratios in multivariate morphometry. Systematic Biology 60: 813–825. https://doi.org/10.1093/sysbio/syr061

Chèvre M (2015) The contact zone of the grass snake (*Natrix natrix*) in Switzerland. Master thesis, Université de Neuchâtel, Neuchâtel, 97 pp.

Dubey S, Ursenbacher S, Schuerch J, Golay J, Aubert P, Dufresnes C (2017) A glitch in the *Natrix*: Cryptic presence of alien grass snakes in Switzerland. Herpetology Notes 10: 205–208.

Dufresnes C, Ambu J, Galán P, Sequeira F, Viesca L, Choda M, Álvaret D, Alar B, Suchan T, Künzel S, Martínez-Solano I, Vences M, Nicieza A (2024) Delimiting phylogeographic diversity in the genomic era: Application to an Iberian endemic frog. Zoological Journal of the Linnean Society: zlad170. https://doi.org/10.1093/zoolinnean/zlad170

Dufresnes C, Poyarkov N, Jablonski D (2023) Acknowledging more biodiversity without more species. Proceedings of the National Academy of Sciences of the United States of America 120: e2302424120. https://doi.org/10.1073/pnas.2302424120

Earl DA, vonHoldt BM (2012) STRUCTURE HARVESTER: A website and program for visualizing structure output and implementing the Evanno method. Conservation Genetics Resources 4: 359–361. https://doi.org/10.1007/s12686-011-9548-7

Evanno G, Regnaut S, Goudet J (2005) Detecting the number of clusters of individuals using the software STRUCTURE: A simulation study. Molecular Ecology 14: 2611–2620. https://doi.org/10.1111/j.1365-294X.2005.02553.x

Fritz U, Grismer LL, Asztalos M (2023) Hybrid zones of *Natrix helvetica* and *N. natrix*: Phenotype data from iNaturalist and genetics reveal concordant clines and the value of species-diagnostic morphological traits. Vertebrate Zoology 73: 383–395. https://doi.org/10.3897/vz.73.e103319

Fritz U, Schmidtler JF (2020) The Fifth Labour of Heracles: Cleaning the Linnean stable of names for grass snakes (*Natrix astreptophora*, *N. helvetica*, *N. natrix* sensu stricto). Vertebrate Zoology 70: 621–665. https://doi.org/10.26049/vz70-4-2020-07

Gebiola M, Monti MM, Johnson RC, Woolley JB, Hunter MS, Giorgini M, Pedata PA (2017) A revision of the *Encarsia pergandiella* species complex (Hymenoptera: Aphelinidae) shows cryptic diversity in parasitoids of whitefly pests. Systematic Entomology 42: 31–59. https://doi.org/10.1111/syen.12187

Glaw F, Franzen M, Oefele M, Hansbauer G, Kindler C (2019) Genetischer Erstnachweis, Verbreitung und südalpine Herkunft der Barrenringelnatter (*Natrix helvetica* spp.) in Bayern. Zeitschrift für Feldherpetologie 26: 1–20.

Goudet J (1995) FSTAT (Version 1.2): A computer program to calculate F-statistics. Journal of Heredity 86: 485–486. https://doi.org/10.1093/oxfordjournals.jhered.a111627

Huber C, Baur H (2016) *Nebria* (*Patrobonebria*) *incognita* n. sp. and *Nebria* (*P.*) *hiekeiana* n. sp., two new species from the Western Himalaya, with remarks on *Nebria* (*P.*) *desgodinsi* (Coleoptera, Carabidae, Nebriinae). Entomologische Blätter und Coleoptera 112: 203–214.

Kabisch K (1999) *Natrix natrix* (Linnaeus, 1758) – Ringelnatter. In: Böhme W (Ed.) Handbuch der Reptilien und Amphibien Europas. Band 3/IIA: Schlangen II. Aula-Verlag, Wiebelsheim, 513–580.

Kindler C, Böhme W, Corti C, Gvoždík V, Jablonski D, Jandzik D, Metallinou M, Široký P, Fritz U (2013) Mitochondrial phylogeography, contact zones and taxonomy of grass snakes (*Natrix natrix*, *N. megalocephala*). Zoologica Scripta 42: 458–472. https://doi.org/10.1111/zsc.12018

Kindler C, Chèvre M, Ursenbacher S, Böhme W, Hille A, Jablonski D, Vamberger M, Fritz U (2017) Hybridization patterns in two contact zones of grass snakes reveal a new Central European snake species. Scientific Reports 7: 7378. https://doi.org/10.1038/s41598-017-07847-9

Kindler C, de Pous P, Carranza S, Beddek M, Geniez P, Fritz U (2018a) Phylogeography of the Ibero-Maghrebian red-eyed grass snake (*Natrix astreptophora*). Organisms, Diversity & Evolution 18: 143–150. https://doi.org/10.1007/s13127-017-0354-2

Kindler C, Fritz U (2018) Phylogeography and taxonomy of the barred grass snake (*Natrix helvetica*), with a discussion of the subspecies category in zoology. Vertebrate Zoology 68: 269–281. https://doi.org/10.3897/vz.68.e31615

Kindler C, Graciá E, Fritz U (2018b) Extra-Mediterranean glacial refuges in barred and common grass snakes (*Natrix helvetica*, *N. natrix*). Scientific Reports 8: 1821. https://doi.org/10.1038/s41598-018-20218-2

Klingenberg CP (2011) MORPHOJ: An integrated software package for geometric morphometrics. Molecular Ecology Resources 11: 353–357. https://doi.org/10.1111/j.1755-0998.2010.02924.x

Klingenberg CP (2013) Visualizations in geometric morphometrics: How to read and how to make graphs showing shape changes. Hystrix 24: 15–24. https://doi.org/10.4404/hystrix-24.1-7691

László Z, Baur H, Tótmérész B (2013) Multivariate ratio analysis reveals *Trigonoderus pedicellaris* Thomson (Hymenoptera, Chalcidoidea, Pteromalidae) as a valid species. Systematic Entomology 38: 753–762. https://doi.org/10.1111/syen.12026

Neumann A, Asztalos M, Fritz U, Glaw F (2024) A spotlight on the hybrid zone of grass snakes (*Natrix helvetica sicula* and *Natrix natrix*) in southern Bavaria – the Prien Valley. Salamandra 60: 17–28.

Pokrant F, Kindler C, Ivanov M, Cheylan M, Geniez P, Böhme W, Fritz U (2016) Integrative taxonomy provides evidence for the species status of the Ibero-Maghrebian grass snake *Natrix astreptophora*. Biological Journal of the Linnean Society 118: 873–888. https://doi.org/10.1111/bij.12782

Pritchard JK, Stephens M, Donnelly P (2000) Inference of population structure using multilocus genotype data. Genetics 155: 945–959. https://doi.org/10.1093/genetics/155.2.945

Pritchard JK, Wen W (2002) Documentation for STRUCTURE Software: Version 2. University of Chicago Press, Chicago, IL, 29 pp.

R Core Team (2017) R: A language and environment for statistical computing. R Foundation for Statistical Computing, Vienna. https://www.R-project.org/

Rohlf FJ (2013) TPSUtility program, version 1.56. Department of Ecology and Evolution, State University of New York, Stony Brook, NY.

Rohlf FJ (2017) TPSDig2, version 2.30. Department of Ecology and Evolution, State University of New York, Stony Brook, NY.

Schultze N, Spitzweg C, Corti C, Delaugerre M, Di Nicola MR, Geniez P, Lapini L, Liuzzi C, Lunghi E, Novarini N, Picariello O, Razzetti E, Sperone E, Stellati L, Vignoli L, Asztalos M, Kindler C, Fritz U (2020) Mitochondrial ghost lineages blur phylogeography and taxonomy of *Natrix helvetica* and *N. natrix* in Italy and Corsica. Zoologica Scripta 49: 395–411. https://doi.org/10.1111/zsc.12417

Seguinot J, Ivy-Ochs S, Jouvet G, Huss M, Funk M, Preusser F (2018) Modelling last glacial cycle ice dynamics in the Alps. Cryosphere 12: 3265–3285. https://doi.org/10.5194/tc-12-3265-2018

Sidlauskas BL, Mol JH, Vari RP (2011) Dealing with allometry in linear and geometric morphometrics: A taxonomic case study in the *Leporinus cylindriformis* group Characiformes: Anostomidae) with description of a new species from Suriname. Zoological Journal of the Linnean Society 162: 103–130. https://doi.org/10.1111/j.1096-3642.2010.00677.x

Thorpe RS (1979) Multivariate analysis of the population systematics of the ringed snake, *Natrix natrix* (L). Proceedings of the Royal Society of Edinburgh 78B: 1–62. https://doi.org/10.1017/S026972700001294X

van Buuren S, Groothuis-Oudshoorn K (2011) mice: Multivariate imputation by chained equations in R. Journal of Statistical Software 45: 1–67. https://doi.org/10.18637/jss.v045.i03

van Riemsdijk I, Struijk RPJH, Pel E, Janssen IAW, Wielstra B (2020) Hybridisation complicates the conservation of *Natrix* snakes in the Netherlands. Salamandra 56: 78–82.

Venables WN, Ripley BD (2002) Modern Applied Statistics with S. Fourth Edition. Springer, New York, NY, 497 pp. https://doi.org/10.1007/978-0-387-21706-2

Waser LE, Schweizer M, Haas A, Hertwig ST (2017) From a lost world: An integrative phylogenetic analysis of *Ansonia* Stoliczka, 1870 (Lissamphibia: Anura: Bufonidae), with the description of a new species. Organisms Diversity & Evolution 17: 287–303. https://doi.org/10.1007/s13127-016-0294-2

## Supplementary material 1

### Supplementary information

Authors: Andreas Schild, Hannes Baur, Stefan T. Hertwig, Uwe Fritz, Sylvain Ursenbacher

Data type: docx

Explanation note: **fig. S1.** Landmark positions. **fig. S2.** STRUCTURE HARVESTER results indicating the optimal number of microsatellite clusters (K). **fig. S3.** Wireframe graph showing shape changes along the canonical variate 1 (CV1) for dorsal landmarks. **fig. S4.** Wireframe graph showing the shape changes along the canonical variate 1 (CV1) for lateral landmarks. **table S2.** Morphological variables measured. Illustrations from Chèvre (2015). **table S3.** Pairwise *FST* values between microsatellite clusters of *Natrix helvetica* (E-GE, E-ML, C-VS and C-TI) and *N. natrix*. **table S4.** Morphological assignment of specimens (horizontal rows) to microsatellite clusters of *Natrix natrix* and *N. helvetica* (E, C-VS, C-TI, vertical columns) based on all morphological variables using a Linear Discriminant Analysis (LDA). **table S5.** Mean and standard deviation (SD) of different morphological traits for Swiss barred grass snakes (*Natrix helvetica*).

Link: https://doi.org/10.3897/zookeys.1205.123911.suppl1

ZooKeys 1205: 239–251 (2024)
DOI: 10.3897/zookeys.1205.127164

Research Article

# Taxonomic notes on the collection of the tribe Lamiini (Coleoptera, Cerambycidae) housed in the Natural History Museum, London

Guanglin Xie[1,2], Maxwell V. L. Barclay[2], Wenkai Wang[3]

1 *Institute of Entomology, College of Agriculture, Yangtze University, Jingzhou, Hubei, 434025, China*
2 *Department of Life Sciences, Natural History Museum, London, SW7 5BD, UK*
3 *Hubei Engineering Research Center for Pest Forewarning and Management, Yangtze University, Jingzhou, Hubei, 434025, China*
*Corresponding authors: Maxwell V. L. Barclay (m.barclay@nhm.ac.uk); Wenkai Wang (wwk@yangtzeu.edu.cn)*

## Abstract

In the present paper, the genus *Mimomyagrus* Breuning, 1970 is synonymized with *Combe* Thomson, 1864, and *Mimomyagrus pfanneri* Breuning, 1970 is considered a junior synonym of *Combe brianus* (White, 1858). The female of *Arctolamia sinica* Bi & Chen, 2022 is described for the first time and this species is reported as new to Myanmar. Type material of *Lamia punctator* Fabricius, 1776 [= *Anoplophora chinensis* (Forster, 1771)], *Cerambyx galloprovincialis* Olivier, 1800 [= *Monochamus galloprovincialis* (Olivier, 1800)] and *Melanauster granulipennis* Breuning, 1938 [= *Monochamus guerryi* Pic, 1903] are confirmed to be preserved in Natural History Museum, London.

**Key words:** Lamiinae, longhorned beetles, new synonym, taxonomy, type material, zoological collections

**Academic editor:** Francesco Vitali
**Received:** 9 May 2024
**Accepted:** 9 June 2024
**Published:** 26 June 2024

**ZooBank:** https://zoobank.org/BFCBF680-68CB-4E0A-A009-23256BE5DDD0

**Citation:** Xie G, Barclay MVL, Wang W (2024) Taxonomic notes on the collection of the tribe Lamiini (Coleoptera, Cerambycidae) housed in the Natural History Museum, London. ZooKeys 1205: 239–251. https://doi.org/10.3897/zookeys.1205.127164

## Introduction

As one of the largest natural history museums, the Natural History Museum, London [formerly British Museum, Natural History (BMNH), and hereafter NHMUK] houses abundant specimens of longhorn beetles from all over the world.

The first author had an opportunity to visit the NHMUK in 2022, and carried out research related to Cerambycidae for one year under the direction of the second author, Maxwell V. L. Barclay, the Senior Curator in Charge of Coleoptera at the NHMUK; the current paper is part of the research findings, together with four other separately published papers.

On the basis of the study of specimens of the tribe Lamiini preserved in the NHMUK, we propose a genus-level and a species-level new synonymy and confirm that the type material of three species, considered to be ‘lost’ and marked as ‘depositary not known’ (Tavakilian and Chevillotte 2023), are in fact deposited in the NHMUK.

## Material and methods

The material examined in this study is deposited in the NHMUK, and has already been identified by earlier specialists, except for the holotypes of *Combe fulgurata* Thomson, 1864, *Mimomyagrus pfanneri* Breuning, 1970 and *Combe brianus* m. *rufoantennatus* Breuning, 1954 used for comparison in this study, which are deposited in the Muséum national d'Histoire naturelle, Paris, Muséum cantonal des sciences naturelles, Lausanne and Royal Belgian Institute of natural sciences, Brussels, respectively.

The label text, which is reproduced verbatim without corrections or additions, is given in single quotation marks for all studied specimens. Individual labels are separated by a semicolon, and data on different rows by a single slash. Additional and explanatory comments by the authors are given in square brackets.

Photographs were taken using a Canon 7D Mark II DSLR camera with a Canon EFS 100 mm lens and edited using Adobe Photoshop 2020 release. Extended depth of field at magnifications was achieved by combining multiple images from a range of focal planes using Combine ZP or Helicon Focus software.

## Results

Based on our study on the tribe Lamiini preserved in the NHMUK, one genus-level synonym and one species-level synonym have been found, the female of one species is newly described with a new distribution record, and the type material of three species previously thought to be lost, has been confirmed to be preserved in the NHMUK. The details are as follows:

### Genus *Combe* Thomson, 1864

*Combe* Thomson, 1864: 83; Pascoe 1866: 252; Lacordaire 1869: 344; Gemminger and Harold 1873: 3028; Aurivillius 1921: 119; Breuning 1961: 347. Type species:*Combe fulgurata* Thomson, 1864 [= *Combe brianus* (White, 1858)].

*Mimomyagrus* Breuning, 1970: 88. Type species: *Mimomyagrus pfanneri* Breuning, 1970. Syn. nov.

### ***Combe brianus*** **(White, 1858)**

Figs 1–3

*Monohammus brianus* White, 1858: 409. Type locality: Nepal.

*Combe Fulgurata* [sic] Thomson, 1864: 83. Type locality: unspecified.

*Combe Brianus* [sic]: Pascoe 1866: 244; Lacordaire 1869: 344; Gemminger and Harold 1873: 3028; Aurivillius 1921: 119.

*Combe brianus*: Breuning 1961: 347; Weigel 2006: 502; Barševskis 2018: 288, 2020: 178.

*Combe brianus* m. *rufoantennatus* Breuning, 1954: 7; 1961: 347. Type locality: Sumatra, Indonesia. Unavailable name.

*Mimomyagrus pfanneri* Breuning, 1970: 88. Type locality: Cameron highlands, Malaysia. Syn. nov.

**Type material examined.** ***Holotype*** of *Monohammus brianus* White, 1858, female: 'Type [p, label circular, red frame]; Brianus / n. o [h]; Mon. Brianus White / Nepal [h]; NHMUK013460997 [p]'; ***holotype*** of *Combe fulgurata* Thomson, 1864, female: 'HOLOTYPE [p, label rectangular, red]; Th. / TYPE [p, black frame]; Ex. Musaeo / JAMES THOMSON [p, black frame]; Ch. J. Gahan / vidit 1895. [p]; Combe / Brianus White / comp. with type / C. J. G. [h]; Brianus / White / Fulguratus / Type Thoms. / Malas. [h, label rectangular, red frame]; Muséum Paris / 1952 / coll. R. Oberthür [p]; HOLOTYPE / *Combe* / *fulgurata* Thomson, 1864 [p]; MNHN, Paris / EC23123 [p]'; ***holotype*** of *Combe brianus* m. *rufoantennatus* Breuning, 1954, female: 'Holotype [p, label rectangular, red, black frame]; Solok / Sumatra / EX COLL. F. SCHNEIDER [p, black frame]; Coll. R. I. Sc. N. B. / Sumatra [p]; S. Breuning det., 195

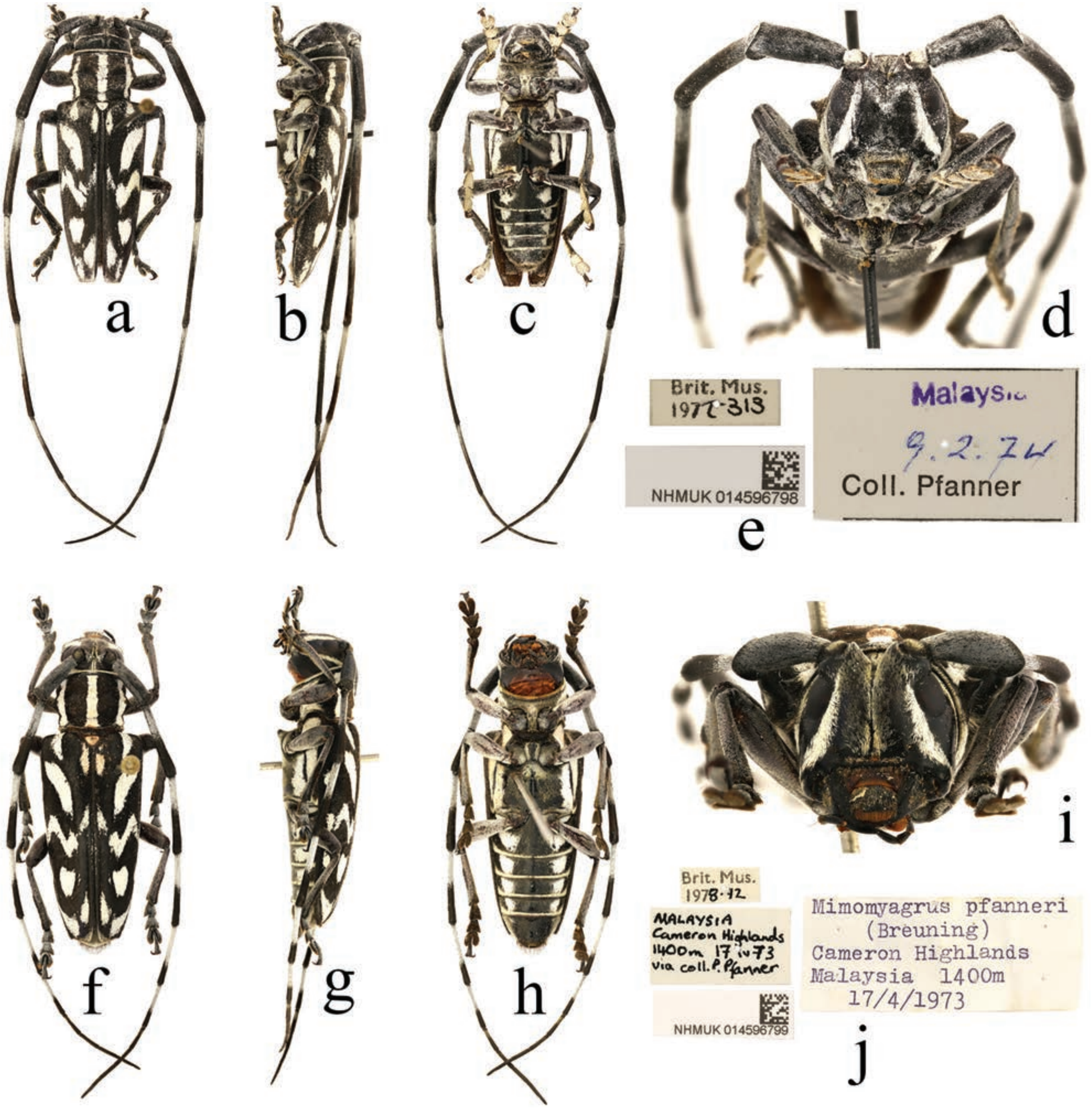

Brit. Mus.
197Ꞇ-313

NHMUK 014596798

Malaysia
9.2.74
Coll. Pfanner

Brit. Mus.
1978-12

MALAYSIA
Cameron Highlands
1400m 17 iv73
via coll. P. Pfanner

NHMUK 014596799

Mimomyagrus pfanneri
(Breuning)
Cameron Highlands
Malaysia 1400m
17/4/1973

**Figure 1.** Habitus of *Combe brianus* (White, 1858) **a–d** male **f–i** female **e, j** labels.

[p] 4 [h] / Combe / brianus / rufoantennatus / mihi Typ [h]; L: Bull. Inst. r. sci. Nat. Belg. 1954, 30, 11: F. [h]'; ***holotype*** of *Mimomyagrus pfanneri* Breuning, 1970, female: 'TYPE [p,label rectangular, red]; Rég. Orientale / Malaisie [h] / Chassot [p] 7. 1968 [h]; GBIFCH / 00338292 [p]'; ***paratype*** of *Mimomyagrus pfanneri* Breuning, 1970, female: 'Para- / type [p, label circular, yellow frame]; PARATYPE [p, label rectangular, red]; Brit. Mus. / 19 [p] 77–313 [h]; Malaysia [p] / Cameron / h'lds iv/74 [h] / Coll. Pfanner [p]; *Mimomyagrus pfanneri* Breuning [h]'.

**Non-type material examined.** Thirteen specimens (5 males, 8 females) identified as '*Combe brianus*' in NHMUK: Malaysia: 1 male: 'MALAY PENIN: / Selangor. / Bukit Kutu / 3500 [h] ft. / 14 . 3. [h] 1931 [1 with handwriting] / H. M. Pendlebury. [p]; Ex Coll: / F. M. S. / Museum. [p, reverse side]; Ex F. M. S. Museum. B. M. 1955–354 [p, reverse side]] / NHMUK013461006 [p]'; 1 male: 'Mal. / P. [h]; Pascoe / Coll. / 93–60 [p]; Combe / brianus / White [h, reverse side]; NHMUK013460999 [p]'; 1 male: 'Penang [h, label circle]; Bowring. / 63. 47* [p] / Combe / brianus, White [h]; NHMUK013461002'; 1 male: 'MALAY PENIN. / Kedah Perak. / 1000–2000 [h] ft. / 19 # March, 1928. [p]; Ex F. M. S. / Museum. / B. M. 1955–354 [p]; NHMUK 013461004 [p]'; 1 male: 'MALAY PENIN [p] / Perak, F. M. S. / Maxwell Hill 3000 / June–July 1916 [h]; 332 [h]; Ex F. M. S. / Museum. / B. M. 1955–354. [p]; NHMUK013387052 [p]'; 1 female: 'Rantau Panjang / Selangor. / H. C. Robinson. [p] / (12. 16 / V / 04) [h] / 1904–327.[p]; (4 / 1107)[p]; NHMUK013387035 [p]'; 1 female: 'Malay / Penang [p]; Fry Coll. / 1905. 100. [p]; 17783 [h]; NHMUK013460998 [p]'; 1 female: 'MALAY PENIN: [p] / Penang F. M. S. / Maxwell Hill 3000 / June–July 1916 [h]; 331 [h]; Ex F. M. S. / Museum. / B. M. 1955–354. [p]; Combe / Brianus, White / 2 [h]; NHMUK013387050 [p]'; 1 female: 'Malay Penin / Panang, F. M. S. [p] j, / Gap / 2900 / May 1915 [h] 193 [p]2 [h] ; Ex F. M. S. / Museum. / B. M. 1955–354 [p]; NHMUK 013461000 [p]'; 1 female: 'Malay / Penang [p]; Data unreliable / See Brit. Mus. / 1949–314. [p, label yellow]; Combe / brianus [h]; NHMUK013461003 [p]'; 1 female: 'Malay / Penang / Batu Feringgi / catchment area [p] / 25 Aug 1963 [h] / H. T. Pagden; Pres by / Com Inst Ent / B. M. 1964-2 [p]; 119 [p]; Combe / brianus White [h] / E. A. J. Duffy det. 1964 [p]; NHMUK013461001 [p]'; 1 female: 'MALAYA / Kuala Lumpur [p]/ Ampang Village [h] / Feb. 26th[h]19[p]35[h]; Ex F. M. S. / Museum. / B. M. 1955–354 [p]; NHMUK 013387047 [p]';1 female: 'MALAY PENIN: / Selangor. / Bukit Kutu / 3300–3500 [h] ft. / 14 . 3. [h] 1931. / H. M. Pendlebury. [p]; Ex Coll: / F. M. S. / Museum. [p, reverse side]; Ex F. M. S. Museum. M. 1955–354 [p, reverse side]; NHMUK013461005 [p]'.

Two specimens (1 male, 1 female) identified as '*Mimomyagrus pfanneri* Breuning, 1970' in NHMUK: Malaysia: 1 male (Fig. 1a–e): 'Malaysia [p] / 9. 2. 74 [h] / Coll. Pfanner [p]; NHMUK014596798 [p]'; 1 female (Fig. 1f–j): 'Malaysia / Cameron Highlands / 1400m 17 iv 73 / via coll. P. Pfanner [h]; Mimomyagrus pfanneri / (Breuning) / Cameron Highlands / (Malaysia 1400 m / 17/4/1973) [p]; Brit. Mus. / 1978.72 [p]; NHMUK014596799 [p]'.

**Comments.** White (1858) described *Monohammus brianus* (Fig. 2a–d) based on a female specimen without head from Nepal. Thomson (1864) established the genus *Combe* for *Combe fulgurata* (Fig. 2e–i) based on a female specimen without indicating locality. Pascoe (1866) transferred *Monohammus brianus* to the genus.

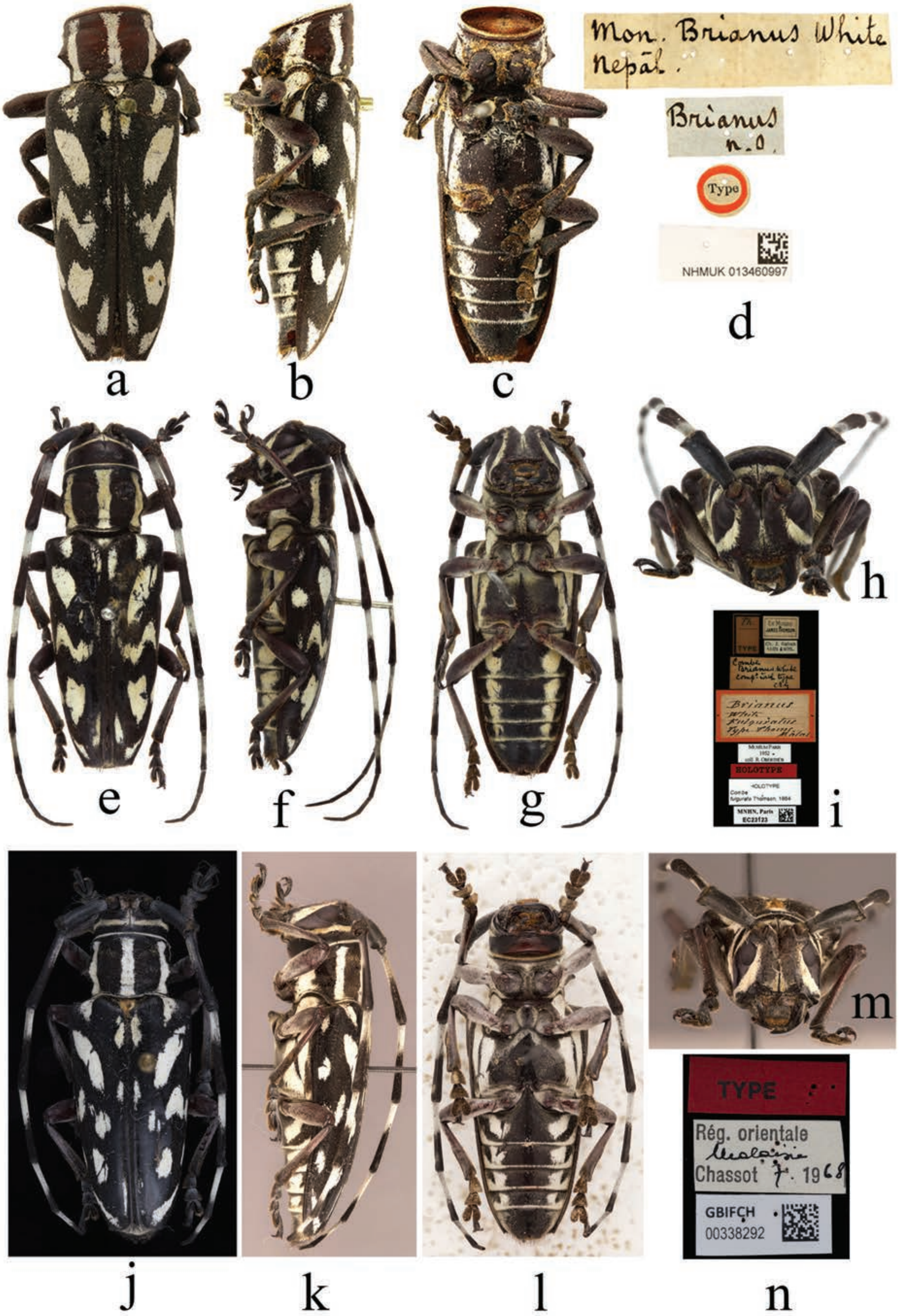

**Figure 2.** Habitus of *Combe brianus* (White, 1858) **a–c** holotype of *Monohammus brianus* White, 1858, female **e–h** holotype of *Combe fulgurata* Thomson, 1864, female **j–m** holotype of *Mimomyagrus pfanneri* Breuning, 1970, female **d, i, n** labels.

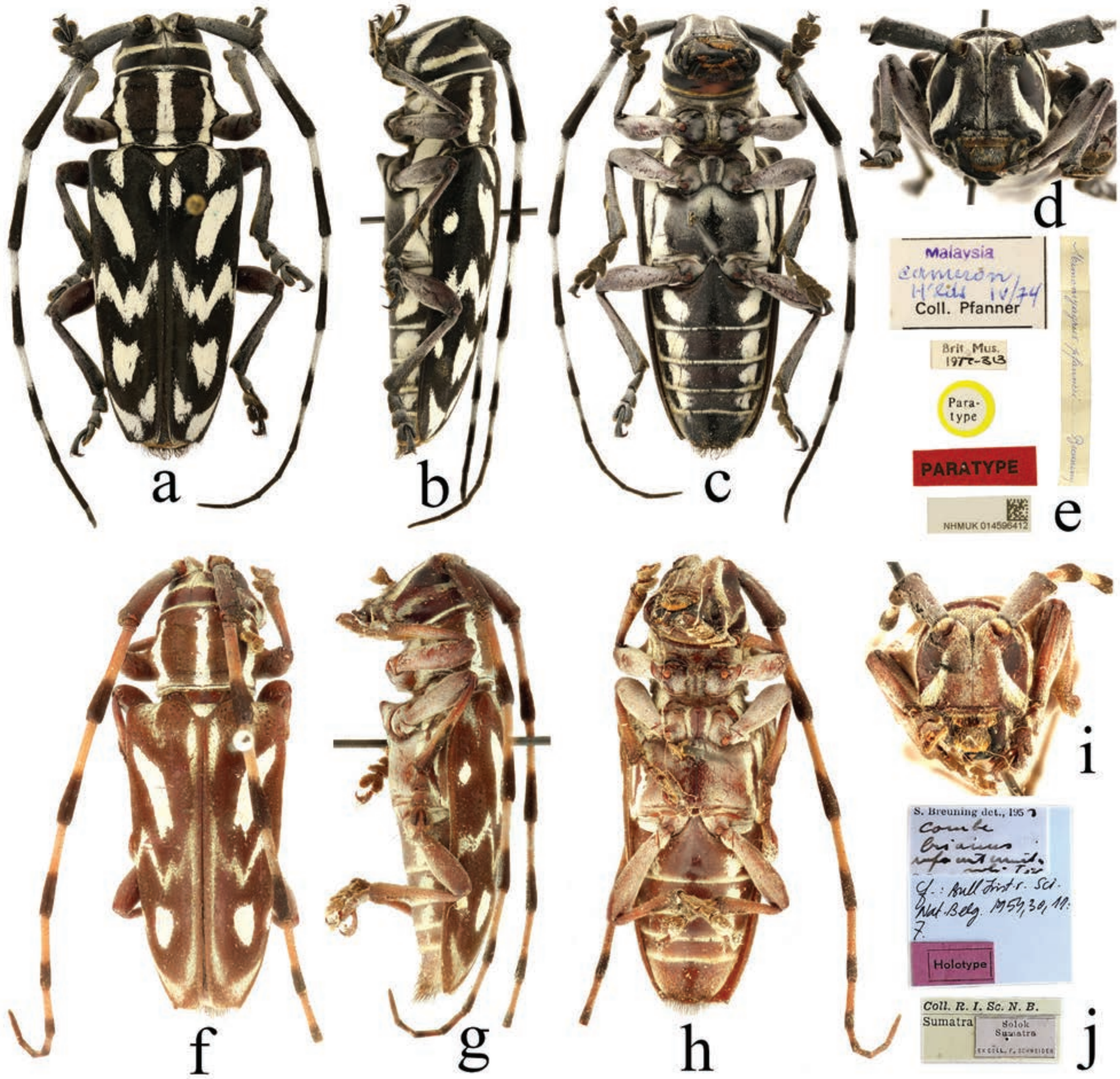

**Figure 3.** Habitus of *Combe brianus* (White, 1858) **a–d** paratype of *Mimomyagrus pfanneri* Breuning, 1970, female **f–i** holotype of *Combe brianus* m. *rufoantennatus* Breuning, 1954, female **e, j** labels.

*Combe* and synonymized *Combe fulgurata* with it based on the male and female specimens from Malacca, Malaysia. Breuning (1954) described a morph, *Combe brianus* m. *rufoantennatus* (Fig. 3f–j), based on a specimen of reddish-brown colour from Sumatra. Subsequently, Breuning (1970) described *Mimomyagrus pfanneri* based on specimens from Cameron Highlands, Malaysia. Through studying these series of type and non-type specimens, we found that, in fact, they belong to the same species. Thus, here we propose the species *Mimomyagrus pfanneri* as a junior synonym of *Combe brianus*.

Since *Mimomyagrus pfanneri* is the type species of *Mimomyagrus*, this genus becomes a junior synonym of the genus *Combe*.

Breuning (1954) regarded the type specimen of *Combe brianus* m. *rufoantennatus* as a male. However, based on the ratio of the antennal length to body length, and the shape of the abdomen, it appears to be a female.

A questionable paratype of *Mimomyagrus pfanneri* (Fig. 3a–e) is present in the collection of the NHMUK. According to the label, a handwritten collection date indicates that the specimen was collected in April, 1974 (Fig. 3e). The species was described in 1970 and the collection date was clearly recorded as 'IV–V 1969' in the original publication by Breuning, although on the label of the holotype a similarly handwritten date is given as 'July 1968'. In any case, it is impossible for the collection date of the claimed paratype to appear after the publication date. Therefore, this specimen cannot be considered as a paratype.

### ***Arctolamia sinica*** **Bi & Chen, 2022**

Figs 4a–j, 5f, i

*Arctolamia sinica* Bi & Chen, 2022: 199.

**Description.** Female: similar to male, body length 33.5 mm, humeral width 12.0 mm. Body black, mostly densely clothed with reddish-brown pubescence, each puncture bearing a black or reddish-brown erect hair; glabrous areas showing black integument; elytra provided with five black pubescent patches. Frons, gena and vertex with black hairs, mouthparts with hairs lighter in colour, nearly yellowish-brown. Antennae with scape clothed with reddish-brown pubescence only on lateral margin; antennomeres III–V clothed with reddish-brown pubescence on basal half, antennomeres VI–VIII on basal half and antennomere XI on extreme apex clothed with greyish-yellow pubescence; antennomeres III–IV clothed with black pubescence on apical half, antennomeres V–VIII clothed with pubescence fading to chestnut on apical half; antennomeres IX–X and most of antennomere XI clothed with chestnut pubescence; scape and pedicel clothed with a black long hair on each puncture, denser on inferior margin; antennomeres III–VI fringed with long hairs below, reddish-brown on base and black on apex, antennomeres III–IV tufted with black hairs around apex. Pronotum clothed with black erect hairs on anterior, lateral and posterior margin, more on anterior margin; disc barely clothed with hairs on calli. Scutellum clothed with reddish-brown pubescence, without hairs. Elytra densely clothed with reddish-brown and black hairs, glabrous only on basal granules; each puncture bearing a long erect black or reddish-brown hair, black hairs short and stiff, reddish-brown hairs long and soft, arranged intermixed with each other; elytra with five black pubescent patches: a basal one located around scutellum, subangular; a lateral one on basal quarter after each humerus, smallest, oblique, not reaching the lateral margin; a large oblique one on each side behind the middle, not reaching suture and lateral margin. Underside densely clothed with reddish-brown pubescence, slightly greyish-yellow on mesosternum and mesoepisternum; ventrites furnished with greyish-yellow and black erect hairs. Legs mostly clothed with reddish-brown pubescence, tibiae and tarsi furnished with sparse black bristles.

Head sparsely punctate; frons transverse, slightly convex, with a distinct median sulcus extending to occiput. Eyes coarsely faceted, lower eye lobe transverse, about as long as gena; vertex uneven, with irregular wrinkles. Antennae distinctly shorter than body; antennal insertions conspicuously elevated, broadly separated; scape stout, gradually thickened apically, longest; antennomere III slightly shorter than antennomere IV, antennomere IV about as long as antennomere V,

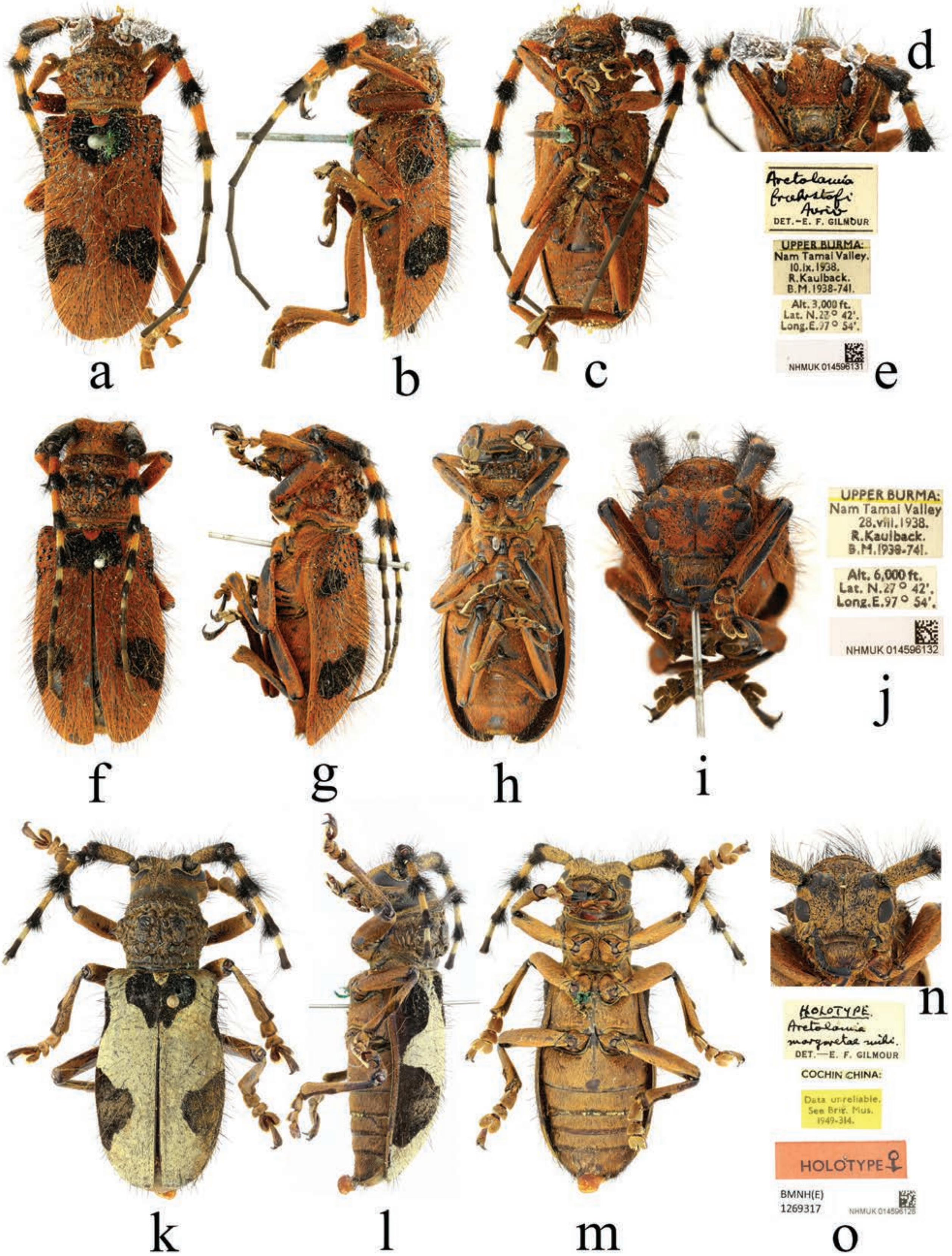

Arctolamia fruhstorferi Auriv.
DET.-E. F. GILMOUR

UPPER BURMA:
Nam Tamai Valley.
10.ix.1938.
R.Kaulback.
B.M.1938-741.

Alt. 3,000 ft.
Lat. N.27° 42'.
Long.E.97° 54'.

NHMUK 014596131

UPPER BURMA:
Nam Tamai Valley
28.viii.1938.
R.Kaulback.
B.M.1938-741.

Alt. 6,000 ft.
Lat. N.27° 42'.
Long.E.97° 54'.

NHMUK 014596132

HOLOTYPE.
Arctolamia margaretae n.sp.
DET.—E. F. GILMOUR

COCHIN CHINA:

Data unreliable.
See Brit. Mus.
1949-314.

HOLOTYPE ♀

BMNH(E)
1269317

NHMUK 014596128

**Figure 4.** Habitus of *Arctolamia* spp. **a–j** *Arctolamia sinica* Bi & Chen, 2022 **k–o** holotype of *Arctolamia margaretae* Gilmour, 1950 **a–d** male **f–i, k–n** female **e, j, o** labels.

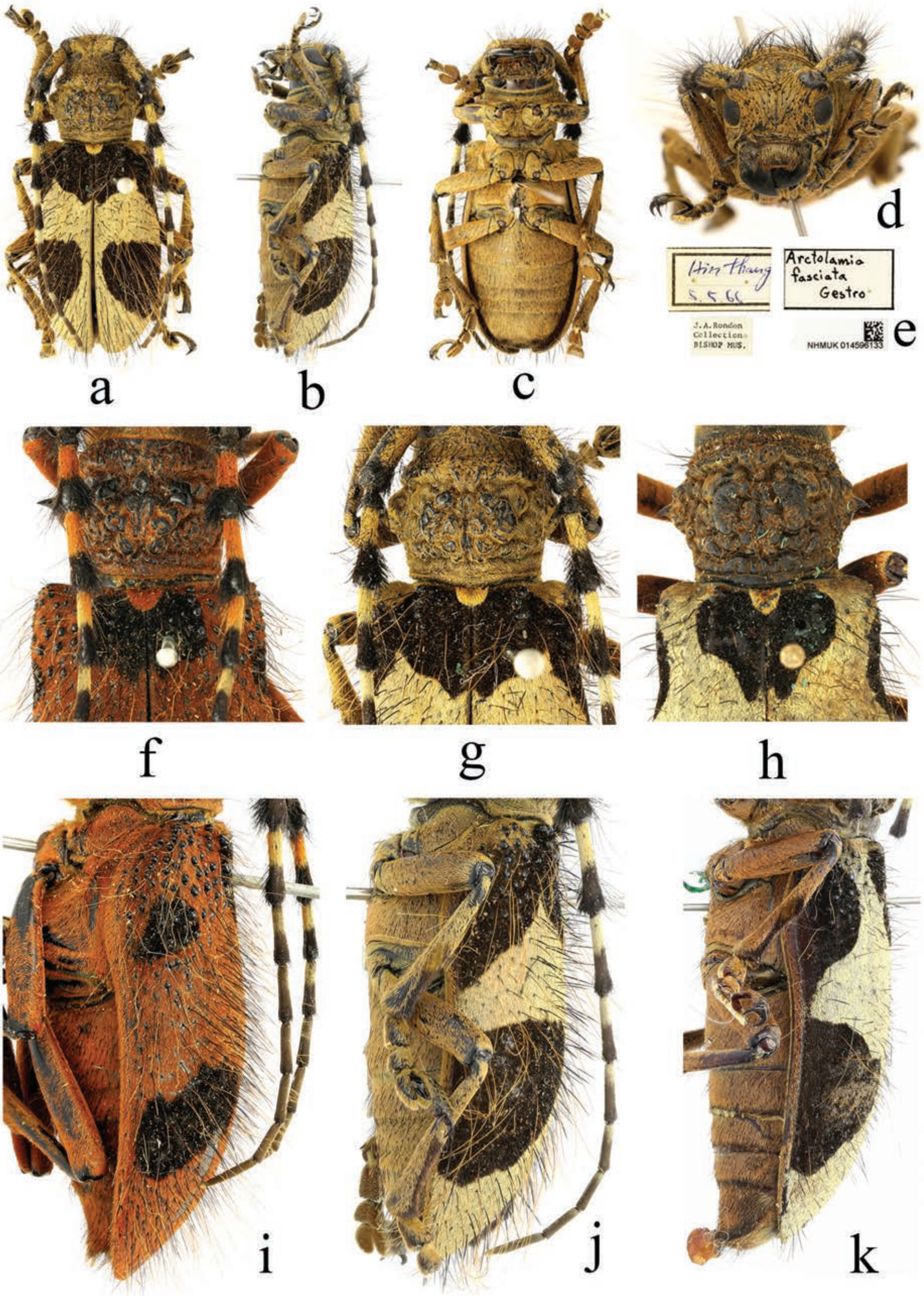

**Figure 5.** Habitus of *Arctolamia* spp. **a–d**, **g, j** *Arctolamia fruhstorferi* Aurivillius, 1902 **f, i** *Arctolamia sinica* Bi & Chen, 2022 **h, k** holotype of *Arctolamia margaretae* Gilmour, 1950 **e** labels **a–d**, **f–k** female.

antennomeres V–X gradually shortened in length, antennomere XI about as long as antennomere VII. Pronotum transverse, with a pointed lateral spine on middle of each side; disc convex, coarsely rugose, with developed calli. Scutellum semicircular. Elytra broad, lateral margins gradually expanding outward at basal quarter after humeri, then convergent backward from middle to apices, apices conjointly rounded; about basal fourth provided the sparse, glabrous granules, of which several large granules regularly arranged in a row near the scutellum. Abdomen with first ventrite distinct longer than second and third ventrite, distal ventrite with apical centre slightly depressed, apical margin nearly straight. Legs moderately long and thick, metafemur reaching the middle of fourth ventrite.

**Non-type material examined.** Myanmar: 1 male: 'UPPER BURMA: / Nam Tamai Valley / 28. viii. 1938. / R. Kaulback. / B. M. 1938–741. [p]; Alt. 6,000 ft. / Lat. N. 27°42'. / Long. E. 97°54'. [p]; Arctolamia / fruhstorferi / Auriv [h] / DET. –E. F. GILMOUR [p]; NHMUK014596131'; 1 female: 'UPPER BURMA: / Nam Tamai Valley / 28. viii. 1938. / R. Kaulback. / B. M. 1938–741. [p]; Alt. 6,000 ft. / Lat. N. 27°42'. / Long. E. 97°54'. [p]; NHMUK014596132'.

**Comments.** Gilmour (1950) misidentified the above pair of specimens as *Arctolamia fruhstorferi* Aurivillius, 1902 (Fig. 4a–j) and, using this as a comparison, described another species, *Arctolamia margaretae* Gilmour, 1950 (Fig. 4k–o). In fact, *A. margaretae* is a junior synonym of *A. fruhstorferi*, as shown by Pu (1981), whereas the specimens misidentified by Gilmour as *A. fruhstorferi* represent *A. sinica* Bi & Chen, 2022.

Bi and Chen (2022) indicated that *A. sinica* can be differentiated from *A. fruhstorferi* by the absence of light-coloured pubescence on the dorsal surface of the scape and numerous large granules on the base of elytra. However, a male specimen of *A. sinica* from Myanmar shows the scape distinctly clothed with reddish-brown pubescence on dorsal surface (Fig. 4a, b, d) and there is a female specimen in the NHMUK identified as *A. fasciata* Gestro, 1891 that is actually supposed to be *A. fruhstorferi* (maybe it is a transitional form), which also has some large granules on the elytral base (Fig. 4a–e). This seems to imply that, given current knowledge, the main feature that distinguishes *A. sinica* from *A. fruhstorferi* is the reddish-brown pubescence on its body.

*Arctolamia sinica*, is also recorded in Myanmar for the first time based on the pair of specimens mentioned above.

## Additional discoveries

Type specimens of *Lamia punctator* Fabricius, 1776 [= *Anoplophora chinensis* (Forster, 1771)] (Fig. 6a–e) and *Cerambyx galloprovincialis* Olivier, 1800 [= *Monochamus galloprovincialis* (Olivier, 1800)] (Fig. 6f–k) and the holotype of *Melanauster granulipennis* Breuning, 1938 [= *Monochamus guerryi* Pic, 1903] (Fig. 6l–p) are confirmed to be preserved in the NHMUK; all were considered to be 'lost' and marked as 'depositary not known' (Tavakilian and Chevillotte 2023). *Lamia punctator* Fabricius, 1776 and *Cerambyx galloprovincialis* Olivier, 1800 are marked as having (missing) 'holotypes' by Tavakilian and Chevillotte (2023) and are labelled at the NHMUK with standard red framed 'type' discs, but there is no evidence of a holotype or of there being only one specimen in their original descriptions, so they are treated as syntypes. *Melanauster granulipennis* Breuning, 1938 is described from a single female, and this specimen is a holotype.

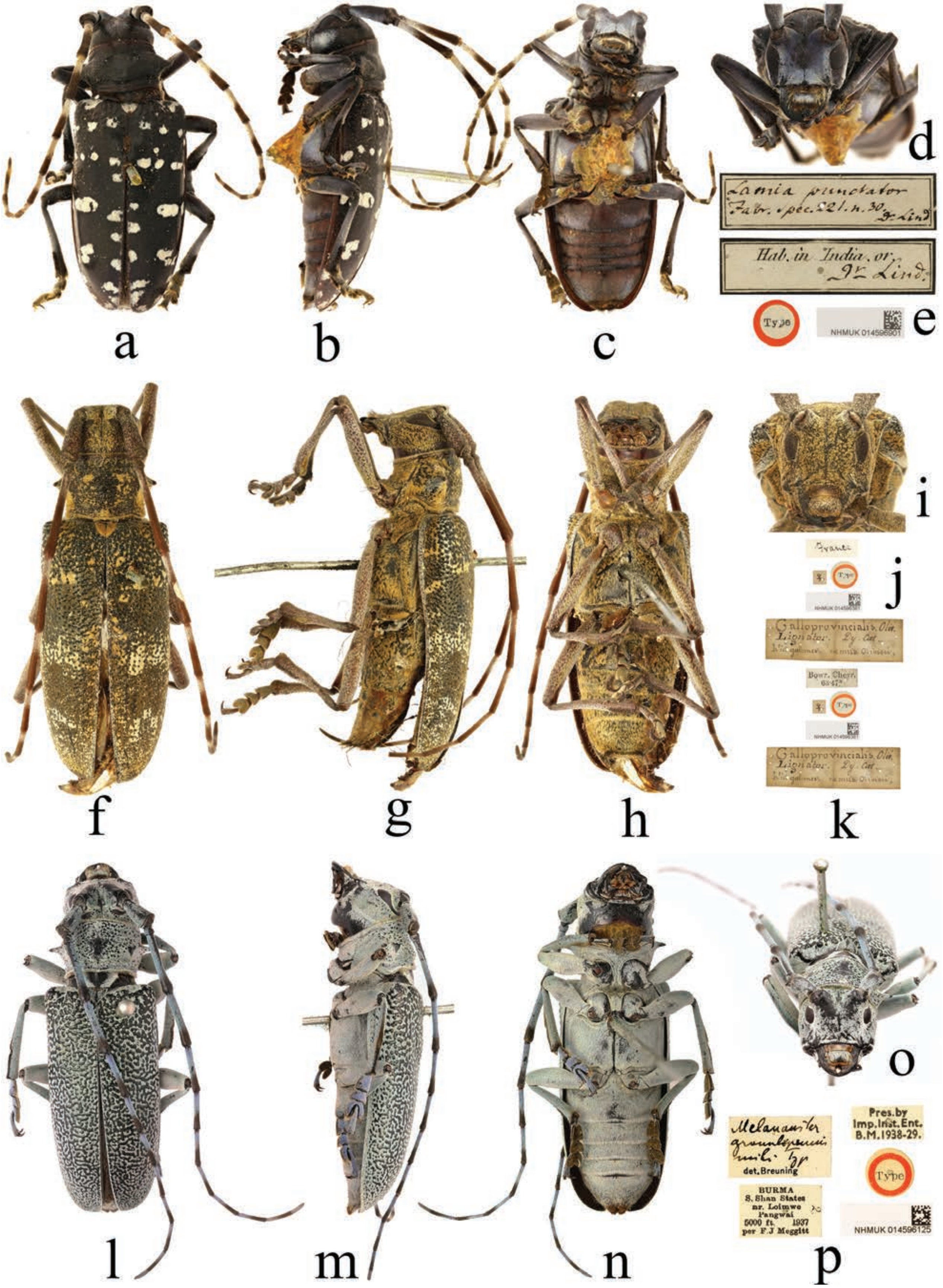

**Figure 6.** **a–d** type specimen of *Lamia punctator* Fabricius, 1776, female **f–i** type specimen of *Cerambyx galloprovincialis* Olivier, 1800, female **l–o** holotype of *Melanauster granulipennis* Breuning, 1938, female **e, j, k, p** labels.

## Acknowledgments

We wish to express our sincere thanks to Antoine Mantilleri and Christophe Rivier (Muséum national d'Histoire naturelle, Paris) for taking the holotype photographs of *Combe fulgurata* Thomson, to Alain Drumont and Julien Lalanne (Royal Belgian Institute of Natural Sciences, Brussels) for taking the holotype photographs of *Combe brianus* m. *rufoantennatus* Breuning, and to Anne Freitag (Muséum cantonal des sciences naturelles, Lausanne) for taking the holotype photographs of *Mimomyagrus pfanneri* Breuning, 1970, and especially to Francesco Vitali (Musée national d'histoire naturelle de Luxembourg, Luxembourg), subject editor of ZooKeys, for carefully revising and patiently handling the manuscript. We also wish to express our special thanks to the Coleoptera curatorial team of the NHMUK, past and present, for maintaining and developing the collection and particularly to Keita Matsumoto and Michael Geiser for supporting the first author during his study at the Natural History Museum, London.

## Additional information

### Conflict of interest

The authors have declared that no competing interests exist.

### Ethical statement

No ethical statement was reported.

### Funding

This research was supported by the China Scholarship Council (202008420315) and the National Natural Science Foundation of China (No. 31672327).

### Author contributions

Conceptualization: GX. Funding acquisition: WW. Resources: MVLB. Writing - original draft: GX. Writing - review and editing: MVLB, WW.

### Data availability

All of the data that support the findings of this study are available in the main text.

## References

Aurivillius C (1921) Cerambycidae: Lamiinae I. Coleopterorum Catalogus auspiciis et auxilio W. Junk, pars 73, Schenkling S Ed., Berlin, 1–322. https://www.biodiversitylibrary.org/page/10202648

Barševskis A (2018) To the knowledge of Long-Horned beetles (Coleoptera: Cerambycidae) of the Oriental Region. Part 1. Acta Biologica Universitatis Daugavpiliensis 18(2): 285–294.

Barševskis A (2020) To the knowledge of Long-Horned Beetles (Coleoptera: Cerambycidae) of the Oriental Region. Part 3. Acta Biologica Universitatis Daugavpiliensis 20(2): 173–188.

Bi WX, Chen CC (2022) Description of one New Species of *Arctolamia* Gestro, 1888 from China (Coleoptera: Cerambycidae: Lamiinae). Japanese Journal of Systematic Entomology 28(2): 199–200.

Breuning S (1938) Nouveaux Cerambycidæ (Col.). Novitates Entomologicae 9: 30–63.

Breuning S (1954) Nouvelles formes de Lamiaires (cinquième partie). Bulletin de l'Institut Royal des Sciences Naturelles de Belgique 30(11): 1–23.

Breuning S (1961) Catalogue des Lamiaires du Monde (Coleoptera, Cérambycidae). 5 Lieferung. Verlag des Museum G. Frey, Tutzing bei München, 96 pp [287–382].

Breuning S (1970) Descriptions de nouveaux Lamiinae de la collection Chassot (Coleoptera Cerambycidae). Bulletin de la Societe Entomologique de Mulhouse (novembre-décembre), 87–90.

Fabricius JC (1776) Genera insectorum eorumque characteres naturales secundum numerum, figuram, situm et proportionem omnium partium oris adiecta mantissa specierum nuper detectarum. MF Bartsch, Kiel, 1–310. https://doi.org/10.5962/bhl.title.65743

Gemminger M, von Harold E (1873) Catalogus coleopterorum hucusque descriptorum synonymicus et systematicus 10, Munich: 2989–3232. http://www.biodiversitylibrary.org/item/38704

Gilmour EF (1950) New and rare Lamiinae. Longicornia I, Lechevalier P, Paris, 537–556.

Lacordaire JT (1869) Histoire Naturelle des Insectes. Genera des Coléoptères ou exposé méthodique et critique de tous les genres proposés jusqu'ici dans cet ordre d'insectes. Famille des longicornes (suite). Librairie Encyclopédique de Roret, Paris, 9(1): 1–409. http://www.biodiversitylibrary.org/item/36757

Olivier GA (1800) Entomologie ou Histoire Naturelle des Insectes, avec leurs caractères génériques et spécifiques, leur description, leur synonymie et leur figure enluminée. Coléoptères. Imprimerie de Lanneau, Paris 4: 125–492. https://www.biodiversitylibrary.org/item/105397#page/177/mode/1up

Pascoe FP (1866) Longicornia Malayana; or, a Descriptive Catalogue of the Species of the three Longicorn Families Lamiidæ, Cerambycidæ and Prionidæ collected by Mr. A. R. Wallace in the Malay Archipelago. (Part III). The Transactions of the Entomological Society of London 3: 225–336. http://www.biodiversitylibrary.org/item/51218 [Third series]

Pu FJ (1981) Notes on Chinese Longicorn Beetles of the genus *Arctolamia* (Coleoptera: Cerambycidae). Dong Wu Fen Lei Xue Bao 6(4): 433–436.

Tavakilian G, Chevillotte H (2023) Titan: base de données internationales sur les Cerambycidae ou Longicornes. Version 3.0. http://titan.gbif.fr/index.html

Thomson J (1864) Systema Cerambycidarum, ou exposé de tous les genres compris dans la famille des Cérambycides et familles limitrophes. Mémoires de la Société Royale des Sciences de Liège 19: 1–540. https://doi.org/10.5962/bhl.title.48458

Weigel A (2006) Checklist and bibliography of Longhorn Beetles from Nepal (Insecta: Coleoptera: Cerambycidae). In: Hartmann M, Weipert J (Eds) Biodiversität und Naturausstattung im Himalaya II. Verein der Freunde und Förderer des Naturkundemuseums Erfurt e. V., Erfurt, 495–510.

White A (1858) Descriptions of *Monohammus Bowringii*, *Batocera Una*, and other Longicorn Coleoptera, apparently as yet unrecorded. Proceedings of the Zoological Society of London 26: 398–413. https://doi.org/10.1111/j.1469-7998.1858.tb06396.x

ZooKeys 1205: 253–265 (2024)
DOI: 10.3897/zookeys.1205.127999

Research Article

# Two new species of the genus *Kingdonella* Uvarov, 1933 (Orthoptera, Acridoidea) and the first reported male of *Kingdonella qinghaiensis* Zheng, 1990

Jianyu Chen[1], Yulong Zhang[1], Xinjiang Li[1]

1 *The Key Laboratory of Zoological Systematics and Application, School of Life Sciences, Institute of Life Sciences and Green Development, Hebei University, Baoding 071002, China*

*Corresponding author: Xinjiang Li (hbulxj@163.com)*

## Abstract

Two new species of the genus *Kingdonella* and the first report of a male *K. qinghaiensis* Zheng, 1990 are presented. The new species *K. gandensis* **sp. nov.** has similar morphological features to *K. wardi* Uvarov, 1933, but it differs from the latter in having 1) the hind tibia black; 2) the epiproct, in males, with a median groove in the basal 1/2 and in the apical 1/4; 3) the denticles of the male epiproct black; 4) the outside of the hind femur reddish-brown on the basal 1/4 and black on the apical 3/4; and 5) the ventral face of the hind femur black on the outer side. The second new species, *K. biruensis* **sp. nov.**, is morphologically close to *K. pienbaensis* Zheng, 1980 but differs from the latter in having 1) the length of the middle segment (12th segment) of antennae 1.2 times longer than its width; 2) the subgenital plate sharp-cornered in males; 3) the ovipositor smooth; 4) the upper half of hind femur outside surface with two black spots; and 5) the ventral face of the hind femur black on its outer side, red on the basal 2/3, and black on the apical 1/3 of its inner side. Finally, we provide a key to all known species of *Kingdonella*.

**Key words:** Grasshopper, identification key, Melanoplinae, taxonomy

Academic editor: Jun-Jie Gu
Received: 21 May 2024
Accepted: 5 June 2024
Published: 27 June 2024

ZooBank: https://zoobank.org/63BA78D8-2ED1-4C8C-AB12-433CF824E7FB

Citation: Chen J, Zhang Y, Li X (2024) Two new species of the genus *Kingdonella* Uvarov, 1933 (Orthoptera, Acridoidea) and the first reported male of *Kingdonella qinghaiensis* Zheng, 1990. ZooKeys 1205: 253–265. https://doi.org/10.3897/zookeys.1205.127999

## Introduction

The genus *Kingdonella* was established by Uvarov in 1933 with *K. wardi* Uvarov, 1933 as the type species (Uvarov 1933). *Kingdonella* is endemic to the Qinghai-Xizang Plateau. All species in this genus lack tegmina, wings, and a tympanum, which are representative evolutionary adaptations to the plateau environment at altitudes of 3000–5000 m.

*Kingdonella* was extensively studied in the 20th century, and 17 species in the genus have been described (Uvarov 1933, 1935, 1939; Mishchenko 1952; Zheng 1980, 1990; Huang 1981; Yin 1984; Li and Xia 2006; Li and Yin 2009). Due to the absence of tegmina and wings, these species have restricted capacity for dispersion and migration across the plateau, leading to narrow distribution ranges. Upon meticulously examining our collected specimens, we identified two new species of *Kingdonella* in the locales of Gande, Qinghai and Biru, Xizang. Additionally, we encountered the male of *K. qinghaiensis* within the confines of Zhiduo, Qinghai, which is the precise location where the holotype was collected. Finally, a key to the genus *Kingdonella* is revised and presented.

## Materials and methods

All samples were collected from Qinghai and Xizang, China. After collection, samples were dried for morphological and color description. Potassium cyanide was used during the drying process to preserve the natural colors. The type specimens were deposited in the School of Life Sciences, Hebei University, Baoding, China. The specimens were photographed using a Fujifilm XH2 camera with an XF 30 mm macro lens.

In the morphological analyses, measurements were made using the MATO software (Liu et al. 2023) for the following body characters:

Body length – dorsally from the fastigium vertex to the distal end of the abdomen.
Pronotum length – dorsally, along the median carina.
Hind femur length – laterally, maximum possible measurement of the hind femur.

## Results

### Taxonomy

**Acridoidea MacLeay, 1821**
**Acrididae MacLeay, 1821**
**Melanoplinae Scudder, 1897**
**Podismini Jacobson, 1905**

***Kingdonella gandensis* sp. nov.**
https://zoobank.org/75C1D661-EA93-41AE-87D6-C61B988C6416
Fig. 1

**Type material.** ***Holotype*:** CHINA • 1♂; Qinghai, Gande; 33.96°N, 99.93°E; 22.VIII.2008; coll. Xinjiang Li, Jiantao Xiao, Yongchao Zhi; catalogue number 080822015.

***Paratypes*:** CHINA 8♂ 11♀, same data as the holotype; catalogue numbers 080822016–080822035.

**Etymology.** The species is named after Gande, the type locality.

**Diagnosis.** The new species resembles *K. wardi* in having a small and obtuse furcula in the male epiproct and long cerci that nearly reach the tip of the epiproct, but it can be distinguished by the characters presented in Table 1.

**Description. Male:** body medium-sized (Fig. 1A, B). Head shorter than pronotum, and frons slightly oblique in profile. Frontal costa distinct and concave on the level of median ocellus (Fig. 1C). Vertical diameter of eyes 1.1 times that of transverse and subocular furrows. Antennae filiform, with 24 segments, slightly longer than head and pronotum combined; length of a middle segment (12th segment) 2.0 times its width. Pronotum rough, nearly straight on anterior margin, and slightly depressed on median posterior

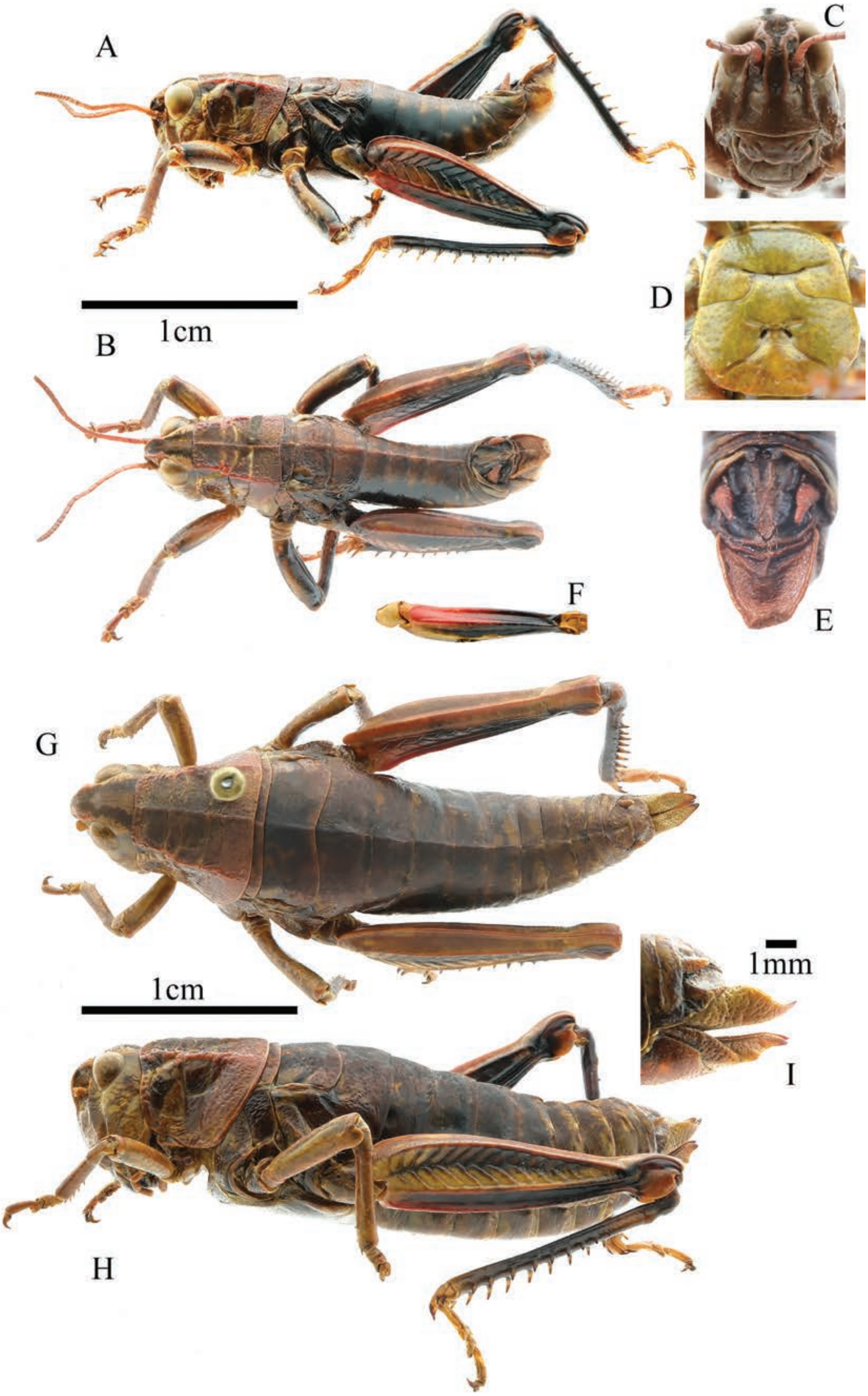

**Figure 1.** *Kingdonella gandensis* sp. nov. male **A** lateral view of holotype **B** dorsal view of holotype **C** head of holotype **D** sternal plate of male holotype, ventral view **E** terminal of abdomen, dorsal view **F** Hind femur, ventral view **G** dorsal view of female paratype **H** lateral view of paratype **I** ovipositor, lateral view.

**Table 1.** Comparison of *Kingdonella gandensis* sp. nov. and *K. wardi* Uvarov, 1933.

| Characters | ***K. gandensis*** **sp. nov.** | ***K. wardi*** |
|---|---|---|
| Colors of hind tibia | Black | Red |
| Epiproct in male | With median groove on basal 1/2 and apical 1/4 | With median groove on base |
| Denticles of male epiproct | Black | Red |
| Outer side of hind femur | Basal 1/4 reddish-brown and apical 3/4 black | Basal 2/3 red and apical 1/3 black |
| Outer side of ventral face of hind femur | Black | Red |

margin. Median carina distinct, slightly cut by last transverse sulci; lateral carinae conspicuous, gradually expanding outward; prozona 2.0 times that of metazona in length. Prosternal process conical, bluntly round at apex. Width of metasternal lobes 1.5 times the length; minimum width of mesosternal interspace 1.6 times the length. Metasternal lobes separated and distinct (Fig. 1D). Tegmina and wings absent. Upper carina of hind femur smooth. Hind femur 4.0 times longer than wide. Outer side of upper basal lobe of hind femur distinctly longer than the lower one. Hind tibia with nine spines on inner and eight on outer side; external apical spine absent. Arolium between claws large, widely rounded, nearly reaching the apex of claws. Posterior margin of 10th abdominal tergite with distinct furcula (Fig. 1E). Tympanal organ absent. Epiproct with denticles on the middle of both sides, with a longitudinal groove in basal 1/2 and in apical 1/4, apically sharp-cornered. Cerci long, conical, and nearly reaching tip of epiproct. Subgenital plate long, sharp-cornered, and protruding backwards. In phallic complex, apical valves of penis slightly longer than cingulum valves; apodemes longer than basal valves of penis, with slightly enlarged and flaky ends; lateral view of basal valves of penis reveals a reniform shape (Fig. 4A–C). Bridge of the epiproct straight, wide, and short; ancorae angular, curving inward, with non-sharp tips; anterior projections semicircular, lateral plates straight, and posterior projections conical; lophi large and flaky, extending towards the medial and lower sides, protruding noticeably in the overall plane, with evident tumor protrusions along edge (Fig. 4D–F). **Female:** body robust, larger than male (Fig. 1G, H). Eyes small, with vertical diameter equal to transverse diameter, and 0.8 times longer than subocular furrows. Pronotum wider, trapezoidal, last transverse sulci not cutting median carina. Minimum mesosternal interspace width 2.8 times length. Ovipositor margin smooth, with a hook-like apex (Fig. 1I). Other characteristics resemble the male.

**Coloration.** Body reddish-brown. Eyes yellowish-brown. Antennae light red. Apex and lateral margins of fastigium red. Pronotum lateral carinae red. Upper side of femur reddish-brown. Inner side of hind femur red at the base and the remaining black. Outer side of hind femur reddish-brown (yellow in females) on basal 1/4 and black on apical 3/4; Ventral face of hind femur red on basal 1/2 and black on apical 1/2 (Fig. 1F). Upper lateral genicular lobe black, other brown. Lower lateral genicular lobe red. Hind tibia black and tarsus brown. Denticles of male epiproct black.

**Measurements.** Shown in Table 2.

**Distribution.** Gande, Qinghai Province, China.

**Table 2.** Measurement of *Kingdonella gandensis* sp. nov.

| Number of specimens | Male | | | Female | | |
|---|---|---|---|---|---|---|
| | Body length | Pronotum length | Hind femur length | Body length | Pronotum length | Hind femur length |
| 1 | 17.53 | 4.18 | 10.56 | 29.00 | 5.27 | 12.48 |
| 2 | 18.04 | 4.28 | 10.64 | 25.29 | 5.82 | 12.98 |
| 3 | 18.88 | 4.20 | 10.02 | 25.51 | 6.24 | 12.27 |
| 4 | 18.15 | 4.44 | 10.55 | 26.73 | 5.50 | 12.91 |
| 5 | 18.90 | 4.22 | 10.22 | 22.43 | 5.74 | 12.59 |
| 6 | 18.39 | 4.20 | 10.33 | 27.91 | 5.40 | 12.93 |
| 7 | 19.41 | 4.53 | 10.95 | 22.87 | 5.09 | 12.73 |
| 8 | 17.71 | 4.42 | 9.88 | 25.85 | 5.51 | 13.06 |
| 9 | 18.54 | 4.17 | 10.94 | 27.42 | 5.54 | 13.24 |
| 10 | – | – | – | 23.64 | 5.38 | 12.55 |
| 11 | – | – | – | 28.90 | 5.46 | 14.16 |
| Min | 17.53 | 4.17 | 9.88 | 22.43 | 5.09 | 12.27 |
| Max | 19.41 | 4.53 | 10.95 | 29.00 | 6.24 | 13.24 |
| Median | 18.39 | 4.22 | 10.55 | 25.85 | 5.51 | 12.91 |

### *Kingdonella biruensis* sp. nov.

https://zoobank.org/0C7A3718-969C-4541-9389-F452156A1D1D
Fig. 2

**Type material.** ***Holotype*:** China • 1♂; Xizang, Biru; 93.91°N, 31.27°E, 8.VIII.2009, coll. Daochuan Zhang and Yulong Zhang; Catalogue number: #090808001.

***Paratypes:*** China 8♂ 8♀, same data as the holotype; Catalogue number: #090808002— #090808017.

**Etymology.** The species is named after Biru, the type locality.

**Diagnosis.** The new species *Kingdonella biruensis* sp. nov. resembles *K. pienbaensis* in having the male epiproct with large denticles, but it can be distinguished by the characters presented in Table 3.

**Description. Male:** body medium-sized (Fig. 2A, B), head shorter than pronotum, and frons slightly oblique in profile. Frontal costa distinct and concave on the level of median ocellus (Fig. 2D). Vertical diameter of eyes 1.1 times that of transverse and equal to subocular furrows. Antennae filiform, with 23 segments, slightly longer than the head and pronotum combined; length of middle segment (12th segment) 1.2 times its width (Fig. 2C). Pronotum rough, nearly straight on anterior margin and slightly depressed on median posterior margin. Median carina distinct, slightly cut by 1st and 3rd transverse sulci; lateral carinae strongly distinct, lateral carinae parallel before 1st transverse sulci and later gradually expanding outward; prozona 2.1 times of metazona in length. Prosternal process conical and slightly sharp at apex. Mesosternal interspace at least 1.7 times wider than long (Fig. 2E). Metasternal lobes separated and distinct. Tegmina and wings absent. Upper carina of hind femur smooth. Hind femur 3.8 times longer than wide. Outer side of upper basal lobe of hind femur distinctly longer than lower one. Hind tibia with nine spines on inner and eight spines on outer side; external apical spine absent. Arolium between claws large, wide, round,

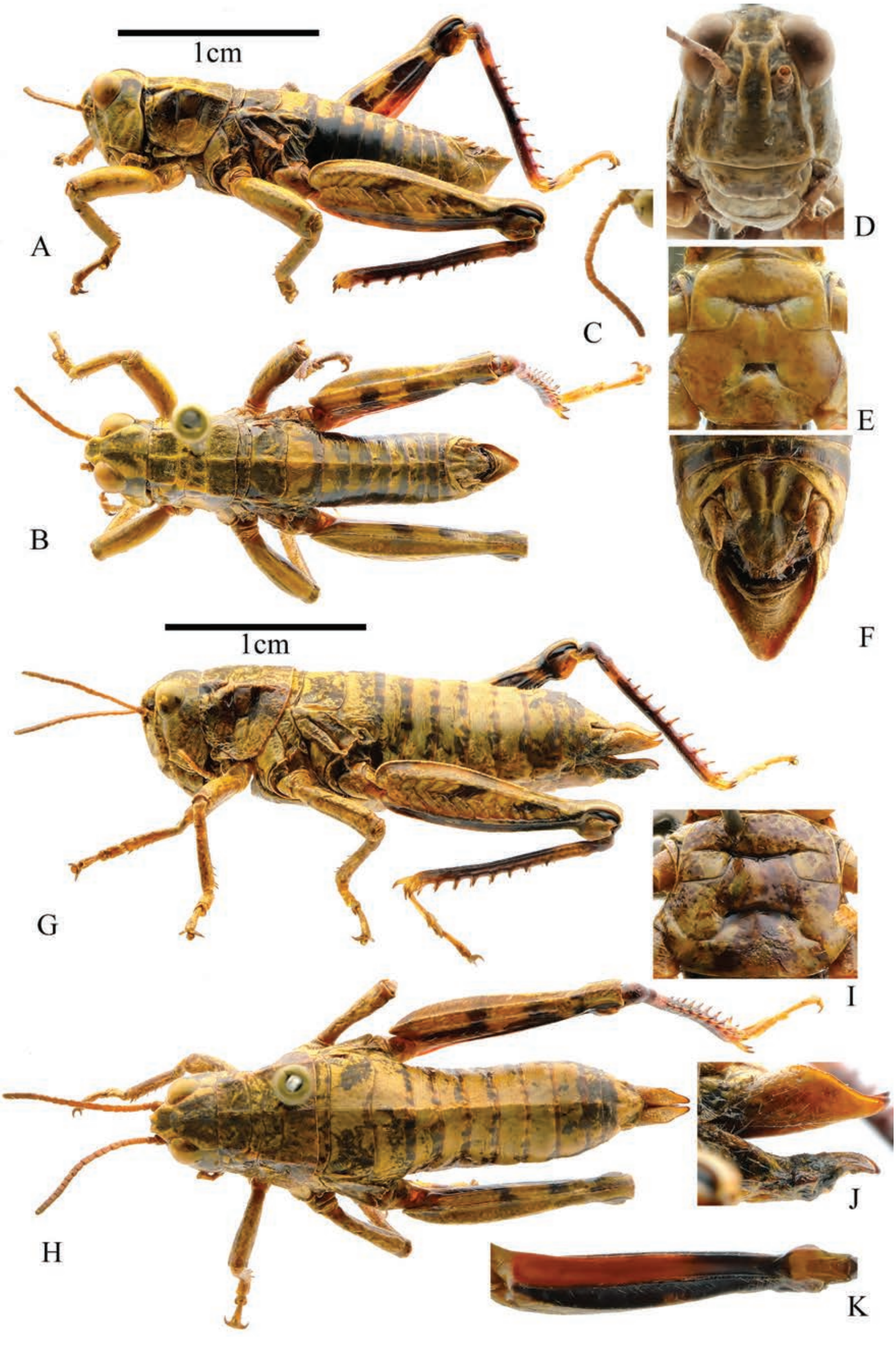

**Figure 2.** *Kingdonella baigasis* sp. nov. **A** dorsal view of male holotype **B** lateral view of male holotype **C** antennae, dorsal view **D** head of holotype **E** sternal plate of male holotype, ventral view **F** terminal of abdomen, dorsal view **G** lateral view of female paratype **H** dorsal view of female paratype **I** sternal plate of female paratype, ventral view **J** ovipositor of paratype, lateral view **K** hind femur of female paratype, ventral view.

**Table 3.** Comparison of *Kingdonella biruensis* sp. nov. and *K. pienbaensis* Zheng, 1980.

| Characters | ***Kingdonella biruensis* sp. nov.** | ***K. pienbaensis*** |
|---|---|---|
| Length of 12th segment in male antennae | 1.2 times the width | 1.6 times the width |
| Subgenital plate in male | Sharp-cornered | Bluntly rounded |
| Ovipositor | Smooth | Blunt spines in the upper valves |
| Upper outside of hind femur color | Yellow with two black spots | Dark |
| Ventral face of hind femur | Black on outer side, red on basal 2/3, and black on apical 1/3 of inner sides | Red |

reaching apex of claws. Posterior margin of 10th abdominal tergite without distinct furcula (Fig. 2E). Tympanal organ absent. Epiproct nearly triangular, longer than wide, bending inward at proximal part to form an obtuse angle terminally; epiproct with large denticles on the middle of both sides, denticles base wider than half of the distance between two denticles base, bluntly rounded at apex; epiproct with longitudinal groove basally, disappearing in the middle. Cerci process conical, sharp at apex, and not reaching tip of epiproct. Subgenital plate long, sharp-cornered, and bluntly rounded at apex (Fig. 2E). In phallic complex, length of apical valves of penis slightly exceeds that of cingulum valves; apodemes longer than basal valves of penis, terminating in sword-like ends. Llateral view of basal valves of penis reveals a reniform shape and distal apodemes (Fig. 4G–I). Bridge of epiproct straight, thin, and elongated; ancorae angular, extending forward, with non-sharp tips; anterior projections extending forward but not surpassing ancorae length; lateral plates straight and posterior projections extending outward. Lophi large and flaky, extending towards medial sides, protruding noticeably in overall plane. In dorsal view, they appear trapezoidal, with evident tumor protrusions along the edge (Fig. 4J–L). **Female:** body robust, larger than male in size (Fig. 2G, H). Vertical diameter of eyes 1.1 times that of the transverse diameter and 0.9 times that of subocular furrows. Mesosternal interspace at least 2.8 times wider than long (Fig. 2I). Ovipositor margin smooth, with a hook-like apex (Fig. 2J). Other characteristics resemble those of the male.

**Coloration.** Body yellow or reddish-brown. Upper part of pronotum lobes darker in color than lower part. Two black spots on each of inner and outer sides of hind femur. Ventral face of hind femur black on outer side, red on basal 2/3 of inner and black on apical 1/3 of inner sides (Fig. 2K). Upper lateral genicular lobe black. Lower lateral genicular lobe dark yellow. Hind tibia purple above and dark brown below, with a lighter spot near the base of hind tibia. All tarsi yellowish, and sometimes 1st tarsomere purple.

**Measurements.** Shown in Table 4.

### *Kingdonella qinghaiensis* Zheng, 1990

Fig. 3

**Examined material.** CHINA • 4♂; Qinghai, Zhiduo; 33.76°N, 95.12°E, 19.VIII.2008; coll. Xinjiang Li, Jiantao Xiao, Yongchao Zhi; Catalogue number: #080819173 — #080819177. (first report of male)

**Diagnosis.** The male *Kingdonella qinghaiensis* resembles *K. parvula* Yin, 1984. The main differences are listed in Table 5.

**Table 4.** Measurement of *Kingdonella biruensis* sp. nov.

| Number of specimens | Male |  |  | Female |  |  |
|---|---|---|---|---|---|---|
|  | Body length | Pronotum length | Hind femur length | Body length | Pronotum length | Hind femur length |
| 1 | 15.75 | 3.33 | 9.13 | 19.76 | 3.66 | 10.35 |
| 2 | 17.03 | 3.42 | 9.05 | 22.69 | 3.78 | 10.60 |
| 3 | 15.77 | 3.05 | 8.89 | 22.34 | 3.86 | 10.27 |
| 4 | 15.13 | 3.14 | 9.61 | 22.58 | 4.29 | — |
| 5 | 15.27 | 3.04 | 9.14 | 23.78 | 4.37 | 10.51 |
| 6 | 14.60 | 3.14 | 8.88 | 21.12 | 3.88 | 10.70 |
| 7 | 16.89 | 3.19 | 9.89 | 22.49 | 4.85 | 10.96 |
| 8 | 15.55 | 3.32 | 8.55 | 21.36 | 4.12 | 11.50 |
| 9 | 16.12 | 3.52 | 9.33 | — | — | — |
| Min | 14.60 | 3.04 | 8.55 | 19.76 | 3.66 | 10.27 |
| Max | 17.03 | 3.52 | 9.89 | 23.78 | 4.85 | 11.50 |
| Median | 15.75 | 3.19 | 9.13 | 22.46 | 4.00 | 10.60 |

**Table 5.** Comparison the male of *Kingdonella qinghaiensis* Zheng, 1990 and *K. parvula* Yin, 1984.

| Characters | *Kingdonella qinghaiensis* | *K. parvula* |
|---|---|---|
| Width of mesosternal interspace | 2.0 times than length | 1.6 times than length |
| Outside of hind femur | Longitudinal dark spot present | Longitudinal dark spot absent |
| Hind tibia color | purple above and dark brown below | Yellowish-brown |

**Redescription. Male:** body small size (Fig. 3A, B). Head shorter than pronotum, with frons slightly oblique in profile. Frontal costa slightly shrunken in front of median ocellus. Eyes nearly elliptical, vertical diameter 1.2 times that of transverse diameter and subocular furrow length. Antennae filiform, 22–23 segments, longer than head and pronotum combined, length of a middle segment (12th segment) 1.5 times its width. Pronotum rough, slightly depressed medially on the anterior and posterior margins. Median carina distinct, lateral carinae nearly absent in metazona, lateral carinae cut by all transverse sulci and median carina cut by last transverse sulci; prozona 2.1 times longer than metazona. Prosternal process conical and blunt at apex. Width of mesothernal lobes 2.0 times the length (Fig. 3C). Width of mesothernal interspace 2.0 times length. Tegmina and wings absent. Upper median carina of hind femur smooth. Hind tibia with nine spines on inner and eight spines on outer sides; external apical spine absent. Arolium between claws large, nearly reaching apex. Posterior margin of 10th abdominal tergite with distinct furcula (Fig. 3D). Tympanal organ absent. Epiproct of male with larger denticles on middle of both sides; basally, denticles width nearly equal to half of length between denticles base, bluntly rounded at apex. Subgenital plate long and slightly sharp at apex (Fig. 3D). In phallic complex, length of the apical valves of penis slightly exceeds that of cingulum valves; apodemes longer than basal valves of penis, terminating in sword-like ends. The lateral view of the basal valves of the penis reveals a reniform shape and distal apodemes (Fig. 4M–O). Bridge of epiproct

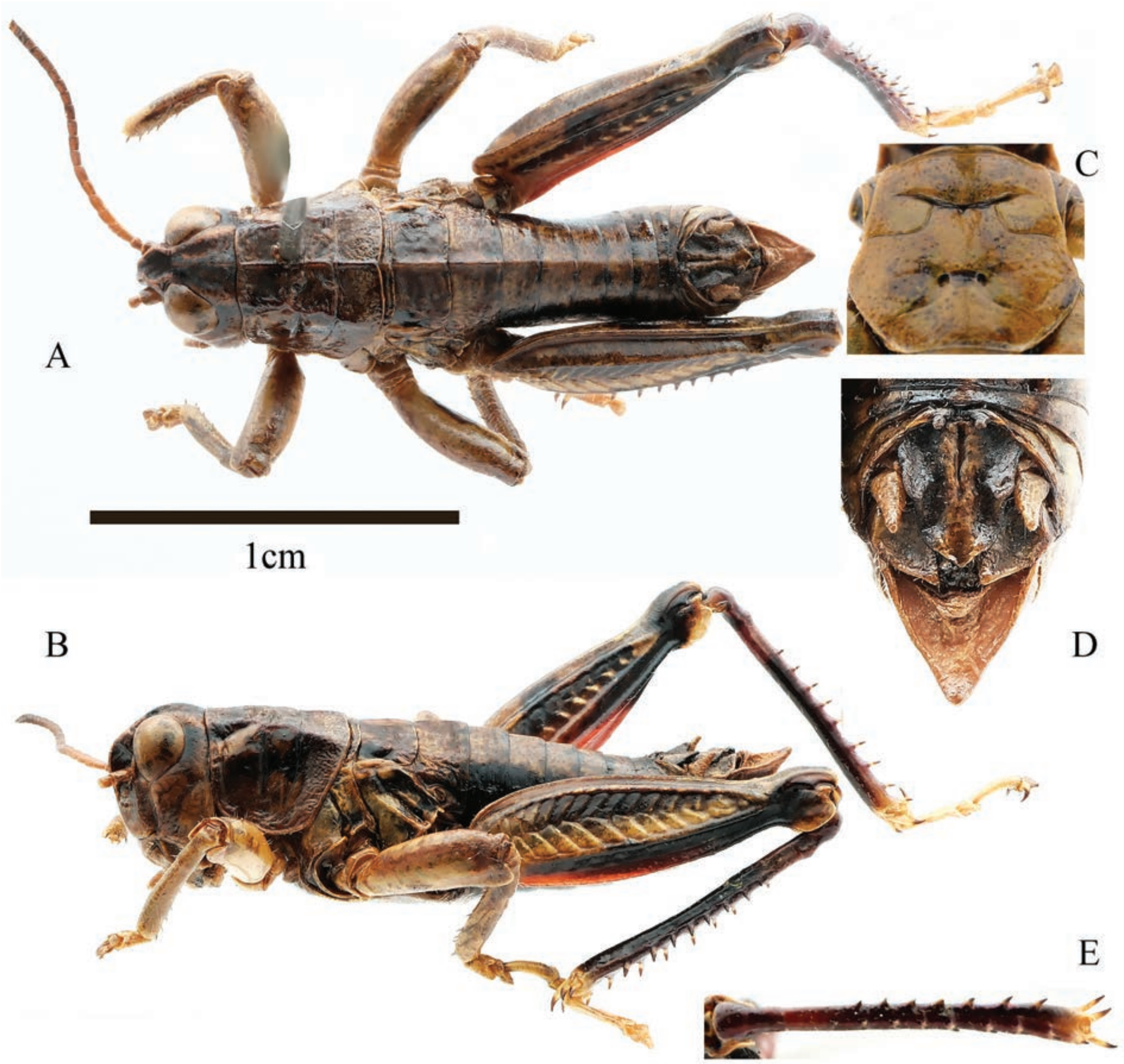

**Figure 3.** *Kingdonella qinghaiensis* Zheng, 1990, male **A** dorsal view **B** lateral view **C** sternal plate, ventral view **D** terminal of abdomen, dorsal view **E** hind tibia, dorsal view.

straight, wide, and short; ancorae angular, curving inward, with sharp tips; anterior projections not extending beyond length of ancorae; lateral plates incline outwards, and posterior projections extending outward. Lophi large and flaky, extending towards medial sides, protruding noticeably in overall plane. In dorsal view, inner length of the lophi longer than outer length, with evident tumor protrusions along edge (Fig. 4P–R).

**Coloration.** Body reddish-brown. Area behind the eyes with a black band. Antennae brown, apex black. Lateral lobes of pronotum with a black spot in center; remaining brown. Outer side of hind femur with a long dark spot, inner side base red, remaining black. Median and apical 3/4 of hind femur dorsal face with dark spot; ventral face of hind femur red on inner and black on outer side. Hind tibia purple above and dark brown below (Fig. 3E). All tarsi yellow.

**Measurements.** Shown in Table 6.

**Distribution.** Zhiduo, Qinghai Province, China.

**Table 6.** Measurement of male *Kingdonella qinghaiensis* Zheng, 1990.

| | Male | | |
|---|---|---|---|
| **Number of specimens** | **Body length** | **Pronotum length** | **Hind femur length** |
| 1 | 14.97 | 3.37 | 8.20 |
| 2 | 16.16 | 3.51 | 8.54 |
| 3 | 15.40 | 3.29 | 8.76 |
| 4 | 13.54 | 3.62 | 8.60 |
| min | 13.54 | 3.29 | 8.20 |
| max | 16.16 | 3.62 | 8.76 |
| median | 15.19 | 3.44 | 8.57 |

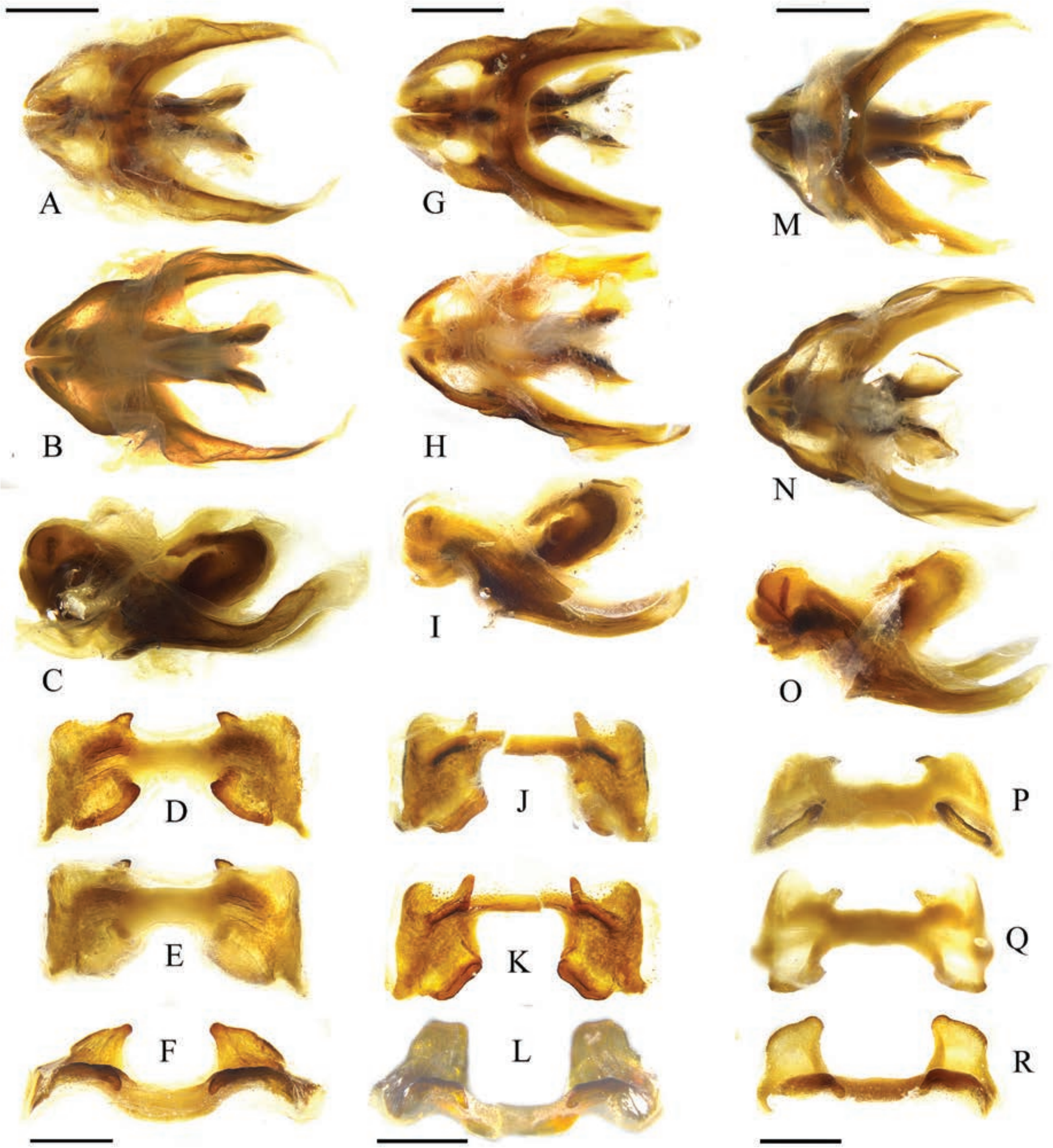

**Figure 4.** *Kingdonella gandensis* sp. nov. male **A–C** dorsal, ventral, and lateral views of phallic complex **D–F** dorsal, ventral, and axial views of epiphallus. *Kingdonella baigasis* sp. nov. male **G–I** dorsal, ventral, and lateral views of phallic complex **J–L** dorsal, ventral, and axial views of epiphallus. *Kingdonella qinghaiensis* male **M–O** dorsal, ventral, and lateral views of phallic complex **P–R** dorsal, ventral, and axial views of epiphallus.

## Key to species of *Kingdonella* Uvarov, 1933 (Li and Xia 2006)

1 In male, furcula at the end of 10th abdominal absent (Fig. 2F); epiproct with a transverse suture in the middle. Lateral carina of pronotum almost fully absent in both sexes, if distinct, epiproct of male with denticles on both ends of transverse suture ........ **2**

– In male, furcula at the end of 10th abdominal tergite distinct (Fig. 1E), epiproct without transverse suture in the middle. Lateral carinae of pronotum at least partly distinct ........ **5**

2 Median carina of pronotum almost fully absent between 1st and 3rd transverse sulci in both sexes. Lateral carina of pronotum almost fully absent. Ventral face of hind femur dark yellow on inner side. Epiproct of male without denticles at both ends of transverse suture ........ ***K. modesta***

– Median and lateral carine in pronotum fully distinct (Fig. 2A). Ventral face of hind femur red on the inner side (Fig. 2K). Epiproct of male with denticles at both ends of transverse suture ........ **3**

3 Mesosternal interspace wider in male; minimum width 2.5 times as long as length. Epiproct of male with small denticles at both ends of transverse suture ........ ***K. afurcula***

– Mesosternal interspace same width in both sexes; minimum width 1.7 times as long as length. Epiproct of male with larger denticles at both ends of transverse suture ........ **4**

4 Subgenital plate of male sharp-cornered (Fig. 2F). Ovipositor smooth (Fig. 2J) ........ ***K. biruensis* sp. nov.**

– Subgenital plate of male bluntly rounded. Ovipositor with blunt spines in upper valve ........ ***K. pienbaensis***

5 In males, epiproct without upward raised denticles in middle of both sides. Upper part of hind tibia in female greyish black ........ ***K. saxicola***

– In males, epiproct with upward raised denticles in middle of both sides (Fig. 1E). upper part of hind tibia of female not greyish black ........ **6**

6 Large and acute furcula at the end of 10th abdominal tergite in male. Epiproct of male with small denticles in middle of both sides. Ventral face of the hind femur in both sexes with only a small red spot at the base, remaining part black ........ **7**

– Small and obtuse furcula at the end of 10th abdominal tergite in male. Epiproct of male with large denticles in middle of both sides. Ventral face of hind femur in both sexes, at least on basal half, bright red or dark red ........ **8**

7 Epiproct of male without longitudinal groove in middle of base ........ ***K. hanburyi***

– Epiproct of male with longitudinal groove in middle of base ........ ***K. rivuna***

8 Eyes nearly circular in both sexes, vertical diameter nearly equal to transverse one in length ........ ***K. pictipes***

– Eyes elliptical in both sexes, vertical diameter 1.1–1.5 times as long as transverse one in length ........ **9**

9 Cerci longer, nearly reaching the tip of epiproct (Fig. 1E) ........ **10**

– Cerci shorter, far from reaching the tip of epiproct ........ **11**

10 Hind tibia in both sexes bright red ........ ***K. wardi***

– Hind tibia in both sexes black (Fig. 1A) ........ ***K. gandensis* sp. nov.**

11 Median carina of pronotum only cut by the 3rd transverse sulci in both sexes .................... **12**
– Median carina cut by the three transverse sulci in both sexes.................... **14**
12 Hind tibia yellowish-brown .................... ***K. parvula***
– Hind tibia black or purple (Fig. 3E) .................... **13**
13 Median carina of pronotum fully distinct (Fig. 3A) .................... ***K. qinghaiensis***
– Median carina of pronotum indistinct between 1st and 3rd transverse sulci .................... ***K. nigrotibia***
14 Ventral face of hind femur in both sexes bright red on inner side. Body small, in male less than 21 mm, in female less than 29 mm .................... **15**
– Ventral face of hind femur dark red on inner side of basal 3/5 in female. Body large, length of body more than 30 mm in females .................... ***K. maga***
15 Subgenital plate of male with conical spine projection at apex in male.................... **16**
– Subgenital plate of male without conical spine projection at apex in male.... **17**
16 Subgenital plate of male with short conical spine projection at apex. Posterior margin of end abdominal tergite with longe furcula. Frontal ridge almost parallel .................... ***K. concia***
– Subgenital plate of male with long conical spine projection at apex. Posterior margin of end abdominal tergite with shorter furcula. Frontal ridge slightly widened between antennae .................... ***K. longiconica***
17 Inner sides of hind femora in both sexes black. Subgenital plate of male relatively wider at apex.................... ***K. nigrofemora***
– Inner sides of hind femora in both sexes yellowish-brown or yellow-green, with two indistinct dark spots on inner sides. Subgenital plate in male relatively more acute and slender .................... **18**
18 Epiproct of male with smaller denticles in middle of both sides; width at base less than 1/5 width of epiproct at denticles ....................***K. kozlovi***
– Epiproct of male with larger denticles in middle of both sides; width at base less than 1/3 width of epiproct at denticles .................... ***K. bicollina***

## Acknowledgements

We thank Jiantao Xiao and Dr Yongchao Zhi for their collection of specimens of the *Kingdonella* genus in the Qinghai-Xizang area.

## Additional information

### Conflict of interest

The authors have declared that no competing interests exist.

### Ethical statement

No ethical statement was reported.

### Funding

This research is funded by the National Natural Science Foundation of China (no. 32070473) and the Hebei Provincial Innovation Capacity Enhancement Program Special Project for High-level Talent Team Building (no. 225A2904D).

## Author contributions

Conceptualization: JC. Data curation: JC. Funding acquisition: XL, YZ. Resources: YZ, XL. Validation: JC. Writing - original draft: JC. Writing - review and editing: JC.

## Author ORCIDs

Jianyu Chen https://orcid.org/0000-0002-4993-3544
Yulong Zhang https://orcid.org/0009-0002-7983-515X
Xinjiang Li https://orcid.org/0000-0001-5204-0491

## Data availability

All of the data that support the findings of this study are available in the main text.

## References

Huang C (1981) Insects of Xizang, Orthoptera: Acrididae, Catantopinae, Pyrgomorphinae, Oedipodinae. 1. Science Press, Beijing, 82–83.

Li HC, Xia KL (2006) Orthoptera, Acridoidea, Catantopidae. Fauna Sinica. Insecta 43: 431–451.

Li XJ, Yin XC (2009) A taxonomic study of the subfamily Conophyminae (Orthoptera: Caelifera: Acridoidea) from Eurasia. Acta Entomologica Sinica 52(10): 1139–1144.

Liu L, Wang Q, Zhang Z, He X, Yu Y (2023) MATO: An updated tool for capturing and analyzing cytotaxonomic and morphological data. The Innovation Life 1(1): 1–7. https://doi.org/10.59717/j.xinn-life.2023.100010

Mishchenko (1952) Locusts and grasshoppers, Catantopinae. Fauna of the U.S.S.R. 4(2): 453–462.

Uvarov (1933) *Kingdonella wardi*, gen. et sp. n., a new grasshopper (Orthoptera, Acrididae) from the Assam Himalayas. Annals and Magazine of Natural History, London (Series 10) 11(64): 468–470. https://doi.org/10.1080/00222933308673677

Uvarov (1935) Three new grasshoppers from South-eastern Tibet (Orthoptera: Acrididae). Annals and Magazine of Natural History, London 10 15: 192–196. https://doi.org/10.1080/00222933508655036

Uvarov (1939) Some Acrididae from south-eastern Tibet. Zoological Journal of the Linnean Society 40(3): 561–574. https://doi.org/10.1111/j.1096-3642.1939.tb01693.x

Yin XC (1984) Grasshoppers and locusts from Qinghai-Xizang Plateau of China, Science Press, Beijing, 79–93.

Zheng Z (1980) New species of grasshoppers from China (Orthoptera: Acrididae). Acta Entomologica Sinica 23(2): 191–194.

Zheng Z (1990) Three new species of grasshoppers from Hengduanshan Range of China (Orthoptera: Acridoidea). Dong Wu Fen Lei Xue Bao 15(2): 197–200.

ZooKeys 1205: 267–298 (2024)
DOI: 10.3897/zookeys.1205.120033

Research Article

# A first revision of the *Andrena* of Iraq (Hymenoptera, Andrenidae), with the description of two new species from Iraqi Kurdistan and additional records from surrounding countries

Thomas J. Wood[1], Halgurd R. Ismael[2], Daniele Baiocchi[3], Mudhafar I. Hamad[4],
Tahseen T. Bapir[2], Marco Selis[5]

1 Naturalis Biodiversity Center, 2333 CR, Leiden, Netherlands
2 Department of Plant Protection, College of Agricultural Engineering Sciences, University of Duhok, Duhok, Kurdistan Region, Iraq
3 Via Matteo Babini 26, 00139, Roma, Italy
4 Khabat Technical Institute, Erbil Polytechnic University, Erbil, Kurdistan Region, Iraq
5 Via dei Tarquini 22, 01100 VT, Viterbo, Italy
Corresponding author: Thomas J. Wood (thomas.wood@naturalis.nl)

## Abstract

Iraq is a large country in the Middle East region that borders both Turkey and Iran, countries known to host two of the largest bee faunas globally, as expected for a group of insects that favour dry to Mediterranean climates. Despite this huge regional species richness, the bee fauna of Iraq is chronically understudied and poorly known, both in relative and absolute terms. This is true for the hyper-speciose bee genus *Andrena*, for which only 17 species have been previously published for Iraq. This work is the first modern contribution to the revision of the *Andrena* fauna of Iraq. Based on new specimen collections in Duhok Governorate (Iraqi Kurdistan) during 2023, a revised total of 59 *Andrena* species for Iraq (42 species recorded for the first time) is presented, including the description of two new species: *Andrena* (*Aciandrena*) *duhokensis* Wood, **sp. nov.** and *Andrena* (*Notandrena*) *baiocchii* Wood, **sp. nov.** The unknown males of *A.* (*Micrandrena*) *elam* Wood, 2022, *A.* (*Micrandrena*) *obsidiana* Wood, 2022, and *A.* (*Notandrena*) *ayna* Wood, 2023 are described. *Andrena bakrajoensis* Amin & Mawlood, 2019, **syn. nov.** is synonymised with *A.* (*Holandrena*) *variabilis* Smith, 1853. Additional records are presented from nearby Middle Eastern countries, particularly Lebanon. These results highlight the fundamentally understudied nature of the Iraqi *Andrena* fauna.

**Key words:** Middle East, pan trap, solitary bees, taxonomy, understudied fauna

OPEN ACCESS

Academic editor: Thorleif Dörfel
Received: 1 February 2024
Accepted: 23 April 2024
Published: 1 July 2024

ZooBank: https://zoobank.org/1093570E-D1C7-4918-BD8F-0BC3D3F486E5

Citation: Wood TJ, Ismael HR, Baiocchi D, Hamad MI, Bapir TT, Selis M (2024) A first revision of the *Andrena* of Iraq (Hymenoptera, Andrenidae), with the description of two new species from Iraqi Kurdistan and additional records from surrounding countries. ZooKeys 1205: 267–298. https://doi.org/10.3897/zookeys.1205.120033

## Introduction

*Andrena* is the second largest genus of bees with approximately 1,700 species following recent revisions (e.g., Pisanty et al. 2022a; Wood and Monfared 2022; Wood 2023, 2024). *Andrena* are known for their explosive radiation and rapid rate of speciation (Bossert et al. 2022), and are likely to have evolved in the Middle East region ca 25 million years ago (Pisanty et al. 2022b). In line with this expected point of origin, the *Andrena* faunas of several Middle Eastern countries are very large, with ca 220 species known from Israel, 215 species known from Iran, and 388 species known from Turkey (Pisanty et al. 2022a; Wood and Monfared 2022; Wood 2023, 2024; Wood, unpublished data). The *Andrena* fauna of Syria is also large, but has not been comprehensively revised, and many species are present which have not yet had their occurrence formally published, with ~ 154–166 species known but not yet fully demonstrated or confirmed (Wood 2020; Wood et al. 2020; Pisanty et al. 2022a; Wood and Monfared 2022; Wood, unpublished data).

In contrast, the published *Andrena* fauna of the country of Iraq is extremely small, with only 17 species mentioned across various literature sources (Morice 1921a, 1921b; Derwesh 1965; Warncke 1969; Khalaf and Al-Omar 1974; Moalif 1994; Gusenleitner and Schwarz 2002; Scheuchl and Willner 2016; Augul 2018; Amin and Mawlood 2019; Ascher and Pickering 2023), some of which primarily cite previous publications without adding any new information, or which never present detailed specimen records at all. The Iraqi *Andrena* fauna has very rarely received dedicated attention, most frequently with species listed without supporting specimens or mentioned museum depositories, in strong contrast to neighbouring Turkey (e.g., Warncke 1965, 1974, 1975; Scheuchl and Gusenleitner 2009; Scheuchl and Hazir 2012; Hazir et al. 2014; Wood 2023) and to a lesser extent Iran and Syria (e.g., Popov 1967; Khodarahmi Ghahnavieh and Monfared 2019; Wood et al. 2020; Wood 2020; Radchenko et al. 2021; Wood and Monfared 2022).

Given the very high *Andrena* species richness found in nearby countries, it is clearly implausible that the Iraqi *Andrena* fauna is so small. In order to counter this knowledge deficit, we conducted new collections in northern Iraq during spring 2023, and critically reviewed the literature and museum collections in order to produce an updated faunal total.

## Materials and methods

*Andrena* specimens were collected from various localities in Duhok province, Iraq (Kurdistan region) during May 2023 (Fig. 1: locations 1, 2, and 3). Specimens were collected using yellow pan traps which were filled with water and placed adjacent to vegetation (Fig. 2C).

Morphological terminology follows Michener (2007). The following abbreviations are used in the species descriptions: **A** = antennal segments, **S** = metasomal sterna, and **T** = metasomal terga. In diagnoses, the defining characters of a species are given, with those of the indicated comparison species given in parentheses. Subgeneric concepts follow Pisanty et al. (2022b). Specimens were measured from the centre of the clypeus at the front of the head to the apical tip of the metasoma to the nearest 0.5 mm. In the faunal list, taxa are presented alphabetically, first by subgenus and then by species. In the full faunal list, species entries followed by an asterisk (*) indicate the first record for Iraq. Likewise, for the global distributions of species, countries marked with an asterisk (*) indicate the first published record for that country. All specimens were identified by T.J. Wood.

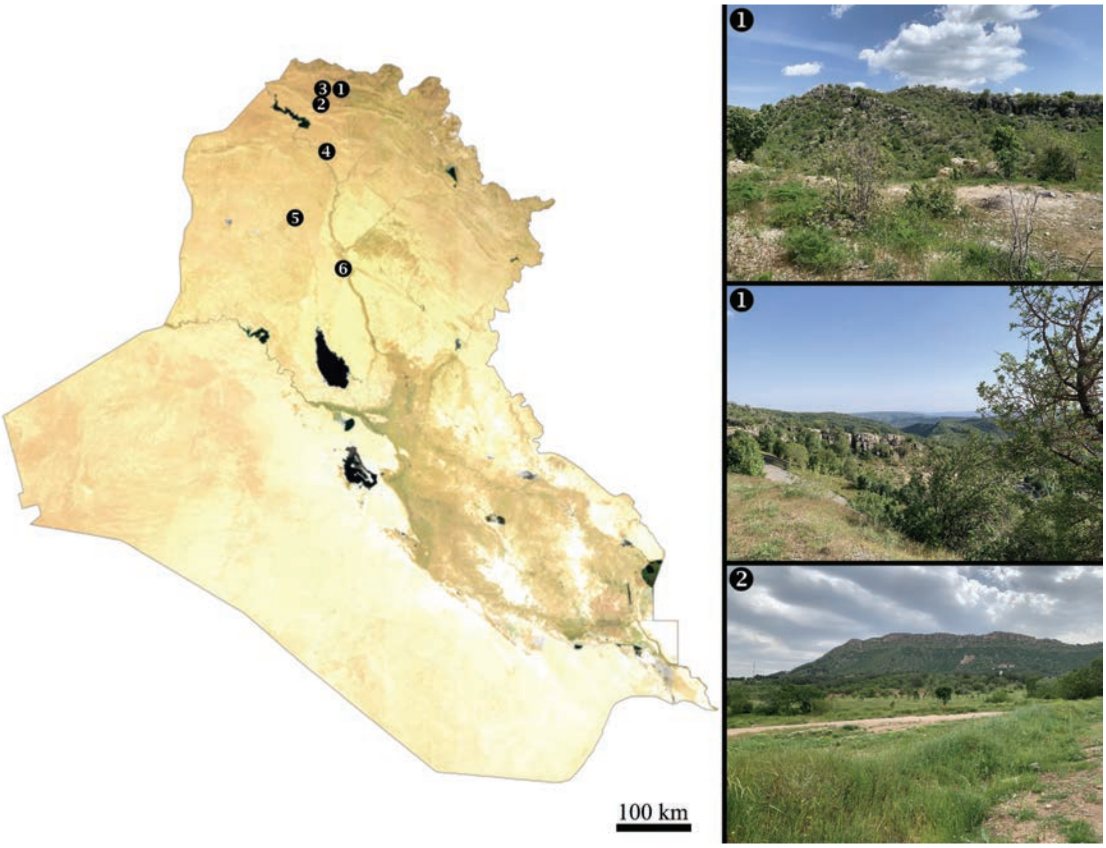

**Figure 1.** Map of Iraq with novel data sites marked. New data locations: 1. Mount Gara, south of Sarsing, Duhok Governorate; 2. Besereh, Bablo, Duhok Governorate; 3. Mangesh, Duhok Governorate; 4. Mosul, Nineveh Governorate; 5. Hatra, Nineveh Governorate; 6. Baiji, Saladin Governorate. Landscape photographs correspond to localities 1 and 2.

**Figure 2.** Sampling participants in Duhok Governorate during May 2023 **A** sampling participants from left to right: Mudhafar Hamad, Daniele Baiocchi, Gianluca Magnani, Halgurd Ismael, Pierpaolo Rapuzzi **B** selection of sampling sites **C** yellow pan trap placed adjacent to vegetation **D** pan trap collection and inspection.

Photographs were taken using an Olympus E-M1 Mark II with a 60 mm macro lens. Additional close-ups were taken with the addition of a Mitutoyo M Plan Apo 5X infinity corrected objective lens. Photographs were stacked using Helicon Focus B (HeliconSoft, Ukraine) and plates were prepared in GNU Image Manipulation Program (GIMP) 2.10. Post-processing of some images was made in Photoshop Elements (Adobe Systems, USA) in order to improve lighting to highlight specific characters. The map of Iraq was taken from GISGeography (2024).

### Abbreviations of depositories

| | |
|---|---|
| **DUMAI** | University of Duhok, Museum of Agriculture College, Duhok, Iraq |
| **MSVI** | Personal collection of Marco Selis, Viterbo, Italy |
| **NHMUK** | Natural History Museum, London, United Kingdom |
| **OÖLM** | Oberösterreiches Landesmusum, Linz, Austria |
| **RMNH** | Naturalis Biodiversity Center, Leiden, the Netherlands |
| **TJWC** | Personal collection of Thomas J. Wood, Leiden, the Netherlands |

## Results

### Full Iraqi faunal list

#### 1. *Andrena* (*Aenandrena*) *aeneiventris* Morawitz, 1872

**Literature records.** Gusenleitner and Schwarz (2002: dot map 11); Scheuchl and Willner (2016); Ascher and Pickering (2023).

**Remarks.** We have not examined any specimens of this species, but the presence of this species in Iraq is highly plausible based on its known global distribution, the map records indicated by Gusenleitner and Schwarz (2002), and the presence of this species in neighbouring Turkey and Iran.

**Distribution.** West and Central Palearctic (Gusenleitner and Schwarz 2002; Osytshnjuk et al. 2005).

#### 2. *Andrena* (*Notandrena*) *aerinifrons* Dours, 1873 *

**Material examined. Iraq:** Mosul, edges of a river, 7.iv.1988, 1♂, leg. Olejníček, OÖLM; **Lebanon:** Balbek-Hermel, Sefri, Haouch Snaid, AUB farm, 33.9244°N, 36.0754°E, 1000 m, 6.iv.2023, 1♂, 8♀, leg. T.J. Wood, TJWC.

**Remarks.** The status of the subspecies *levantina* Hedicke, 1938 (which nominally occurs in the Middle East) is unclear, and may not be merited, although *A. aerinifrons* sensu lato shows high and difficult-to-interpret intraspecific variation in its mitochondrial DNA barcode (Wood, unpublished data).

**Distribution.** *Andrena aerinifrons* sensu lato is distributed from Iberia and North Africa to the Middle East including Iraq* and Iran (Gusenleitner and Schwarz 2002; Wood and Monfared 2022).

### 3. *Andrena* (*Taeniandrena*) *afzeliella* (Kirby, 1802)

**Literature records.** Gusenleitner and Schwarz (2002: dot map 345, as *A. ovatula* (Kirby, 1802)); Ascher and Pickering (2023).

**Remarks.** We have not examined any specimens of this historically confused species (see Praz et al. 2022), but the presence of this species in Iraq is highly plausible based on its known global distribution, the map records indicated by Gusenleitner and Schwarz (2002), and the presence of this species in neighbouring Turkey and Iran where it is abundant.

**Distribution.** Somewhat unclear due to historical taxonomic confusion, but probably West and Central Palearctic (Praz et al. 2022; Wood and Monfared 2022; Ascher and Pickering 2023).

### 4. *Andrena* (*Melandrena*) *albifacies* Alfken, 1927

**Literature records.** Warncke (1969); Gusenleitner and Schwarz (2002: dot map 17); Grace (2010); Augul (2018); Wood and Monfared (2022); Ascher and Pickering (2023).

**Remarks.** We have not examined any specimens of this species, but the presence of this species in Iraq is highly plausible based on its known global distribution, the mention of this species from southern Iraq (Warncke 1969), the map records indicated by Gusenleitner and Schwarz (2002), and the presence of this species in neighbouring Iran.

**Distribution.** Morocco, Algeria, Tunisia, Libya, Egypt, Israel and West Bank, Jordan, Syria, Iraq, Iran (Warncke 1969; Gusenleitner and Schwarz 2002; Wood and Monfared 2022; Ascher and Pickering 2023).

### 5. *Andrena* (*Truncandrena*) *albopicta* Radoszkowski, 1874

**Literature records.** Gusenleitner and Schwarz (2002: dot map 18); Grace (2010); Augul (2018); Ascher and Pickering (2023).

**Remarks.** We have not examined any specimens of this species, but the presence of this species in Iraq is plausible: the species is present in south-eastern Turkey (see specimen records presented by Wood and Monfared 2022), and the dot map presented by Gusenleitner and Schwarz (2002) seems to indicate the presence of this species in northern Iraq. It is therefore tentatively accepted as present.

**Distribution.** Turkey, Armenia, Iraq, Iran (Gusenleitner and Schwarz 2002; Ascher and Pickering 2023), note that previous records from European Russia were erroneous, see Proshchalykin et al. (2023).

### 6. *Andrena* (*Melandrena*) *albopunctata* (Rossi, 1792)

**Literature records.** Gusenleitner and Schwarz (2002: dot map 19); Ascher and Pickering (2023).

**Remarks.** We have not examined any specimens of this species, but the presence of this species in Iraq is highly plausible based on its known global distribution, the map records indicated by Gusenleitner and Schwarz (2002), and the presence of this species in neighbouring Turkey and Iran.

**Distribution.** West and Central Palearctic (Gusenleitner and Schwarz 2002; Osytshnjuk et al. 2008).

### 7. *Andrena* (incertae sedis) *antilibanotica* Wood, 2020 *

**Material examined. Iraq:** Duhok, Mt. Gara [S of Sarsing], 37.0158°N, 43.3506°E, 1912 m, 11.v.2023, 3♂, leg. D. Baiocchi, MSVI.

**Distribution.** Syria, Turkey, Iraq*, Iran (Wood and Monfared 2022; Wood 2023).

### 8. *Andrena* (*Chlorandrena*) *astica* Warncke, 1967 *

**Material examined. Iraq:** Duhok, Mt. Gara [S of Sarsing], 37.0158°N, 43.3506°E, 1912 m, 11.v.2023, 3♂, leg. D. Baiocchi, MSVI/TJWC; **Lebanon:** Bekaa, Qob Elias valley, 33.7989°N, 35.8192°E, 900 m, 5.iv.2023, 1♂, leg. M. Boustani, TJWC.

**Distribution.** Greece, Turkey, Cyprus, Israel and West Bank, Lebanon*, Georgia, Iraq*, Iran (Schwenninger 2015; Wood and Monfared 2022).

### 9. *Andrena* (*Notandrena*) *ayna* Wood, 2023 *

**Material examined. Iraq:** Duhok, Mt. Gara [S of Sarsing], 37.0158°N, 43.3506°E, 1912 m, 11.v.2023, 3♂, leg. D. Baiocchi, MSVI/TJWC.

**Remarks and diagnosis.** Wood (2023) described *A. ayna* from south-eastern Turkey (province of Hakkâri) based on two female specimens. Three male specimens from northern Iraq are now available. They are recognisable as *Notandrena* due to the short and broad head (Fig. 3B; 1.25× wider than long), the apex of the clypeus narrowed and slightly upturned, the at least partially yellow-marked clypeus, the broadened and weakly carinate gena (Fig. 3C; broader than the diameter of the compound eye), and the pronotum with a strong humeral angle. As in the female sex, *A. ayna* is immediately recognisable due to the sculpture of the scutum and scutellum which are almost entirely smooth and shiny over their entirely area, with scattered and sparse punctures (Fig. 3D).

**Description. Male.** ***Body length*:** 6.5–7 mm (Fig. 3A). ***Head*:** Dark, 1.25× wider than long (Fig. 3B). Clypeus variably yellow-marked, from medial ½ with yellow spot which does not extend to lateral margins to almost entirely dark with small pale dot medio-apically. Clypeus broadly flattened medially, surface densely and shallowly punctate, punctures separated by 0.5–1 puncture diameter, surface dull; apical margin narrow, projecting, anterior margin slightly upturned, weakly emarginate. Process of labrum tiny, trapezoidal, slightly wider than long, surface polished and shining. Gena 1.5× wider than diameter of compound eye, posterior margin weakly carinate, surface covered with curved striations (Fig. 3C); ocelloccipital distance subequal to diameter of lateral ocellus. Head covered with sparse light brownish pubescence, hairs not equalling length of

**Figure 3.** *Andrena* (*Notandrena*) *ayna* Wood, 2023 male **A** habitus, lateral view **B** face, frontal view **C** head, lateral view **D** scutum, dorsal view **E** terga, dorsal view **F** genital capsule, dorsal view.

scape. Antennae basally dark, A4–13 ventrally lightened by presence of greyish-brown scales; A3 exceeding A4, shorter than A4+5.

***Mesosoma*:** Scutum and scutellum polished and shining over almost entire surface, scutum weakly shagreened anteriorly; scutum with scattered irregular punctures, punctures separated by 1–5 puncture diameters, scutellum almost impunctate (Fig. 3D). Pronotum with strongly produced humeral angle, deep vertical furrow with surface shining, remaining lateral face of propodeum with longitudinal striations. Mesepisternum irregularly microreticulate, weakly shining. Dorsolateral parts of propodeum shagreened, weakly shining, sculpture overlain by network of irregular raised rugosity; propodeal triangle laterally defined by fine straight carinae, internal surface with network of rugae radiating from base, propodeal triangle not strongly differentiated from remaining propodeum. Mesosoma covered with sparse light brown hairs, none equalling length of scape. Legs dark, apical tarsal segments paler orange-brown, pubescence whitish. Hind tarsal claws with inner tooth. Wings hyaline, stigma and venation orange, nervulus antefurcal.

***Metasoma*:** Tergal discs dark, marginal areas broadly lightened hyaline brown-white (Fig. 3E). Terga with sculpture variable, disc of T1 smooth and shining, T2–4 with base weakly shagreened, sculpture disappearing medially, tergal margins without sculpture. T1 with disc sparsely punctate, punctures separated by 2–3 puncture diameters, discs of T2–4 with punctures separated by 1–2 puncture diameters, marginal areas impunctate. Tergal discs with scattered pale hairs, not forming hairbands. T6–7 with light brown hairs overlying pseudopygidial plate. S8 columnar, short, apical margin truncate, ventral surface with sparse short brown hairs. Genital capsule compact, gonocoxae with inner margins almost forming rounded 90° angle, very weakly projecting (Fig. 3F). Gonostyli narrow basally, strongly broadening and flattened apically, inner margin raised, outer surface with short golden-brown hairs. Penis valves occupying ½ space between gonostyli, outer margins slightly thickened, progressively narrowing apically.

**Distribution.** South-eastern Turkey (Hakkâri) and northern Iraq* (Wood 2023).

### 10. *Andrena* (*Notandrena*) *baiocchii* Wood, sp. nov. *

https://zoobank.org/6005A148-DD6C-45CE-8284-4DB733F080F1

**Material examined.** ***Holotype*: IRAQ:** Duhok, Mt. Gara [S of Sarsing], 37.0158°N, 43.3506°E, 1912 m, 11.v.2023, 1♀, leg. D. Baiocchi, RMNH. ***Paratypes*: IRAQ:** Same information as holotype, 5♀, MSVI/RMNH/TJWC/DUMAI.

**Diagnosis.** *Andrena baiocchii* can be recognised as part of the subgenus *Notandrena* Pérez, 1890 due to the dorsolateral angle of the pronotum with a strong transverse ridge (= pronotum with a strong humeral angle), dull impunctate terga (Fig. 4F; hence placing it closer to members of the former subgenus *Carandrena* Warncke, 1968), scutum with distinct but weakly shining to dull green-purple metallic reflections (Fig. 4D), hind tibiae which weakly but distinctly broaden medially and apically, resembling a crude isosceles triangle and covered with simple scopal hairs, and lack of any other distinctive characters. This combination of characters places it close to *A. schlettereri* Friese, 1896 (Central Europe to Turkey), *A. purpureomicans* Alfken, 1935 (Turkey), *A. trimarginata* (Radoszkowski, 1886) (= *A. zostera* Warncke, 1975; Middle East and Central Asia, see below), and *A. aerinifrons* Dours, 1873 sensu lato (Iberia, North Africa, and the Middle East). *Andrea baiocchii* can be separated from all these comparison species by the shape of the head which is almost round, only 1.1× wider than long (Fig. 4B; in comparison species is the head shorter, 1.2–1.4× wider than long) and the clypeus has contrasting surface sculpture, shagreened and weakly shining basally but becoming smooth and shining in its apical half AND with

**Figure 4.** *Andrena* (*Notandrena*) *baiocchii* sp. nov. female **A** habitus, lateral view **B** face, frontal view **C** clypeus, frontal view detail **D** scutum, dorsal view **E** propodeum, dorsal view **F** terga, dorsal view.

punctures becoming sparse, in the apical 1/3 of the clypeus with punctures separated by 1–3 puncture diameters (Fig. 4C). In comparison species the clypeus usually has a uniform sculpture, typically dull, never smooth and shining in its apical half (with the exception of *A. trimarginata*) and the clypeal punctures are consistently denser. *Andrena trimarginata* can be separated by the overall shape of the head (clearly wider than long) and by the density of clypeal punctures which are separated by a consistent 0.5–1 puncture diameters over the entire surface of the clypeus. Some individual species can also be separated with additional characters, as *A. baiocchii* has a small body size of 7–8 mm (usually 8–9 mm in *A. aerinifrons*), the propodeal triangle has a network of finely raised rugae covering ¾ of its surface (Fig. 4E; surface smooth in *A. aerinifrons*), and the tarsi are dark and the terga are completely impunctate (with the tarsi lightened orange and the terga with shallow but distinct punctures in *A. purpureomicans*). The male is unknown, but is expected to share the relatively elongate head which is unusual within this group of species.

**Description. Female.** ***Body length*:** 7–8 mm (Fig. 4A). ***Head*:** Dark, 1.1× wider than long (Fig. 4B). Clypeus domed, variably sculptured, in basal ½ with fine granular shagreen, weakly shining, in apical ½ smooth and shining, polished; surface punctate, punctures separated by 1–3 puncture diameters (Fig. 4C). Process of labrum small, rounded trapezoidal, 2× wider than long, apical margin weakly emarginate. Gena marginally exceeding diameter of compound eye; ocelloccipital distance equals ½ diameter of lateral ocellus. Foveae dorsally occupying slightly < ½ space between compound eye and lateral ocellus, slightly narrowing ventrally, separated from inner margin of compound eye by distance subequal to its own diameter; foveae filled with brown hairs. Face, gena, vertex, and scape with sparse light brown hairs, none equalling length of scape. Antennae basally dark, A5–12 ventrally lightened by presence of grey-orange scales; A3 slightly exceeding A4+5, slightly shorter than A4+5+6.

***Mesosoma*:** Scutum and scutellum with dense fine granular microreticulation, weakly shining to dull, laterally and anteriorly with weak but distinct green-purple metallic reflections; surface irregularly and obscurely punctate, punctures separated laterally by 1–3 puncture diameters, medially by 3–5 puncture diameters (Fig. 4D). Pronotum with strong humeral angle. Mesepisternum and dorsolateral parts of propodeum with dense granular microreticulation, dull; propodeal triangle delineated by change in surface sculpture, predominantly covered with finely raised rugae over ¾ of its surface (Fig. 4E). Mesosoma with light brown hairs, longest on mesepisternum, not equalling length of scape. Propodeal corbicula incomplete, dorsal fringe composed of long plumose light brown hairs, internal surface with scattered light brown hairs. Legs predominantly dark, apical tarsal segments lightened brownish, pubescence light brown. Flocculus complete but relatively sparse, composed of light brown plumose hairs; femoral and tibial scopae composed of light brown-golden simple hairs. Hind tarsal claws with very small inner tooth. Wings hyaline, stigma bright orange, venation dark orange, nervulus antefurcal.

***Metasoma*:** Terga dark, apical margins weakly but distinctly depressed, partially lightened brown; tergal discs with regular granular microreticulation, weakly shining, essentially impunctate, with very weak and sparse punctures disappearing into background sculpture (Fig. 4F). Terga with scattered short white hairs, not forming apical hairbands. Apical fringe of T5 and hairs flanking pygidial plate orange. Pygidial plate large, broadly rounded triangular, lateral margin weakly raised and impunctate, internal surface densely punctate, punctures separated by < 0.5 puncture diameters.

**Male.** Unknown.

**Etymology.** The species is named after Daniele Baiocchi who has collected insects across much of the Mediterranean basin and Middle East, and who led bee collection during the expedition to Duhok Governorate in May 2023.

**Distribution.** Iraq (Kurdistan region).

### 11. *Andrena* (*Plastandrena*) *bimaculata* (Kirby, 1802)

**Literature records.** Gusenleitner and Schwarz (2002: dot map 55); Scheuchl and Willner (2016); Ascher and Pickering (2023).

**Remarks.** We have not examined any specimens of this species, but the presence of this species in Iraq is highly plausible based on its known global distribution, the map records indicated by Gusenleitner and Schwarz (2002), and the presence of this species in neighbouring Turkey and Iran. We note however that the species concept of *A. bimaculata* is unclear, and all Old World members of the subgenus *Plastandrena* require revision using molecular markers. It should therefore be considered in a sensu lato at the present time.

**Distribution.** In a sensu lato, West and Central Palearctic to Mongolia (Gusenleitner and Schwarz 2002; Ascher and Pickering 2023).

### 12. *Andrena* (*Cryptandrena*) *brumanensis* Friese, 1899 *

**Material examined.** **Iraq:** Duhok, Bessre [Besereh], Bablo, 36.8675°N, 43.1206°E, 1065 m, 5–6.v.2023, 1♀, leg. D. Baiocchi, MSVI; Duhok, E Mangesh, 37.0230°N, 43.1505°E, 1046 m, 8.v.2023, 1♂, leg. D. Baiocchi, MSVI.

**Distribution.** Southern Europe to Turkey and the Near East, including Iraq* and Iran (Gusenleitner and Schwarz 2002; Wood and Monfared 2022).

### 13. *Andrena* (*Truncandrena*) *caneae* Strand, 1915 *

**Material examined.** **Iraq:** Duhok, Mt. Gara [S of Sarsing], 37.0158°N, 43.3506°E, 1912 m, 11.v.2023, 1♂, leg. D. Baiocchi, MSVI/TJWC.

**Distribution.** Greece, Turkey, Cyprus, Syria, Iraq* (Gusenleitner and Schwarz 2002).

### 14. *Andrena* (*Micrandrena*) *cedricola* Wood, 2020 *

**Material examined.** **Iraq:** Duhok, Mt. Gara [S of Sarsing], 37.0158°N, 43.3506°E, 1912 m, 11.v.2023, 2♂, leg. D. Baiocchi, MSVI/TJWC.

**Distribution.** Israel, Lebanon, Syria, Turkey, Iraq* (Pisanty et al. 2022a).

### 15. *Andrena* (*Chlorandrena*) *cinereophila* Warncke, 1965 *

**Material examined.** **Iraq:** Duhok, Mt. Gara [S of Sarsing], 37.0158°N, 43.3506°E, 1912 m, 11.v.2023, 1♂, leg. D. Baiocchi, MSVI; **Lebanon:** Balbek-Hermel, Sefri, Haouch Snaid, AUB farm, 33.9244°N, 36.0754°E, 1000 m, 6.iv.2023, 11♀, leg. T.J. Wood, TJWC; Beqaa, Anjar, 1 km E, Armenian Cemetary, 33.7372°N, 35.9503°E, 900 m, 7.iv.2023, 1♀, leg. T.J. Wood, TJWC; Beqaa, Beqaa valley, Mansourah, Aammiq wetland preserve, 33.7321°N, 35.7853°E, 850 m, 3.iv.2023, 1♂, leg. T.J. Wood, TJWC; Beqaa, Beqaa valley, Qaraoun dam, 33.5483°N, 35.6851°E, 850 m, 6.iv.2023, 3♂, leg. T.J. Wood, TJWC.

**Distribution.** East Mediterranean to Central Asia, including Lebanon* and Iraq* (Gusenleitner and Schwarz 2002; Osytshnjuk et al. 2005; Wood and Monfared 2022).

### 16. *Andrena* (*Cordandrena*) *cordialis* Morawitz, 1878

**Literature records.** Morice (1921b); Derwesh (1965), mentioning "Survey of Iraq Fauna 1915–1919"; Augul (2018).

**Material examined.** **Iraq:** Baiji [Saladin Governorate, 35.0299°N, 43.4489°E], 1–31.iii.1986, 1♀, leg. M. Carl, OÖLM; Baiji, 1–30.iv.1986, 2♂, leg. M. Carl, OÖLM.

**Remarks.** *Andrena cordialis* is part of a tricky group of species to identify, with the species *A. cypria* Pittioni, 1950 and *A. torda* Warncke, 1965 described after the 1915–1919 survey was conducted. Morice (1921b) specifically mentioned the species from Basrah in southern Iraq. Based on our examined material, we can confidently confirm both *A. cordialis* and *A. torda* from Iraq, and so the record of Morice (1921b) is considered plausible. We note here that the "Survey of Iraq Fauna 1915–1919" is represented by the publications of Morice (1921a; 1921b), only Morice (1921b) dealing with the *Andrena* fauna.

**Distribution.** Eastern Europe through Turkey and the Caucasus to Central Asia, including Iraq and Iran (Gusenleitner and Schwarz 2002; Osytshnjuk et al. 2005; Wood and Monfared 2022)

### 17. *Andrena* (*Poecilandrena*) *crassana* Warncke, 1965 *

**Material examined.** **Iraq:** Duhok, Mt. Gara [S of Sarsing], 37.0158°N, 43.3506°E, 1912 m, 11.v.2023, 2♂, leg. D. Baiocchi, MSVI; **Lebanon:** Beqaa, Beqaa valley, Qaraoun, 3.5 km W of Madjal Balhis, 33.5377°N, 35.7038°E, 900 m, 4.iv.2023, 1♂, leg. T.J. Wood, TJWC.

**Remarks.** Specimens from Iraq nominally belong to *A. crassana* s. str. And the specimen from Lebanon nominally belongs to ssp. *Inka* Warncke, 1969 (Levant). It is not clear if *inka* merits subspecific status.

**Distribution.** *Andrena crassana* sensu lato has a distribution of North Macedonia, Greece, Turkey, Cyprus, Israel and West Bank, Lebanon*, Jordan, Syria, Iraq*, Iran (Gusenleitner and Schwarz 2002; Pisanty et al. 2018; Wood and Monfared 2022).

### 18. *Andrena* (*Aciandrena*) *curviocciput* Pisanty & Wood, 2022 *

**Material examined.** **Iraq:** Duhok, Mt. Gara [S of Sarsing], 37.0158°N, 43.3506°E, 1912 m, 11.v.2023, 12♂, leg. D. Baiocchi, MSVI/TJWC.

**Remarks.** Known from the Tanin-Tanin pass in south-eastern Turkey (Pisanty et al. 2022a), so its presence in northern Iraq was expected.

**Distribution.** Israel, Lebanon, Turkey, Iraq* (Pisanty et al. 2022a).

### 19. ***Andrena* (incertae sedis) *discordia* Wood, 2023 ***

**Material examined. Iraq:** Duhok, Mt. Gara [S of Sarsing], 37.0158°N, 43.3506°E, 1912 m, 11.v.2023, 1♂, leg. D. Baiocchi, MSVI.

**Distribution.** Turkey, Iraq*, Iran (Wood 2023).

### 20. ***Andrena* (*Aciandrena*) *duhokensis* Wood, sp. nov. ***

https://zoobank.org/3C35CEE1-7063-4C23-8577-1BA21A6CCAFE

**Material examined.** ***Holotype*: Iraq:** Duhok, Mt. Gara [S of Sarsing], 37.0158°N, 43.3506°E, 1912 m, 11.v.2023, 1♂, leg. D. Baiocchi, RMNH. ***Paratypes*: Iraq:** Same information as holotype, 7♂, MSVI/RMNH/TJWC/DUMAI.

**Diagnosis.** *Andrena duhokensis* can be recognised as part of the subgenus *Aciandrena* Warncke, 1968 due to the small body size, dark integument with the exception of the pale-marked clypeus (Fig. 5A), finely shagreened propodeal triangle (Fig. 5D; without lateral or basal rugae), more or less impunctate terga (Fig. 5E), strongly antefurcal nervulus, and typical simple genital capsule (Fig. 5F; e.g., without completely reduced gonocoxae as in most members of the subgenus *Graecandrena* Warncke, 1968). Identification of *Aciandrena* species is extremely challenging due to the large number of often cryptic species found in dry environments, their often very local distributions, and lack of good characters in the female sex. Fortunately, males are a little easier to identify through the examination of the genital capsule. *Andrena duhokensis* can be initially recognised due to its almost entirely yellow-marked clypeus (with the exception of two small black marks [sometimes absent] and some narrow black areas at the edges of the clypeus), placing it closest to *A. tenuis* Morawitz, 1877 which was described from the Caucasus. However, *A. duhokensis* can be recognised due to the unique form of the genital capsule which has the gonocoxal teeth with their apexes strongly truncate and asymmetrical so that they diverge from each other (Fig. 5F); in other words, they form somewhat pointed but flattened and diverging teeth. In comparative species of *Aciandrena*, the gonocoxal teeth are either strongly produced and truncate (e.g., *A. deminuta* Wood 2022 from Iran), produced into narrowly pointed or more broadly rounded teeth (e.g., *A. tenuis* from Turkey and the Caucasus, *A. aciculata* Morawitz, 1886 from Europe to the Caucasus), or reduced and truncate but never forming diverging teeth (e.g., *A. judaea* Scheuchl & Pisanty, 2016 from Israel). In this context, *A. duhokensis* can be separated from all similar species.

**Description. Female.** Unknown.

**Male.** Body length 4–5 mm (Fig. 5A). ***Head*:** Dark, 1.25× wider than long (Fig. 5B). Clypeus weakly domed, predominantly yellow or pale yellow marked with exception of two black dots (sometimes absent) and narrow black markings laterally; surface finely shagreened and weakly shining, irregularly punctate, punctures separated by 1–3 puncture diameters. Process of labrum small, rounded trapezoidal, 2× wider than long, apical margin weakly emarginate. Gena subequal to diameter of compound eye; ocelloccipital distance equals diameter of lateral ocellus. Head covered with dirty white hairs, none equalling length of scape. Antennae basally dark, A4–13 ventrally lightened by presence of grey scales; A3 exceeding length of A4, shorter than A4+5; A4 sub-square, shorter than long, A5 quadrate, as long as broad.

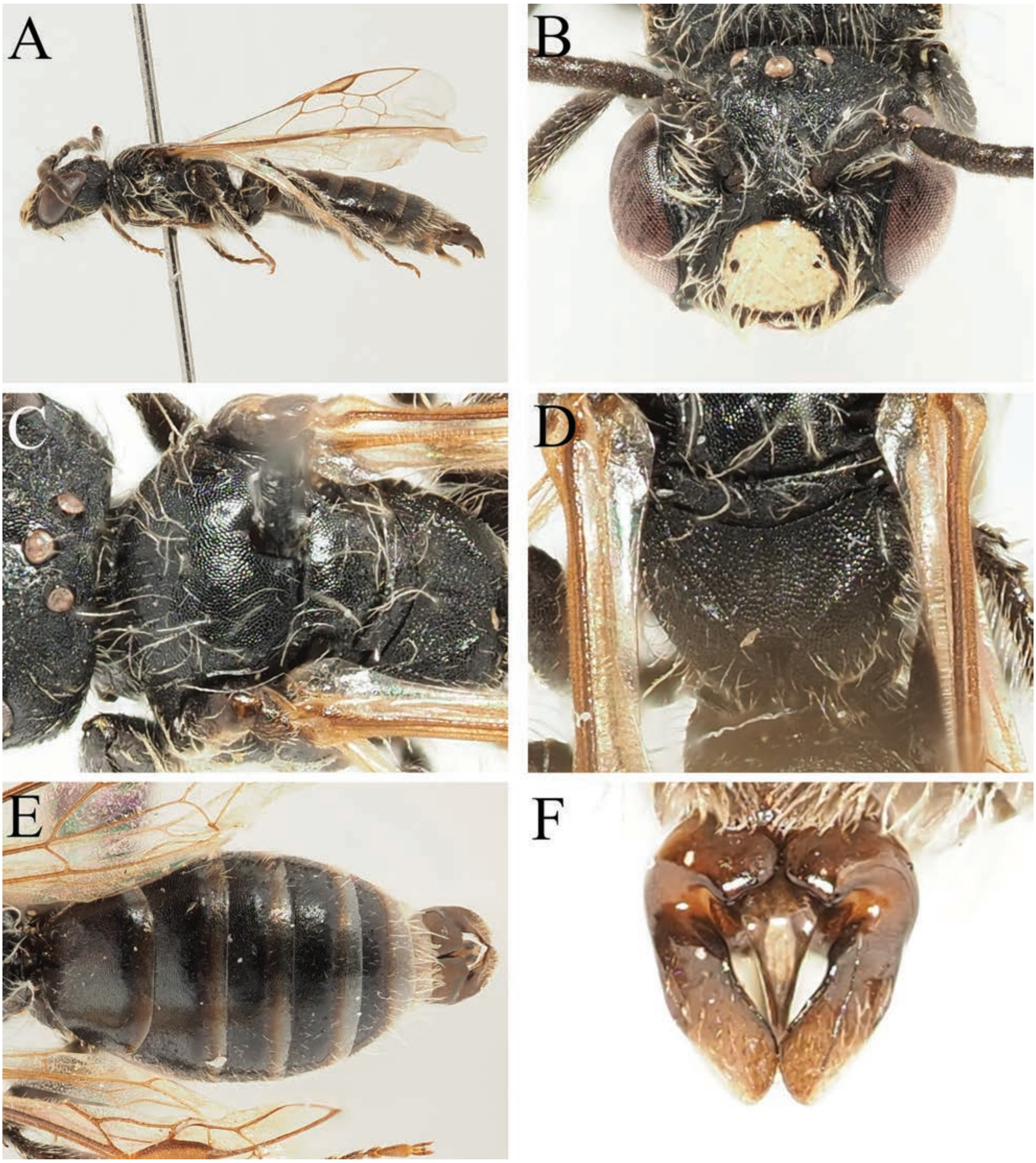

**Figure 5.** *Andrena* (*Aciandrena*) *duhokensis* sp. nov. male **A** habitus, lateral view **B** face, frontal view **C** scutum, dorsal view **D** propodeum, dorsal view **E** terga, dorsal view **F** genital capsule, dorsal view.

***Mesosoma*:** Scutum and scutellum with fine granular shagreen, weakly shining, irregularly punctate, punctures separated by 1–4 puncture diameters (Fig. 5C). Mesepisternum and dorsolateral parts of propodeum with regular but large microreticulation, dull to weakly shining; propodeal triangle large, indicated by change in surface sculpture, internal surface with fine granular microreticulation, in some parts with weakly raised network of carinae between microreticulation, surface dull (Fig. 5D). Mesosoma with sparse short whitish hairs. Legs predominantly dark, apical tarsal segments slightly lightened orange, pubescence white. Hind tarsal claws with strong inner tooth. Wings hyaline, stigma, and venation pale orange, nervulus very strongly antefurcal.

***Metasoma*:** Terga predominantly dark, tergal margins weakly but distinctly depressed, broadly lightened hyaline yellow-brown (Fig. 5E). Tergal discs finely microreticulate to shagreened, weakly shining, surface essentially impunctate, with scattered obscure punctures disappearing into underlying sculpture. Terga with sparse scattered short hairs, not forming hairbands. T6 and T7 with long light brown hairs overlying pseudopygidial plate of T7. S8 narrow, apex slightly broadened like a fish-tail, truncate, ventral surface with dense lateral fan of brown hairs. Genital capsule compact, gonocoxae produced into apical teeth, teeth strongly truncate, apexes angled and diverging from each other to form angular anteriorly projecting teeth (Fig. 5F). Gonostyli flattened and spatulate, internal margins raised, forming slight bump on inner margin basally. Penis valves moderate, occupying ½ space between gonostyli basally, strongly tapering apically.

**Etymology.** The name is derived from the city of Duhok which gives its name to the province in which these specimens were collected.

**Distribution.** Iraq (Kurdistan region).

### 21. *Andrena* (*Micrandrena*) *elam* Wood, 2022 *

**Material examined. Iraq:** Duhok, Mt. Gara [S of Sarsing], 37.0158°N, 43.3506°E, 1912 m, 11.v.2023, 23♂, 1♀, leg. D. Baiocchi, MSVI/TJWC.

**Remarks and diagnosis.** Wood in Wood and Monfared (2022) described *A. elam* in the female sex from western and southern Iran, and Wood (2023) reported further specimens from southern and south-eastern Turkey. Numerous male specimens from northern Iraq are now available. They can be recognised as *Micrandrena* due to the small body size, dark integument (including clypeus Fig. 6B), entirely rugose propodeal triangle (Fig. 6D), and normal genital capsule. As in the female sex, they can be separated from other *Micrandrena* species by the combination of smooth and shining scutum and scutellum with moderately dense punctures (Fig. 6C), the tergal discs with extremely strong and dense reticulation (Fig. 6E), this reticulation becoming much weaker on the marginal areas, with punctures visible on the discs of T3–4 (though comparatively weaker and less visible than in the female), and by the tergal margins becoming progressively more strongly depressed. Additionally, the genital capsule is distinctive (Fig. 6F), somewhat elongate, with the gonocoxae produced into weak angular teeth, with thickened gonostyli with a weak rounded bump on their inner margins and outer surface lightened and covered with short golden hairs. It resembles the form of two former *Fumandrena* (= *Micrandrena*) species (*A. fabrella* Pérez, 1895 (western Mediterranean) and *A. tomora* Warncke, 1975 (eastern Mediterranean)), but these have the gonostyli apically flattened, not thickened. It is very close to *A. subviridula* Wood, 2022 (northern Iran, see illustrations in Wood and Monfared 2022), but can be separated by the gonocoxae produced into apical points (in *A. subviridula* with the gonocoxae apically truncate), by the weaker bump on the inner margins of the gonostyli (in *A. subviridula* with this bump comparatively more pronounced), and by the more extensively shiny scutum which lacks subtle greasy green-metallic reflections (in *A. subviridula* with the scutum more extensively shagreened anteriorly and laterally).

**Description. Male.** ***Body length*****:** 6 mm (Fig. 6A). ***Head*****:** Dark, 1.45× wider than long (Fig. 6B). Clypeus domed, densely punctate, punctures separated by < 0.5–1 puncture diameter, surface with weakly raised latitudinal striations between punctures, surface weakly shining. Process of labrum trapezoidal, 2× wider than long, anterior margin weakly emarginate, surface smooth and shining. Gena equalling diameter of compound eye; ocelloccipital distance equalling diameter of lateral ocellus. Head with sparse whitish hairs, none equalling length of scape; clypeus in fresh individuals with moderate “beard” of ventrally projecting pale hairs. Antennae dark, A5–13 ventrally lightened by presence of silver-grey scales; A3 exceeding length of A4, shorter than A4+5.

***Mesosoma*****:** Scutum and scutellum polished and shining over almost entire surface, scutum weakly shagreened anteriorly; irregularly punctate, punctures separated by 1–3 puncture diameters (Fig. 6C). Pronotum rounded. Mesepisternum microreticulate, dull. Dorsolateral parts of propodeum microreticulate, dull, sculpture overlain by network of irregular raised rugosity; propodeal triangle laterally defined by irregular carinae, internal surface densely covered with network of evenly-spaced rugae, propodeal triangle thus well-differentiated from dorsolateral parts of propodeum (Fig. 6D). Mesosoma covered with sparse light brown hairs, none equalling length of scape. Legs dark, apical tarsal segments paler dark brown, pubescence whitish. Hind tarsal claws with inner tooth. Wings hyaline, stigma dark brown, venation orange-brown, nervulus interstitial.

***Metasoma*****:** Tergal discs dark, marginal areas with apical rim narrowly lightened brown (Fig. 6E). Tergal discs strongly reticulate, reticulation strongest on T1, surface dull, becoming progressively weaker on subsequent terga, discs of T5 and T6 weakly shining; marginal areas shagreened, weakly shining. Tergal discs obscurely punctate, T1 almost impunctate, punctures progressively more visible on subsequent terga, punctures on disc of T4 separated by 1–2 puncture diameters. Tergal discs with scattered pale hairs, not forming hairbands. T6 and T7 with light brown hairs overlying pseudopygidial plate. S8 columnar, apical margin truncate, ventral surface with sparse short brown hairs. Genital capsule somewhat elongate, gonocoxae with apical margins produced into slightly projecting narrow apical teeth (Fig. 6F). Gonostyli robust, thickened, with weak bump on internal margins basally, apically weakly flattened, apical ½ lightened hyaline yellowish. Penis valves narrow, occupying ½ space between gonostyli, uniformly narrowing towards apex.

**Distribution.** Southern and south-eastern Turkey, northern Iraq*, and western and southern Iran (Wood and Monfared 2022; Wood 2023).

### 22. *Andrena* (*Lepidandrena*) *elisaria* Gusenleitner, 1998 *

**Material examined.** **IRAQ:** Duhok, Mt. Gara [S of Sarsing], 37.0158°N, 43.3506°E, 1912 m, 11.v.2023, 1♂, leg. D. Baiocchi, MSVI.

**Distribution.** Israel, Turkey, Iraq*, Iran (Gusenleitner 1998; Pisanty et al. 2018; Wood and Monfared 2022).

### 23. *Andrena* (incertae sedis) *euzona* Pérez, 1895

**Literature records.** Wood and Monfared (2022).

**Figure 6.** *Andrena* (*Micrandrena*) *elam* Wood, 2022 male **A** habitus, lateral view **B** face, frontal view **C** scutum, dorsal view **D** propodeum, dorsal view **E** terga, dorsal view **F** genital capsule, dorsal view.

**Distribution.** Morocco, Algeria, Tunisia, Libya, Egypt, Israel and West Bank, Jordan, Syria, Iraq, Iran (Gusenleitner and Schwarz 2002; Wood and Monfared 2022).

### 24. *Andrena* (*Plastandrena*) *eversmanni* Radoszkowski, 1867

**Literature records.** Wood and Monfared (2022).

**Distribution.** Turkey, Armenia, Iraq, Iran, Russia (European part), Turkmenistan, Uzbekistan, Kazakhstan, Tajikistan, Pakistan, Mongolia, China (Wood and Monfared 2022; Ascher and Pickering 2023).

### 25. *Andrena* (*Hoplandrena*) *ferox* Smith, 1847 *

**Material examined. Iraq:** Duhok, Mt. Gara [S of Sarsing], 37.0158°N, 43.3506°E, 1912 m, 11.v.2023, 1♀, leg. D. Baiocchi, MSVI; **Lebanon:** Beqaa, Beqaa valley, Mansourah, Aammiq wetland preserve, 33.7321°N, 35.7853°E, 850 m, 3.iv.2023, 1♀, leg. T.J. Wood, TJWC.

**Distribution.** West Palaearctic to the Middle East, including Lebanon*, Iraq*, Iran (Gusenleitner and Schwarz 2002; Scheuchl and Willner 2016; Wood and Monfared 2022).

### 26. *Andrena* (*Melandrena*) *flavipes* Panzer, 1799

**Literature records.** Morice (1921b); Derwesh (1965), mentioning "Survey of Iraq Fauna 1915–1919"; Gusenleitner and Schwarz (2002: dot map 161); Scheuchl and Willner (2016); Augul (2018); Ascher and Pickering (2023).

**Remarks.** We have not examined any specimens of this species, but the presence of this species in Iraq is extremely plausible based on its known global distribution, its abundance in a wide variety of habitats, the map records indicated by Gusenleitner and Schwarz (2002), and the presence of this species in neighbouring Turkey and Iran.

**Distribution.** West and Central Palearctic (Gusenleitner and Schwarz 2002; Ascher and Pickering 2023).

### 27. *Andrena* (*Bryandrena*) *florea* Fabricius, 1793 *

**Material examined. Iraq:** Duhok, Mt. Gara [S of Sarsing], 37.0158°N, 43.3506°E, 1912 m, 11.v.2023, 1♂, leg. D. Baiocchi, MSVI.

**Distribution.** West Palaearctic, from Morocco to Iraq*, Iran, Turkmenistan, and the Ural mountains (Gusenleitner and Schwarz 2002).

### 28. *Andrena* (*Ulandrena*) *fulvitarsis* Brullé, 1832

**Literature records.** Gusenleitner and Schwarz (2002: dot map 177); Ascher and Pickering (2023).

**Remarks.** We have not examined any specimens of this species, but the presence of this species in Iraq is plausible based on its known global distribution, the map records indicated by Gusenleitner and Schwarz (2002), and the presence of this species in neighbouring Turkey.

**Distribution.** East Mediterranean, from Italy to Crimea, Turkey, the Levant, Iraq (Gusenleitner and Schwarz 2002).

### 29. ***Andrena*** **(incertae sedis)** ***garrula*** **Warncke, 1965 ***

**Material examined. Iraq:** Duhok, Mt. Gara [S of Sarsing], 37.0158°N, 43.3506°E, 1912 m, 11.v.2023, 1♀, leg. D. Baiocchi, MSVI.

**Remarks.** This specimen appears to be *A. garrula* s. str. as opposed to the Levantine ssp. *lomvia* Warncke, 1969; the difference between the two subspecies is difficult to distinguish in the female sex.

**Distribution.** Bulgaria, Turkey, Israel and West Bank, Lebanon, Jordan, Syria, Iraq*, Iran (Gusenleitner and Schwarz 2002; Wood et al. 2020; Wood and Monfared 2022).

### 30. ***Andrena*** **(*Melandrena*)** ***grandilabris*** **Pérez, 1903 ***

**Material examined. Iraq:** Duhok, Mt. Gara [S of Sarsing], 37.0158°N, 43.3506°E, 1912 m, 11.v.2023, 4♂, leg. D. Baiocchi, MSVI.

**Remarks.** Turkey, Iraq*, Iran (Wood and Monfared 2022).

### 31. ***Andrena*** **(*Euandrena*)** ***hermonella*** **Scheuchl & Pisanty, 2016 ***

**Material examined. Iraq:** Duhok, Mt. Gara [S of Sarsing], 37.0158°N, 43.3506°E, 1912 m, 11.v.2023, 2♀, leg. D. Baiocchi, MSVI.

**Remarks.** The original female specimens described by Pisanty et al. (2016) actually belonged to *A. gageae* Wood & Pisanty, 2022 (see Pisanty et al. 2022a). The true female of *A. hermonella* is being described from south-eastern Turkey (Wood, in press). This extends the range from south-eastern Turkey into northern Iraq.

**Distribution.** Israel, Turkey, Iraq* (Pisanty et al. 2016; Wood, unpublished data).

### 32. ***Andrena*** **(incertae sedis)** ***hosseiniiae*** **Wood & Monfared, 2022 ***

**Material examined. Iraq:** Duhok, Mt. Gara [S of Sarsing], 37.0158°N, 43.3506°E, 1912 m, 11.v.2023, 1♀, leg. D. Baiocchi, MSVI.

**Remarks.** The first record of this species outside of Iran, with all previous records coming from close to Yasuj (Kohgiluyeh and Boyer-Ahmad Province) in southern Iran.

**Distribution.** Iraq* and Iran (Wood and Monfared 2022).

### 33. ***Andrena*** **(*Poecilandrena*)** ***hybrida*** **Warncke, 1975 ***

**Material examined. Iraq:** Duhok, Mt. Gara [S of Sarsing], 37.0158°N, 43.3506°E, 1912 m, 11.v.2023, 1♀, leg. D. Baiocchi, MSVI.

**Remarks.** Multiple subspecies are described for *A. hybrida*; their statuses require further study, but this is limited by the scarcity of material. Iraqi material conforms to *A. hybrida* s. str.

**Distribution.** Ukraine, Russia (European part), Turkey, Iraq*, Iran (Gusenleitner and Schwarz 2002; Wood and Monfared 2022).

### 34. ***Andrena* (*Graecandrena*) *hyemala* Warncke, 1973 ***

**Material examined. Iraq:** Duhok, Mt. Gara [S of Sarsing], 37.0158°N, 43.3506°E, 1912 m, 11.v.2023, 7♂, leg. D. Baiocchi, MSVI; Mosul, edges of a river, 7.iv.1988, 3♀, leg. Olejníček, OÖLM.

**Remarks.** The specimens presented here appear to be *A. hyemala* s. str. The statuses of the subspecies *repressa* Warncke, 1975 (Levant) and *kushika* Osytshnjuk, 1994 (Central Asia) require further study.

**Distribution.** *Andrena hyemala* sensu lato is distributed from south-eastern Europe through the Middle East (including Iraq* and Iran) to Central Asia (Gusenleitner and Schwarz 2002; Osytshnjuk et al. 2008; Wood and Monfared 2022).

### 35. ***Andrena* (*Ulandrena*) *kriechbaumeri* Schmiedeknecht, 1883 ***

**Material examined. Iraq:** Duhok, E Mangesh, 37.0230°N, 43.1505°E, 1046 m, 8.v.2023, 1♂, leg. D. Baiocchi, MSVI; **Syria:** Apamea, 65 km NW Hama, 270 m, 18.iv.1992, 1♂, leg. K. Warncke, OÖLM; **Turkey:** Siirt, 5 km E Eruh, 1000 m, 26.v.1983, 1♂, leg. K. Warncke, OÖLM.

**Remarks.** The finding of *A. kriechbaumeri* in Iraq is notable. One of the most common and abundant *Andrena* species in the southern Balkans, *A. kriechbaumeri* is much less common in Turkey where it is largely restricted to western Turkey (see distribution map of Gusenleitner and Schwarz 2002). Examination of undetermined material in the OÖLM collection produced specimens from northern Syria and a specimen from near to Siirt in eastern Turkey. To our knowledge, this is the most easterly specimen known from Turkey. In this context, the presence of *A. kriechbaumeri* in northern Iraq represents less of an outlier, though it is clear that *A. kriechbaumeri* has a population centre in the Balkan Peninsula.

**Distribution.** Europe from Italy to Turkey, Syria*, and Iraq* (Gusenleitner and Schwarz 2002).

### 36. ***Andrena* (*Poecilandrena*) *laticeps* Morawitz, 1878 ***

**Material examined. Iraq:** Duhok, Mt. Gara [S of Sarsing], 37.0158°N, 43.3506°E, 1912 m, 11.v.2023, 3♂, leg. D. Baiocchi, MSVI.

**Distribution.** Turkey, Georgia, Armenia, Iraq*, Iran (Wood and Monfared 2022; Ascher and Pickering 2023).

### 37. ***Andrena* (*Melandrena*) *limata* Smith, 1853 ***

**Material examined. Iraq:** Baiji [Saladin Governorate, 35.0299°N, 43.4489°E], 1–31.iii.1986, 3♀, leg. M. Carl, OÖLM.

**Distribution.** West and Central Palearctic including Iraq* and Iran (Gusenleitner and Schwarz 2002; Osytshnjuk et al. 2008; Wood and Monfared 2022).

### 38. *Andrena* (*Micrandrena*) *luscinia* Warncke, 1975 *

**Material examined. Iraq:** Duhok, Mt. Gara [S of Sarsing], 37.0158°N, 43.3506°E, 1912 m, 11.v.2023, 1♀, leg. D. Baiocchi, MSVI; **Lebanon:** Beqaa, Rachaiya, 5 km S, Mount Hermon nature reserve, 33.4586°N, 35.8395°E, 1500 m, 8.iv.2023, 2♀, leg. T.J. Wood, TJWC.

**Distribution.** Israel, Lebanon*, Turkey, Iraq*, Iran (Pisanty et al. 2018; Wood and Monfared 2022).

### 39. *Andrena* (incertae sedis) *monacha* Warncke, 1965 *

**Material examined. Iraq:** Duhok, Mt. Gara [S of Sarsing], 37.0158°N, 43.3506°E, 1912 m, 11.v.2023, 1♂, leg. D. Baiocchi, MSVI.

**Distribution.** Greece, Turkey, Cyprus, Lebanon, Syria, Iraq*, Iran (Gusenleitner and Schwarz 2002; Wood et al. 2020; Wood and Monfared 2022).

### 40. *Andrena* (*Melandrena*) *morio* Brullé, 1832

**Literature records.** Khalaf and Al-Omar (1974); Gusenleitner and Schwarz (2002: dot map 310); Scheuchl and Willner (2016); Augul (2018).

**Remarks.** We have not examined any specimens of this species, but the presence of this species in Iraq is plausible based on its known global distribution, the map records indicated by Gusenleitner and Schwarz (2002), and the presence of this species in neighbouring Turkey and Iran.

**Distribution.** West and Central Palaearctic (Gusenleitner and Schwarz 2002; Osytshnjuk et al. 2008; Wood and Monfared 2022).

### 41. *Andrena* (*Melandrena*) *nitidemula* Scheuchl & Hazir, 2012 *

**Material examined. Iraq:** Duhok, Mt. Gara [S of Sarsing], 37.0158°N, 43.3506°E, 1912 m, 11.v.2023, 1♀, leg. D. Baiocchi, MSVI.

**Distribution.** Greece, Turkey, Syria, Georgia, Armenia, Iraq*, Iran (Wood and Monfared 2022).

### 42. *Andrena* (*Micrandrena*) *obsidiana* Wood, 2022 *

**Material examined. Iraq:** Duhok, Mt. Gara [S of Sarsing], 37.0158°N, 43.3506°E, 1912 m, 11.v.2023, 15♂, 4♀, leg. D. Baiocchi, MSVI/TJWC; **Turkey:** Hakkâri, pass E of Uludere, 6.vi.1977, 1♂, 2♀, leg. K. Warncke, OÖLM/TJWC; Hakkâri, Tanin-Tanin-Pass, 2500 m, 2.vi.1980, 3♂, 1♀, leg. K. Warncke, OÖLM.

**Remarks and diagnosis.** Wood and Monfared (2022) described *A. obsidiana* in the female sex from southern and south-eastern Turkey and western and southern Iran. Numerous male specimens from northern Iraq are now available, as well as some additional specimens from south-eastern Turkey that were not available for study at the time of the original description. One of these *A. obsidiana* specimens from Turkey (a female) was separated by Warncke and labelled as "*A. ferulella* spec. nov.", but this name was never published.

*Andrena obsidiana* can be recognised as *Micrandrena* due to the small body size, dark integument (including clypeus Fig. 7B), entirely rugose propodeal triangle (Fig. 7D), and normal genital capsule (Fig. 7F). Due to the smooth and shining scutum and scutellum with moderately dense punctures (Fig. 7C) and the genital capsule (gonocoxae produced into weak angular teeth, with thickened gonostyli with very small rounded bump on their inner margins, and outer surface lightened and covered with short golden hairs) it is close to *A. elam* and *A. subviridula*, but it can instantly be separated from them by the sculpture of the terga which is almost completely smooth and shining (Fig. 7E), with only superficial shagreenation at the base of the tergal discs. There are also differences in the genital capsule, with that of *A. obsidiana* being comparatively more elongate, with the bump on the inner margin of the gonostyli reduced to a relatively tiny projection.

**Description. Male.** ***Body length*:** 5–6 mm (Fig. 7A). ***Head*:** Dark, 1.25× wider than long (Fig. 7B). Clypeus domed, densely punctate, punctures separated by < 0.5–1 puncture diameter, surface weakly shining. Process of labrum trapezoidal, 2× wider than long, anterior margin weakly emarginate, surface weakly shining. Gena equalling diameter of compound eye; ocelloccipital distance subequal to diameter of lateral ocellus. Head with sparse whitish hairs, none equalling length of scape; clypeus in fresh individuals with moderate "beard" of ventrally projecting pale hairs. Antennae basally dark, A5–13 ventrally lightened by presence of brownish-grey scales; A3 exceeding length of A4, slightly shorter than A4+5.

***Mesosoma*:** Scutum and scutellum polished and shining over almost entire surface, scutum weakly shagreened anteriorly; irregularly punctate, punctures separated by 1–3 puncture diameters, slightly denser on scutum (Fig. 7C). Pronotum rounded. Mesepisternum microreticulate, dull. Dorsolateral parts of propodeum microreticulate, dull, sculpture overlain by dense network of raised rugosity; propodeal triangle poorly defined laterally, without clear linear carinae, internal surface densely covered with dense network of rugae, propodeal triangle thus poorly differentiated from dorsolateral parts of propodeum (Fig. 7D). Mesosoma covered with sparse whitish to light brown hairs, none equalling length of scape. Legs dark, apical tarsal segments paler dark brown, pubescence whitish. Hind tarsal claws with inner tooth. Wings hyaline, stigma dark brown, venation orange-brown, nervulus weakly to strongly antefurcal.

***Metasoma*:** Tergal discs dark, marginal areas with apical rim obscurely lightened dark brown (Fig. 7E). Tergal discs with weak sculpture, T1 polished and shining, base of remaining terga with fine shagreen, otherwise smooth and shining. Terga deeply punctate, T1 with punctures separated by 1–2 puncture diameters, remaining tergal discs with punctures separated by 1 puncture diameter; punctures only partially extending onto marginal areas, becoming weaker on apical terga, marginal area of T5 almost impunctate. Tergal margins progressively more strongly depressed, weakly on T1, strongly on T5. Tergal discs with scattered pale hairs, not forming hairbands. T6 andT7 with light brown hairs overlying pseudopygidial plate. S8 columnar, apical margin rounded, ventral surface with dense fan of short brown hairs. Genital

**Figure 7.** *Andrena* (*Micrandrena*) *obsidiana* Wood, 2022 male **A** habitus, lateral view **B** face, frontal view **C** scutum, dorsal view **D** propodeum, dorsal view **E** terga, dorsal view **F** genital capsule, dorsal view.

capsule somewhat elongate, gonocoxae with apical margins produced into slightly projecting narrow apical teeth (Fig. 7F). Gonostyli robust, thickened, with weak and obscure bump on internal margins basally, apical ½ lightened hyaline yellowish. Penis valves narrow, occupying ½ space between gonostyli, uniformly narrowing towards apex.

**Distribution.** Southern and south-eastern Turkey, northern Iraq*, and western and southern Iran (Wood and Monfared 2022).

### 43. ***Andrena*** **(*Micrandrena*)** ***oedicnema*** **Warncke, 1975 ***

**Material examined. Iraq:** Duhok, Mt. Gara [S of Sarsing], 37.0158°N, 43.3506°E, 1912 m, 11.v.2023, 2♂, leg. D. Baiocchi, MSVI;

**Distribution.** Greece, Turkey, Israel and West Bank, Lebanon, Jordan, Syria, Turkey, Iraq*, Iran (Gusenleitner and Schwarz 2002; Pisanty et al. 2018; Wood and Monfared 2022).

### 44. ***Andrena*** **(*Pallandrena*)** ***pallidicincta*** **Brullé, 1832 ***

**Material examined. Iraq:** Duhok, Mt. Gara [S of Sarsing], 37.0158°N, 43.3506°E, 1912 m, 11.v.2023, 11♀, leg. D. Baiocchi, MSVI/TJWC.

**Distribution.** South-eastern Europe to Turkey, Lebanon, Israel, and Iraq* (Gusenleitner and Schwarz 2002; Wood et al. 2020).

### 45. ***Andrena*** **(*Truncandrena*)** ***pareklisiae*** **Mavromoustakis, 1956 ***

**Material examined. Iraq:** Duhok, Mt. Gara [S of Sarsing], 37.0158°N, 43.3506°E, 1912 m, 11.v.2023, 6♀, leg. D. Baiocchi, MSVI/TJWC.

**Distribution.** Cyprus, Turkey, Lebanon, Syria, Iraq*, Iran (Wood 2023).

### 46. ***Andrena*** **(*Truncandrena*)** ***rufomaculata*** **Friese, 1921 ***

**Material examined. Iraq:** Duhok, Mt. Gara [S of Sarsing], 37.0158°N, 43.3506°E, 1912 m, 11.v.2023, 1♀, leg. D. Baiocchi, MSVI.

**Distribution.** Turkey, Israel and West Bank, Lebanon, Jordan, Syria, Iraq*, Iran (Wood et al. 2020; Wood and Monfared 2022).

### 47. ***Andrena*** **(*Suandrena*)** ***savignyi*** **Spinola, 1838**

**Literature records.** Moalif (1994); Ascher and Pickering (2023).

**Remarks.** We have not examined any specimens of this species, but the listing is plausible due to the presence of multiple specimens of *A. savignyi* in western and southern Iran (Wood and Monfared 2022), and the preference of *A. savignyi* for dry desert and semi-desert habitats.

**Distribution.** West and Central Palaearctic (Wood and Monfared 2022; Ascher and Pickering 2023).

### 48. ***Andrena*** **(*Micrandrena*)** ***sillata histrionica*** **Warncke, 1975 ***

**Material examined. Iraq:** Duhok, Mt. Gara [S of Sarsing], 37.0158°N, 43.3506°E, 1912 m, 11.v.2023, 4♂, 1♀, leg. D. Baiocchi, MSVI.

**Distribution.** Subspecies *histrionica* is found in Turkey, Iraq*, and Iran only (Wood and Monfared 2022). It may merit species status due to differences in the male genital capsule, but genetic data are required.

### 49. *Andrena* (*Euandrena*) *symphyti* Schmiedeknecht, 1883 *

**Material examined. Iraq:** Duhok, Mt. Gara [S of Sarsing], 37.0158°N, 43.3506°E, 1912 m, 11.v.2023, 5♂, 1♀, leg. D. Baiocchi, MSVI.

**Distribution.** West Palaearctic, including Iraq* and Iran (Gusenleitner and Schwarz 2002; Wood and Monfared 2022).

### 50. *Andrena* (*Chlorandrena*) *tadauchii* Gusenleitner, 1998 *

**Material examined. Iraq:** Duhok, E Mangesh, 37.0230°N, 43.1505°E, 1046 m, 8.v.2023, 1♀, leg. D. Baiocchi, MSVI; Duhok, Mt. Gara [S of Sarsing], 37.0158°N, 43.3506°E, 1912 m, 11.v.2023, 14♂, leg. D. Baiocchi, MSVI/ TJWC; **Lebanon:** Balbek-Hermel, Sefri, Haouch Snaid, AUB farm, 33.9244°N, 36.0754°E, 1000 m, 6.iv.2023, 2♂, 20♀, leg. T.J. Wood, TJWC; Beqaa, Anjar, 1 km E, Armenian Cemetary, 33.7372°N, 35.9503°E, 900 m, 7.iv.2023, 1♀, leg. T.J. Wood, TJWC; Beqaa, Beqaa valley, Mansourah, Aammiq wetland preserve, 33.7321°N, 35.7853°E, 850 m, 3.iv.2023, 1♀, leg. T.J. Wood, TJWC; Bekaa, Qob Elias valley, 33.7989°N, 35.8192°E, 900 m, 5.iv.2023, 1♀, leg. T.J. Wood, TJWC; Hrar-Akkar, 34.4572°N, 36.1228°E, 900 m, 17.iv.2021, 1♂, leg. A. Saab, TJWC.

**Remarks.** Confirmed as present in Lebanon after the unclear listing of Grace (2010).

**Distribution.** Israel and West Bank, Lebanon*, Syria, Turkey, Iraq* (Pisanty et al. 2022a).

### 51. *Andrena* (*Ulandrena*) *tadorna callida* Warncke, 1974 *

**Material examined. Iraq:** Hatra [Nineveh Governorate, 35.5759°N, 42.7254°E], 6.iv.1988, 1♂, leg. Olejníček, OÖLM; **Saudi Arabia:** Abha, 2000 m, 31.iii.1980, 1♂, leg. K.M. Guichard, NHMUK; As Nimas [Al Namas], 2450 m, 3–4.iv.1980, 3♂, 3♀, leg. K.M. Guichard, NHMUK; **Syria:** 110 km E of Palmyra, 350 m, 21.iv.1992, 2♀, leg. K. Warncke, OÖLM; 30 km W Palmyra, 580 m, 23.iv.1992, 6♀, leg. M. Kraus and K. Warncke, OÖLM; Suweidaono, ENE 80km, 700 m, 27.iii.1988, 2♂, leg. M. Schwarz, TJWC.

**Remarks.** The status of *A. tadorna callida* is unclear and requires investigation; it may well merit species status due to consistent differences in the shape of the genital capsule (see comments in Gusenleitner and Schwarz 2002).

**Distribution.** *Andrena tadorna* sensu lato is found in Morocco, Algeria, Tunisia, Libya, Egypt, Israel, Jordan, Syria*, Saudi Arabia*, Iraq* Gusenleitner and Schwarz (2002).

### 52. *Andrena* (*Micrandrena*) *tkalcui* Gusenleitner & Schwarz, 2002 *

**Material examined. Iraq:** Duhok, Bessre [Besereh], Bablo, 36.8675°N, 43.1206°E, 1065 m, 5–6.v.2023, 1♀, leg. D. Baiocchi, MSVI; Duhok, Mt. Gara [S of Sarsing], 37.0158°N, 43.3506°E, 1912 m, 11.v.2023, 1♀, leg. D. Baiocchi, MSVI.

**Distribution.** Israel and West Bank, Jordan, Syria, Turkey, Iraq*, Iran (Gusenleitner and Schwarz 2002; Wood and Monfared 2022).

### 53. *Andrena* (*Cordandrena*) *torda* Warncke, 1965 *

**Material examined. Iraq:** Duhok, Mt. Gara [S of Sarsing], 37.0158°N, 43.3506°E, 1912 m, 11.v.2023, 6♂, leg. D. Baiocchi, MSVI/TJWC; **Lebanon:** Beqaa, Beqaa valley, Mansourah, Aammiq wetland preserve, 33.7321°N, 35.7853°E, 850 m, 3.iv.2023, 2♀, leg. T.J. Wood, TJWC; Beqaa, Beqaa valley, Qaraoun, 3.5 km W of Madjal Balhis, 33.5377°N, 35.7038°E, 900 m, 4–5.iv.2023, 2♀, leg. T.J. Wood, TJWC.

**Remarks.** Records from Lebanon, Jordan, and Syria reported by Wood et al. (2020) were incorrectly identified female specimens of *A. cypria* (see Wood and Monfared 2022), with females of *A. torda* and *A. cypria* being challenging to separate morphologically. The female Lebanese specimens presented here were confirmed as *A. torda* through DNA barcoding (BIN: BOLD:AES5002) as distinct from *A. cypria* (BIN: BOLD:AFH0814), this latter BIN containing a barcoded male specimen of *A. cypria* which can be unambiguously recognised due to the combination of its antennal segment ratios and genital capsule.

**Distribution.** Greece, Turkey, Cyprus, Israel and West Bank, Lebanon*, Iraq*, Iran (Wood and Monfared 2022).

### 54. *Andrena* (*Notandrena*) *trimarginata* (Radoszkowski, 1886)

**Literature records.** Wood and Monfared (2022, as *A. zostera* Warncke, 1975).

**Material examined. Lebanon:** Balbek-Hermel, Sefri, Haouch Snaid, AUB farm, 33.9244°N, 36.0754°E, 1000 m, 6.iv.2023, 4♂, leg. T.J. Wood, TJWC.

**Remarks.** A taxonomic work will soon recognise *Halictus trimarginatus* Radoszkowski, 1886 (described from Turkmenistan) as the senior name of *A. zostera* (Wood, in press).

**Distribution.** Israel and West Bank, Syria, Lebanon*, Turkey, Azerbaijan, Iraq, Iran, Turkmenistan, Uzbekistan, Tajikistan (Osytshnjuk et al. 2005 as *A. subsmaragdina* Osytshnjuk, 1984; Wood and Monfared 2022).

### 55. *Andrena* (*Aciandrena*) *turmalina* Pisanty & Wood, 2022 *

**Material examined. Iraq:** Duhok, Bessre [Besereh], Bablo, 36.8675°N, 43.1206°E, 1065 m, 5–6.v.2023, 1♀, leg. D. Baiocchi, MSVI; Duhok, Mt. Gara [S of Sarsing], 37.0158°N, 43.3506°E, 1912 m, 11.v.2023, 4♂, 5♀, leg. D. Baiocchi, MSVI/TJWC; **Lebanon:** Beqaa, Anjar, 1 km E, reforestation area, 33.7311°N, 35.9478°E, 1000 m, 7.iv.2023, 1♀, leg. T.J. Wood, TJWC.

**Remarks.** As suspected by Pisanty et al. (2022a), *A. turmalina* is also present in Lebanon.

**Distribution.** Israel, Lebanon*, Turkey, Iraq*, Iran (Pisanty et al. 2022a).

### 56. *Andrena* (*Holandrena*) *variabilis* Smith, 1853

*Andrena bakrajoensis* Amin & Mawlood, 2019, syn. nov.

**Literature records.** Amin and Mawlood (2019, as *A. bakrajoensis*)

**Remarks.** Amin and Mawlood (2019) described *A. bakrajoensis* from Bakrajo in Iraqi Kurdistan. They diagnosed it against *A.* (*Simandrena*) *vetula* Lepeletier, 1841, but based on the description and the provided photographs it is clearly a member of the subgenus *Holandrena* Pérez, 1890 due to the predominantly declivous propodeum (almost without a dorsal horizontal area), strong tergal hairbands, and compact body with rounded head. Based on the long ocelloccipital distance (3× the diameter of a lateral ocellus), it can only be a single species, *A. variabilis*. *Andrena bakrajoensis* is therefore synonymised with *A. variabilis*. The distribution maps of Gusenleitner and Schwarz (2002) do not positively indicate the presence of *A. variabilis* in Iraq, though some dots are present around the Tigris and Euphrates deltas in southern Iraq. However, *A. variabilis* is a widely distributed species in Turkey and Iran (Gusenleitner and Schwarz 2002; Wood and Monfared 2022), and so its presence in Iraq is expected and demonstrated through this synonymy.

### 57. *Andrena* (*Planiandrena*) *veterana* Pisanty, 2022 *

**Material examined. Iraq:** Duhok, Mt. Gara [S of Sarsing], 37.0158°N, 43.3506°E, 1912 m, 11.v.2023, 1♀, leg. D. Baiocchi, MSVI; **Lebanon:** Beqaa, Rachaiya, 5 km S, Mount Hermon nature reserve, 33.4586°N, 35.8395°E, 1500 m, 8.iv.2023, 10♀, leg. T.J. Wood, TJWC.

**Remarks.** These records markedly expand the range of *A. veterana* which was described from Mount Hermon (Pisanty et al. 2022a).

**Distribution.** Israel, Lebanon*, Iraq* (Pisanty et al. 2022a).

### 58. *Andrena* (*Simandrena*) *vetula* Lepeletier, 1841

**Literature records.** Morice (1921b); Derwesh (1965), mentioning “Survey of Iraq Fauna 1915–1919”; Gusenleitner and Schwarz (2002: dot map 504); Augul (2018); Ascher and Pickering (2023).

**Remarks.** We have not examined any specimens of this species, but the presence of this species in Iraq is highly plausible based on its known global distribution, the map records indicated by Gusenleitner and Schwarz (2002), and the presence of this species in neighbouring Turkey and Iran.

**Distribution.** West and Central Palearctic (Gusenleitner and Schwarz 2002; Wood and Monfared 2022; Ascher and Pickering 2023).

### 59. ***Andrena*** **(*Poecilandrena*)** ***viridescens*** **Viereck, 1916**

**Literature records.** Morice (1921b); Derwesh (1965), mentioning "Survey of Iraq Fauna 1915–1919", as *A. cyanescens* Nylander, 1852 nec. Haliday; Augul (2018).

**Material examined.** **IRAQ:** Duhok, Mt. Gara [S of Sarsing], 37.0158°N, 43.3506°E, 1912 m, 11.v.2023, 5♂, leg. D. Baiocchi, MSVI/TJWC.

**Remarks.** Members of the subgenus *Poecilandrena* Hedicke, 1933 are challenging to identify (e.g., Pisanty et al. 2018), but we can confirm the record of Morice (1921b) through the examination of newly collected material.

**Distribution.** Europe to Turkey, Iraq, Iran (Gusenleitner and Schwarz 2002; Wood and Monfared 2022).

## Species excluded

### ***Andrena*** **(*Melandrena*)** ***sigiella*** **Gusenleitner, 1998**

**Literature records.** Grace (2010); Augul (2018); Ascher and Pickering (2023).

**Remarks.** We have examined no specimens of this species from outside of the Levant (Israel and West Bank, Jordan, Lebanon, Syria; Wood et al. 2020). Neither Grace (2010) or Augul (2018) report precise specimen records and, pending further investigations, we exclude *A. sigiella* from the list of Iraqi *Andrena* as if truly present it would be a considerable range extension from the Levant.

### ***Andrena*** **(*Suandrena*)** ***leucocyanea*** **Pérez, 1895**

**Literature records.** Dylewska (1983).

**Remarks.** Dylewska (1983: 22) revised members of the subgenus *Suandrena* Warncke, 1968, mentioning *A. leucocyanea* from Iraq from Abu Ghuraib [= Abu Ghraib] and Dewania [= Al Diwaniyah]. Given the many taxonomic changes that have occurred in this subgenus since 1983 (e.g., Kratochwil 2021; Pisanty et al. 2022a) and its difficulty of identification, it is unclear what these specimens might actually be. Consequently, we exclude this species from the Iraqi fauna pending inspection of material in light of the currently accepted taxonomic framework for this subgenus.

## Discussion

As a measure of its chronic lack of study, the updated faunal list presented here for Iraqi *Andrena* totals some 59 species, a tiny fraction of the 215 and 388 species known from neighbouring Iran and Turkey, respectively (Wood and Monfared 2022; Wood 2023; Wood, unpublished data), and even of the 154–166 species known from neighbouring Syria. Moreover, to the best of our knowledge, the current work represents the first country records for 42 of the 59 Iraqi *Andrena* species reported here. Indeed, the collection around Duhok in May 2023 produced 38 new country records just for *Andrena*, including the two new species for science. Of these 38 new country records, 12 of these species have been described since 2016, highlighting that not only is Iraq understudied in general, but that it specifically hosts a special *Andrena* fauna containing range-restricted species that has received relatively little attention until recently.

The increase from 17 to 59 *Andrena* species represents a 347% increase in species richness. Should it be applied equally across the entire Iraqi bee fauna, the 101 species listed by Ascher and Pickering (2023) would become 350. Though this is a crude approach, this produced total is plausible and seems reasonable given the huge diversity of bee species known to occur in Turkey (1,786 species as listed by Ascher and Pickering 2023). If anything, it is likely to be an underestimate. Based on the initial determination of other Iraqi bee groups, we will soon report faunal increases of 380% for *Eucera* (Apidae), ~ 666–833% for osmiine bees (Megachilidae), and an estimated 430–530% increase for *Nomada* (Apidae) (M. Selis, unpublished data). When dealing with such a poorly studied but likely species-rich fauna, these massive increases indicate a consistent pattern. We hope that this first focused revision of Iraqi *Andrena* can serve as a model to promote further studies into the Iraqi bee fauna.

## Acknowledgements

We thank Esther Ockermüller and Martin Schwarz (OÖLM) for their continued support at the invaluable Linz collection, as well as Joseph Monks (NHMUK). We thank Alireza Monfared, Christian Schmid-Egger, Christophe Praz, and Erwin Scheuchl for helpful comments which meaningfully improved the manuscript.

## Additional information

### Conflict of interest

The authors have declared that no competing interests exist.

### Ethical statement

No ethical statement was reported.

### Funding

No funding was reported.

### Author contributions

TJW identified specimens, described new species, and lead writing of the manuscript; HRI and DB coordinated fieldwork, conducted fieldwork, and contributed to writing of the manuscript; MIH and TTB conducted fieldwork; MS coordinated and conducted specimen preparation and identification, and contributed to writing of the manuscript.

### Author ORCIDs

Thomas J. Wood https://orcid.org/0000-0001-5653-224X
Marco Selis https://orcid.org/0000-0002-8200-9441

### Data availability

All of the data that support the findings of this study are available in the main text.

## References

Amin HM, Mawlood NA (2019) A New Species of The Sand Bees, *Andrena* Fabricius, 1775 (Hymenoptera, Andrenidae) From Kurdistan Region-Iraq. Journal of University of Garmin 6(2): 343–347. https://doi.org/10.24271/garmian.196228

Ascher JS, Pickering J (2023) Discover Life bee species guide and world checklist (Hymenoptera: Apidae: Anthophila). https://www.discoverlife.org/mp/20q?guide=Apoidea_species&flags=HAS

Augul RS (2018) Study on diversity of bees (Hymenoptera, Apoidea) from different regions of Iraq. Bulletin of the Iraq Natural History Museum 15(1): 57–75. https://doi.org/10.26842/binhm.7.2018.15.1.0057

Bossert S, Wood TJ, Patiny S, Michez D, Almeida EAB, Minckley RL, Packer L, Neff JL, Copeland RS, Straka J, Pauly A, Griswold T, Brady SG, Danforth BN, Murray EA (2022) Phylogeny, biogeography and diversification of the mining bee family Andrenidae. Systematic Entomology 47(2): 283–302. https://doi.org/10.1111/syen.12530

Derwesh AI (1965) A preliminary list of identified insects and arachnids of Iraq. Director General Agriculture Research Projections Baghdad. Bulletin 112: 121–123.

Dylewska M (1983) *Andrena suerinensis* Friese und verwandte Arten (*suerinensis*- Untergruppe) (Hymenoptera, Apoidea, Andrenidae). Entomologische Abhandlungen 47: 15–34.

GISGeography (2024) Iraq Satellite Map. https://gisgeography.com/iraq-map/#Satellite-Map [accessed 27 January 2024]

Grace A (2010) Introductory biogeography to bees of the Eastern Mediterranean and Near East. Bexhill Museum Association, Bexhill, 283 pp.

Gusenleitner F (1998) Neue westpaläarktische *Andrena*-Arten (Hymenoptera: Apidae: Andreninae). Entomofauna 19: 109–144.

Gusenleitner F, Schwarz M (2002) Weltweite Checkliste der Bienengattung *Andrena* mit Bemerkungen und Ergänzungen zu paläarktischen Arten (Hymenoptera, Apidae, Andreninae, Andrena). Entomofauna (Supplement 10): 1–1280.

Hazir C, Keskin N, Scheuchl E (2014) Faunistic, geographical and biological contributions to the bee genus *Andrena* (Hymenoptera, Andrenidae, Andreninae) from Turkey. Journal of Hymenoptera Research 38: 59–133. https://doi.org/10.3897/jhr.38.7288

Khalaf AN, Al-Omar MA (1974) A second list of insects of Iraq. Biological Research Center Publication No. 2., Iraq Government Press, Baghdad, 41 pp.

Khodarahmi Ghahnavieh R, Monfared A (2019) A survey of bees (Hymenoptera: Apoidea) from Isfahan Province, Iran. Journal of Insect Biodiversity and Systematics 5(3): 171–201. https://doi.org/10.52547/jibs.5.3.171

Kratochwil A (2021) Taxonomic re-evaluation of *Andrena cyanomicans* Pérez, 1895, *A. fratella* Warncke, 1968, *A. maderensis* Warncke, 1969, *A. mirna* Warncke, 1969, *A. notata* Warncke, 1968, and *A. portosanctana* Warncke, 1969 (Hymenoptera, Anthophila). Linzer Biologische Beitrage 53: 631–698.

Michener CD (2007) The Bees of the World. 2nd edn. Johns Hopkins University Press, Baltimore, 953 pp.

Moalif AS (1994) The bee fauna of Iraq. Melissa 7: 5–6.

Morice FD (1921a) Annotated lists of Aculeate Hymenoptera (except Heterogyna) and Chrysids recently collected in Mesopotamia and North-west Persia. Journal of the Bombay Natural History Society 27: 816–828.

Morice FD (1921b) Annotated lists of Aculeate Hymenoptera (except Heterogyna) and Chrysids recently collected in Mesopotamia and North-west Persia. (Continued from p. 828, Vol. XXVII.). Journal of the Bombay Natural History Society 28: 192–203.

Osytshnjuk AZ, Romasenko L, Banaszak J, Cierzniak T (2005) Andreninae of the Central and Eastern Palaearctic. Part 1. Polish Entomological Monographs II. Polish Entomological Society, Poznań, Poland, 235 pp.

Osytshnjuk AZ, Romasenko L, Banaszak J, Motyka E (2008) Andreninae of the Central and Eastern Palearctic. Part 2. Polish Entomological Monographs V. Polish Entomological Society, Poznań, Poland, 233 pp.

Pisanty G, Scheuchl E, Dorchin N (2016) Eight new species of *Andrena* Fabricius (Hymenoptera: Apoidea: Andrenidae) from Israel – a Mediterranean hotspot for wild bees. Zootaxa 4189(3): 485–515. https://doi.org/10.11646/zootaxa.4189.3.3

Pisanty G, Scheuchl E, Dorchin N (2018) Taxonomic review of the subgenus *Andrena* (*Poecilandrena*) (Hymenoptera: Andrenidae) in Israel and the Levant. Zootaxa 4374(2): 151–188. https://doi.org/10.11646/zootaxa.4374.2.1

Pisanty G, Scheuchl E, Martin T, Cardinal S, Wood TJ (2022a) Twenty-five new species of mining bees (Hymenoptera: Andrenidae: *Andrena*) from Israel and the Levant. Zootaxa 5185(1): 1–109. https://doi.org/10.11646/zootaxa.5185.1.1

Pisanty G, Richter R, Martin T, Dettman J, Cardinal S (2022b) Molecular phylogeny, historical biogeography and revised classification of andrenine bees (Hymenoptera: Andrenidae). Molecular Phylogenetics and Evolution 170: 107151. https://doi.org/10.1016/j.ympev.2021.107151

Popov VV (1967) The bees (Hymenoptera, Apoidea) of Iran. Trudy Zoologicheskogo Instituta, Leningrad 43: 184–216. [In Russian.]

Praz C, Genoud D, Vaucher K, Bénon D, Monks J, Wood TJ (2022) Unexpected levels of cryptic diversity in European bees of the genus *Andrena* subgenus *Taeniandrena* (Hymenoptera, Andrenidae): Implications for conservation. Journal of Hymenoptera Research 91: 375–428. https://doi.org/10.3897/jhr.91.82761

Proshchalykin MY, Fateryga M, Astafurova YV (2023) Corrections and additions to the catalogue of the bees (Hymenoptera, Anthophila) of Russia. ZooKeys 1187: 301–339. https://doi.org/10.3897/zookeys.1187.113240

Radchenko VG, Allahverdi M, Fekrat L (2021) Revision of the mining bee subgenus *Andrena* (*Longandrena*) (Hymenoptera: Apoidea: Andrenidae). Zootaxa 5032(4): 489–515. https://doi.org/10.11646/zootaxa.5032.4.2

Scheuchl E, Gusenleitner F (2009) *Andrena* (*Margandrena*) *elsei* nov.sp., eine neue türkische Sandbienenart (Hymenoptera, Apidae, Andreninae). Linzer Biologische Beitrage 41: 947–962.

Scheuchl E, Hazir C (2012) Description of three new *Andrena* species (Hymenoptera: Apoidea: Andrenidae) from Turkey. The Florida Entomologist 95(4): 831–838. https://doi.org/10.1653/024.095.0403

Scheuchl E, Willner W (2016) Taschenlexikon der Wildbienen Mitteleuropas – Alle Arten im Porträt. Quelle and Meyer Verlag, Wiebelsheim, 917 pp.

Schwenninger HR (2015) Revision of the Western Palaearctic species of the *Andrena taraxaci*-group with description of four new species (Hymenoptera: Andrenidae). Stuttgarter Beiträge zur Naturkunde A, Neue Serie 8: 251–270.

Warncke K (1965) Beitrag zur Kenntnis der Bienengattung *Andrena* F. in der Türkei (Hymenoptera, Apoidea). Mitteilungen der Münchner Entomologischen Gesellschaft 55: 244–273.

Warncke K (1969) A contribution on the knowledge of the genus *Andrena* (Apoidea) in Israel. Israel Journal of Entomology 4: 377–408.

Warncke K (1974) Die Sandbienen der Türkei (Hymenoptera, Apoidea, *Andrena*), Teil A. Mitteilungen der Münchner Entomologischen Gesellschaft 64: 81–116.

Warncke K (1975) Die Sandbienen der Türkei (Hymenoptera, Apoidea, *Andrena*), Teil B. Mitteilungen der Münchner Entomologischen Gesellschaft 65: 29–102.

Wood TJ (2020) Description of a remarkable new *Andrena* species (Hymenoptera: Andrenidae) from Syria. Zoology in the Middle East 66(3): 262–268. https://doi.org/10.1080/09397140.2020.1782580

Wood TJ (2023) New Old World *Andrena* species, with a focus on Turkey (Hymenoptera: Andrenidae). Zootaxa 5266(1): 1–72. https://doi.org/10.11646/zootaxa.5266.1.1

Wood TJ (2024) New Asian *Andrena* species, with notes on the subgenus *Cnemidandrena* (Hymenoptera: Andrenidae). Zootaxa 5404(1): 167–188. https://doi.org/10.11646/zootaxa.5404.1.11

Wood TJ (in press) Further revisions to the Palaearctic *Andrena* fauna (Hymenoptera: Andrenidae). Zootaxa. [in press]

Wood TJ, Monfared A (2022) A revision of the *Andrena* (Hymenoptera: Andrenidae) fauna of Iran, with the description of 16 new species. European Journal of Taxonomy 843: 1–136. https://doi.org/10.5852/ejt.2022.843.1947

Wood, TJ, Boustani M, Rasmont P (2020) A revision of the *Andrena* (Hymenoptera: Andrenidae) of Lebanon with the description of six new species. Annales de la Société entomologique de France (N.S.) 56: 279–312. https://doi.org/10.1080/00379271.2020.1794960

ZooKeys 1205: 299–331 (2024)
DOI: 10.3897/zookeys.1205.121928

Research Article

# The genus *Nisotra* Baly, 1864 (Coleoptera, Chrysomeliae, Galerucinae, Alticini) in Taiwan, with redescriptions of four Asian species and notes on the immature stages of *N. gemella* (Erichson, 1834)

Chi-Feng Lee[1], Ming-Yao Chiang[1], Michael F. Geiser[2], Kuo-Hung Chuang[3]

1 *Applied Zoology Division, Taiwan Agricultural Research Institute, Taichung 413, Taiwan*
2 *Department of Life Sciences, Natural History Museum, London, UK*
3 *Crop Environment Section, Taoyuan District Agricultural Research and Extension Station,Taoyuan, Taiwan*
*Corresponding author: Kuo-Hung Chuang (khchuang@tydais.gov.tw)*

OPEN ACCESS

**Academic editor:** Caroline Chaboo
**Received:** 29 February 2024
**Accepted:** 19 May 2024
**Published:** 1 July 2024

**ZooBank:** https://zoobank.org/959F762C-4DFB-4693-BC95-BDB9E8E8249C

**Citation:** Lee C-F, Chiang M-Y, Geiser MF, Chuang K-H (2024) The genus *Nisotra* Baly, 1864 (Coleoptera, Chrysomeliae, Galerucinae, Alticini) in Taiwan, with redescriptions of four Asian species and notes on the immature stages of *N. gemella* (Erichson, 1834). ZooKeys 1205: 299–331. https://doi.org/10.3897/zookeys.1205.121928

## Abstract

*Nisotra chrysomeloides* Jacoby, 1885, *N. dohertyi* (Maulik, 1926), *N. gemella* (Erichson, 1834), and *Nisotra nigripes* Jacoby, 1894 are redescribed with illustrations of aedeagi, antennae, gonocoxae, abdominal ventrite VIII, and spermathecae. *Nisotra nigripes* is recorded for the first time from Taiwan. The immature stages and life history of *N. gemella* were studied in the laboratory using a novel rearing design. Four synonyms previously proposed are confirmed: *Sphaeroderma javana* de Motschulsky, 1866, *S. orbiculata* de Motschulsky, 1866, *Nisotra bowringi* Baly, 1876, and *Podagrica hibisci* Bryant, 1941 with *N. gemella* (Erichson, 1834). Lectotypes are designated for *Haltica gemella* Erichson, 1834, *N. chrysomeloides* Jacoby, 1885, *N. bowringi* Baly, 1876, and *Podagrica hibisci* Bryant, 1941.

**Key words:** *Hibiscus rosa-sinensis*, *Hibiscus taiwanensis*, *Hibiscus tiliaceus*, Host plants, Lamiaceae, Malvaceae, *Mesona chinensis*, *Urena lobata*

## Introduction

*Nisotra* Baly, 1864 is a widespread genus of flea beetles occurring in Oriental, Palaearctic, Australian, Madagascar, and Afrotropical regions which contains approximately 90 species (Nadein 2013). Only eight species have been recorded from the Palearctic region (Döberl 2010), of which *N. gemella* (Erichson, 1834) is the only species found in Taiwan (Kimoto and Takizawa 1997). *Nisotra gemella* is one of the most widespread species of the genus, occurring west to India, east to Taiwan and the Philippines, north to China, and south to Indonesia (Sumatra and Java) (Kimoto 2000, 2001). This species was firstly recorded in Taiwan by Chen (1934a) and a number of subsequent records were reported (Kimoto 1966, 1970, 1986, 1987, 1989, 1991; Takizawa et al. 1995). Several different host plant species were recorded to *N. gemella*, including *Hibiscus rosa-sinensis* L. (Malvaceae) by Bryant (1941), *Boehmeria nivea* var. *nivea* (L.)

Gaudich. (Urticaceae) by Takizawa (1979) and Yu et al. (1996), *Urena lobata* L. (Malvaceae) by Kimoto (2003), and *Gonostegia hirta* (Blume) Miq. (Urticaceae) by Takizawa (1979).

Beginning during 2005, Taiwanese populations of the genus have been collected and observed extensively by members of the Taiwan Chrysomelid Research Team (TCRT). The TCRT is composed of ten amateurs interested in producing a complete inventory of chrysomelid species in Taiwan. Adults collected from Kinmen Island (金門) were feeding on leaves of *Hibiscus rosa-sinensis*, but populations in Taiwan were found feeding on those of *H. tiliaceus* L. and *H. taiwanensis* S.Y. Hu (current study). In addition, we observed adults feeding on leaves of *Mesona chinensis* Benth. (Lamiaceae). Most of leaves have not been recorded as host plants of *N. gemella*. A taxonomic revision of Taiwanese populations was therefore deemed necessary.

*Mesona chinensis*, referred to as “mesona” (仙草), is an import crop (Fig. 1A, B) that is made into “grass jelly” (仙草凍), a dessert consumed in Taiwan, Hong Kong, Macau, Vietnam, and Southeast Asia. Grass jelly is made by boiling leaves of mesona for hours and cooling the liquid. In addition, mesona can be made into different drinks and desserts, such as hot grass jelly (燒仙草) and mesona tea (仙草茶). Recently the senior author found adults of *Nisotra* feeding on mesona and causing serious damage (Fig. 1B). Since the plants are small and easily manipulated in the laboratory, we set up some modified equipment for observing immature stages of the beetles as the immature stages of this genus are poorly known. Only *N. basselae* (Bryant, 1941), an agricultural pest of Slippery cabbage, *Abelmoschus manihot* Medicus in the Solomon Islands, has its immature stages briefly described as part of an unpublished dissertation (Vaqalo 2014).

Identification of species of *Nisotra* is problematic due to their similar morphologies. Scherer (1969) was the first to use male aedeagi for identifying species from the Indian Subcontinent. Zhang and Yang (2007) recorded five species of *Nisotra* from China based on examination of the aedeagi and provided a key to *Nisotra* species based on external morphology. In contrast, only one species, *N. gemella*, was identified from China by Gressitt and Kimoto (1963), and Indochina by Kimoto (2000). Medvedev (2009) identified *N. chrysomeloides* and *N. gemella* based only on the male aedeagus.

For clarifying species diversity in Taiwan and species identities in Taiwan, China, and Indochina, species identities of *Nisotra* collected from Indochina and Taiwan were re-evaluated based on specimens from numerous institutions, including the following with large collections of the genus: the Natural History Museum, London, UK (**NHMUK**), the largest collection of leaf beetles globally; the Senckenberg Deutsches Enomologisches Institut, Müncheberg, Germany (**SDEI**), where specimens collected from Taiwan during the 1910s by Sauter and identified by Chen (1933) are housed; and the Kitakyushu Museum of Natural History and Human History, Kitakyushu, Japan (**KMNH**), where specimens collected from Taiwan during 1960s to 1980s identified by Kimoto are housed. Four species recorded from China, *N. gemella*, *N. chrysomeloides*, *N. dohertyi*, and *N. nigripes* are redescribed. In the former studies only aedeagi and spermathecae were studied (Zhang and Yang 2007). During this study antennae, abdominal ventrites VIII in females, and gonocoxae were also examined to evaluate their diagnostic values.

## Materials and methods

To obtain eggs of *N. gemella*, young sprouts of mesona were placed in plastic cups (Pint-sized BugDorm, vol. 720 ml) covered by net screen. Eight pairs of *Nisotra* adults were collected from Hsinpu（新埔）in Hsinchu county and placed with the sprouts (Fig. 1C, D) in one plastic cup.

For laboratory rearing of larvae, young sprouts were dug up and roots were washed with water to remove soil. Roots were then put into 9-cm diameter plastic petri dishes covered with tin foil and with blotter paper lining the bottoms

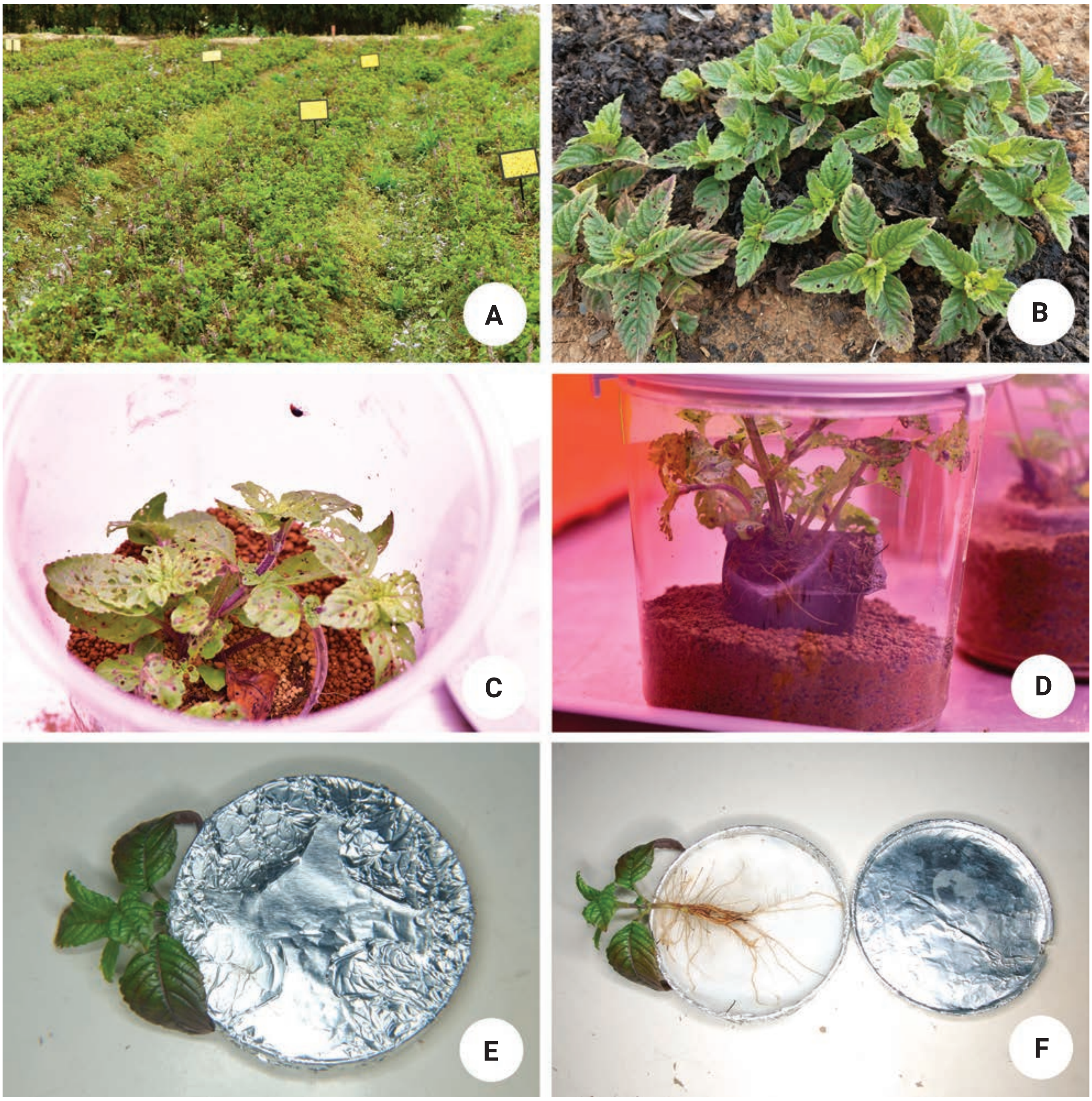

**Figure 1.** Experiments on immature stages of *Nisotra gemella* (Erichson) **A** plantation of mesona (*Mesona chinensis*, 仙草), with yellow sticky insect traps for monitoring populations of *N. gemella* **B** feeding marks made by adults of *N. gemella* **C** young sprouts of mesona placed in plastic cups (Pint-sized BugDorm) as well as adults of *N. gemella*, in dorsolateral view **D** ditto, in lateral view **E** a special design for observing immature stages of *N. gemella* with plastic petri dishes closed **F** ditto, but plastic petri dishes opened.

(Fig. 1E, F). Eggs were put into the petri dishes and kept in darkness and constant temperature (25 ± 1 °C). Larvae were transferred to the plastic petri dishes with roots as mentioned above and observed daily.

For taxonomic study, abdomens of adults were separated from the forebodies and boiled in 10% KOH solution, followed by washing in distilled water to prepare genitalia for illustrations. The genitalia were then dissected from the abdomens, mounted on slides in glycerine, and studied and drawn using a Leica M165 stereomicroscope. For detailed examinations, a Nikon ECLIPSE 50i microscope was used.

At least three males and three females from each species were examined to delimit variability of diagnostic characters. For species collected from more than one locality or with color variations, at least one pair of each sex from each locality and color morph was examined. Length was measured from the anterior margin of the eye to the elytral apex, and width at the greatest width of the elytra. Nomenclature for morphological structures of adults follows Duckett and Daza (2004). Names of plant species follows Taiwan Encyclopedia of Life (2024), TaiEOL.

Terminology of tubercles on larvae follows Kimoto (1962) and Takizawa (1972). Tubercles are defined as sclerotized plates surrounding the bases of primary setae on the body surface. Body surface is divided into five regions: dorsal, dorso-lateral, epipleural, pleural, and sternal regions. The dorsal region has a group of tubercles named group D, which is divided into three tubercles: Da, Dpi, and Dpe, or four tubercles: Dai, Dae, Dpi, and Dpe, where subscripts ‘a’, ‘p’, ‘i’, and ‘e’ denote ‘anterior’, ‘posterior’, ‘interior’, and ‘exterior’, respectively. The dorso-lateral region has tubercle **DL**, which is sometimes divided into two separate tubercles. Epipleural regions have tubercles **EP**, which are also sometimes divided. Pleural regions have a tubercle **P**. The sternal region has three tubercles: parasternal (**PS**), sternellar (**SS**), and eusternal (**ES**) tubercles. Spiracles (**sp**) are present on meso- and metathoraces, and abdominal segments I–VIII.

Specimens studied herein are deposited at the following institutes and collections:

| | |
|---|---|
| **KMNH** | Kitakyushu Museum of Natural History and Human History, Kitakyushu, Japan [Yûsuke Minoshima] |
| **MCSN** | Museo Civico di Storia Naturale “Giacomo Doria”, Genova, Italy [Roberto Poggi] |
| **MCZC** | Museum of Comparative Zoology, Harvard University, Massachusetts, USA [Philip D. Perkins] |
| **MNHUB** | Museum für Naturkunde, Leibniz-Institut für Evolutions- und Biodiversitätsforschung an der Humboldt-Universität zu Berlin, Berlin, Germany [Bernd Jäger] |
| **NHMUK** | The Natural History Museum, London, UK [Michael F. Geiser] |
| **NMNS** | National Museum of Natural Science, Taichung, Taiwan [Bao-Cheng Lai] |
| **SDEI** | Senckenberg Deutsches Enomologisches Institut, Müncheberg, Germany [Mandy Shröter] |
| **SEHU** | Laboratory for Systematic Entomology, Hokkaido University, Sapporo, Japan [Haruo Takizawa] |
| **TARI** | Applied Zoology Division, Taiwan Agricultural Research Insitute, Taichung, Taiwan [Chi-Feng Lee] |

**ZIN** Zoological Institute, Russian Academy of Science, St. Petersburg, Russia [Alexey G. Mosekyo]

Exact label data are cited for all type specimens of described species; a double slash (//) divides the data on different labels and a single slash (/) divides the data in different rows. Other comments and remarks are in square brackets: [p] – preceding data are printed, [h] – preceding data are handwritten, [w] – white label, [y] – yellow label, [g] – green label, [b] – blue label, and [r] – red label. Traditional Chinese fonts are added to the names of localities.

## Taxonomy

### ***Nisotra chrysomeloides*** **Jacoby, 1885**

Figs 2A, B, 3A–C, 4

*Nisotra chrysomeloides* Jacoby, 1885: 36 (Malaysia: Sarawak); Weise 1922: 126 (Indonesia: Java; redescription); Scherer 1969: 150 (India, Myanmar, Vietnam, China; illustration of male aedeagus); Wang 1992: 684 (China: Sichuan, Yunnan); Medvedev 1992: 32 (Nepal); Medvedev 2000: 21 (Nepal).

*Podagrica dohertyi*: Maulik, 1926 (one paratype).

*Nisotra orbiculata* sensu Gressitt and Kimoto 1966: 793 (China: Hainan, Liamui).

*Nisotra gemella* sensu Medvedev 1993: 17 (Philippines: Palawan); Kimoto 2000: 233 (Laos: Umg. Vientiane).

**Types.** *Nisotra chrysomeloides*. ***Lectotype*** ♂ (MCSN, here designated for clarifying its taxonomic status) (Fig. 2A, B), labeled: “Borneo / Sarawak / 1865 66. / Coll. J. Doria [p, w] // Typus [p, w, red letters, with red border] // chrysomeloides / Jac. [p, w] // Nisotra / chrysomeloides / Jac. [h, b] // SYNTYPUS / *Nisotra* / *chrysomeloides* n. sp. / det. M. Jacoby, 1885 [p, r] // Museo Civico / di Genova [p, b]”. Paralectotypes. 3♂, 4♀ (MCSN): “Borneo / Sarawak / 1865 66. / Coll. J. Doria [p, w] // SYNTYPUS / *Nisotra* / *chrysomeloides* n. sp. / det. M. Jacoby, 1885 [p, r] // Museo Civico / di Genova [p, b]”; 2♀ (MCSN): “Sarawak / Doria 65 [p, w] // SYNTYPUS / *Nisotra* / *chrysomeloides* n. sp. / det. M. Jacoby, 1885 [p, r] // Museo Civico / di Genova [p, b]”; 1♀ (NHMUK): “Borneo / Sarawak / 1865 66. / Coll. J. Doria [p, w] // Jacoby Coll. / 1909-28a [p, w] // chrysomeloides Jac [h, b] // SYN- / TYPE [p, w, circle label with blue border]”; 1 (sex undetermined, MCZC): “Borneo / Sarawak / 1865 66. / Coll. J. Doria [p, w] // 1st Jacoby / Coll. [p, w] // chrysomeloides / Jac. [h, b] // Type [p] / 18561 [h, r]”.

*Podagrica dohertyi*. 1♀ (NHMUK): “Co- / type [p, w, circle label with yellow border] // Doherty [p, w] // Birmah / RubyM$^{es}$ [p, w] // Fry Coll. / 1905. 100. [p, w] // *Podagrica* / *dohertyi* M. [h] / S. Mulik det. [p] / type 1926 [h, w]”.

**Additional material examined. Cambodia.** 1♂ (NHMUK), Phnom Bokor, 24–31.X.2007, leg. S. Murzin; 1♀ (NHMUK), Kirirom, 15–17.X.2007, leg. S. Murzin; **China.** Hainan: 2♂, 2♀ (NHMUK), leg. J. Whitehead, 1899.315; 1♀ (KMNH), Liamui, 2.VIII.1933, leg. J. L. Gressitt; Hong Kong: 2♂ (KMNH), Lam Tsuen Valley nr Pak Ngau Shek, 30.V.1965, leg. Y. Miyatake; Yunnan: 1♂ (TARI), Banggunjianshan (邦棍尖山), 20.V.2016, leg. Y.-T. Wang; 2♂, 1♀ (TARI), Bakaliangzi (坝卡梁子), 26.III.2018, leg. Y.-T. Wang; 1♂, 3♀ (TARI), Bakaxiaozhai (巴卡小寨), 2.VIII.2017, leg. Y.-T. Wang; 1♂ (TARI), same but with “18.IX.2017”; 2♀ (TARI), Bangdashan (邦達山), 16.IX.2015, leg. Y.-T. Wang; 2♂, 1♀ (TARI), Bulangshan (布朗山), 28.IX.2017, leg. Y.-T. Wang; 2♀ (TARI), Chinoshan (基諾山), 30.V.2018, leg. Y.-T. Wang; 1♀ (TARI), Luteshan (綠德山), 9.IX.2017, leg. Y.-T. Wang; 2♀ (TARI), Manfen (曼粉), 12.V.2016, leg. Y.-T. Wang; 1♂ (TARI), same but with "20.IX.2017"; 1♂ (TARI), Menglun (勐侖), 2.VIII.2017, leg. Y.-T. Wang; 1♀ (TARI), Mohan (磨憨), 14.V.2016, leg. Y.-T. Wang; 2♂, 6♀ (TARI), Ruili (瑞麗), 6.IX.2014, leg. Y.-T. Wang; **India.** 2♀ (MCSN), Mungphu, 1890, leg. D. Atkinson; Sikkim: 1♀ (KMNH); Uttarakhand: 1♂ (SEHU), Mohand Forest nr Dehra Dun, 7–9.XI.1978; **Indonesia.** Java: 1♀ (SEHU), Bremi, Mt. Argopuro, 31.V.2005, leg. H. Takizawa; 1♂ (MCSN), Buitenzorg (= Bogor), 1878, leg. D. Lansberge; 1♂, 2♀ (MCSN), Sinagar, IV.1876, leg. Beccari; 6♂, 12♀ (MCSN), Tcibodas, X.1874, leg. O Beccari; Sumatra: 2♂, 4♀ (SDEI), coll. Kraatz; 1♂, 1♀ (MCSN), Balighe, X.1890–III.1891, leg. E. Modigliani; 1♂, 1♀ (SEHU), Jambi, Lapak Aur, 6.II.2006, leg. H. Takizawa; 1♀ (MCSN), Mentawei Island, Si Oban, IV.-VIII.1894, leg. Modigliani; 1♀ (MCSN), Padang, 1890, leg. E. Modigliani; 2♂, 1♀ (MCSN), Pangherang -Pisang, X.1890–III.1891, leg. E. Modigliani; 1♂, 1♀ (SEHU), Gunnung Sibayak (Tanah Karo), 11.II.1984, leg. H. Urban, K. Urban, I. Worm, J. Wiesner; 2♂, 2♀ (MCSN), Soekaranda, leg. Dohrn; **Laos.** 1♂, 1♀ (NHMUK), Haut Mekong, Muong Sing, 18.IV.1918, leg. R. V. de Salvaza; 1♀ (KMNH), Umg. Vientiane, III. –VI.1963; Champasak: 2♂, 2♀ (NHMUK), Bolaven Paleau, Rout (No. 23), Pakse-Paksong, Ban Itou env (km 35), 10–18.IV.1999, leg. E. Jendek & O. Šauša; Hua Pan: 5♂, 19♀ (NHMUK), Ban Saleui, Phou Pan Mt., 3–30.VI.2014, leg. C. Holzschuh; 3♂, 5♀ (NHMUK), same but with "27.IV. –1.VI.2011"; Louang Namtha: 1♀ (NHMUK), 20 km NW Louang Namtha, 24–30.V.1997, leg. Jendek; Phongsaly: 9♂, 4♀ (NHMUK), Phongsaly, Phu Fa, 26.VII.2006, leg. M. Geiser; Vientiane: 1♀ (NHMUK), Vang Vieng, 20.VII.2006, leg. A. Strauch; **Malaysia.** Pahang: 3♂, 2♀ (SEHU), Cameron Highland, Gn. Brinchiang, 30.VIII.2016, leg. H. Takizawa; Sabah: 1♂, 1♀ (SEHU), Kota Kinabalu, Kg. Kiapad, Inanam, 26.VI.2010, leg. H. Takizawa; 1♂, 2♀ (SEHU), Ranau, Kundasan, 30.VI.2007, leg. H. Takizawa; Sarawak: 1♀ (SEHU), Kelambit Highland, Bario, 13.VI.2018, leg. A. Abe; **Myanmar.** 3♂, 2♀ (2♂: SDEI; 1♂, 1♀: MCSN; 1♀: NHMUK), Carin Cheba, V.–VII.-(18)88, leg. L. Fea; 1♂ (NHMUK), Karen Mts., leg. Doherty, Fry Coll., 1905.100; 1♂ (NHMUK), Momeit, leg. Doherty, Fry Coll., 1905.100; 1♀ (NHMUK), Pegu, Atkinson Coll.,

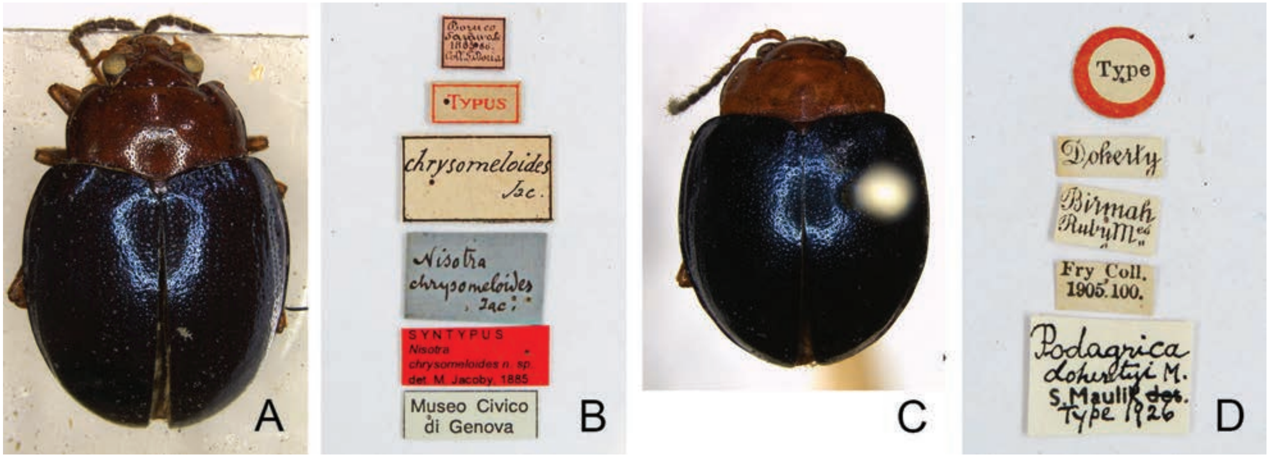

**Figure 2.** Type specimens and labels **A** *Nisotra chrysomeloides* Jacoby, 1885, lectotype **B** labels pinned with lectotype **C** *Podagrica dohertyi* Maulik, 1926, holotype **D** labels pinned with holotype.

1892-3; 1♀ (NHMUK), Toungoo, coll. Andrewes, 1922-221; Kachin State: 2♀ (NHMUK), Nam Tamai, 2.VIII.1938, leg. R. Kaulback; **Nepal.** Bagman Zong: 1♀ (MCSN), Kathmandu valley, Lalitpur Distr., Godawari-Phulchoki, 1–7.VI.1996, leg. P. Čechovský; **Philippines.** Palawan: 1♀ (MCSN), Singapan Basin, Tau't reservation, 11.XII.1990–5.I.1991, coll. Medvedev; **Thailand.** Nakhon Ratchasima: 1♀ (NHMUK), 15.VI.1962, coll. C. I. E.; Nan: 12♂, 11♀ (NHMUK), Doi Phuka N. P., V.2000, leg. local collector; Tak: 1♀ (NHMUK), Mae Chan / Mae Klong confluence, Thung Yai Wildlife Sanctuary, 27.IV.–6.V.1988, leg. M. J. D. Brendell; **Vietnam.** Gia Lai-Kon Tum: 1♀ (MCSN), So Lang, 50 km N Ankhe Ha-Nung, 9.XI.1979, coll. Medvedev; Lao Cai: 1♂ (NHMUK), Cha Pa (= Sa Pa), 13–20. IV.1962, leg. A. Warchalowski; Vinh Phuc: 6♂, 3♀ (NHMUK), Tam Dao, 24–26. IV.1962, leg. A. Warchalowski; 1♀ (NHMUK), same locality, 13.X.1966, leg. A. Jadwiszczak; 2♂ (NHMUK), same locality, 17.X.1966, leg. J. Kania.

**Redescription. Adults.** Length 4.0–4.7 mm, width 2.6–3.2 mm (*n* = 202). General color orange or reddish brown (Fig. 3A–C); elytra, meso- and metathoracic, and abdominal ventrites metallic purple; four basal antennomeres I–IV yellowish brown, V dark brown, VI–XI black. Antennae (Fig. 4A) filiform in males, ratios of lengths of antennomeres I to XI 1.0: 0.6: 0.6: 0.6: 0.6: 0.6: 0.6: 0.6: 0.7: 0.7: 1.0; ratios of length to width from antennomeres I to XI 2.9: 2.3: 2.5: 2.8: 2.6: 2.2: 2.2: 1.8: 2.0: 1.9: 3.0; similar in females, ratios of lengths of antennomeres I to XI (Fig. 4B) 1.0: 0.5: 0.6: 0.5: 0.5: 0.5: 0.6: 0.6: 0.6: 0.6: 1.0; ratios of length to width from antennomeres I to XI 2.6: 2.2: 2.8: 2.3: 2.3: 1.8: 2.0: 1.8: 1.9: 1.9: 3.0. Pronotum 1.9–2.0 × wider than long; disc shining, with sparse, fine punctures, slightly convex; longitudinal groove on each side of apical margin deep, with several coarse punctures along groove; longitudinal groove along basal margin short and shallow; lateral margins rounded; apical margins slightly concave; basal margin medially convex. Elytra 1.2 × longer than wide; disc with coarse punctures arranged into paired longitudinal lines, with fine punctures between coarse punctures; lateral margins rounded, narrowed behind middle. Aedeagus (Fig. 4C–E) wide, ~ 3.8 × longer than wide; parallel sided, moderately narrowed at apical 1/10, apex pointed; moderately curved in lateral view; tectum sclerotized. Endophallic spiculae reduced. Gonocoxae (Fig. 4H) longitudinal and basally connected; apex of each gonocoxa widely rounded, curved dorsally, with nine or ten long setae. Ventrite VIII (Fig. 4F) well sclerotized, short setae arranged into transverse line along sides of apical margin, long setae arranged in transverse line inside apical margin, spiculum extremely long. Spermathecal receptaculum (Fig. 4G) strongly swollen; pump long and curved, with long apical process; sclerotized spermathecal duct moderately long after base of spermathecal gland.

**Diagnosis.** Adults of *Nisotra chrysomeloides* are similar to those of *N. gemella*, with similar body shapes and color patterns, but *N. chrysomeloides* can be distinguished from *N. gemella* by the distinct longitudinal grooves at the sides of the pronotal base with punctures along the grooves (longitudinal grooves almost reduced in *N. gemella*), and less convex pronotum (more convex pronotum in *N. gemella*).The acute apex of the aedeagus in *N. chrysomeloides* (Fig. 4C) differs from the truncate apex and small process in *N. dohertyi* (Fig. 5C) and *N. gemella* (Fig. 7C), and widely rounded apex and small process at middle in *N. nigripes* (Fig. 14C). The moderately curved aedeagus in lateral view differs from the slightly curved aedeagus in *N. nigripes* (Fig. 14D) and strongly

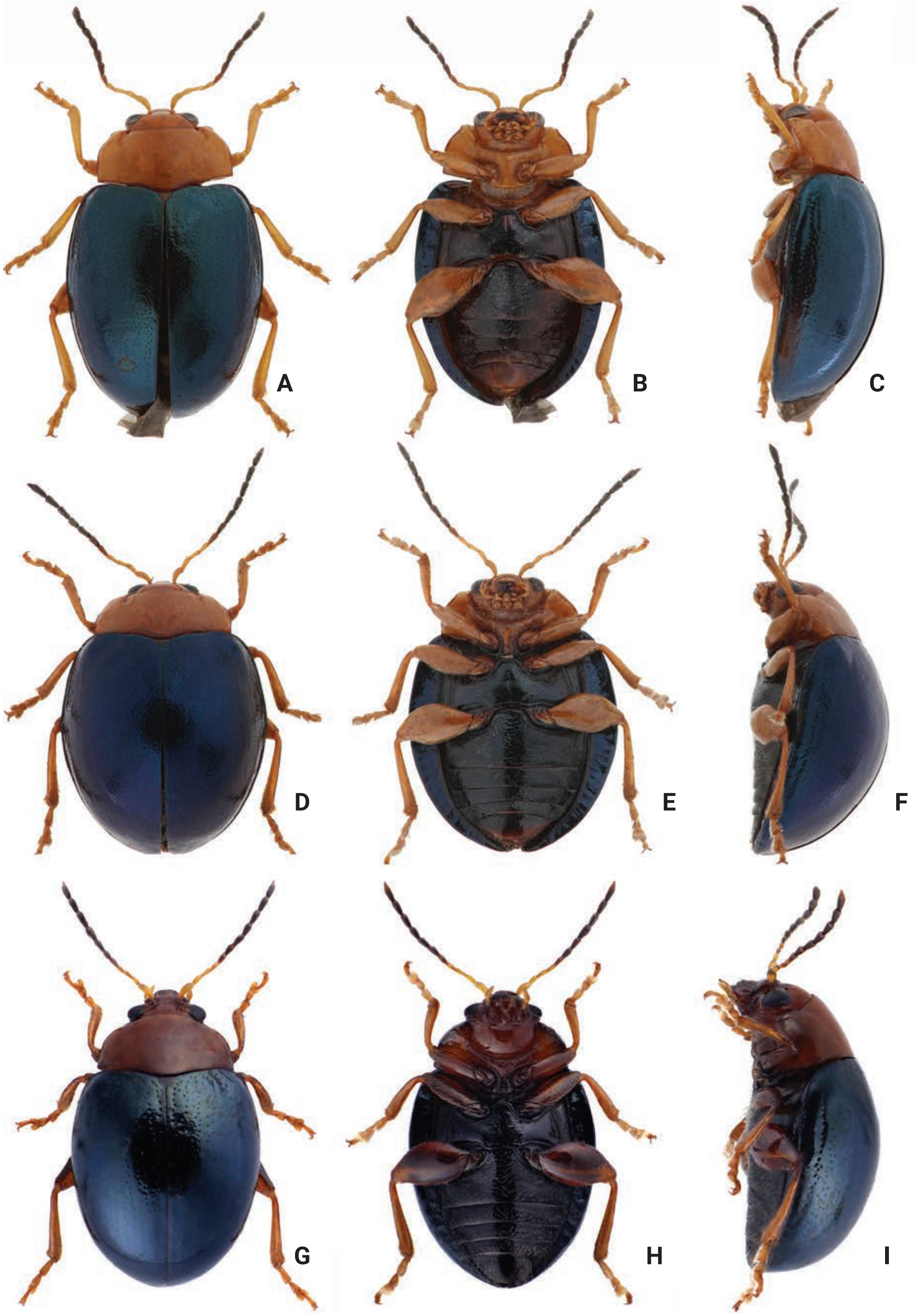

**Figure 3.** Habitus of *Nisotra* species **A** *N. chrysomeloides* Jacoby, female, dorsal view **B** ditto, ventral view **C** ditto, lateral view **D** *N. dohertyi* (Maulik), female, dorsal view **E** ditto, ventral view **F** ditto, lateral view **G** *N. gemella* (Erichson), female, dorsal view **H** ditto, ventral view **I** ditto, lateral view.

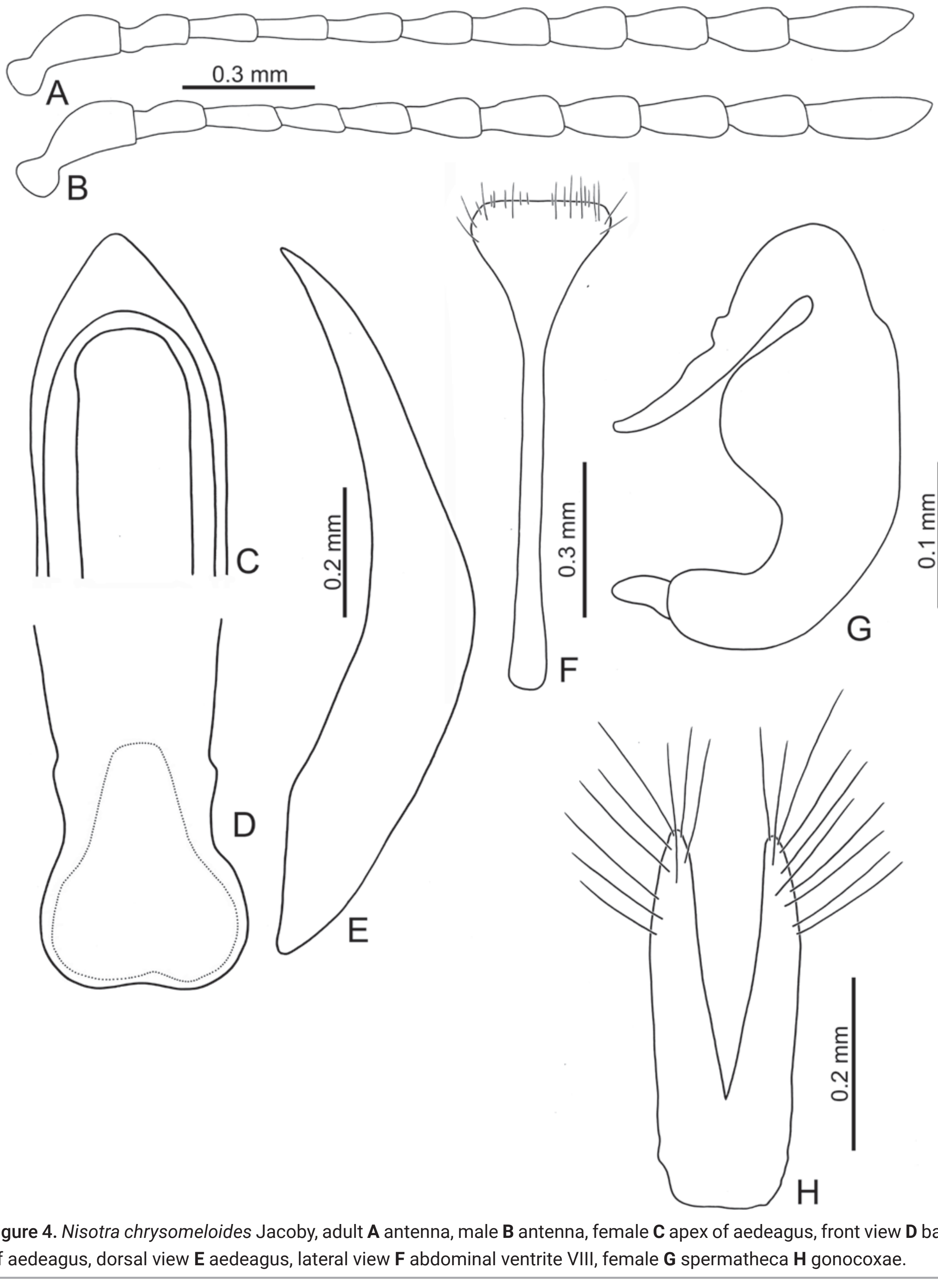

**Figure 4.** *Nisotra chrysomeloides* Jacoby, adult **A** antenna, male **B** antenna, female **C** apex of aedeagus, front view **D** base of aedeagus, dorsal view **E** aedeagus, lateral view **F** abdominal ventrite VIII, female **G** spermatheca **H** gonocoxae.

curved aedeagus in *N. dohertyi* (Fig. 5E). The sclerotized tectum (Fig. 4C) differs from the membranous tectum in others (Figs 5C, 6C, 14C). In females of *N. chrysomeloides*, the dorsally directed apices of the gonocoxae (Fig. 4H) differ from the straight gonocoxae in *N. gemella* (Fig. 7G), the laterally directed apices in *N. nigripes* (Fig. 14G), and inwardly directed apices in *N. dohertyi* (Fig. 5I). Abdominal ventrite VIII, with one transverse line of long setae inside the apical margin and dense short setae along the apical margin (Fig. 4F), differs from ventrite VIII with several pairs of long setae along the apical margin in *N. dohertyi* (Fig. 5F, G).

**Distribution.** Cambodia, China, India, Indonesia (Java, Sumatra), Laos, Malaysia, Myanmar, Nepal, Philippines (Palawan), Thailand, Vietnam.

### ***Nisotra dohertyi*** **(Maulik)**

Figs 2C, D, 3D–F, 5

*Podagrica dohertyi* Maulik, 1926: 280 (Myanmar).

*Nisotra dohertyi*: Scherer 1969: 148; Medvedev 1992: 32 (Nepal); Zhang and Yang 2007: 842 (China: Yunnan).

**Types.** ***Holotype*** ♂ (NHMUK, by original designation) (Fig. 2C, D), labeled: “Type [p, w, circle label with red border] // Doherty [p, w] // Birmah / RubyM$^{es}$ [p, w] // Fry Coll. / 1905. 100. [p, w] // *Podagrica* / *dohertyi* M. [h] / S. Mulik det. [p] / type 1926 [h, w]”. ***Paratypes***. 2♂ (NHMUK): “Co- / type [p, w, circle label with yellow border] // Doherty [p, w] // Birmah / RubyM$^{es}$ [p, w] // Fry Coll. / 1905. 100. [p, w] // *Podagrica* / *dohertyi* M. [h] / S. Mulik det. [p] / type 1926 [h, w]”.

**Additional material examined. China.** Yunnan: 2♂ (TARI), Banggunjianshan (邦棍尖山), 15.IX.2015, leg. Y.-T. Wang; 1♂ (TARI), same but with “17. IX.2015”; 1♀ (TARI), same but with “11.VI.2017”; 1♀ (TARI), same but with “22. IX.2018”; 1♂, 6♀ (TARI), Bulangshan (布朗山), 28.IX.2017, leg. Y.-T. Wang; 3♀ (TARI), Dingiazhai (丁家寨), 27.IV.2018, leg. Y.-T. Wang; 1♀ (TARI), Ruili (瑞麗), 5.IX.2014, leg. Y.-T. Wang; 1♂, 1♀ (TARI), Wuliangshan (無量山), 11.VII.2017, leg. Y.-T. Wang; **Laos.** 1♀ (NHMUK), Haut Mekong, Muong Sing, 18.IV.1918, leg. R. V. de Salvaza; 3♀ (NHMUK), Haut Mekong, Nam Long, 26.IV.1918, leg. R. V. de Salvaza; Hua Pan: 6♂, 20♀ (NHMUK), Ban Saleui, Phou Pan Mt., 3–30. VI.2014, leg. C. Holzschuh; 2♀ (NHMUK), same but with “27.IV. –1.VI.2011”; 1♂ (NHMUK), Phongsaly, Phu Fa, 26.VII.2006, leg. M. Geiser; **Myanmar.** 1♀ (NHMUK), Sadon, 28.VI. –5.VII.1939, leg. R. Malaise; **Vietnam.** Lao Cai: 4♂, 3♀ (NHMUK), Cha Pa (= Sa Pa), 13–20.IV.1962, leg. A. Warchalowski; 1♀ (NHMUK), same locality, 24.IX.2004, leg. M. Geiser.

**Redescription. Adults.** Length 4.0–4.4 mm, width 2.8–3.3 mm ($n$ = 59). General color yellowish brown (Fig. 3D–F); elytra, meso- and metathoracic, and abdominal ventrites metallic purple; four basal antennomeres I–IV yellowish brown, V dark brown, VI–XI black . Antennae (Fig. 5A) filiform in males, ratios of lengths of antennomeres I to XI 1.0: 0.6: 0.6: 0.5: 0.6: 0.6: 0.7: 0.7: 0.8: 0.8: 1.1; ratios of length to width from antennomeres I to XI 2.4: 2.0: 2.3: 2.0: 2.2: 2.2: 2.3: 2.3: 2.5: 2.5: 3.5; similar in females, ratios of lengths of antennomeres I to XI (Fig. 5B) 1.0: 0.6: 0.6: 0.5: 0.6: 0.6: 0.7: 0.7: 0.8: 0.7: 1.0; ratios of length to width from antennomeres I to XI 2.5: 2.4: 2.6: 2.5: 2.6: 2.1: 2.6: 2.3: 2.5: 2.4: 3.7. Pronotum 2.0–2.2 × wider than long; disc dull, with micro-reticulation, less convex; with sparse, fine punctures; longitudinal groove on each side of apical margin deep, with several coarse punctures along groove; longitudinal groove on basal margin short and shallow; lateral margins rounded; apical margins

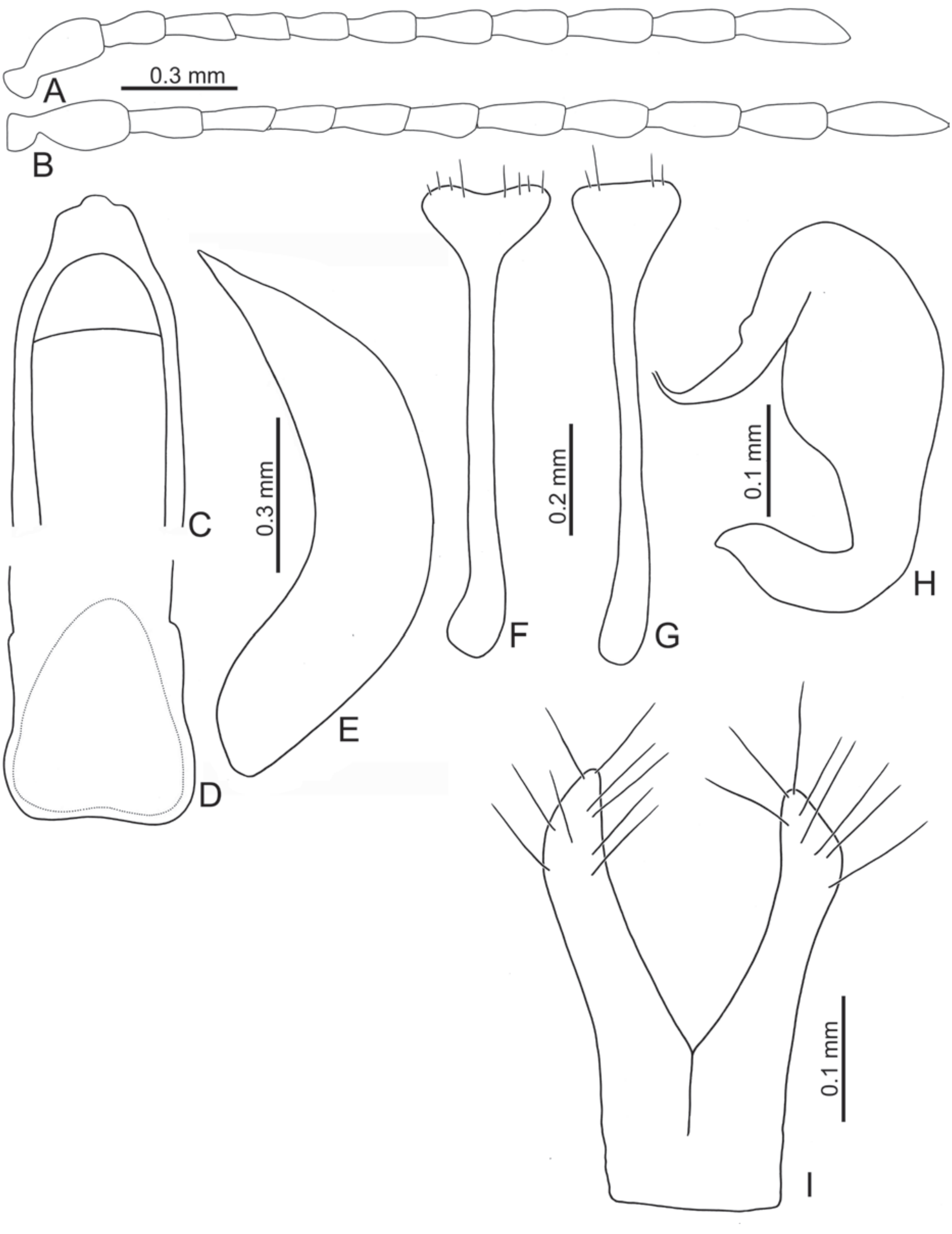

**Figure 5.** *Nisotra dohertyi* (Maulik), adult **A** antenna, male **B** antenna, female **C** apex of aedeagus, front view **D** base of aedeagus, dorsal view **E** aedeagus, lateral view **F** abdominal ventrite VIII, female, from China (Yunnan) **G** abdominal ventrite VIII, female, from China (Laos) **H** spermatheca **I** gonocoxae.

slightly concave; basal margin medially convex. Elytra 1.1 × longer than wide; disc with coarse, confused punctures, mixed with fine punctures; lateral margins rounded, narrowed behind middle. Aedeagus (Fig. 5C–E) wide, ~ 3.7 × longer than wide; parallel sided, moderately narrowed at apical 1/10; apex truncate, but with one median rounded process; extremely strongly curved in lateral view; tectum membranous. Endophallic spiculae reduced. Gonocoxae (Fig. 5U) longer than wide, and basally connected; apex of each gonocoxa widely rounded, curved inwards, with eight or nine long setae. Ventrite VIII (Fig. 5F, G) well sclerotized, 2–4 pairs of setae arranged into transverse line along sides of apical margin, spiculum extremely long. Spermathecal receptaculum (Fig. 5H) strongly swollen; pump long and curved, with long apical process; spermathecal duct sclerotized, moderately long after base of spermathecal gland.

**Diagnosis.** Adults of *Nisotra dohertyi* are characterized by the confused punctures on the elytra (punctures arranged into paired longitudinal lines in other species), dull pronotum with micro-reticulation (shining pronota without micro-reticulation in others), and ovate elytra, 1.1 × longer than wide (oblong elytra, 1.2 × longer than wide in others), although this character is similar in a few adults of *N. chrysomeloides* and *N. gemella* with more ovate bodies. In males of *N. dohertyi*, the truncate apex and small process of the aedeagus (Fig. 5C) differ from the acute apex in *N. chrysomeloides* (Fig. 4C) and widely rounded apex and small medial process in *N. nigripes* (Fig. 14C). The strongly curved aedeagus in lateral view (Fig. 5E) differs from the moderately curved aedeagus in *N. chrysomeloides* (Fig. 4E) and *N. gemella* (Fig. 7D), and slightly curved aedeagus in *N. nigripes* (Fig. 14D). The membranous tectum (Fig. 5C) differs from the sclerotized tectum in *N. chrysomeloides* (Fig. 4C). In females of *N. dohertyi*, the inwardly directed apices of the gonocoxae differ from the straight gonocoxae in *N. gemella* (Fig. 7G), dorsally directed apices in *N. chrysomeloides* (Fig. 4H), and laterally directed apices in *N. nigripes* (Fig. 14G). Abdominal ventrite VIII with several pairs of long setae along apical margin (Fig. 5F, G) differs from the presence of one transverse line of long setae inside the apical margin and dense short setae along the apical margin in others (Figs 4F, 7E, 14E).

**Distribution.** China, Laos, Myanmar, Vietnam. Records in Nepal need further confirmation.

### ***Nisotra gemella*** **(Erichson)**

Figs 3G–I, 6A–N, 7–12

*Haltica gemella* Erichson, 1834: 275 (Philippines: Luzon).

*Nisotra gemella*: Jacoby 1885: 34 (Indonesia: Java); Scherer 1969: 148 (illustration of male aedeagus); Kimoto and Takizawa 1973: 177 (Nepal); Scherer 1979: 138 (India, Bhutan); Gruev 1985: 40 (Nepal); Kimoto 1986: 60 (additional records in Taiwan); Kimoto 1987: 191 (additional records in Taiwan); Kimoto 1989: 263 (additional records in Taiwan); Kimoto 1991: 16 (additional records in Taiwan); Medvedev 1993: 17 (Philippines: Luzon, Palawan (misidentification!)); Kimoto 2000: 233 (Laos, Thailand); Medvedev 2000: 21 (Nepal); Kimoto 2001: 201 (catalogue); Aston 2009: 5 (China: Hong Kong).

*Nisotra gemellata* [sic!]: Duvivier 1885: 49 (Indonesia: Sumatra).

*Sphaeroderma javana* Motschulsky, 1866: 421 (Indonesia: Java). Synonymized with *N. gemella* by Medvedev (2006). Synonym confirmed.

*Podagrica javana*: von Harold 1876: 3481.

*Nisotra javana*: Weise 1922: 126; Ogloblin 1930: 106.

*Sphaeroderma orbiculata* Motschulsky, 1866: 421 (India); Harold 1876: 3548 (catalogue). Synonymized with *N. gemella* by Scherer (1969). Synonym confirmed.

*Nisotra orbiculata*: Ogloblin 1930: 106; Chen 1933: 55 (China: Guandong); Chen 1934a: 181 (Taiwan); Chen 1934b: 278 (South China, Vietnam, India); Chûjô 1935: 474 (catalogue of Taiwan fauna); Gressitt and Kimoto 1963: 793 (China: Sichuan, Jiangxi, Guanxi, Fujian, Hainan Island); Kimoto 1966: 35 (additional records in Taiwan); Scherer 1969: 148 (India); Kimoto 1970: 215 (New Taipei City: Pinglin (坪林)); Takizawa et al. 1995: 14 (additional records in Taiwan).

*Nisotra bowringi* Baly, 1876: 584 (China: Hong Kong); Jacoby 1889: 196 (Myanmar). Synonymized with *N. orbiculata* by Ogloblin (1930). Synonym confirmed.

*Podagrica bowringi*: Maulik 1926: 278 (India).

*Podagrica hibisci* Bryant, 1941: 286 (Malaysia; host plant: *Hibiscus rosa-sinensis* L.). Synonymized with *N. gemella* by Scherer (1969). Synonym confirmed.

**Types.** *Haltica gemella*. ***Lectotype*** ♂ (MNHUB, here designated to preserve stability of nomenclature), labeled (Fig. 6A–C): “Manila / Meyer [h, y] // Paratypus [p, r] // HOLOTYPUS [p, red letters] / Nisotra ♂ / gemella / (Erichson) [h, black letters] / det Dr. G. Scherer 19 [p, red letters] 67 [h, w, black letters]”. Paratypes (MNHUB): three specimens bear same labels as lectotype except “PARATYPUS [p, red letters] / Nisotra ♂ or ♀ / gemella / (Erichson) [h, black letters] / Dr. G. Scherer 19 [p, red letters] 67 [h, w, black letters]”. One specimen labeled (Fig. 6D): “45025 [p, w] // Haltica / gemella / Eri / Manila / Meyer [h, y] // Typus [p, r] // PARATYPUS [p, red letters] / Nisotra ♂/ gemella / (Erichson) [h, black letters] / Dr. G. Scherer 19 [p, red letters] 67 [h, w, black letters]”. Although labels for holotype and paratypes were written by Scherer, but it was not officially published.

*Sphaeroderma javana*. ***Lectotype*** ♂ (ZIN, designated by Medvedev 2006) (Fig. 6E–G): “Sphaeroderma / javana / Motsch. / Java [h, y] // LECTOTYPUS / Nisotra / javana Motsch. / L. Medvedev design. [p, r]”. Medvedev (2006) indicated that there are three paralectotypes female bearing same labels.

*Sphaeroderma orbiculata*. ***Lectotype*** ♂ (ZIN, designated by Medvedev 2006) (Fig. 6H–J): “Sphaeroderma / orbiculata / Motsch / Ind. or. [h, y] // Nisotra / orbiculata Mts / (= borwing Baly / 1927 [h] D. Ogloblin det. [p. w] // LECTOTYPUS / Nisotra / orbiculata Motsch. / L. Medvedev design. [p, r]”.

*Nisotra bowringi*. ***Lectotype*** ♀ (NHMUK, here designated to preserve stability of nomenclature) (Fig. 6K, L), labeled: “Hong / Kong [h, w, circle label] // Nisotra / Bowringi / Baly / Hong Kong [h, b] // Type / H. T. [p, w, circle label with red border]”. ***Paralectotype*:** 1♀ (NHMUK), shared with the same pin as lectotype.

*Podagrica hibisci*. ***Lectotype*** ♀ (NHMUK, here designated to preserve stability of nomenclature) (Fig. 6M, N), labeled: “01880 [h] / Malaya [p] / Kula Lumpur / 16.12. [h] 19 [p] 37 [h] / Entom. Div. [p] / Hibiscus / Rosa-sinensis [h, w] // Type [p, r, circle label with red border] // Pres. by / Imp. Inst. Ent. / B. M. 1941-61. [p, w] // Podagrica / hibisci / Bryant [h] / Det. G. E. Bryant [p, w] // NHMUK015024484 [p, w, with QR-Code]”. ***Paralectotype*.** 1♀ (NHMUK), bearing same labels as lectotype but without type and QR-Code labels.

**Additional material examined. China.** Fujian: 1♀ (TARI), Chishui (赤水), 20.VI.2014, leg. Y.-T. Chung; 1♂ (KMNH), Chungan: Bohea Hills, 11.I.1940, leg.

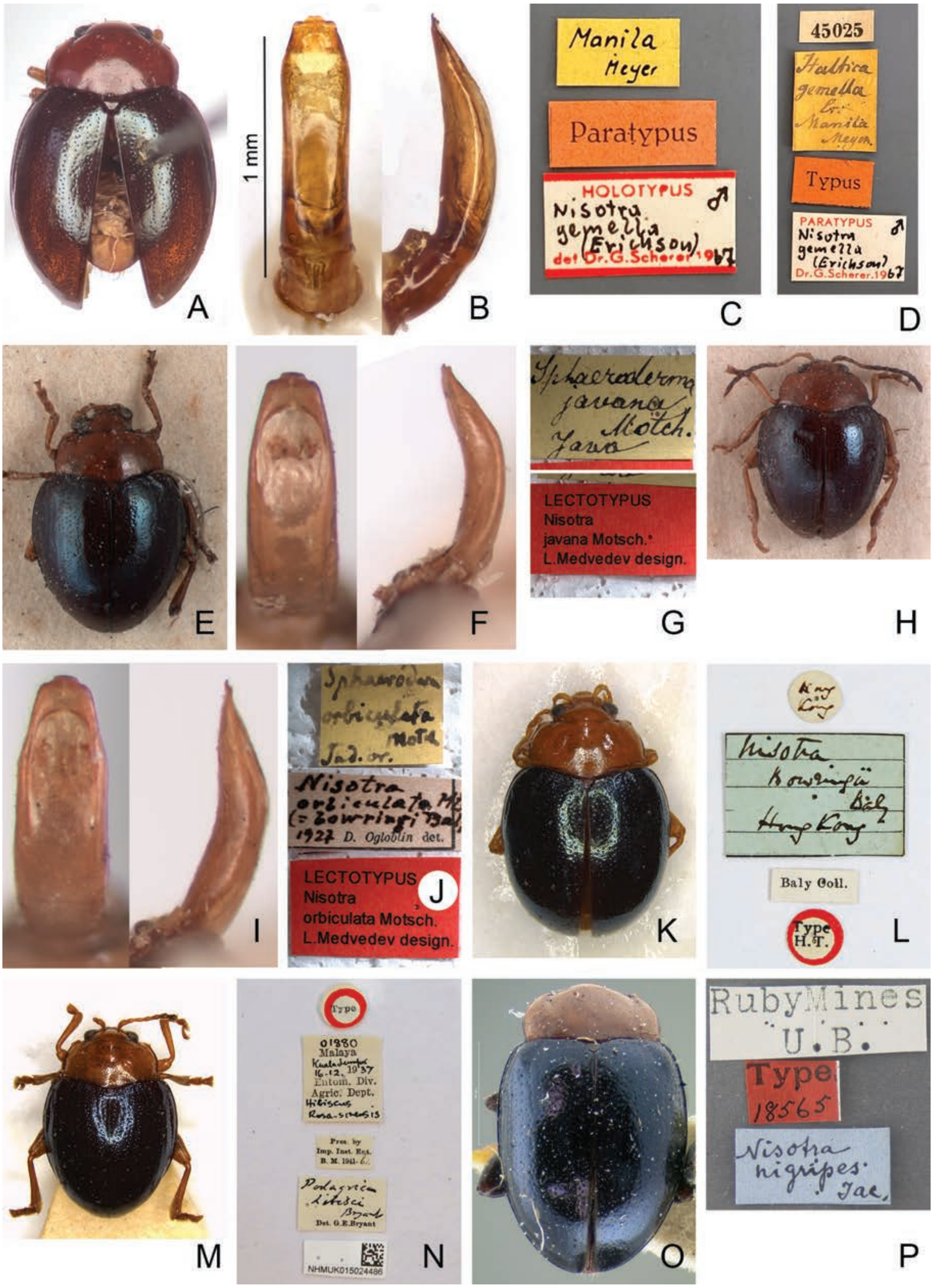

**Figure 6.** Type specimens and labels **A** *Haltica gemella* Erichson, 1834, lectotype **B** aedeagus dissected from lectotype, left: dorsal view; right: lateral view **C** labels pinned with lectotype **D** labels pinned with a paralectotype **E** *Sphaeroderma javana* Motschulsky, 1866, lectotype **F** aedeagus dissected from lectotype, left: dorsal view; right: lateral view **G** labels pinned with lectotype **H** *Sphaeroderma orbiculata* Motschulsky, 1866, lectotype **I** aedeagus dissected from lectotype, left: dorsal view; right: lateral view **J** labels pinned with lectotype **K** *Nisotra bowringi* Baly, 1876, lectotype **L** labels pinned with lectotype **M** *Podagrica hibisci* Bryant, 1941 **N** labels pinned with lectotype **O** *Nisotra nigripes* Jacoby, 1894, holotype **P** labels pinned with holotype.

T. C. Maa; 1♀ (TARI), Zhaizhong (宅中), 24.VIII.2014, leg. Y.-T. Wang; Guandong: 1♀ (KMNH), Fei-ha to Fei-loi, 1.VII.1950, leg. J. L. Gressitt; 1♀ (NHMUK), nr. Canton (= Guanzhou, 廣州), 27.IX.1980, leg. P. M. Hammond, B.M. 1980-491; Guanxi: 1♂ (NHMUK), Huanjiang Xian, Maonan, leg. M. Häckel; Hainan: 1♀ (TARI), Nanhsitsum (南喜村), 15.XI.2018, leg. Y.-T. Wang; Hong Kong: 1♂, 1♀ (NHMUK), coll. Walker, 1893—58; Hunnan: 1♀ (NHMUK), mts. Daiongshan, Xinhua, VII.2004, leg. Jing; Yunnan: 1♂ (TARI), Bakaxiaozhai (巴卡小寨), 1.VIII.2017, leg. Y.-T. Wang; 1♂ (TARI), Chinoshan (基諾山), 31.V.2018, leg. Y.-T. Wang; 4♂ (TARI), Manfen (曼粉), 20.IX.2017, leg. Y.-T. Wang; 1♀ (TARI), Menglun (勐侖), 2.VIII.2017, leg. Y.-T. Wang; 1♀ (TARI), same but with “20.IV.2018”; 2♀ (TARI), same but with “2.V.2019”; 1♀ (TARI), Mohan (磨憨), 14.V.2016, leg. Y.-T. Wang; 1♀ (TARI), Nabang (那邦), 25.IX.2018, leg. Y.-T. Wang; 2♀ (TARI), Ruili (瑞麗), 15.IX.2014, leg. Y.-T. Wang; Zhejiang: 3♂ (NHMUK), Da-Laen-Saen, near Ning-Po, col. Walker, 1893-18; 2♂ (NHMUK), same locality, leg. J. J. Waliker, G. C. Champion Coll., B.M. 1927-409; **India.** Andaman Islands: 3♂ (NHMUK), Capt. Wimberley, Fry Coll. 1905 100; 2♂, 1♀ (NHMUK), same locality, leg. F. A. de Roepstorff, 1884-15; 1♂, 1♀ (NHMUK), Port Blair, 10.X.1989, leg. B. S. Bhumannava, feeding on *Urena lobata*; Assam: 1♀ (KMNH), Kaziranga nödl. Mikir-Hills, Brahmaputra, V.1961, leg. G. Scherer; Sikkim: 1♀ (NHMUK), Dikchu, 23.IV.1924, leg. R. W. G. Hingaton; Tamil Nadu: 5♂ (SEHU), Nilgiri, Mettupalayam, 30.II.1978; Uttarakhand: 1♀ (NHMUK), Ranikhet, Kumaon, coll. H. G. Champion, 1953-156; 1♂ (SEHU), Mohand Forest nr Dehar Dun, 7–9.XI.1978; 3♂, 1♀ (SEHU): FRI, Dehra Dun, 10–13.XI.1978; **Indonesia.** Java: 1♀ (SEHU), Bremi, Mt. Argopuro, 31.V.2005, leg. H. Takizawa; 9♂, 12♀ (MCSN), Buitenzorg (= Bogor), 1875, leg. G. B. Ferrari; 1♀ (MCSN), same but with “X.1872”; 1♀ (MCSN), same locality, 1878, leg. D. Lansberge; 1♂, 1♀ (SDEI); Sulawesi: 1♀ (SEHU), Kendari: Amoito, 1.XII.1974, leg. K. Kusigemati; 1♂ (SEHU), Kendari: Andonuhu, 3.XII.1974, K. Kusigemati; 3♂, 3♀ (MCSN), Kandari, III.(18)74, leg. O. Beccari; Sumatra: 2♂ (SEHU), Aceh, Kota Cane, 26–28.IV.1998, leg. H. Takizawa; 3♂, 4♀ (MCSN), Ayer Manicior (= Ajer Mantjoer), VIII.1878, leg. O. Beccari; 2♂, 1♀ (SDEI), Bangkei Island, 1885, leg. H. Kühn; 1♀ (MCSN), Benculen, IV.1891, leg. E. Modigliani; 1♂, 1♀ (SEHU), Bukit Gompong, Sukarami, NE 20 km from Padang, 19.VIII.1998, leg. M. Ohara; 1♂ (SEHU), Jambi, Lapak Aur, 6.II.2006, leg. H. Takizawa; 1♂ (MCSN), Padang, 1890, leg. E. Modigliani; 1♂ (MCSN), Sing Hara, X.1878, leg. O. Beccari; 1♂, 2♀ (SDEI), Tebing Tinggi, leg. Schultheiss; **Laos.** 3♂, 4♀ (NHMUK), Betw. Vientiane & Luang Prabang, end of 1919, leg. R. V. de Salvaza; Attapu: 1♂ (NHMUK), Bolaven Plateau, 15 km SE of Ban Huang Kong, Nong Lom (lake), 18–30.IV.1999, leg. E. Jendek & O. Šauša; Bolikhamsai: 1♂, 1♀ (NHMUK), Lak Sao, 18.VIII.2004, leg. M. Geiser; Borikhan: 1♂ (NHMUK), Borikhan env., 20 km N of Muang Pakxan, 18.V.2003, leg. O. Šafránek; Champasak: 1♀ (NHMUK), Bolaven Paleau, Rout (No. 23), Pakse-Paksong, Ban Itou env (km 35), 10–18.IV.1998, leg. E. Jendek & O. Šauša; Hua Pan: 1♀ (NHMUK), Ban Saleui, Phou Pan Mt., 11.IV.-15.V.2012, leg. C. Holzschuh; 1♂ (NHMUK), same but with “27.IV. –1.VI.2011”; Phongsaly: 1♂ (NHMUK), Phongsaly, Phu Fa, 26.VII.2006, leg. M. Geiser; Savannakhét: 1♂ (SEHU), 1.V.2006, leg. K. Maruyama; Vientiane: 1♀ (SEHU), Vang vieng, 28–29.V.2004, leg. T. Tsuru; 1♀ (NHMUK), same locality, 20.VII.2006, leg. M. Geiser; 2♂, 1♀ (NHMUK), same but with “21.VII.2006”; **Malaysia.** Kuala Lumpur: 1♂ (SEHU), Labu, 31.III.2007, leg. H. Takizawa; Perak: 4♂, 2♀ (MCSN), 25 km NE of Ipoh, Banjaran Titi Wangsa mts., Korbu mt., 27.I.–

2.II.1999, leg. P. Čechovský; 3♂, 2♀ (MCSN), same but with "4–13.III.1998"; Sabah: 1♂, 2♀ (SDEI), Kinabalu, S. W. 11, leg. H. Rolle; **Myanmar.** 1♂, 1♀ (SDEI), Carin Cheba, V.–VII.-(18)88, leg. L. Fea; 1♂, 1♀ (NHMUK), same locality, coll. Fry, 1905.100; 1♀ (MCSN), Carin, Asciuii Cheba, I.(18)88, leg. L. Fea; 4♂, 4♀ (SDEI), Palon, Pegu, VIII.–IX.(18)87, leg. L. Fea; 1♀ (NHMUK), Momeit, leg. Doherty, Fry Coll., 1905.100; 1♀ (NHMUK), Paungde, coll. Andrewes, 1922-221; 1♂, 2♀ (NHMUK), Prome, coll. Andrewes, 1922–221; 2♂, 2♀ (SDEI), Rangoon (= Yangon), 1887, leg. Fea; 1♀ (NHMUK), same but with "Atkinson Coll., 1892–3"; 2♀ (NHMUK), same but with "coll. Fry, 1905.100"; 1♂ (NHMUK), same locality, 1933–34, leg. F. J. Meggitt; 4♂, 4♀ (4♂, 2♀: SDEI; 1♀: MCSN; 1♀: NHMUK), Teinzo, V.1886, leg. Fea; 1♂, 2♀ (NHMUK), Tharrawaddy, leg. H. Swale, 1913-117; 4♀ (NHMUK), same locality, leg. H. E. Andrewes, 1922-221; 2♂, 3♀ (NHMUK), same locality, 26.XII.1953, leg. H. G. Champion; 1♀ (NHMUK), Toungoo, 26.XII.1953, leg. H. G. Champion; Kachin State: 1♂ (MCSN), VIII.1885, leg. Fea; 1♀ (NHMUK), Bhamo, VIII.1885, leg. Fea; 2♂, 1♀ (NHMUK), Nam Tamai, 2.VIII.1938, leg. R. Kaulback; Kayin Sate: 1♀ (TARI), Than Daung Gyi, 18.V.2017, leg. Y.-T. Wang; Yangon: 2♂, 2♀ (NHMUK), Shwentha, 23.VII.1988, leg. T. T. Nwe, collected from *Urena lobata*; **Nepal.** 3♂, 2♀ (SEHU), Balaju Kathmandu Valley, 11.IX.1987, leg. H. Takizawa; **Papua New Guinea.** 1♀ (SDEI), Haveri, VII.–XI.(18)93, leg. Loia; 1♀ (SDEI), Ighibirei, VII.-VIII.(18)90, leg. Loria; 1♂ (TARI), West Highland, Begesin Missions station 43 km 237° von Madan, Kulturlandschan, 6.V.1996, leg. H. Deumer; **Philippines.** Luzon. Kalinga: 1♂ (MCSN), Tulgao, 23.VI.1988, coll. Medvedev; **Singapore.** 3♂, 1♀ (NHMUK), leg. C. J. Saunders, B. M. 1933-227; **Taiwan.** Hsinchu: 3♂, 3♀ (TARI), Hsinpu (新埔), 2.I.2010, leg. K.-H. Chuang; 18♂, 23♀ (TARI), same but with "5.X.2021"; 12♂, 14♀ (TARI), same but with "18.XII.2021"; Kinmen: 2♂, 7♀ (TARI), Kinmen Island (金門島), 18.VI.2014, leg. Y.-T. Chung; 4♂, 8♀ (TARI), same island, Jhongshanlin (中山林), 28.VI.2023, leg. C.-F. Lee; 5♀ (TARI), 太武苗圃(= Kinmen Botanical Gardens, 金門植物園), 24.IV.2002, leg. H. T. Shih; 1♀ (TARI), same but with "Taiwushan (太武山)"; Matsu: 1♀ (TARI), Beigan Island (北竿島), 14.V.2018, leg. H.-T. Fang; New Taipei City: 1♀ (KMNH), Pinglin (坪林), 23.VI.1965, leg. Y. Kurosawa; 4♂ (TARI), Watzuwei (挖仔尾), 28.VI.2008, leg. H. Lee; 1♂ (KMNH), Urai (烏來), 31.V.1976, leg. H. Makihara; Nantou: 1♀ (SDEI), Fuhosho (= Wucheng, 五城), IX.1909, leg. Sauter; Pingtung: 1♂, 1♀ (TARI), Shantimen (三地門), 1–5.III.1982, leg. K. C. Chou & C. C. Pan; 1♀ (TARI), Tahan trail (大漢林道), 10.IV.2023, leg. J.-C. Chen; Taipei: 1♀ (SDEI), Hokuto (= Peitou, 北投), III.1912, leg. Sauter; Taitung: 2♀ (SDEI), Paroe (= Tawu, 大武), IX.1912, leg. H. Sauter; Taoyuan: 1♀ (TARI), Tayuan (大園), 15.VIII.2011, leg. L.-F. Chu; **Thailand.** Chiang Mai: 1♀ (NHMUK), Fah Luan Univ. Campus, 20–22.VII.2009, leg. D. Quicke & B. et R. Butcher; 1♀ (NHMUK), Queen Sirikit Botanic Gardens, VII.2006, leg. H. Mendel & M. V. L. Barclay; 1♂ (NHMUK), Tha Ton Env., 20.IV.2003, leg. O. Šafránek; Kanchanaburi: 1♂, 1♀ (NHMUK), Thongpapoom, 11–12.VII.2009, leg. D. Quicke & B. et R. Butcher; Mae Hong Son: 1♂ (NHMUK), Mae Hong Son, 17–21.VI.1993, leg. Schneider; Nakhon Nayok: 2♂, 1♀ (SEHU), Ban Na, 27.VII.1997, leg. S. Ohmomo; Nan: 1♂, 2♀ (NHMUK), Doi Phuka N. P., V.2000, leg. local collector; Songkhla: 1♀ (NHMUK), Chon Thong, 24–27.IV.1991, leg. L. Dembický; Yala: 1♂ (NHMUK), Betong, Gunung Cang Dun vill., 25.III. –22.IV.1993, leg. J. Horák; **Vietnam.** Băc Giang: 2♂, 2♀ (TARI), Tây Yên Tủ, 2.VI.2014, leg. Y.-T. Wang; Hà Nôi: 1♂, 1♀ (TARI), Huyên Mê Linh, 30.V.2014, leg. Y.-T. Wang; Hòa Binh: 3♀

(NHMUK), VIII.1918, leg. R. V. de Salvaza; 1♂ (MCSN), Ha Son-Binh, 10 km SW Hoa Binh, 17.X.1976, leg. L. Medvedev; Lao Cai: 2♂ (NHMUK), Bao Ha, 12.IV.1962, leg. A. Warchalowski; 1♂ (NHMUK), same but with "4.IV.1962"; 2♂, 5♀ (NHMUK), Cha Pa (= Sa Pa), 14.IV.1962, leg. A. Warchalowski; Nam Dinh: 1♀ (NHMUK), Van Diem, 19.III.1962, leg. A. Warchalowski; 1♂ (NHMUK), same but with "7.II.1962"; Ninh Binh: 1♂ (NHMUK), Cuc Phuong, 8.VI.1966, leg. R. Bizlawski & B. Pisarski; Quang Ninh: 1♂ (TARI), 10 km SE Tien Yen, 1–14.IV.2004, leg. H. Mühle; Vinh Phuc: 1♂, 2♀ (NHMUK), Tam Dao, 25.IV.1962, leg. A. Warchalowski; 1♂, 1♀ (NHMUK), same locality, 17.X.1966, leg. J. Kania.

**Redescription. Adults.** Length 3.1–3.9 mm, width 2.0–2.5 mm (*n* = 376). General color yellowish brown (Fig. 3G–I); elytra, meso- and metathoracic, and abdominal ventrites metallic purple; four basal antennomeres I–IV yellowish brown, V dark brown, VI–XI black. Antennae (Fig. 7A) filiform in males, ratios of lengths of antennomeres I to XI 1.0: 0.5: 0.6: 0.5: 0.5: 0.5: 0.5: 0.6: 0.6: 0.7: 1.0; ratios of length to width from antennomeres I to XI 3.2: 2.4: 2.9: 2.6: 2.2: 2.2: 2.2: 2.6: 2.6: 2.6: 4.2; similar in females, ratios of lengths of antennomeres I to XI (Fig. 7B) 1.0: 0.5: 0.5: 0.5: 0.5: 0.5: 0.6: 0.6: 0.6: 0.6: 1.0; ratios of length to width from antennomeres I to XI 3.6: 2.3: 2.9: 2.5: 2.4: 1.9: 2.0: 2.2: 2.6: 2.2: 3.8. Pronotum 1.8–1.9 × wider than long; disc shining, moderately convex, with sparse, fine punctures; longitudinal groove on each side of apical margin reduced; longitudinal groove on basal margin short and shallow; lateral margins rounded; apical margins slightly concave; basal margin medially convex. Elytra 1.2 × longer than wide; disc with coarse punctures arranged into longitudinal lines, with fine punctures between coarse punctures; lateral margins rounded, narrowed behind middle. Aedeagus (Fig. 7C, D) wide, ~ 4.8 × longer than wide; parallel sided, but slightly wider at apical 1/7, and then moderately and apically narrowed; apex truncate, but with one median rounded process; strongly curved in lateral view, apex directed upward; tectum membranous, with several stout setae at apex of internal sac. Endophallic spiculae reduced. Gonocoxae (Fig. 7G) longer than wide, and basally connected; apex of each gonocoxa widely rounded, with eight long setae along apical margin and outer margin. Ventrite VIII (Fig. 7E) with apex weakly sclerotized, with one semicircular membranous area at middle of apical margin, several long setae arranged into transverse line near apical margin, and several shorter setae along apical margin, both types of setae absent medially. Spiculum extremely long. Spermathecal receptaculum (Fig. 6F) strongly swollen; pump long and curved, with long apical process; sclerotized spermathecal duct moderately long after base of spermathecal gland.

**Variations.** Adults in some populations have more ovate body shapes (elytra 1.1 × as long as wide), including those on the Andaman Islands (India).

***Remarks*.** Adults of *N. gemella* are characterized by more convex pronotum and reduced longitudinal grooves on the sides of the apical margins (less convex pronotum and long, deep longitudinal grooves on sides of apical margins in others). In males of *N. gemella*, the truncate apex of the aedeagus bears a small process (Fig. 7C) that differs from the acute apex in *N. chrysomeloides* (Fig. 4C) and the widely rounded apex and small medial process in *N. nigripes* (Fig. 14C). The moderately curved aedeagus in lateral view (Fig. 7D) differs from the strongly curved aedeagus in *N. dohertyi* (Fig. 5E) and slightly curved aedeagus in *N. nigripes* (Fig. 14D). The membranous tectum (Fig. 7C) differs from the sclerotized tectum in *N. chrysomeloides* (Fig. 4C). In females of *N. gemella*,

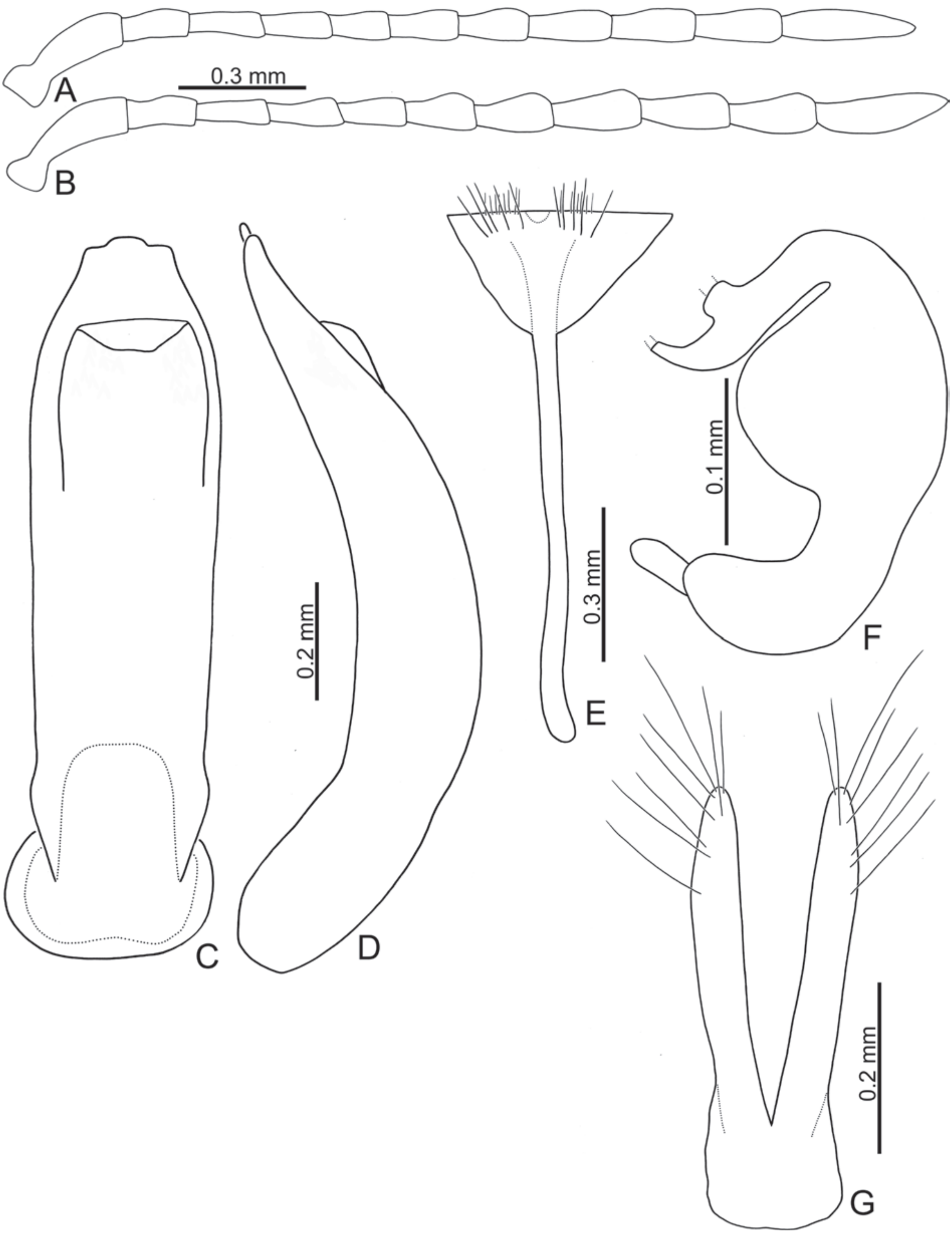

**Figure 7.** *Nisotra gemella* (Erichson), adult **A** antenna, male **B** antenna, female **C** aedeagus, dorsal view **D** aedeagus, lateral view **E** abdominal ventrite VIII, female **F** spermatheca **G** gonocoxae.

the straight gonocoxae (Fig. 7G) differ from the dorsally directed gonocoxal apices in *N. chrysomeloides* (Fig. 4H), the inwardly directed apices in *N. dohertyi* (Fig. 5I), and laterally directed apices in *N. nigripes* (Fig. 14G). Abdominal ventrite VIII, with one transverse line of long setae inside the apical margin and dense short setae along the apical margin (Fig. 7E), differs from ventrite VIII of *N. dohertyi* (Fig. 5F, G), with several pairs of long setae along the apical margin.

Third-instar larvae. Length 4.8 mm, width 1.0 mm, cylindrical, cream colored, with tubercles well-developed, head dark brown (Fig. 8A, B). Head (Fig. 9A) hypognathous, rounded, strongly sclerotized; surface generally smooth. Endocarina (ec) visible, extending into clypeus. Frontal suture (fs) V-shaped, starting from apical 1/3 of endocarina; apically abbreviated halfway between endocarina and lateral margin. Vertex with four pairs of setae (v1–v4). Frons with three pairs of setae (f1–f3). Sides with five pairs of setae (s1–s5). Clypeus transverse, apical margin straight, with one pair of small setae at sides. Labrum transverse, apical margin irregular, with two pairs of long setae; epipharynx (Fig. 9E) with several setae at sides, and flattened, apically pointed setae. Mandible (Fig. 9F) robust; five-toothed, with tiny serrations on mesal margins of teeth; two setae on opposite sides; mola reduced; prostheca composed of several flattened, slender setae. Maxillary palpus (mp) (Fig. 9B) three-segmented, palpomere II with one long seta at one side and one short seta at opposite side; palpifer (pf) with one long seta at opposite sides; mala (ml) with two-segmented conical sensorium and surrounding by three pairs of short setae, mesal side margined with one row of elongate, flattened setae with rounded apices; stipes (st) with one long seta and one short seta. Labial palp (lp) two-segmented, palpomere II cylindrical, palpomere I much wider than II; ligula (lg) rounded, with one pair of short setae; prementum (prm) with one pair of long setae; postmentum (pom) with two pair of long setae. Stemmata reduced and invisible. Antenna (Fig. 9C, D) three-segmented, one tubercle with one prominent and several tiny conical sensoria on antennomere II, one large conical sensorium on antennomere III.

Prothorax (Fig. 10) with dorsal, dorso-lateral, and anterior epipleural tubercles fused, D-DL-EPa type; basal and apical margins with two pairs of setae, lateral margins with four pairs of setae; epipleural region with one small tubercle EPp, with one seta; trochantin (ti) with one seta; sternal regions with two tubercles: ES and SS, ES not divided medially, with one pair of setae, SS separated, with one seta on each tubercle; one additional seta between ES and SS. Meso- and metathoraces with dorsal tubercle divided into Dai, Dae, Dpi, and Dpe; with one pair of setae on each tubercle, except Dae; DL tubercle not divided, with two setae; epipleuron with one tubercle, EP, surrounding spiracle, with one seta; trochantin (ti) without setae; sterna with two tubercles, ES and SS, separated medially, with one seta on each tubercle. Legs (Fig. 8C) five-segmented, coxa (co) with four long setae apically and two short setae basally; trochanter (tr) with four long mesal setae, one long seta apically, and one short seta at lateral area; femur (fe) with three pairs of apical setae on opposite; tibia (tb) with one short mesal seta near margin, two pairs of setae near outer margin, and one pair of setae apically; tarsungulus (ta) slightly curved, with broad base, with one mesal seta near margin of broad base.

Abdominal segment I–VIII (Fig. 10) with dorsal tubercles divided into three tubercles: Da, Dpi, and Dpe, Da and Dpi not divided medially, Da with two pairs of setae, Dpi with one pair of setae, Dpe with one seta; dorso-lateral region with two tubercles: DLa and DLp, with one seta on each tubercle; epipleural tubercle with one seta separated from spiracle, spiracle rounded, tubercle P with one seta; sternal region with three tubercles: PS, ES, and SS; ES and SS not divided medially, ES with one pair of setae but SS with two pairs of setae; PS

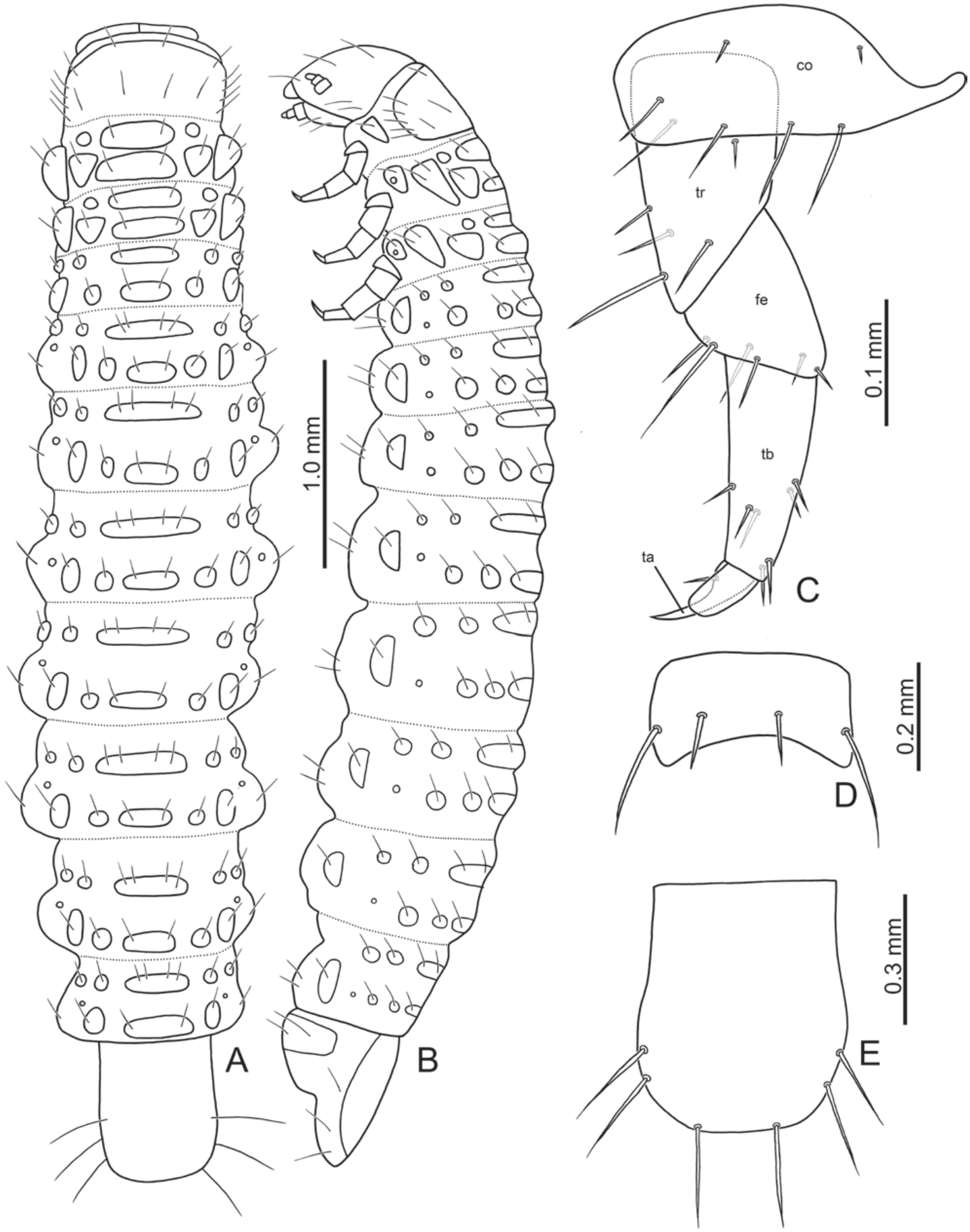

**Figure 8.** *Nisotra gemella* (Erichson), third-instar larva **A** larva in dorsal view **B** larva in lateral view **C** leg **D** abdominal ventrite IX **E** pygopod. Abbreviations: co- coxa; fe- femur; ta- tarsungulus; tb- tibia; tr- trochanter.

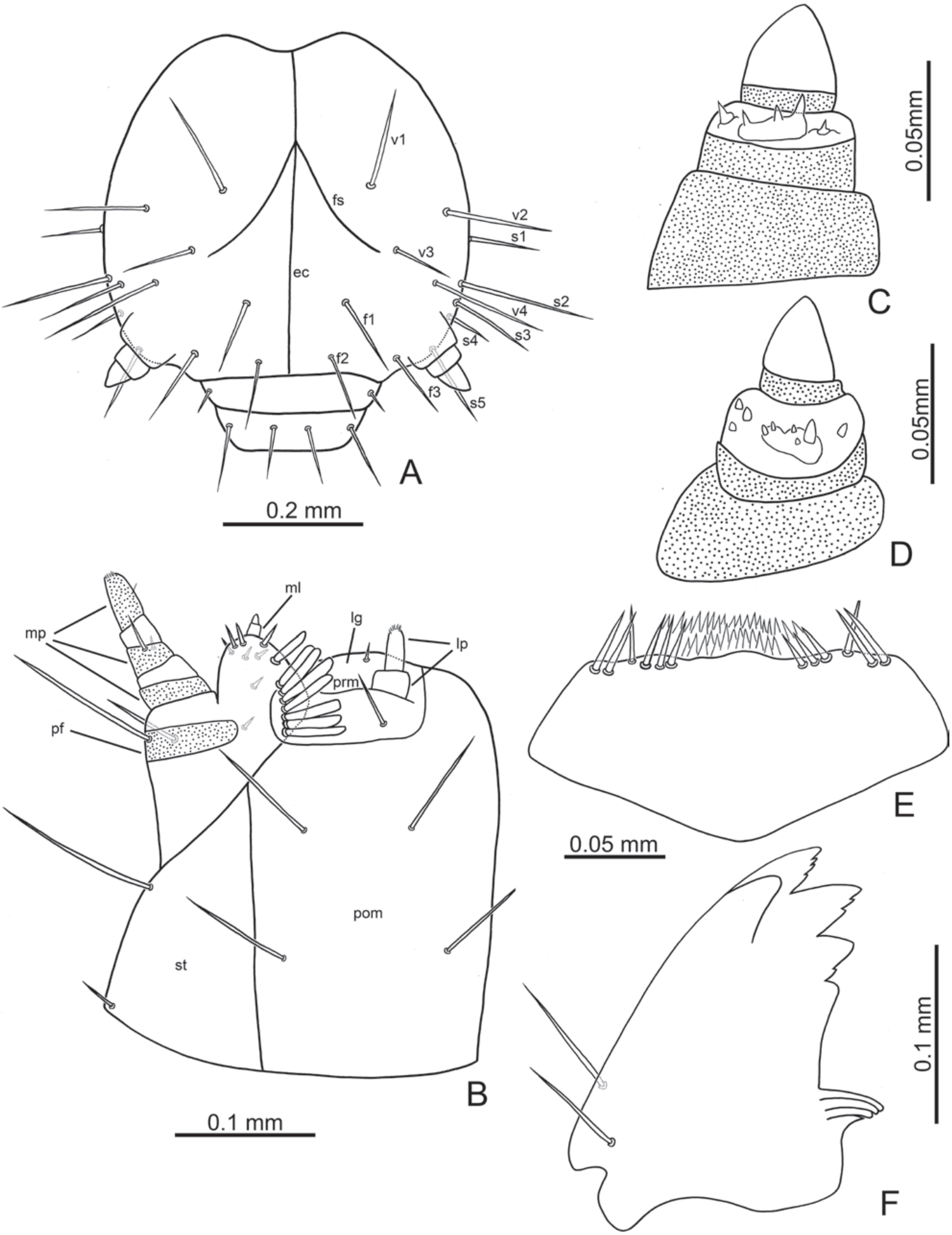

**Figure 9.** *Nisotra gemella* (Erichson), third-instar larva **A** head **B** maxilla and labium **C** antenna, in lateral view **D** antenna, in dorso-lateral view **E** epipharynx **F** mandible. Abbreviations: ec- endocarina; f1–f3- setae on frontal area; fs- frontal suture; lg- ligula; lp- labial palp; ml- mala; mp- maxillary palp; pf- palpifer; pom- postmentum; prm- prementum; s1–s5- setae on sides of head; st- stripes; v1–v4- setae on vertex.

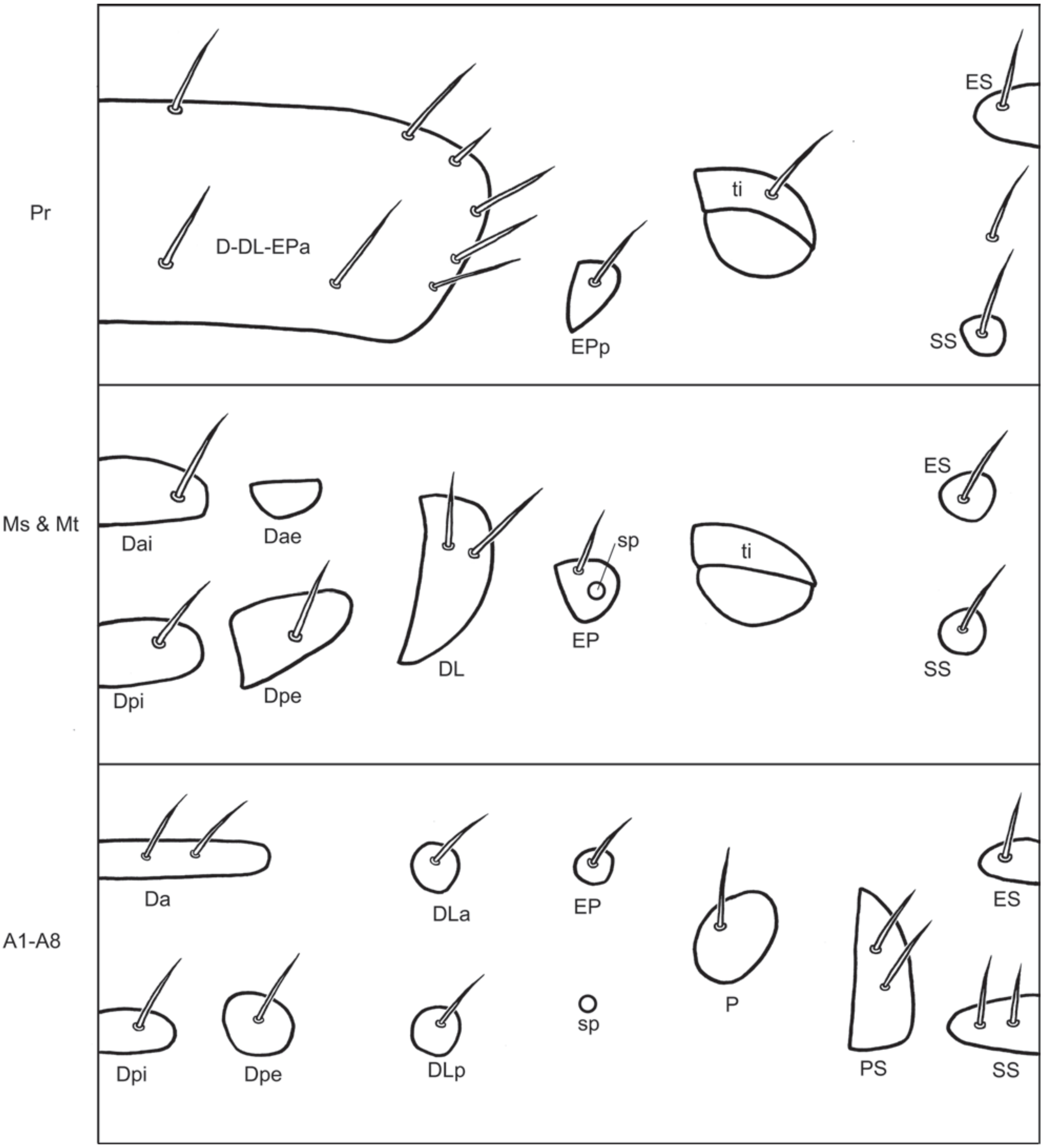

**Figure 10.** *Nisotra gemella* (Erichson), third-instar larva: location of tubercles and body chaetotaxy. Abbreviations: Pr- prothorax; Ms- mesothorax; Mt- metathorax; A1–A8- abdominal segments I–VIII.

large and with two setae. Abdominal segment IX covered by pygopod dorsally (Fig. 7E); pygopod oblong, slightly and apically widened, with three pairs of setae margined apically; ventral region (Fig. 8D) sclerotized and not divided, with two pairs of setae.

**Pupa.** Length 3.8 mm; width 1.4 mm, yellowish white. Head (Fig. 11B) with three pairs of setae: one pair on vertex, one pair on mesal margins of eyes, the other pair between antennae. Prothorax (Fig. 11A) with five pairs of setae on outer margin; one pair on baso-lateral angles; two pairs near basal margin and

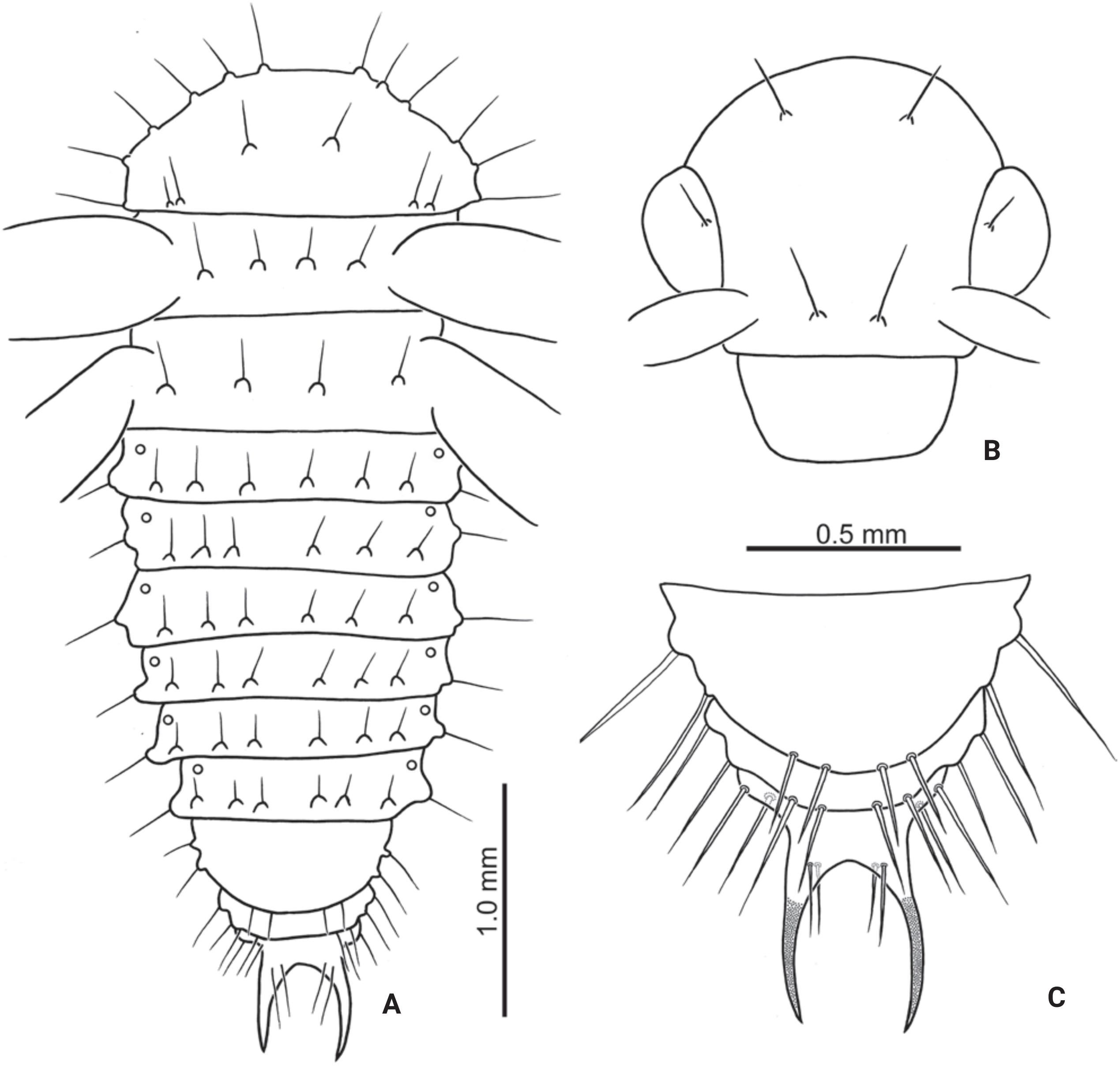

**Figure 11.** *Nisotra gemella* (Erichson), pupa **A** dorsal view **B** head **C** abdominal segments VII–IX.

close to each other, outer pair shorter; one pair at central part near middle line. Meso- and metathoraces with two pairs of setae. Abdominal segment I–VIII (Fig. 11A) with four pairs of setae; setae on abdominal segment I–VI near posterior margin; VII (Fig. 11C) expanded posteriorly, setae along posterior margin; VIII similar to VII but narrower; IX with apical processes sclerotized at apex and strongly pointed, two pairs of setae at sides, two pairs on base of apical processes, one on each, dorsal and ventral surfaces, respectively. Bases of femora of front and middle legs with three pairs of setae, but only two pairs of setae on bases of femora of hind legs.

**Host plants.** Malvaceae: *Hibiscus rosa-sinensis* (Bryant 1941 and current study) (Fig. 11F), *H. tiliaceus* (current study), *Urena lobata* (Kimoto 2003), and Lamiaceae: *Mesona chinensis* (current study). Takizawa (1979) recorded two species of Urticaceae (*Boehmeria nivea* var. *nivea* and *Gonostegia hirta*) as host plants for Taiwanese populations of *Nisotra orbiculata* (= *N. gemella*) but this

**Figure 12.** *Nisotra gemella* (Erichson) **A** female depositing eggs on soil **B** eggs **C** larvae feeding on roots **D** mature larvae crawling into soil and constructing underground chamber for pupation **E** pupa **F** adults attacking *Hibiscus rosa-sinensis*.

may be incorrect because flea beetles collected from both plants belong to the genus *Euphitrea* Baly. Both plants were also regarded as host plants for *Neorthaea* (= *Euphitrea*) *nisotroides* Chen and *Neorthaea flavicornis* Chen in the same paper (Takizawa 1979). We assessed five plants for adults of *Nisotra gemella*, which fed originally on *Mesona chinensis* in the laboratory. These five were *Hibiscus rosa-sinensis*, *H. tiliaceus*, *Urena lobata* (Malvaceae), *Boehmeria nivea* var. *nivea* (Urticaceae), and *Mentha canadensis* (Lamiaceae). They did not feed on leaves of *Boehmeria nivea* var. *nivea* or *Mentha canadensis*.

**Biology.** Females deposited eggs on the soil or leaf litter (Fig. 12A). Each egg (Fig. 12B) was oblong and pale yellow, 1.0 mm in length and 0.5 mm in width. Larvae hatched after 10–14 days, and have three instars Larvae were pale yellow with black heads, pronota, and pygopods (Fig. 12C). They fed on roots. Larval durations varied from 25–46 days. Mature larvae (Fig. 12D) crawled into the soil and constructed underground chambers for pupation. Pupal stage (Fig. 12E) durations were 7–8 days. Adults fed by cutting the leaf lamina. They jumped promptly when disturbed. Adults remained on the adaxial side of leaves.

**Remarks.** The specimens collected from Palawan, Philippines (Medvedev 1993) and Vietnam, were misidentified and represent *Nisotra chrysomeloides*. The same error has been made by other taxonomists.

**Distribution.** Cambodia, China, India (including Andaman and Nicobar islands), Indonesia (Sumatra, Java, Sulawesi), Laos, Malaysia, Myanmar, Nepal, Papua New Guinea, Philippines (Luzon), Singapore, Thailand, Taiwan, and Vietnam.

### ***Nisotra nigripes* Jacoby**

Figs 6O, P, 13, 14

*Nisotra nigripes* Jacoby, 1894: 293 (Myanmar); Medvedev 2000: 21 (Nepal); Zhang and Yang 2007: 844 (China: Yunnan).

*Nisotra orbiculata* sensu Kimoto 1970: 215 (Taitung: Chipen (知本); Chiayi: Fenchihu (奮起湖)); Kimoto 1989: 263 (Kaohsiung: Liu Kui (六龜)).

**Type.** ***Holotype*** (sex undetermined, based on photographs, MCZC, fixed by monotypy) (Fig. 2O, P): “Ruby Mines / U. B. [p, w] // Type [p] / 18565 [h, r] // Nisotra / nigripes / Jac. [h, b]”.

**Additional material examined.** **Laos.** Vientiane: 1♂ (NHMUK), 1 km W Vang Vieng, 15.VIII.2004, leg. M. Geiser; **Myanmar.** 3♀ (NHMUK), Toungoo, coll. Andrewes, 1922-221; 1♂ (NHMUK), Ruby Mines, leg. Doherty, Fry Coll., 1905.100; Kachin State: 2♂, 2♀ (NHMUK), Nam Tamai, 2.VIII.1938, leg. R. Kaulback; Naga: 1♂, 1♀ (SEHU), Somura, 1–2.V.2005, leg. A. Abe; **Taiwan.** Chiayi: 1♂ (KMNH), Fenchihu (奮起湖), 12.IV.1965, leg. T. Saigusa; Hsinchu: 6♂, 2♀ (TARI), Tahunshan (大混山), 24.II.2009, leg. S.-F. Yu; 1♂ (TARI), Talu trail (大鹿林道), 22.X.2008, leg. H.-J. Chen; Kaohsiung: 1♀ (TARI), Chungchihkuan (中之關), 16.IV.2012, leg. L.-P. Hsu; 2♀ (KMNH), Liu Kui (六龜), 31.III.1986, leg. K. Baba; 2♂, 3♀ (TARI), Namahsia (納瑪夏), 1.IX.2012, leg. Y.-T. Chung; 1♀ (TARI), Peitawushan (北大武山), 27.V.2013, leg. Y.-T. Chung; 2♀ (TARI), same but with “1.IX.2016”; 1♂ (TARI), Shihshan logging trail (石山林道), 1–3.X.2008, leg. M.-H. Tsao; 2♂, 3♀ (TARI), Tengchih (藤枝), 2–5.VI.2008, leg. C.-F. Lee; 1♂ (TARI), same locality, 8.VI.2013, leg. W.-C. Liao; Nantou: 2♂, 1♀ (NMNS), Hsitou (溪頭), 21.VIII.2006, leg. W. T. Jin; 1♂ (KMNH), Lushan Wenchuan (盧山溫泉), 6.VI.1976, leg. H. Makihara; 1♂ (TARI), same locality, 27–31.V.1980, leg. K. S. Lin & L. Y. Chou; 3♂, 2♀ (TARI), Tungpu (東埔), 28.IV. –2.V.1981, leg. T. Lin & C. J. Lee; 1♀ (TARI), same locality, 18–23.XI.1981, leg. T. Lin & W. S. Tang; 1♂, 3♀ (TARI), same locality, 19–23.VII.1982, leg. L. Y. Chou & T. Lin; 2♂, 2♀ (TARI), same locality, 16–20.IV.1984, leg. K. C. Chou & C. H. Yung; 1♂, 6♀ (TARI), same locality, 23–27.VII.1984, leg. K. C. Chou & C. H. Yang; Pingtung: 6♂, 4♀ (TARI), Laii (來義), 23.IV.2008, leg. W.-T. Liu; 2♂, 4♀ (TARI), Wutai (霧台), 12.IV.2009, leg. U. Ong; Taichung: 1♂ (TARI), Chiapotai (佳保台), 14–18.X.1980, leg. K. S. Lin & C. H. Wang; Taitung: 2♂, 1♀ (KMNH), Chipen (知本), 10.VIII.1966, leg. H. Kamiya; 1♂, 2♀ (TARI), Lichialintao (利嘉林道), 24.IV.2008, leg. C.-L. Hsiao;

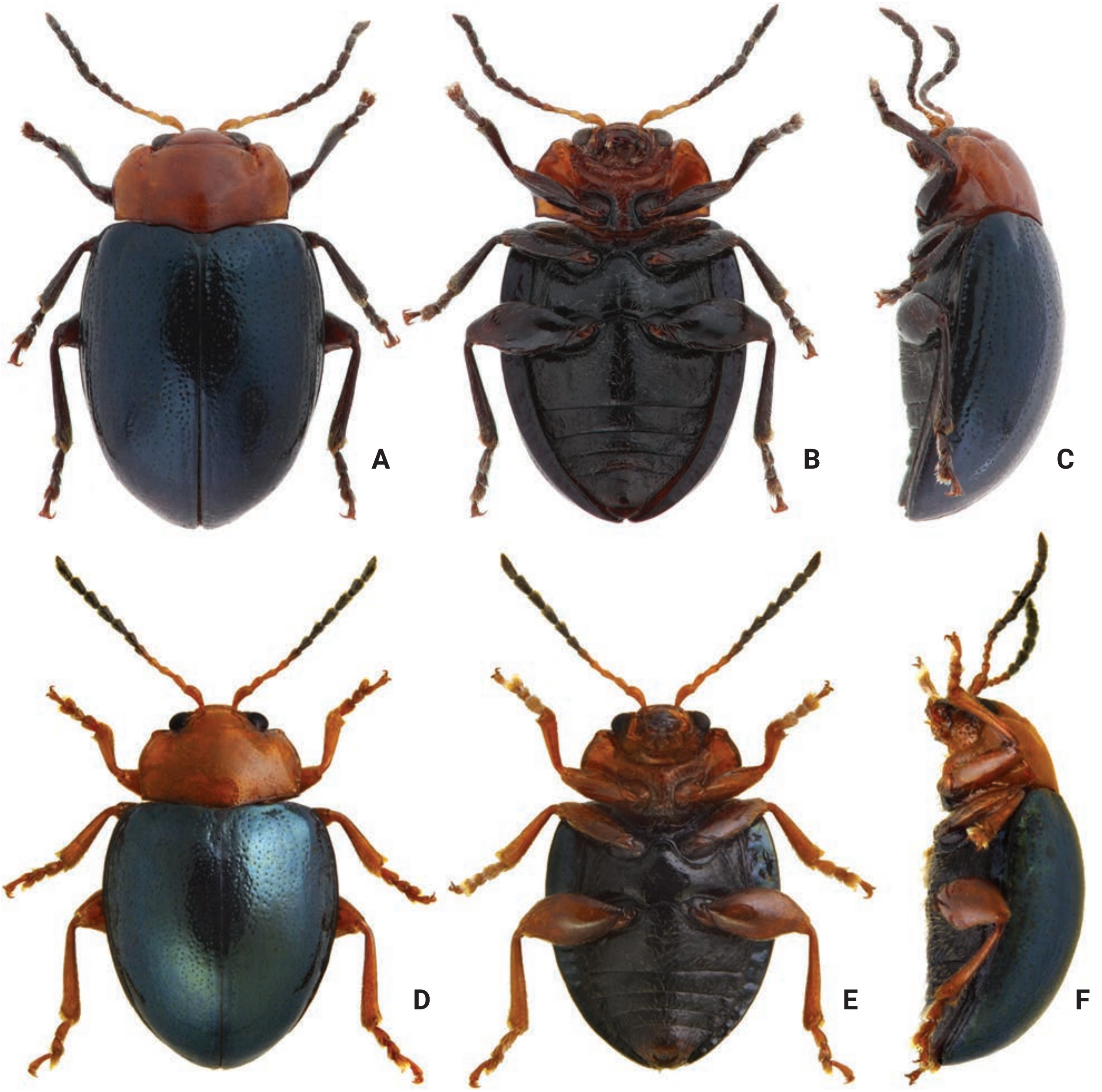

**Figure 13.** Habitus of *Nisotra nigripes* Jacoby **A** female, from Myanmar, dorsal view **B** ditto, ventral view **C** ditto, lateral view **D** male, from Taiwan, dorsal view **E** ditto, ventral view **F** ditto, lateral view.

2♂, 1♀ (TARI), Liyuan (栗園), 28.III.2014, leg. W.-C. Huang; **Thailand.** Siam: 2♀ (KMNH), Tak, 20.VIII.1961.

**Redescription. Adults.** Length 3.6–4.4 mm, width 2.3–2.7 mm (*n* = 92). General color yellowish brown (Fig. 13A–C); elytra, meso- and metathoracic and abdominal ventrites metallic purple; legs black. four basal antennomeres I–IV yellowish brown, V dark brown, VI–XI black. Antennae (Fig. 14A) filiform in males, ratios of lengths of antennomeres I to XI 1.0: 0.5: 0.5: 0.5: 0.6: 0.5: 0.6: 0.6: 0.6: 0.6: 0.9; ratios of length to width from antennomeres I to XI 2.9: 2.1: 2.5: 2.1: 2.2: 2.1: 2.0: 1.9: 1.8: 1.9: 3.1; similar in females, ratios of lengths of antennomeres I to XI (Fig. 14B) 1.0: 0.4: 0.4: 0.4: 0.5: 0.5: 0.5: 0.5: 0.6: 0.6: 0.8; ratios of length to width from antennomeres I to XI 3.3: 2.2: 2.8: 2.4: 2.7: 2.1: 2.2: 1.9: 2.1: 1.9: 2.8. Pronotum 1.8–1.9 × wider than long; disc shining, with sparse, fine

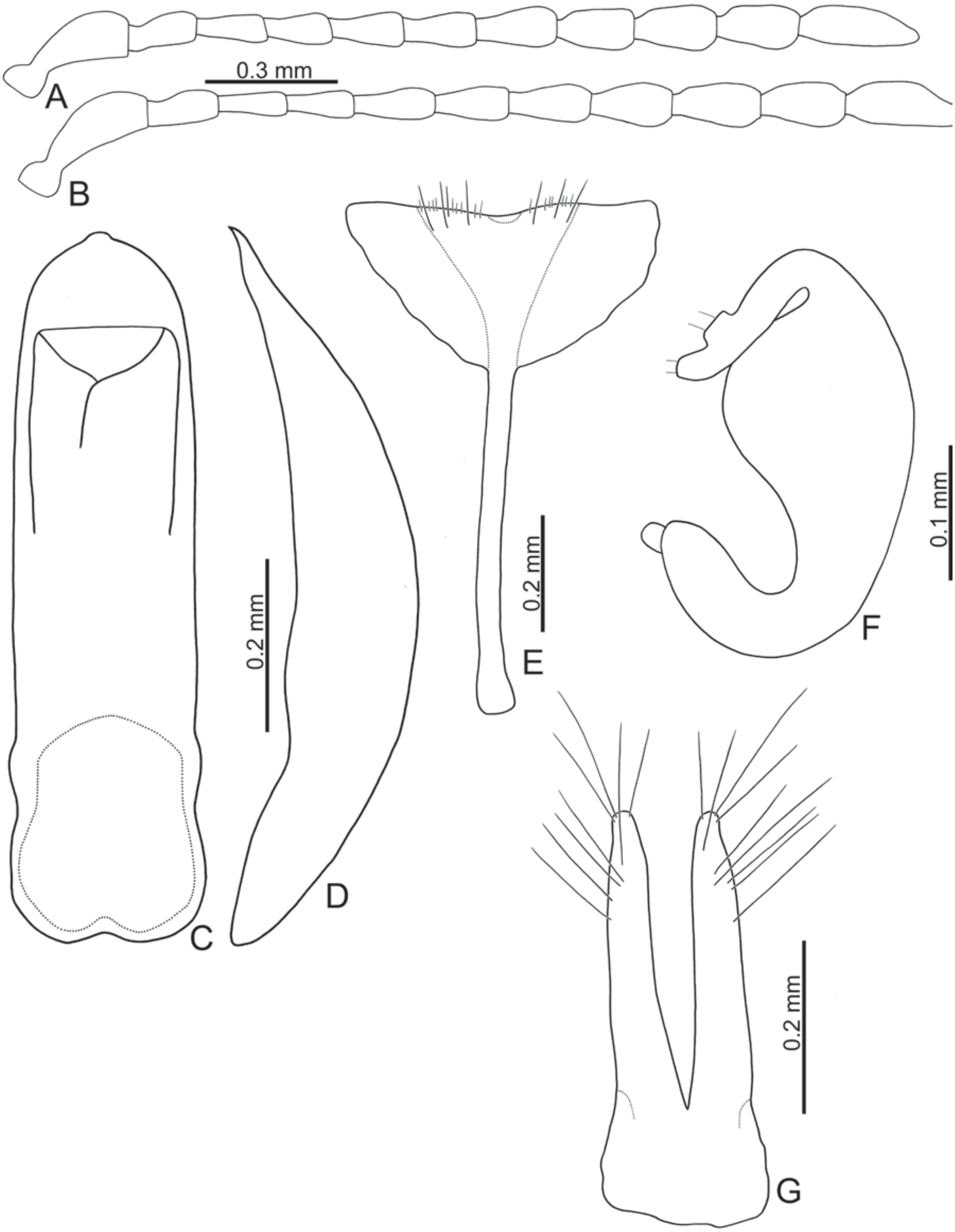

**Figure 14.** *Nisotra nigripes* Jacoby, adult **A** antenna, male **B** antenna, female **C** aedeagus, dorsal view **D** aedeagus, lateral view **E** abdominal ventrite VIII, female **F** spermatheca **G** gonocoxae.

punctures, less convex; longitudinal groove on each side of apical margin shallow, with several coarse punctures along longitudinal groove; short and shallow longitudinal groove on basal margin; lateral margins rounded; apical margins slightly concave; basal margin medially convex. Elytra 1.2 × longer than wide; disc with coarse punctures arranged into longitudinal lines, with fine punctures between coarse punctures; lateral margins rounded, narrowed behind middle.

Aedeagus (Fig. 14C, D) wide, ~ 4.2 × longer than wide; parallel sided, subapically narrow, apex with one median rounded process; slightly curved in lateral view, apex directed inward; tectum membranous, internal sac without stout setae. Endophallic spiculae reduced. Gonocoxae (Fig. 14G) longer than wide, and basally connected; each gonocoxa subapically narrowed and apex truncate, and curved outwards, with eight or nine long setae along apical and outer margins. Ventrite VIII (Fig. 14E) with apex weakly sclerotized, with one semicircular membranous area at middle of apical margin and several long setae in a transverse line near apical margin, with several setae along apical margin, both types of setae absent medially, spiculum extremely long. Spermathecal receptaculum (Fig. 14F) strongly swollen; pump long and curved, with small apical process; spermathecal duct sclerotized, short after base of spermathecal gland.

**Variation.** Adults from Taiwan have yellowish brown legs (Fig. 13D–F) that are different from those of the Asian continent, which possess black legs.

**Diagnosis.** Most adults of *N. nigripes* Jacoby are similar to those of *N. chrysomeloides* but differ in possessing black legs (yellowish brown legs in others). However, Taiwanese populations of *N. nigripes* is not distinguishable from those of *N. chrysomeloides*, which is not recorded from Taiwan. In males of *N. nigripes*, the widely rounded apex of the aedeagus bearing a small process at the middle (Fig. 14C) differs from the truncate apex and small process in *N. gemella* (Fig. 7C) and *N. dohertyi* (Fig. 5C), and acute apex in *N. chrysomeloides* (Fig. 4C). The slightly curved aedeagus in lateral view (Fig. 14D) differs from the moderately curved aedeagus in *N. gemella* (Fig. 7D) and *N. chrysomeloides* (Fig. 4E), and strongly curved aedeagus in *N. dohertyi* (Fig. 5E). The membranous tectum (Fig. 14C) differs from the sclerotized tectum in *N. chrysomeloides* (Fig. 4C). In females of *N. nigripes*, laterally directed apices of and gonocoxae (Fig. 14G) are different from the straight gonocoxae in *N. gemella* (Fig. 7G), dorsally directed apices in *N. chrysomeloides* (Fig. 4H), and inwardly directed apices in *N. dohertyi* (Fig. 5I). The setae of abdominal ventrite VIII, with one transverse line of long setae inside the apical margin and dense short setae along the apical margin (Fig. 14E) differs from the presence of several pairs of long setae along the apical margin in *N. dohertyi* (Fig. 5F, G).

**Host plant.** Adults in Taiwan feed on leaves of *Hibiscus taiwanensis*, which is an endemic plant.

**Distribution.** China, Laos, Myanmar, Taiwan, and Thailand.

Zhang and Yang (2007) provided a key to Chinese species of *Nisotra*. We think most of the key is appropriate, but lengths of bodies and some coloration characters are too variable for reliable diagnoses. It is modified to include species from Taiwan as follows:

1 Distinct longitudinal groove on each side of anterior margin of pronotum; pronotum less convex .......... **2**

– Inconspicuous longitudinal groove on each side of anterior margin of pronotum .......... **5**

2 Body ovate (1.1 × longer than wide); confused punctures on elytra; pronotum dull and with micro-reticulation .......... ***N. dohertyi* (Maulik)**

– Body oblong (1.2 × longer than wide); punctures on elytra arranged into paired longitudinal rows; pronotum shining and lacking micro-reticulation .......... **3**

3 Legs black........................................................................ ***N. nigripes*** **Jacoby**
– Legs yellowish brown.....................................................................................**4**
4 Specimens collected from Taiwan................................. ***N. nigripes*** **Jacoby**
– Specimens collected from other areas............ ***N. chrysomeloides*** **Jacoby**
5 Longitudinal groove of each side of basal margin of pronotum inconspicuous and short, < 1/5 of pronotum .......................... ***N. gemella*** **(Erichson)**
– Longitudinal groove of each side of basal margin of pronotum distinct and long, > 1/5 of pronotum ................................ ***N. xinjiangana*** **Zhang & Yang**

## Discussion

*Nisotra chrysomeloides*, *N. dohertyi*, *N. gemella*, and *N. nigripes* represent more than 95% of museum specimens in historical collections collected from Southeast Asia, China, and Taiwan. Many identified specimens are misidentified, probably because few diagnostic characters can be used for reliable species identifications. Moreover, diagnostic characters can be variable. Doubtfully identified specimens must be dissected for identification. Distributions of each will require updating based on the present study. *Nisotra gemella* recorded from Taiwan is confirmed, and *N. nigripes* is newly recorded from Taiwan. Only aedeagi and spermathecae were used as diagnostic characters in the former studies (e.g., Scherer 1969; Zhang and Yang 2007). The results show that spermathecae are less diagnostic in species identities but more diagnostic in supraspecific classification. Abdominal ventrite VIII in females and gonocoxae are diagnostic for species identities. We suggest that both structures are needed in current and future taxonomy.

*Nisotra gemella* is one of the most widespread flea beetles of the genus ocurring from China and Taiwan to Papua New Guinea. Such widespread distribution might be result of two host plants. *Hibiscus tiliaceus* are adapted to the sea-shore habits. The colonization of *N. gemella* on many islands and coastal areas across the Pacific and Indian Oceans is likely associated with this peculiar feature of their host. In Taiwan, adults are not only found in mainland, but also Kinmen Island (金門島) and Beigan Island (北竿島). Its distribution is similar to another leaf beetle, *Phola octodecimguttata* (Fabricius, 1775) (Lee and Geiser 2023) adapted to seashore habitats. The second plant is *H. rosa-sinensis* which is a popular ornamental plant in Asia. Humans planted substantial populations surrounding structures and gardens. Thus, adults have become common due to associations with the plant. In the present study we found this species also fed on one important crop, *Mesona chinensis*. It has become a major pest where mesona has been planted in large areas. Clarification of species identity will contribute to managing this pest in the future.

*Nisotra nigripes* is not a common species and was not studied by Scherer (1969) due to lack of specimens. Zhang and Yang (2007) were the first to illustrate the male aedeagus based on specimens collected from Yunnan. In Taiwan, adults of *N. nigripes* are more common at many localities than those of *N. gemella*. This is a result of the common occurrence of its host plant *Hibiscus taiwanensis* in mountainous areas. By contrast, although the host plants for *N. gemella* are common in lowlands of Taiwan and around human habitations, adults of *N. gemella* are not common, probably due to sensitivity to human disturbance or chemicals. A host plant shift to *Mesona chinensis* seems to have ensured survival of *N. gemella* populations.

## Acknowledgements

We are grateful to the Taiwan Chrysomelid Research Team (TCRT) and citizen scientists, including Hou-Jay Chen (陳厚潔), Yi-Ting Chung (鍾奕霆), Hsueh Lee (李雪), Wen-Chuan Liao (廖文泉), Ui-Ka Ong (王惟加), Mei-Hua Tsou (曹美華), and Su-Fang Yu (余素芳) for assistance in collecting material. We thank Hsing-Tzung Cheng (鄭興宗) for photos of specimens, Hsing-Tzung Cheng (鄭興宗) for field photography, and Chih-Kai Yang for identification of host plants. We would like to thank all curators listed above for giving us the opportunity to study the specimens from their collections. We thank Chang-Chin Chen (陳常卿) for assisting our study in various ways. We thank Chris Carlton for reading the draft and editing for American English style. Finally, we thank Jan Bezděk and one anonymous reviewer for reviewing the manuscript, and Caroline Chaboo for editing the manuscript.

## Additional information

### Conflict of interest

The authors have declared that no competing interests exist.

### Ethical statement

No ethical statement was reported.

### Funding

This study was supported by the National Science and Technology Council NSTC 112-2313-B-055-001-MY3 and the Animal and Plant Health Inspection Agency, Ministry of Agriculture 113AS-5.5.4-VP-01.

### Author contributions

Investigation: MFG, MYC. Project administration: KHC. Writing - original draft: CFL.

### Author ORCIDs

Chi-Feng Lee https://orcid.org/0000-0003-1996-0557
Ming-Yao Chiang https://orcid.org/0000-0002-1514-7086

### Data availability

All of the data that support the findings of this study are available in the main text.

## References

Aston P (2009) Chrysomelidae of Hong Kong Part 2 Alticinae. Hong Kong Entomological Journal 1: 1–13. http://hkentsoc.org/bulletin/HKEB1(1)_chrysomelidae_part2_aston.pdf

Baly JS (1876) Descriptions of a new genus and of species of Halticinae. Transactions of the Royal Entomological Society of London 1876(4): 581–602. https://doi.org/10.1111/j.1365-2311.1876.tb01931.x

Bryant GE (1941) New species of Chrysomelidae (Coleoptera) from Malaya and Java. Annals & Magazine of Natural History 8(11): 283–288. https://doi.org/10.1080/03745481.1941.9727970

Chen S-H (1933) Some species of Halticinae from Canton. Peking Natural History Bulletin 8(1933–1934): 43–58.

Chen S-H (1934a) Coléopères Halticinae recueillis par M. H. Sauter à Formosae. Annales de la Société Entomologique de France 103: 176–185.

Chen S-H (1934b) Revision of the Halticinae (Col. Chrysomelidae) of Yunnan and Tonkin. Sinensia 5: 225–416.

Chûjô M (1935) Studies on the Chrysomelidae in the Japanese Empire (VIII). Subfamily Halticinae (3). Transactions of the Natural History Society of Formosa 25: 459–476.

de Motschulsky V (1866) Essai d'un catalogue des insects de l'île de Ceylan. Supplément. Bulletin de la Société Impériale des Naturalistes de Moscou 39(2): 393–446.

Döberl M (2010) Alticinae. In: Löbl I, Smetana A (Eds) Catalogue of Palaearctic Coleoptera, Vol. 6. Apollo Books, Stenstrup, 491–563.

Duckett CN, Daza JD (2004) A new species of flea beetle in the genus *Alagoasa* Bechyné (Coleoptera: Chrysomelidae: Galerucinae) from highland Costa Rica. Coleopterists Bulletin 58(1): 84–96. https://doi.org/10.1649/608

Duvivier A (1885) Phytophages (Halticides et Galérucides) recueillis par M. J. Weyers, a fort de Kock, Païnan (Sumatra) et a l'île Bodjo. Bulletin ou Comptes-Rendus des Scéances de la Société Entomologique de Belique 1885: 48–54.

Erichson WF (1834) Coleopteren. In: Meyen F (Ed.) Beiträge zur Zoologie, gesammelt auf einer Reise um die Erde. Nova Acta Physico-Media Academia Caesarea Leopoldino Carolinae Naturae Curiosorum 16 Supplementum, 219–277.

Gressitt JL, Kimoto S (1963) The Chrysomelidae (Coleopt.) of China and Korea. Part 2. Pacific Insects Monograph 1B: 301–1026.

Gruev B (1985) Leaf-beetles collected by P. Beron and S. Andreev from the National Museum (Natural History)—Sofia in India, Sir Lanka, Nepal, Burma and Thailand in 1981 and 1984 (Coleoptera, Chrysomelidae). Entomological Review of Japan 40: 35–47. https://www.cabidigitallibrary.org/doi/full/10.5555/19870544190

Jacoby M (1885) Descriptions of new genera and species of phytophagous Coleoptera from the Indo-Malayan and Austro-Malayan subregions, contained in the Genoa Civic Museum. Second Part. Annali del Museo Civico di Storia Naturale di Genova 22: 20–76. https://doi.org/10.5962/bhl.part.6180

Jacoby M (1889) Viaggio di Leonardo Fea in Birmania e reioni vicine. – List of the phytophagous Coleoptera obtained by Signor L. Fea at Burmah and Tenasserim, with descriptions of the new species. Annali del Museo Civico di Storia Naturale di Genova 27: 147–237.

Jacoby M (1894) Descriptions of new genera and species of phytophagous Coleoptera obtained by W. Doherty in the Malayan Archipelago. Novitates Zoologicae 1: 267–330. https://doi.org/10.5962/bhl.part.24565

Kimoto S (1962) A phylogenetic consideration of Chrysomelinae based on immature stages of Japanese species (Coleoptera). Journal of the Faculty of Agriculture, Kyushu University 12(2): 67–88. https://doi.org/10.5109/22694

Kimoto S (1966) A list of the chrysomelid specimens of Taiwan preserved in the Zoological Museum, Berlin. Esakia 5: 21–38. https://doi.org/10.5109/2351

Kimoto S (1970) Notes on the Chrysomelidae from Taiwan IV. Kontyû 38: 205–221.

Kimoto S (1986) The Chrysomelidae (Insecta: Coleoptera) collected by the Nagoya University Scientific Expedition to Taiwan in 1984. Kurume University Journal 35: 53–62. https://www.cabidigitallibrary.org/doi/full/10.5555/19870542501

Kimoto S (1987) The Chrysomelidae (Insecta: Coleoptera) collected by the Nagoya University Scientific Expedition to Taiwan in 1986. Kurume University Journal 36: 183–194. https://www.cabidigitallibrary.org/doi/full/10.5555/19891115201

Kimoto S (1989) The Taiwanese Chrysomelidae (Insecta: Coleoptera) collected by Dr. Kintaro Baba, on the occasion of his entomological survey in 1983 and 1986. Kurume University Journal 38: 237–272. https://cir.nii.ac.jp/crid/1520853832925934976

Kimoto S (1991) The Taiwanese Chrysomelidae (Insecta: Coleoptera) collected by Dr. Kintaro Baba, on the occasion of his entomological survey in 1987, 1988 and 1989. Kurume University Journal 40: 1–27. https://cir.nii.ac.jp/crid/1520290882041451392

Kimoto S (2000) Chrysomelidae (Coleoptera) of Thailand, Cambodia, Laos and Vietnam. VII. Alticinae. Bulletin the Institute of Comparative Studies of International Cultures and Societies 26: 103–299. https://cir.nii.ac.jp/crid/1520290884031616640

Kimoto S (2001) Check-list of Chrysomelidae of south east Asia, south of Thailand and West of Irian-Jaya of Indonesia, IX. Alticinae. Bulletin the Institute of Comparative Studies of International Cultures and Societies 27: 153–249. https://cir.nii.ac.jp/crid/1520572358852237696

Kimoto S (2003) The leaf beetles (Chrysomelidae) of Thailand and Indochina. Tokai University Press, Tokyo, 150 pp.

Kimoto S, Takizawa H (1973) The chrysomelid-beetles of Nepal, collected by the Hokkaido University scientific expedition to Nepal Himalaya, 1968 part II. Kontyû 41: 170–180. https://cir.nii.ac.jp/crid/1542824520143079424

Kimoto S, Takizawa H (1997) Leaf beetles (Chrysomelidae) of Taiwan. Tokai University Press, Tokyo, 581 pp.

Lee C-F, Geiser MF (2023) Taxonomic review of the genus *Phola* Weise, 1890 (Coleoptera: Chrysomelidae: Chrysomelinae). Taiwan Nongye Yanjiu 72(3): 197–218. https://doi.org/10.6156/JTAR.202309_72(3).0002

Maulik S (1926) The Fauna of British India, including Cleyon and Burma. Coleoptera. Chrysomelidae (Chrysomelinae and Halticinae). Taylor and Francis, London, 442 pp.

Medvedev LN (1992) Chrysomelidae from the Nepal Himalayas, III (Insecta: Coleoptera). Stuttgarter Beitrage zur Naturkunde, Serie A, Biologie 485: 1–36. https://www.biodiversitylibrary.org/item/104387#page/8/mode/1up

Medvedev LN (1993) Alticinae of the Philippine Islands (Coleoptera Chrysomelidae), Part 2. Russian Entomological Journal 2: 11–32.

Medvedev LN (2000) Chrysomelidae from the Nepal Himalayas, with revision of the genus *Haplosomoides* (Insecta: Coleoptera). Stuttgarter Beitrage zur Naturkunde, Serie A, Biologie 616: 1–32.

Medvedev LN (2006) To the knowledge of Chrysomelidae (Coleoptera) described by V. Motschulsky. Russian Entomological Journal 15: 409–417.

Medvedev LN (2009) Alticinae of Indochina. KMK Scientific Press Ltd., Moscow, 223 pp.

Nadein KS (2013) Catalogue of Alticini genera of the World (Coleoptera: Chrysomelidae). Beetles and Coleopterists website, Zoological Institute, Saint-Petersburg. http://www.zin.ru/Animalia/Coleoptera/eng/alticinw.htm [Accessed 18 June 2024]

Ogloblin DA (1930) De quelques expèces de Halticinae (Col. Chrysomelidae) de la collection de V. Motschoulsky. Eos. Revista Espanola de Entomologia 6: 83–112.

Scherer G (1969) Die Alticinae des indischen Subkontinentes. Pacific Insects Monograph 22: 1–251.

Scherer G (1979) Ergebnisse der Bhutan-Expedition 1972 des Naturhistorischen Museums in Basel. Entomologica Basiliensia 4: 127–139.

Taiwan Encyclopedia of Life (2024) TaiEOL. https://taieol.tw/ [Accessed 11 June 2024]

Takizawa H (1972) Descriptions of larvae of glanduliferous group of Galerucinae in Japan, with notes on subdivisions of the subfamily (Coleoptera: Chrysomelidae). Insecta Matsumurana (Supplement 10): 1–14. https://eprints.lib.hokudai.ac.jp/dspace/bitstream/2115/22238/1/10_P1-14.pdf

Takizawa H (1979) Notes on Taiwanese Chrysomelidae, III. Kontyû 47: 340–351.

Takizawa H, Nakamura S, Kojima K (1995) The Taiwanese chrysomelid beetles preserved in Hiwa Museum for Natural History (Chrysomelidae: Coleoptera). Miscellaneous Reports of the Hiwa Museum for Natural History 33: 1–16.

Vaqalo M (2014) Biology and ecology of *Nisotra basselae* (Bryant) on *Abelmoschus manihot* Medicus in Solomon Islands. Doctorate dissertation, The University of Queensland, Australia, 163 pp.

von Harold E (1876) Chrysomelidae (Pars II). In: Gemminger M, Harold B (Eds) Catalogus Coleopterorum. Vol. XII: Chrysomelidae (Pars II), Languriidae, Erotylidae, Endomychidae, Coccinellidae, Corylophidae, Platypsyllidae. Theodor Ackermann, Manachii, 3479–3676.

Wang S (1992) Coleoptera: Chrysomelidae-Alticinae. In: Chen S-H (Ed.) Insects of Hengduan Mountain Region. Volume I. Science Press, Beijing, 675–753.

Weise J (1922) Chrysomeliden der indo-malayischen Region. Tijdschrift voor Entomologie 65: 39–130.

Yu P, Wang S, Yang X (1996) Economic Insect Fauna of China. Fasc. 54, Coleoptera: Chrysomeloidea (II). Scinece Press, Beijing, 324 pp. [In Chinese]

Zhang Y, Yang X (2007) A key to species of *Nisotra* Baly (Coleoptera: Chrysomelidae: Alticinae) from China, with description of a new species and two new records from China. Proceedings of the Entomological Society of Washington 109(4): 841–846.

ZooKeys 1205: 333–348 (2024)
DOI: 10.3897/zookeys.1205.124183

Research Article

# Two new oonopid spiders (Arachnida, Araneae) from Xishuangbanna tropical rainforest, Yunnan, China

Yanfeng Tong[1], Yongbo Shao[1], Dongju Bian[2], Shuqiang Li[3]

1 College of Life Science, Shenyang Normal University, Shenyang 110034, China
2 Key Laboratory of Forest Ecology and Management, Institute of Applied Ecology, Chinese Academy of Sciences, Shenyang 110016, China
3 Institute of Zoology, Chinese Academy of Sciences, Beijing 100101, China
Corresponding author: Yanfeng Tong (tyf68@hotmail.com); Dongju Bian (biandongju@163.com)

## Abstract

A new species of the genus *Bannana* Tong & Li, 2015 and a new species of the genus *Trilacuna* Tong & Li, 2007 are recorded from Xishuangbanna, Yunnan Province: *Bannana zhengguoi* Tong & Li, **sp. nov.** (♂♀) and *Trilacuna aoxian* Tong & Li, **sp. nov.** (♂♀). An identification key to species of the genus *Bannana* from Xishuangbanna is provided. Detailed diagnoses, descriptions, and photomicroscopy images of new species are provided.

**Key words:** Biodiversity, goblin spiders, taxonomy

## Introduction

Goblin spiders (Araneae, Oonopidae) are small (usually <3 mm), six-eyed, haplogyne, non-web-building spiders. They have a nearly worldwide distribution and occur mainly in leaf litter, under bark, and in the tree canopy (Jocqué and Dippenaar-Schoeman 2006; Ubick and Dupérré 2017). Currently, 1952 extant described species in 115 genera of oonopid spiders have been recorded in the world, in which 17 genera and 118 species are distributed in China (WSC 2024).

Xishuangbanna, located in southern Yunnan Province, has the best-preserved tropical rainforest in China and belongs to the Indo-Burma biodiversity hotspot (Myers 1988). The survey of oonopid spiders from Xishuangbanna has started relatively recently. To date, 28 species in five genera have been recorded from Xishuangbanna (Huang et al. 2021; Tong et al. 2021; Song et al. 2024).

The genus *Bannana* was established by Tong and Li (2015). Only three species have been described, *B. crassispina* Tong & Li, 2015, *B. parvula* Tong & Li, 2015, and *B. songxiaobini* Tong & Li, 2019. All three species are endemic to Xishuangbanna, Yunnan (Tong and Li 2015; Sun et al. 2019). The genus *Trilacuna* Tong & Li, 2007 currently comprised 43 species. All species are known from Iran to the Korean Peninsula and south to Sumatra (Tong and Li 2007; Eichenberger and Kranz-Baltensperger 2011; Grismado et al. 2014; Malek-Hosseini et al. 2015). In China, the genus is represented by 21 species, of which 12 species are known in Yunnan Province (Tong et al. 2019; Ma et al. 2023). There are no distribution records of this genus in Xishuangbanna until now. The present paper describes two new species of *Bannana* and *Trilacuna* from this region.

Academic editor: Dimitar Dimitrov
Received: 29 March 2024
Accepted: 27 May 2024
Published: 1 July 2024

ZooBank: https://zoobank.org/AA2B0FE9-C13A-4712-972C-9EAEF9909FE0

Citation: Tong Y, Shao Y, Bian D, Li S (2024) Two new oonopid spiders (Arachnida, Araneae) from Xishuangbanna tropical rainforest, Yunnan, China. ZooKeys 1205: 333–348. https://doi.org/10.3897/zookeys.1205.124183

## Materials and methods

All the specimens used in this study were collected by pitfall trapping or searching by hand in forest leaf litter and later examined using a Leica M205C stereomicroscope. Details of body parts and measurements were studied under an Olympus BX51 compound microscope. Photos were made with a Canon EOS 750D zoom digital camera (18 megapixels) mounted on an Olympus BX51 compound microscope. Left palps were detached for taking images. Endogyne were cleared in 85.0–90.0% lactic acid at normal temperature. Scanning electron microscope images (SEM) were taken under high vacuum with a Hitachi TM3030 after critical-point drying and gold-palladium coating. All measurements in the text are expressed in millimeters. All materials studied are deposited in Shenyang Normal University (**SYNU**) in Shenyang, China.

Taxonomic descriptions follow Tong and Li (2015) and Tong et al. (2020). The following abbreviations are used in the text and figures: **ALE** = anterior lateral eyes; **ALE–PLE** = distance between ALE and PLE; **ap** = apodemes; **as** = anterior sclerite; **boc** = booklung covers; **cls** = comb-like structure; **cmp** = clypeus median projection; **db** = dorsal branch; **dep** = deep depressions; **emb** = embolus; **glo** = tube-like globular structure; **ldi** = labium deep incision; **pb** = posterior branch; **PLE** = posterior lateral eyes; **PME** = posterior median eyes; **se** = serrula; **spb** = slender posterior branch; **tba** = transverse bars; **tp** = triangular plate; **tsc** = transverse sclerite; **vb** = ventral branch; **XNNR** = Xishuangbanna National Natural Reserve; **XTBG** = Xishuangbanna Tropical Botanical Garden.

## Taxonomy

### Family Oonopidae Simon, 1890

### Genus *Bannana* Tong & Li, 2015

**Type species.** *Bannana crassispina* Tong & Li, 2015; gender feminine.

## Key to species of *Bannana* from Xishuangbanna, China

Male of *B. songxiaobini* is unknown.

1 Male........................................................................................................**2**
– Female.....................................................................................................**4**
2 Eyes not reduced (Fig. 1B, D); with group of thick setae on epigastric region and short comb-like structure on dorsal branch of bulb (Figs 1G, 4F) ................................................................................ ***B. zhengguoi* sp. nov.**
– Without the aforementioned character........................................................**3**
3 With rows of setae on the central part of sternum and thick bristles on palpal tibiae (Tong and Li 2015: figs 1C, 2A, D) ..........***B. crassispina* Tong & Li, 2015**
– Without aforementioned characters ..................***B. parvula* Tong & Li, 2015**
4 Eyes not reduced (Fig. 2B, G); posterior spiracles not connected by groove (Figs 2H, 3D) ..............................................................***B. zhengguoi* sp. nov.**
– Eyes reduced (Tong and Li 2015: figs 3E, D, 5A, D); posterior spiracles connected by groove (Tong and Li 2015: fig. 6D, E) ..........................................**5**

5 Postepigastric scutum long, nearly quadrangular, the distance between the groove connected posterior spiracles to posterior margin nearly three times the distance to anterior margin (Sun et al. 2019: fig. 1G) ........................................................................................ ***B. songxiaobini* Tong & Li, 2019**

– Postepigastric scutum short, only around epigastric furrow, the distance between the groove connected posterior spiracles to posterior margin nearly equal to or shorter than the distance to anterior margin (Tong and Li 2015: figs 3G, 5G) ........................................................................ **6**

6 Dorsal scutum covering about 5/6 of abdomen, about equal to the abdomen width (Tong and Li 2015: fig. 5E); the distance between the groove connected posterior spiracles to posterior margin nearly equal to the distance to anterior margin (Tong and Li 2015: figs 5I, 6D) ........................................................................................ ***B. parvula* Tong & Li, 2015**

– Dorsal scutum covering about 3/4 of abdomen, about 2/3 of abdomen width (Tong and Li 2015: fig. 3A); the distance between the groove connected posterior spiracles to posterior margin nearly equal to half the distance to anterior margin (Tong and Li 2015: figs 2H, 3H) ........................................................................................ ***B. crassispina* Tong & Li, 2015**

### *Bannana zhengguoi* Tong & Li, sp. nov.

https://zoobank.org/37E10DC8-C19D-4237-830B-FE6C2DA9E78E
Figs 1–4

**Type materials.** ***Holotype*** ♂ (SYNU-1051): China, Yunnan Prov., Menglun, XTBG, primary tropical seasonal rain forest, searching by hand, 21°55.035'N, 101°16.500'E, 558 m, Guo Zheng leg., 4–11/5/2007. ***Paratypes*:** 1♂1♀ (SYNU-1052–1053), same data as holotype; 1♂ (SYNU-1040), XNNR, secondary tropical montane evergreen broad-leaved forest, pitfall traps, 21°54.767'N, 101°11.431'E, 880 m, Guo Zheng leg., 16–31/4/2007; 1♀ (SYNU-1037), XTBG, primary tropical seasonal rain forest, searching by hand, 21°55.035'N, 101°16.500'E, 558 m, Guo Zheng leg., 4–11/5/2007; 1♂ (SYNU-1038), XNNR, primary tropical seasonal rain forest, pitfall traps 21°57.669'N, 101°11.893'E, 790 m, Guo Zheng leg., 1–15/4/2007; 1♀ (SYNU-1039), XTBG, primary tropical seasonal rain forest, searching by hand, 21°55.035'N, 101°16.500'E, 558 m, Guo Zheng leg., 19–26/5/2007; 3♂ (SYNU-1041–1043), XNNR, primary tropical seasonal rain forest, pitfall traps, 21°57.669'N, 101°11.893'E, 790 m, Guo Zheng leg., 1–15/5/2007; 1♀ (SYNU-1044), XNNR, secondary tropical seasonal moist forest, searching by hand, 21°54.607'N, 101°17.005'E, 633 m, Guo Zheng leg., 19–26/5/2007; 1♀ (SYNU-1045), XTBG, primary tropical seasonal rain forest, searching by hand, 21°55.035'N, 101°16.500'E, 558 m, Guo Zheng leg., 1–15/7/2007; 1♂ (SYNU-1046), XTBG, primary tropical seasonal rain forest, pitfall traps, 21°55.035'N, 101°16.500'E, 558 m, Guo Zheng leg., 16–31/4/2007; 1♂ (SYNU-1047), XTBG, rubber-tea plantation (about 20 yr.), pitfall traps, 21°55.551'N, 101°16.923'E, 561 m, Guo Zheng leg., 16–31/6/2007.

**Diagnosis.** The new species can be distinguished from all the congeners in having the eyes not reduced (Figs 1D, 2G), vs reduced eyes (Tong and Li 2015: figs 1F, 3D, 4C, 5D; Sun et al. 2019: fig. 1H). Furthermore, males of the new species can be distinguished from those of *B. crassispina* and *B. parvula* by

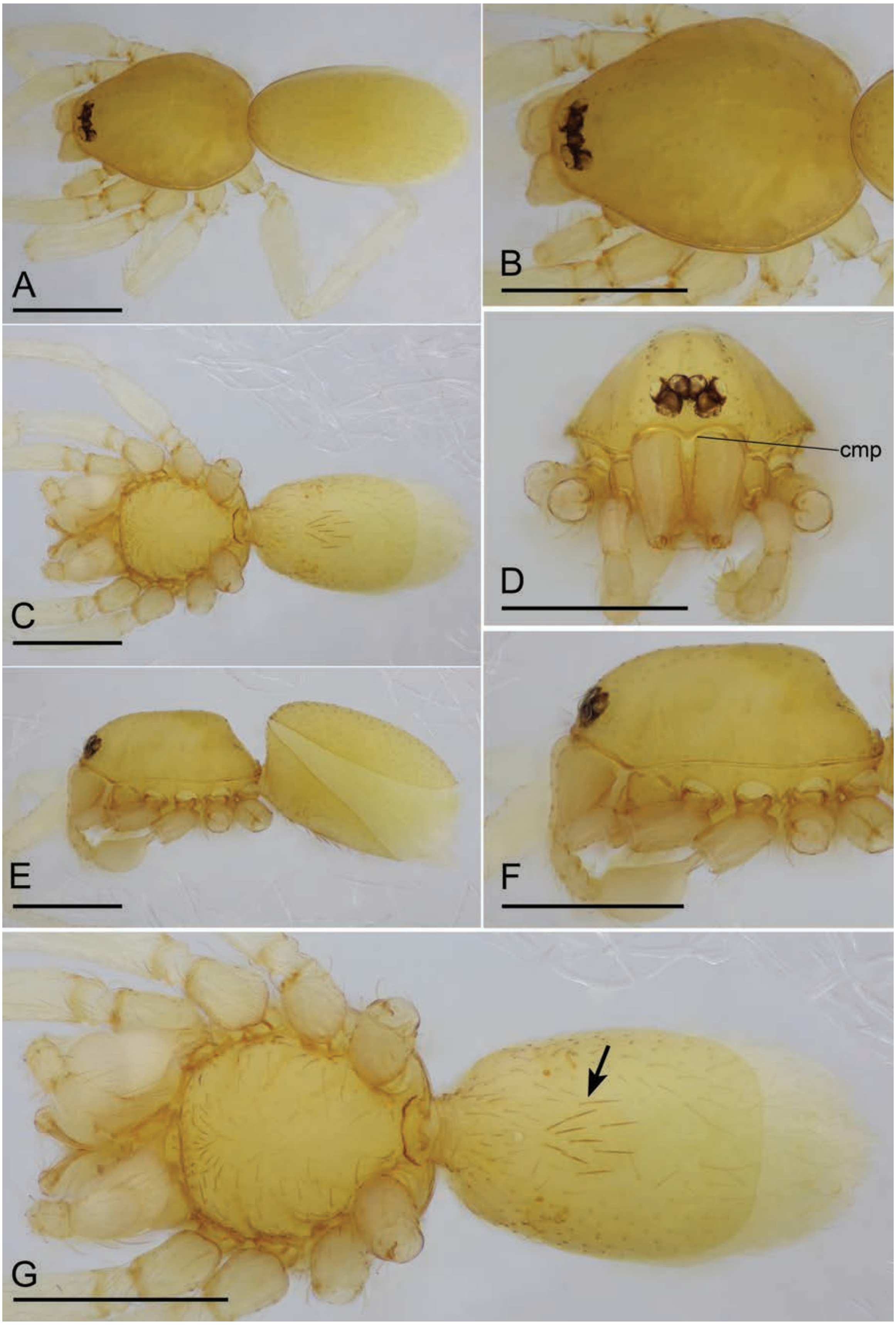

**Figure 1.** *Bannana zhengguoi* sp. nov., male holotype **A, C, E** habitus in dorsal, ventral, and lateral views **B, D, F** prosoma in dorsal, anterior and lateral views **G** habitus in ventral view, black arrow shows the group of thick setae. Abbreviation: cmp = clypeus median projection. Scale bars: 0.4 mm (**A–G**).

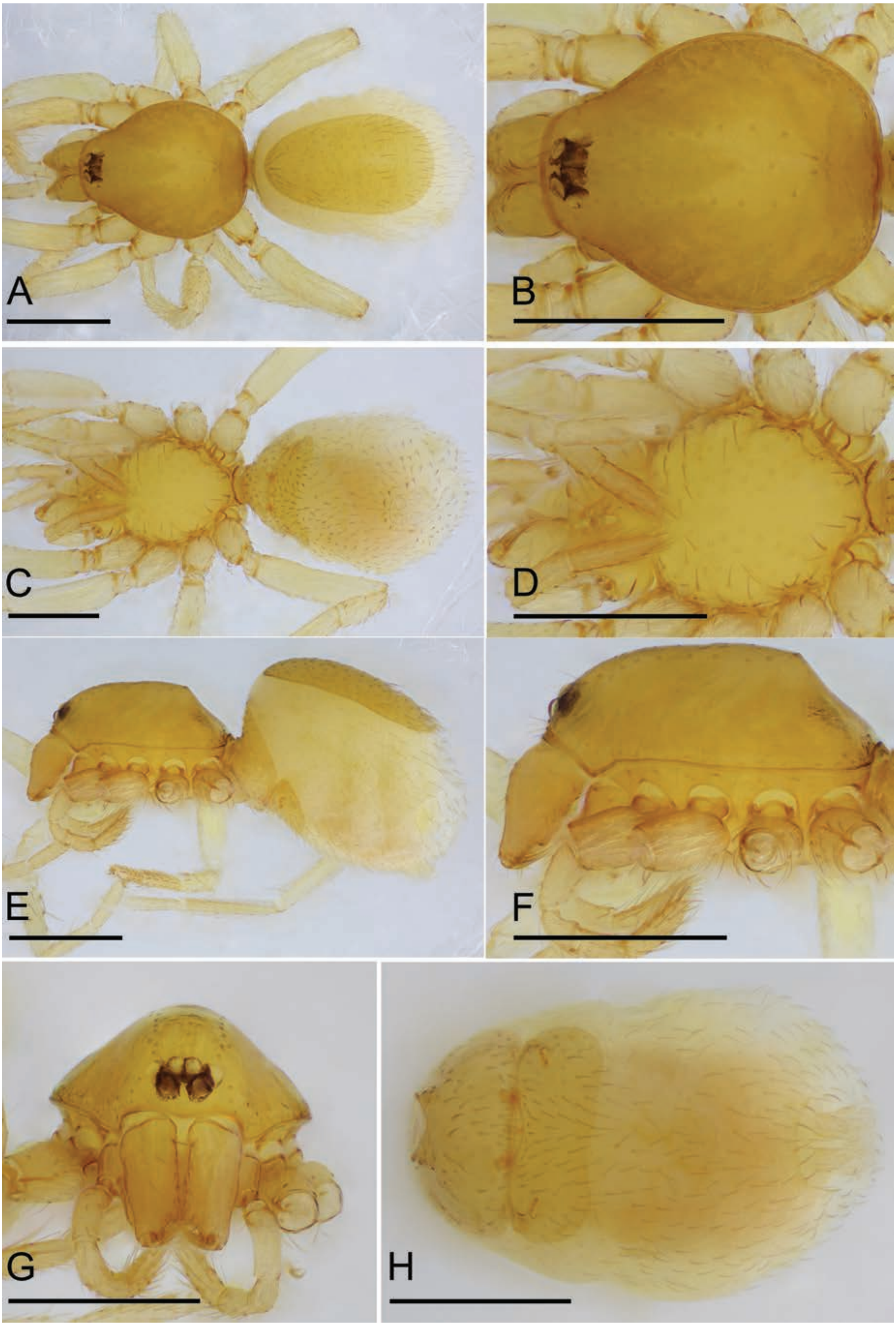

**Figure 2.** *Bannana zhengguoi* sp. nov., female paratype (SYNU-1053) **A, C, E** habitus in dorsal, ventral, and lateral views **B, D, F, G** prosoma in dorsal, ventral, lateral and anterior views **H** abdomen in ventral view. Scale bars: 0.4 mm (**A–H**).

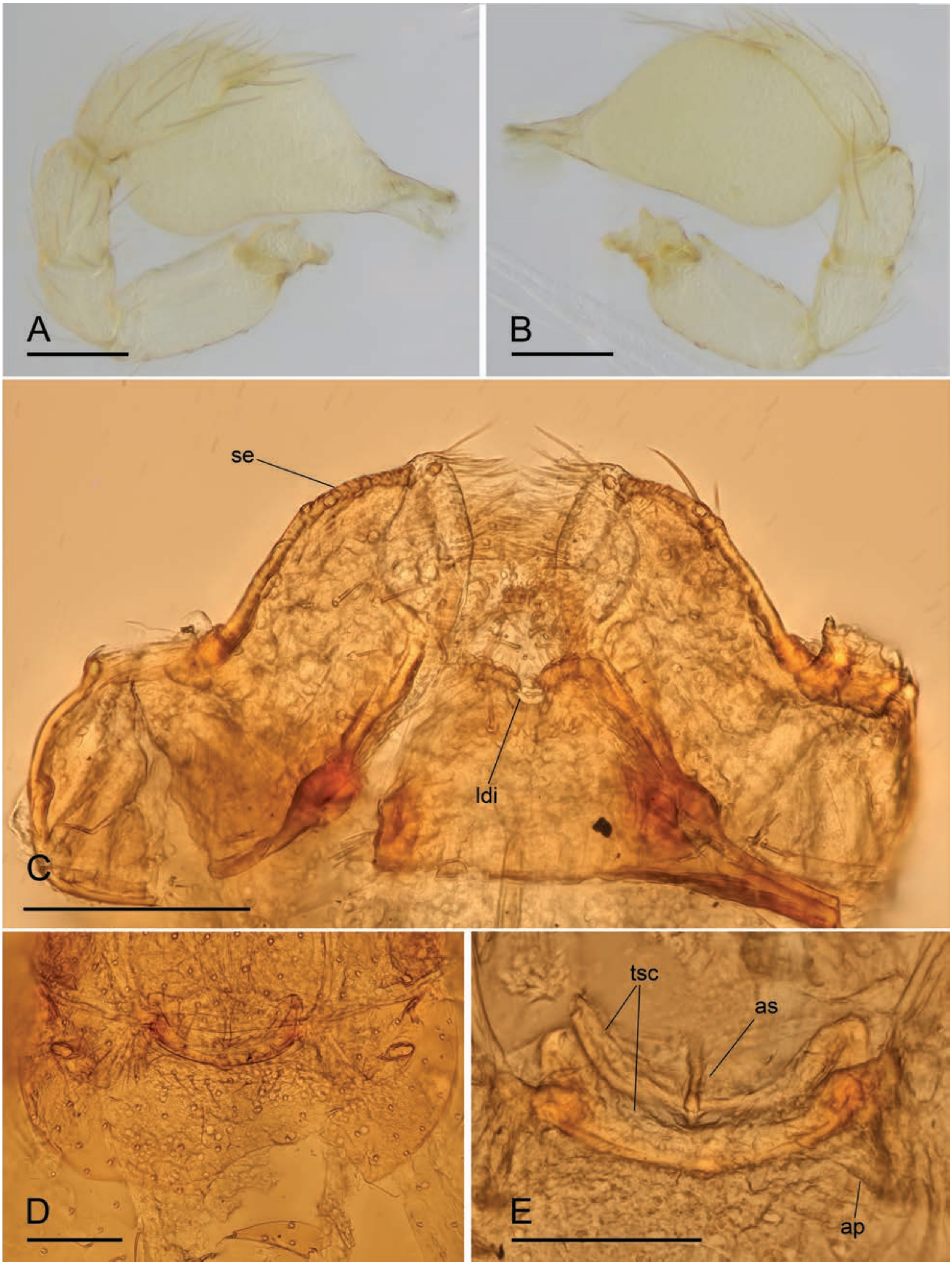

**Figure 3.** *Bannana zhengguoi* sp. nov. **A** male left palp, prolateral view **B** male left palp, retrolateral view **C** male endites and labium, ventral view **D, E** endogyne in ventral and dorsal views. Abbreviations: ap = apodemes; as = anterior sclerite; ldi = labium deep incision; se = serrula; tsc = transverse sclerite. Scale bars: 0.1 mm (**A–E**).

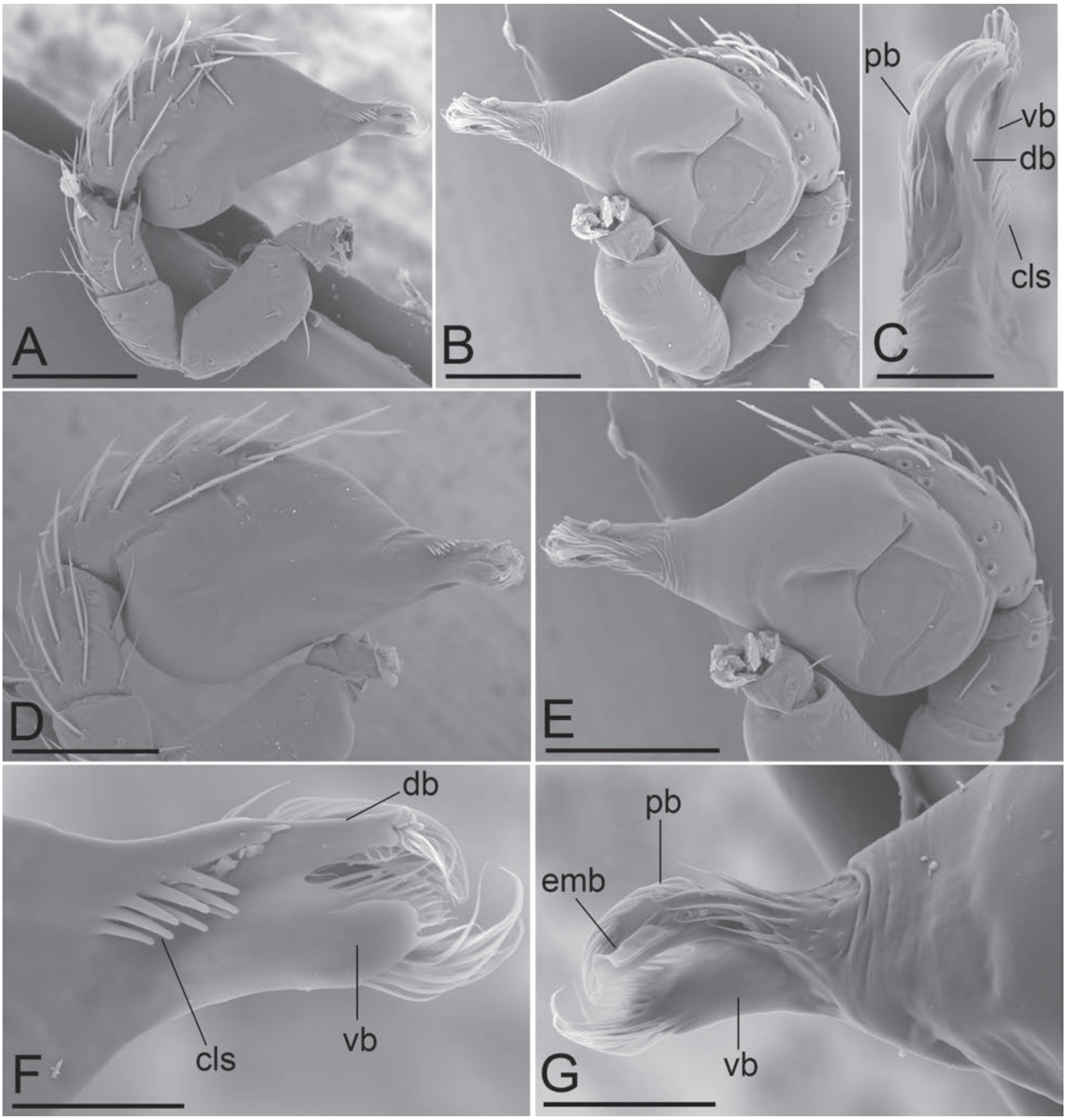

**Figure 4.** *Bannana zhengguoi* sp. nov., male left palp, SEM **A, B** prolateral and retrolateral views **C, F, G** distal part of bulb, dorsal, prolateral and retrolateral views **D, E** bulb, prolateral and retrolateral views. Abbreviations: cls = comb-like structure; db = dorsal branch; emb = embolus; pb = posterior branch; vb = ventral branch. Scale bars: 0.1 mm (**A, B, D, E**); 0.03 mm (**C, F, G**).

the short comb-like structure on dorsal branch of bulb and group of thick setae on epigastric region (Figs 1G, 4F), vs without comb-like structure and group of thick setae (Tong and Li 2015: figs 1G, 2E, 4F, 6A); females of the new species can be distinguished from those of *B. crassispina*, *B. parvula*, and *B. songxiaobini* by the posterior spiracles not connected by groove (Figs 2H, 3D), vs connected (Tong and Li 2015: figs 3G, H, **I**, 5G; Sun et al. 2019: fig. 1G).

**Description. Male (holotype).** ***Body*** yellow, chelicerae, sternum, and legs lighter; habitus as in Fig. 1A, C, E; body length 1.45. ***Carapace*** (Fig. 1B, F): 0.68

long, 0.50 wide; pars cephalica almost flat in lateral view, surface smooth. ***Eyes*** (Fig. 1B, D): ALE largest; PLE and PME nearly equal in size; ALE–PLE separated by less than ALE radius; PME touching each other; posterior eye row recurved as viewed from above, straight as viewed from front. ***Clypeus*** (Fig. 1D): height about 0.5 times of ALE diameter, with a triangular clypeus median projection (cmp). ***Mouthparts*** (Fig. 3C): labium deeply incised. ***Sternum*** (Fig. 1G): surface finely reticulate. Abdomen (Fig. 1A, C, E, G): 0.82 long, 0.45 wide; dorsal scutum nearly covering full length of abdomen, postepigastric and epigastric scutum fused, covering 5/6 of abdomen length; book lung covers ovoid, surface smooth; epigastric region with a group of thick setae, posterior spiracles not connected by groove. ***Palp*** (Figs 3A, B, 4A–G): pale-orange; 0.48 long (0.15, 0.09, 0.08, 0.16); femur elongated (width/length = 0.48); bulb oval, tapering apically; embolus system complicated, with a cluster of short comb-like structures on dorsal branch, many hair-like structure on ventral and posterior branches.

**Female (SYNU-1053).** Same as male except as noted. ***Body*** habitus as in Fig. 2A, C, E; body length 1.51. ***Carapace*** (Fig. 2B, F): 0.66 long, 0.53 wide. ***Abdomen*** (Fig. 2A, C, E, H): 0.84 long, 0.56 wide; dorsal scutum covering about 4/5 of abdomen length, about 2/3 of abdomen width; postepigastric scutum rectangular, posterior margin nearly straight. ***Epigaster*** (Fig. 3D): surface without external features. ***Endogyne*** (Fig. 3E): with two narrow, transverse sclerites (tsc) and an anterior stick-shaped sclerite (as); lateral apodemes (ap) present.

**Etymology.** The specific name is named in honor of the collector, Mr Guo Zheng.

**Distribution.** Known only from the type locality.

### Genus *Trilacuna* Tong & Li, 2007

**Type species.** *Trilacuna rastrum* Tong & Li, 2007; gender feminine.

### *Trilacuna aoxian* Tong & Li, sp. nov.

https://zoobank.org/0E605FF2-B545-407D-B8AD-775025FD0E03
Figs 5–8

**Type materials.** ***Holotype*** ♂ (SYNU-989): China, Yunnan Prov., Menglun, XNNR, primary tropical seasonal rain forest, pitfall traps, 21°57.669'N, 101°11.893'E, 790 m, Guo Zheng leg.,16–31/3/2007; ***Paratypes*****:** 1♀ (SYNU-990), XTBG, primary tropical seasonal rain forest, searching by hand, 21°55.035'N, 101°16.500'E, 558 m, Guo Zheng leg., 5–12/1/2007; 1♀ (SYNU-991), XTBG, primary tropical seasonal rain forest, searching by hand, 21°55.035'N, 101°16.500'E, 558 m, Guo Zheng leg., 19–25/11/2006; 1♀ (SYNU-992), XTBG, primary tropical seasonal rain forest, searching by hand, 21°55.035'N, 101°16.500'E, 558 m, Guo Zheng leg., 5–12/12/2006; 1♂ (SYNU-993), XNNR, secondary tropical montane evergreen broad-leaved forest, pitfall traps, 21°54.767'N, 101°11.431'E, 880 m, Guo Zheng leg., 1–15/3/2007; 1♀ (SYNU-994), XNNR, secondary tropical seasonal moist forest, pitfall traps, 21°54.607'N, 101°17.005'E, 633 m, Guo Zheng leg., 16–31/6/2007; 1♀ (SYNU-995), XNNR, primary tropical seasonal rain forest, pitfall traps, 21°55.035'N, 101°16.500'E, 558 m, Guo Zheng leg., 1–15/4/2007;

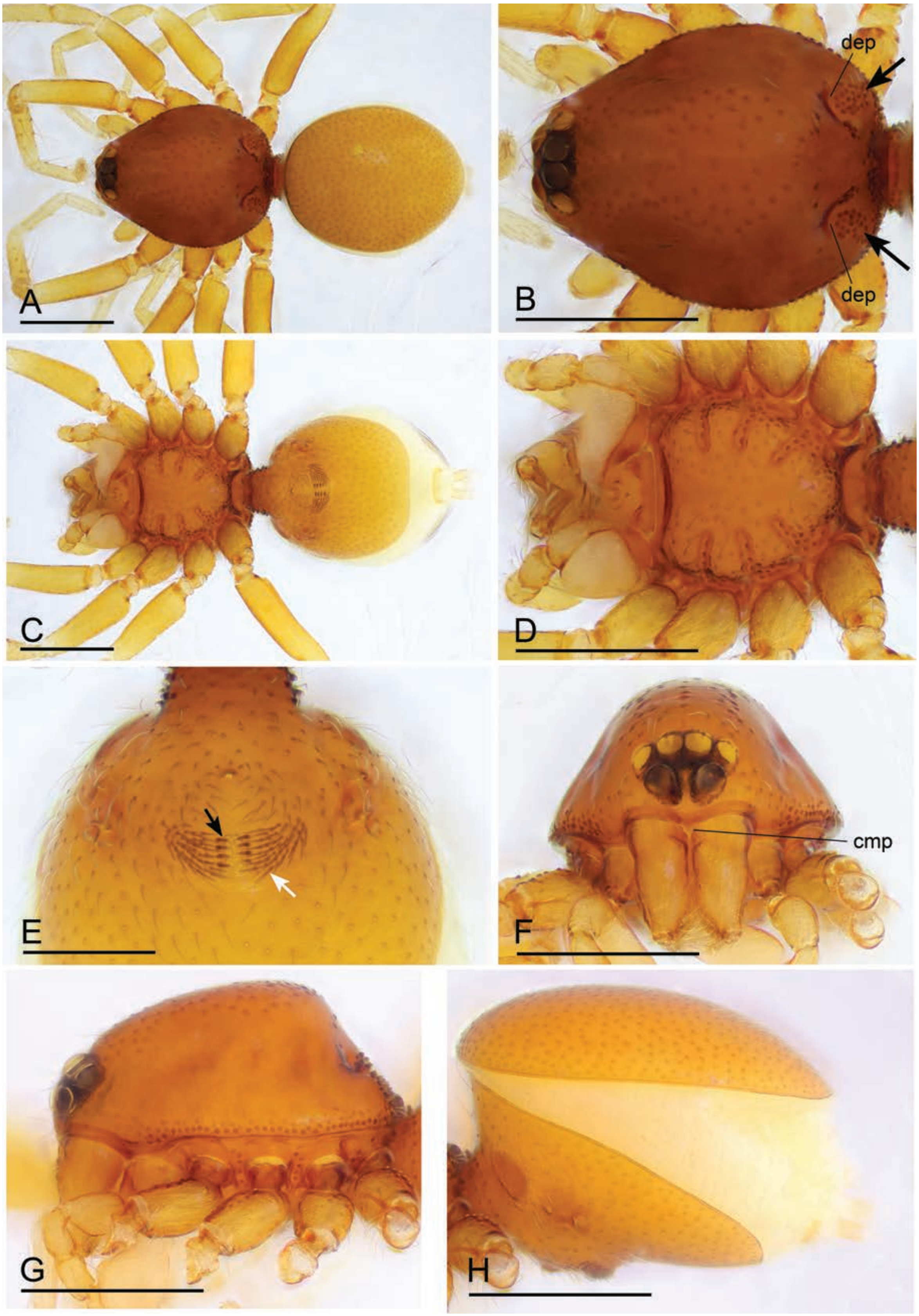

**Figure 5.** *Trilacuna aoxian* sp. nov., male holotype **A, C** habitus in dorsal and ventral views **B, D, F, G** prosoma in dorsal, ventral, anterior and lateral views, black arrows show large hair bases **E, H** abdomen in ventral and lateral views, black arrow shows the rows of short, black thorn-like setae, white arrow shows cluster of short setae. Abbreviations: cmp = clypeus median projection; dep = deep depressions. Scale bars: 0.4 mm (**A–D, F–H**); 0.2 mm (**E**).

4♂ (SYNU-996–999), XTBG, primary tropical seasonal rain forest, pitfall traps, 21°55.035'N, 101°16.500'E, 558 m, Guo Zheng leg., 1–15/1/2007; 3♂ (SYNU-1000–1002), XTBG, primary tropical seasonal rain forest, pitfall traps, 21°55.035'N, 101°16.500'E, 558 m, Guo Zheng leg., 16–31/2/2007; 1♂ (SYNU-1003), XNNR, primary tropical seasonal rain forest, pitfall traps, 21°57.445'N, 101°12.997'E, 744 m, Guo Zheng leg., 16–31/2/2007; 1♀ (SYNU-1004), XTBG, primary tropical seasonal rain forest, searching by hand, 21°55.035'N, 101°16.500'E, 558 m, Guo Zheng leg., 19–25/11/2006; 1♂ (SYNU-1005), XNNR, secondary tropical seasonal moist forest, pitfall traps, 21°54.607'N, 101°17.005'E, 633 m, Guo Zheng leg., 1–15/3/2007; 2♂1♀ (SYNU-1006–1008), XTBG, primary tropical seasonal rain forest, pitfall traps, 21°55.035'N, 101°16.500'E, 558 m, Guo Zheng leg., 16–31/1/2007; 1♂ (SYNU-1009), XNNR, primary tropical seasonal rain forest, pitfall traps, 21°57.669'N, 101°11.893'E, 790 m, Guo Zheng leg., 16–31/2/2007; 2♂1♀ (SYNU-1010–1012), XTBG, primary tropical seasonal rain forest, pitfall traps, 21°55.035'N, 101°16.500'E, 558 m, Guo Zheng leg., 1–15/1/2007; 1♂ (SYNU-1013), XNNR, secondary tropical seasonal moist forest, searching by hand, 21°54.607'N, 101°17.005'E, 633 m, Guo Zheng leg., 19–25/2/2007; 3♂ (SYNU-1014–1016), XNNR, primary tropical seasonal rain forest, pitfall traps, 21°57.445'N, 101°12.997'E, 744 m, Guo Zheng leg., 16–31/2/2007; 3♂ (SYNU-1017–1019), XNNR, primary tropical seasonal rain forest, pitfall traps, 21°57.669'N, 101°11.893'E, 790 m, Guo Zheng leg., 1–15/2/2007; 1♂ (SYNU-1023), XNNR, primary tropical seasonal rain forest, pitfall traps, 21°57.445'N, 101°12.997'E, 744 m, Guo Zheng leg., 16–31/2/2007; 1♀ (SYNU-1024), XNNR, secondary tropical seasonal moist forest, pitfall traps, 21°54.607'N, 101°17.005'E, 633 m, Guo Zheng leg., 1–15/7/2007; 1♀ (SYNU-1027), XNNR, primary tropical seasonal rain forest, searching by hand, 21°57.669'N, 101°11.893'E, 790 m, Guo Zheng leg., 19–25/10/2006; 1♂ (SYNU-1028), XNNR, primary tropical seasonal rain forest, searching by hand, 21°57.445'N, 101°12.997'E, 744 m, Guo Zheng leg., 19–25/1/2007; 1♂ (SYNU-1029), XTBG, primary tropical seasonal rain forest, pitfall traps, 21°55.035'N, 101°16.500'E, 558 m, Guo Zheng leg., 16–31/2/2007; 1♀ (SYNU-1030), XTBG, primary tropical seasonal rain forest, pitfall traps, 21°55.035'N, 101°16.500'E, 558 m, Guo Zheng leg., 16–31/2/2007; 1♀ (SYNU-1031), XNNR, primary tropical seasonal rain forest, searching by hand, 21°57.669'N, 101°11.893'E, 790 m, Guo Zheng leg., 19–25/2/2007; 1♂ (SYNU-1032), XNNR, primary tropical seasonal rain forest, pitfall traps, 21°57.669N, 101°11.893'E, 790 m, Guo Zheng leg., 1–15/1/2007; 1♀ (SYNU-1033), XNNR, primary tropical seasonal rain forest, searching by hand, 21°57.445'N, 101°12.997'E, 744 m, Guo Zheng leg., 10–20/6/2007; 3♂ (SYNU-1034–1036), XNNR, primary tropical seasonal rain forest, pitfall traps, 21°57.669'N, 101°11.893'E, 790 m, Guo Zheng leg., 16–31/2/2007; 2♂1♀ (SYNU-1048–1050), XTBG, primary tropical seasonal rain forest, pitfall traps, 21°55.035'N, 101°16.500'E, 558 m, Guo Zheng leg., 1–15/1/2007.

**Diagnosis.** The new species is similar to *Trilacuna changzi* Tong & Li, 2020 in having long, thick setae on male endites, the tortuous, tube-like globular structure of endogyne, and the deep depressions on carapace, but it can be distinguished by the densely mucronate structure on sub-distal area of bulb (Fig. 8F, H) vs without mucronate structure (Tong et al. 2020: figs 5A, C, E), the rows of short, black thorn-like setae and cluster of short setae on epigastric

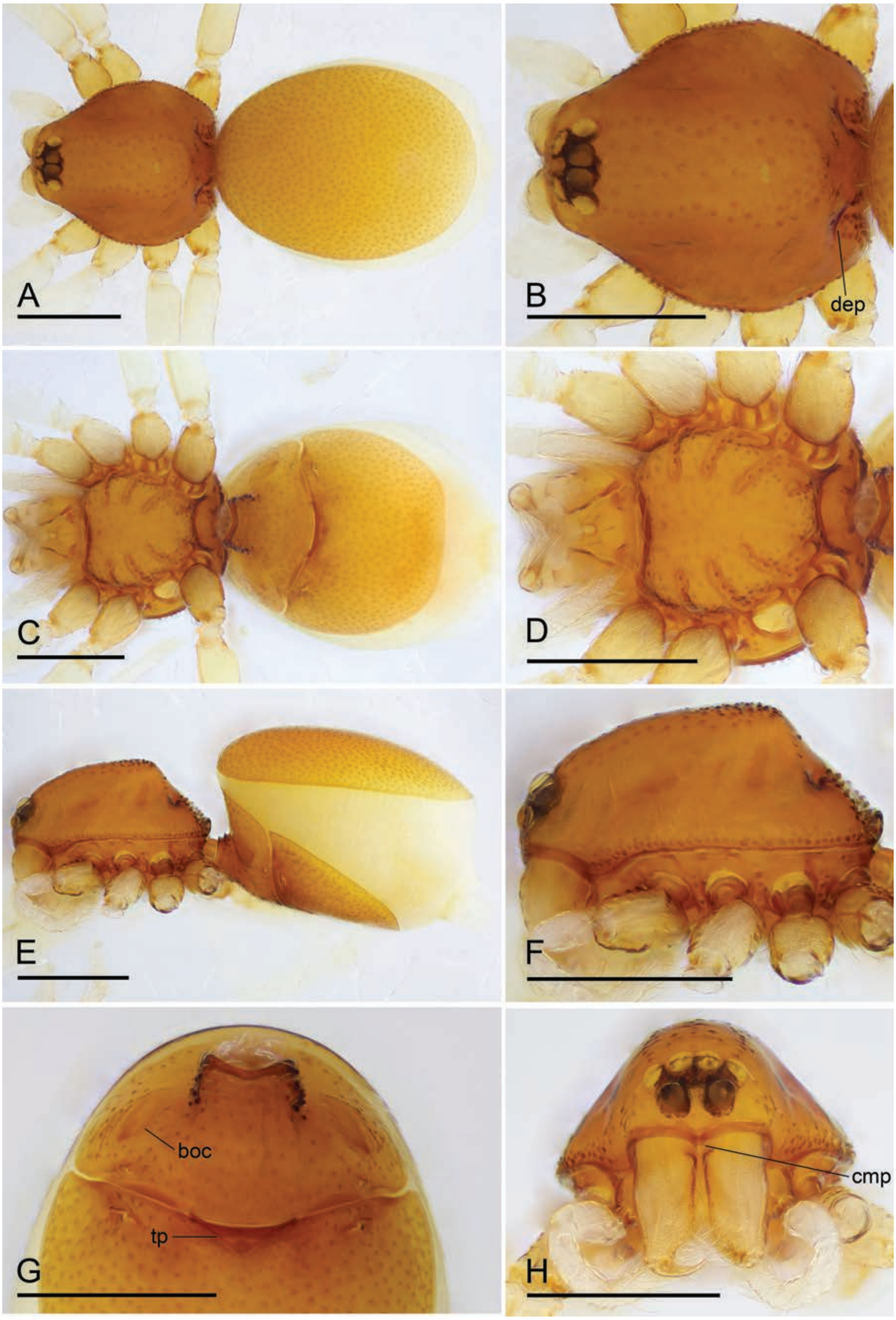

**Figure 6.** *Trilacuna aoxian* sp. nov., female paratype (SYNU-990) **A, C, E** habitus in dorsal, ventral, and lateral views **B, D, F, H** prosoma in dorsal, ventral, lateral and anterior views **G** abdomen in ventral view. Abbreviations: boc = booklung covers; cmp = clypeus median projection; dep = deep depressions; tp = triangular plate. Scale bars: 0.4 mm (**A–H**).

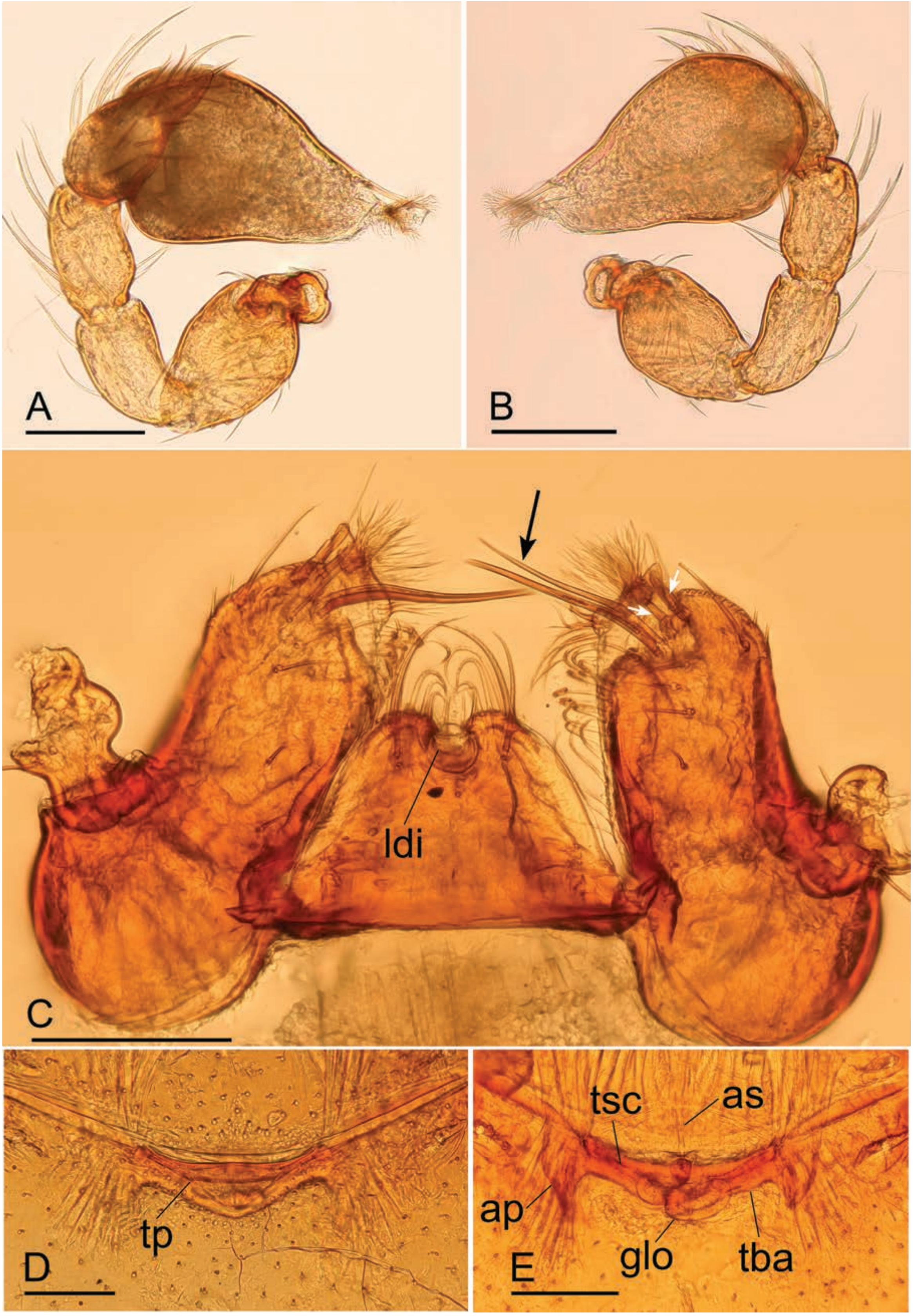

**Figure 7.** *Trilacuna aoxian* sp. nov. **A** male left palp, prolateral view **B** male left palp, retrolateral view **C** male endites and labium, ventral view, white arrow shows the short, thick setae, black arrow shows two very long, thick setae **D, E** endogyne in ventral and dorsal views. Abbreviations: ap = apodemes; as = anterior sclerite; glo = tube-like globular structure; ldi = labium deep incision; tba = transverse bars; tp = triangular plate; tsc = transverse sclerite. Scale bars: 0.1 mm (**A–E**).

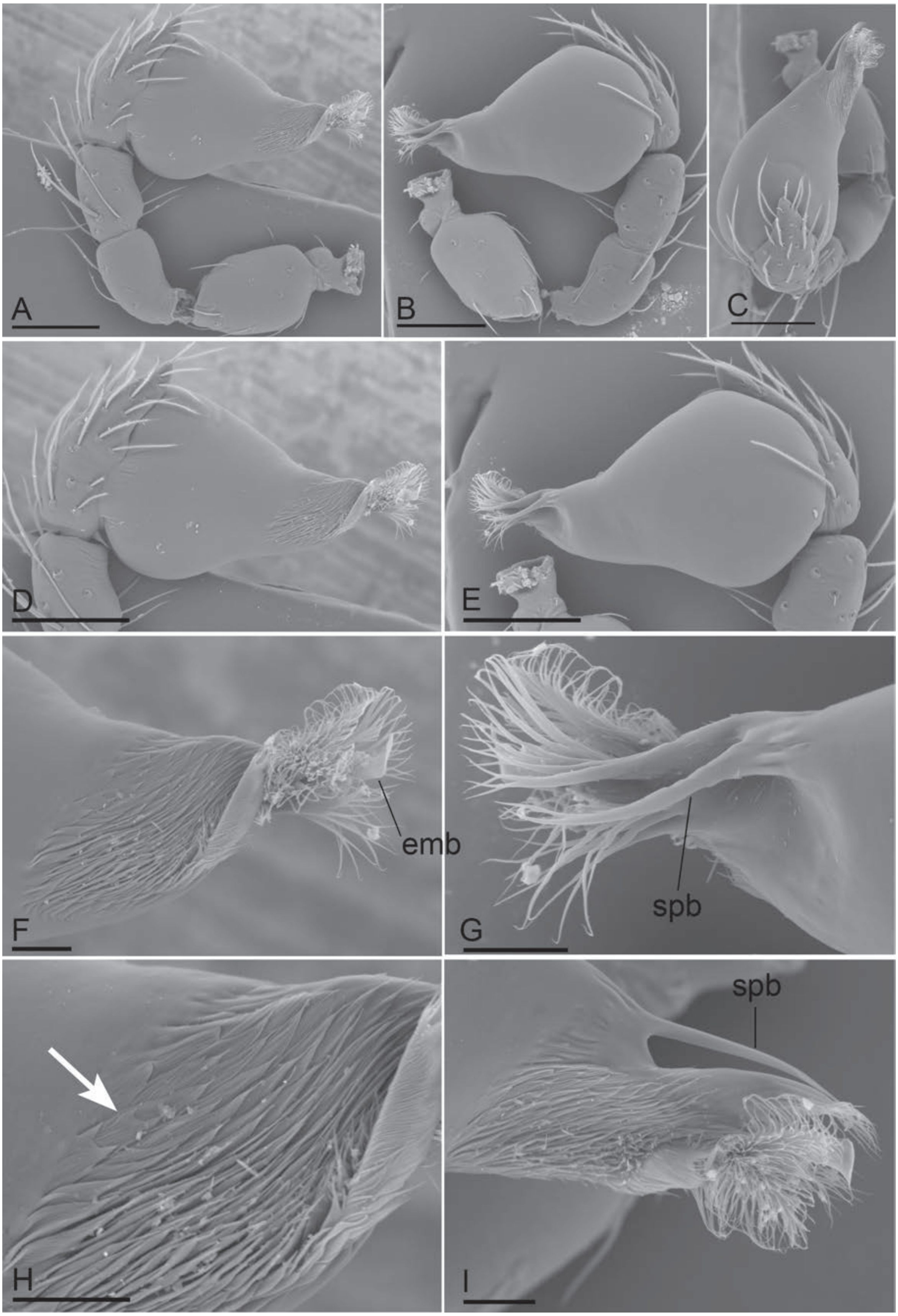

**Figure 8.** *Trilacuna aoxian* sp. nov., male left palp, SEM **A, B, C** prolateral, retrolateral and dorsal views **D, E** bulb, prolateral and retrolateral views **F, G, I** distal part of bulb, prolateral, retrolateral and dorsal views **H** detail of bulb, arrow shows the mucronate structure. Abbreviations: emb = embolus; spb = slender posterior branch. Scale bars: 0.1 mm (**A–E**); 0.02 mm (**F–I**).

region of male (Fig. 5E) vs a cluster of dense, short setae behind epigastric region (Tong et al. 2020: arrow in fig. 4C), and the triangular plate on epigastric region of female having the height/length = 0.33 (Fig. 6G), vs the height/length = 0.45 in *T. changzi* (Tong et al. 2020: fig. 6G).

**Description. Male (holotype).** ***Body*** yellowish brown, chelicerae, sternum and legs lighter; habitus as in Fig. 5A, C; body length 1.62. ***Carapace*** (Fig. 5B, G): 0.77 long, 0.63 wide; sides smooth; lateral margin with small denticles; posterior surface with deep depressions and group of large hair bases. ***Eyes*** (Fig. 5B, F): ALE largest; PLE and PME nearly equal in size; ALE–PLE separated by less than ALE radius; PME touching each other; posterior eye row recurved as viewed from above, procurved as viewed from front. ***Clypeus*** (Fig. 5F): height about 0.75 times of ALE diameter, with a triangular, pointed, clypeus median projection (cmp). ***Mouthparts*** (Fig. 7C): labium deeply incised, endites with two short, thick setae and two very long, thick setae. ***Sternum*** (Fig. 5D): surface smooth. ***Abdomen*** (Fig. 5A, C, E, H): 0.86 long, 0.66 wide; booklung covers ovoid, surface smooth; epigastric region strongly elevated, with two rows of short, black thorn-like setae and cluster of short setae. ***Palp*** (Figs 7A, B, 8A–I): orange; 0.57 long (0.15, 0.13, 0.11, 0.18); femur elongated (width/length = 0.64); bulb oval, with densely mucronate structure on sub-distal area; embolus system with many hair-like structure and a single slender posterior branch.

**Female (SYNU-990).** Same as male except as noted. ***Body*** habitus as in Fig. 6A, C, E; body length 1.81. ***Carapace*** (Fig. 6B, F): 0.73 long, 0.65 wide. ***Abdomen*** (Fig. 6A, C, E, G): 1.08 long, 0.82 wide. ***Epigaster*** (Figs 6G, 7D): with a triangular plate, the height/length = 0.33. ***Endogyne*** (Fig. 7E): with narrow, transverse sclerite (tsc), an anterior stick-shaped sclerite (as), and a posterior tortuous, tube-like globular structure (glo); transverse bars (tba) with two lateral apodemes (ap).

**Etymology.** The specific name comes from Chinese pinyin, “aoxian”, which means “depression” and is in reference to the deep depression on posterior surface of carapace; noun in apposition.

**Distribution.** Known only from the type locality.

## Acknowledgements

The manuscript benefitted greatly from comments by Marc Milne (University of Indianapolis, USA) and Dimitar Dimitrov (University of Bergen, Norway).

## Additional information

### Conflict of interest

The authors have declared that no competing interests exist.

### Ethical statement

No ethical statement was reported.

### Funding

This study was supported by the National Natural Science Foundation of China (NSFC32370479, 31972867).

## Author contributions

YT designed the study. YT and SL performed morphological species identification. YT and YS finished the descriptions and took the photos. YT and DB drafted and revised the manuscript.

## Author ORCIDs

Yanfeng Tong https://orcid.org/0000-0002-4348-7029
Yongbo Shao https://orcid.org/0009-0005-1156-6725
Dongju Bian https://orcid.org/0000-0002-9324-8026
Shuqiang Li https://orcid.org/0000-0002-3290-5416

## Data availability

All of the data that support the findings of this study are available in the main text.

## References

Eichenberger B, Kranz-Baltensperger Y (2011) New *Trilacuna* species from Thailand, Malaysia and Sumatra (Araneae, Oonopidae). Zootaxa 2823(1): 1–31. https://doi.org/10.11646/zootaxa.2823.1.1

Grismado CJ, Deeleman-Reinhold CL, Piacentini LN, Izquierdo MA, Ramírez MJ (2014) Taxonomic review of the goblin spiders of the genus *Dysderoides* Fage and their Himalayan relatives of the genera *Trilacuna* Tong and Li and *Himalayana*, new genus (Araneae, Oonopidae). Bulletin of the American Museum of Natural History 387: 1–108. https://doi.org/10.1206/843.1

Huang Y, Bian D, Tong Y, Zhang Z, Li S (2021) Two new species of the genus *Trilacuna* (Araneae: Oonopidae) from Jinyun Mountain of Chongqing, China. European Journal of Taxonomy 748: 1–14. https://doi.org/10.5852/ejt.2021.748.1337

Jocqué R, Dippenaar-Schoeman AS (2006) Spider Families of the World. Musée Royal de l'Afrique Central, Tervuren, 336 pp.

Ma J, Bian D, Tong Y, Yang Z, Zhang Z (2023) Three new species of the genus *Trilacuna* Tong & Li, 2007 (Araneae, Oonopidae) from Yunnan Province, China. ZooKeys 1174: 289–300. https://doi.org/10.3897/zookeys.1174.106130

Malek-Hosseini MJ, Grismado CJ, Sadeghi S, Bakhshi Y (2015) Description of the first cave dwelling species of the spider genus *Trilacuna* Tong & Li from Iran (Araneae: Oonopidae). Zootaxa 3972(4): 549–561. https://doi.org/10.11646/zootaxa.3972.4.6

Myers N (1988) Threatened biotas: "hot spots" in tropical forests. The Environmentalist 8(3): 1–20. https://doi.org/10.1007/BF02240252

Song C, Tong Y, Bian D, Li S (2024) A survey of the genus *Orchestina* Simon, 1882 (Araneae, Oonopidae) from Xishuangbanna, China, with descriptions of five new species. Zoosystematics and Evolution 100(1): 255–277. https://doi.org/10.3897/zse.100.117968

Sun X, Lin Y, Tong Y, Li S (2019) First report of a new myrmecophile spider (Araneae, Oonopidae) from Xishuangbanna, China. Acta Arachnologica Sinica 28(1): 37–40.

Tong Y, Li S (2007) One new genus and four new species of oonopid spiders from southwest China (Araneae: Oonopidae). Annales Zoologici, Warszawa 57: 331–340.

Tong Y, Li S (2015) One new genus and two new species of oonopid spiders from Xishuangbanna Rainforest, southwestern China (Araneae, Oonopidae). ZooKeys 494: 1–12. https://doi.org/10.3897/zookeys.494.9183

Tong Y, Chen H, Bai S, Zhang Z, Li S (2019) Seven new species of the genus *Trilacuna* Tong & Li, 2007 from Yunnan, China (Araneae, Oonopidae). ZooKeys 821: 11–44. https://doi.org/10.3897/zookeys.821.29599

Tong Y, Li S, Bian D (2020) Taxonomic studies on the genus *Trilacuna* (Araneae, Oonopidae) from Myanmar. ZooKeys 960: 39–62. https://doi.org/10.3897/zookeys.960.54053

Tong Y, Sun X, Li S, Bian D (2021) Taxonomic study of the genus *Ischnothyreus* (Araneae, Oonopidae) from Xishuangbanna Rainforest, southwestern China. ZooKeys 1034: 165–197. https://doi.org/10.3897/zookeys.1034.63388

Ubick D, Dupérré N (2017) Oonopidae. In: Ubick D, Paquin P, Cushing P, Roth V (Eds) Spiders of North America: an Identification Manual (2nd edition). American Arachnological Society, Keene, New Hampshire, 181–182.

WSC (2024) World Spider Catalog. Version 25.0 Natural History Museum Bern. http://wsc.nmbe.ch [Accessed on 27 March 2024]

ZooKeys 1205: 349–371 (2024)
DOI: 10.3897/zookeys.1205.125639

Research Article

# A new species of *Cincticostella* Allen, 1971 (Ephemeroptera, Ephemerellidae) from Yunnan, China and establishment of a new species complex

Ye-Kang Sun[1], Rong-Long Yang[1], Zhi-Wei Tan[2], Xian-Fu Li[1,3,4], Luke M. Jacobus[5]

1 *Institute of Eastern-Himalaya Biodiversity Research, Dali University, Dali 671000, Yunnan, China*
2 *Yunnan Key Laboratory for Pollution Processes and Control of Plateau Lake-Watersheds, Yunnan Academy of Ecological and Environmental Sciences, Kunming 650034, Yunnan, China*
3 *Collaborative Innovation Center for Biodiversity and Conservation in the Tree Parallel Rivers Region of China, Dali University, Dali, Yunnan, China*
4 *Research Center of Ecology and Governance for Er'hai Lake Streams, Dali, Yunnan, China*
5 *Division of Science, Indiana University Columbus, Columbus 47203, IN, USA*
*Corresponding authors: Xian-Fu Li (lixf@eastern-himalaya.cn); Zhi-Wei Tan (tanzhiweitt@163.com)*

## Abstract

*Cincticostella jianchuan* **sp. nov.** from Dali Bai Autonomous Prefecture, Yunnan Province, China, is described based on chorionic structure, nymph, and winged stages. The new species is closely related to *C. fusca* (Kang & Yang, 1995), but it can be distinguished in the male imago stage by its mesonotum and penes morphology, coloration, and the forking point of the stem of MA+Rs on the forewing; in the nymph stage, it can be distinguished by the length of the posterolateral projections of abdominal segment IX and the setation of the abdominal terga. Compared to other congeners, nymphs and male imagoes of the new species and *C. fusca* share several morphological characteristics, such as a larger body, mesothorax with medially notched anterolateral projections, forefemur without a subapical band of transverse spines of the nymphs, the area between C, Sc and R1 of the forewings distinctly pigmented, and an apical sclerite on the ventral face of the penes of the male imagoes, supporting the proposition of a new species complex, the *jianchuan* complex. The systematics of *Cincticostella* and related genera are discussed briefly.

**Key words:** Eastern-Himalaya, Ephemerellidae, Hengduan Mountains, Mayfly, Taxonomy

Academic editor: Ben Price
Received: 18 April 2024
Accepted: 7 June 2024
Published: 1 July 2024

ZooBank: https://zoobank.org/996E28FC-8FA0-4585-AA18-0B8708A86096

Citation: Sun Y-K, Yang R-L, Tan Z-W, Li X-F, Jacobus LM (2024) A new species of *Cincticostella* Allen, 1971 (Ephemeroptera, Ephemerellidae) from Yunnan, China and establishment of a new species complex. ZooKeys 1205: 349–371. https://doi.org/10.3897/zookeys.1205.125639

## Introduction

The genus *Cincticostella* Allen, 1971 (Ephemeroptera: Ephemerellidae: Ephemerellinae: Ephemerellini) includes 22 species from throughout the eastern Palearctic and Indomalayan regions (Auychinda et al. 2022). The distinctive nymphs have the anterolateral angles of the prothorax projecting anteriorly and have a pair of large, wide, mesothoracic anterolateral processes (Jacobus and McCafferty 2008; Xie et al. 2009). Recent years have seen increased study of this genus, with nine of its species being described for the first time in the last five years (Martynov et al. 2019, 2021; Auychinda et al.

2020a, 2022). Also, several male adults have been described for the first time (Zhang et al. 2020, 2021; Zheng and Zhou 2021), resulting in a better understanding of this and related genera.

Due to uncertain relationships of species in the genus *Cincticostella* and possible polyphyly, the term “complex” has been used at various times to indicate distinctly different groups of species (Allen 1975; Martynov et al. 2019, 2021). According to Allen (1975), representatives of the *nigra*-group lack head tubercles and their middle and hind pairs of femora are narrow, not enlarged and the margins are without serration; ones of the *insolta*-group have suboccipital head tubercles and the middle and hind pairs of femora being enlarged with serrated margins and/or protuberances. But *C. gosei* (Allen, 1975) did not fit into either of these two complexes (Martynov et al. 2021). Therefore, the monotypic *C. gosei* complex was proposed by Martynov et al. (2021), according to *C. gosei* had a combination of characters. Up to now, the genus *Cincticostella* has three complexes. Martynov et al. (2021) and Auychinda et al. (2022) had reviewed the species included in each complex. The *nigra* complex is the largest, with 14 species (Martynov et al. 2021; Auychinda et al. 2022). Zhang et al. (2020) described the male imago of *C. fusca* Kang & Yang, 1995, a species within this group. They remarked about the unique form of the genitalia, but they did not recognize a new species complex for it. Li et al. (2020) noted a novel gene arrangement pattern in its mitochondrial genome.

During our recent survey of the mayfly fauna of the Hengduan Mountains area, at the eastern end of the Himalayas, a not yet described species of *Cincticostella* similar to *C. fusca* was found in Jianchuan County, Dali Bai Autonomous Prefecture, western Yunnan, China, at an altitude of more than 2200 m. Here, we describe this new *Cincticostella* species based on imago, subimago, nymph, and chorionic structure. Based on these new data and previous data for *C. fusca* (Zhang et al. 2020), we propose a new species complex within *Cincticostella*.

## Material and methods

*Cincticostella* nymphs were collected with a D-frame net from the riffle and running habitats of the Jinlong River, in Jianchuan County, Dali Bai Autonomous Prefecture, western Yunnan, China. Following the guidelines of Li et al. (2022) and Yang et al. (2023), the habitat photographs were taken using the mobile phone equipped with a Kase 40–75 mm macro lens. Water pH was measured with a YSI Professional Plus Multiparameter. Some specimens were dissected under a stereomicroscope and were mounted on slides with Hoyer’s Solution for examination under higher light magnification. Slide-mounted specimens were examined, photographed and measured under a Keyence VHX-S550E digital microscope. Eggs were dissected from female imagoes. Eggs were dried, coated with gold, observed and photographed by scanning electron microscopy (SEM). The final plates were prepared with Adobe Photoshop CC 2018.

All imagoes were collected by rearing the mature nymphs in the laboratory. All materials are stored in 95% ethanol. Holotype and paratype specimens are deposited in the Museum of Biology, Institute of Eastern-Himalaya Biodiversity Research, Dali University (MBDU). Species hypotheses utilize a morphological species concept.

## Results

**Ephemeroptera Latreille, 1810**
**Ephemerellidae Klapálek, 1909**

### *Cincticostella jianchuan* sp. nov.

https://zoobank.org/87E98558-629C-4512-8224-A2BD9C29791C
Figs 1–20

**Material examined.** ***Holotype*:** male imago, with final nymphal instar exuviae (in ethanol), China, Yunnan Province, Dali City, Jianchuan County, Jinlong River, 26°35'2.7"N, 99°51'45.0"E, 2371 m a.s.l., 09.V.2022, coll. Xian-Fu Li and Rong-Long Yang. ***Paratypes*:** 40 nymphs, 24 imagos and 20 subimagos reared from nymphs with same data as holotype.

**Diagnosis.** The new species is similar to *C. fusca*. These two species can be differentiated from other *Cincticostella* species by the following combination of characters in the nymph: 1) caudal filaments length subequal to or slightly shorter than body length, 2) genae developed into obvious extensions, 3) mesothoracic projection with notch, 4) forefemur without transverse row of setae on upper surface, and 5) all articulations of caudal filaments with spines; and by the following combination of characters in the male imago: 1) area between C, Sc and R1 of forewings colored, 2) styliger plate with median convex lobe-like posterior projection, and 3) general shape of penes, especially the form of the apical sclerite on the ventral face.

The new species can be distinguished from *C. fusca* in the male imago stage by its coloration, its mesonotal scutellum morphology, and by the shape of genitalia. In the nymphal stage, the two species can be distinguished by the setation of abdominal terga and the shapes of posterolateral projections of tergum IX. Specifically:

1. Cells of costal and subcostal fields of the forewing of *C. jianchuan* sp. nov. are brown (Figs 7E, 10D, 17A, B), whereas these cells are dark brown in *C. fusca* (Zhang et al. 2020: fig. 4A, B).
2. The mesonotum of *C. jianchuan* sp. nov. clearly has three projections on the posterior margin (Fig. 8A), while *C. fusca* has only two projections apparent (Zhang et al. 2020: fig. 4D).
3. *Cincticostella jianchuan* sp. nov. has two subapical hemispherical grooves on the ventral face of the penes (Fig. 9B, E), but *C. fusca* has two additional large ventral projections on the upper middle of the ventral face of the penes (Zhang et al. 2020: fig. 5C, E).
4. In terms of wing venation, the stem of the MA+Rs fork of *C. jianchuan* sp. nov. occurs at a slightly more distal location than the fork of MP (Fig. 7E). However, in *C. fusca*, the MP fork and the stem of the MA+Rs fork are equidistant from the base of the wings to the margin (Zhang et al. 2020: fig. 6A).
5. The posterolateral projections of abdominal segment IX of the nymph of *C. jianchuan* sp. nov. (Fig. 5A, C, D) are longer than the same posterolateral projections on *C. fusca* (Kang and Yang 1995: fig. 3H).

6. Also on the nymph, each lateral margin of abdominal segments IV–VIII and median area of terga II–X of *C. fusca* nymph has setae (Kang and Yang 1995: fig. 3G). In contrast, the nymph of *C. jianchuan* sp. nov. lacks setae in the corresponding locations (Fig. 5A, B).

**Descriptions.** ***Last instar nymph*** (in alcohol). Last instar nymph: head width, male 3.1–3.3 mm; female 3.4–3.5 mm; body length (excluding tails), male 15.3–16.7 mm, female 18.0–18.9 mm; cerci length, male 8.9–11.6 mm, female 10.5–12.8 mm, middle caudal filament, male 9.3–10.9 mm, female 10.6–11.5 mm. Body color reed green to brown (Fig. 1A–C).

***Head*:** base color reed green to brown, genae expanded into lobes (Fig. 2A); middle portion of antennae with tiny setae on articulations (Fig. 2C), basal (Fig. 2B) and apical (Fig. 2D) portions of antennae without such setae. Labrum width equal to about 1/3 head width, setae on dorsal and ventral surfaces; those on ventral surface and anterolateral margin relatively longer and more densely arranged (Fig. 2E). Mandible: both mandibles with numerous short hair-like setae on dorsal and lateral surfaces; trifurcated outer incisor and bifurcated inner incisor (Fig. 2F, G). Left mandible without seta near mola, prostheca comprised of two tufts of spines with common stem (Fig. 2F). Right mandible with row of irregular hair-like setae under mola, prostheca with one tuft of hair-like setae on common base (Fig. 2G). Hypopharynx (Fig. 2H): lingua recumbent oval, with shallow anteromedian concavity, short setae densely situated on anterolateral margins, apical 1/4 with pale spot; superlinguae with slight curved outer, anterior margin and surface densely covered with long setae. Maxilla (Fig. 2I–K): apex with 2 large canine teeth and slightly curved plate, apical margin of plate crenate (Fig. 2K); tuft of stout setae at apex; galea-lacinia with several setae near base; lateral margins of stipes and cardo with fine setae; three-segmented maxillary palp covered with hair-like setae and sharp setae, segment III very small and short, segment length ratio from base to apex = 5.3: 4.7: 1.0 (Fig. 2I–K). Labium (Fig. 2L): paraglossae semicircular, apical half of dorsum with closely set sharp setae; apical three quarters of venter with loose set of fine setae; glossae long and ellipsoid with setae; labial palp with 3 segments, surfaces of segments I and II with sharp setae; segment II slightly enlarged; segment III very small, segment length ratio from base to apex = 7.2: 5.1: 1.0.

***Thorax*** general color yellowish to reed green. Pronotum with paired small brownish green irregular stripes, anterolateral corners produced anteriorly (Fig. 1A, B); mesonotum with medial pale stripe, paired small brownish green dots and irregular stripes (Fig. 1A, B), lateral margins each with blunt projection near anterolateral corner (Figs 1A, B, 3A). Prosternum with pair of hole-like structures (Fig. 3B, indicated by black arrow). Legs: posterolateral angles of fore and middle coxae each with acute projection (Fig. 1A). Dorsal surface of femur of each leg with setae on median, posterior and anterior areas (Fig. 4A–C), ratio of overall femur width of foreleg: middle-leg: hindleg = 1.0: 1.0: 1.1. Ratio of femur: tibia: tarsus of foreleg = 1.9: 1.8: 1.0, ratio of femur: tibia: tarsus of middle-leg = 2.4: 2.4: 1.0, ratio of femur: tibia: tarsus of hindleg = 2.6: 3.0: 1.0. Claws pale, apices dark brown, with 4–5 blunt denticles medially (Fig. 4D, E).

***Abdomen*:** abdominal segments II–IX each with posterolateral projection with clavate setae; largest posterolateral projection on segment VIII, long and divergent posterolateral projections on segment IX (Fig. 5A). Posterior margins of segments II–IX each with pair of sharp tubercles, progressively longer

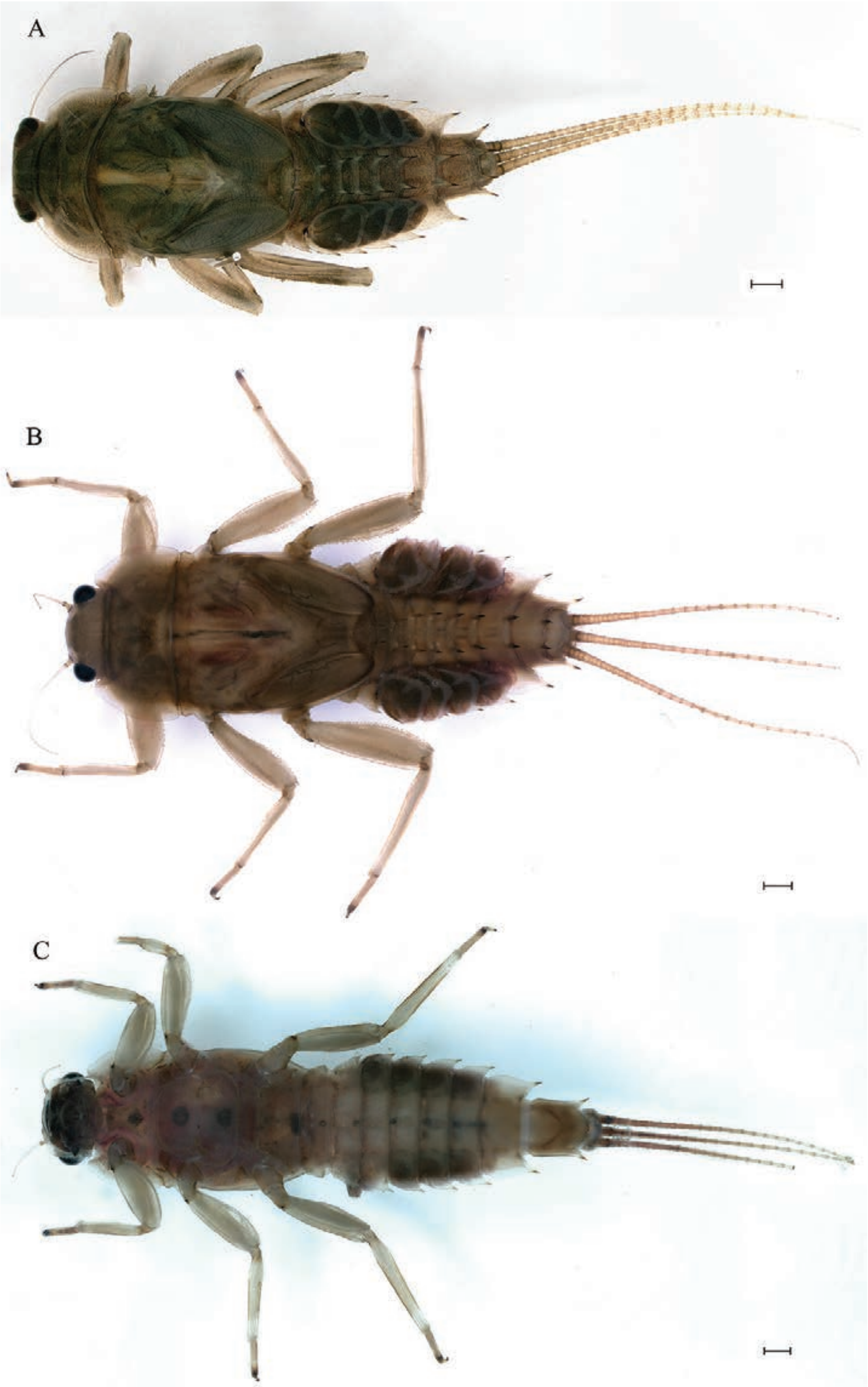

**Figure 1.** Last nymphal instar of *Cincticostella jianchuan* sp. nov. **A** dorsal habitus of male **B** dorsal habitus of female **C** ventral habitus of male. Scale bar: 1000 μm (**A, B**).

on segments II–VIII (Fig. 5A). Each tergum without setae on posterior margin and dorsal area (Fig. 5A, B), but posterior margin of tergum I with long fine setae. Posterior margin of sternum IX of male wavy (Fig. 5C); posterior margin of sternum IX of female concave (Fig. 5D). Gills III–V subequal in size, dorsal lamellae oblique oval, ventral lamellae each with deep cleft (Fig. 6A–C); gill VI dorsal lamella rounded, ventral lamella without deep cleft (Fig. 6D); gill VII

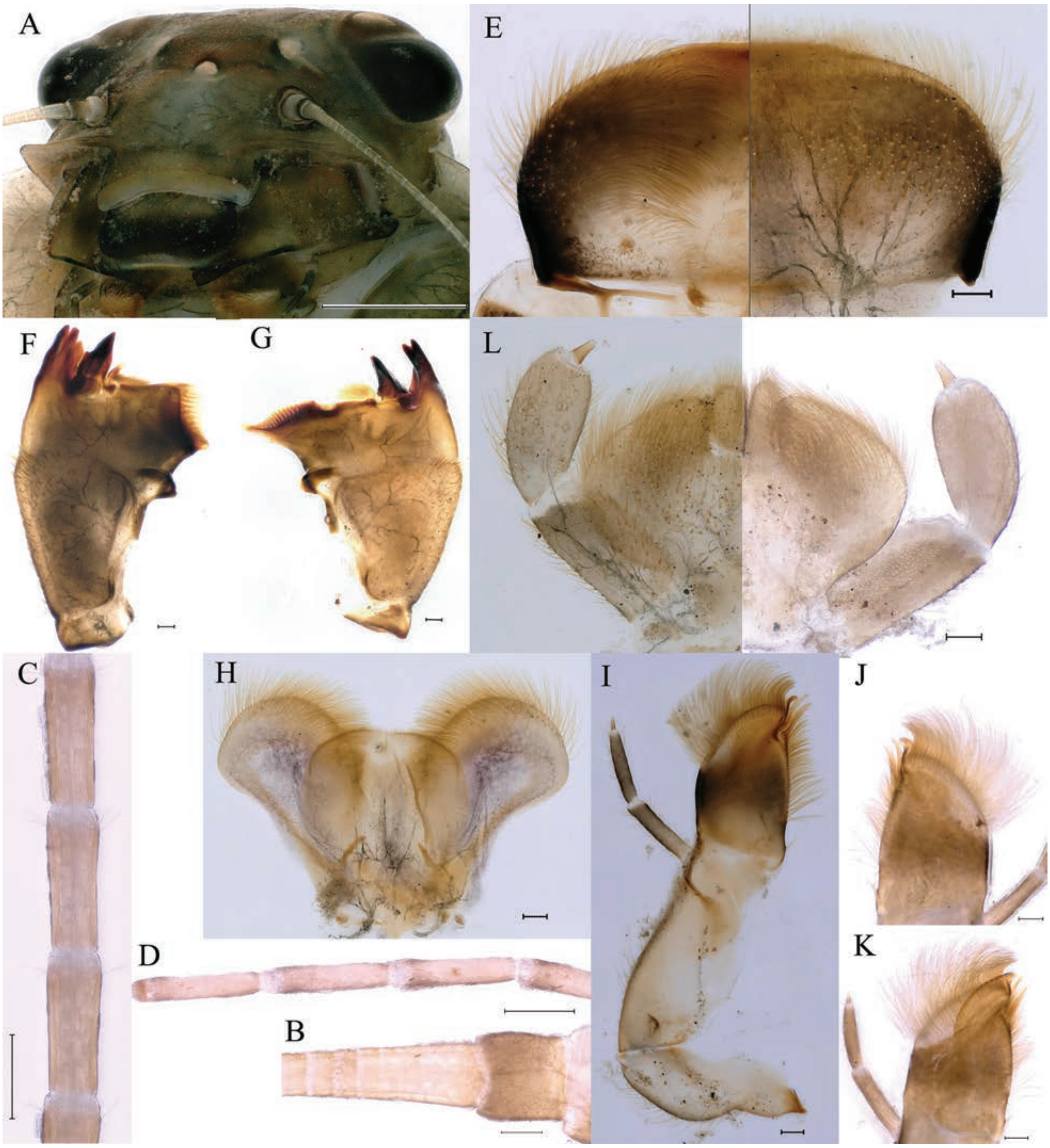

**Figure 2.** Nymphs of *Cincticostella jianchuan* sp. nov. **A** head **B** basal part of antenna **C** middle part of antenna **E** apical part of antenna **E** labrum **F** left mandible **G** right mandible **H** hypopharynx (ventral view) **I** left maxilla **J** apex of right maxilla (dorsal view) **K** apex of right maxilla (ventral view) **L** labium (ventral view). Scale bar: 1000 μm (**A**); 100 μm (**B–K**).

small, somewhat heart-shaped but rounded (Fig. 6E). Distal part of caudal filaments darkly colored, each segment with whorled acute setae at apex and few sharp setae near middle area, median segments with long fine setae on lateral margins loosely arranged (Fig. 6F).

***Male imago*** (in ethanol). Body length 18.3–18.8 mm (excluding tails), head width 3.1–3.3 mm, forewing length 19.4–20.0 mm, hindwing length 5.4–5.9 mm, cerci length 8.9–11.6 mm, middle caudal filament 9.3–10.9 mm. Body color brown to dark brown (Figs 7A–C, 17A).

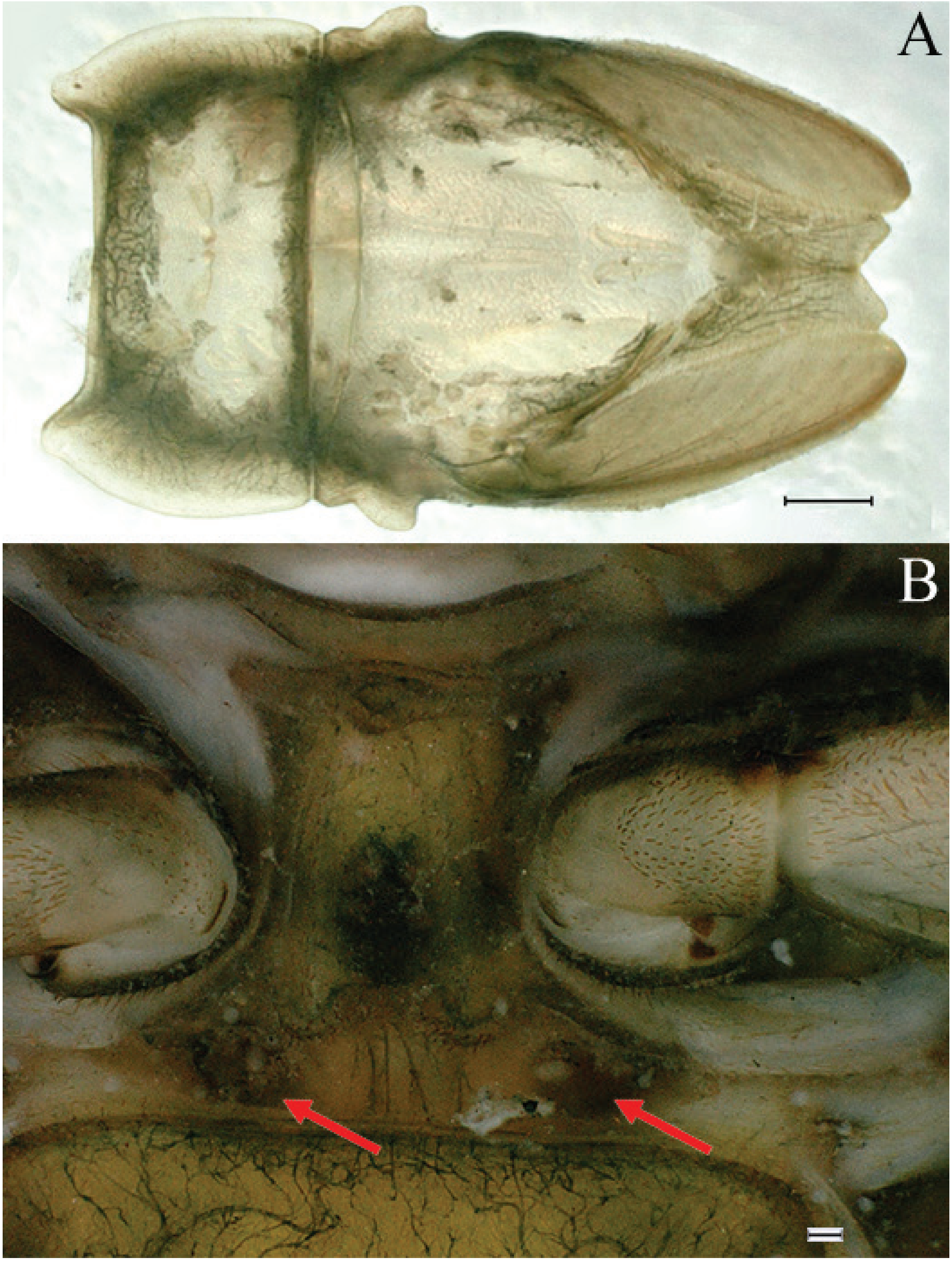

**Figure 3.** Nymphs of *Cincticostella jianchuan* sp. nov. **A** thorax of last nymphal instar (dorsal view) **B** ventral view of pronotum with hole-like structures. Scale bar: 1000 μm (**A**); 500 μm (**B**).

***Head*.** Compound eyes contiguous, upper portion brown and lower portion black (Fig. 7B, D).

***Thorax*.** Pronotum with expanded posterolateral air sac-like structure (Fig. 7A–D, indicated by red arrow). Mesonotum with three projections on posterior margin, middle projection short (Fig. 8A, indicated by red arrow). Forewings generally hyaline, veins brown; all cells of costal and subcostal fields tinted with brown, 2/3 cells from base to margin of subcostal and radial fields

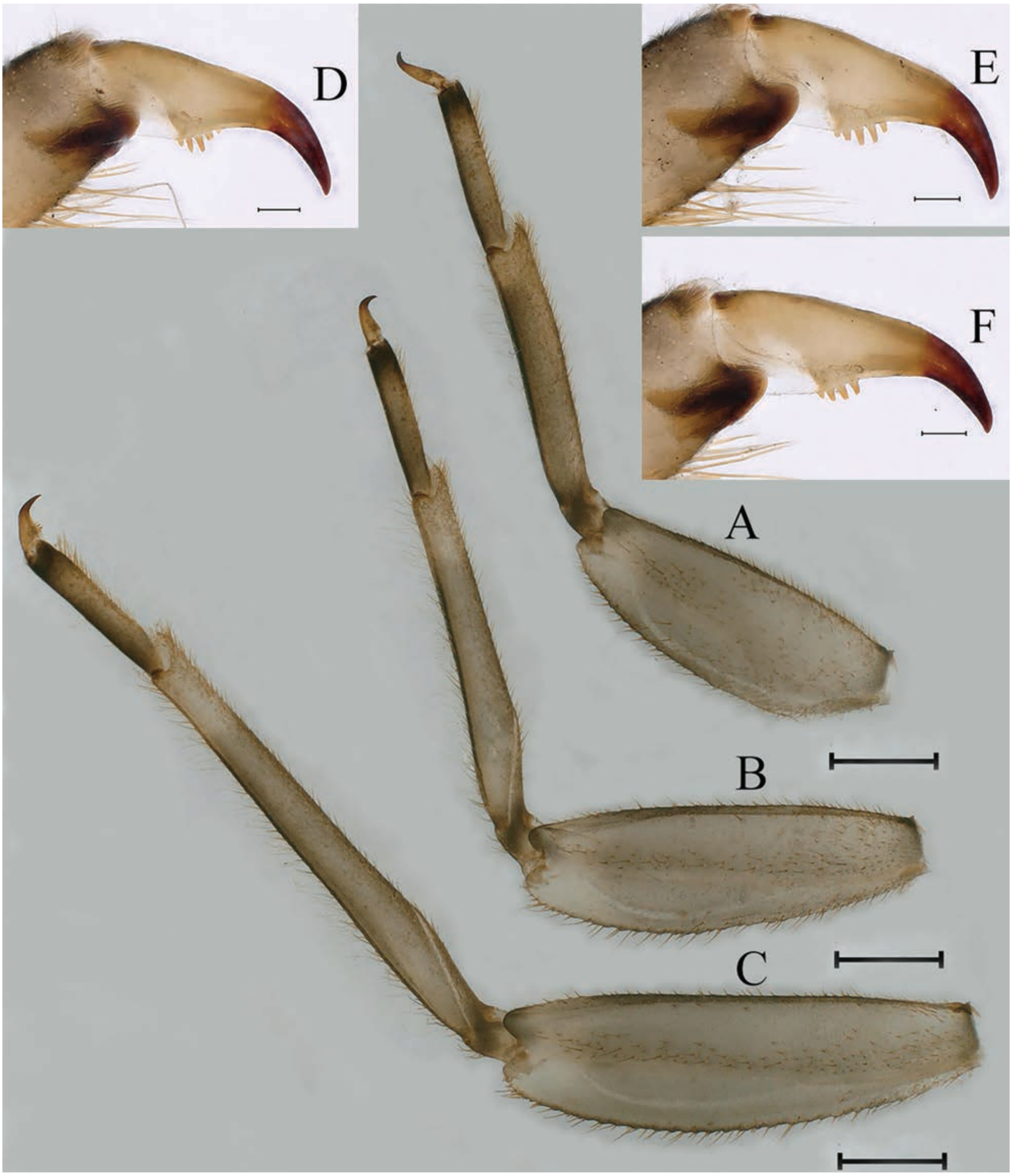

**Figure 4.** Nymphs of *Cincticostella jianchuan* sp. nov. **A** foreleg **B** midleg **C** hindleg **D** claw of foreleg **E** claw of midleg **F** claw of hindleg. Scale bar: 1000 μm (**A–C**); 100 μm (**D–F**).

tinted with brown; cross veins in stigmatic area slightly oblique, and those between costal and subcostal areas separated into two rows of cells. MA forked 2/3 of distance from base to margin; stem of MA+Rs fork at very base, just slightly more distal than fork of MP (Fig. 7E). Hindwing totally hyaline, leading margin slightly concave; MA single, MP forked symmetrically (Fig. 7F). Forelegs brown to dark brown (Fig. 8B), mid- and hindlegs brown (Fig. 8C, D).

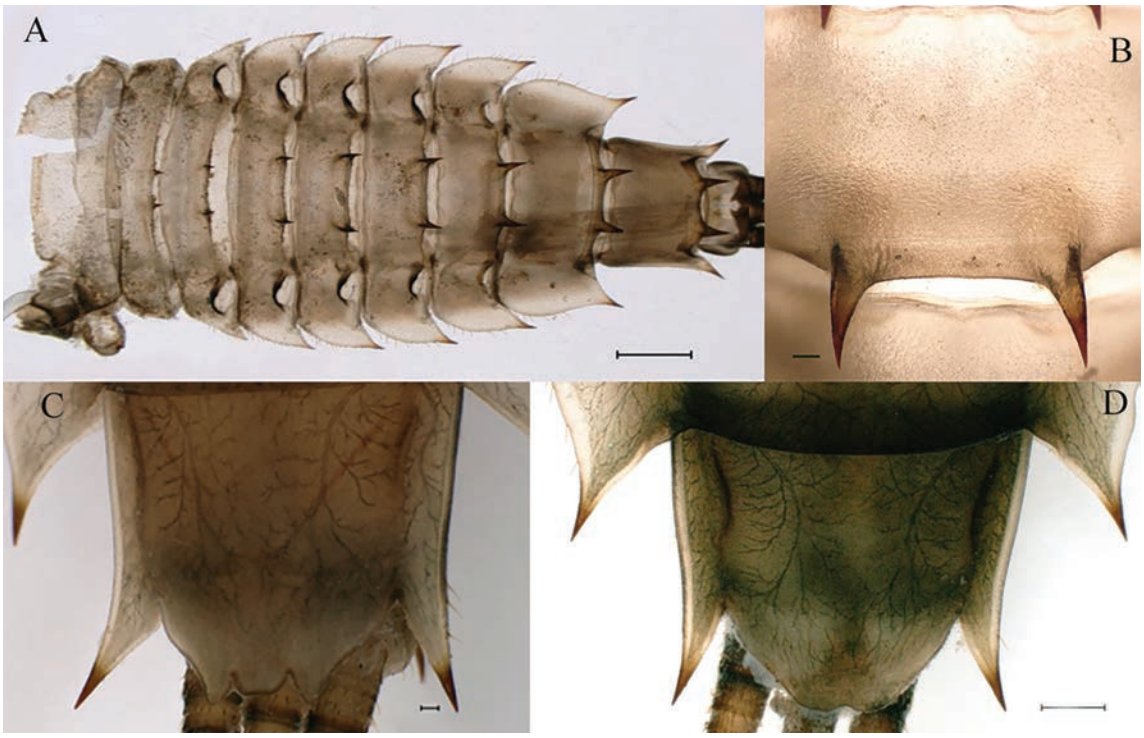

**Figure 5.** Nymphs of *Cincticostella jianchuan* sp. nov. **A** abdomen (dorsal view) **B** abdominal terga VII enlarged **C** posterior part of abdomen of male (ventral view) **D** posterior part of abdomen of female (ventral view). Scale bar: 1000 μm (**A**); 500 μm (**D**); 100 μm (**B, C**).

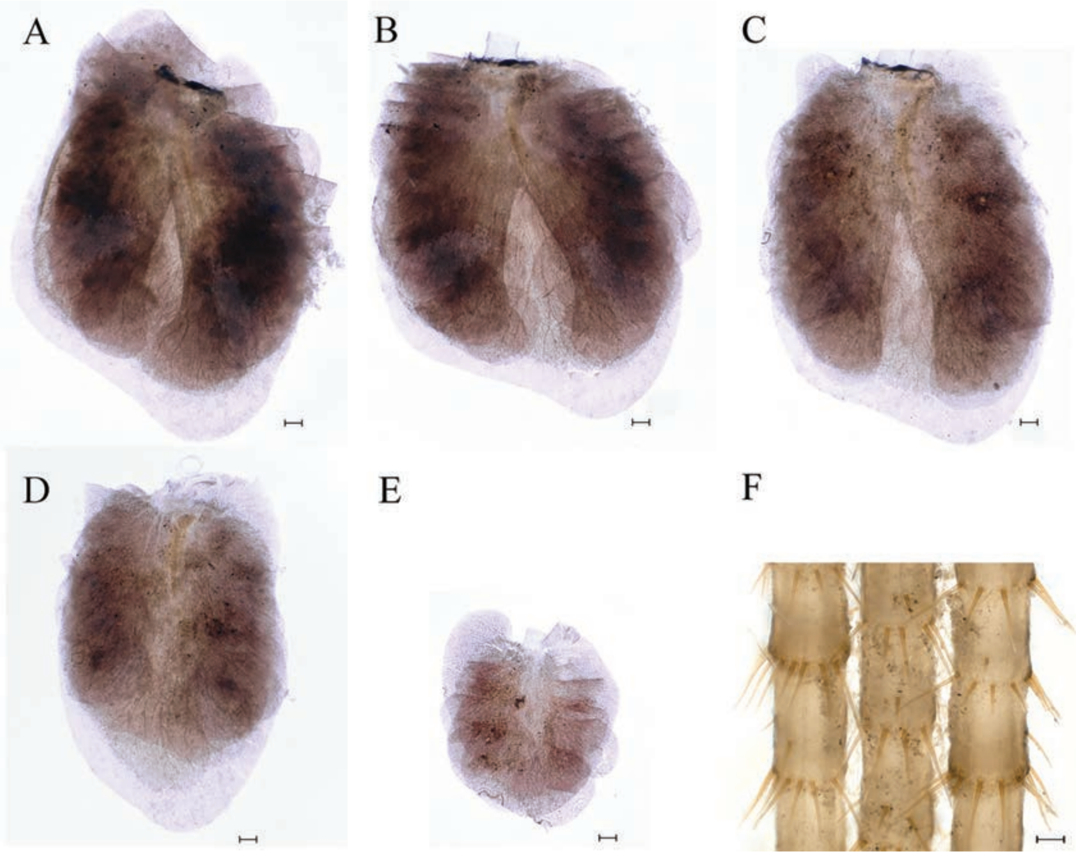

**Figure 6.** Nymphs of *Cincticostella jianchuan* sp. nov. **A** gill III **B** gill IV **C** gill V **D** gill VI **E** gill VII **F** caudal filaments. Scale bar: 100 μm (**A–F**).

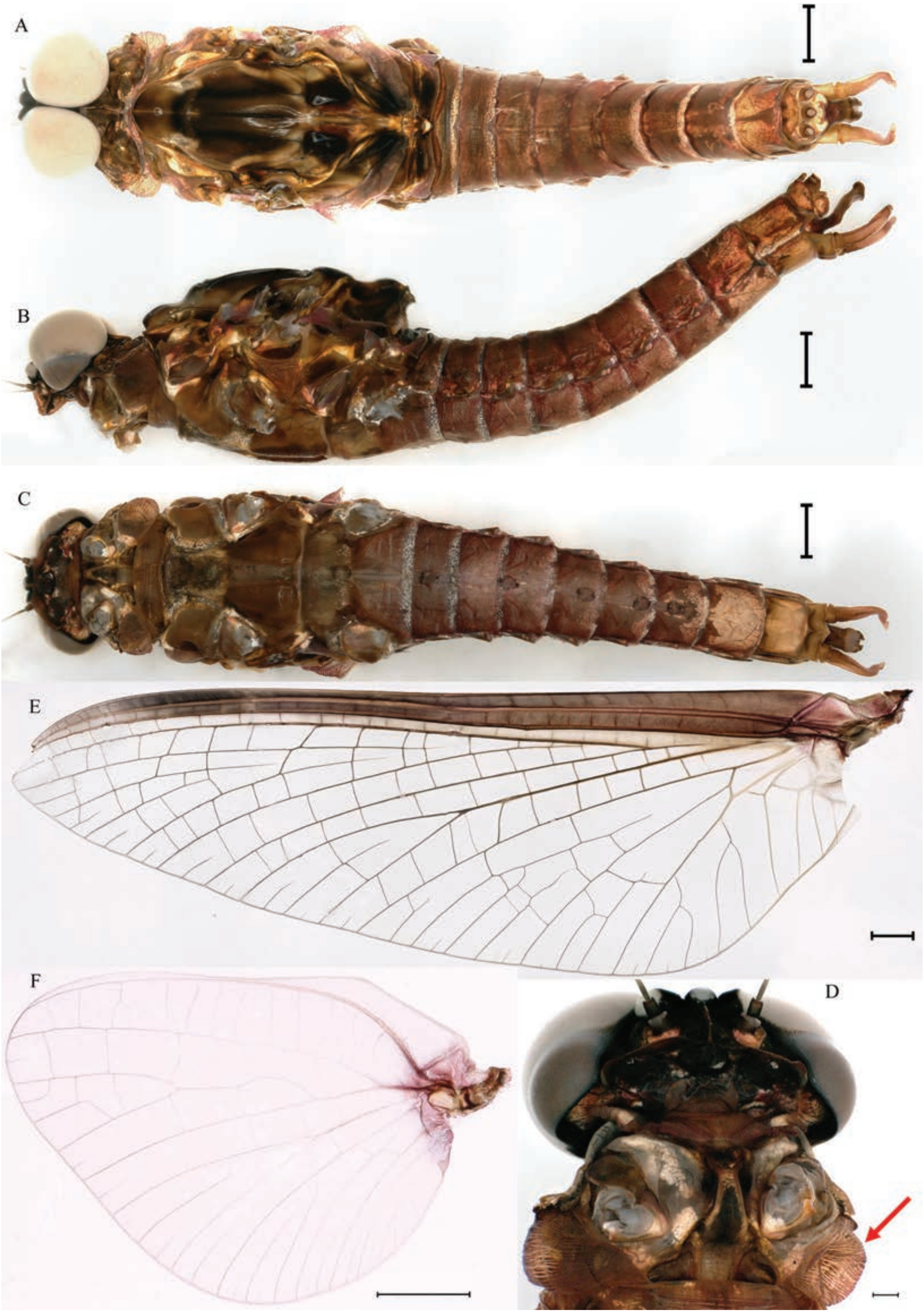

**Figure 7.** Male imago of *Cincticostella jianchuan* sp. nov. **A** dorsal view of body **B** lateral view of body **C** ventral view of body **D** ventral view of head and pronotum, with air sac-like structure indicated by red arrow **E** forewing **F** hindwing. Scale bar: 1000 µm (**A–F**).

Femur: tibia: tarsus of foreleg = 1.0: 1.3: 1.6, tarsal segments from basal to apical = 1.0: 5.4: 5.0: 3.5: 1.8; femur: tibia: tarsus of midleg = 2.2: 2.3: 1.0, tarsal segments arranged in decreasing order = 1.0: 1.4: 1.3: 1.0: 2.5; femur: tibia: tarsus of hindleg = 2.6: 3.0: 1.0, tarsal segments arranged in decreasing order = 1.0: 1.3: 1.5: 1.1: 2.9. Claws of all legs similar, one blunt and one hooked.

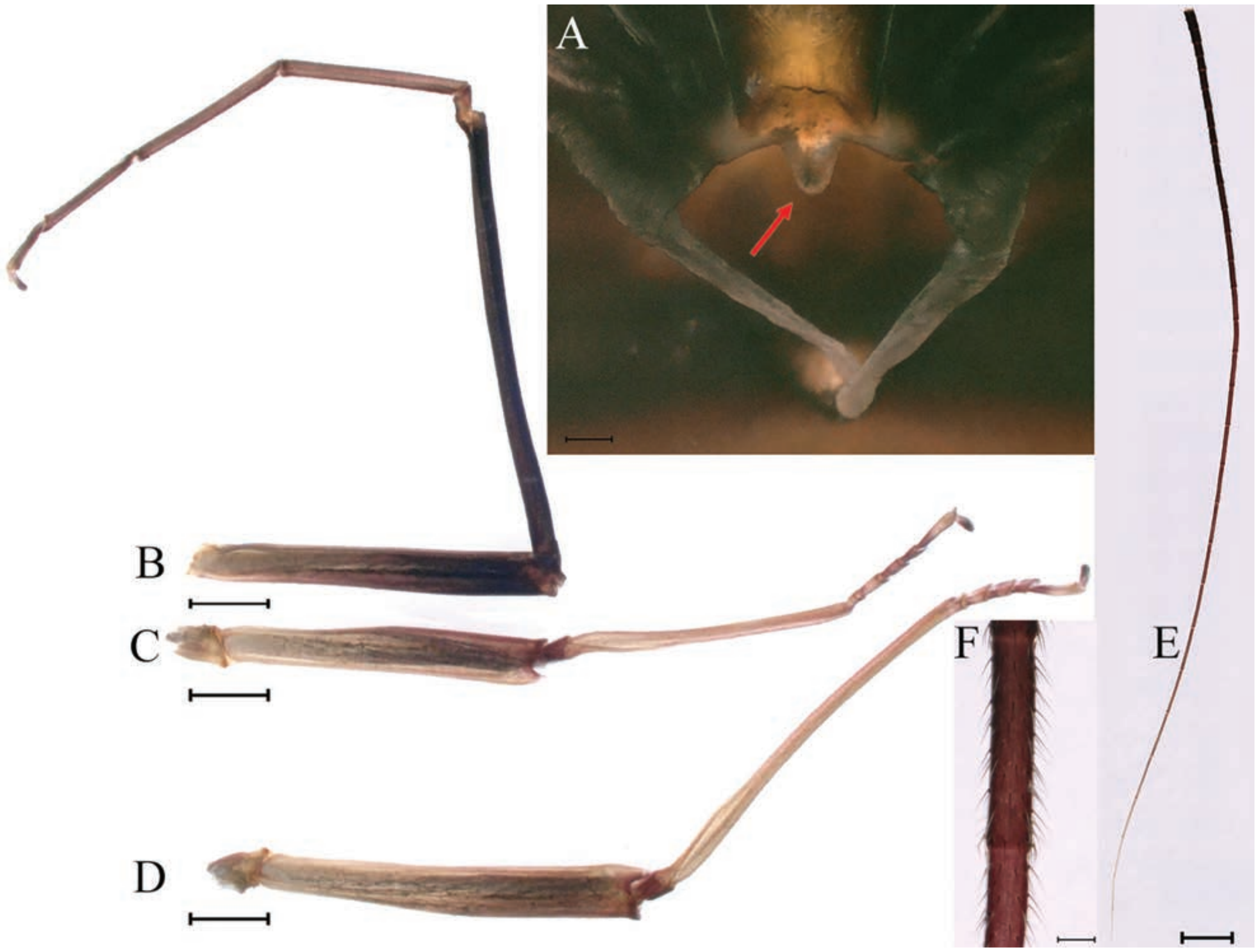

**Figure 8.** Male imago of *Cincticostella jianchuan* sp. nov. **A** lateral scutellar projections, middle one indicated by red arrow **B** foreleg **C** midleg **D** hindleg **E** cerci **F** cerci enlarged. Scale bar: 100 μm (**A, F**); 1000 μm (**B–E**).

***Abdomen*.** Terga II–V each with pale stripe on posterior margin, pair of diffuse dark dots near posterior margins of terga II–IX; diffuse dark stripes on middle and lateral faces of terga VIII–IX (Fig. 7A, B). Dark ganglionic marks on sterna I–VII (Fig. 7C). Small portion of sternum VII and most of sterna VIII–IX light colored (Fig. 7C). Styliger plate with middle projection (Fig. 7C). Caudal filaments brown to dark brown, with spines (Fig. 8E, F).

***Genitalia*.** Forceps covered with stout setae; segment 3 globular; segment 2 angled inward distally and with slight subapical constriction (Fig. 9A–C). Penis lobes compact, with linear groove on apical 1/2 of dorsal face (Fig. 9A, D), apical sclerite (Fig. 9C, F), two subapical hemispherical grooves (Fig. 9B, E, indicated by red arrows), one basal obvious bump (Fig. 9B, E), one subapical large pale plate on ventral face (Fig. 9C, F), lobes separated by slight cleft (Fig. 9C, F).

***Female imago*** (in ethanol). Color pattern similar to male (Figs 10A–F, 11 A–C, 17B); body length 19.1–22.9 mm (excluding tails), head width 2.9–3.5 mm, cerci length 17.6–23.7 mm, middle caudal filament 17.3–22.1 mm, forewing 19.9–23.4 mm, hindwing 5.5–6.1 mm. Lengths of femur: tibia: tarsus of foreleg = 1.9: 1.6: 1.0, tarsal segments from basal to apical = 1.0: 2.0: 1.7: 1.1: 2.3; femur: tibia: tarsus of midleg = 2.4: 2.4: 1.0, tarsal segments from basal to apical = 1.0: 1.2: 1.2: 1.1: 3.2; femur: tibia: tarsus of hindleg = 2.7: 3.1: 1.0, tarsal segments from basal to apical = 1.0: 1.1: 1.4: 1.0: 2.7. Compared with male, pronotum

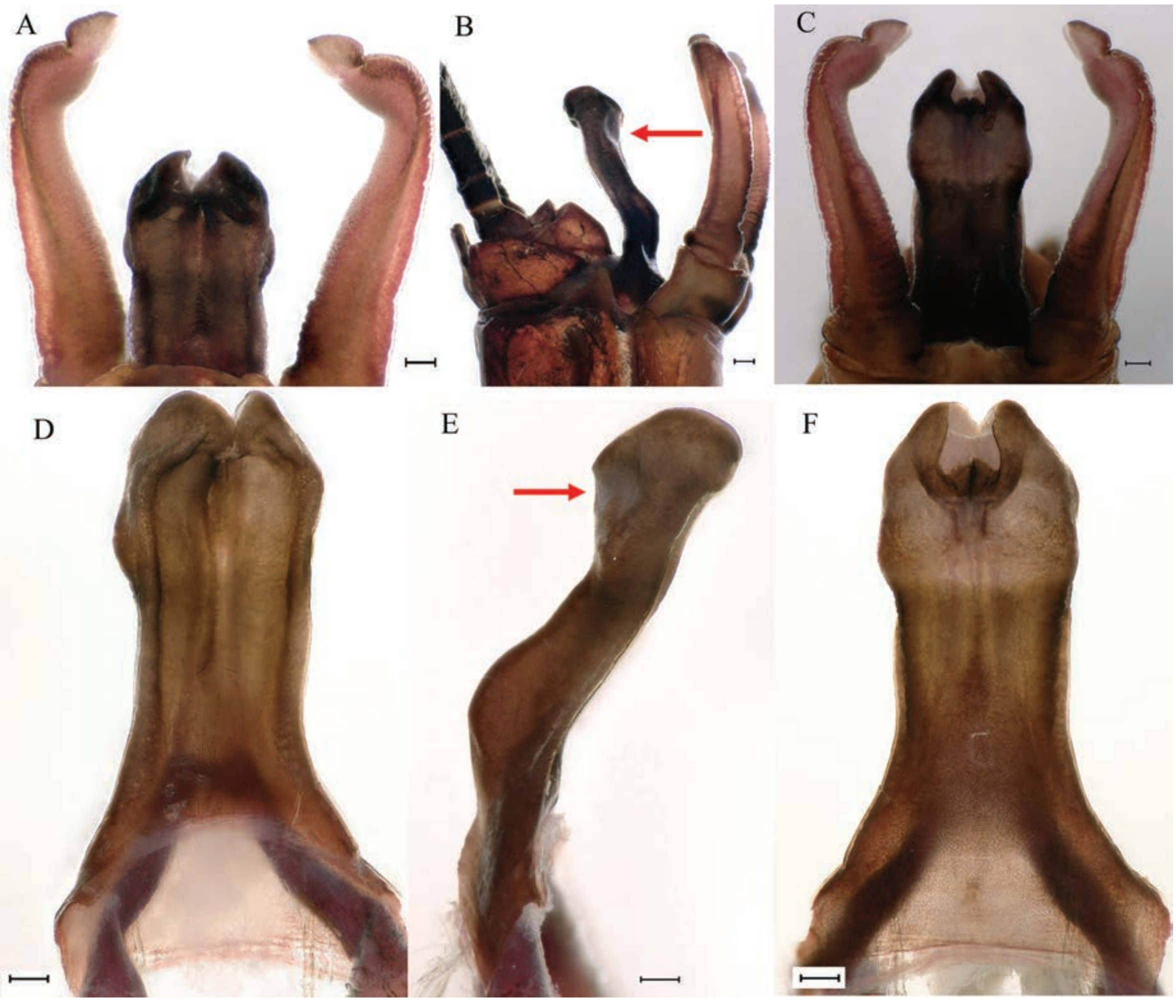

**Figure 9.** Male imago of *Cincticostella jianchuan* sp. nov. **A** genitalia (dorsal view) **B** genitalia (lateral view) with groove indicated by arrow **C** genitalia (ventral view) **D** penes (dorsal view) **E** penes (lateral view), with position of groove indicated by arrow **F** penes (ventral view). Scale bar: 100 μm (**A–F**).

with nonexpanded posterolateral air sac-like structures; inner margin of femur of foreleg covered with spines. Posterior margin of subgenital plate produced to 1/5 length of sternum VIII. Posterior margin of subanal plate with obvious median cleft (Fig. 10F). Color pattern of caudal filaments similar to male.

***Male subimago.*** Body color taupe gray to dark brown (Figs 12A–C, 17B). Front portions of forewing and hindwing taupe gray and rear portions nearly white (Fig. 13A, B). Pronotum with nonexpanded posterolateral air sac-like structures; scutellum with three long, pointed posterior prolongations (Fig. 12A, B). Caudal filaments with relative densely spines (Fig. 14E). Apical sclerite of penes incomplete (Fig. 13C). Body length 13.0–14.5 mm (excluding tails), head width 2.6–3.0 mm, cerci length 8.0–16.5 mm, middle caudal filament 8.5–16.4 mm, forewing 19.4–19.8 mm, hindwing 4.6–5.1 mm (Fig. 12A–C, 13A–C, 14A–E). Margins of femur and tibia of foreleg, midleg and hindleg all densely covered with spines (Fig. 14A–D). Length of femur: tibia: tarsus of foreleg = 1.3: 1.4: 1.0, tarsal segments from basal to apical = 1.0: 2.7: 2.5: 1.8: 2.2; femur: tibia: tarsus of midleg = 2.4: 2.3: 1.0, tarsal segments from basal to apical = 1.2: 1.7: 1.3: 1.0: 2.9; femur: tibia: tarsus of hindleg = 3.1: 3.6: 1.0, tarsal segments from basal to apical = 1.0: 3.0: 3.0: 2.0: 6.2.

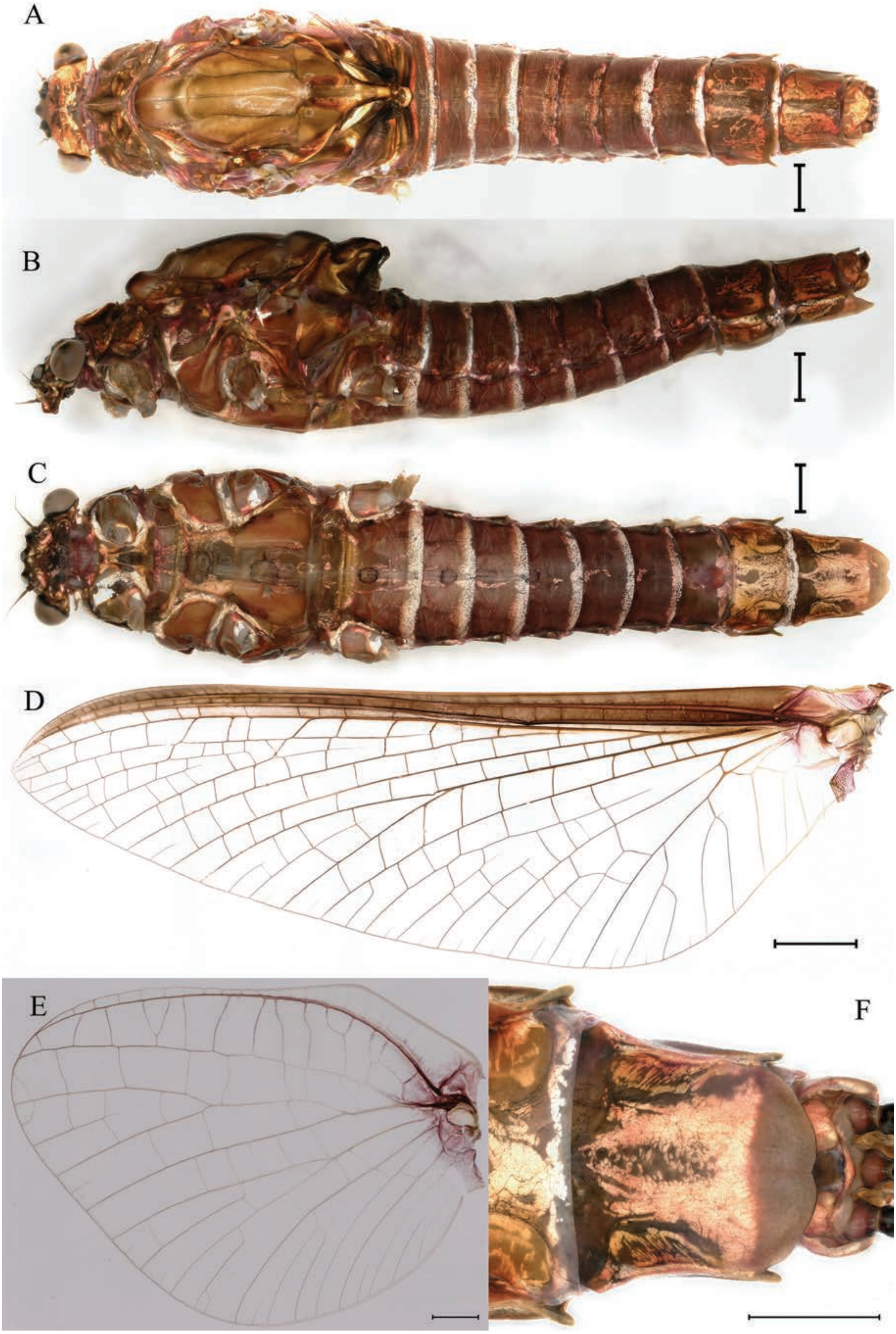

**Figure 10.** Female imago of *Cincticostella jianchuan* sp. nov. **A** dorsal view **B** lateral view **C** ventral view **D** forewing **E** hindwing **F** posterior part of abdomen (ventral view). Scale bar: 2000 μm (**D**); 1000 μm (**A–C, F**); 500 μm (**E**).

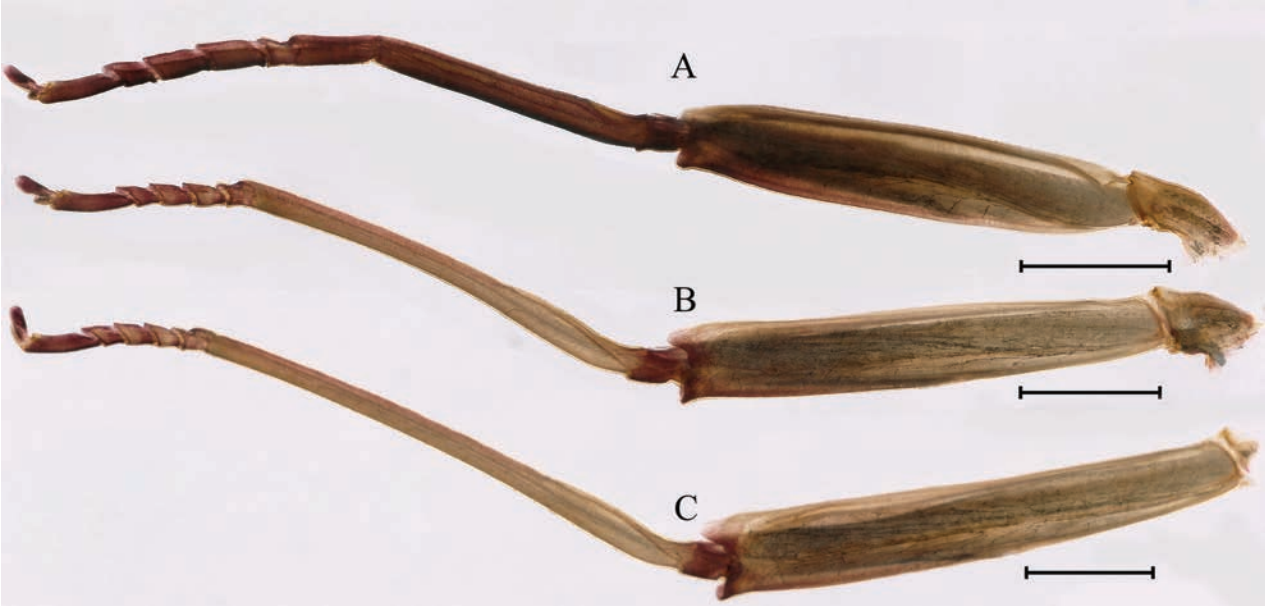

**Figure 11.** Female imago of *Cincticostella jianchuan* sp. nov. **A** foreleg **B** midleg **C** hindleg. Scale bar: 1000 µm (**A–C**).

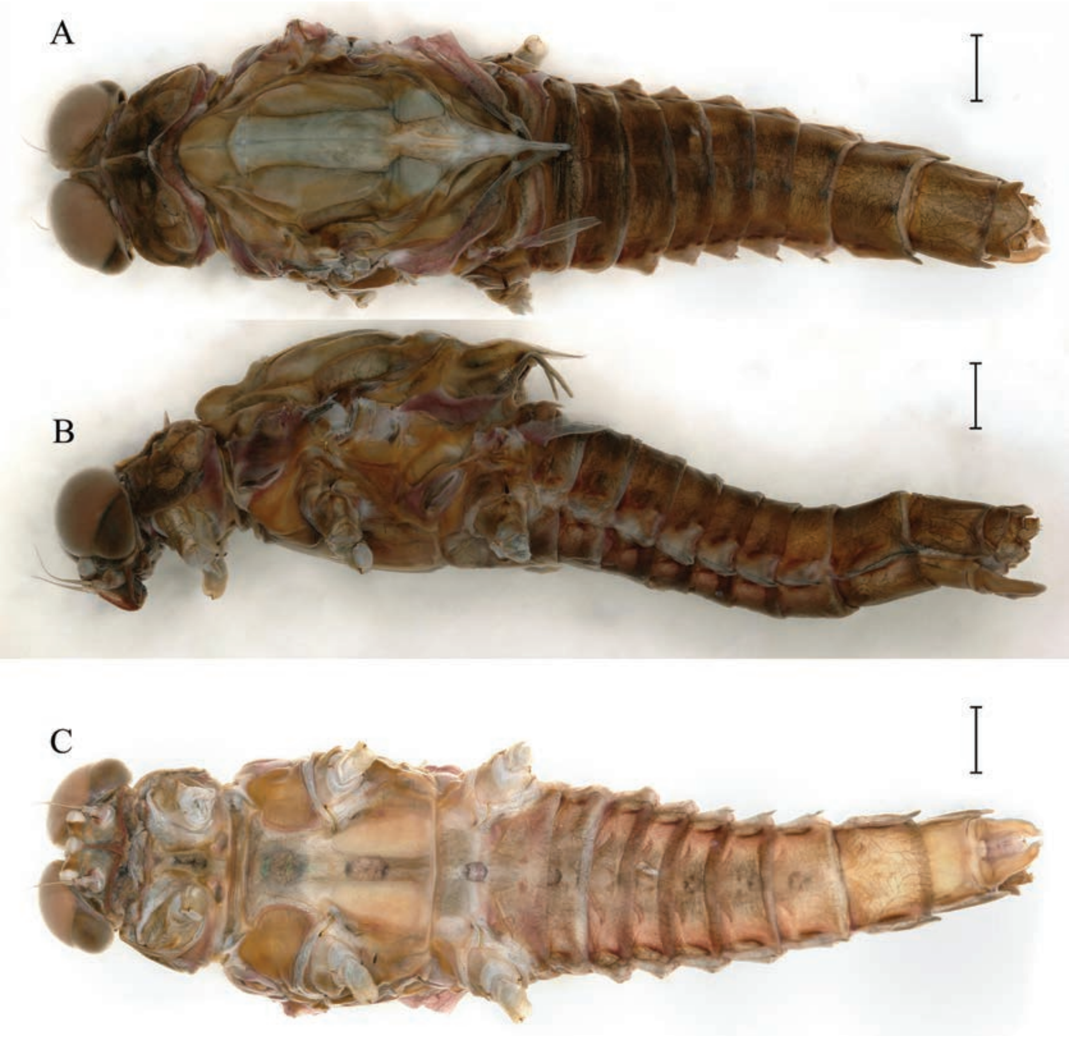

**Figure 12.** Male subimago of *Cincticostella jianchuan* sp. nov. **A** dorsal view **B** lateral view **C** ventral view. Scale bar: 1000 µm (**A–C**).

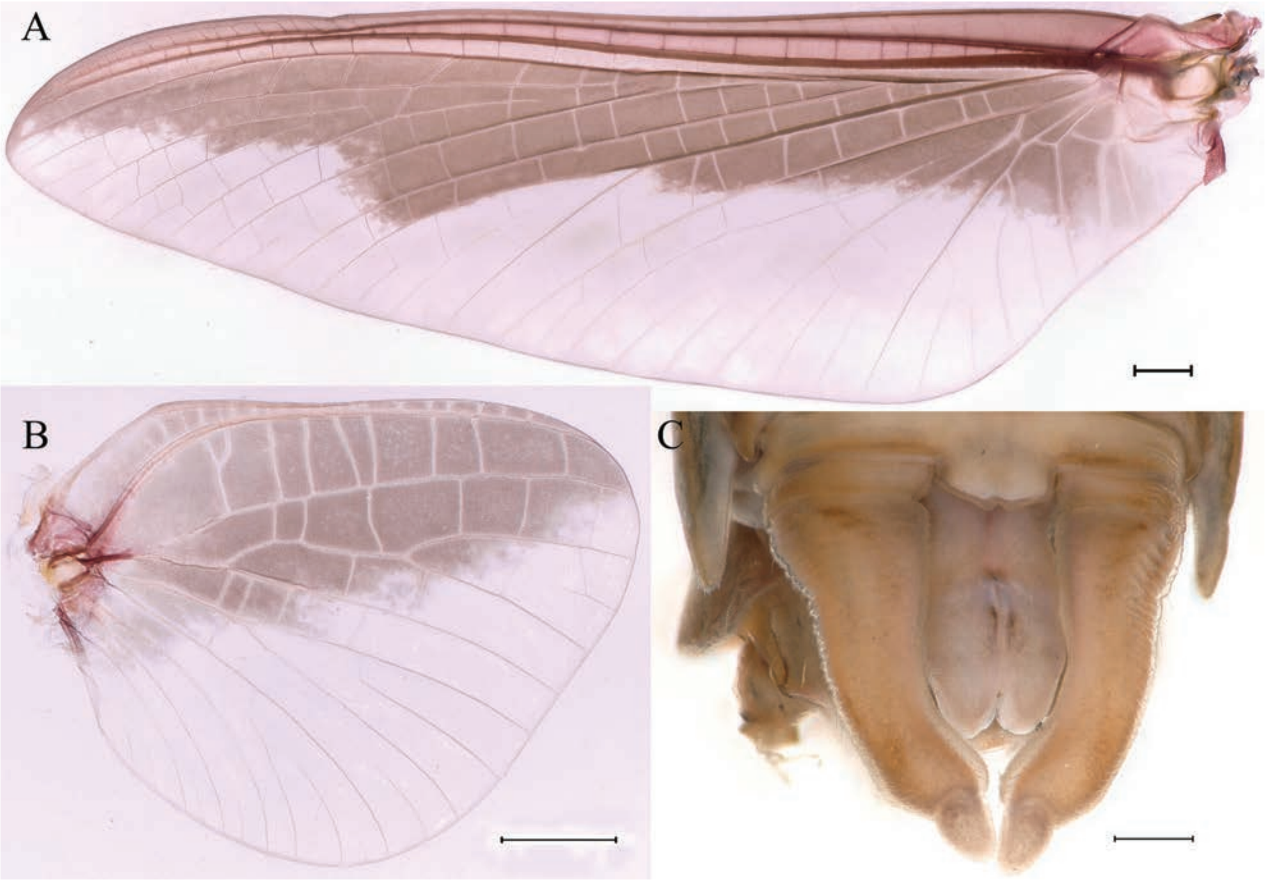

**Figure 13.** Male subimago of *Cincticostella jianchuan* sp. nov. **A** forewing **B** hindwing **C** ventral view of genitalia. Scale bar: 1000 µm (**A, B**); 200 µm (**C**).

***Female subimago*** (in alcohol). Similar to male subimago except for usual sexual differences (Figs 15A–C, 16A–E, 17C). Length of femur: tibia: tarsus of foreleg = 1.7: 1.6: 1.0, tarsal segments from basal to apical = 1.0: 1.7: 1.4: 1.0: 2.1; femur: tibia: tarsus of midleg = 2.4: 2.5: 1.0, tarsal segments from basal to apical = 1.0: 1.3: 1.3: 1.2: 2.8; femur: tibia: tarsus of hindleg = 3.1: 3.6: 1.0, tarsal segments from basal to apical = 1.0: 1.7: 1.4: 1.3: 3.2. Inner margins of tarsus of foreleg, midleg and hindleg densely covered with spines (Fig. 8D–F, J). Head width 2.9–3.6 mm, body length 17.5–19.7 mm (excluding tails), forewing length 18.6–22.2 mm, hindwing length 3.8–5.7 mm, cerci length 12.2–13.8 mm, middle caudal filament 13.0–13.8 mm.

***Eggs*:** dissected from female imago. Length 142–207 µm, width 96–120 µm. Ovoid with polar cap composed of dense filaments, each filament with intumescent terminal (Fig. 18A, B). Chorion with irregular polygonal ridges except subpolar areas (Fig. 18A–D); mesh with variety of tubercles medially; knobs of attachment structure and micropyle distributed near equator (Fig. 18A, C).

**Persistent mouthparts of winged stages.** The new species presents persistent but vestigial mouthparts in the winged stages; in ventral view of head, the labium is present and clearly visible (Fig. 19A–D, indicated by red arrow).

**Etymology.** The specific epithet is named after the type locality, Jianchuan County, Dali Bai Autonomous Prefecture, Yunnan Province, China. The English common name of this species is the Jianchuan spiny crawler mayfly. The Chinese name is 剑川带肋蜉.

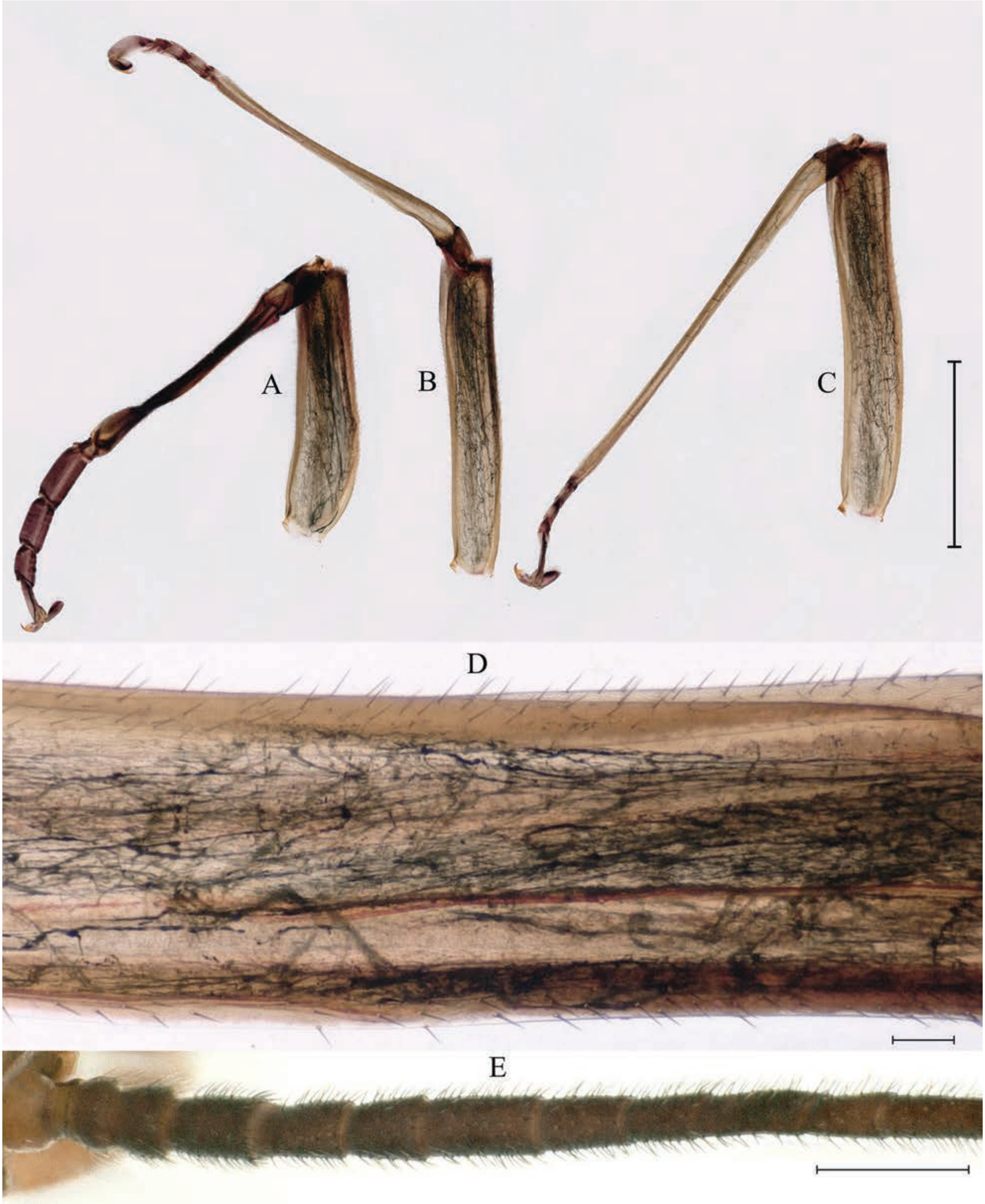

**Figure 14.** Male subimago of *Cincticostella jianchuan* sp. nov. **A** foreleg **B** midleg **C** hindleg **D** closer view of femur of midleg **E** cerci. Scale bar: 2000 μm (**A–C**); 500 μm (**E**); 100 μm (**D**).

**Distribution.** Yunnan, China.

**Ecology.** The nymphs of this new species were collected from upstream reaches of the Jinlong River in Jinchuan County, Dali Bai Autonomous Prefecture, Yunnan Province. The nymphs prefer run and riffle habitats containing

**Figure 15.** Female subimago of *Cincticostella jianchuan* sp. nov. **A** dorsal view **B** lateral view **C** ventral view. Scale bar: 1000 µm (**A–C**).

stones of various sizes (Fig. 20A, B). Sampling sites were located at high altitudes (above 2300 m); the river and associated riparian zone passed through relatively natural habitat or traditional agriculture; width of the river was 3.0–9.7 m, but can reach 15 m during the flood season (Fig. 20A); the water quality tended to be alkaline (pH = 9.04). In the laboratory, the mature nymphs quickly completed the molting process on the water surface from 9 pm to 12 pm at night. The subimago stage persisted until the third noon or afternoon, with the observed lifespan of imagoes being about 3–4 days.

## Discussion

As discussed to some extent in the diagnosis section, *C. jianchuan* sp. nov. is closely related to *C. fusca*, whose nymph and imago share the following characters. In the nymph: 1) larger body size; 2) a pair of hole-like structures on the prosternum (Fig. 3B); 3) mesothorax with medially notched anterolateral projections (Fig. 3A; Kang and Yang 1995: fig. 3B; Zhang et al. 2020: fig. 1C); 4) forefemur without a transverse band of setae on the upper surface (Fig. 4A; Kang and Yang 1995: fig. 3D; Zhang et al. 2020: fig. 3A); and 5) without serration

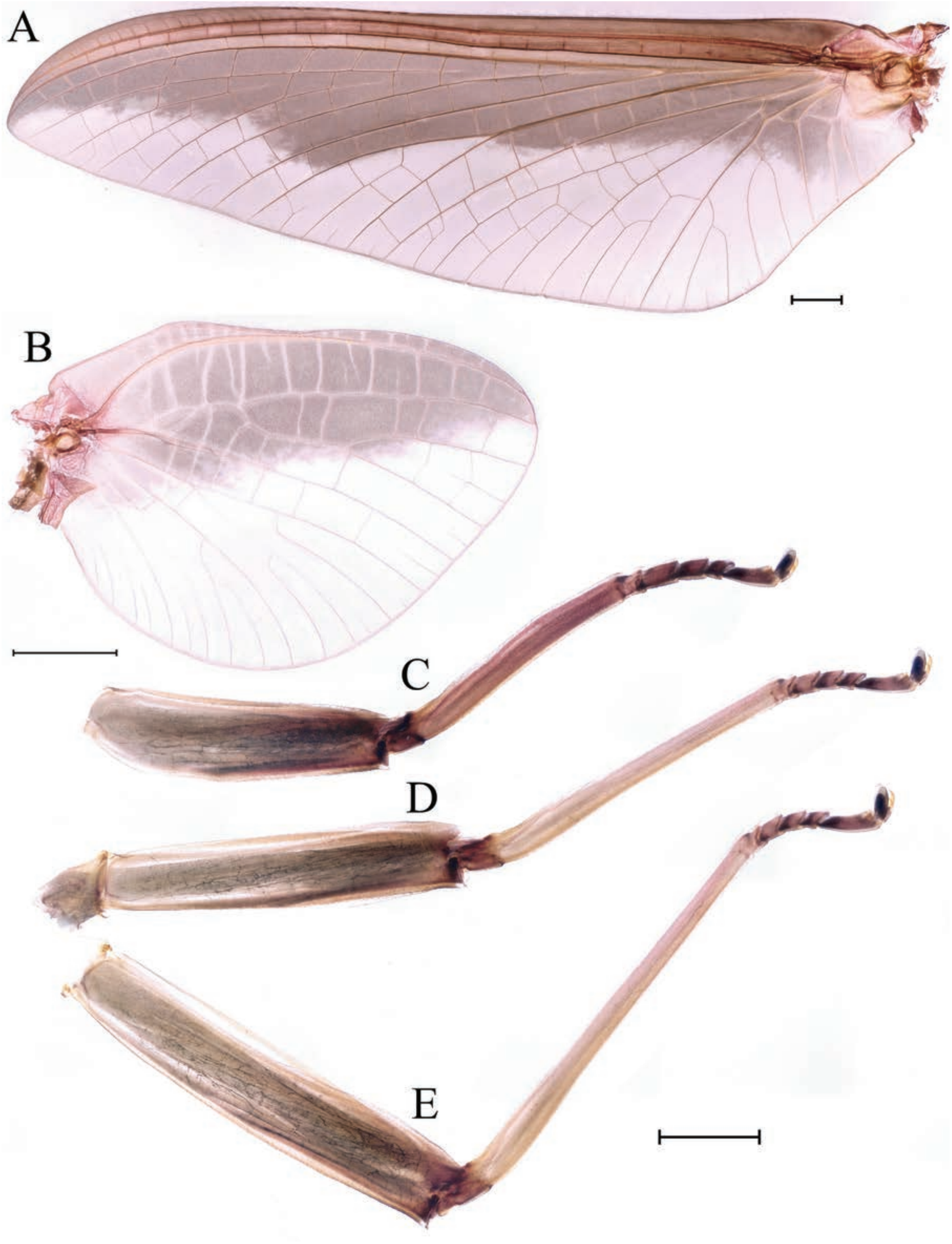

**Figure 16.** Female subimago of *Cincticostella jianchuan* sp. nov. **A** forewing **B** hindwing **C** foreleg **D** midleg **E** hindleg. Scale bar: 1000 μm (**A–E**).

of margins of middle femora (Fig. 4B; Zhang et al. 2020: fig. 3B) and hind femora (Fig. 4C; Zhang et al. 2020: fig. 3C). In the male imago: 1) larger body size; 2) area between C, Sc and R1 distinctly pigmented (Fig. 7E, 10D, 17A, B; Zhang et al. 2020: fig. 4A, B, 5A, 6A); and 3) with apical sclerite on ventral face of the penes (Fig. 9C, F; Zhang et al. 2020: fig. 5C, E, 6C, D).

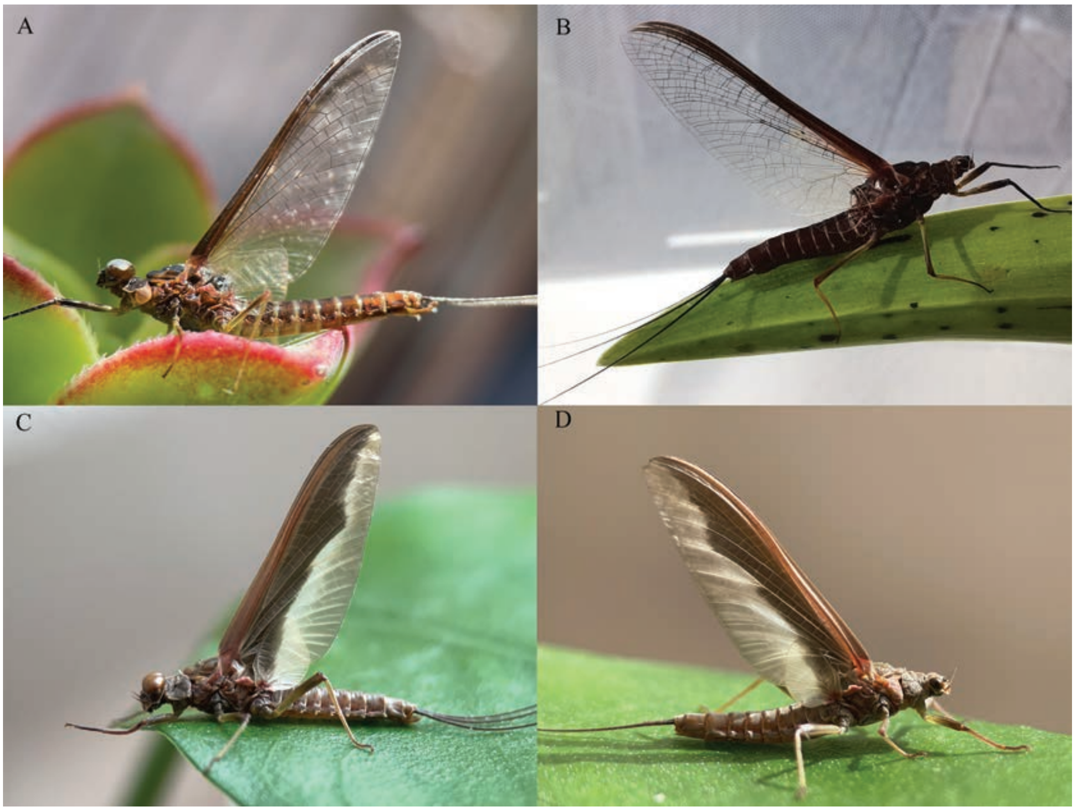

**Figure 17.** Winged stages of *Cincticostella jianchuan* sp. nov. (living) **A** male imago **B** female imago **C** male subimago **D** female subimago.

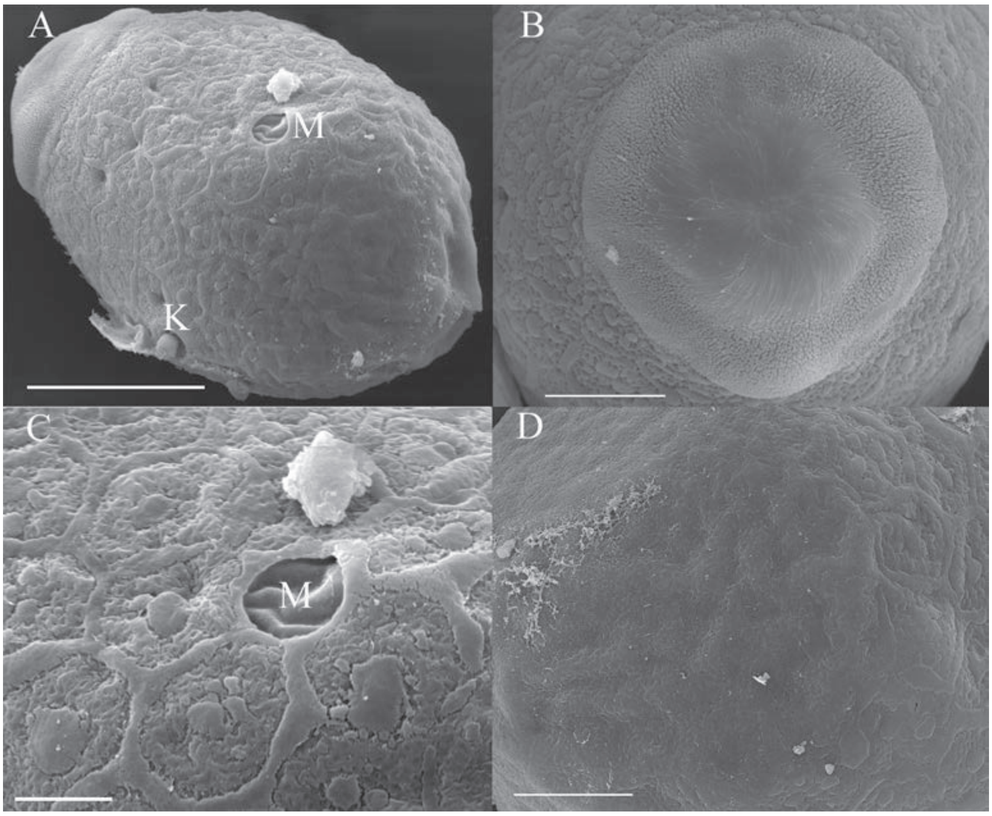

**Figure 18.** Egg of *Cincticostella jianchuan* sp. nov. **A** lateral view with micropyle (M) and knob of attachment structure (K) **B** polar cap **C** micropyle (M) enlarged **D** bottom view. Scale bar: 50 μm (**A**); 20 μm (**B–D**); 10 μm (**C**).

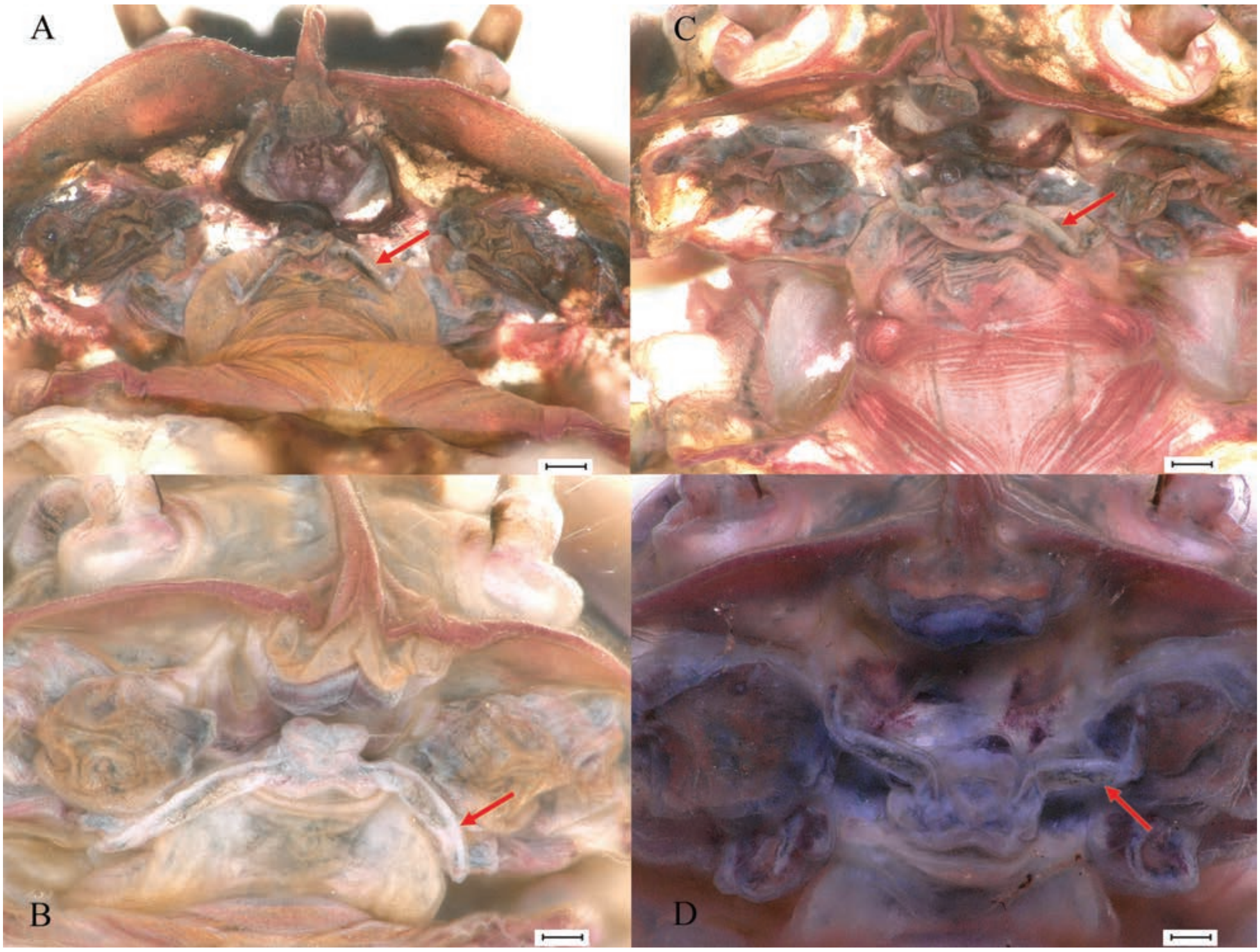

**Figure 19.** Persistent mouthparts of *Cincticostella jianchuan* sp. nov. Labium indicated by arrow. **A** male imago **B** female imago **C** male subimago **D** female subimago. Scale bars: 100 µm (**A–D**).

*Cincticostella jianchuan* sp. nov. and *C. fusca* differ from all other described *Cincticostella* species in these combinations of characters, which offer support for the recognition of a new species complex, the *jianchuan* complex. Although representatives of the *jianchuan* complex fit into the *nigra*-group, according to Allen (1975), they lack head tubercles and their middle and hind pairs of femora are narrow, not enlarged, and the margins are without serrations. But through our field investigations of the central, southern, and southwestern regions of China, the following characteristics demonstrate their stable uniqueness. The body size of the *jianchuan* complex is larger than the other complexes of *Cincticostella*. Mesothoracic anterolateral projections of the *C. insolta* complex (such as Martynov et al. 2019: figs 3, 4), *C. nigra* complex (such as Martynov et al. 2021: fig. 1C, D) and *C. gosei* complex (Martynov et al. 2021: fig. 13C, D) are not notched. The forefemora of the *C. nigra* complex (such as Martynov et al. 2021: fig. 3A) and *C. gosei* complex (Zhang et al. 2021: fig. 2D) have subapical bands of transverse setae, and the *C. insolta* complex (such as Martynov et al. 2019: figs 15, 16) and *C. gosei* complex (Zhang et al. 2021: fig. 2E, F) have serrations on the margins of middle and hind femora. The area between C, Sc and R1 of the *C. insolta* complex (Zheng and Zhou 2021: fig. 4A), *C. nigra* complex (pers. obs., Xian-Fu Li) and *C. gosei* complex (Zhang et al. 2021: fig. 3A, B) are semihyaline. The *Cincticostella insolta* complex (Zheng and Zhou 2021: fig. 6C),

**Figure 20.** Habitat of *Cincticostella jianchuan* sp. nov. **A** general habitat of Jinlong River **B** nymphs on the cobblestone, indicated by arrows.

*C. nigra* complex (pers. obs., Xian-Fu Li) and *C. gosei* complex (Zhang et al. 2021: fig. 4F) male imagoes lack the apical sclerite on the ventral face of the penes. In addition, the forewing (Figs 13A, 16A, 17C) and the hindwing (Figs 13B, 16B, 17D) of the subimago of *C. jianchuan* sp. nov. have clear differences from the *C. insolta* complex (Zheng and Zhou 2021: fig. 4B), *C. nigra* complex (pers. obs., Xian-Fu Li) and *C. gosei* complex (Zhang et al. 2021: fig. 3C, D).

The *jianchuan* complex species are at least superficially similar to species currently placed in four other genera related to *Cincticostella*, which include *Adoranexa* Jacobus & McCafferty, 2008, *Ephacerella* Paclt, 1994, *Spinorea* Jacobus & McCafferty, 2008, and *Notacanthella* Jacobus & McCafferty, 2008, based on their large size, abdominal armature of nymphs, male imago genital forceps morphology and other features. All of the species in these five genera, except for the type species of *Notacanthella*, have nymphs with a denticulate blade on the apex of the maxilla (Jacobus and McCafferty 2008). Distinctions between these genus groups (Jacobus and McCafferty 2008) were based mostly on exact combinations of nymphal thoracic projections and questionable qualities of the maxillary blade, at least some of which have been shown to be unreliable (Auychinda et al. 2020b). Zhang et al. (2021) also showed that some species based on male adults had been incorrectly assigned to genus. These facts, along with the number of species in the genus *Cincticostella* nearly doubling in very recent years, would suggest that systematics of this genus complex and the specific composition of various nominal genus groups (including their current junior synonyms) should be re-evaluated based on morphology and perhaps also with molecular data (Ogden et al. 2009).

## Additional information

### Conflict of interest

The authors have declared that no competing interests exist.

### Ethical statement

No ethical statement was reported.

### Funding

This work was supported by the National Natural Science Foundation of China (31960255) and the Second Tibetan Plateau Scientific Expedition and Research Program (2019QZKK0402).

### Author contributions

Data curation: RLY. Funding acquisition: ZWT. Writing - original draft: YKS. Writing - review and editing: LMJ, XFL.

### Author ORCIDs

Xian-Fu Li https://orcid.org/0000-0002-1258-1573
Luke M. Jacobus https://orcid.org/0000-0002-7201-3922

### Data availability

All of the data that support the findings of this study are available in the main text.

## References

Allen RK (1971) New Asian Ephemeroptera with notes (Ephemeroptera: Ephemerellidae). Canadian Entomologist 103(4): 512–528. https://doi.org/10.4039/Ent103512-4

Allen RK (1975) *Ephemerella* (*Cincticostella*): A revision of the nymphal stages (Ephemeroptera: Ephemerellidae). The Pan-Pacific Entomologist 51(1): 16–22.

Auychinda C, Muranyi D, Li W, Sartori M, Gattolliat J-L (2020a) A new species of *Cincticostella* (Ephemeroptera, Ephemerellidae) from China. Alpine Entomology 4: 129–138. https://doi.org/10.3897/alpento.4.50597

Auychinda C, Sartori M, Boonsoong B (2020b) Review of *Notacanthella* Jacobus & McCafferty, 2008 (Ephemeroptera: Ephemerellidae) in Thailand, with the redescription of *Notacanthella commodema* (Allen, 1971). Zootaxa 4731(3): 414–424. https://doi.org/10.11646/zootaxa.4731.3.9

Auychinda C, Sartori M, Boonsoong B (2022) *Cincticostella ebura* sp. nov., a new species of mayfly (Ephemeroptera, Ephemerellidae) from Thailand. ZooKeys 1130: 191–204. https://doi.org/10.3897/zookeys.1130.91039

Jacobus LM, McCafferty WP (2008) Revision of Ephemerellidae genera (Ephemeroptera). Transactions of the American Entomological Society 134(1): 185–274. https://doi.org/10.3157/0002-8320(2008)134[185:ROEGE]2.0.CO;2

Kang SC, Yang CT (1995) Ephemerellidae of Taiwan (Insecta, Ephemeroptera). Bulletin of National Museum of Natural Science 5: 95–116.

Klapálek F (1909) Ephemeridae, Eintagsfliegen. In: Brauer A (Ed.) Die Süsserwasserfauna Deutchlands. Verlag von Gustav Fischer, Jena, 8, 1–32.

Li R, Zhang W, Ma Z, Zhou C (2020) Novel gene rearrangement pattern in the mitochondrial genomes of *Torleya mikhaili* and *Cincticostella fusca* (Ephemeroptera:

Ephemerellidae). International Journal of Biological Macromolecules 165: 3106–3114. https://doi.org/10.1016/j.ijbiomac.2020.10.124

Li XF, Sun YK, Liu ZY, Jacobus LM, Xiao W (2022) A new species of *Notacanthella* Jacobus & McCafferty, 2008 (Ephemeroptera, Ephemerellidae) from Yunnan, China. ZooKeys 1103: 25–44. https://doi.org/10.3897/zookeys.1103.82984

Martynov AV, Selvakumar C, Subramanian KA, Sivaramakrishnan KG, Chandra K, Palatov DM, Sinha B, Jacobus LM (2019) Review of the *Cincticostella insolta* (Allen, 1971) complex (Ephemeroptera: Ephemerellidae), with description of three new species from northern India and Nepal. Zootaxa 4551(2): 147–179. https://doi.org/10.11646/zootaxa.4551.2.2

Martynov AV, Selvakumar C, Palatov DM, Subramanian KA, Sivaramakrishnan KG, Vasanth M, Jacobus LM (2021) Overview of Indian and Nepali representatives of the *Cincticostella nigra* (Ueno, 1928) complex (Ephemeroptera, Ephemerellidae), with discussion about *Cincticostella* Allen, 1971 species complexes. ZooKeys 1040: 123–166. https://doi.org/10.3897/zookeys.1040.64280

Ogden TH, Osborne JT, Jacobus LM, Whiting MF (2009) Combined molecular and morphological phylogeny of Ephemerellinae (Ephemerellidae: Ephemeroptera), with remarks about classification. Zootaxa 1991(1): 28–42. https://doi.org/10.11646/zootaxa.1991.1.2

Paclt J (1994) *Ephacerella*, a replacement name for *Acerella* Allen, 1971 (Ephemeroptera), nec Berlese, 1909 (Protura). Entomological News 105: 283–284.

Xie H, Jia YY, Chen P, Jacobus LM, Zhou CF (2009) Two new *Cincticostella* species from China with a larval key to species of the genus (Ephemeroptera: Ephemerellidae). Zootaxa 2299(1): 53–61. https://doi.org/10.11646/zootaxa.2299.1.5

Yang K, Li XF, Tong XL, Cai QH (2023) A new species of *Siphlonurus* Eaton, 1868 (Ephemeroptera, Siphlonuridae) from Yunnan, China. ZooKeys 1166: 121–139. https://doi.org/10.3897/zookeys.1166.102847

Zhang W, Han N, Zhang M, Wang YF, Zhou CF (2020) The imaginal and detailed nymphal characters of *Cincticostella fusca* (Kang & Yang, 1995) (Ephemeroptera: Ephemerellidae). Zootaxa 4729(2): 277–285. https://doi.org/10.11646/zootaxa.4729.2.8

Zhang M, Li WJ, Ying XL, Zhou CF (2021) The imaginal characters of *Cincticostella gosei* (Allen, 1975) linking the genus *Cincticostella* Allen, 1971 to *Ephacerella* Paclt, 1994 (Ephemeroptera: Ephemerellidae). Zootaxa 5081(1): 131–140. https://doi.org/10.11646/zootaxa.5081.1.5

Zheng X, Zhou C (2021) First detailed description of adults and nymph of *Cincticostella femorata* (Tshernova, 1972) (Ephemeroptera: Ephemerellidae). Aquatic Insects 42(1): 23–36. https://doi.org/10.1080/01650424.2020.1871026